

Assessment of the DCH Issue for Plants with Ice Condenser Containments

Sandia National Laboratories

**U.S. Nuclear Regulatory Commission
Office of Nuclear Regulatory Research
Washington, DC 20555-0001**



AVAILABILITY NOTICE

Availability of Reference Materials Cited in NRC Publications

NRC publications in the NUREG series, NRC regulations, and *Title 10, Energy, of the Code of Federal Regulations*, may be purchased from one of the following sources:

1. The Superintendent of Documents
U.S. Government Printing Office
P.O. Box 37082
Washington, DC 20402-9328
<http://www.access.gpo.gov/su_docs>
202-512-1800
2. The National Technical Information Service
Springfield, VA 22161-0002
<<http://www.ntis.gov>>
1-800-553-6847 or locally 703-605-6000

The NUREG series comprises (1) brochures (NUREG/BR-XXXX), (2) proceedings of conferences (NUREG/CP-XXXX), (3) reports resulting from international agreements (NUREG/IA-XXXX), (4) technical and administrative reports and books [(NUREG-XXXX) or (NUREG/CR-XXXX)], and (5) compilations of legal decisions and orders of the Commission and Atomic and Safety Licensing Boards and of Office Directors' decisions under Section 2.206 of NRC's regulations (NUREG-XXXX).

A single copy of each NRC draft report for comment is available free, to the extent of supply, upon written request as follows:

Address: Office of the Chief Information Officer
Reproduction and Distribution
Services Section
U.S. Nuclear Regulatory Commission
Washington, DC 20555-0001

E-mail: <DISTRIBUTION@nrc.gov>
Facsimile: 301-415-2289

A portion of NRC regulatory and technical information is available at NRC's World Wide Web site:

<<http://www.nrc.gov>>

After January 1, 2000, the public may electronically access NUREG-series publications and other NRC records in NRC's Agencywide Document Access and Management System (ADAMS), through the Public Electronic Reading Room (PERR), link <<http://www.nrc.gov/NRC/ADAMS/index.html>>.

Publicly released documents include, to name a few, NUREG-series reports; *Federal Register* notices; applicant, licensee, and vendor documents and correspondence; NRC correspondence and internal memoranda; bulletins and information notices; inspection and investigation reports; licensee event reports; and Commission papers and their attachments.

Documents available from public and special technical libraries include all open literature items, such as books, journal articles, and transactions, *Federal Register* notices, Federal and State legislation, and congressional reports. Such documents as theses, dissertations, foreign reports and translations, and non-NRC conference proceedings may be purchased from their sponsoring organization.

Copies of industry codes and standards used in a substantive manner in the NRC regulatory process are maintained at the NRC Library, Two White Flint North, 11545 Rockville Pike, Rockville, MD 20852-2738. These standards are available in the library for reference use by the public. Codes and standards are usually copyrighted and may be purchased from the originating organization or, if they are American National Standards, from—

American National Standards Institute
11 West 42nd Street
New York, NY 10036-8002
<<http://www.ansi.org>>
212-642-4900

DISCLAIMER

This report was prepared as an account of work sponsored by an agency of the United States Government. Neither the United States Government nor any agency thereof, nor any of their employees, makes any warranty, expressed or implied, or assumes

any legal liability or responsibility for any third party's use, or the results of such use, of any information, apparatus, product, or process disclosed in this report, or represents that its use by such third party would not infringe privately owned rights.

Assessment of the DCH Issue for Plants with Ice Condenser Containments

Manuscript Completed: September 1999
Date Published: April 2000

Prepared by
M. M. Pilch, K. D. Bergeron, J. J. Gregory

Sandia National Laboratories
Albuquerque, NM 87185

R. Y. Lee, NRC Project Manager

Prepared for
Division of Systems Analysis and Regulatory Effectiveness
Office of Nuclear Regulatory Research
U.S. Nuclear Regulatory Commission
Washington, DC 20555-0001
NRC Job Code J6027



ABSTRACT

This report (NUREG/CR-6427) addresses the Direct Containment Heating (DCH) issue for all Westinghouse plants with ice condenser containments. There are ten operating ice condenser plants located at five sites in the U.S. DCH phenomena in ice condenser plants are different in some important aspects from DCH phenomena in other Pressurized Water Reactors (PWRs) in that they have ice beds to suppress Design Basis Accident (DBA) steam loads, AC-powered igniters to control hydrogen concentrations in the atmosphere, small containment volumes, and containment buildings with low ultimate capacities to withstand internal pressures.

Unlike PWRs with large dry or subatmospheric containments, the DCH issue for ice condenser plants could not be resolved by a probabilistic comparison of containment loads versus containment strength. The approach taken here is to provide an expansion of a probabilistic framework, which represents a simplification of the NUREG-1150 containment event tree for Sequoyah. The containment event tree is intended to give each containment challenge its proper probabilistic weighting based on plant specific core damage frequencies, phenomenological probabilities, and plant specific fragility curves. The probabilistic framework addresses DCH-induced overpressure failures in the context of all significant early containment failure modes. These include DCH overpressure failures, thermal failures of the containment liner, non-DCH hydrogen combustion overpressure failures, and non-explosive steam spike overpressure failures.

The most significant finding of this study was that the early containment failure probability is dominated by non-DCH hydrogen combustion events rather than DCH events. This is because the HPME probability is small, the SBO probabilities are small, and because containment loads in non-station blackouts are not containment threatening.

The CONTAIN code was used exclusively to calculate containment loads resulting from DCH, non-DCH hydrogen combustion, and non-explosive steam spikes for representative station blackout and non-station blackout scenarios. CONTAIN calculations show that no ice condenser plant is inherently robust to all credible DCH or hydrogen combustion events in station blackouts. CONTAIN predictions show that containment loads in nonstation blackout are not containment threatening for any reasonable plant damage state.

Consistent with perceptions of the technical community, this study shows that ice condenser plants are substantially more sensitive to early containment failure than PWRs with large dry or subatmospheric containments. A plant-specific evaluation of the containment event tree showed that all plants, except McGuire, have an early failure probability within the range 0.35% to 5.8% for full power internal events. The early containment failure probability was 13.9% for McGuire. The higher containment failure probability is dominated by the relatively higher station blackout probability and relatively weaker containment for McGuire.

Reduction in the probability of a struck open power-operated relief valve (PORV) after uncovering of the top of active fuel (UTAF) had no significant impact on the conclusions of this study. Reduction in the hot leg failure probability increases the probability of early containment failure for those plants with a large SBO frequency, but not to the point that conclusions regarding compliance with NRC goals would change. An additional sensitivity study assuming

Abstract

intentional depressurization by the operators after UTAF also had no impact on the conclusions of this study. All plants, especially McGuire, would benefit from reducing the station blackout frequency or some means of hydrogen control that is effective in station blackouts. The risk reduction was greater than an order of magnitude for all plants; however, NRC goals are generally achieved without such actions. If the igniters and air return fans are not available (e.g., SBOs), uncertainties in containment loads are dominated by uncertainties in hydrogen combustion phenomena and the amount of clad oxidized during core degradation

CONTENTS

| <u>Section</u> | <u>Page</u> |
|--|-------------|
| ABSTRACT | iii |
| EXECUTIVE SUMMARY | xv |
| ACKNOWLEDGMENTS | xxi |
| ACRONYMS | xxiii |
| NOMENCLATURE | xxv |
| 1.0 INTRODUCTION | 1 |
| 2.0 ASSESSMENT METHODOLOGY | 5 |
| 3.0 ASSESSMENT OF ICE CONDENSER CONTAINMENT PHENOMENA | 9 |
| 3.1 Introduction | 9 |
| 3.2 Phenomenological Overview | 10 |
| 3.2.1 Global Scaling Parameters: Large Dry Containment vs. Ice Condenser Containments | 12 |
| 3.2.2 Specific Issues Involving HPME in Ice Condenser Containments | 17 |
| 3.2.2.1 Availability of ESFs | 17 |
| 3.2.2.2 HPME Threats Other Than DCH | 22 |
| 3.2.2.3 Other Phenomenological Issues | 25 |
| 4.0 QUANTIFICATION OF THE PROBABILISTIC FRAMEWORK | 29 |
| 4.1 HPME Tree | 33 |
| 4.1.1 RCS Leak Size at Uncovery of Top of Active Fuel (UTAF) | 33 |
| 4.1.2 Stuck Open PORV During Cycling at SSP | 46 |
| 4.1.3 Temperature-Induced Leak in RCP Seals | 48 |
| 4.1.4 Intentional Depressurization of the RCS | 49 |
| 4.1.5 Temperature-Induced Failure of the Surge Line or Hot Leg | 52 |
| 4.1.6 RCS Pressure Prior to Possible Vessel Breach | 54 |
| 4.1.7 AC Power Recovery After UTAF and Before Vessel Breach | 56 |
| 4.1.8 Core Damage Arrest | 58 |
| 4.2 Containment Failure Tree | 60 |
| 4.2.1 Vessel Breach Mode and Size | 60 |
| 4.2.2 Cavity Water | 62 |
| 4.2.3 DCH Overpressure Failures | 64 |
| 4.2.4 Containment Liner Failure | 68 |
| 4.2.5 Non-DCH Overpressure Failure at Vessel Breach | 70 |
| 5.0 CONTAIN CALCULATIONS IN SUPPORT OF CONTAINMENT LOADS AT VESSEL BREACH AND ICE INVENTORY | 73 |

| | | |
|------------|--|-----|
| 5.1 | Introduction | 73 |
| 5.2 | CONTAIN Code..... | 74 |
| | 5.2.1 Capabilities of the CONTAIN Code | 74 |
| | 5.2.2 Overview of Calculations..... | 75 |
| | 5.2.3 CONTAIN Options and Model Parameters | 77 |
| 5.3 | Containment Response for DCH-Relevant Scenarios..... | 83 |
| | 5.3.1 Scenario VI-c: Non-Station Blackouts | 83 |
| | 5.3.2 Scenario VI-d: Station Blackouts | 89 |
| 5.4 | Insights on Predictions of Ice Inventory at Vessel Breach | 92 |
| | 5.4.1 Historical Perspective..... | 93 |
| | 5.4.2 Analytic Insights on Ice Inventory..... | 96 |
| 5.5 | Containment Response for Non-DCH Relevant Scenarios..... | 97 |
| 5.6 | Conclusions from the CONTAIN Studies..... | 100 |
| 6.0 | QUANTIFICATION OF CONTAINMENT FRAGILITY | 101 |
| 7.0 | RESULTS AND SENSITIVITIES..... | 105 |
| 7.1 | Benchmark Evaluations..... | 105 |
| 7.2 | Extrapolation Evaluations | 105 |
| 7.3 | Sensitivity Studies | 113 |
| 8.0 | SUMMARY AND RECOMMENDATION | 121 |
| 9.0 | REFERENCES..... | 127 |
| Appendix A | Extension of Zion SCDAP/RELAP5 Analysis Supporting DCH Issue Resolution for PWRs with Ice Condenser Containments..... | A-1 |
| Appendix B | CONTAIN Code Analyses of DCH in Ice Condenser Plants..... | B-1 |
| Appendix C | Plant Geometry..... | C-1 |
| Appendix D | A Splinter Scenario Approach to DCH Resolution of DCH. | D-1 |
| Appendix E | Peer Review Comments | E-1 |

FIGURES

| <u>Figure</u> | <u>Page</u> |
|--|-------------|
| 3.1 Layout of a typical ice condenser containment (taken from Sequoyah IPE) | 11 |
| 3.2 Screening margin and pressure energy ratio..... | 16 |
| 3.3 Hydrogen and Zr/UCO ₂ ratio parameters..... | 16 |
| 4.1 HPME probability for slow station blackouts in Sequoyah | 34 |
| 4.2 Early containment failure for slow station blackouts in Sequoyah..... | 35 |
| 4.3 HPME probability for fast station blackouts in Sequoyah..... | 36 |
| 4.4 Early containment failure for fast station blackouts in Sequoyah..... | 37 |
| 4.5 HPME probability for LOCAs in Sequoyah..... | 38 |
| 4.6 Early containment failure for LOCAs in Sequoyah | 39 |
| 4.7 HPME probability for transients in Sequoyah..... | 40 |
| 4.8 Early containment failure for transients in Sequoyah | 41 |
| 4.9 HPME probability for ATWS in Sequoyah..... | 42 |
| 4.10 Early containment failure for ATWS blackouts in Sequoyah..... | 43 |
| 4.11 HPME probability for internal floods in Sequoyah..... | 44 |
| 4.12 Early containment failure for internal floods in Sequoyah | 45 |
| 4.13 NUREG-1150 quantification of probability of liner failure as a function of melt mass dispersed into the ICIR..... | 69 |
| 5.1 CONTAIN nodalization of the Sequoyah containment (UP and LP are the upper and lower plena)..... | 78 |
| 5.2 Comparison of predictions using CONTAIN 1.2 and CONTAIN 2.0 for Scenario VIa | 82 |
| 5.3 SCDAP/RELAP-5Upper containment pressure for Case VI using original SCDAP/RELAP-5 sources | 85 |
| 5.4 Energy injected into containment from coolant | 86 |

FIGURES (Continued)

| <u>Figure</u> | <u>Page</u> |
|---|-------------|
| 5.5 Predicted ice inventory in non-SBOs with bounding steam sources representative of scenarios with ARFs and no auxiliary feedwater | 87 |
| 5.6 DCH pressure excursion in the upper compartment for Scenario VI-d for different deck leakage assumptions..... | 91 |
| 5.7 Ice remaining for different deck leakage assumptions | 91 |
| 5.8 Peak hydrogen concentrations for Scenario VI-d (SBOs)..... | 92 |
| 5.9 Prediction of ice inventory for various modeling approaches..... | 98 |
| 6.1 Fragility curves for all Westinghouse plants with ice condenser containments | 104 |
| B.1 CONTAIN nodalization of the Sequoyah containment | B-41 |
| B.2 Pressure histories in the upper and lower compartments for the reference case | B-42 |
| C.1 Schematic drawings of the IDCOR cavity groups | C-20 |
| C.2 Layout of an ice condenser typical containment (taken from the Watts Bar IPE)..... | C-21 |
| D.1 The probabilistic framework for containment failure under direct containment heating scenarios. The (J) and (F) are the “joint” and “function” operations, respectively. | D-4 |
| D.2 Splinter DCH scenarios used in NUREG/CR-6075 | D-34 |
| D.3 Splinter DCH scenarios reflecting working group recommendations. | D-35 |
| D.4 Further definition of splinter scenarios for ice condenser plants..... | D-36 |
| D.5 Timing of key core melt progression events for a SBO with a 250 gpm/pump leak..... | D-37 |
| D.6 Distribution for fraction of Zr oxidized (core-wide) in Scenarios V and VI | D-38 |
| D.7 Crucible formation in a flooded RPV-Scenarios V, Va, and Vb..... | D-39 |
| D.8 Distribution of molten UO ₂ in the lower plenum at the time of vessel rupture for Scenarios V, Va, and Vb..... | D-40 |

FIGURES (Concluded)

| <u>Figure</u> | <u>Page</u> |
|---|-------------|
| D.9 Crucible formation in wet core scenarios with partial operator invention-Scenarios VI, Via, and VIb,..... | D-41 |
| D.10 Distribution for molten UO ₂ in the lower plenum at the time of vessel rupture for Scenarios VI, VIa, and VIb,..... | D-42 |
| D.11 Validation of the two-cell equilibrium model against all experiments with compartmentalized geometry..... | D-54 |
| D.12 Potential impact of codispersed water on DCH loads. | D-55 |
| D.13 Validation of the coherence ratio for scenarios without coejected water. | D-56 |
| D.14 Validation of the hole ablation model..... | D-57 |
| D.15 Fragility curves for all Westinghouse plants with ice condenser containments. | D-61 |

TABLES

| <u>Table</u> | <u>Page</u> |
|---|-------------|
| 4.1 Mean core damage frequency and fractional contribution of various core damage initiators to core damage | 31 |
| 4.2 Comparison of leak size characteristics..... | 46 |
| 4.3 Initiator leak sizes at UTAF ¹ : Sequoyah NUREG-1150..... | 47 |
| 4.4 Leak sizes associated with LOCAs as a CDI in all ice condenser plants | 48 |
| 4.5 Quantification of a stuck open PORV issue..... | 48 |
| 4.6 NUREG-1150 Quantification of Westinghouse reactor coolant pump leaks for station blackout accidents | 50 |
| 4.7 Sequoyah and Watts Bar quantification of temperature- induced RCP leaks for station blackout accidents | 51 |
| 4.8 Temperature-induced reactor coolant pump leaks following UTAF..... | 51 |
| 4.9 Intentional depressurization of the RCS..... | 52 |
| 4.10 Probability of temperature induced failure of the surge line or hot leg | 53 |
| 4.11 Mapping of leak sizes to RCS pressure prior to possible vessel breach..... | 55 |
| 4.12 SNL recommended collapsed mapping of leak sizes into RCS pressure prior to possible vessel breach | 56 |
| 4.13 Probability of AC recovery after UTAF and before vessel breach in SBOs | 57 |
| 4.14 Assessment of AC Recovery recovery and Core core Damage damage arrest in ice condenser plants | 58 |
| 4.15 Quantification of core damage arrest/invessel..... | 59 |
| 4.16 NUREG-1150 quantification of vessel breach mode and size..... | 61 |
| 4.17 Inferred NUREG-1150 quantification of cavity water at vessel breach | 63 |
| 4.18 Recommended quantification of cavity water at vessel breach | 63 |
| 4.19 NUREG-1150 quantification of DCH containment overpressure failure probability for NUREG-1150 scenarios with “medium” core fraction and ice condenser effective | 65 |

TABLES (Continued)

| <u>Table</u> | <u>Page</u> |
|---|-------------|
| 4.20 Recommended DCH loads at vessel breach based on CONTAIN analyses | 66 |
| 4.21 Recommended DCH containment overpressure failure probabilities for extrapolation evaluations assuming a DCH event occurs | 67 |
| 4.22 Quantification of liner melt through given a HPME event for different vessel pressures and a non-flooded cavity..... | 69 |
| 4.23 NUREG-1150-like quantification of containment over pressure failure probabilities for non-DCH events..... | 72 |
| 4.24 SNL recommended containment overpressure failure probabilities for non-DCH event | 72 |
| 5.1 DCH-relevant scenarios for CONTAIN calculations..... | 76 |
| 5.2 CONTAIN representation of the ice condenser doors | 80 |
| 5.3 Recommended parameters from long-term Waltz Mill analyses | 81 |
| 5.4 Dry-Cavity DCH pressures for Scenario VI-c; non-SBO | 88 |
| 5.5 NUREG/CR-4551, Vol. 5, Rev. 1, Part 2, Quantification (Q29) of ice remaining at vessel breach for the NUREG-1150 study | 93 |
| 5.6 SCDAP/RELAP5 sequence timings for case of best estimate (250 gpm/pump) RCP leaks . | 94 |
| 5.7 Conditions assumed for steam spike | 99 |
| 5.8 Cases without DCH (combustion enabled at VB)..... | 99 |
| 6.1 Containment fragility | 103 |
| 7.1 Detailed comparison of (benchmark) lower head failure probabilities with Full NUREG-1150 results | 106 |
| 7.2 Comparison of (benchmark) early containment failure modes with full NUREG-1150 results..... | 107 |
| 7.3 Summary of base case results using Sequoyah IPE input | 109 |
| 7.4 Early containment failure probability for all ice condenser plants | 111 |
| 7.5 Comparison of external events and internal events core damage frequencies | 112 |

TABLES (Continued)

| <u>Table</u> | <u>Page</u> |
|--------------|---|
| 7.6 | Summary of key phenomenological assumptions, uncertainties, and their implications..... 117 |
| 7.7 | Simplified snapshot of DCH assessments for McGuire..... 119 |
| B.1 | CONTAIN representation of the Sequoyah containment B-34 |
| B.2 | RCS initial conditions for Sequoyah DCH calculations B-35 |
| B.3 | Timing and coherence information for debris, steam, and water sources B-36 |
| B.4 | Ice condenser containment fragility measures..... B-36 |
| B.5 | Containment conditions at vessel breach B-36 |
| B.6 | Containment pressurization from blowdown alone B-37 |
| B.7 | Reference calculations for comparison with TCE/LHS..... B-37 |
| B.8 | Summary of Scenario V and Scenario Va results B-38 |
| B.9 | Summary of Scenario VI and VIa results B-39 |
| B.10 | Cases without igniters B-40 |
| C.1 | Cavity dispersal summary..... C-17 |
| C.2 | Validation of melt retention by freezing during cavity dispersal..... C-18 |
| C.3 | Input for coherence ratio correlation..... C-18 |
| C.4 | Cavity water summary C-18 |
| D.1 | Definition of Probability Levels D-3 |
| D.2 | Description of TCE/LHS summary quantifications. D-25 |
| D.3 | Model input for Scenario V D-27 |
| D.4 | Model input for Scenario Va D-28 |

TABLES (Concluded)

| <u>Table</u> | <u>Page</u> |
|---|-------------|
| D.5 Model input for Scenario Vb | D-29 |
| D.6 Model input for Scenario VI..... | D-30 |
| D.7 Model input for Scenario VIa | D-31 |
| D.8 Model input for Scenario Vib | D-32 |
| D.9 Distribution of molten UO ₂ mass at the time of vessel breach for Scenario V, and Va, andVb..... | D-33 |
| D.10 Distribution of molten UO ₂ mass at the time of vessel breach for Scenario VI, VIa, and Vib | D-33 |
| D.11 Comparison with prior work for Zion | D-33 |
| D.12 Survey of DCH-relevant experiments | D-50 |
| D.13 CONTAIN/TCE comparisons | D-52 |
| D.14 Experiments insights on “cojected” water for Calvert Cliffs geometry..... | D-53 |
| D.15 Applicability of the database to reactors..... | D-53 |
| D.16 Validation of melt retention by freezing during cavity dispersal..... | D-53 |
| D.17 Containment fragility | D-60 |
| D.18 CCFO results using TCE/LHS with the small dry assumption..... | D-65 |
| D.19 CCFP results biasing TCE predictions to be more representative of CONTAIN predictions with the small dry approximation | D-65 |
| D.20 CCFP results biasing TCE predictions to match point comparisons with CONTAIN assuming ice remains in the ice chest | D-65 |
| D.21 Comparison of NUREG-1150 loads elicitation with DCH predicted in this study..... | D-66 |

EXECUTIVE SUMMARY

In a light-water reactor core melt accident, if the reactor pressure vessel (RPV) fails while the reactor coolant system (RCS) is at high pressure, the expulsion of molten core debris may pressurize the reactor containment building (RCB) beyond its failure pressure. A failure in the bottom head of the RPV, followed by melt expulsion and blowdown of the RCS, will entrain molten core debris in the high-velocity steam blowdown gas. This chain of events is called a high-pressure melt ejection (HPME). Four mechanisms may cause a rapid increase in pressure and temperature in the reactor containment: (1) blowdown of the RCS, (2) efficient debris-to-gas heat transfer, (3) exothermic metal/steam and metal/oxygen reactions, and (4) hydrogen combustion. These processes, which lead to increased loads on the containment building, are collectively referred to as direct containment heating (DCH). It is necessary to understand factors that enhance or mitigate DCH because the pressure load imposed on the RCB may lead to early failure of the containment.

NUREG/CR-6075 and its supplement, "The Probability of Containment Failure by Direct Containment Heating in Zion," established the methodology and success criterion for resolving the DCH issue for nuclear power plants (NPP) with large dry containments. NUREG/CR-6109, "The Probability of Containment Failure by Direct Containment Heating in Surry," applied the same methodology to the Surry plant (subatmospheric containment) as a second demonstration of the DCH resolution methodology. DCH was examined in a broader way for all Westinghouse (W) plants, excluding plants with ice condenser containments, in NUREG/CR-6338, "Resolution of the Direct Containment Heating Issue for all Westinghouse Plants with Large Dry Containments or Subatmospheric Containments." Most recently, the DCH issue was examined for all Combustion Engineering (CE) and Babcock & Wilcox (B&W) plants in NUREG/CR-6475, "Resolution of the Direct Containment Heating Issue for Combustion Engineering Plants and Babcock & Wilcox Plants." In the vast majority of PWRs with large dry or subatmospheric containments, DCH is the dominant mode of early containment failure, and the DCH issue was resolved through plant specific probabilistic comparisons of DCH loads versus containment strength without taking credit for low HPME probabilities. In a few cases, recourse to elementary assessments of HPME probabilities or other supplementary arguments was required to ensure that the DCH issue was adequately resolved.

This report (NUREG/CR-6427) addresses the DCH issue for all Westinghouse plants with ice condenser containments. There are ten ice condenser operating plants located at five sites in the U.S. DCH phenomena in ice condenser plants are different in some important aspects from DCH phenomena in plants with large dry or subatmospheric containments. Ice condenser plants are unique among PWRs in that they have ice beds to suppress Design Basis Accident (DBA) steam loads, AC-powered igniters to control hydrogen concentrations in the atmosphere, small containment volumes, and containment buildings with low ultimate capacities for pressure.

The most significant finding of this study was that the early containment failure probability is dominated by non-DCH hydrogen combustion events (which only occur during station blackouts) rather than by DCH events. This is because the station blackout (SBO) probability is small, the HPME probability is small, and because containment loads are non-threatening for any reasonable plant damage state (PDS) associated with a non-SBO.

Executive Summary

Initially, the methodology developed in NUREG/CR-6075 and NUREG/CR-6075, Supplement 1, was used to perform a load versus strength evaluation for each of these plants using plant-specific data gathered from Individual Plant Examinations (IPEs), Final Safety Analysis Reports (FSARs), and direct contacts with plant personnel (when necessary). The same enveloping accident scenarios (splinters) that were used in NUREG/CR-6075, Supplement 1, and NUREG/CR-6109 were used for these plant evaluations under the assumption that a DCH event occurs. One additional splinter scenario, unique to plants with ice condenser containments, was also considered. These splinter scenarios establish important input parameters for the DCH load calculations, e.g., the RCS pressure at vessel breach, the melt mass and composition, the RPV breach size, the containment pressure and atmosphere composition at vessel breach, etc. The initial approach taken was to model the ice condenser plant as a small dry containment without taking credit for the passive pressure suppression afforded by the ice beds or the active pressure suppression afforded by containment sprays. Scenarios with deeply flooded cavities were not analyzed.

Assuming core damage and a HPME/DCH event, all ice condenser plants exceeded the metric (conditional containment failure probability, CCFP ≤ 0.1) based on DCH-induced overpressure failures alone. Consequently, the DCH issue could not be resolved based on load/strength evaluations alone if a DCH event was postulated, and credit for ice beds, sprays, and igniters is not taken.

This initial assessment of DCH in ice condenser plants was reviewed by a NRC-sponsored panel of six experts who are familiar with the phenomenology and the DCH issue resolution process. Reviewer comment and recommendations fell into three general categories:

1. Expand the probabilistic framework to include sequence probabilities,
2. Validate CONTAIN's ice condenser models if CONTAIN is to be used in the load calculations, and
3. Model the ice condenser explicitly in the loads calculations.

This revision of draft NUREG/CR-6427 explicitly addresses these peer review comments. The approach taken is to provide an expansion of the probabilistic framework, which represents a simplification of the NUREG-1150 containment event tree for Sequoyah. The probabilistic framework addresses DCH-induced overpressure failures in the context of all significant early containment failure modes. These include DCH overpressure failures, thermal failures of the containment liner, non-DCH hydrogen combustion overpressure failures, and non-explosive steam spike overpressure failures.

The following practical approach was adopted for assessing the importance of HPME/DCH to early containment failure for all ice condenser plants.

1. Develop a simplified version of the NUREG-1150 containment event tree (CET) that operates on each core damage initiator (CDI) as a class (e.g., LOCAs) and not on the hundreds of plant damage states (PDS) that might be members of a given class.

2. Benchmark the simplified tree by demonstrating that the simplified tree, with NUREG-1150 consistent input, reproduces (in a reasonable fashion) the results documented in NUREG-1150 for Sequoyah. This ensures that all significant top events have been identified from the NUREG-1150 study.
3. Update specific quantifications in the simplified CET if significant new work since the time of NUREG-1150 justifies the revision. Significant quantifications that were updated include the hot leg failure probability and a reassessment of containment loads using CONTAIN. Additional simplifications of the CET are possible to produce a more scrutable result for extrapolation evaluations.
4. Use the more simplified logic tree to evaluate, in a consistent manner, the early containment failure probabilities for all ice condenser plants (including a reevaluation for Sequoyah) using plant specific information (e.g., fragility and CDI frequencies) to the extent that information is available from the IPEs.

A simplified CET was developed to quantify the HPME probability and the early containment failure probability for each of the six CDI classes: slow station blackout, fast station blackout, loss of coolant accident (LOCAs), transients, anticipated transients without scram (ATWS), and internal floods. We focus on full power internal events and exclude bypass events such as interfacing LOCAs and steam generator tube ruptures. The HPME portion of the CET quantifies whether core damage is arrested in vessel and at what RCS pressure does vessel failure occur if core damage is not arrested in vessel. The top events are:

1. RCS leak size at UTAF,
2. Stuck open PORV during cycling at system setpoint (SP),
3. Temperature-induced leak in reactor coolant pump (RCP) seals,
4. Intentional depressurization of the RCS,
5. Temperature-induced failure of the surge line or hot leg,
6. RCS pressure prior to possible vessel failure,
7. AC power recovery after UTAF and before vessel breach, and
8. Core damage arrest in vessel.

The containment failure portion of the CET addresses vessel breach mode/size, the quantity of water in the cavity, and each of the four containment failure mechanisms noted above.

The CONTAIN code was used exclusively to calculate containment loads resulting from DCH, non-DCH hydrogen combustion, and non-explosive steam spikes for representative station blackout and non-station blackout scenarios. The ice condenser model in CONTAIN was recently benchmarked against Waltz Mill data (full-height tests for ice condenser performance)

Executive Summary

for DBA conditions. CONTAIN has also been benchmarked against key experiments that emphasize each of the three sources of containment loads noted above. However, there are no integral DCH tests in ice condenser geometry to fully validate CONTAIN for this application.

Steam sources were taken from a SCDAP/RELAP5 SBO calculation and used as input to a CONTAIN code model of the ice condenser containment. CONTAIN predicted that approximately half the ice remained at the time of vessel breach. A fully consistent calculation of ice inventory for non-SBO events was not performed as part of this study, but a review of NUREG-1150 quantifications shows that 10-50% of the ice remains at the time of predicted vessel breach for DCH relevant scenarios. NUREG-1150 quantifications showed total or almost total ice melt for a number of scenarios; these tended to be cases involving large LOCAs or induced large LOCAs that preclude DCH.

CONTAIN calculations performed in support of the present effort show that there is a potential for the ice to be considerably more effective in preventing threatening DCH loads than indicated by the earlier studies, provided igniters (and ARFs) are operating prior to vessel breach. The principal reason is that the combination of limited metal in the melt and oxygen starvation in the lower containment resulted in a much smaller contribution from the combustion of DCH-produced hydrogen, and the ice was calculated to be very effective in suppressing pressurization owing to superheated gas and steam.

CONTAIN calculations showed that no ice condenser plant is inherently robust to all credible DCH or hydrogen combustion events in a station blackout (SBO) accident. The containment is threatened by hydrogen combustion events alone because igniters, which are AC-powered, are not available to mitigate the accumulation of very high concentrations of hydrogen in the containment. Hydrogen combustion, initiated by and in conjunction with a DCH event is even more threatening. The ice beds were found to significantly reduce DCH loads in a SBO accident, but not to a level that did not threaten the containment. CONTAIN predicted non-threatening containment loads for non-SBOs provided ice or one train of containment sprays is available. If the refueling water storage tank has emptied and approximately 50% or more of the ice is melted, the reactor cavity will be deeply flooded and the nature of containment loads change from DCH to non-threatening steam spikes.

The containment event tree is intended to give each containment challenge its proper probabilistic weighting based on plant specific core damage frequencies, phenomenological probabilities, and plant specific fragility curves. The CET event tree was benchmarked against NUREG-1150 to ensure that all significant top events were reasonably represented in a simplified CET patterned after NUREG-1150. Detailed comparisons proved this to be the case. The CET was further simplified by introducing some conservative assumptions and specific quantifications were updated based on more recent NRC-sponsored research.

A plant-specific evaluation of the CET showed that all plants, except McGuire, had an early failure probability (given core damage) within the range 0.35% to 5.8% for full power internal events. These integral estimates of early containment failure are qualitatively consistent with published IPE results for these plants. The early containment failure probability, as computed here, was 13.9% for McGuire. This higher containment failure probability for McGuire is

dominated by the relatively high SBO frequency and the relatively weak containment for McGuire. The IPE assessments of early containment failure at McGuire (2%) are significantly lower than our assessments; however, we have not investigated the reasons for this difference.

Phenomenological uncertainties are large, but a fully integrated uncertainty study was outside the scope of this effort. However, selected sensitivity studies were performed here to illuminate the importance of certain quantifications and to examine the importance of certain accident management procedures that might be proposed. Reduction in the hot leg failure probability and the probability of a stuck open power-operated relief valve (PORV) after uncovering of the top of actual fuel (UTAF) had no significant impact on the results of this study. Reduction in the hot leg failure probability increases the probability of early containment failure for those plants with a large SBO frequency, but not to the point that conclusions regarding compliance with NRC goals would change. An additional sensitivity study assuming intentional depressurization by the operators after UTAF also had no impact on the conclusions of this study. All plants, especially McGuire, would benefit from a reduction in SBO frequency or some means of hydrogen control that is effective in SBOs. The resulting risk reduction is greater than an order of magnitude for all plants.

Assuming igniters and air return fans are not operational (e.g. SBOs), uncertainties in containment loads are dominated by uncertainties in hydrogen combustion phenomena and the amount of clad oxidized during core degradation. For non-SBOs, uncertainties in containment loads are dominated by uncertainties in modeling, the availability of sprays, the ice inventory at vessel breach, and the melt mass. We use the mean fragility curves as reported in the IPEs, which have not been reviewed. These fragility curves are steep with a short low-end tail, and any uncertainties in these fragility curves could have a significant impact on computed containment failure probabilities.

Consistent with perceptions of the technical community, this study shows that ice condenser plants are substantially more sensitive to early containment failure than PWRs with large dry or subatmospheric containments. These perceptions, however, are not consistent with IPE results summarized in NUREG-1560 that show many PWRs with large dry or subatmospheric containments report early containment failure probabilities in excess of 10% given a core damage accident, while none of the ice condenser plants reported early failures greater than 2.4%. NUREG-1560 cites DCH processes as the main contribution to early containment failure in PWRs with large dry or subatmospheric containments. In light of more recent NRC estimates of DCH-induced containment failure probabilities, we conclude that many utilities with large dry or subatmospheric containments were overly conservative in their treatment of HPME probabilities and DCH loads.

To develop a more integrated perspective for risk-informed regulation, it is recommended that the insights of this study be factored into more complete Level II analyses for each significant plant damage state and that the evaluation of early containment failure be evaluated not only for internal events, but also for external events, low power shutdown events, and bypass events. For completeness, we recommend that a formal uncertainty study be performed to quantify the impact of identified uncertainties on early containment failure; however, uncertainties in the fundamental DCH processes of dispersal, fragmentation, and debris/gas heat

Executive Summary

transfer are not likely to contribute significantly to the overall uncertainty in early containment failure because these DCH processes are such a small contributor to early containment failure. Containment sprays are important in mitigating loads in non-SBOs if the ice inventory is depleted, but it remains to be confirmed that plants with identified vulnerabilities in switching to recirculation mode have implemented proposed remediations.

ACKNOWLEDGMENTS

The authors would like to acknowledge M.D. Allen, D.C. Williams, K.S. Quick,* and S.W. Hong,** who contributed significantly to an earlier draft of this report. Their contributions, in part, are acknowledged in the current report by their listed authorship of appendices. The authors would like to thank J.J. Gregory and R.G. Cox, who reviewed the first report and provided numerous helpful comments. A.L. Camp and L.L. Humphries reviewed this revised draft of the report. Energy Research, Inc., summarized some key insights from the IPEs and reviewed large format (paper) versions of the event tree used in our benchmark calculations. The authors are especially grateful for the constructive comments received from an NRC-sponsored peer review consisting of R.E. Henry, M. Ishii, S. Levy, M. Modarres, F. Moody, and D. Stamps. M.L. Garcia typed, compiled, and edited the first manuscript, and R.F. Yellowrobe assumed the responsibilities for the revised manuscript.

Much of the successful resolution of the DCH issue is the result of an extensive experimental program managed by M.D. Allen and T.K. Blanchat. The DCH experiments were reviewed as part of a Nuclear Regulatory Commission (NRC)-sponsored effort known as the Severe Accident Scaling Methodology (SASM) Program that was chaired by N. Zuber (NRC). As a result of SASM recommendations, the NRC-sponsored experimental programs were redirected toward performing integral counterpart experiments at two different physical scales at Sandia National Laboratories and Argonne National Laboratory. These experiments included detailed (geometrically scaled) simulations of the Zion, Surry, and Calvert Cliffs subcompartment structures and had initial conditions closely tied to postulated accident scenarios. Additional guidance for the Zion and Surry experiment programs was provided by a five-member DCH Experiment Technical Review Group (TRG) that included R.E. Henry, M. Ishii, F.J. Moody, T.G. Theofanous, and B.R. Sehgal. Guidance for the Calvert Cliffs experiment program was provided by a five-member DCH Experiment TRG that included R.E. Henry, M. Ishii, F.J. Moody, S. Levy, and M.L. Corradini.

This work was sponsored by the Safety Margins and Systems Analysis Branch of the Office of Research of the U.S. Nuclear Regulatory Commission. Input and valuable guidance were supplied by R.Y. Lee and C.G. Tinkler.

* Idaho National Engineering Laboratory.

** On special assignment from Korea Atomic Energy Research Institute (KAERI).

ACRONYMS

| | |
|-------|--|
| ANL | Argonne National Laboratory |
| ANS | American Nuclear Society |
| ARFs | air return fans |
| ATWS | anticipated transients without scram |
| BSR | bulk spontaneous reaction |
| B&W | Babcock & Wilcox |
| CCFP | conditional containment failure probability |
| CDA | core damage arrest |
| CDF | core damage frequency |
| CDI | core damage initiator |
| CE | combustion engineering |
| CET | containment event tree |
| CLCH | convection limited containment heating |
| CR1 | causal relation |
| CTTF | Containment Technology Test Facility |
| CWTI | corium/water thermal interaction |
| DBA | design basis accident |
| DCH | direct containment heating |
| DDT | deflagration-to-detonation transition |
| DFB | diffusion flame burning |
| DPD | discrete probability distribution |
| ECCS | emergency core cooling system |
| EPRI | Electric Power Research Institute |
| ESF | engineered safety features |
| FAI | Fauske and Associates, Inc. |
| FCI | fuel coolant interaction |
| FSAR | final safety analysis report |
| GPM | gallons per minute |
| HIPS | high pressure streaming |
| HP | high pressure |
| HPIS | high pressure injection system |
| HPME | high-pressure melt ejection |
| ICIR | incore instrument room |
| IET | Integral Effects Test |
| INEL | Idaho National Engineering Laboratory |
| IPE | Individual Plant Examination |
| IPEEE | individual plant examinations of external events |
| LB | lower bound |
| LERF | large early release fraction |
| LFP | Limited Flight Path |
| LHS | Latin hypercube sampling |
| LOCA | loss of coolant accident |
| LP | low pressure |

ACRONYMS (concluded)

| | |
|----------|---|
| LPIS | low pressure safety injection system |
| LWR | light water reactor |
| NPP | nuclear power plant |
| NRC | Nuclear Regulatory Commission |
| NSSS | nuclear steam supply system |
| OTSG | once-through steam generator |
| PARS | passive autocatalytic recombiners |
| PDF | probability density function |
| PDS | Plant damage states |
| PORV | power-operated relief valve |
| PRA | probabilistic risk assessment |
| PSA | plant safety assessment |
| PSAR | preliminary safety analysis report |
| PWR | pressurized water reactor |
| QS | quench spray |
| RCB | reactor containment building |
| RCDT | reactor coolant drain tank |
| RCP | reactor coolant pump |
| RCS | reactor coolant system |
| RHR | residual heat removal |
| RPV | reactor pressure vessel |
| RWST | refueling water storage tank |
| SAGs | Severe Accident Guidelines |
| SASM | Severe Accident Scaling Methodology |
| SBLOCA | small break loss-of-coolant accident |
| SBO | station blackout accident |
| SG | steam generator |
| SNL | Sandia National Laboratories |
| SP | setpoint |
| SRV | |
| SSP | system setpoint pressure |
| STR | seal table room |
| TCE | Two-Cell Equilibrium |
| TDS | Technology Development Tests |
| TMI-II | Three Mile Island-II |
| TMLB | |
| TPG | Technical Program Group |
| TRG | DCH Experiment Technical Review Group |
| TSC | technical support center |
| USNRC | United States Nuclear Regulatory Commission |
| UTAF | Uncovery of Top of Active Fuel |
| VB | vessel breach |
| <u>W</u> | Westinghouse |

NOMENCLATURE

| | |
|--------------|---|
| A_h | = breach area in RPV |
| A_s | = surface area of the reactor cavity |
| C_d | = discharge coefficient (0.6) |
| $C_{d,h}$ | = discharge coefficient |
| $C_{p,w}$ | = heat capacity of RPV steel |
| $C_{R\tau}$ | = constant in coherence correlation |
| C_v | = constant-volume molar heat capacity of the containment atmosphere |
| D_h^0 | = initial hole diameter |
| . | |
| D_h | = characteristic ablation rate |
| e_{bias} | = relative bias |
| . | |
| E_{HT} | = characteristic heat transfer rate to structure |
| . | |
| E_{H2} | = energy release rate from combustion of pre-existing hydrogen |
| f_{coh} | = fraction of blowdown steam coherent with debris dispersal |
| f_d | = fraction dispersed |
| f_{disp} | = fraction of debris dispersed from cavity |
| f_{pre} | = fraction of pre-existing hydrogen burned on DCH timescales |
| f_{Zr} | = fraction of Zr mass oxidized core-wide |
| F_f | = failure frequency |
| $h_{d,w}$ | = debris/wall heat transfer coefficient during ablation (see Appendix J, NUREG/CR-6075) |
| $h_{f,w}$ | = heat of fusion for RPV steel |
| M_{CRM} | = mass of control rod material in melt at vessel failure |
| . | |
| M_d | = melt ejection rate from RPV |
| $M_{g,e}$ | = gas remaining in the RCS at the end of debris dispersal |
| M_d^0 | = initial melt mass |
| M_g^0 | = initial RCS gas mass |
| M_{Zr}^0 | = mass of Zr initially in core |
| M_s | = mass of steel in melt at vessel failure |
| M_{ss} | = mass of steel |
| $M_{s,LP}$ | = mass of steel in lower plenum |
| M_{UO2} | = mass of UO_2 in melt at vessel failure |
| $MW_{g,RCS}$ | = molecular weight of RCS gas |
| M_{Zr} | = mass of Zr in melt at vessel failure |
| M_{ZrO2} | = mass of ZrO_2 in melt at vessel failure |
| N_{ATM}^0 | = atmosphere moles in containment just prior to vessel failure |
| N_{H2} | = mole of hydrogen produced from Zr oxidation |
| P | = initial containment pressure |
| P_f | = failure probability |
| $P_{0.01}$ | = pressure corresponding to a 1 percent failure probability on the fragility curve |

NOMENCLATURE (continued)

| | |
|-------------|--|
| P_c^0 | = initial containment pressure |
| P_{RCS}^0 | = initial RCS pressure |
| $P_{e,RCS}$ | = RCS pressure at the end of debris dispersal |
| R | = universal gas constant |
| R_τ | = coherence ratio |
| R_u | = universal gas constant |
| T | = initial containment temperature |
| T_d^0 | = debris temperature |
| T_{RCS}^0 | = RCS gas temperature |
| $T_{mp,w}$ | = melting temperature of RPV steel |
| T_w | = temperature of RPV lower head at vessel failure |
| U^0 | = total internal energy of containment atmosphere |
| V | = containment volume |
| V_c | = cavity volume |
| V_{cav} | = cavity volume |
| V_{LP} | = volume of lower plenum |
| V_{RCS} | = RCS volume |
| X_{H_2} | = hydrogen concentration in the containment atmosphere |
| X_{stm} | = steam concentration in the containment atmosphere |
| X_{Zr} | = mass fraction Zr |

Greek

| | |
|---------------------|---|
| α_c | = thermal diffusivity of frozen core material |
| δ | = thickness of frozen core debris on cavity walls |
| $\Delta U_{0.01}$ | = energy input required to threaten containment |
| ρ_{CRM} | = mass density of control rod material |
| ρ_d | = mass density of debris |
| ρ_d | = density of molten core debris |
| ρ_{UO_2} | = mass density of UO_2 |
| ρ_{UO_2/ZrO_2} | = mass density of UO_2/ZrO_2 eutectic |
| ρ_w | = mass density of RPV steel |
| ρ_{Zr} | = mass density of Zr |
| ρ_{ZrO_2} | = mass density of ZrO_2 |
| τ_b | = characteristic blowdown time |
| τ_c | = characteristic entrainment interval |
| τ_D | = characteristic time to double the initial hole size by ablation |
| τ_e | = characteristic entrainment interval |
| τ_e | = characteristic debris dispersal interval |
| τ_M | = characteristic time to eject melt from RPV in the absence of ablation |

NOMENCLATURE (concluded)

| | |
|-------------|---|
| λ_c | = growth rate constant for conduction limited freezing of a superheated liquid on an infinite substrate |
| Φ_{H2} | = global scaling parameter for potential to develop high hydrogen concentrations |
| Φ_m | = robustness of the issue resolution provided by accepting a screening study CCFP ≤ 0.01 as indicating the true CCFP ≤ 0.1 |
| Φ_R | = pressurization energy ratio |
| Φ_{Zr} | = normalized Zr/UO ₂ ratio |
| η | = pressurization efficiency |
| η_c | = combustion efficiency |
| Ψ | = debris/atmosphere heat capacity ratio |
| γ | = ratio of molar specific heats, C_p/C_v |

1.0 INTRODUCTION

In a light-water reactor core melt accident, if the reactor pressure vessel (RPV) fails while the reactor coolant system (RCS) is at high pressure, the expulsion of molten core debris may pressurize the reactor containment building (RCB) beyond its failure pressure. A failure in the bottom head of the RPV, followed by melt expulsion and blowdown of the RCS, will entrain molten core debris in the high-velocity steam blowdown gas. This chain of events is called a high-pressure melt ejection (HPME). Four mechanisms may cause a rapid increase in pressure and temperature in the reactor containment: (1) blowdown of the RCS, (2) efficient debris-to-gas heat transfer, (3) exothermic metal-steam and metal-oxygen reactions, and (4) hydrogen combustion. These processes, which lead to increased loads on the containment building, are collectively referred to as direct containment heating (DCH) when they have the potential to occur simultaneously. It is necessary to understand factors that enhance or mitigate DCH because the pressure load imposed on the RCB may lead to early failure of the containment.

DCH is a prominent severe accident issue because of its potential for early containment failure. Although the RPV did not fail at Three Mile Island II (TMI-II), some important and necessary conditions for HPME/DCH existed, e.g., the relocation of approximately 20 mt of core material to the lower head and high (approximately 10 MPa) RCS pressures. The Nuclear Regulatory Commission (NRC) has identified DCH as a major issue for resolution in the Revised Severe Accident Research Plan (NRC 1992) and has sponsored programs at Sandia National Laboratories (SNL) to resolve the DCH issue.

NUREG-1150 was the first attempt to treat DCH from a probabilistic risk assessment (PRA) perspective that integrates sequence probabilities with uncertainties associated with initial/boundary conditions and phenomenological uncertainties associated with predicting containment loads. NUREG-1150 addressed only a small number of reference plants and the DCH database was largely nonexistent at the time, so there was no way to validate these early attempts to predict DCH loads. More recently, the IPEs have also addressed the DCH issue from a PRA perspective. Their strength is that plant-specific sequence information is fully integrated into the assessment for every plant. On the other hand, the approaches taken to assess containment loads are inconsistent and poorly tied to the existing database.

Section 2.0 of this report presents the overall methodology and success criteria for resolution of the DCH issue. Historically, the first step in the DCH issue resolution process for PWRs with large dry or subatmospheric containments was the writing and public review of NUREG/CR-6075 and its supplement, "The Probability of Containment Failure by Direct Containment Heating in Zion." NUREG/CR-6109, "The Probability of Containment Failure by Direct Containment Heating in Surry," applied the same methodology to the Surry plant as a second demonstration of the DCH resolution methodology. DCH was examined in a broader way for all Westinghouse (W) plants, excluding plants with ice condenser containments, in NUREG/CR-6338, "Resolution of the Direct Containment Heating Issue for all Westinghouse Plants With Large Dry Containments or Subatmospheric Containments." Most recently, the DCH issue was examined for all Combustion Engineering (CE) and Babcock & Wilcox (B&W) plants in NUREG/CR-6475, "Resolution of the Direct Containment Heating Issue for Combustion Engineering Plants and Babcock & Wilcox Plants." In the vast majority of PWRs with large dry

Introduction

or subatmospheric containments, DCH is the dominant mode of early containment failure, and the DCH issue was resolved through plant specific probabilistic comparisons of DCH loads versus containment strength without taking credit for low HPME probabilities or active pressure suppression afforded by containment sprays. In a few cases, recourse to elementary assessments of HPME probabilities or other supplementary arguments was required to ensure that the DCH issue was adequately resolved.

This report (NUREG/CR-6427) addresses the DCH issue for all Westinghouse plants with ice condenser containments. There are ten operating ice condenser plants located at five sites in the U.S. DCH phenomena in ice condenser plants are different in some important aspects from DCH phenomena in plants with large dry or subatmospheric containments. A quantitative assessment of these differences is given in Section 3.0.

Initially, the methodology developed in NUREG/CR-6075 and NUREG/CR-6075, Supplement 1, was used to perform a probabilistic load versus strength evaluation for each of these plants using plant-specific data gathered from IPEs, Final Safety Analysis Reports (FSARs), and direct contacts with plant personnel (when necessary). The same enveloping accident scenarios (splinters) that were used in NUREG/CR-6075, Supplement 1, and NUREG/CR-6109 were used for these plant evaluations. One additional splinter scenario, unique to plants with ice condenser containments, was also considered. These splinter scenarios establish important input parameters for the load calculations, e.g., the RCS pressure at vessel breach, the melt mass and composition, the RPV breach size, the containment pressure and atmosphere composition at vessel breach, etc.

The initial approach taken was to model the ice condenser plant as a small dry containment without taking credit for the passive pressure suppression afforded by the ice beds or active pressure suppression afforded by containment sprays. Scenarios with deeply flooded cavities were not analyzed as part of the effort documented in Appendix D. Assuming a HPME/DCH event for these assumptions, all ice condenser plants violated the success criteria ($CCFP \leq 0.1$) based on DCH-induced overpressure failures alone. Those sections of draft NUREG/CR-6427 that deal with this splinter scenario approach are preserved in their entirety as Appendix D of this report. We acknowledge that the underlying assumptions of Appendix D are overly conservative and physically inconsistent with the expected evolution of accident scenarios in ice condenser plants. Sensitivity studies performed as part of Appendix D show that ice beds could be effective at suppressing DCH loads if the igniters are also operational.

Appendix D also documents peer review comments on draft NUREG/CR-6427. Reviewer comment and recommendations fell into three general categories:

- (1) Expand the probabilistic framework to include sequence probabilities,
- (2) Validate CONTAIN's ice condenser models if CONTAIN is to be used in the load calculations, and
- (3) Model the ice condenser explicitly in the loads calculations.

This revision of draft NUREG/CR-6427 explicitly addresses these peer review comments. The approach taken is to provide a best-estimate expansion of the probabilistic framework, which represents a simplification of the NUREG-1150 containment event tree for Sequoyah. The probabilistic framework addresses DCH-induced overpressure failures in the context of all significant early containment failure modes. The simplified containment event tree (CET) and its quantification is presented in Section 4.0.

Available SCDAP/RELAP5 SBO calculations for Zion were used to provide steam sources to the containment for the case of best estimate RCP leaks. The steam sources, with some modification, were taken as input conditions for a CONTAIN simulation of containment response for the steam loads. For non-SBOs, these steam sources maximize the load on the ice chest and minimize the ice inventory because auxiliary feedwater was not represented in the SCDAP/RELAP5 calculation. These calculations were used to define the ice inventory, the containment base pressure, and the DCH pressure rise at the time of vessel breach. These assessments are described in Section 5.0. We acknowledge that loss of auxiliary feedwater has a low probability in non-SBO events; consequently, this report will address additional non-SBO scenarios where significant ice inventory remains in the ice chest.

The containment fragility curve was extracted from the IPE for each plant. The fragility assessments are summarized in Section 6.0 and are compiled previously in Appendix C (Pilch et al. 1996). Containment loads, for each end state in the containment loads tree, are convoluted with the plant specific fragility curve to determine the corresponding overpressure failure probability. The results of these calculations are presented in Section 7.0. The summary and conclusions are given in Section 8.0. Comments from a NRC-sponsored peer review of this revised document by experts in Reactor Safety are published in Appendix E.

2.0 ASSESSMENT METHODOLOGY

Based on recommendations of the NRC, the methodology has traditionally aimed at grouping each PWR into one of two categories:

- (1) PWRs in which the threat of early containment failure, conditional on core damage, is shown to be ≤ 0.1 , and
- (2) PWRs in which the threat is > 0.1 .

We emphasize that the containment failure probability is conditional on core damage. More recently, the NRC has placed greater emphasis on the large early release fraction (LERF) of $< 10^{-5}$ as a safety goal. Ultimately, the resolution of any safety issue is based on a risk-informed assessment of the plant performance against safety goals, uncertainties in the plant performance relative to those safety goals, and cost/benefit analyses associated with any proposed changes in the plant. The metric used in this study is the CCFP for early containment failure, which serves the purpose here as a common metric by which the relative vulnerability of reactor containments can be assessed so that the results of this study can be compared to those of previous DCH resolution studies. We expect that the insights of this study ultimately will be factored into utility PRAs, and the revised results presented in the format that best addresses the regulatory goals in place at the time.

We recognize that DCH must be considered in the plant-specific context of all early containment failure modes¹ when the CCFP criterion is applied; however, DCH is thought to dominate early containment failure for most PWR plants with large dry or subatmospheric containments. Consequently, reasonable demonstration that the containment failure probability given a DCH event is less than 0.1 is sufficient to classify a plant into the first category. The DCH issue was previously resolved for all PWRs with large dry or subatmospheric containments through plant-specific probabilistic comparisons of DCH loads versus containment strength assuming that a HPME event occurred. For the vast majority of these plants, the containment failure probability was less than a 0.01 screening criteria without recourse to sequence or HPME probabilities. Although not examined in a general way, it was recognized that the DCH containment failure probability would be at least an order of magnitude lower if DCH was considered conditional on core damage (rather than conditional on a HPME event) because of the low HPME probability.

The DCH issue for ice condenser plants could not be resolved based on plant-specific probabilistic comparisons of DCH loads versus containment strength assuming that a HPME event occurs (for the very limiting assumptions of no ice and a dry cavity). An initial attempt along these lines is documented as Appendix D for reference. NUREG/CR-4551 for the Sequoyah plant was carefully reviewed for possible insights to an assessment methodology. Four key observations can be summarized as follows:

¹ We conservatively define early containment failure as occurring shortly after vessel breach. We note that the NRC is considering defining early in terms of the public evacuation time scale instead of vessel breach.

Assessment Methodology

- (1) Given a "typical" DCH event, NUREG-1150 says there is approximately a 34% probability of containment overpressure failure; and if the containment does not fail by overpressure, then there is approximately 24% probability that the accumulation of dispersed debris against the containment liner will result in a thermal failure.
- (2) The probability of vessel breach with RCS pressure greater than 200 psi is approximately 35%.
- (3) The total mean early containment failure probability (weighted by the probability of all plant damage states) is approximately 7.6% with non-HPME failures making up about half of the total.
- (4) The uncertainties are large with the early containment failure probability ranging from approximately 0.02% to approximately 70% for the 5% and 95% confidence limits, respectively.

The implications for a DCH assessment study focused on ice condenser plants are fivefold:

- (1) Revised load/strength analyses for a small number of bounding "splinter scenarios" (assumed to be conditional on a DCH event) cannot produce DCH resolution because liner failures alone are greater than the 10% criteria for early containment failure.
- (2) It is unlikely that DCH resolution will be achieved in a general way based on HPME probabilities alone (although there is now a technical basis to take more credit for hot leg failures).
- (3) DCH assessment must be approached from an integrated perspective that addresses all significant modes of early containment failure in a framework that places all significant failure modes in the proper and consistent probabilistic framework. This framework should take into account all relevant research carried out in recent years.
- (4) We must acknowledge that the uncertainties in early containment failure might be large, but it is outside the scope of this study to quantify uncertainties.
- (5) The DCH issue itself might be judged of secondary importance if the frequency-weighted DCH overpressure failures are shown to be small compared to other frequency-weighted contributors to early failure, even if the probability of all early failures is comparable to or exceeds a CCFP of 10%.

The best way to address these needs is through detailed and credible Level I and Level II probabilistic analyses, specific to each individual plant. This is outside the scope of the current assessment, and a cursory review of the IPE's for ice condenser plants shows that the Level II decompositions and quantifications differ from plant to plant. In this work, the following is proposed as a practical approach for assessing the importance of HPME/DCH to early containment failure for all ice condenser plants.

- (1) Develop a simplified version of the NUREG-1150 event tree that operates on each core damage initiator (CDI) as a class (e.g., LOCAs) and not on the more numerous plant damage states (PDS) that might exist at the time of core uncovering.
- (2) Benchmark the simplified tree by demonstrating that the simplified tree, with NUREG-1150 consistent input, reproduces (in a reasonable fashion) the results documented in NUREG-1150 for Sequoyah.
- (3) Update specific quantifications (e.g., hot leg failure probabilities) in the simplified tree if significant new work since the time of NUREG-1150 justifies the revision.
- (4) Calculate the probability of DCH containment failure in reference to other modes of early containment failure and reference the results to previous NUREG-1150 results.

This approach for assessing DCH in ice condenser plants is developed more fully in Section 4.0.

This report focuses on full power interval events. We acknowledge that risk-informed regulation must also address external events (fire and seismic) and low power shutdown events,² but these are outside the scope of the current effort. Core damage frequencies for full power internal events were previously quantified by the utilities in the individual plant examinations (IPEs), while CDFs for external events were more recently quantified by some utilities in the individual plant examinations of external events (IPEEEs). In some cases, the CDF for external events can be comparable to the CDF for internal events. The CDF for low power shutdown events has not been systematically evaluated for all light water reactors (LWRs); but in a few cases where quantifications have been performed, the CDF can again be comparable to the CDF for full power internal events. As this study will show for full power internal events, the CCFPs for ice condenser plants can be comparable to or exceed the CCFP < 0.1 success criteria; consequently, a comprehensive assessment of early containment failure would benefit from additional consideration of external events and low power shutdown events. External events and low power shutdown events as initiators could introduce more early containment failures, which when combined with early failures for internal events, could exceed 10% of all core damage accidents. This is because external events could have a disproportionately large number of SBO-like sequences, which have a significant probability of early containment failure from hydrogen deflagrations even in the absence of DCH processes.

² Level II and Level III risks have not been assessed for low power shutdown accidents; however, DCH would not normally be possible in low power shutdown events because the RCS pressure is low.

3.0 ASSESSMENT OF ICE CONDENSER CONTAINMENT PHENOMENA

3.1 Introduction

The United States Nuclear Regulatory Commission (USNRC) and others have invested considerable effort towards understanding and resolving the DCH issue for commercial US power plants over the past ten years. These efforts have focused primarily on the phenomena that might occur during a HPME sequence in PWRs with large dry containments. In particular, the later phases of the experimental effort were guided by the Severe Accident Scaling Methodology (SASM) program which emphasized DCH in the large dry containments; subsequent experimental efforts focused on the study of DCH phenomena as they would be manifest in large dry containments and the initial conditions were defined to be appropriate for large dry containments. There were good reasons for that focus; DCH was shown by NUREG-1150 (NRC 1989) to be the only important mechanism of concern that could lead to early containment failure for large dry containments. Other plant types (i.e., the "pressure suppression containments"—BWRs and PWRs with ice condenser containments) had smaller populations in the plant fleet and had other early containment failure concerns associated with them.

At the present time, efforts toward resolution of the DCH issue for plants with large dry or subatmospheric containments are complete, and it is now appropriate to review how those results might be applied to these other plant types and what additional work might be needed to pursue resolution for the pressure suppression containments. Care must be taken in translating the results for plants with large dry containments to these specialized containments. Each has a different phenomenological "signature" in response to an HPME event. These differences could have a strong bearing on the relevance or applicability of the substantial knowledge base that has been developed to date for the large dry containments. None of the special characteristics of the pressure suppression containments have been factored into the experimental programs, and they received at most passing attention in the SASM effort. Hence, there is less of a validation base for whatever analytical tools are available for addressing the specialized features of the pressure suppression containments.

The starting point for such an assessment should be a basic discussion of the nature of the threat posed by HPME to ice condenser containments, with a particular emphasis on the differences from the large dry containments. This section provides such a review for the ice condensers. Its purpose is not to delve deeply into any particular phenomenological sub-issue, but rather to provide a general context in which to view HPME in ice condensers compared with previous work on DCH in large dry containments.

We make an important distinction here between HPME and DCH. HPME is a mode of vessel failure that is the end point of the in-vessel part of the event trees used in PRAs. DCH is a set of phenomena that subsequently occur in the containment that represent a potential threat to containment integrity through global overpressurization. Other containment failure mechanisms besides DCH but resulting from HPME have been considered for plants with large dry containments, e.g., hydrogen combustion and in-vessel steam explosions. However, they have been largely dismissed on the basis of loads evaluations and probabilistic considerations.

For ice condensers, we will explain below that the spectrum of threats caused by HPME is not as narrowly confined to the DCH threat as is true for the large dry containments. This fact has important implications for the nature of issue resolution and for the appropriate process to pursue it. Equally relevant is the fact that the DCH process itself may have a different nature, both qualitatively and quantitatively, for ice condensers than for large dry containments; that is to say, the set of phenomena occurring may be different, and the strength of their interactions may be different. Under these circumstances, it is important to avoid misunderstandings stemming from vague terminology. One of the central contributions of the Severe Accident Scaling Methodology was to introduce a degree of rigor into such discussions of severe accident issues. In the discussion to follow, we will attempt to be as precise as possible with terminology and to be clear about the limitations of the present cursory scoping assessment. We will also borrow heavily from analyses performed for the NUREG-1150 study (Gregory et al. 1990), though we will update the discussion with research results that have emerged since the time of that work.

In Section 3.2, we will summarize current thinking on the numerous sub-issues that are subordinate to the larger issue of HPME in ice condensers. This begins with a discussion of global scaling of the critical containment parameters for large dry containments and ice condensers. This is followed by a brief discussion of each of the specific phenomena that could occur during HPME in ice condensers that have been hypothesized to be of potential importance in various studies to date. Throughout, we will attempt to compare and contrast the corresponding processes in ice condensers and large dry containments, because one of the goals is to understand the relevance to the former of the large knowledge base developed for the latter. This discussion will cover not only the events in ice condensers that more or less correspond to DCH in large dry containments, but will also touch on containment threats that have no corresponding role for large dry containments.

In Section 3.3, we draw some general conclusions about how this brief review sheds light on the appropriate directions for pursuing assessment of this severe accident issue. This discussion is intended to motivate the overall approach followed in the remainder of the report, as well as our recommendations for possible follow-on work.

3.2 Phenomenological Overview

A brief introduction to the design and layout of an ice condenser plant is essential to a phenomenological discussion of HPME and DCH. Figure 3.1 shows a layout of the Sequoyah containment building, which is representative of all ice condenser plants. The containment comprises of a lower compartment containing the RPV and the main components of the RCS, the upper dome with spray headers,³ and an annular ice compartment containing ice for pressure suppression. In a DBA, steam released from the RCS must flow through the ice beds. There are air return fans (ARFs) that help circulate flow from the upper compartment back to the lower compartment, AC-powered igniters are provided throughout the upper and lower compartments (but not in the ice beds) to prevent hydrogen concentrations from exceeding flammable limits.

³ We note that D.C. Cook is unique among ice condenser plants in that it also has spray systems in the lower compartment.

Sequoyah Unit 1 Individual Plant Examination

Revision 0

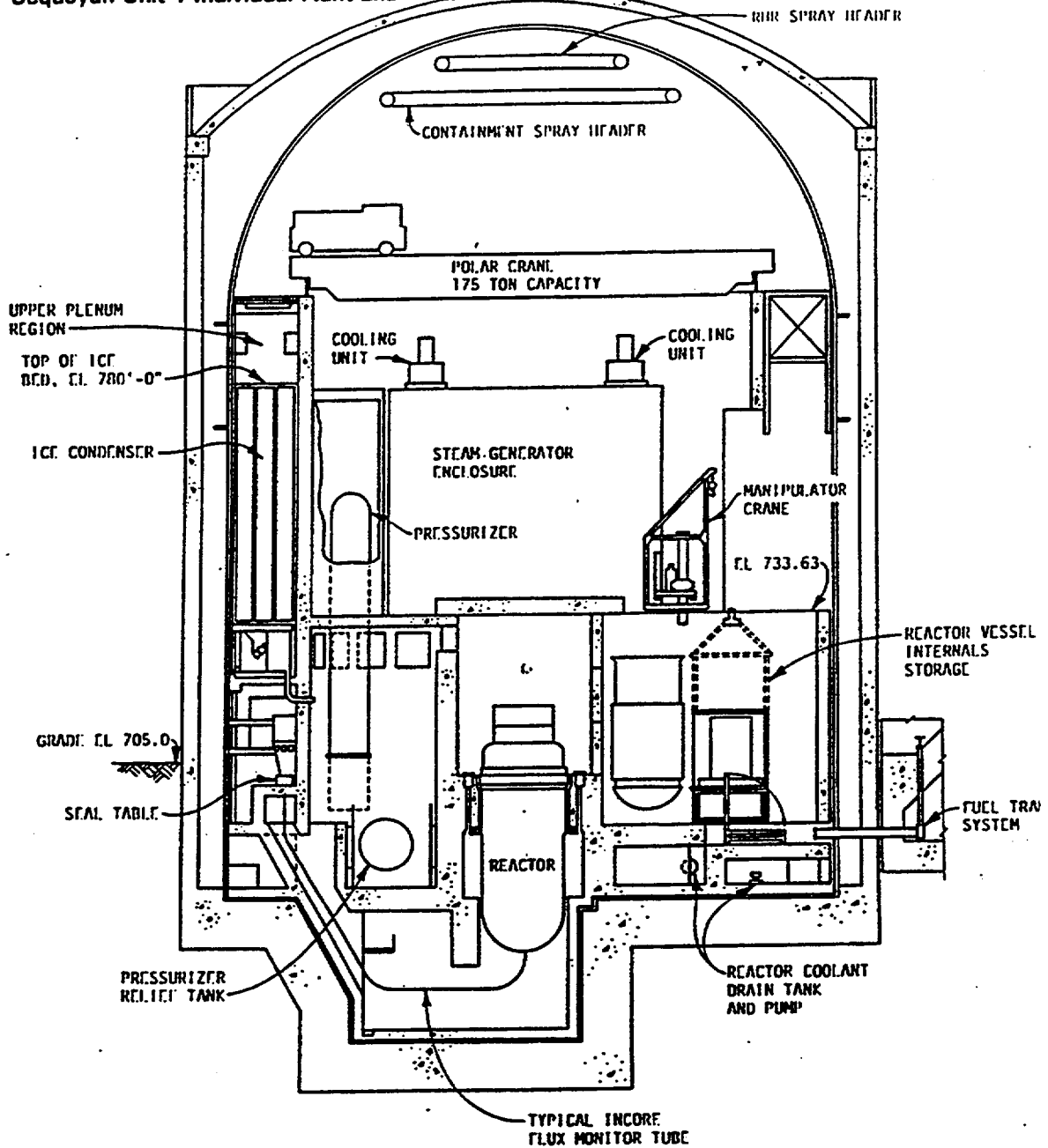


Figure 3.1 Layout of a typical ice condenser containment (taken from Sequoyah IPE)

Differences in HPME phenomenology between ice condenser and large dry containments can be grouped into two categories. The first involves phenomena that are associated specifically with the ice condenser and that have no close analogue in the large dry containments; e.g., the effects of rapid steam condensation in the ice condenser during a DCH event. The second involves phenomena that can occur in both types of containments, but with the boundary conditions for the processes being sufficiently different that quite different behaviors may actually result. A consideration of global scaling parameters provides some useful insights into the second class of differences, and we consider these in the next section. Specific instances of both classes of phenomena are then discussed in Section 3.2.2.

3.2.1 Global Scaling Parameters: Large Dry Containment vs. Ice Condenser Containments

In this section, we define three global scaling parameters that reflect containment resistance toward DCH, sensitivity of the margin to DCH uncertainties, and concentration regimes for hydrogen phenomenology. We then present two-dimensional maps comparing the location of the ice condenser containments with the location of Westinghouse large dry and subatmospheric containments in the parameter space defined by the scaling parameters. We conclude that ice condenser plants are smaller and weaker and are susceptible to containment failure during hydrogen combustion events alone when active hydrogen control (igniters) is not operational. The ice beds can be effective at mitigating DCH loads when hydrogen control is also available. In addition, many scenarios in ice condenser plants lead to deeply flooded cavities. Deeply flooded cavities lead to steam spike loads on the containment, which are more easily suppressed by the remaining ice.

Containment Pressurization Energy Ratio. One measure of a containment's resistance toward DCH can be defined by considering the ratio of the energy required to result in a pressure rise sufficient to threaten containment integrity to the energy available in the core debris. In the screening approach that was adopted for previous issue resolution efforts, the screening criterion has been that the conditional containment failure probability (CCFP) be less than 0.01 (conditional on core damage and a HPME event); hence, we define a "threatening" pressure to be $P_{0.01}$, the pressure corresponding to a 1% failure probability on the fragility curve. The energy input required to threaten the containment, $\Delta U_{0.01}$, is then given by

$$\begin{aligned}\Delta U_{0.01} &= V C_v \Delta P_{0.01} / R, \\ \Delta P_{0.01} &= P_{0.01} - P_c^0,\end{aligned}\tag{3.1}$$

where V is the containment volume, C_v is the constant-volume molar heat capacity of the containment atmosphere, R is the universal gas constant, P_c^0 is the containment pressure immediately prior to vessel breach, and where the number of moles of gas in containment is constant (neglects steam and hydrogen addition). Following NUREG/CR-6338 (Pilch et al. 1996), we take P_c^0 to be 0.25 MPa and 0.15 MPa for atmospheric and subatmospheric large dry containments, respectively; both values assume active engineered safety features (ESFs) are not available. Based upon CONTAIN calculations described in Appendix B, we take P_c^0 to be 0.18 MPa for ice condenser containments when active ESFs are unavailable.

The total energy (thermal and chemical) potentially available depends upon the core debris mass and the composition. For present purposes, we are interested only in relative measures, and we assume that the various energy sources scale as the core size, for which we take the measure to be the mass of UO_2 (M_{UO_2}). A possible concern is that there is some variation in the ratio of zirconium inventory (M_{Zr}) to UO_2 inventory among the various plants and that this could distort comparisons based upon M_{UO_2} alone, because M_{Zr} largely governs the potential for hydrogen production and hydrogen can be a very important contributor to DCH loads. We examine this question further in connection with hydrogen phenomenology below and accept this approximation for now.

Because we are interested in relative measures, we define a "pressurization energy ratio," ϕ_R , by taking the ratio of $\Delta U_{0.01}/M_{UO_2}$ for the plant of interest to the value of $\Delta U_{0.01}/M_{UO_2}$ for the Zion plant, which we use as a typical PWR large dry containment for reference purposes:

$$\phi_R = \frac{M_{UO_2, Zion} \Delta P_{0.01} V}{M_{UO_2} (\Delta P_{0.01} V)_{Zion}}, \quad (3.2)$$

where we have neglected any differences in C_v for different plant atmospheres. We note that Eq. (3.2) takes no credit for passive pressure suppression afforded by the ice beds, and the results must be interpreted accordingly.

Margin Provided by CCFP ≤ 0.01 in Screening Studies. The operational definition of "issue resolution" adopted in this program has been demonstration that the $CCFP \leq 0.1$. The value of 0.01 was adopted for previous screening studies in order to allow for uncertainties owing to plant-specific features that may not have been adequately considered and to allow for phenomenological uncertainties in the loads modeling. A question of some importance is then how robust this margin is toward DCH modeling uncertainties. That is, by how much would some unacknowledged uncertainty have to increase the efficiency of DCH in order to yield an actual $CCFP \geq 0.1$ when the screening calculations gave $CCFP \leq 0.01$? A measure ϕ_m of the robustness of this margin can be obtained by replacing $\Delta P_{0.01}$ in the definition of ϕ_R by $\delta P_m = P_{0.1} - P_{0.01}$, where $P_{0.1}$ is the pressure corresponding to a 10% failure probability on the containment fragility curve; thus,

$$\phi_m = \frac{M_{UO_2, Zion} \delta P_m V}{M_{UO_2} (\delta P_m V)_{Zion}}. \quad (3.3)$$

A small value of ϕ_m results when the containment fragility curve is steep, implying that the pressures corresponding to the 10% and 1% failure probabilities do not differ greatly. A small value of ϕ_m does not necessarily imply a weak containment. Again, Eq. (3.3) takes no credit for passive pressure suppression afforded by the ice beds, and the results must be interpreted accordingly.

Hydrogen Phenomenology. We consider here the global hydrogen concentrations that can accumulate in the containment when igniters are not operational. Such scenarios are largely confined to SBO events, which are a relatively small contributor to the set of all core damage accidents. In first approximation, the potential for hydrogen production scales as the mass of zirconium in the core, M_{Zr} . In defining ϕ_R above, we assumed that the ratio M_{Zr}/M_{UO_2} is the same in all PWR plants, and that M_{UO_2} could therefore be taken as a measure of the relative variation in total energy available for DCH among the various plants. In order to investigate this issue, we define a normalized Zr/UO₂ ratio, ϕ_{Zr} , from the relation

$$\phi_{Zr} = \frac{M_{Zr} / M_{UO_2}}{(M_{Zr} / M_{UO_2})_{Zion}} \quad (3.4)$$

If values of ϕ_{Zr} show sufficiently small variability, we may conclude that variations in the Zr/UO₂ mass ratios among the plants will not seriously perturb the ϕ_R values calculated from Eq. (3.2). Similar considerations apply to the adequacy of Eq. (3.3) used to define the margin parameter, ϕ_m .

There are many features of hydrogen phenomenology for which ϕ_{Zr} is not a useful scaling parameter because these features show strong nonlinear dependencies upon the hydrogen mole fraction. Examples include burn completeness, burn rates, and the potential for flame acceleration and deflagration-to-detonation transition (DDT) that could produce dynamic containment loads. Flame speeds and burn completeness increase rapidly with increasing concentration; for example, burn completeness is very low near the upward flammability limit (approximately 4% H₂) but increases rapidly with mole fraction, becoming almost 100% complete for concentrations greater than or equal to 7-10% (Wong 1988). The likelihood of flame acceleration and/or DDT are sensitive to hydrogen concentration and can show an approximate threshold behavior; for example, the NUREG-1150 study assessed DDT in certain Sequoyah scenarios and concluded DDT to be impossible for hydrogen concentrations less than 14% while the probability of DDT was taken to be greater than 0.6 if a deflagration initiated at concentrations greater than or equal to 16% for the scenarios considered. We note, however, that if global hydrogen concentrations are high enough to support detonations then a deflagration with the same hydrogen concentration is sufficient to fail the containment with a high probability. As a practical matter, little is lost by ignoring global detonations in the upper dome.

In comparing the ice condenser and large dry containments, therefore, it is useful to define a global scaling parameter that reflects the potential for developing high hydrogen concentrations. A comparative measure for this purpose may be defined by taking the ratio of M_{Zr} to the number of moles of containment atmosphere and assuming that the latter is proportional to $P_c^0 V / T_c^0$:

$$\phi_{H_2} = \frac{M_{Zr} T_c^0 (P_c^0 V)_{Zion}}{(M_{Zr} T_c^0)_{Zion} P_c^0 V} \quad (3.5)$$

where T_c^0 is the initial containment temperature. Eq. (3.5) takes no credit for active hydrogen control (AC igniters) and the results must be interpreted accordingly.

Mapping of Ice Condenser and Large Dry Containments. In this section, we compare ice condenser and large dry containments in terms of the global scaling parameters defined above. The "large dry containments" considered are limited to the atmospheric and subatmospheric containments for Westinghouse plants, which are the plants that were addressed in NUREG/CR-6338. In the plots to be presented, some of the data points represent two containments when there are two units that are identical with respect to the scaling parameters.

In Figure 3.2, ϕ_m is plotted against ϕ_R for ice condenser containments (open symbols) and large dry containments (closed symbols). For the latter, all data required to evaluate the scaling parameters were taken from Tables 4.3 and 6.1 of NUREG/CR-6338 (Pilch et al. 1996). The values assumed for containment pressure at vessel breach are those that correspond to accident scenarios without active containment ESFs operating.

It is immediately obvious that the ice condenser and large dry containments fall in quite different regions of the scaling parameter space. Much of this separation is because of the differences in ϕ_R . For the large dry containments, ϕ_R varies from 0.58 for H. B. Robinson to 1.74 for Seabrook. For the ice condensers, the range is only 0.16 to 0.27. For Sequoyah, $\phi_R = 0.24$; this means that DCH need be only 24% as efficient to threaten containment integrity in Sequoyah as is required in Zion, and only approximately 40% as efficient as is required in H.B. Robinson. These differences occur because ice condenser containments are not as strong or as big as large dry containments.

Unlike the case for ϕ_R , there is a slight overlap between the ranges spanned by ϕ_m for ice condensers (0.12-0.27) and the large dry containments (0.20-1.0). However, the ice condenser values are all at or below the low end of the range for large dry containments. Sequoyah has the smallest value of ϕ_m , 0.12. In Sequoyah, therefore, the margin provided by screening with a CCFP of 0.01 could be overcome by uncertainties in DCH efficiency that are almost an order of magnitude smaller than those required to overcome the margin in Zion. Even for Watts Bar ($\phi_m = 0.27$), the difference with respect to Zion is almost a factor of four.

The separation in Figure 3.2 of ice condenser containments from large dry and subatmospheric containments derives from the treatment of ice condenser plants as small dry containments. In reality, ice beds are a passive pressure suppression feature that are inherent to the design of ice condenser containments. The potential for ice beds to mitigate DCH loads is realized by the following simple calculations. For an upper bound melt mass of 87 mt, the total latent and sensible heat ($\Delta e \sim 1.3$ MJ/kg) is 0.113×10^6 MJ. If all this energy is transferred to ice, then only 30% of the initial ice inventory is required to fully mitigate the DCH event. Although an oversimplification, this calculation shows that any realistic analysis of DCH in ice condenser plants must take proper credit for the ice beds.

Values of ϕ_{H2} are plotted against ϕ_{Zr} in Figure 3.3. It is seen that the values ϕ_{Zr} do not span a wide range; in fact, the standard deviation in ϕ_{Zr} among all the plants considered is only 7%.

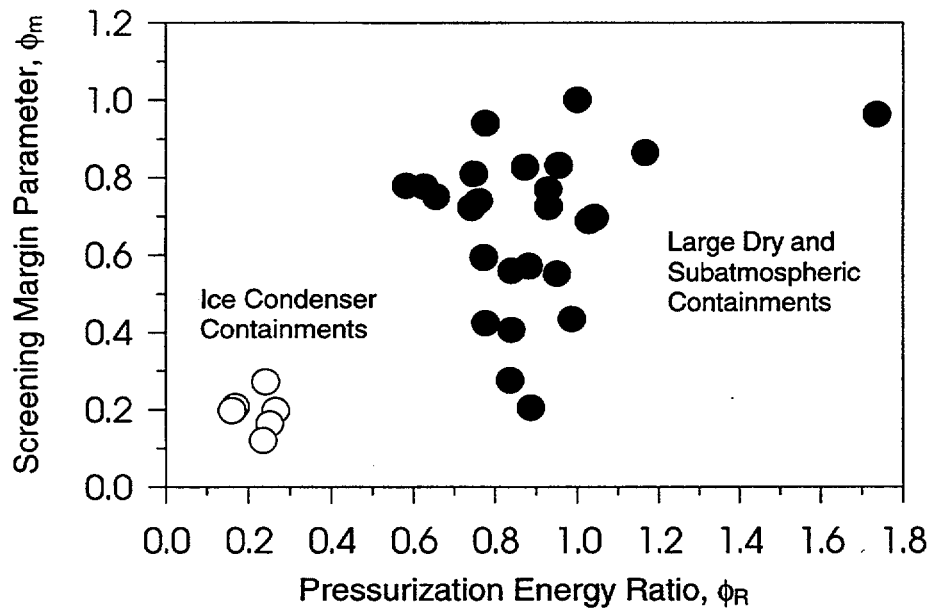


Figure 3.2 Screening margin and pressure energy ratio (no credit taken for passive pressure control effort by ice beds in ice condenser plants)

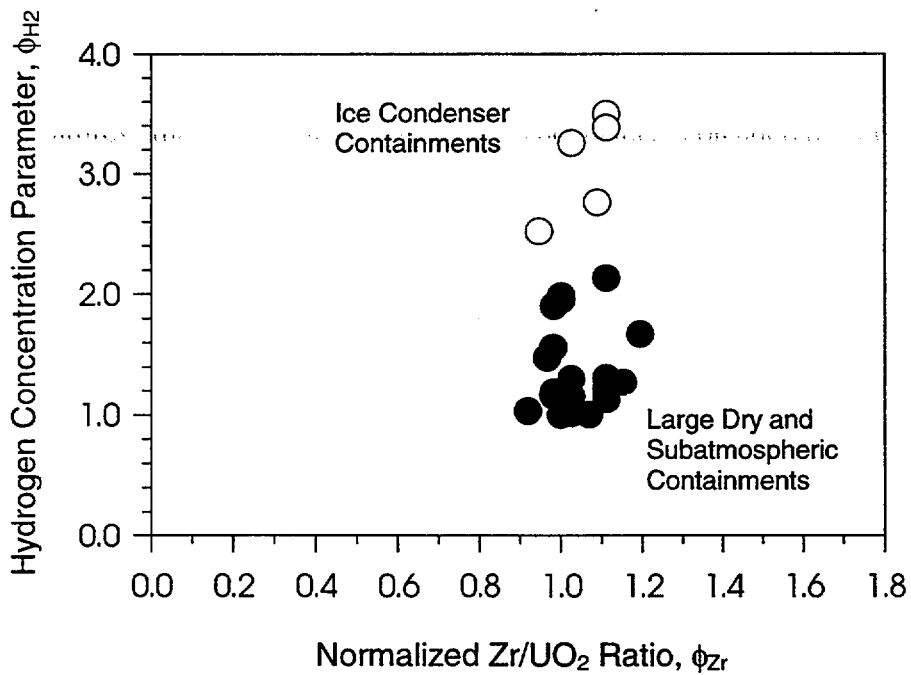


Figure 3.3 Hydrogen and Zr/ VO_2 ratio parameters (applies to SBO scenarios with no hydrogen control in ice condenser plants)

Furthermore, there is no significant tendency for the ice condenser plants to differ from the large drys with respect to this parameter. Hence, we can conclude that variations in ϕ_{Zr} do not significantly perturb the comparisons presented in Figure 3.2 for ϕ_R and ϕ_m .

In contrast, the values of the hydrogen concentration parameter ϕ_{H_2} for the ice condenser plants (2.5-3.5, assuming no hydrogen control) are outside the ranges spanned by the large dry containments (1.0-1.7 for the atmospheric containments, 1.9-2.0 for the subatmospheric containments). In the absence of igniters, global hydrogen concentrations in the ice condenser plants can be approximately 2.5 times as great as in Zion, for equivalent metal oxidation fractions. This difference is large enough to put the containment into quite different phenomenological behavior regimes in Sequoyah. The value of ϕ_{H_2} does depend on the containment pressure at vessel breach, which in turn depends upon various details of the accident sequence including especially engineered safety feature availability. However, these variations will be insufficient to alter the conclusion that the range of ϕ_{H_2} values that must be considered for ice condenser plants is considerably higher than the range that has been necessary to consider in large dry containments.

The separation in Figure 3.3 of ice condenser containments from large dry and subatmospheric containments derives from the assumption that hydrogen control is not available for the ice condenser plants. In reality, ice condenser plants are equipped with AC-powered igniters that are highly effective at maintaining hydrogen concentrations below flammable limits for those scenarios when power is available. The results depicted in Figure 3.3 apply only to SBO accidents where power is not available. SBO scenarios are only small contributors to the core damage frequency; consequently, proper probabilistic weighting of SBO scenarios could greatly diminish the increased concern of hydrogen combustion events in ice condenser plants.

3.2.2 Specific Issues Involving HPME in Ice Condenser Containments

In what follows, we consider the various issues relating to HPME and DCH in ice condenser plants in greater detail and compare them with analogous issues, if any, in large dry containments. First, we consider issues related to the availability of various ESFs. Next we consider HPME threats other than DCH pressure loads, and we conclude by considering other containment phenomenology. The latter phenomena are considered primarily in the context of DCH pressure loads. Much of what follows is based upon assessments performed for the NUREG-1150 effort, supplemented by more recent work where possible.

3.2.2.1 Availability of ESFs

In addition to the ice condenser itself, ice condenser containments include three other ESFs: ARFs, igniters, and sprays. Except for containment sprays, there is no analogue for these ESFs in large dry or subatmospheric containments. A large number of combinations of various levels of ESF availability are possible. The effect of these combinations on DCH threats can be complex and has not been fully delineated, nor has the question of ESF availability for the spectrum of events of potential interest to DCH and HPME been systematically addressed.

Assessment of Ice Condenser Containment Phenomena

Insights from NUREG-1150 have been factored into the simplified CETs developed in Section 4.0 of this report.

Effectiveness of Ice in the Ice Condenser. Prior to vessel breach, the ice condenser is expected to provide an efficient means of condensing steam released from the primary system. If the air return fans are operating, pressures, temperatures, and steam concentrations within containment at vessel breach may not be substantially greater than for normal operating conditions. If ice is exhausted, pressures and steam concentrations will rise. However, if ice is exhausted prior to vessel breach, it is expected this will not happen until relatively late in the period preceding vessel breach; hence, large additional releases of steam and energy to the containment are not likely to occur between the time ice is exhausted and the time vessel breach occurs. Hence, very high pressures and steam concentrations at vessel breach are not expected, and the dome usually will not be inerted against hydrogen combustion. We note, however, that scenarios with significant ice melting will result in a deeply flooded cavity that changes the nature of containment loads from DCH to a steam spike.

By design, the ice in the ice condenser is configured so as to provide for efficient condensation of steam in a DBA. This configuration also favors rapid transfer of thermal energy from the atmosphere in the ice chest. In a DCH event, superheated gas and steam are generated in the lower compartment, forcing flow through the ice condenser. There is a potential that the ice condenser will remove much of the energy and the steam from the gas flowing through it, substantially mitigating DCH. Note, however, that the ice condenser cannot remove hydrogen, although the removal of steam and sensible heat from the gases entering the ice condenser can delay the rate at which hydrogen from the lower compartment reaches the dome

Early CONTAIN calculations (Williams et al. 1987) indicated that the ice condenser could mitigate DCH significantly, but containment-threatening loads were still calculated for many of the scenarios considered. These calculations used melt mass representative of complete core melt and significant melting of structural steel. In the NUREG-1150 study, ΔP values were assumed to be 30-70% higher, depending upon the scenario, if ice were completely ineffective than if it were fully effective. An ice bed is considered ineffective if the ice is completely melted or if uneven melting allows gases to largely bypass any remaining ice. A more detailed CONTAIN study (Williams and Gregory 1990) yielded qualitatively similar results. Nonetheless, in these calculations, the presence of ice did not prevent containment-threatening loads from developing in many of the scenarios considered, even if igniters were available prior to vessel breach. An important factor was that the melts assumed in these prior studies contained considerably more metal than our current assessments.⁴ Hydrogen produced during the DCH event itself was an important contributor to the calculated ΔP , and the ice condenser can have at most only a limited effect upon this component of the pressurization.

⁴ The melt composition in this earlier study was taken from BMI-2104. Based on inventory arguments BMI-2104 assumed that all unoxidized cladding (~12 mt) and all structural steel (~62 mt) would be in the melt. Using more mechanistic modeling, current best estimate codes predict that most unoxidized cladding will be retained in an in-core crucible and that melting of structural steel is largely limited to small quantities of thin steel within the core regions.

In contrast, CONTAIN calculations performed in support of the present effort (Section 5.0 and Appendix B) implied that there is a potential for the ice to be considerably more effective in preventing threatening DCH loads than indicated by the earlier studies, provided igniters (and ARFs)⁵ are operating prior to vessel breach. The principal reason is that the combination of limited metal in the melt and oxygen starvation in the lower containment resulted in a much smaller contribution from the combustion of DCH-produced hydrogen, and the ice was calculated to be very effective in suppressing pressurization owing to superheated gas and steam. Containment threatening loads are still calculated for SBOs because DCH can only worsen an already threatening hydrogen combustion event.

Impaired Ice Condenser Efficiency. The preceding discussion of DCH mitigation by the ice condenser presumes that the ice condenser is in a condition to be effective at the time HPME occurs. There are three ways in which ice condenser effectiveness can be defeated:

- (1) Ice may be totally melted prior to vessel breach.
- (2) Ice may still be present, but uneven ice melting may have opened up sufficient channels that the remaining ice is effectively bypassed at vessel breach.
- (3) Detonations in the ice condenser at vessel breach may open up channels bypassing the remaining ice.

These issues were considered in some detail in the NUREG-1150 analyses. The detonation issue was addressed in Williams and Gregory 1990 who concluded that detonable gas compositions under adverse circumstances could not be ruled out. Ice was totally or almost totally depleted in a number of scenarios; however, these tended to be cases involving large LOCAs or induced large LOCAs, which would preclude DCH. Cases in which any LOCAs were sufficiently small that primary system pressures were in the intermediate or high range at vessel breach generally had considerable ice remaining at vessel breach.

The NUREG-1150 (NRC 1990) analysts also considered the bypass issues. Except when ice was almost depleted (greater than or equal to 90% ice melt), they concluded that any channeling would result in a bypass of less than 10% for both the uneven ice melt and the detonation-induced bypass case. However, calculations using the HECTR code (Dingman and Camp 1985) and the CONTAIN code (Williams and Gregory 1990) showed quite strong tendencies for recirculation flows to produce highly uneven ice melt in some of the scenarios considered. The degree to which control volume codes such as HECTR and CONTAIN can model these effects quantitatively is uncertain, and there is also uncertainty as to how much channeling can be tolerated without seriously degrading the ice condenser performance in the context of DCH mitigation.

Modeling of the Ice Condenser During DCH. To date, quantitative analyses of mitigation of DCH by the ice condenser have been limited to various analyses performed with the CONTAIN

⁵ The availability of igniters is greater than 99% and the availability of ARFs is greater than 99% given that there is power in the plant.

code. There has been recent effort to validate the CONTAIN ice condenser model for DBA conditions; however, a prototypic data base for validation under DCH conditions is nonexistent. The model includes a user-specifiable multiplier on the heat and mass transfer coefficients for the ice, and it also includes a user-specifiable water film thickness on the ice. Heat conduction limitations through this water film can limit the rates of heat and mass transfer to the ice.

In the calculations described in Appendix B of this report, a major motivation was to determine whether the ice condenser offered the potential for significant mitigation; no claim is made that the calculations demonstrate a fully validated capability for DCH events. In this context, artificially eliminating a potentially promising mitigation effect by using overly conservative modeling assumptions was considered undesirable. Hence the heat/mass transfer multiplier was set to its default value (5) and the effect of limited heat transfer rates through the water film (which is very uncertain) was virtually eliminated by setting the film thickness to a very small value. Although the results obtained indicate a very promising potential for DCH mitigation by the ice condenser, uncertainties in the modeling should be considered. Subsequent benchmarking of the CONTAIN code against Waltz Mill data (full-height ice bed experiments) confirmed these parameter selections.

Ice Condenser Doors. Flows from the lower containment through the ice condenser and to the dome are controlled by three sets of doors. These are located between the lower compartment and the lower plenum, between the ice chest and the upper plenum, and between the upper plenum and the dome. The doors open under a forward pressure and are nominally reversible, reclosing when the forward pressure is relaxed. However, if the doors are opened with sufficient force, they may reclose incompletely or not at all. If the lower plenum doors remain partially open during the period prior to vessel breach, the recirculation flows that lead to uneven ice melt can be affected (generally increased), and atmospheric conditions in the lower compartment can be altered (Williams and Gregory 1990). The initial flow surge during a DCH event will open the doors, but it has not been established whether all the doors will reclose fully afterwards.

Williams and Gregory (1990) argued that if the doors do reclose fully, pressures in the lower compartment may decline considerably more rapidly than the dome pressures after the DCH event, resulting in a substantial pressure differential between the upper and lower compartments. The implications of this pressure differential for the integrity of containment structures, including the doors, have not been established.

Igniters. Igniters are provided to intentionally ignite hydrogen, thereby burning it off before concentrations can reach dangerous levels. They require AC power to operate and operator action to activate. Procedures direct the operators to turn on the igniters under accident conditions except in the case of recovered station blackout accidents, in which case the igniters are to be turned on only if hydrogen concentrations have not yet exceeded 6%. Based upon human reliability analysis, it was assumed in NUREG-1150 that the operators would act correctly in 99% of the cases when AC power is available at the initiation of the accident. In a recovered SBO, the operators are instructed not to re-energize the igniters unless non-flammable hydrogen concentrations exist in the containment and the technical support center (TSC) concurs with the operator decision to re-energize the igniters.

If igniters are not available and other ignition sources are absent, large amounts of hydrogen can accumulate in the containment prior to vessel breach in some accident scenarios. This hydrogen can greatly augment DCH loads; in fact, combustion of this hydrogen by itself can threaten the containment. Furthermore, the ice condenser cannot mitigate this component of the containment loading to any great extent. Hence the availability of ignition sources prior to vessel breach can be crucial in evaluating the loads associated with HPME.

Corresponding Large Dry Issues. Large dry containments are not required to have igniters. Chance ignition (as in the TMI-II accident) can occur if the atmosphere is flammable. In NUREG/CR-6338, it was concluded that, in general, the atmosphere will be flammable at vessel breach only if some degree of containment heat removal is available. The issue of burning off hydrogen prior to vessel breach is much less dominant in large dry containments and this question did not play an important role in NUREG/CR-6338 (it was assumed that the hydrogen would not burn prior to vessel breach). Flammable hydrogen concentrations can accumulate in the containment prior to vessel breach in some Combustion Engineering plants.

Air Return Fans. The ARFs require AC power. They actuate automatically when containment pressures reach 3 psig and will actuate in a recovered station blackout if other failures do not prevent their doing so. The ARFs will assure a generally well-mixed containment except at times of rapid influx of large quantities of steam and/or hydrogen from the primary system. Immediately prior to vessel breach, available SCDAP/RELAP5 calculations do not predict strong sources from the primary system, suggesting that the containment will be reasonably well mixed prior to vessel breach if the ARFs operate. If ARFs do not operate, steam concentrations will be considerably higher in the lower compartment than in the dome, and the lower compartment may be inert toward combustion prior to vessel breach as judged by conventional inerting criteria (these criteria probably do not apply at the very high temperatures that quickly develop in the lower compartment during DCH). Operation of the ARFs will decrease hydrogen concentrations in the ice beds and increase the degree of ice melt prior to vessel breach.

Containment Sprays. Long-term heat removal for the Sequoyah plant is provided by containment sprays with associated heat exchangers. Like the ARFs, they require AC power and actuate automatically when the containment pressure exceeds 3 psig, assuming they are in an operable condition. If sprays are operating, the refueling water storage tank (RWST) generally will have been exhausted prior to vessel breach, in which case the cavity will probably contain water, with the amount depending upon the amount of ice melted. There are penetrations for nuclear instrumentation in the biological shield wall that will allow water to leak into the cavity. If the RWST has emptied and approximately 50% or more of the ice has melted, water will overflow the cavity exit and deeply flood the cavity, in which case DCH was assumed to be prevented in NUREG-1150. We have endorsed this assumption in the present study also.

If sprays are operating at the time of vessel breach, there will be some airborne water in the dome atmosphere and evaporation of this water will tend to cool the dome and reduce pressures during DCH. The extent of this mitigation is addressed in Section 5.0 where it is shown that sprays are effective at mitigating DCH loads to non-threatening levels provided the igniters are operational, even when ice is depleted prior to vessel breach. Spray operation is stated to reduce

ice melt in the NUREG-1150 study (sprays remove heat from the atmosphere that otherwise would go into ice melting), but a quantitative effect cannot be derived from the results given. Sprays operate only in the dome (except for the D.C. Cook Plant), and most of the gas and steam normally reaches the dome only after passing through the ice condenser. Nonetheless, Section 5.0 of this report shows that spray operation in the upper dome has a relatively small effect at preserving the ice inventory.

Corresponding Large Dry Issues. Of the active ESFs in Sequoyah, the sprays are the only systems for which reasonable counterparts exist in large dry containments. Their direct effects upon DCH loads were not considered in NUREG/CR-6338; however, some of the possible consequences associated with spray operation (reduced containment pressures and steam concentrations at vessel breach, extent of cavity flooding) were considered.

3.2.2.2 HPME Threats Other Than DCH

Global Hydrogen Combustion in the Upper Dome. Hydrogen combustion is a potential threat in ice condenser plants only for those scenarios (largely SBOs) where igniters are not operational. The more common core damage scenarios involve AC power in the plants; consequently, power is generally available for hydrogen control. The igniters are effective at maintaining hydrogen concentrations below flammable levels when AC power is available.

Igniters do not function in SBO accidents; consequently, the large values (2.5-3.5) of the global hydrogen scaling parameter ϕ_{H_2} noted above suggests that hydrogen deflagration (and even possibly detonations) in the upper dome are more credible in ice condenser plants than in large dry containments. The initial conditions calculated by CONTAIN (Appendix B of this report) include molar hydrogen concentrations of 14-18% if ignition sources are absent. The calculations made use of hydrogen sources calculated by SCDAP/RELAP5 in which in-vessel zirconium oxidation was predicted to be 58%. This value is greater than the median (approximately 40%) assumed in NUREG/CR-6338, but it is less than the value of 75% that is postulated for the NRC's hydrogen rule for ice condenser plants (10 CFR 50.44). Operating igniters or the presence of other ignition sources preclude development of the high global hydrogen concentrations required for global detonations, whatever the extent of in-vessel zirconium oxidation.

In NUREG-1150, deflagration-to-detonation transition (DDT) in the ice condenser or the upper plenum was considered likely (probability greater than or equal to 0.45) whenever ignition occurred with hydrogen concentrations greater than or equal to 14%. DDT may be less likely in the open volumes of the dome (obstacles and channel geometries favor DDT) but turbulence and/or elevated temperatures associated with the DCH event could enhance detonability. Furthermore, a detonation initiated in the ice condenser or upper plenum region could propagate into the dome if gas compositions and temperatures there are within the detonable regime.

Accelerated flames occur when the combustion front accelerates to near-sonic velocities but does not become supersonic. Considerations for flame acceleration resemble those for DDT but the requirements are somewhat less stringent. Flame acceleration has been observed with hydrogen concentrations down to 10%, even with substantial steam present. Other things being

equal, peak dynamic pressures for accelerated flames are lower than for detonations but the integrated dynamic load (i.e., the impulse) can be comparable.

Global flame acceleration and/or detonations apparently were not considered in NUREG-1150. If they occur, the threat to containment integrity would presumably be substantial because, at the high hydrogen concentrations required, even a simple deflagration can be threatening. Consequently, little is achieved by distinguishing between deflagrations and detonations.

Obviously, if detonable hydrogen concentrations have developed, the potential threat is not limited to HPME events; any ignition source could initiate combustion and DDT. However, as noted above, HPME may provide conditions more favorable to detonation (turbulence and/or elevated temperatures) than would otherwise exist. If nothing else, HPME assures an ignition source.

Corresponding Large Dry Issues. Global detonations are generally not considered an important threat for PWR large dry containments because it is difficult to achieve the high hydrogen concentrations required in the larger containment volumes. Nonetheless, threats of dynamic loads are considered minimal for large dry containments and have received little emphasis in recent work.

Local Detonations. Because the ice condenser can strip steam from the entering gas mixture, detonable gas compositions can develop in the ice condenser and the upper plenum even if atmospheric compositions are not susceptible to detonation elsewhere within containment. Although a potential detonation threat can develop independently of HPME, the occurrence of HPME may promote detonability as discussed under global detonations and, in any case, it will provide an ignition source. As noted previously, the NUREG-1150 containment loads expert panel considered DDT in the ice condenser and/or upper plenum to be likely if ignition occurred with hydrogen concentrations exceeding 14%. Given a detonation, the distribution of impulsive loadings overlapped the distribution of containment fragility with respect to impulse as defined by the structural response experts. Hence, containment failure as a result of detonations in the ice condenser and/or the upper plenum were an acknowledged failure mode.

It is generally assumed that, if igniters and ARFs are both operating, the containment will be sufficiently well mixed that high hydrogen concentrations cannot develop in the ice chest even though there are no igniters there. In principle, this may not be true for short periods of time during very rapid release of steam and hydrogen from the primary system (Williams and Gregory 1990). The likelihood that this will happen just prior to vessel breach is probably sufficiently small that it may be discounted.

If igniters operate but ARFs do not, the lower compartment is typically steam-inerted; hence the igniters located there are ineffective. Code calculations (Dingman and Camp 1985; Williams and Gregory 1990) indicate that hydrogen can reach detonable concentrations in the ice condenser before concentrations in the upper plenum (where the closest igniters are located) are high enough to initiate a burn that can propagate downward into the ice condenser. If HPME occurs while these conditions exist, DDT may follow ignition. However, the detonation would be limited to the ice condenser in this scenario, and the NUREG-1150 structural response panel

Assessment of Ice Condenser Containment Phenomena

considered the containment boundary in the ice condenser to be less vulnerable to impulsive loading than in the plenum, although failure was still possible.

During an HPME event, the mixture flowing into the ice condenser will include high concentrations of steam mixed with varying amounts of hydrogen. Condensation of steam can then lead to gas mixtures exiting the ice condenser with high concentrations of hydrogen immediately after the HPME event. Since the HPME event will have depleted gas entering the ice condenser of oxygen, the high hydrogen concentrations are not necessarily combustible. However, if gases from the dome subsequently mix with the hydrogen-rich gas in the ice condenser, detonable compositions may develop at some point.

Corresponding Large Dry Issues. Large dry containments include no features capable of causing a large, local concentration of hydrogen analogous to the ice condenser. The flow paths between the lower compartments and the upper dome generally favor well mixed conditions in the atmosphere. Analyses of the IET experiments conclude that mixing processes would likely preclude the possibility of detonations in large dry containments.

Containment Failure by Direct Contact with Molten Debris. In the Sequoyah plant, debris traveling up the in-core instrumentation tunnel in an HPME event can strike the seal table. It is possible that the seal table and/or adjacent paneling will fail owing to thermal and mechanical loading, in which case molten debris can enter the seal table room (STR). The STR is located in the annulus between the crane wall and the containment shell, below the lower plenum. Debris accumulating against the shell inner surface could then heat it, causing a thermal failure resulting in loss of containment integrity.

Past analyses have indicated that this may not be a very low-probability event, given the requisite conditions. Tarbell et al. (1986) cited analyses from which they concluded failure is "assured" if 35 mt of debris enter the STR. Based, in part, upon these results in NUREG-1150, it was assumed that shell failure probabilities were in the range 0.3-0.6 for debris quantities entering the STR in the range 20-60 mt. Overall, the contribution to the CCFP from just this scenario was not broken out in the reported results; however, it was of the same order of magnitude as the probability of failure owing to overpressure associated with HPME.

This failure mode is favored by some of the same parameters that would favor an overpressure failure resulting from DCH: large melt mass, high RPV pressure, etc. Obviously, this mode does not matter greatly if the containment has already failed as a result of overpressure. However, the DCH loads are potentially sensitive to many issues that do not affect the direct contact mode; e.g., ice effectiveness, igniters, and operating ARFs. A deeply flooded cavity is assumed to preclude this failure mode.

Corresponding Large Dry Issues. Most large containments do not have dispersal pathways such that large quantities of debris can accumulate against the containment liner in a concentrated region. One exception is ANO-1 (B&W), where the IPE noted that the reactor cavity ducts material directly to the containment liner. The IPE concluded that water on the floor would preclude liner failure. This potential failure mechanism was not in NUREG/CR-6475

(Pilch et al. 1997), but it was not considered as an integral part of the DCH containment failure probabilities.

Vessel Launch as a Rocket. NUREG-1150 considered the possibility that massive failure of the vessel lower head while at high pressure could result in launching the vessel as a rocket, failing the containment. They defined several cases and completely ruled out the "rocket" failure except for the most severe case, in which the probability was still very low (0.01). It was considered slightly more plausible (probability 0.05) that an event of this type could result in damage to the missile shield, causing loss of seal between the upper and lower compartments and, hence, causing ice condenser bypass. Even this possibility was assigned sufficiently low probabilities that it is unlikely that it could significantly alter the overall risk associated with HPME. Occurrence of any "rocket" scenario was considered to be contingent upon gross failure of the lower head. Recent experiments (Chu and Pilch et al. 1999) confirm that localized failures are to be expected in plants with lower head penetrations.

Corresponding Large Dry Issues. Analogous events have been considered for large dry containments, with similar conclusions being reached with respect to the threat to containment integrity. The question of ice condenser bypass, however, has no large dry containment analogue.

Ex-Vessel Steam Explosions and FCIs. When there is water in the cavity, ex-vessel steam explosions can occur following vessel breach. Even if a true "steam explosion" does not occur, severe cavity pressurization may result from the FCIs following HPME, especially if the cavity is heavily flooded. NUREG-1150 considered the possibility that an ex-vessel steam explosion could cause containment failure. The only failure mode identified was the possibility that blast traveling up the in-core instrument tunnel to the seal table could create missiles that might fail the containment. This event was considered incredible except for the combination of a melt mass greater than or equal to 20% of the core being ejected into a deeply flooded cavity, and even in this case a conditional probability of only 0.01 was assigned.

Various experiments involving HPME and water have demonstrated a capability for severe cavity pressurization. Typically, the interactions have not been truly explosive, but cavity pressures of several MPa have resulted. The possibility of vessel displacement and its implications may merit further investigation for these conditions. The fragility of the cavity walls (if the walls are free standing) has not been addressed. The potential for missile generation, should the cavity walls fail, has also not been assessed.

Corresponding Large Dry Issues. For the specific failure mode identified in NUREG-1150, there is probably no analogue in large dry containments because the STR is located inside the crane wall. Any missile would have to penetrate the crane wall and still possess sufficient energy to fail the containment.

3.2.2.3 Other Phenomenological Issues

Here we briefly summarize other phenomenological issues affecting DCH loads in order to identify any potentially significant differences between large dry containments and ice condenser

plants. We do not explicitly consider the effect of ice in the ice condenser, which was discussed in Section 3.2.2.1; however, we note that some of the effects mentioned here may be of significance only for scenarios in which ice is depleted.

Oxygen Depletion Prior to Vessel Breach. If igniters operate, or if other ignition sources are present, hydrogen burns prior to vessel breach may substantially reduce the available oxygen supply at the time of vessel breach. For example, given 58% in-vessel zirconium oxidation as in the calculations cited in Appendix B, combustion of all this hydrogen prior to vessel breach would consume about 56% of the initial inventory of oxygen in the containment. Complete combustion of the hydrogen is not to be expected; however, the CONTAIN calculations of initial conditions in Appendix B predict that over 40% of the oxygen will be consumed prior to vessel breach.

Although global oxygen starvation during a DCH event is not expected to occur, local oxygen starvation is expected in the lower compartment and the ice condenser. This can be a significant mitigator of DCH. In the Surry-geometry SNL/IET experiments performed in the CTTF, the measured ΔP values ranged from 0.283 MPa to 0.43 MPa, and CONTAIN analyses of these experiments indicated that over half of this range could be attributed to the differences in the initial oxygen inventories in these experiments, even though oxygen starvation on a global basis did not occur in any of the experiments.

In this context, a high degree of in-vessel zirconium oxidation is *nonconservative* in accident scenarios with igniters operating. This point needs to be kept in mind when assessing the conservatism or nonconservatism of assumptions made concerning the extent of zirconium oxidation.

Corresponding Large Dry Issues. In large dry containments, depletion of oxygen prior to vessel breach is not an important issue and it is conservative to assume high levels of zirconium oxidation, because this maximizes the pre-existing hydrogen available at vessel breach. This is true because the melt on the lower head contains little zirconium at vessel breach, regardless of the amount of incore clad oxidation.

Combustion of Pre-Existing Hydrogen. As noted previously, a very strong combustion event may occur at vessel breach if igniters had not been operating. If igniters operate prior to vessel breach, it was assumed in NUREG-1150 that hydrogen would burn when concentrations reached 5.5%. Burns initiated at these concentrations are not complete, and some hydrogen will always remain. For scenarios with igniters, the CONTAIN calculations described in Appendix B predict that hydrogen concentrations of approximately 3.7-5.0 m/o would exist at vessel breach.

Corresponding Large Dry Issues. The hydrogen concentrations cited for scenarios with operating igniters are within the range that can arise in large dry containments and radically different behavior is not expected. If there is no containment heat removal, steam concentrations in the dry containments may be higher, however.

Combustion of DCH-Produced Hydrogen. Phenomenologically, the issues involved in the combustion of DCH-produced hydrogen are similar for ice condenser plants and large dry

containments. However, as was noted above, the oxygen inventory everywhere in ice condenser plants may be partially depleted owing to prior hydrogen burns. In addition, the lower compartment is less open to recirculation flows (assuming ARFs are not running) that might replenish oxygen than are the subcompartments in some large dry containments, and the relatively large volume of the lower containment (approximately one third of the total containment volume) may increase hydrogen hold-up in the lower compartment. These factors may make combustion of DCH-produced hydrogen less complete than is the case for many large dry containments.

Debris-Water Interactions. Debris-water interactions may arise in either the context of co-dispersed cavity water or co-ejected RPV water. Cavity water is potentially important only if the cavity contains some water, but not sufficient water to completely flood it. In Sequoyah, no cavity flooding is expected if the RWST has not dumped, while complete cavity flooding is expected if the RWST has dumped and 50% or more of the ice is melted. Even with RWST dump, little cavity water is expected if ice melt is less than or equal to 25%. It is possible that the range of scenarios in which cavity water is important may be quite limited, but only more detailed identification of the spectrum of accident sequences of significance to DCH can determine whether this is the case.

Both simple phenomenological arguments and code calculations (e.g., CONTAIN) indicate that, if moderate amounts of water interact with the debris, DCH loads in compartmentalized geometries can be enhanced. The reason is that the enhanced steam supply can enhance the extent of debris-gas thermal and chemical interactions, and can accelerate transport of energy and hydrogen to the dome, reducing the effects of mitigation by atmosphere-structure heat transfer. On the other hand, large amounts of water are more likely to mitigate loads by quenching the debris, suppressing the combustion of hydrogen, and cooling the atmosphere by evaporation of aerosolized water. No fully mechanistic models are available for calculating the effect of water on DCH loads. Limited experiments suggest that DCH loads are insensitive to cavity water in large dry containments. If the ice beds are functional at vessel breach, there may be a net mitigative benefit in converting direct heating (i.e., an atmospheric temperature rise) into a scenario with additional steam loading. This is because the ice beds can be more efficient at condensing steam than cooling hot gases.

Corresponding Large Dry Issues. No important qualitative differences between ice condenser plants and large dry containments have been identified in connection with debris-water interactions.

Atmosphere-Structure Heat Transfer. Atmosphere-structure heat transfer has been found to be an important mitigator in the CONTAIN analyses of the DCH IET experiments in both the Zion and Surry geometries. Delay of hydrogen combustion owing to hold-up in oxygen-starved subcompartments contributed to this effect by prolonging the time period over which heat transfer could act. Deleting the combined heat transfer and hydrogen hold-up effects increased the calculated ΔP by 60-75%. Because ice condenser containments represent a compartmentalized containment geometry, qualitatively similar mitigation effects are expected for these containments also.

Debris Transport to the Dome. Pilch et al. (1994b) have concluded that debris transport to the dome in large dry containments will be insufficient to have an important impact upon DCH loads except in cases in which line-of-sight paths connecting the cavity exits to the dome are important. No such line-of-sight transport paths exist in ice condenser containments. The only potentially significant pathway for dispersed debris to enter the upper dome is for it to pass through the ice compartment. Tutu et al. (1986) concluded, through extrapolation of experiment results, that approximately 80% of all debris entering the ice chest would be trapped by the ice baskets alone before entering the dome. Examination of the lower compartment geometry in an ice condenser plant suggests that particles would have a hard time negotiating the turns necessary for gas to carry melt particles into the ice chest. Furthermore, the gas expands and slows down significantly as it exits the cavity and enters the lower compartment, which further reduces the potential for debris (approximately 1 mm) to follow gas into the ice chest. Hence, the carryover of dispersed debris to the dome is not believed to be an important issue in ice condenser plants. This has been confirmed by CONTAIN calculations that assume (as a bound) that debris moves with gas and without slip into the ice chest, subject only to gravitational settling in the lower compartment. CONTAIN predicts very little debris transport to the upper dome.

RPV Insulation. In the SNL/IET-11 experiment, the stainless steel insulation surrounding the RPV was simulated. The insulation was almost totally stripped away, apparently by melting ablation, and the ablated insulation may have contributed to hydrogen production (Blanchat et al. 1994). However, the ablated insulation did not contribute to experiment loads in any significant or decisive fashion. In large dry containments, some of the ablated insulation can enter the dome via the annular gap around the RPV. This is not possible in ice condenser plants, which may reduce the potential contribution of the insulation to DCH loads.

Other DCH Phenomena. Other DCH-related phenomena include the rates of thermal and chemical interactions of gas and steam with airborne and nonairborne debris, debris airborne residence times, fraction of debris dispersed from the cavity, and coherence between debris dispersal and blowdown steam. No major differences between large dry containments and ice condenser containments have been identified concerning these phenomena.

4.0 QUANTIFICATION OF THE PROBABILISTIC FRAMEWORK

The best way to address the integration needs is through detailed and credible Level I and Level II probabilistic analyses, specific to each individual plant. This is outside the scope of the current assessment, and a cursory review of the IPE's for Ice Condenser plants shows that the Level II decompositions and quantifications for one plant are not always consistent with the decomposition and quantifications of another plant. To address these needs, the following practical approach was adopted for assessing the importance of HPME/DCH to early containment failure for all Ice Condenser plants.

- (1) Develop a simplified version of the NUREG-1150 event tree that operates on each CDI as a class (e.g., LOCAs) and not on the hundreds of PDS that might be members of a given class.
- (2) Benchmark the simplified tree by demonstrating that the simplified tree, with NUREG-1150 consistent input, reproduces (in a reasonable fashion) the results documented in NUREG-1150 for Sequoyah. This ensures that all significant top events have been identified in the NUREG-1150 study.
- (3) Update specific quantifications (e.g., hot leg failure probabilities) in the simplified tree if significant new work since the time of NUREG-1150 justifies the revision. Additional simplifications of the CET are possible to produce a more scrutable result for extrapolation evaluations.
- (4) Use the more simplified logic tree to evaluate, in a consistent manner, the early containment failure probabilities for all ice condenser plants (including a reevaluation for Sequoyah) using plant specific information (e.g., fragility and CDI frequencies) to the extent that information is available from the IPEs.

The DCH issue for ice condenser plants must be examined from the perspective of all early containment failure modes. The significant modes of early containment failure considered in NUREG-1150 and the current assessments are:

- (1) DCH overpressure failures,
- (2) Thermal failures of the containment liner resulting from accumulation of dispersed debris against the containment liner following HPME,
- (3) Non-DCH hydrogen combustion overpressure failures in scenarios where core damage is arrested in vessel or when the RPV fails at low pressures, and
- (4) Non-DCH steam spike overpressure failures when the lower head fails at low (less than 200 psi) RCS pressures.

NUREG-1150 also considered α -mode failures, but the early containment failure probabilities were small and could be ignored in the current assessments.

Quantification of the Probabilistic Framework

A CET was developed to quantify the HPME probability and the early containment failure probability for each of the six CDI classes,

- (1) Slow station blackout,
- (2) Fast station blackout,
- (3) LOCAs,
- (4) Transients,
- (5) ATWS, and
- (6) Internal floods

that do not represent bypass events; consequently, we exclude interfacing LOCAs and steam generator tube ruptures. Consistent with the IPEs, the internal floods are included in our study even though internal floods were not treated as an internal event in NUREG-1150. A review of the IPEs shows that internal floods are evaluated with the same event tree and quantifications as transients. We do the same. Table 4.1 summarizes the mean core damage frequency for each plant. The fractional contribution of each core damage initiator is also summarized. We note that McGuire and Watts Bar have SBO fractions that are substantially higher than the rest of the plants.

We operate on each CDI as a class (e.g., LOCAs) and not on the more numerous Plant Data States (PDS) that might exist at the time of core uncovering. This implies that there is only one dominant PDS for each CDI. This is reasonable for SBOs where active systems (igniters, ARFs, sprays, auxiliary feedwater, HPSI, LPSI, etc.) are not available. Only the passive system, the ice condenser, is assumed available in SBOs.

The assumption of a single dominant PDS for each of the non-SBO CDIs is clearly not correct. For the purpose of convenience, we define a base case where igniters, ARFs, sprays, and LPSI are assumed available in non-SBOs. No auxiliary feedwater (implying no secondary side cooling during the core degradation transient) is also assumed for convenience even though many sequences will have auxiliary feedwater available. We will address these cases in our loads quantifications, and in Section 7.0, we will perform one-at-a-time sensitivity studies to explore the potential impact of different PDS for non-SBOs. The key results of this study are insensitive to the PDS chosen for non-SBOs.

The simplified CETs used in this study was developed with the software, Precision Tree Pro⁶ version 1.0a. Precision Tree is an add-on to spreadsheet programs such as Microsoft Excel. The event trees are developed in a graphical format that becomes impractical for very large trees. As a practical matter, two separate trees were developed for each of the six CDI classes noted above: an HPME tree and a containment failure tree.

⁶ Copyright © 1996-1997, Palisade Corporation, 31 Decker Road, Newfield, NY, 14867, Ph. 607-277-8000, WEB <http://www.palisade.com>.

Table 4.1 Mean core damage frequency and fractional contribution of various core damage initiators to core damage

| Core Damage Initiator | Sequoyah N-1150 | Sequoyah IPE | Catawba IPE | DC Cook IPE | McGuire IPE | Watts Bar IPE |
|------------------------------|----------------------------|-------------------------|------------------------|------------------------|------------------------|--------------------------|
| 1 Slow SBO | 0.0827 | 0.0103 | 0.0034 | 0.0060 | 0.0790 | 0.0601 |
| 2 Fast SBO | 0.1671 | 0.0207 | 0.0069 | 0.0121 | 0.1598 | 0.1566 |
| 3 LOCAs | 0.6289 | 0.1802 | 0.1289 | 0.5599 | 0.3842 | 0.3005 |
| 4 Interfacing LOCA | 0.0117 | 0.0001 | 0.0013 | 0.0009 | 0.0002 | 0.0006 |
| 5 Transients | 0.0413 | 0.6684 | 0.6017 | 0.2592 | 0.3382 | 0.2705 |
| 6 ATWS | 0.0377 | 0.0413 | 0.0171 | 0.0456 | 0.0384 | 0.0476 |
| 7 STGR | 0.0306 | 0.0395 | 0.0000 | 0.1131 | 0.0002 | 0.0501 |
| 8 Internal Flood | NA | 0.0395 | 0.2407 | 0.0032 | 0.0000 | 0.1140 |
| Total | 1.0000 | 1.0000 | 1.0000 | 1.0000 | 1.0000 | 1.0000 |
| Mean CD Freq | 5.57E-05 | 1.70E-04 | 5.80E-05 | 6.26E-05 | 4.00E-05 | 8.00E-05 |

Quantification of the Probabilistic Framework

For the NUREG-1150 benchmark calculation, the HPME tree is intended to quantify the following information (conditional on the CDI):

- (1) The probability of vessel breach with the RCS at system setpoint pressure (SSP = 2500 psi).
- (2) The probability of vessel breach with "high" RCS pressures ($1000 \text{ psi} < P < 2000 \text{ psi}$).
- (3) The probability of vessel breach with "intermediate" RCS pressure ($200 \text{ psi} < P < 1000 \text{ psi}$),
- (4) The probability of vessel breach with "low" RCS pressures ($P < 200 \text{ psi}$), and
- (5) The probability of core damage arrest in vessel.

The containment failure tree starts with output from the HPME tree to calculate early containment failure. The CET was simplified even further for the extrapolation evaluations producing a more scrutable and focused result.

The threshold for debris dispersal and significant DCH processes was taken as 200 psi (1.36 MPa) in the NUREG-1150 study. Recent HPME/DCH experiments by Blanchat et al. (1999) in the highly dispersive Bechtel annular cavity (e.g., the Calvert Cliffs Plant) demonstrated that cavity dispersal and DCH loads decreased significantly when the RCS-equivalent pressure was reduced to 2 MPa. The reactor cavity geometry typical of ice condenser plants is less dispersive than the Bechtel annular cavity design; however, we retain for convenience the more conservative NUREG-1150 threshold of 200 psi in our basic logic.

Sections 4.1 and 4.2 define and quantify the top events for each containment event sub-tree, respectively. The discussions focus on NUREG-1150 quantifications, IPE insights when available, and our synthesis of recent research. From this, we recommend revisions to NUREG-1150 quantifications as appropriate. The NUREG-1150 benchmark is, in format, too voluminous for report publication; however, large format (paper) versions of the tree have been independently reviewed by Energy Research, Inc., and SNL staff familiar with NUREG-1150. These reviewers agree to the following:

- (1) That the simplified event tree logic reasonably captures the key processes modeled in NUREG-1150 that relate to RCS pressure at vessel breach and early containment failure,
- (2) That the quantifications in the CET for the Sequoyah benchmark calculations reasonably represent the NUREG-1150 intent, and
- (3) That the results of the Sequoyah benchmark calculation are in reasonable agreement with the NUREG-1150 results.

An independent SNL reviewer examined and verified the implementation of key input to the benchmark CET. The even more simplified CET for the extrapolation evaluations is presented in

Figures 4.1-4.12 for the Sequoyah plant for each of the six CDIs. The logic is the same for all other plants while some quantifications will be plant specific or sensitivity study specific. A detailed description of the quantifications is given below. While the simplifications and extrapolation are considered reasonable, these trees should not be considered equivalent to detailed CETs, and the results should be considered approximate and scoping in nature.

4.1 HPME Tree

The HPME tree quantifies whether core damage is arrested in vessel and at what RCS pressure does vessel failure occur if core damage is not arrested in vessel. The top events in this tree are:

- (1) RCS leak size at UTAF,
- (2) Stuck open PORV during cycling at system setpoint (SP),
- (3) Temperature-induced leak in RCP seals,
- (4) Intentional depressurization of the RCS,
- (5) Temperature-induced failure of the surge line or hot leg,
- (6) RCS pressure prior to possible vessel failure,
- (7) AC power recovery after UTAF and before vessel breach, and
- (8) Core damage arrest in vessel.

Quantification of these HPME-related events is presented in Sections 4.1.1 to 4.1.8.

4.1.1 RCS Leak Size at Uncovery of Top of Active Fuel (UTAF)

Definitions and terminology for leak sizes differ between NUREG-1150 and the IPE's. Table 4.2 maps the IPE definitions and characteristics onto the NUREG-1150 definitions and characteristics. We will use the NUREG-1150 definitions and characteristics as our default because our simplified CET and many of the quantifications are patterned after NUREG-1150.

Leak sizes associated with initiating events are addressed in the NUREG-1150 study for Sequoyah as Question 1 (Q1⁷) in Gregory et al. (1990). Table 4.3 summarizes the NUREG-1150 quantifications for Sequoyah. Note that NUREG-1150 did not explicitly consider Internal Floods as part of its internal events analysis. In NUREG-1150, initiating leaks are sometimes associated with CDIs that are not LOCAs. Table 4.4 addresses leak sizes at UTAF as obtained from the IPEs. Induced or intentional leaks after UTAF are addressed in Sections 4.1.2, 4.1.3, and 4.1.4.

⁷ We adopt, from this point forward, the standard that "Q_n" represents the nth top event question in Gregory et al. (1990).

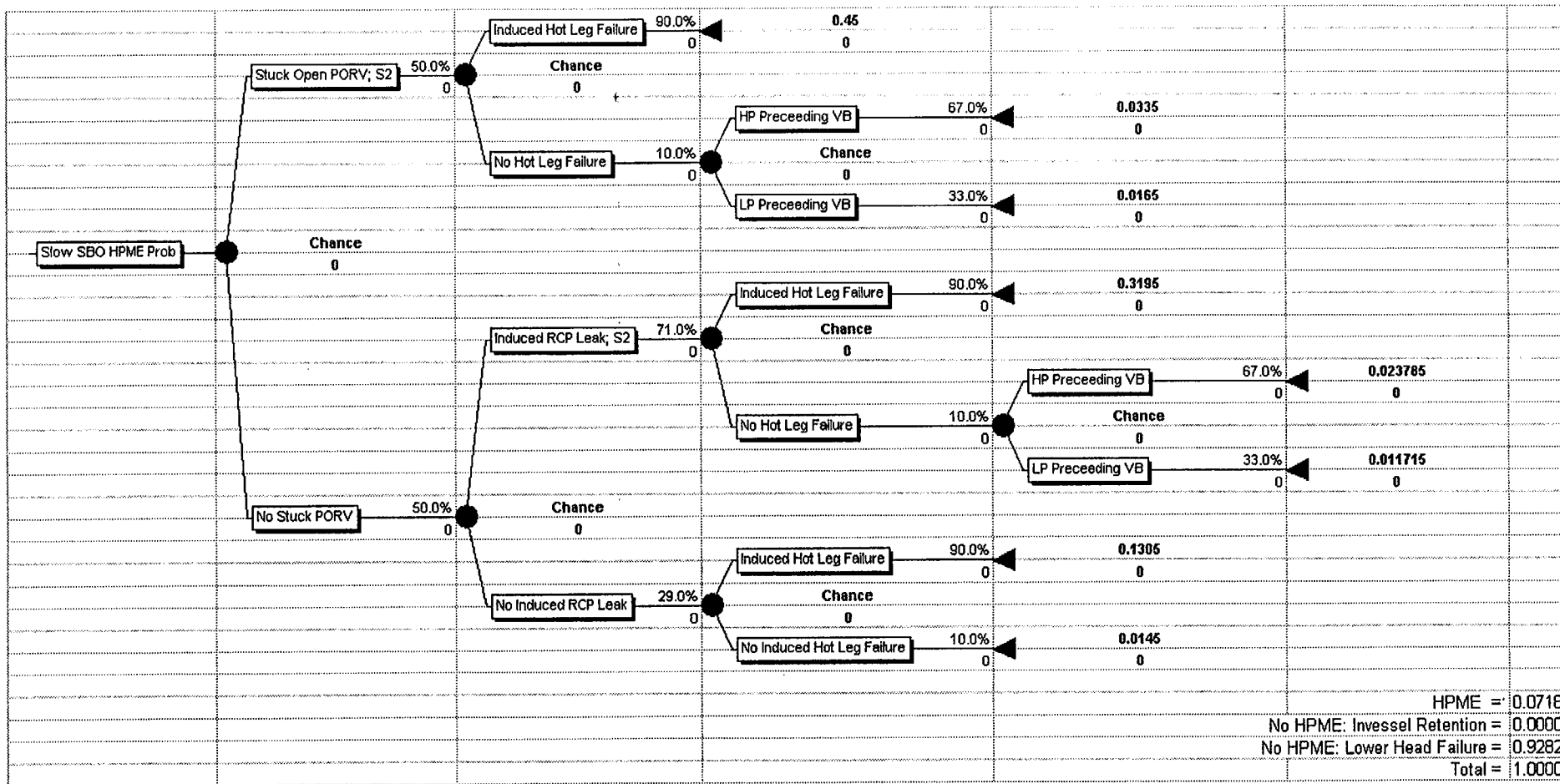


Figure 4.1 HPME probability for slow station blackouts in Sequoyah

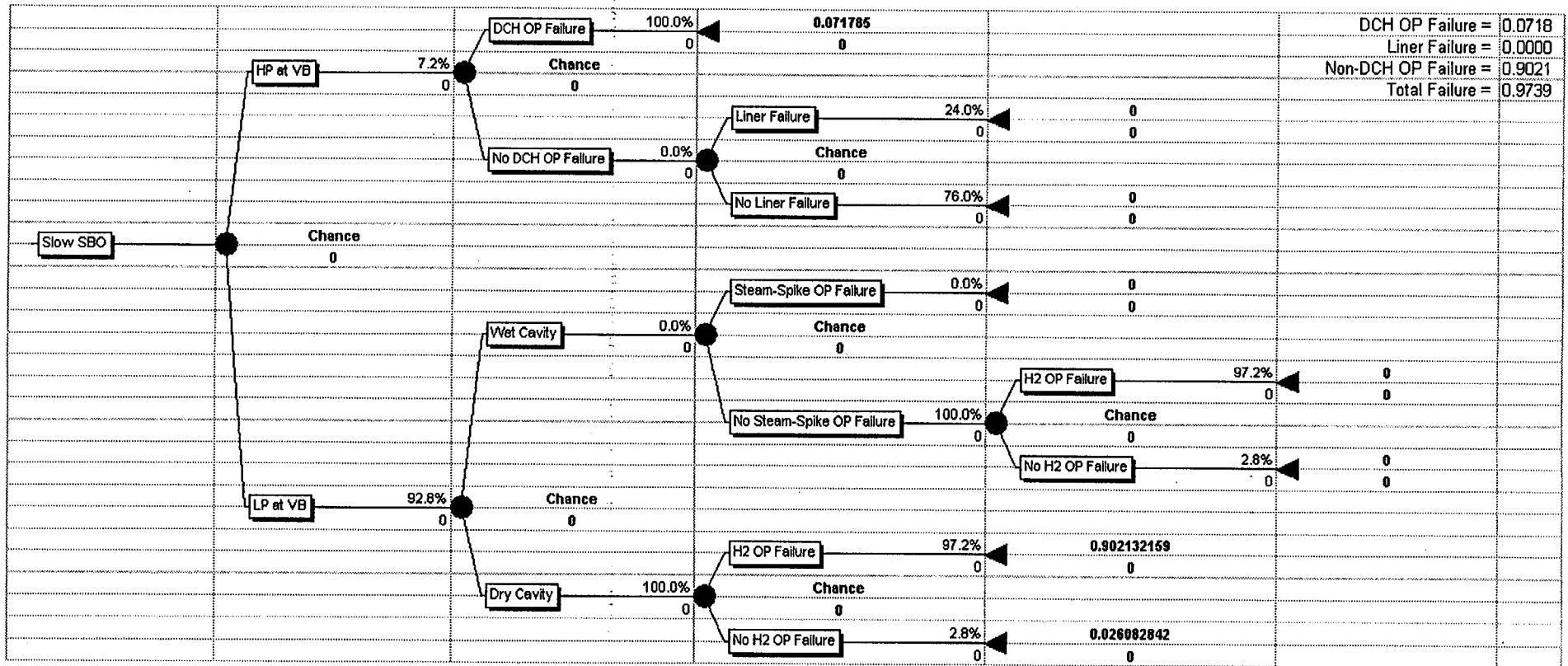


Figure 4.2 Early containment failure for slow station blackouts in Sequoyah

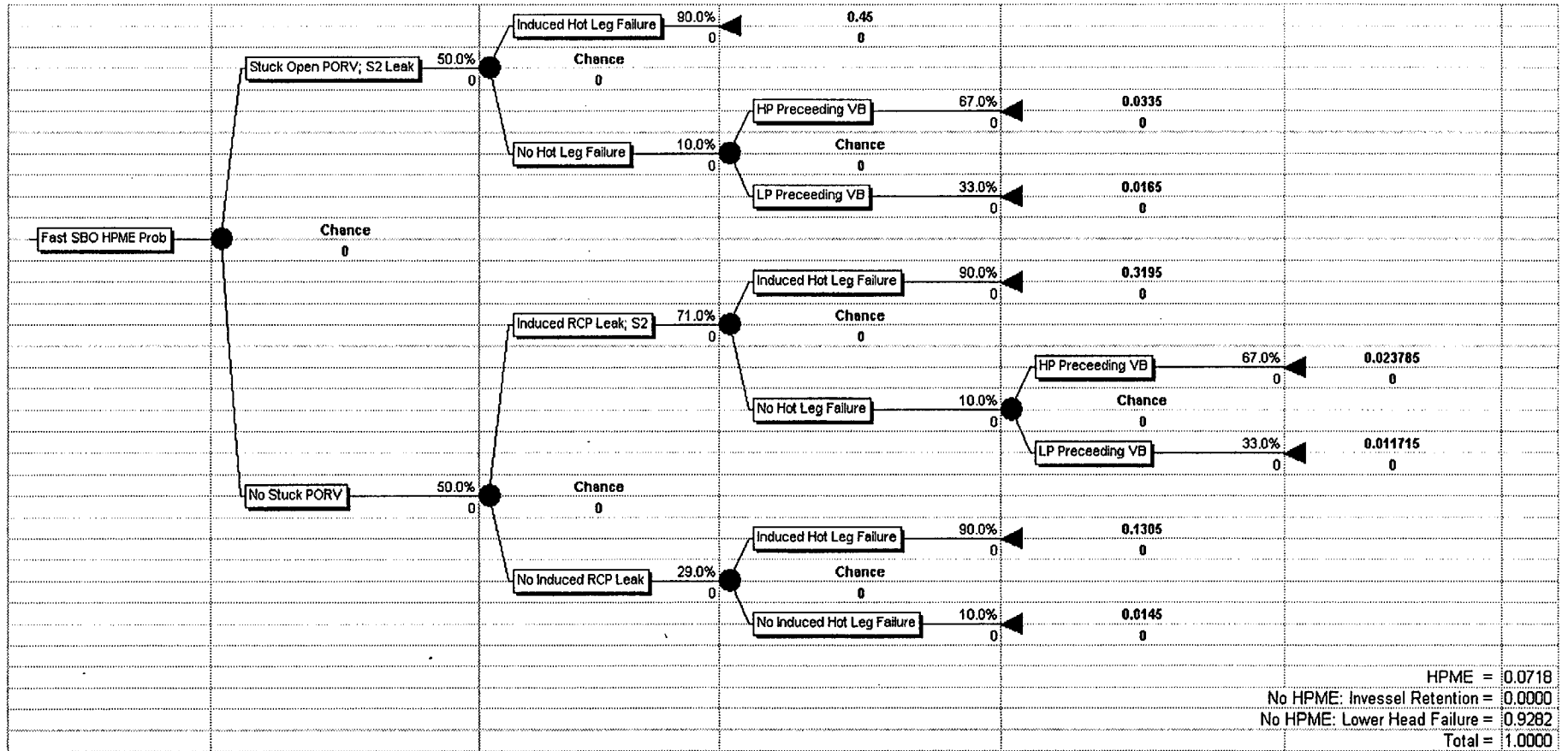


Figure 4.3 HPME probability for fast station blackouts in Sequoyah

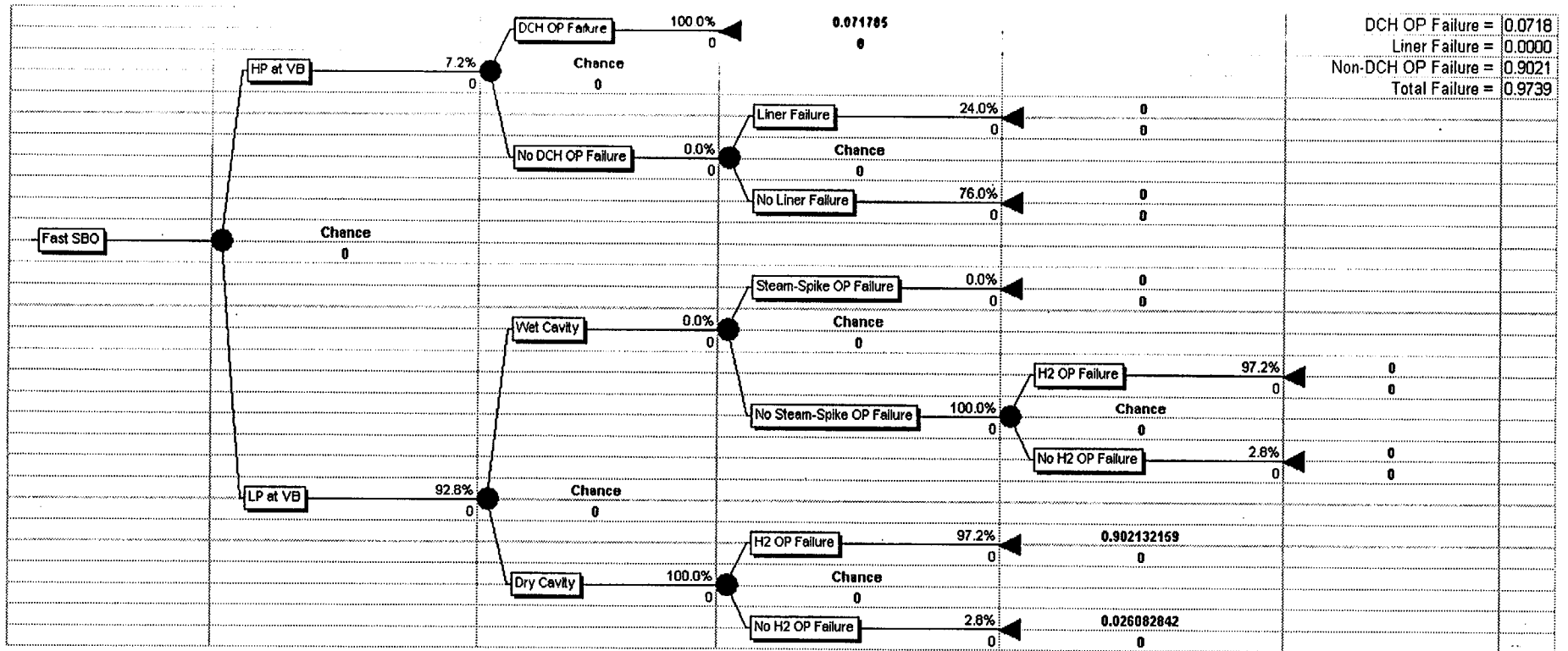


Figure 4.4 Early containment failure for fast station blackouts in Sequoyah

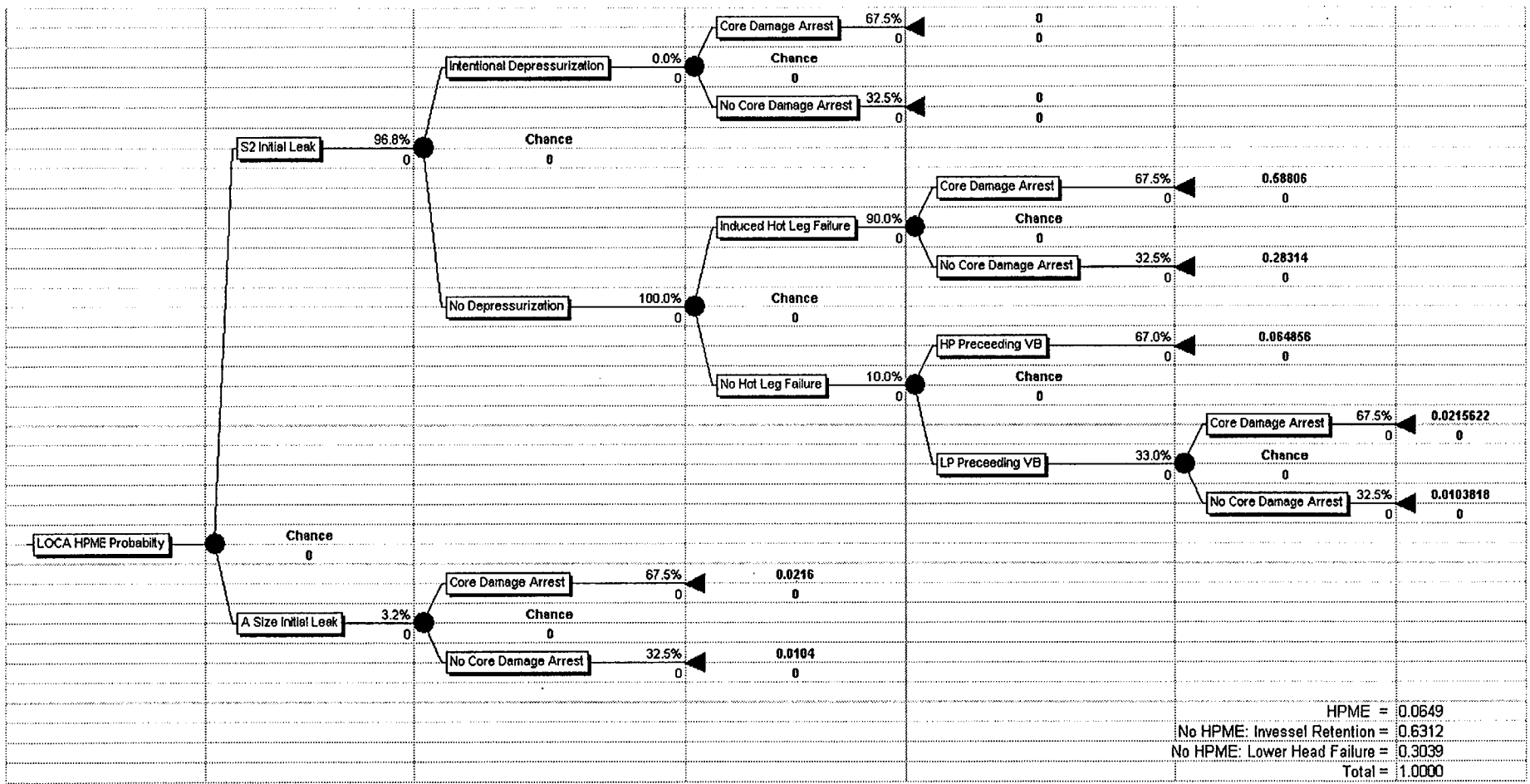
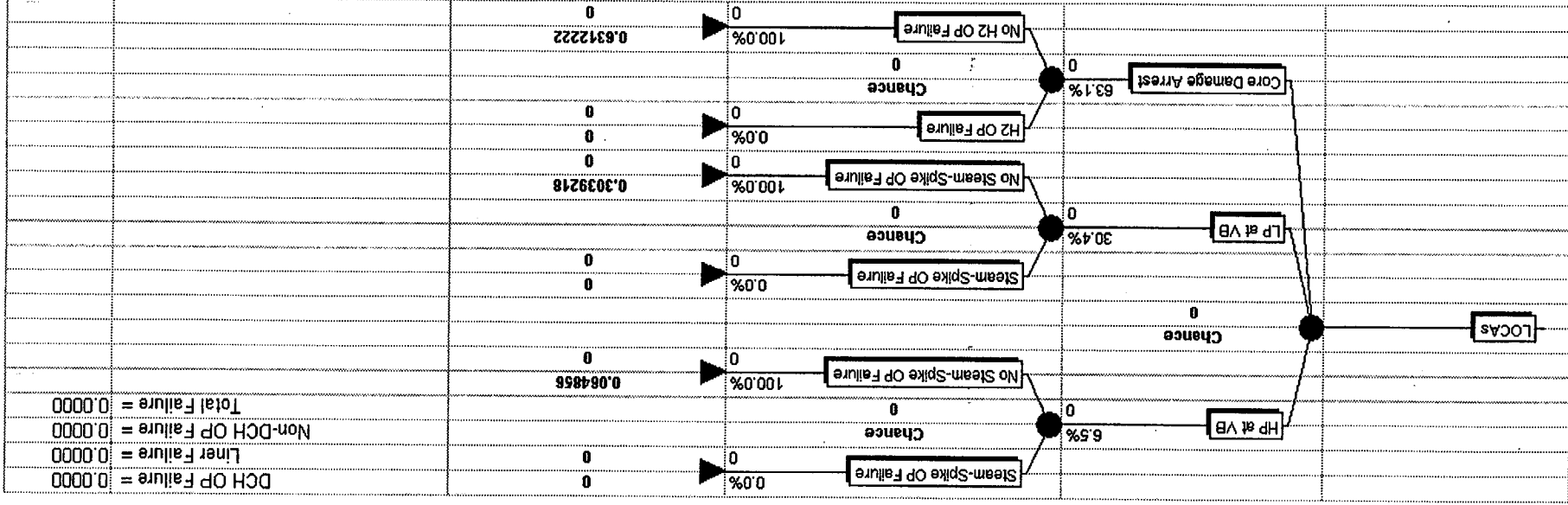


Figure 4.5 HPME probability for LOCAs in Sequoyah

Figure 4.6 Early containment failure for LOCAs in Sequoyah



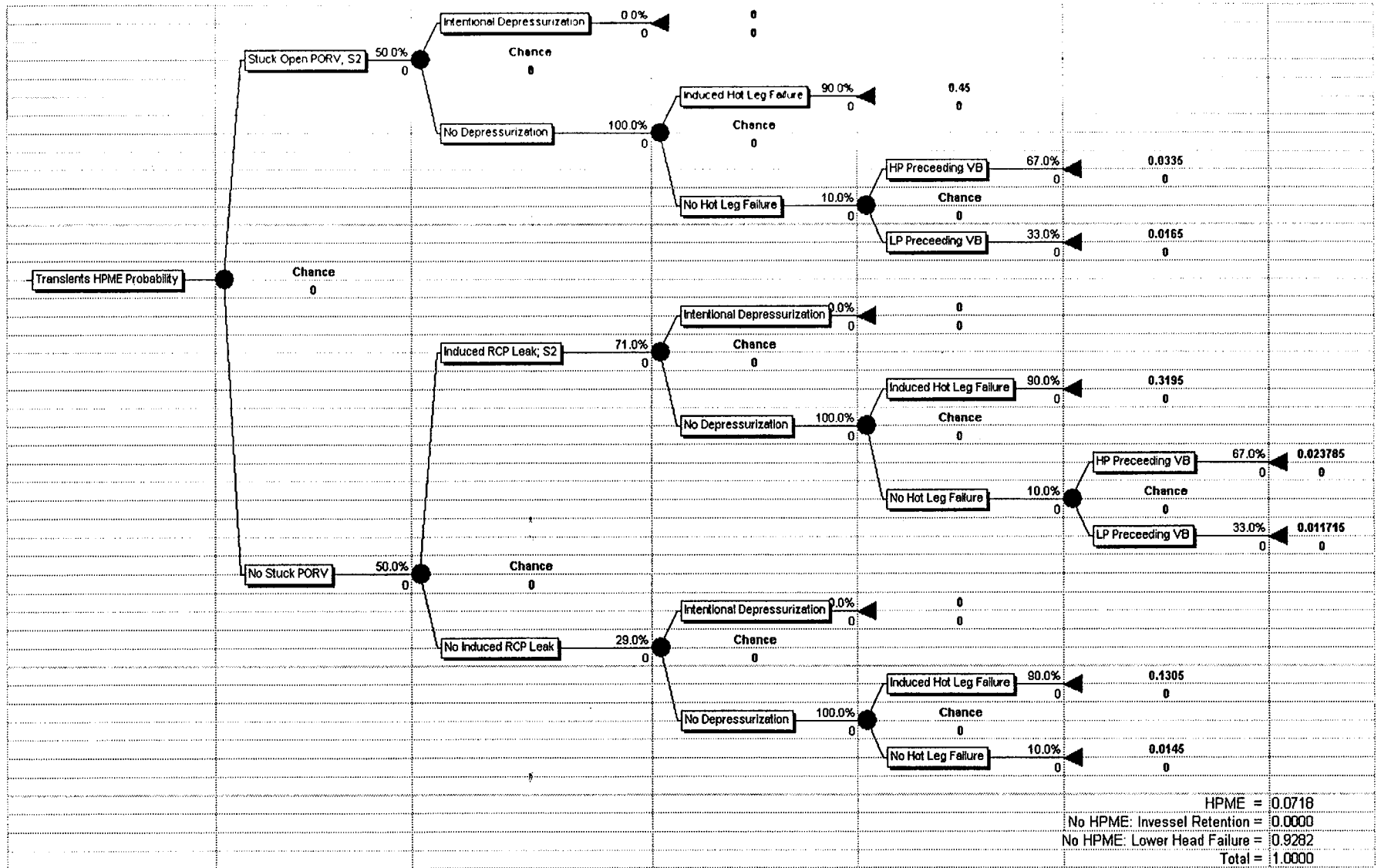


Figure 4.7 HPME probability for transients in Sequoyah

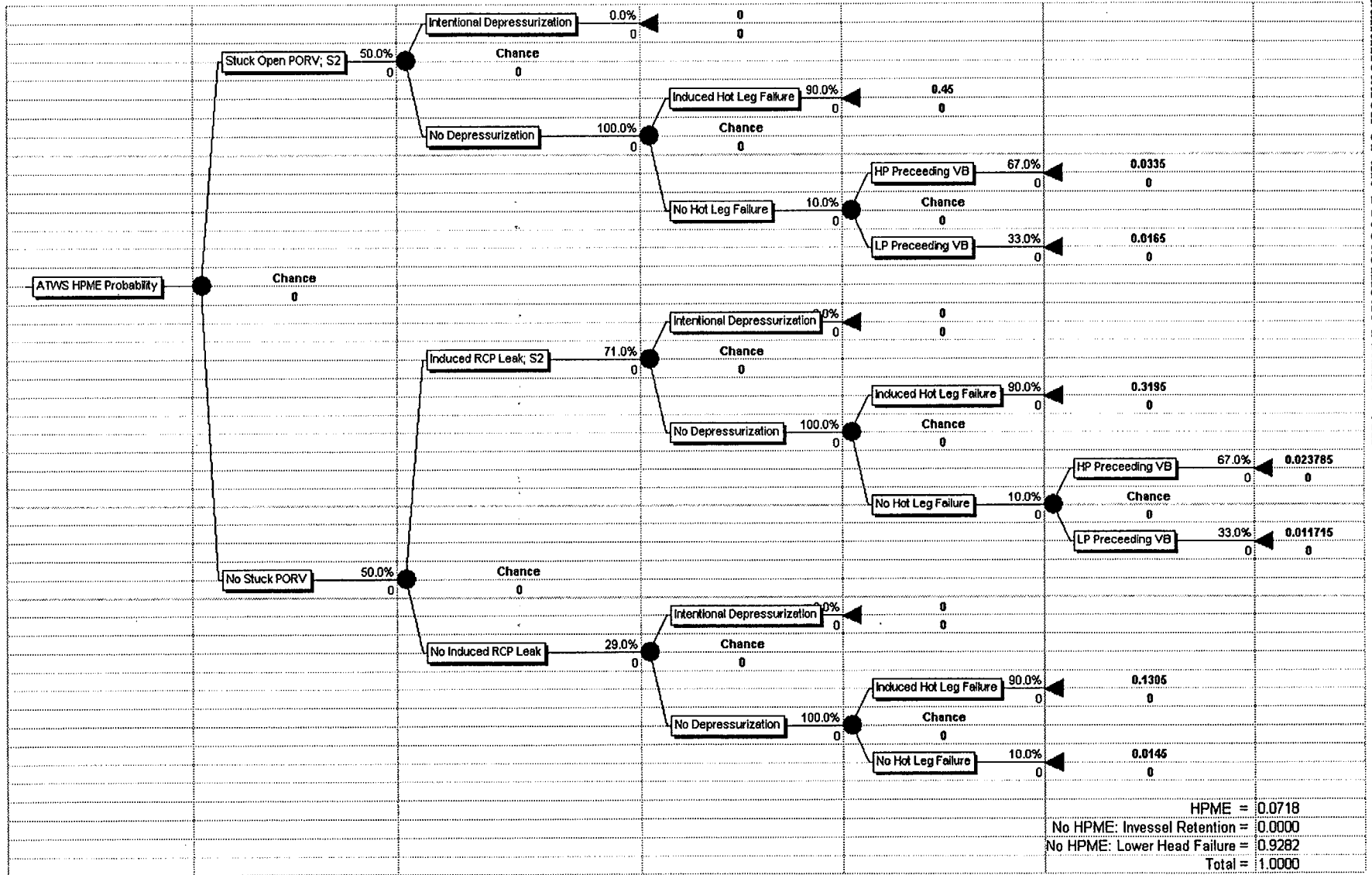


Figure 4.9 HPME probability for ATWS in Sequoyah

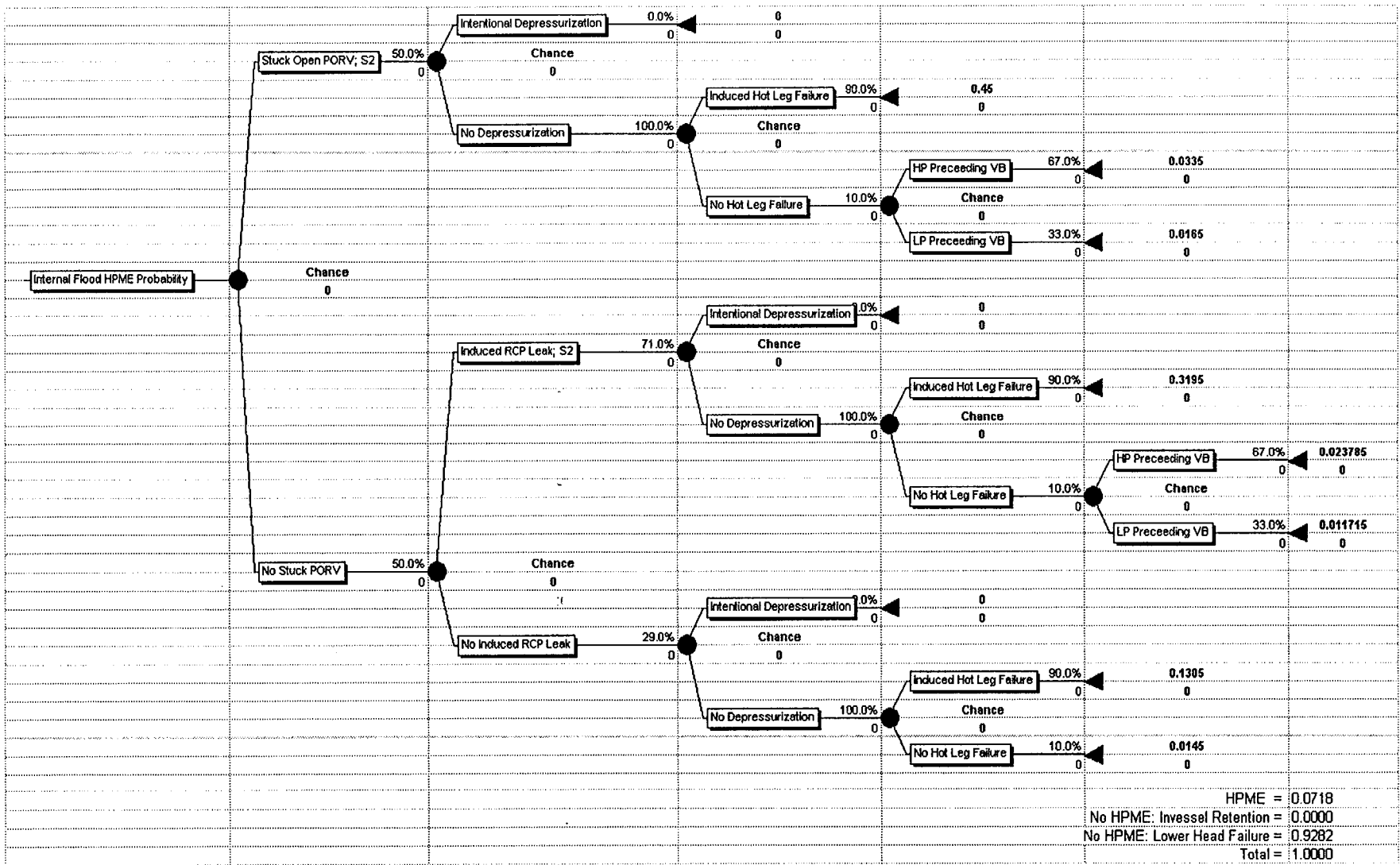


Figure 4.11 HPME probability for internal floods in Sequoyah

Table 4.2 Comparison of leak size characteristics

| NUREG-1150 | IPE's |
|----------------------------------|--|
| Very small break: S3 D < 0.5" | |
| Small break: S2 0.5" ≤ D < 2" | Small LOCA 0.375" < D < 2" |
| Large Break: A 2" < D | Medium LOCA 2" < D < 6" Large LOCA 6" < D |

The IPEs, however, appear to associate initiator leaks only with LOCAs. This simplifies the CET used for the extrapolation evaluations. Table 4.3 summarizes these initiator LOCA leak sizes for all plants as obtained from the IPEs. NUREG-1150 says that S3 leaks dominate for Sequoyah while the IPEs are consistent in their assessment that S2 leaks dominate LOCA initiators. For this study, we accept IPE assessments of LOCA leak sizes, as this information can only be obtained from a careful review of plant plumbing.

4.1.2 Stuck Open PORV During Cycling at SSP

PORVs and SRVs stick open occasionally in normal service. After core melt begins, they will be operating at temperatures much higher than those they encounter in normal service, so the single-cycle failure-to-reclose probability is higher than under normal operating conditions. Further, the valves are expected to cycle many times during core melt. The distribution for the PORVs or SRVs sticking open during core melt was determined in NUREG-1150 (Q17). Plausible rates of failure for a single cycle were estimated by increasing the normal failure rate to account for degraded performance at above-design temperatures. The number of cycles was estimated from code simulations. The probability estimates for the PORVs or SRVs sticking open during core melt obtained in this manner ranged from 0.1 to 1.0. In the absence of any data on the operation of these valves at the temperatures in questions, a uniform distribution from 0.0 to 1.0 (with a mean value of 0.5) was used in NUREG-1150.

Table 4.5 summarizes the NUREG-1150, IPE, and recommended quantifications for this issue.⁸ The IPEs generally cite the NUREG-1150 study for their quantification; consequently, we also adopt the NUREG-1150 quantifications for our study. In Section 7.0 of this report (Results and Sensitivities), a sensitivity study (case 5) is performed setting to zero the probability of a PORV sticking open.

⁸ In this table and all subsequent tables in Section 4.0, a blank entry means that the authors could not readily find the required information in the plant IPE.

Table 4.3 Initiator leak sizes at UTAF¹: Sequoyah NUREG-1150

| Core Damage Initiators | | Large Break (D>2"): A | Small Break (0.5"<D<2"): S2 | Very Small Break (D<0.5"): S3 | Interfacing LOCA Break | Steam Generator Tube Rupture | No Break: PORV Cycling | Total |
|------------------------|----------------|-----------------------|-----------------------------|-------------------------------|------------------------|------------------------------|------------------------|-------|
| 1 | Slow SBO | 0.000 | 0.028 | 0.954 | 0.000 | 0.000 | 0.018 | 1.000 |
| 2 | Fast SBO | 0.000 | 0.000 | 0.000 | 0.000 | 0.000 | 1.000 | 1.000 |
| 3 | LOCAs | 0.226 | 0.168 | 0.606 | 0.000 | 0.000 | 0.000 | 1.000 |
| 4 | Transients | 0.000 | 0.000 | 0.000 | 0.000 | 0.000 | 1.000 | 1.000 |
| 5 | ATWS | 0.000 | 0.000 | 0.757 | 0.000 | 0.135 | 0.108 | 1.000 |
| 6 | Internal Flood | | | | | | | |

¹Induced or intentional LOCAs after UTAF are addressed in Sections 4.1.2, 4.1.3, and 4.1.4.

Table 4.4 Leak sizes associated with LOCAs as a CDI in all ice condenser plants

| | Leak Size | | |
|-------------------|----------------|---------------------|-------------|
| | S3 D < 0.5" | S2 0.5" < D < 2" | A 2" < D |
| Sequoyah (N-1150) | 0.606 | 0.168 | 0.226 |
| Sequoyah | 0.000 | 0.968 | 0.032 |
| Catawba | 0.000 | 0.827 | 0.173 |
| DC Cook | 0.000 | 0.842 | 0.158 |
| McGuire | 0.000 | 0.759 | 0.241 |
| Watts Bar | 0.000 | 0.977 | 0.023 |

Table 4.5 Quantification of a stuck open PORV issue

| | Probability of Sticking | Leak Size |
|---------------------|-------------------------|-----------|
| NUREG-1150 (Q17) | 0.5 | S2 |
| Sequoyah, Watts Bar | 0.5 | – |
| Catawba, McGuire | 0.5 | S2 |
| DC Cook | – | – |
| SNL Quantification | 0.5 | S2 |

The PORV capacity in Ice Condenser plants is either 22.5 kg/s/PORV or 25.5 kg/s/PORV of saturated steam at the PORV setpoint. To achieve these flow rates, SCDAP/RELAP5 would model the PORV with a diameter of either 1.28" or 1.38", respectively. Leaks of this size are classified as S2 leaks in NUREG-1150 or as small leaks in the IPEs.

Conditions for PORV cycling at UTAF normally are associated with accident initiators with no initiating leak. In the NUREG-1150 study for Sequoyah, 75.7% of ATWS initiators have S3 leaks. The core is at full power in these events; consequently, NUREG-1150 assumes that PORVs will cycle for S3 initiator leaks in ATWS events.

4.1.3 Temperature-Induced Leak in RCP Seals

One of the secondary effects of a station blackout situation for Westinghouse plants is the possibility of a LOCA created by failure of the RCP seals to maintain a restricted flow between the primary system and the containment. Westinghouse RCP seals are designed to use mechanical components, in the form of rings and plates, and elastomer gaskets in the form of O-rings and channel seals to restrict leakage from the RCPs. Normal operation of a pump allows

for small amounts of leakage of primary water through the pump shaft seals (3 gpm). Furthermore, cooling water maintains the temperature of the seal components well below that of the primary systems. In the event of station blackout, the cooling water to the seals would be lost resulting in an initial leak rate of 21 gpm because of minor changes in seal geometry. Without cooling, there is concern that the shaft seals could fail to restrict flow, possibly leading to significant leakage of up to 480 gpm of each pump.

A NUREG-1150 elicitation panel addressed the issue of temperature-induced RCP leaks (Wheeler et al. 1989, Issue 4). The experts considered combinations of component failures, seal failures, and multiple pump failures in deriving a probability distribution of RCP leakage rates. The NUREG-1150 quantifications are summarized in Table 4.6. The off-normal leakage probability and leakage rate are a strong function of the O-ring material. The old O-rings are off-the-shelf components that are known to soften and degrade significantly with temperature if RCP cooling is not available. The new O-rings are custom made by Westinghouse and qualified for higher temperatures. The NRC has not required Westinghouse and Westinghouse has not committed to using the new O-rings; consequently, each utility is free to choose which O-rings to employ. We were not able to confirm if each ice condenser plant uses the old O-rings or the new O-rings.

In a station blackout accident, Table 4.6 says there is ~70% probability that the old O-rings will leak beyond normal rates, and there is approximately 19% probability that the new O-rings will leak. The mean (and most probable) leak rates are 211 gpm (253 most probable) and 176 gpm (172 gpm) for old and new O-rings, respectively. Table 4.7 summarizes similar quantifications taken from the Sequoyah and Watts Bar IPEs. The probability of off-normal leakage is consistent with NUREG-1150, assuming the old O-rings were employed; however, the most probable leak rate is more consistent with the new O-ring material.

Table 4.8 summarizes the NUREG-1150, IPE, and recommended quantifications for this issue. We have not been able to confirm if all ice condenser plants use the old O-rings or the new O-rings. Lacking better information, our recommended quantifications are patterned after NUREG-1150 values assuming the old O-ring material was employed in all plants. We note, however, that NUREG-1150 classified temperature-induced RCP leaks as S3 ($D < 0.5''$) leaks, which appears to be inconsistent with the expected value or most probable RCP leaks (Table 4.5). We will treat RCP leaks as S3 leaks for the NUREG-1150 benchmark calculations for consistency, and we will treat RCP leaks as S2 leaks in the extrapolation assessments. This classification of leaks sizes has implications on the expected RCS pressure at vessel breach (see Section 4.1.6).

4.1.4 Intentional Depressurization of the RCS

The end point of the emergency operating procedure directs the operators to latch open the pressurizer PORVs when the core exit thermocouples reach 1200°F (933 K), which characterizes temperatures well above normal operation (580°F), but just before significant clad oxidation is initiated. Intentional depressurization will delay core damage and reduce the RCS pressure to the point where Low Pressure Safety Injection Systems (LPIS) are effective (if available) at restoring cooling.

Table 4.6 NUREG-1150 Quantification of Westinghouse reactor coolant pump leaks for station blackout accidents

| Total gpm | gpm/Pump | Old O-rings Discrete Prob | New O-rings Discrete Prob | Comments |
|---------------------------------|----------|------------------------------|------------------------------|--|
| 12 | 3 | | | Normal operation leakage |
| 84 | 21 | 0.30200 | 0.81000 | Normal shutdown leakage |
| 244 | 61 | 0.14800 | 0.01400 | Off-normal leakage |
| 313 | 78 | 0.00000 | 0.01000 | Off-normal leakage |
| 433 | 108 | 0.01100 | 0.00060 | Off-normal leakage |
| 480 | 120 | 0.00130 | 0.00000 | Off-normal leakage |
| 543 | 136 | 0.00000 | 0.00260 | Off-normal leakage |
| 705 | 176 | 0.00120 | 0.14600 | Most probable (new O-rings), off-normal leakage |
| 796 | 199 | 0.00000 | 0.00270 | Off-normal leakage |
| 1013 | 253 | 0.53000 | 0.00830 | Most probable (old O-rings), off-normal leakage |
| 1230 | 308 | 0.00000 | 0.00000 | Off-normal leakage |
| 1920 | 480 | 0.00420 | 0.00420 | Off-normal leakage |
| Probability of off-normal leak= | | 0.69570 | 0.18840 | Off-normal conditions only |
| EV total gpm = | | 844 | 689 | Off-normal conditions only |
| EV gpm/pump= | | 211 | 172 | Off-normal conditions only |

Table 4.7 Sequoyah and Watts Bar quantification of temperature- induced RCP leaks for station blackout accidents

| Total gpm | gpm/Pump | Discrete Probability | Comment |
|----------------------------------|-----------------------|----------------------|-----------------------------------|
| 84 | 21 | 0.290 | Normal shutdown leakage |
| Other (320 assumed) | other (80 assumed) | 0.170 | Off-normal leakage |
| 750 | 188 | 0.535 | Most probable, off-normal leakage |
| 1440 | 360 | 0.005 | Off-normal leakage |
| Probability of off-normal leak = | | 0.710 | Off-normal conditions only |
| EV total gpm = | | 844 | Off-normal conditions only |
| EV gpm/pump = | | 211 | Off-normal conditions only |

Table 4.8 Temperature-induced reactor coolant pump leaks following UTAF

| | Probability of Leak | Leak Size |
|---------------------|---------------------|---|
| NUREG-1150 (Q18) | 0.71 | 253 gpm/pump (most probable) $D_{equiv} = 1.09''$; S3 |
| Sequoyah, Watts Bar | 0.71 | 188 gpm/pump (most probable) $D_{equiv} = 0.94''$; S2 |
| Catawba, McGuire | -- | -- |
| D.C. Cook | -- | -- |
| SNL Quantification | 0.71 | 250 gpm/pump $D_{equiv} = 1.08''$; S2 |

Table 4.9 summarizes the NUREG-1150, IPE, and SNL-recommended quantifications for the probability that operators will intentionally depressurize the RCS. With one exception, NUREG-1150 took no credit for intentional depressurization by the operators. The exception is represented by one PDS associated with an ATWS initiator where the PORV stuck open after cycling initially. The rationale for taking very limited credit for intentional depressurization in NUREG-1150 is twofold. At the time of NUREG-1150, procedures prohibited intentional depressurization unless at least one centrifugal charging pump or safety injection pump was running. AC power is required for operation of the pumps; consequently, deliberate

Table 4.9 Intentional depressurization of the RCS

| | Probability of Depressurization |
|---------------------|------------------------------------|
| NUREG-1150 (Q19) | 0.0 (0.9*) |
| Sequoyah, Watts Bar | 0.0 |
| Catawba, McGuire | > 0.9 |
| D.C. Cook | — |
| SNL Quantification | 0.0 |

*Intentional depressurization credited for only one PDS for the ATWS initiator.
No credit for all other PDS and CDI initiators.

depressurization is not credible for station blackouts. For other CDIs, no credit was taken for intentional depressurization after UTAF because the operators already failed to follow procedures to depressurize (in Level I analyses); consequently, the operators were not given credit to follow similar procedures after UTAF.

Since the time of NUREG-1150, Westinghouse has provided the plants with a set of Severe Accident Guidelines (SAGs) that pick up where the EOPs end. The SAGs have been approved by the NRC and operators are currently being trained on the SAGs. The Sequoyah and Watts Bar IPEs noted that operator depressurization after the onset of core uncover could be included in the CET after accident management concerns were addressed (the SAGs were not fully implemented at the time of the IPEs). Catawba and McGuire, on the other hand, took significant credit for intentional depressurization in the CET.

We have examined the relevant SAGs and note that they are just that, guidelines and not procedures. The operators are asked in the SAGs to make a subjective assessment of the pros and cons of depressurization before taking any action. From a human reliability perspective, guidelines do not carry the same weight that procedures imply. Lacking a credible human reliability analysis built on the EOPs, SAGs, and operator interaction with the TSC, we have chosen to take no credit for operator intentional depressurization after UTAF. As a sensitivity study (case 4 in Section 7.0), we will consider a case of operator intentional depressurization after UTAF (with 90% probability) for all CDIs excluding only SBOs. We assume that intentional depressurization will lead to "low" RCS pressures at vessel breach.

4.1.5 Temperature-Induced Failure of the Surge Line or Hot Leg

After much of the core is uncovered, the upper portion of the vessel and the piping connected to it will be subjected to temperatures well above the design temperature. The core will be above 2000°F, so temperatures higher than 1000°F are possible in the vicinity of the hot leg nozzles and the surge line. If the RCS remains at high pressure during degradation, the hoop stress on the hot leg and the surge line will be high, and the elevated temperatures will weaken

the metal considerably. It is possible that the piping may fail before vessel breach. Both the hot leg and the surge line are large pipes, so that all failures are of "A" size.

Table 4.10 summarizes NUREG-1150, IPE, and SNL-recommended quantifications for this issue. NUREG-1150 considered surge line or hot leg failures likely only when the RCS was at the system setpoint pressure (no leak except for cycling PORVs), and only limited credit was given for RCS pressures above 2000 psi (13.6 MPa). Surge line or hot leg failures were considered incredible when RCS pressures were below 2000 psi (13.6 MPa). We note also that NUREG-1150 assigns the same probability of surge line or hot leg failure to all CDIs. The IPEs generally adopted the NUREG-1150 quantifications with only minor adjustment of the probabilities while accepting the assessment that surge line or hot leg failures are only likely at system setpoint pressures.

Since the time of NUREG-1150, best estimate SCDAP/RELAP5 calculations have been performed for the spectrum of pump seal leaks in both Zion (Pilch et al. 1994b) and Surry (Pilch et al. 1995), which are both Westinghouse plants. The calculations all showed hot leg failure after the onset of core damage but well before core relocation to the lower plenum and well before lower head failure. The resulting depressurization of the RCS precludes HPME/DCH processes. The impact of varying key modeling parameters affecting core melt progression was examined in Pilch et al. (1995). For SBO sequences in Surry, the probability of hot leg failure was quantified as $P = 0.98$ for system setpoint pressures; $P = 0.98$ for 250 gpm RCP leaks; and $P = 1.0$ for stuck open or latched open PORVs.

We conclude from these calculations that hot leg or surge line failure is essentially assured for the full spectrum of RCS leak sizes that could leave the RCS at DCH-relevant pressures at vessel breach. We note that hot leg or surge line failure did not occur in TMI-II; and consistent with TMI-experience, the operators have means at hand that could disrupt natural and forced convective flows in the RCS if AC power is available. Consequently, we recommend that the hot leg or surge line failure probability be set to 90% for all CDIs and all leaks capable of leaving the RCS at DCH-relevant pressures at vessel breach. As a sensitivity study (case 6, Table 7.4, Section 7.0), the probability of hot leg or surge line failure will be reduced conservatively to 50% for SBOs and to 10% for non-SBOs.

Table 4.10 Probability of temperature induced failure of the surge line or hot leg

| | Probability of Failure | | |
|---------------------|------------------------|---------|---------|
| | No Leak | S3 Leak | S2 Leak |
| NUREG-1150 (Q21) | 0.768 | 0.035 | 0.000 |
| Sequoyah, Watts Bar | 0.768 | – | – |
| Catawba, McGuire | 0.900 | 0.001 | 0.001 |
| D.C. Cook | – | – | – |
| SNL Quantification | 0.900 | 0.900 | 0.900 |

In some scenarios, the cavity can be deeply flooded. Exvessel cooling will delay and possibly prevent lower head failure. We note in Section 4.2.2 that no credit is taken from prevention or delay of lower head failure. Delaying lower head failure would increase the likelihood that the hot leg, surge line, or even the upper head would fail and completely depressurize the RCS before lower head failure.

4.1.6 RCS Pressure Prior to Possible Vessel Breach

The RCS pressure just prior to vessel breach may be considerably higher than during some prior phases of the core degradation process. Cycles of accumulator discharge and core relocation to the lower plenum are events that could cause significant repressurization just prior to vessel breach. This pressure decreases at a rate primarily dependent upon the size of the hole(s) in the RCS pressure boundary. Therefore, the RCS pressure at breach may depend strongly upon the time between slump and breach because the length of this period determines where on the decreasing pressure curve the breach occurs. There is considerable uncertainty in the RCS pressure at vessel breach for situations with S_3 or S_2 breaks.

Table 4.11 summarizes the NUREG-1150 and SNL-recommended quantifications for this issue. In NUREG-1150, the RCS pressure at vessel breach is a unique function of the CDI leak size *or* the size of induced leaks, whichever is larger. For example, a stuck open PORV (S_2 leak) followed by a temperature-induced RCP leak (S_2 leak) is treated as a single S_2 leak in terms of defining the RCS pressure at vessel breach. The Sequoyah and Watts Bar IPEs provide different probability quantifications for the case of single leaks and compound leaks. The entries in Table 4.11 for Sequoyah and Watts Bar are for single leaks only so the entries can be compared directly to the NUREG-1150 quantifications.

We adopt the NUREG-1150 “*or* logic” for the current study. We believe this decision is generally conservative in that it favors somewhat higher RCS pressures at vessel breach. A practical consequence of this decision is that our CET can be simplified further for the extrapolation evaluations by eliminating branches for additional leaks if these leaks are similar or smaller than previously defined leaks.

The NUREG-1150 and available IPE quantifications are consistent in that A-sized leaks always lead to low RCS pressures (LP) at vessel breach and that no leaks (i.e., cycling PORVs) always lead to system setpoint pressures at vessel breach. The Sequoyah and Watts Bar IPEs generally favor higher RCS pressures at vessel breach (relative to NUREG-1150) for S_3 and S_2 leaks. Our recommended quantifications favor higher RCS pressures at vessel breach relative to NUREG-1150 quantifications.

The RCS pressure prior to vessel breach is used to define downstream logic or to quantify downstream results relating to

- (1) Containment loads at vessel breach (see Sections 4.2.3 and 4.2.5), and
- (2) Containment failure resulting from liner meltthrough.

Table 4.11 Mapping of leak sizes to RCS pressure prior to possible vessel breach

| | | Probability of Vessel Breach in Stated Pressure Range | | | |
|------------------------|-----------------|---|-------------------------------|----------------------------|------------------------|
| | | SSP | HP | IP | LP |
| Leak Size ¹ | | 2500 psi 17 MPa | 1000-2000 psi 6.8-13.6 MPa | 200-600 psi 1.4-4.1 MPa | < 200 psi < 1.4 MPa |
| NUREG-1150 (Q25) | A | 0.000 | 0.000 | 0.000 | 1.000 |
| | S ₂ | 0.000 | 0.000 | 0.200 | 0.800 |
| | S ₃ | 0.000 | 0.330 | 0.340 | 0.330 |
| | NL ² | 1.000 | 0.000 | 0.000 | 0.000 |
| Sequoyah, Watts Bar | A | 0.000 | 0.000 | 0.000 | 1.000 |
| | S ₂ | 0.000 | 0.250 | 0.500 | 0.250 |
| | S ₃ | 0.290 | 0.170 | 0.536 | 0.005 |
| | NL | 1.000 | 0.000 | 0.000 | 0.000 |
| Catawba, McGuire | --- | --- | --- | --- | |
| D.C. Cook | -- | --- | -- | --- | |
| SNL Quantification | A | 0.000 | 0.000 | 0.000 | 1.000 |
| | S ₂ | 0.000 | 0.330 | 0.340 | 0.330 |
| | S ₃ | 0.330 | 0.340 | 0.330 | 0.000 |
| | NL | 1.000 | 0.000 | 0.000 | 0.000 |

¹ Initiator Leak or induced leak.

² NL means no leak except for a cycling PORV.

Quantification of the Probabilistic Framework

As in NUREG-1150, the CET for our benchmark activity quantifies these two issues for all four pressure ranges. For the extrapolation study, it is sufficient to consider only two pressure ranges; low pressure, $P < 200$ psi (1.4 MPa) characteristic of non-DCH processes; and a modified high pressure (HP*), $P > 200$ psi (1.4 MPa) that is relevant to DCH processes. This simplification of the CET necessitates some conservative choices in some later quantifications, which will be discussed in the appropriate sections. Table 4.12 summarizes the collapsed mapping of leak sizes to RCS pressure prior to vessel breach. These values are used in the extrapolation study.

4.1.7 AC Power Recovery After UTAF and Before Vessel Breach

There is some probability of recovering AC power in both short-term SBOs and long-term SBOs. Restoration of core AC recovery has the potential to

- (1) restore core cooling and arrest core damage in vessel,
- (2) induce hydrogen combustion and possible containment failure before vessel breach, and
- (3) reduce DCH loads if the lower head fails.

Procedures prohibit energizing the igniters in a recovered SBO unless the hydrogen concentrations are non-flammable and the TSC concurs with the decision to re-energize the igniters. However, the air return fans will reboot automatically after a few minutes and other systems will also be re-energized. NUREG-1150 quantifications (Q48, Q49, Q50, and Q51) imply that there is approximately 89% probability of random ignition somewhere in the plant if flammable concentrations of hydrogen are present during a recovered SBO. This precombustion of hydrogen in the containment atmosphere before vessel breach could fail the containment, and it will significantly reduce the subsequent DCH loads relative to scenarios where DCH occurs in conjunction with high concentrations (approximately 12%) of hydrogen in the containment.

Table 4.13 summarizes NUREG-1150, IPE, and SNL-recommended quantifications for this issue. As considered in NUREG-1150, key times in the SBO sequences are

- (1) Fast SBO: early period = 1 hr, UTAF = 1.6 hr, VB = 2.6 hr, and
- (2) Slow SBO: early period = 4 hr, UTAF = 8.6 hr, VB = 10.4 hr.

Table 4.12 SNL recommended collapsed mapping of leak sizes into RCS pressure prior to possible vessel breach

| Leak Size ¹ | HP* | LP |
|------------------------|------------------------|------------------------|
| | > 200 psi > 1.4 MPa | < 200 psi < 1.4 MPa |
| A | 0.00 | 1.00 |
| S ₂ | 0.67 | 0.33 |
| S ₃ | 1.00 | 0.00 |
| NL | 1.00 | 0.00 |

¹ Initiator Leak or induced leak.

Table 4.13 Probability of AC recovery after UTAF and before vessel breach in SBOs

| | Probability of AC Recovery | |
|---------------------|----------------------------|----------|
| | Fast SBO | Slow SBO |
| NUREG-1150 (Q22) | 0.41 | 0.721 |
| Sequoyah, Watts Bar | Explicitly not addressed | |
| Catawba, McGuire | No "credit" taken | |
| D.C. Cook | --- | --- |
| SNL Quantification | 0.00 | 0.00 |

Note that NUREG-1150 calculated the probability of AC recovery after UTAF using a time window that starts 0.6 hr to 4.6 hr prior to UTAF. This was done to provide continuity with the Level I analysis, but it does result in an artificially high probability of AC recovery for the Level II analysis. We use these probabilities in the benchmark calculations because our intent is to reproduce NUREG-1150 results.

The Sequoyah and Watts Bar IPEs took credit for AC recovery before UTAF in their Level I analyses; however, the IPE did not address the issue in their Level II analysis stating that the time window for AC recovery and core damage arrest (CDA) was too small. The Catawba and McGuire IPEs also took "no credit" for AC recovery because there is a "fairly short time period" between UTAF and vessel breach.

Table 4.14 summarizes our own assessments of AC recovery and CDA for ice condenser plants. These independent assessments are motivated by the fact that modern best-estimate systems codes like SCDAP/RELAP5 generally predict a much longer time interval between core uncover and vessel breach when compared to the code predictions available at the time of NUREG-1150. The time for UTAF is controlled by boiloff of the secondary and part of the primary coolant inventory. The listed times are adopted from the NUREG-1150 study; however, the time to UTAF in a fast SBO are also consistent best estimate SCDAP/RELAP5 calculations for Zion (Pilch et al. 1994b). The timing (relative to UTAF) of core damage (onset of clad oxidation) is taken from the same Zion calculation. This Zion calculation also predicted hot leg failure well before core relocation and lower head failure; consequently, we must speculate on the timing of vessel breach under the assumption that hot leg failure does not occur. The listed vessel breach time assumes that core relocation would have occurred shortly after predicted hot leg failure and that the predicted time between relocation and vessel breach remains unchanged.

New power recovery curves were recently published by Atwood et al. (1998). The curves were based on sixteen years (1980-1996) of actual plant experience. Working directly with Figure 3-9 in Atwood et al., we computed the probability of AC recovery and the probability of core damage arrest given AC power recovery. We assume that AC recovery must occur before core damage (i.e., onset of clad oxidation) to ensure CDA.

Table 4.14 Assessment of AC Recovery recovery and Core core Damage damage arrest in ice condenser plants

| | Fast SBO | Slow SBO |
|----------------------------|----------|----------|
| UTAF (hr) | 1.6 | 8.6 |
| Core Damage (hr) | 2.23 | 9.23 |
| Vessel Breach (hr) | 5.4 | 12.4 |
| Prob of AC Recovery | 0.34 | 0.00 |
| Prob of CDA Given Recovery | 0.45 | 0.00 |

Table 4.14 shows that there is essentially no chance of AC recovery or CDA in a slow SBO. The power recovery curve is essentially flat, characteristic of weather related SBOs, for the time window (8.6-12.4 hrs⁹) associated with slow SBOs. There is a finite probability of AC recovery and core damage arrest in a fast SBO; however, the total probability ($0.34 \times 0.45 = 0.153$) is small. Consequently, our simplified CET ignores the probability of AC recovery and CDA (see Table 4.15) for all SBOs. This is also conservative because it assumes that the hydrogen combustion event occurs in conjunction with the DCH event.

We note that there is some small probability of ignition prior to vessel breach even if AC recovery does not occur. An obvious ignition source is the hot lower head itself, which must reach temperatures of ~1000 K before rupture occurs. However, the lower compartment is typically steam inerted to deflagrations. Even if deflagrations are not possible, the lower head could act as a catalyst for local hydrogen/oxygen recombination.

4.1.8 Core Damage Arrest

It is possible to arrest the core damage process, avoid vessel breach, and achieve a safe, stable state (as at TMI-II) if adequate coolant injection is restored before the core degradation process has gone too far. Recovery of injection is caused by one of two events. Recovery of injection capability follows the restoration of offsite power in SBO accidents, which we judged to be of insignificant probability in Section 4.1.7. In other types of accidents, an injection system is operating when core degradation commences, but no injection is taking place because the RCS pressure is too high.¹⁰ If a break in the RCS pressure boundary allows the RCS pressure to decrease to the point where the operating system can inject, there is some chance of arresting the core degradation process. The probability of arresting core degradation depends on the time the injection starts relative to the state of the core. We note that core relocation to the lower plenum at TMI-II occurred at a time when the core was already resubmerged in water.

⁹ The length of a slow SBO can be very plant specific.

¹⁰ The maximum HPIS pressure for any of the ice condenser plants is 1700 PSI; therefore, some depressurization from the RCS setpoint of 2400 PSI is required before significant injection can occur.

Table 4.15 Quantification of core damage arrest/invessel

| CDI | HPIS Avail? | LPIS Avail? | NUREG-1150 | | | SNL Recommendation |
|--------------------------|-------------|---------------|---------------------------|---|-------------|--------------------|
| | | | CDA Given Injection (Q26) | Prob of ECCS Recovery Given AC Recovery (Q23) | Prob of CDA | |
| Recovered Slow SBO | Yes | Yes | 0.9 | 0.95 | 0.855 | NA |
| Recovered Fast SBO | Yes | Yes | 0.9 | 0.95 | 0.855 | NA |
| LOCAs | No | 0.75% of time | 0.9 | 1.0 | 0.675 | 0.675 |
| Transients | Yes | Yes | 0.9 | 1.0 | 0.900 | NA |
| ATWS | | | | | | |
| PORV Cycles @ Initiation | No | Yes | 0.9 | 1.0 | 0.900 | NA |
| S ₃ Initiator | No | No | 0.9 | 1.0 | 0.900 | NA |
| Internal Floods | Yes | Yes | NA | 1.0 | NA | NA |

Quantification of the Probabilistic Framework

Table 4.15 summarizes quantifications relevant to core damage arrest in vessel. The table entries are based on NUREG-1150, except for the last column and the last row. The IPEs are not explicit in how they treat this issue. The last column lists our recommendations, which are largely patterned after NUREG-1150. Internal floods were not treated in NUREG-1150. As noted previously, we treat internal floods in a manner consistent with transients. The NA (not applicable) entry for SNL recommendations emphasizes that there are no initiator leaks for any CDI (except for LOCAs), so there is no possibility for sufficient depressurization in time to ensure CDA.

NUREG-1150 assumes that injection occurs in time to arrest core damage only if initiator leaks depressurize the RCS. Induced leaks are not assumed to depressurize the RCS in time to arrest core damage. If high pressure injection systems (HPIS) are available, then any initiator leak is sufficient to depressurize the RCS to the point that injection can begin. CDA in these scenarios preclude DCH events and liner meltthrough events. For LPIS to be effective, an initiator leak must be sufficiently large that it would lead to low RCS pressure. CDA for these scenarios avoids high steam spike loads, in conjunction with a possible hydrogen burn, that occur when low pressure lower head failure occurs with a wet or deeply flooded cavity.

4.2 Containment Failure Tree

The containment failure tree starts with output from the HPME tree to calculate early containment failure. The top events in the containment failure tree are

- (1) Vessel breach mode and size,
- (2) Cavity water,
- (3) DCH overpressure failures,
- (4) Containment liner failures, and
- (5) Non-DCH overpressure failures.

Quantification of these containment failure related events is presented in Sections 4.2.1 to 4.2.5.

4.2.1 Vessel Breach Mode and Size

In NUREG-1150, the DCH loads at vessel breach were an explicit function of hole size, and the hole size is largely a function of the mode of vessel breach. Table 4.16 summarizes the relevant NUREG-1150 quantifications.

NUREG-1150 considered three modes of vessel failure: bottom failure, unzipping, and pour. A bottom failure is characterized by failure of one or more of the penetrations that pass through the lower head or by a small rupture of the lower head. In either case, the listed hole size is what you get after ablation of steel during melt ejection. The unzipping mode is characterized by a large rupture or large circumferential tearing of the lower head, and ablation contributes little to the final hole size. Both these modes are associated with high pressure melt ejection (HPME) from the RPV into the reactor cavity and with direct containment heating (DCH) processes coupled with RCS blowdown.

Table 4.16 NUREG-1150 quantification of vessel breach mode and size

| RCSP @ VB | Mode Q65 | Mode Prob Q65 | Hole Size | Hole Size Prob, Q65 & Q72 |
|----------------------|---------------------|--------------------------|-------------------|--|
| SSP | | | | |
| | Bottom Hole | 0.790 | small, D ~ 0.36 m | 0.711 |
| | Unzipping | 0.130 | large, D ~ 1.6 m | 0.209 |
| | Pour | 0.080 | Irrelevant | 0.080 |
| HP & IP | | | | |
| | Bottom Hole | 0.600 | small, D ~ 0.36 m | 0.540 |
| | Unzipping | 0.13 | large, D ~ 1.6 m | 0.190 |
| | Pour | 0.270 | Irrelevant | 0.270 |
| LP | | | | |
| | Irrelevant | Irrelevant | Irrelevant | Irrelevant |

Prototype experiments addressing RPV failure in a severe accident have been performed (Chu et al. 1999) since the time of NUREG-1150. These experiments show that

- (1) Local failure at an incore instrument guide tube occurs before rupture of the lower head.
- (2) For uniform or hot spot heating of the lower head, a rupture (assuming no incore instrument penetrations) is attracted to non-uniformities in temperature or vessel thickness, and the rupture size is smaller than the region that sees substantial temperatures.
- (3) Side ruptures (reduced melt ejection) or even unzipping of the lower head are possible for conditions more consistent with low RCS pressures. Since we are focused on high RCS pressure events and all ice condenser plants have lower head penetrations, we conclude that a local penetration failure (followed by ablation) is most likely for DCH relevant conditions. Such failures can be characterized by holes approximately 0.4 m equivalent diameter. This is close to the "small" hole category in NUREG-1150.

The pour mode of vessel breach is normally associated with low pressure failure of the lower head; however, NUREG-1150 also considered a pour mode associated with high pressure failure of the lower head. The scenario envisaged is that of lower head failure before the bulk of the core debris relocates in the bottom head of the vessel. The failure occurs because of a small amount of molten debris that "dribbles" to the bottom head along an instrumentation tube causing lower head failure at a penetration. The RCS then blows down through this break, but no core debris is expelled. After the blowdown, the bulk of the debris locates to the lower head and pours into the cavity. Although there could be a small driving force caused by the gas pressure in the RCS, the pour failure mode is distinguished by the fact that gravity is the primary force causing the molten core debris to leave the vessel. This high pressure pour mode greatly reduces the number of DCH events in NUREG-1150, and we have included this mechanism in our benchmark calculations.

We believe, however, that this high pressure pour mode is not phenomenologically supported. In addition, a much better understanding of DCH processes and loads has evolved since the time of NUREG-1150, with experiments and analyses suggesting that the DCH loads are not a strong function of hole size. Consequently, the CET is simplified by eliminating vessel breach mode and hole size as top events in extrapolation studies.

4.2.2 Cavity Water

In NUREG-1150, the pressure loads at vessel breach are a function of the amount of water in the cavity at vessel breach. The quantity of cavity water is classified in one of three ways:

- (1) Dry; condensate levels of water in the cavity,
- (2) Wet; intermediate between a dry cavity and a flooded cavity, and
- (3) Flooded; reactor cavity full of water.

The manway to the reactor cavity stands approximately 13 feet above the floor of the subcompartment; consequently, water cannot flow into the cavity unless significant water accumulates on the subcompartment floor. Typically, the RCS boiloff inventory plus the contents of the RWST plus approximately 50% ice melt is required to deeply flood the reactor cavity.

A deeply flooded reactor cavity will (at least partially) submerge the lower head, leading to the possibility that core melt can be retained within the lower head. NUREG-1150 and the Sequoyah/Watts-Bar IPE explicitly take no credit for this invessel retention. A recent OECD/CSNI-sponsored workshop (OECD 1998) on this issue concluded that invessel retention by exvessel cooling could not be assured for large core masses characteristic of many US pressurized water reactors (PWRs). Consequently, we take no credit in our studies for invessel retention resulting from exvessel cooling. Even if exvessel cooling does not prevent lower head failure, it is likely to delay the failure. This increases the likelihood that the hot leg, surge line, or even the upper head will fail leading to complete depressurization of the RCS before lower head failure. No credit is taken for this in the current study.

NUREG-1150 computes the amount of cavity water based on several PDS-specific conditionalities; the most important of which are the fraction of ice melted and whether the RWST is fully injected into the containment. The latter requires AC power; consequently, wet or deeply flooded cavities cannot be expected in unrecovered SBOs. These quantifications are themselves dependent on other PDS-specific parameters. We have extracted summary values of cavity water from the NUREG-1150 output files themselves (Table 4.17). Table 4.17 shows that a flooded cavity is not possible in SBOs because AC power is required for containment sprays or emergency core cooling; consequently, the RWST cannot be injected into the containment. The probabilities of a wet cavity (in NUREG-1150) follow closely the probabilities of AC recovery (Table 4.14) suggesting a partial discharge of the RWST. With AC power in the plant, a dry cavity is not likely while a deeply flooded cavity is possible when large (but not total) ice inventories are melted.

Table 4.17 Inferred NUREG-1150 quantification of cavity water at vessel breach

| | Probability | | |
|------------|-------------|------|---------|
| | Dry | Wet | Flooded |
| Slow SBO | 0.55 | 0.45 | 0.00 |
| Fast SBO | 0.86 | 0.14 | 0.00 |
| LOCA's | 0.00 | 0.24 | 0.76 |
| Transients | 0.00 | 0.11 | 0.89 |
| ATWS | 0.00 | 0.19 | 0.81 |

Our benchmark evaluations use Table 4.17 entries for all branches that lead to vessel breach. We simplify the CET even further for the extrapolation evaluations. Recovered SBOs are low probability events that are ignored here, so there is no possibility of wet or deeply flooded cavities. In any case, we note that DCH loads (see Section 4.2.3) are insensitive to cavity water; consequently, we do not consider cavity water for branches that lead to failure of the lower head with RCS pressures greater than 200 psi (1.4 MPa). CONTAIN calculations described in Section 5.0 show that the ice beds are completely melted in non-SBOs if auxiliary feedwater is not available. Because AC power is available, the RWST tank can be fully injected into the containment. Consequently, for the limiting case of no auxiliary feedwater, we expect a deeply flooded cavity because the RWST is drained into the containment and the ice is fully melted. Our recommended quantifications for the extrapolation evaluations are listed in Table 4.18.

We chose the more limiting case of no auxiliary feedwater as our base case for convenience (as described in Section 5.0) while acknowledging that many PDSs for non-SBO could have auxiliary feedwater available. If auxiliary feedwater is available, the steam load on the ice chest is reduced and the potential for significant ice at vessel breach exists. This scenario is treated as a sensitivity (case 10, Section 7.3).

Table 4.18 Recommended quantification of cavity water at vessel breach

| | Probability | | |
|-----------------|-------------|------|---------|
| | Dry | Wet | Flooded |
| Slow SBO | 1.00 | 0.00 | 0.00 |
| Fast SBO | 1.00 | 0.00 | 0.00 |
| LOCA's | 0.00 | 0.00 | 1.00 |
| Transients | 0.00 | 0.00 | 1.00 |
| ATWS | 0.00 | 0.00 | 1.00 |
| Internal Floods | 0.00 | 0.00 | 1.00 |

4.2.3 DCH Overpressure Failures

Containment loads at vessel breach are a function of the RCS pressure at vessel breach. DCH processes dominate containment loads if the RCS pressure is not low (i.e., $P > 200$ psi, 1.4 MPa) at the time of vessel breach. Contributions to DCH loads include blowdown of the RCS, direct transfer of thermal energy from dispersed melt to the containment atmosphere, oxidation of metals in the melt, combustion of DCH produced hydrogen, and combustion of hydrogen pre-existing in the containment atmosphere.

Table 4.19 summarizes DCH containment-overpressure failure probabilities as inferred from NUREG-1150 data. Containment load distributions are a function of

- (1) RCS pressure at vessel breach (Section 4.1.6),
- (2) Hole size (Section 4.2.1),
- (3) Concentration of pre-existing hydrogen in the atmosphere,
- (4) Quantity of cavity water (Section 4.2.2), and
- (5) Ice inventory (Section 5.0).
- (6) In-vessel clad oxidation – *there was little sensitivity of loads to this variable so the dependency is not included in Table 4.19.*
- (7) Core Melt Fraction – *“Medium” core fractions implemented for this study.*

In NUREG-1150, the concentration of pre-existing hydrogen in the containment atmosphere is a function of in-core zirconium oxidation, the operation of containment igniters, and the existence of random ignition sources. When AC power is available, the containment igniter system is almost always available (Q13); and if it is not available, there are significant sources of random ignition from energized equipment. Consequently, the concentration of pre-existing hydrogen in the containment is “low” (i.e., $X < 5.5\%$) when AC power is available. Igniters are not available in unrecovered SBOs, so the hydrogen concentration is considered “high” (i.e., X approximately 12%). NUREG-1150, however, concludes that there is a 15% probability of random ignition in the lower compartment that propagates throughout the containment. This would reduce the hydrogen concentration to “low” values. In our benchmark evaluations, we weighed the DCH overpressure failure probabilities in SBOs by the chance of random ignition. There is no need to do this to other CDIs because an ignition source is assured.

All entries in Table 4.19 assume sufficient ice inventory remains to significantly mitigate DCH loads. This is consistent with NUREG-1150 quantifications (Q29) for scenarios that are DCH relevant. This issue was the focus of peer review comments on draft NUREG/CR-6427 (Section D.8). Section 5.0 of this report addresses this issue of ice inventory in greater detail. We conclude that significant quantities of ice remain in SBOs and that little or no ice remains in any sequence where the ARFs are operational. These conclusions will be reflected in our extrapolation evaluations for non-SBO scenarios.

Table 4.19 NUREG-1150 quantification of DCH containment overpressure failure probability for NUREG-1150 scenarios with “medium” core fraction and ice condenser effective

| | RCS Pat VB | Hole Size | Pre-existing Hydrogen | Cavity Water | NUREG-1150 Cases (Harper et al. 1991) | DCH OP Fail. Prob |
|----|--------------|-----------|-----------------------|--------------|---------------------------------------|-------------------|
| 1 | SSP + High | Small | High | Dry | 7,8,9 | 0.184 |
| 2 | SSP + High | Large | High | Dry | 4,5,6 | 0.340 |
| 3 | SSP + High | Small | Low | Dry | 7,8,9 | 0.184 |
| 4 | SSP + High | Large | Low | Dry | 4,5,6 | 0.340 |
| 5 | SSP + High | Large | High | Wet | 1,2,3 | 0.264 |
| 6 | SSP + High | Large | Low | Wet | 1,2,3 | 0.264 |
| 7 | SSP + High | Small | High | Wet | 1,2,3 | 0.264 |
| 8 | SSP + High | Small | Low | Wet | 1,2,3 | 0.264 |
| 9 | Intermediate | Small | High | Dry | 21,22,23 | 0.164 |
| 10 | Intermediate | Large | High | Dry | 15,16,17 | 0.293 |
| 11 | Intermediate | Small | Low | Dry | 7,8,9 | 0.151 |
| 12 | Intermediate | Large | Low | Dry | 4,5,6 | 0.252 |
| 13 | Intermediate | Large | High | Wet | 10,11,12 | 0.218 |
| 14 | Intermediate | Large | Low | Wet | 1,2,3 | 0.192 |
| 15 | Intermediate | Small | High | Wet | 13 | 0.345* |
| 16 | Intermediate | Small | Low | Wet | 1,2,3 | 0.192 |

*Load distribution provided in NUREG-1150 for high core fraction only.

For our benchmark evaluations, the DCH containment-overpressure failure probabilities were computed by convoluting the distribution for maximum containment pressure (i.e., base pressure and pressure rise) following vessel breach and the containment fragility curve specific to Sequoyah, as defined in NUREG-1150 (Breeding et al. 1992). The distributions for pressure rise at vessel breach were taken from NUREG-1150 (Harper et al. 1991). The distributions selected for pressure rise correspond to best estimate or “medium” core melt masses in NUREG-1150. The resulting DCH containment-overpressure failure probabilities are summarized in Table 4.19.

Table 4.19 shows no entries for a deeply flooded cavity. It was the intent of NUREG-1150 to evaluate high pressure lower head failures with a deeply flooded cavity as equivalent to low pressure lower head failures with a deeply flooded cavity (Section 4.2.5). We have discovered an

implementation error in NUREG-1150 in that DCH loads for a flooded cavity were treated as low pressure lower head failures with a wet (not a flooded cavity). Our benchmark calculations reflect what was actually implemented in NUREG-1150.

Table 4.19 shows an insensitivity of DCH-induced containment failures to the level of pre-existing hydrogen. With vessel breach at system setpoint or high RCS pressures, NUREG-1150 experts judged that there was no sensitivity to levels of pre-existing hydrogen in the containment atmosphere. The sensitivity is small for intermediate RCS pressures. This insensitivity to hydrogen concentrations in the containment atmosphere are not consistent with best estimate DCH calculations, with the high concentrations (approximately 12%) of hydrogen in the atmosphere for unrecovered SBOs. Table 4.19 also shows a large sensitivity to RCS hole size, which is not supported by more recent experiments or analyses. Because of these apparent inconsistencies in NUREG-1150 for DCH loads, we rely on CONTAIN calculations, as documented in Section 5.0, for DCH load estimates at vessel breach.

The quantification of DCH loads for this study can be greatly simplified for the extrapolation evaluations. Tables 4.20 and 4.21 summarize our recommendations, which are only a function of the level of pre-existing hydrogen in the atmosphere. This is possible because the plants all have similar size, geometry, and cores. The base pressure and pressure rise are estimated as point values (for upper bound melt masses) from best estimate CONTAIN calculations (Section 5.0). The base pressure is higher in SBOs because containment sprays are not operational. The pressure rise at vessel breach is higher for SBOs because igniters are not available to control hydrogen concentrations prior to vessel breach. In all SBO cases, ice is available at vessel breach to potentially mitigate loads. The failure probabilities are a function of the plant only through the use of the plant-specific fragility curve (see Section 6.0).

The hole size controls dispersal for low RCS pressures. The hole size controls the coherence of dispersed melt and RCS blowdown, which in turn, limits the amount of metals in the dispersed melt that become oxidized. A larger hole means more metal oxidation; however, nominal holes approximately 0.4m in diameter typically lead to complete oxidation of any metals in the melt for the melt compositions that have been considered in DCH resolution activities (e.g., Pilch et al. 1994b).

Table 4.20 Recommended DCH loads at vessel breach based on CONTAIN analyses

| | Base P (MPa)at VB | Press Rise (MPa) at VB | Total P (MPa) at VB |
|-------------------------------|------------------------------|-----------------------------------|--------------------------------|
| SBO (High H ₂) | 0.287 | 0.533 | 0.820 |
| Non-SBO (Low H ₂) | 0.116 | 0.150 | 0.266 |

Table 4.21 Recommended DCH containment overpressure failure probabilities for extrapolation evaluations assuming a DCH event occurs

| | SBO Fraction of Core Damage | DCH OP Failure Probabilities | |
|-----------|-----------------------------|------------------------------|---------|
| | | SBO | Non-SBO |
| Catawba | 0.0103 | 1.000 | 0.000 |
| D.C. Cook | 0.0181 | 0.820 | 0.000 |
| McGuire | 0.2388 | 0.980 | 0.000 |
| Sequoyah | 0.0103 | 0.998 | 0.000 |
| Watts Bar | 0.2167 | 0.999 | 0.000 |

Limited experiments and analyses have shown that DCH loads with significant quantities of cavity water are comparable to dry cavity DCH loads; however, the nature of the containment pressurization is better characterized as a saturated steam spike rather than superheating of the containment atmosphere, which is the traditional perspective of DCH loads. In an ice condenser plant, we believe that dry-cavity DCH loads will bound wet/flooded DCH loads because the pressure suppression system (assuming ice inventory remains) was designed to accommodate sudden large releases of steam. Consequently, we focus on the bounding DCH loads associated with dry reactor cavity as encompassing the wet cavity case as well.

Best estimate SCDAP/RELAP5 calculations have been performed for the Zion plant, which is a four-loop Westinghouse plant, typical of the ice condenser plants as well. Steam sources from a 250 gpm/pump seal leak (NUREG-1150 best estimate based on various combinations of stage failures) were sourced into a CONTAIN code containment model of the Sequoyah plant. The CONTAIN code has been validated against Waltz Mill data for DBA analyses in ice condenser plants.

The resulting containment loads prior to vessel breach and as a consequence of the DCH event are summarized in Table 4.20. The DCH loads were computed using the upper limit of the melt distribution (87.5 mt) used in prior DCH resolution studies. Hydrogen released to the containment prior to vessel breach corresponds to 49% oxidation of clad.

The containment failure probabilities listed in Table 4.21 were based on these loads and the plant-specific fragility curves discussed in Section 6.0. Containment failure probabilities based on current generation codes are significantly higher than NUREG-1150 quantifications for SBOs. This results from a more consistent treatment of hydrogen combustion during a DCH event and the higher base pressure. Containment failure probabilities are generally lower for non-SBOs because the sprays are effective at mitigating loads even when ice is completely melted and because the plant-specific fragility curves generally imply a stronger containment relative to Sequoyah/NUREG-1150.

Quantification of the Probabilistic Framework

We note from Table 4.21 that no plant is inherently robust to all credible DCH events in a SBO accident. McGuire and Watts Bar have relatively high SBO frequencies so we anticipate that DCH events will contribute to a higher early containment failure probability in these plants. Dry-cavity DCH loads for non-SBOs are not containment threatening because of the mitigation derived from containment sprays (as discussed in Section 5.0).

The Sequoyah and Watts Bar IPEs used DCH loads from NUREG-1150 in conjunction with their own fragility curves; consequently, the containment failure probabilities are less than those listed in Table 4.21. The Catawba and McGuire IPE judged it "likely" that the ice condenser can handle the DCH pressure spike. The Catawba and McGuire IPEs assigned a probability of 10% to DCH overpressure failures; however, this failure probability is conditional on the probability of sufficient fragmentation for DCH ($P = 0.5$) and the probability that debris is transported to the upper dome ($P = 0.1$). We believe that these additional conditionalities are phenomenologically unsupported.

4.2.4 Containment Liner Failure

The ejection of molten corium under high pressure from the vessel at breach may lead to a containment failure involving direct thermal attack of the containment liner in the in-core instrumentation room, where the seal table is located. This failure mode is described in detail in Tarbell et al. 1986. One of the ways for dispersed debris to exit the reactor cavity is directly through the personnel access to the instrumentation tunnel. Another exit from the cavity is deemed possible if the seal table fails. The seal table is the plate at which the instrumentation tubes terminate. In this scenario, seal table failure is assumed to occur by a combination of thermal attack and mechanical loads. Debris is then inertially driven to enter the instrumentation room and accumulates on the floor. If a substantial amount of debris piles up against the wall, the debris may melt through the 1.5 in.-thick steel containment wall.

Table 4.22 summarizes the NUREG-1150, IPE, and SNL-recommended quantifications for this issue. NUREG-1150 (Q78) quantified the probability of liner failure as a function of melt mass dispersed into the incore instrument room (ICIR). The mean values of the distribution are reproduced here as Figure 4.13. The melt mass dispersed into the ICIR is the product of the core mass, core fraction molten and ejected from the RCS ($f_{BE} = 0.30$, Q66), and the fraction of dispersed mass carried into the ICIR (Q68). The latter is a weak function of RCS pressure at vessel breach for DCH relevant RCS pressures:

| | |
|---------------------------|--------------------|
| SSP, High RCS Pressure | $f_{ICIR} = 0.417$ |
| Intermediate RCS Pressure | $f_{ICIR} = 0.325$ |
| Low RCS Pressure | $f_{ICIR} = 0.000$ |

The Sequoyah and Watts Bar IPEs appear to have adopted the same logic and quantifications as NUREG-1150; however, their liner failure probabilities are somewhat higher than those that we computed with NUREG-1150 quantifications. These differences have not been resolved. The Catawba and McGuire IPE adopted a different logic structure and quantifications. The overall liner failure probability was assumed independent of core mass and

Table 4.22 Quantification of liner melt through given a HPME event for different vessel pressures and a non-flooded cavity

| | Probability of Liner Melt through | | | |
|---------------------|-----------------------------------|-------|--------------|-------|
| | SSP | High | Intermediate | Low |
| NUREG-1150 | 0.240 | 0.240 | 0.170 | 0.000 |
| Sequoyah, Watts Bar | 0.332 | 0.332 | 0.243 | 0.000 |
| Catawba, McGuire | 0.066 | 0.066 | 0.066 | – |
| D.C. Cook | – | – | – | – |
| SNL Recommendation | 0.240 | 0.240 | 0.240 | 0.000 |

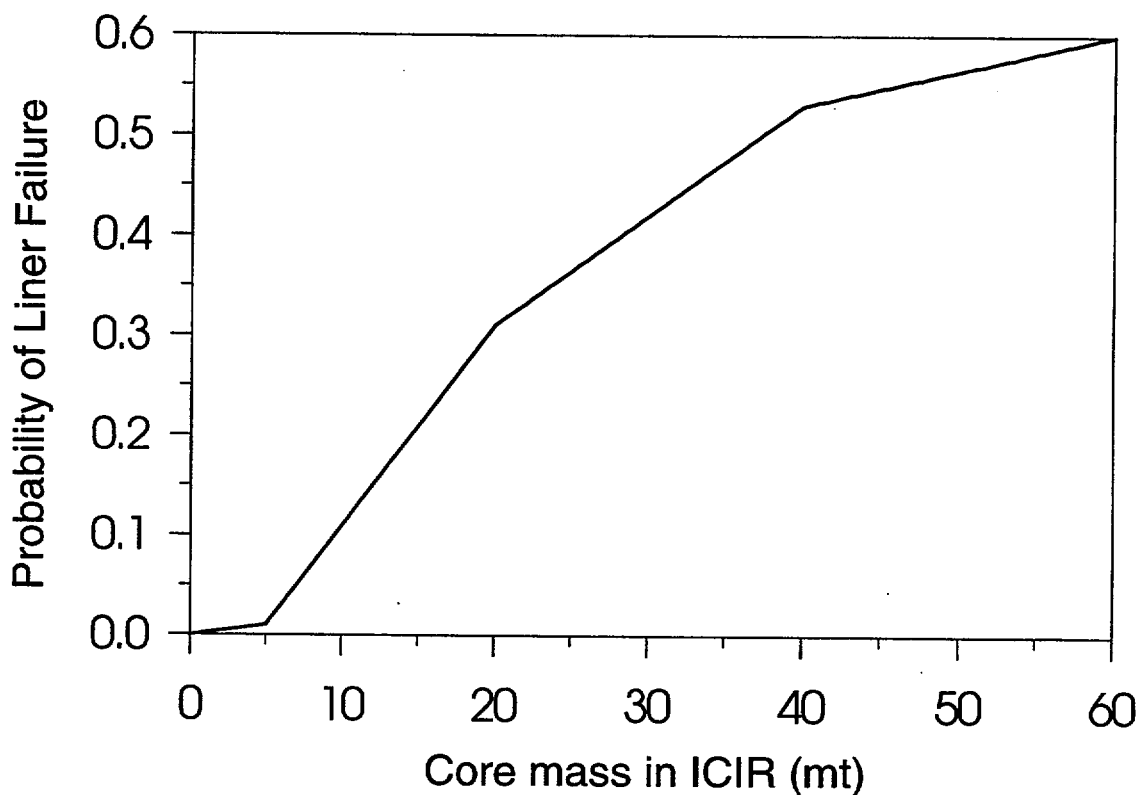


Figure 4.13 NUREG-1150 quantification of probability of liner failure as a function of melt mass dispersed into the ICIR

Quantification of the Probabilistic Framework

RCS pressure at vessel breach; however, unjustified credit was taken for mitigative features of the cavity and obstructions that limit the possibility that debris accumulates against the containment liner.

For benchmark evaluations, we use the NUREG-1150 quantifications for the best estimate core fraction melted and ejected into the reactor cavity. The CET was simplified previously (Section 4.1.6) by considering only two pressure ranges for extrapolation evaluations: DCH relevant RCS pressure at vessel breach and low pressures at vessel breach. For the simplified CET, we conservatively recommend using NUREG-1150 liner meltthrough probabilities associated with SSP and high RCS pressures. NUREG-1150 also assumed that there would be no liner failure if the cavity was deeply flooded or if there was an exvessel steam explosion. We adopted this logic for the current study.

4.2.5 Non-DCH Overpressure Failure at Vessel Breach

Non-DCH pressure loads on the containment can occur in two scenarios:

- (1) The lower head does not fail, but there is a hydrogen combustion event, and
- (2) The lower head fails and melt "pours" into the reactor cavity creating a steam spike followed by a hydrogen combustion event if the sequence is a SBO where power is recovered after vessel breach.

NUREG-1150 treats early hydrogen combustion through a series of top events. By early combustion, we refer to a hydrogen combustion event that occurs after UTAF but prior to vessel breach if it were to occur. These top events quantify the clad fraction oxidized, the hydrogen and steam concentrations throughout containment, the probability of random ignitions (SBOs only) throughout the containment, and combustion completeness if ignition occurs. This complex logic quantifies the containment pressure caused by hydrogen combustion if the lower head does not fail and the hydrogen concentration in the containment at the time of vessel breach if the lower head does fail. The Sequoyah and Watts Bar IPEs appear to adopt a similar logic structure and similar quantifications. The Catawba and McGuire PIEs address similar top events in the context of a simpler binary logic structure.

The NUREG-1150 logic structure and quantifications have been simplified for our CET. Table 4.23 summarizes quantifications used in our benchmark evaluations. For hydrogen combustion events prior to vessel breach, we use as a surrogate for the NUREG-1150 logic. We use the NUREG-1150 dry-cavity quantifications for containment loads at vessel breach and low RCS pressures. These loads are dominated by hydrogen combustion and are tabulated for high and low levels of pre-existing hydrogen in the containment. As noted in Section 4.2.3, high levels of pre-existing hydrogen are exclusively assigned to SBO events because igniters are unavailable.

In the case of lower head failure with the pour mode of melt relocation to the cavity, the hydrogen combustion event is coupled with a steam spike. Table 4.23 shows that loads are maximized for a wet cavity in the NUREG-1150 study. Note also that hydrogen combustion is

suppressed for a deeply flooded cavity; in which case, the loads come entirely from a steam spike.

Table 4.24 shows SNL-recommended containment overpressure failure probabilities for non-DCH events. These quantifications are intended to be used in the extrapolation evaluations. Quantification of containment loads is derived from CONTAIN calculations (Section 5.5), while the containment failure probability is based on the plant specific fragility curve. We note that a steam spike is not possible in SBO because the cavity is always dry and significant quantities of ice remain at vessel breach. Two evaluations for the steam spike are listed for non-SBOs; one assuming sprays are operational and the other assuming that sprays are non-operational if there is a failure to switch to recirculation mode. Base case extrapolation evaluations will be performed with a steam spike pressure rise scaled to the expected (i.e., BE = best estimate) value of melt mass.

The assumption of steam spike loads in our base case assessments follows from the assumptions of no auxiliary feedwater and the complete melting of the ice inventory before vessel breach. As a sensitivity (case 10, Section 7.3), we will explore the implications of PDS in non-SBO where the ice inventory is not completely depleted. We note, however, that it takes only 50% ice melt in a non-SBO to deeply flood the cavity; consequently, it is likely that the cavity is deeply flooded and still have significant quantities of ice remaining. Any sensitivity to upper bound steam spikes will be eliminated when significant ice remains.

D.C. Cook is unique among ice condenser plants in that it has lower compartment sprays in addition to upper compartment sprays common to all ice condenser plants. Our limited calculations were performed assuming that only upper compartment sprays are available. We anticipate that plant-specific calculations for D.C. Cook, which also take credit for lower compartment sprays, would predict loads for D.C. Cook that are even lower than those listed in Table 4.24.

We note that no ice condenser plant is inherently robust to all credible hydrogen combustion events in an SBO accident. McGuire and Watts Bar have relatively high SBO frequencies so we anticipate that hydrogen combustion overpressure failures will contribute to a higher early containment failure probability for these plants.

Table 4.23 NUREG-1150-like quantification of containment over pressure failure probabilities for non-DCH events

| Cavity Water | Base Pressure (MPa) | SBO, High H ₂ | | | Other CDIs, Low H ₂ | | |
|--------------|---------------------|--------------------------|---------------------|--------------|--------------------------------|---------------------|--------------|
| | | NUREG-1150 Case | Pressure Rise (MPa) | OP Fail Prob | NUREG-1150 Case | Pressure Rise (MPa) | OP Fail Prob |
| Flooded | 0.145 | 1 | 0.248 | 0.123 | 1 | 0.248 | 0.123 |
| Wet | 0.145 | 4 | 0.325 | 0.264 | 3 | 0.135 | 0.025 |
| Dry | 0.145 | 6 | 0.215 | 0.056 | 5 | 0.223 | 0.000 |

Table 4.24 SNL recommended containment overpressure failure probabilities for non-DCH event

| SBO Frac of CD | | | Catawba | D.C. Cook | McGuire | Sequoyah | Watts Bar |
|-----------------------------|---------------------|--------------------|---------------------------------|-----------|---------|----------|-----------|
| | | | 0.0103 | 0.0181 | 0.2388 | 0.0310 | 0.2167 |
| | Base Pressure (MPa) | Max Pressure (MPa) | Containment Failure Probability | | | | |
| SBO | | | | | | | |
| H ₂ Burn | 0.287 | 0.644 | 0.286 | 0.935 | 0.551 | 0.972 | 0.222 |
| Steam Spike | 0.287 | 0.287 | 0.000 | 0.000 | 0.000 | 0.000 | 0.000 |
| Non-SBO | | | | | | | |
| H ₂ Burn | 0.116 | 0.116 | 0.000 | 0.000 | 0.000 | 0.000 | 0.000 |
| Steam Spike ¹ BE | 0.116 | 0.266 | 0.000 | 0.000 | 0.000 | 0.000 | 0.000 |
| Steam Spike ² BE | 0.231 | 0.403 | 0.000 | 0.084 | 0.000 | 0.000 | 0.000 |

¹ Spray operational

² Fail to switch to recirculation mode, spray inoperable after 36 minutes

5.0 CONTAIN CALCULATIONS IN SUPPORT OF CONTAINMENT LOADS AT VESSEL BREACH AND ICE INVENTORY

5.1 Introduction

The probabilistic framework defined in Section 4.0 requires, for completion, the quantifications of DCH loads, non-DCH related hydrogen combustion loads, and non-DCH related steam spike loads. The loads must be specified for two dominant scenarios: station blackouts and non-station blackouts. SBOs are characterized by high hydrogen concentrations, significant ice inventory remaining, and no active containment cooling (i.e., sprays). Non-SBOs are characterized by low hydrogen concentrations, potentially a more limited ice inventory, and containment sprays in the base case. Previous discussions noted that with auxiliary feedwater available, significant ice could remain at vessel breach and the cavity could still be flooded. Various deviations from the base case will also be quantified here.

Peer reviewers criticized the original draft of this report because DCH loads calculations were performed using the TCE model under the assumption of no ice and no sprays for all scenarios. Peer reviewers recommended

- (1) Validation of CONTAIN's ice condenser models if CONTAIN is to be used in the load calculations, and
- (2) Model the ice condenser explicitly in the loads calculations.

The peer reviewers were explicit in their belief that significant ice would be present at vessel breach in all credible scenarios.

This section addresses these peer review comments in two ways. First, containment loads calculations were performed with the CONTAIN code so that appropriate credit can be taken for the ice condenser and containment sprays. Since the time of the draft report, the CONTAIN code has been benchmarked against Waltz Mill data for ice condenser performance (WEC 1974). The CONTAIN code had also been validated previously for hydrogen combustion and steam spike events. The CONTAIN code has also been benchmarked against the existing DCH database for large dry containments, and key code parameters were selected in a manner consistent with other DCH resolution activities.

Secondly, this section will address peer reviewer comments that significant ice will remain at vessel breach in all credible scenarios. NUREG-1150 quantifications and other available code calculations were reviewed. An expanded set of CONTAIN calculations were performed with steam sources taken from SCDAP/RELAP5 (SBO sequence) to better define the scenarios when ice would or would not be present at vessel breach. A simple hand calculation was used to lend credibility to code calculations that the ice inventory will be depleted before vessel breach in non-SBOs when auxiliary feedwater is not available. Lastly, the modeling capabilities of core melt progression have changed significantly since the time of NUREG-1150. These differences are reviewed with regard to its potential impact on quantifying the ice inventory at vessel breach.

5.2 CONTAIN Code

5.2.1 Capabilities of the CONTAIN Code

The simultaneous interactions among numerous phenomena that would occur during a reactor accident involving DCH are highly complex and difficult to account for without sophisticated computational simulation tools. The CONTAIN code was developed to model these complex interactions so that an understanding of the controlling phenomena and the dominant uncertainties could be obtained (Murata et al. 1997). Phenomena treated in the code include the following:

- flow of steam/non-condensable gas mixtures via multiple paths through the containment;
- condensation of steam on ice surfaces and subsequent ice melting and drainage;
- opening and closing of the three levels of doors in the ice condenser system;
- ejection of debris, steam, and water into the reactor cavity at the time of vessel breach;
- trapping of debris on solid surfaces in the lower containment and (possibly) re-entrainment;
- entrainment of water in the reactor cavity into the debris ejected from the cavity;
- chemical interactions between the molten debris and steam or oxygen while the debris is suspended in the steam-air mixture;
- radiation and convective heat transfer among the debris, atmosphere and structural heat sinks;
- hydrogen combustion induced by igniters and/or contact with ejected debris;
- effects of containment sprays and air return fans.

For thermal-hydraulic phenomena in ice condenser systems, version 2.0 of CONTAIN was previously assessed against PNL data (Russell and Williams 1990) for ice condenser performance. More recently, CONTAIN was assessed against tests performed by Westinghouse at the Waltz Mill test facility (Tills et al. to be published). These full-height tests were designed to demonstrate the effectiveness of ice condenser systems in dealing with design basis accidents (DBAs) and involve the thermal-hydraulic interactions between steam-air mixtures and the ice condenser system. The ice condenser benchmark analyses (Tills et al. to be published) are in the final stages of review by the NRC as part of a broader effort to formally qualify and document the CONTAIN code for DBA analyses.

Despite this extensive effort to validate CONTAIN 2.0 for ice condenser DCH analysis, the existing experimental data base is far from sufficient for establishing a true predictive capability for CONTAIN or any other code. No integral DCH experiments in ice condenser geometry are available to validate code predictions of DCH phenomena in ice condenser plants. The range of phenomena involved is diverse; interactions among them are strong and non-linear; the parameter space of possible initial and boundary conditions is very large. While the current understanding of DCH phenomenology has been advanced significantly by the NRC's codes and experiments and corresponding nuclear industry efforts, it is essential to acknowledge the significant residual uncertainty concerning DCH phenomenology. Computational studies must be

guided and interpreted in the light of expert judgement and realistic appreciation of phenomenological uncertainties.

More traditional applications of CONTAIN are predictions of containment response to steam sources and non-DCH related combustion of hydrogen (deflagrations not detonations) in containment. Murata et al. (1997) lists the extensive validation base for these processes, which include ISP-16 for the HDR steam source tests and the NTS large scale hydrogen combustion tests as examples. Given the importance of hydrogen combustion in ice condenser plants, we note that the correlations for flame speed and combustion completeness are largely derived from the large-scale NTS tests, which were conducted for the full range of hydrogen and steam concentrations that are relevant to deflagrations in the accident scenarios considered here.

CONTAIN's modeling of DCH phenomenology has been extensively assessed with respect to NRC-sponsored DCH tests at Sandia and elsewhere (Williams et al. 1995a, 1995b; Boyack 1995). The existing database, however, is restricted to plants with large dry or subatmospheric containments. There is no database to assess the performance of the ice chest for DCH events; consequently, some extrapolation of CONTAIN models outside its validation base is required for this study. We believe that this validation is justified given the CONTAIN's validation for related phenomena and related geometries. The phenomena encompassed by these tests included interactions of the ejected debris with water in the reactor cavity (but not deeply flooded cases), the containment atmosphere, and solid structures, but not any interactions involving ice.

5.2.2 Overview of Calculations

A simplified probabilistic methodology modeled on the more detailed NUREG-1150 approach is adopted in Section 4.0 of this report. The CONTAIN calculational study presented here is intended to support the probabilistic analysis with detailed, mechanistic calculations that can shed light on the controlling phenomena influencing critical elements of the probabilistic analysis. Only a limited number of calculations could be carried out within the scope of this project, so it was important that the accident sequences studied are carefully selected.

The CONTAIN calculations address a small number of accident scenarios and each scenario is in turn studied with a number of sensitivity calculations. Most of the calculations were performed with version 1.2 of the CONTAIN code. These were the calculations in the draft report that was reviewed by the peer review committee in 1997. These earlier calculations are fully documented without change in Appendix B of this report. Following peer review feedback, a new series of calculations was undertaken with CONTAIN 2.0. These calculations had the benefit of validation against the Waltz Mill tests, as well as some improvements in modeling compared to the older CONTAIN 1.2 code. Table 5.1 lists the scenarios addressed in the two series of calculations: the 1.2 Series are the calculations carried out with CONTAIN 1.2 as reported in Appendix B; the 2.0 Series is a smaller set performed with CONTAIN 2.0 and reported in this chapter.

The various scenarios listed in Table 5.1 for the CONTAIN 1.2 series of calculations are distinguished by bifurcations in core melt progression and conditions in the containment as

Table 5.1 DCH-relevant scenarios for CONTAIN calculations

| | Scenario | Pressure at Vessel Breach | Igniters | Air Return Fans | Sprays | Comments |
|------------|----------|---------------------------|----------|-----------------|--------|--------------------------------|
| 1.2 Series | V | 16 MPa | On | Off | Off | Low H ₂ /High steam |
| | V-a | 16 MPa | On | On | Off | Low H ₂ /Low steam |
| | V-b | 16 MPa | Off | On | Off | High H ₂ /Low steam |
| | VI | 8 MPa | On | Off | Off | Low H ₂ /High steam |
| | VI-a | 8MPa | On | On | Off | Low H ₂ /Low steam |
| | VI-b | 8MPa | Off | On | Off | High H ₂ /Low steam |
| 2.0 Series | VI-c | 8 MPa | On | On | On | Non-SBO/Low H ₂ |
| | VI-d | 8 MPa | Off | Off | Off | SBO/High H ₂ |

discussed more fully in Section D.3. These scenarios were defined for the purpose of enveloping RCS pressure, melt mass and composition, and steam/hydrogen concentrations in the containment without regard to the probabilistic significance (or likelihood) of any individual scenario. Performing load/strength evaluations for these enveloping scenarios (with an assumption of no ice) did not lead to closure of the DCH issue.

Responding to peer reviewer comments, an expanded framework was developed in Section 4.0 that defines scenarios more in terms of their probabilistic significance rather than their bounding characteristics. The two scenarios listed in Table 5.1 for the CONTAIN 2.0 series of calculations are more representative of credible DCH-relevant states.

Steam and gas sources from the primary system are needed for the CONTAIN calculations to establish initial conditions in the containment at the time of vessel failure. Detailed in-vessel calculations that were specific to an ice condenser PWR were not available for this purpose, but we did have some calculations from SCDAP/RELAP5 for a SBO in the Zion plant, which has a similar NSSS configuration (Knudson, 1993). Some scaling of these sources was necessary; however, because of differences between Zion and typical ice condenser plants. Details are provided in Appendix B.

The 2.0 Series involved many fewer calculations than the 1.2 Series, and the scenarios studied were slightly different. No fully pressurized cases (Scenario V) were considered. This was for two reasons:

- (1) The earlier results indicated that DCH loads from the intermediate pressure cases were about the same as for the high pressure cases; and
- (2) The likelihood of operator actions resulting in the conditions postulated for the high pressure scenarios was judged to be relatively low.

For the Scenario VI-c runs, there was one difference between the 2.0 Series and the earlier work: this was the inclusion of containment sprays in the upper containment. These were added because it was judged unlikely that the air return fans and the igniters would both be available but the containment sprays would not be available.

A new scenario in the 2.0 Series is the intermediate pressure case with no available engineered safety features, identified as VI-d. This is an important scenario because it represents the fully unrecovered station blackout. The emphasis will be on the CONTAIN 2.0 calculations in the detailed discussions to follow in the next section. However, general insights from the 1.2 Series will also be identified as needed.

5.2.3 CONTAIN Options and Model Parameters

Only a relatively few CONTAIN calculations will be discussed in the main body of this report (many more are discussed in Appendix B). In this section, the key assumptions about code parameters, modeling options, and initial conditions for the CONTAIN calculations will be described.

Containment Nodalization. For the containment nodalization, we built upon a 6-cell CONTAIN plant deck that was developed for the study performed by Williams and Gregory (1990). It is based on the Sequoyah nuclear power plant (see Figure 3.1). A block diagram of the current 9-cell nodalization is shown in Figure 5.1. Some modifications to the earlier deck were made to reflect improvements to the CONTAIN code and to allow better understanding of some heat transfer issues. Williams and Gregory (1990) found that the DCH loads calculated using 6-cell and 26-cell representations did not differ very significantly, and thus their results support the use of the 9-cell representation in the present work. Their results also indicated that the more detailed representation would be needed if it were desired to expand the scope of the ice condenser DCH analyses to include issues involving uneven melting of ice and gas distribution issues, including existence of detonable gas mixtures in parts of the containment. Consideration of these questions is outside the scope of the present study. Again, Appendix B provides details.

Modeling of the Shield Building. The Sequoyah containment is a free-standing steel shell which is surrounded by a concrete shield building; there is a substantial gap (approximately 1.5 m) between the shield building and the shell. In the earlier work, the shield building was not modeled. However, more recent studies of passively-cooled containments with a similar configuration have indicated that radiative heat transfer from the shell to the shield building can be important. Although this heat transfer is much too slow to affect the DCH response directly, it was thought that it could affect the containment initial conditions for DCH. Modeling of the shield building was therefore included.

In order to model the shield building, a cell (Cell 8) was added to the deck to represent the annular gap. Steel structures representing the outer surface of the shell were provided as were concrete structures representing the shield building. The steel structures were connected to the corresponding structures representing the shell in the various interior cells, in order to model thermal conduction through the shell. The radiative energy transfer between the shell and the

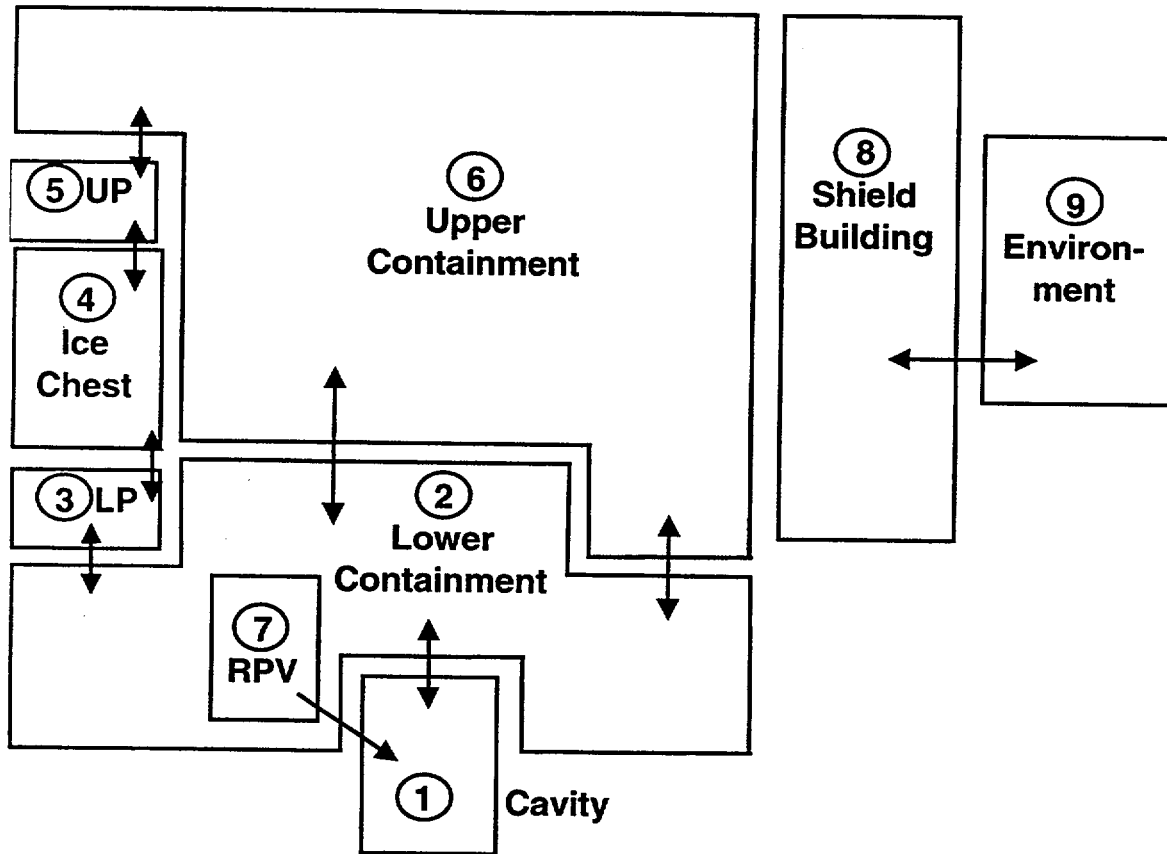


Figure 5.1 CONTAIN nodalization of the Sequoyah containment (UP and LP are the upper and lower plena)

shield building was modeled using the CONTAIN net enclosure model. The cell representing the shield building annulus was connected by a 0.1 m^2 flow path to a very large "environment" cell in order to permit pressure equalization with the environment.

Containment Volume. Based upon information from the Sequoyah individual plant examination (IPE), the free volume of the containment interior was taken to be $3.37 \times 10^4 \text{ m}^3$. The volumes of the various cells in the CONTAIN representation are summarized in Table B.1.

Initial Atmosphere. At the time of reactor shutdown ($t=0 \text{ s}$ in the calculations), the containment pressure was assumed to be 0.1 Mpa . The atmosphere temperature was taken to be 311 K , except for the ice condenser volumes, which were at 273.5 K .

Bypass Paths. The design intent of the containment is to force flow between the lower compartment and the dome to pass through the ice condenser. However, a limited amount of direct flow between the lower containment and the upper containment is possible. When the total flow rates are large (which includes flows during DCH), the great majority of the flow does pass through the ice condenser. However, when flow rate are low, and the ice condenser doors therefore closed, much of what flow does exist may pass to the upper containment via the paths

that bypass the ice condenser. As described in Williams and Gregory 1990, this bypass flow can have a considerable effect on conditions at vessel breach if the air return fans (ARFs) are not operating. Containment pressures and dome steam concentrations are increased by the bypass flow. If the ARFs are operating, the bypass flow is too small relative to the flow forced by the fans to have a significant effect.

Two sources of bypass are modeled. One bypass flow path is the refueling drains, modeled as a flow path from Cell 2 to Cell 6 at an elevation of 6.47 m. The other is defined in the FSAR as unspecified deck leakage with an effective flow area $\leq 0.29 \text{ m}^2$. A value of 0.29 m^2 is used here. Since the FSAR value is an upper bound, actual leakage could be substantially smaller. A sensitivity calculation was therefore performed with an effective deck leakage flow area of 0.029 m^2 .

Because the refueling drains are located at a relatively low elevation in the lower compartment, they are expected to flood when the volume of water exceeds about 750 m^3 , which happens well before vessel breach in the calculations. Flooding terminates the contributions of this flow path to the bypass flow. This flooding could not be directly modeled in the older versions of CONTAIN; however, it was modeled in the present calculations using the new pool tracking capabilities of CONTAIN 2.0.

Air Return Fans. In ice condenser plants, air return fans are provided which return air from the dome to the lower compartment, forcing enhanced flow through the ice condenser. This promotes containment mixing and helps to prevent detonable hydrogen concentrations from developing in the ice condenser volumes. It also accelerates steam and energy transport to the ice condenser and therefore enhances ice melt. In Sequoyah, the fans boot automatically when the containment pressure rises to 3 psig (Gregory et al. 1990); however, the fans are not always available in some core melt accidents of potential interest for DCH. The ARFs were modeled by defining a flow path between Cells 2 and 6 with a user specified flow rate from Cell 6 to Cell 2 of $54.7 \text{ M}^3/\text{s}$. This flow rate corresponds to full operation of both trains of fans operating.

Igniters. The Sequoyah plant is equipped with igniters for intentional ignition of hydrogen in the lower compartment, the upper plenum, and the dome; there are no igniters in the cavity, lower plenum, or ice condenser. In CONTAIN, availability of igniters was modeled by allowing ignition whenever the gas composition was within the flammable range. CONTAIN default flammability limits were used except for the minimum combustible mole fraction for ignition, which was set to 5.5 mole percent (m/o). This value is the same as what was assumed in the NUREG-1150 (NRC 1990) analyses of the Sequoyah plant (Gregory et al. 1990). In cells that contained no igniters, ignition was prevented by setting the ignition criteria to impossible values. Burns initiating in cells with igniters could still propagate into the cells without igniters, however. (In CONTAIN, criteria for propagation are specified independently of the ignition criteria, and the propagation criteria were left at default values.) For calculations in which it was assumed that igniters do not operate, all hydrogen combustion prior to vessel breach was suppressed.

Ice Condenser. The initial height of the ice column was taken to be 14.53 m, the initial ice mass was $1.11 \times 10^6 \text{ kg}$, and the effective surface area available for heat transfer was $2.48 \times 10^4 \text{ m}^2$.

CONTAIN Calculations

As ice melts, these three quantities are decreased proportionately in the CONTAIN model. In some sensitivity studies, it was desired to run the DCH calculation with amounts of ice that differed from the amounts CONTAIN calculated to remain at the time of vessel breach. This was accomplished by restarting the calculation at vessel breach with the desired quantities of ice specified. The ice condenser is modeled as Cell 4 in Figure 5.1. The potential for countercurrent natural circulation in the ice chest was not modeled.

Ice Condenser Doors. There are three sets of doors that open in response to a forward pressure. The first set is between the lower compartment and the lower plenum (between Cells 2 and 3); it is hinged to open with a minimal forward pressure. Unless the hinges are damaged, they can fully reclose, although a slight back pressure is required for full closure. The hinges are crushable and can deform if the doors are opened with sufficient violence, in which case they will not reclose. It has not been assessed whether this should be expected to occur in a DCH event. In the present study, the doors have been assumed to reclose in the absence of a continuing forward pressure.

There are also doors between the ice condenser and the upper plenum (between Cells 4 and 5), and between the upper plenum and the upper containment (between Cells 5 and 6). These require a larger forward pressure to open them and, if fully opened, they will only partially reclose.

In CONTAIN, all three sets of doors were modeled using flow paths in which the flow area is a function of the forward pressure differential. The lower plenum doors were assumed to be fully reversible. The partially irreversible behavior of the other two sets of doors was modeled. Table 5.2 quantifies the behavior of ice condenser doors in the CONTAIN model.

Containment Sprays. Ice condenser plants have two redundant sprays systems in the upper dome. It was assumed here that only one of the two systems was operational. For Sequoyah and our analyses, the spray system was assumed to operate at 4750 gpm. RHR sprays were not modeled. Sprays were modeled in Cell 6 in Figure 5.1.

Table 5.2 CONTAIN representation of the ice condenser doors

| Door | | Flow Area (m ²) | | ΔP Range Over Which Doors Open (Pa) | | | | |
|----------------------------|------------|-----------------------------|-------|-------------------------------------|--------|-------|-------|---------|
| | | Min. | Max. | Min. | Max. | | | |
| Intermed. Deck | Reversible | 1.86 | 70.24 | 263. | 28498. | | | |
| | Irrev. | 0.0 | 22.79 | 28498. | 37910. | | | |
| Upper Plenum | Reversible | 1.86 | 93.9 | 263. | 4441. | | | |
| | Irrev. | 0.0 | 92.08 | 4441. | 8619. | | | |
| Lower Plenum Doors: | | | | | | | | |
| ΔP (Pa) | ≤ -14.0 | 0.0 | 4.788 | 9.576 | 19.15 | 28.73 | 38.30 | ≥ 46.92 |
| Area (m ²) | 0.00403 | 2.0 | 2.60 | 3.75 | 6.23 | 20.24 | 44.6 | 78.0 |

We note that D.C. Cook is unique in that a redundant set of lower compartment sprays are also available. All calculations performed here do not model the lower compartment sprays. The implications for D.C. Cook are that the lower compartment sprays will reduce the steam load on the ice chest and mitigate loads (especially steam spike loads) relative to other ice condenser plants.

Ice Condenser Modeling. The principal value of assessing CONTAIN against the Waltz Mill experiments performed by Westinghouse was to validate the code's ability to predict flows, pressures, temperatures, and rate of ice melting under DBA conditions. The comparison also was intended to provide guidance to users on good choices for key adjustable parameters. There were two such key parameters. The first is the "heat transfer multiplier," which is the factor multiplying the condensation rate onto the ice surface compared to the condensation rate onto a flat plate with the same nominal geometric area. This multiplier was set to a default value of 5.0 in the standard release of CONTAIN 2.0. It is needed because flow in the region of the ice/steam surface is tortuous and usually turbulent, and the actual ice surface is highly convoluted and porous. The second key parameter is the thickness of the liquid film surface that forms on the ice during condensation. This film limits the total heat transfer coefficient from the atmosphere to the ice when the atmosphere is nearly pure steam.

Two time scales were investigated in the Waltz Mill tests. In the short-term analyses (corresponding to a large break LOCA), figures of merit were lower compartment pressure and exit temperature of the melted ice. For the long-term analyses, the quantities of interest were upper containment pressure and temperature, and time at which ice was completely melted. Parameter regimes for both time scales were developed from the Waltz Mill CONTAIN studies, but it is the long-term results that are most important for the current study. Table 5.3 provides the recommended values. Note that the long-term recommendations are the same as the original default values. Most of the calculations in the 1.2 Series used these defaults; thus, the 1.2 Series and the 2.0 Series are expected to be quite comparable.

An important difference between the 2.0 Series and the 1.2 Series involves a change in DCH modeling capabilities in the new code. In the 1.2 Series, the atmosphere emissivity was artificially set to a high value (0.8) to reflect the enhancement of emissivity due to aerosols created during the DCH event itself. Unfortunately, this quantity is fixed throughout a CONTAIN 1.2 calculation, so that radiation heat transfer between gases and solid surfaces was overestimated during the period before vessel breach. In the CONTAIN 2.0 code, the option exists to force an increase in gas emissivity only during the DCH event. The result was slightly higher temperatures during the part of the accident before the DCH event and comparable

Table 5.3 Recommended parameters from long-term Waltz Mill analyses

| Parameter | Value |
|-------------------------------|----------------------|
| Heat/Mass transfer multiplier | 5.0 |
| Liquid Film Thickness (m) | 5.0×10^{-5} |

CONTAIN Calculations

pressures and temperatures during the DCH event. Consequently, upgrading from CONTAIN 2.0 did not significantly change predicted containment conditions before or during the DCH event (see Figure 5.2).

Other parameters characterizing the ice condenser were taken from the Sequoyah IPE. This included the ice mass, height, and initial temperature. The default value of the exit temperature of the melted ice (350 K) was used, though this parameter generally has little impact because the code will not allow the melt temperature to exceed the ice compartment atmosphere temperature or be lower than its dewpoint. The draining of melted ice into the lower compartment could condense additional steam before this steam reaches the ice beds. This was not modeled in the current calculations because the efficiency of the process is dependent on the degree to which the water is "spray" into the lower compartment.

DCH Modeling. Because of the high uncertainty associated with DCH processes, the CONTAIN code has many adjustable parameters and user options that must be set for each calculation. A great deal of effort has been made to utilize available experimental data to develop a

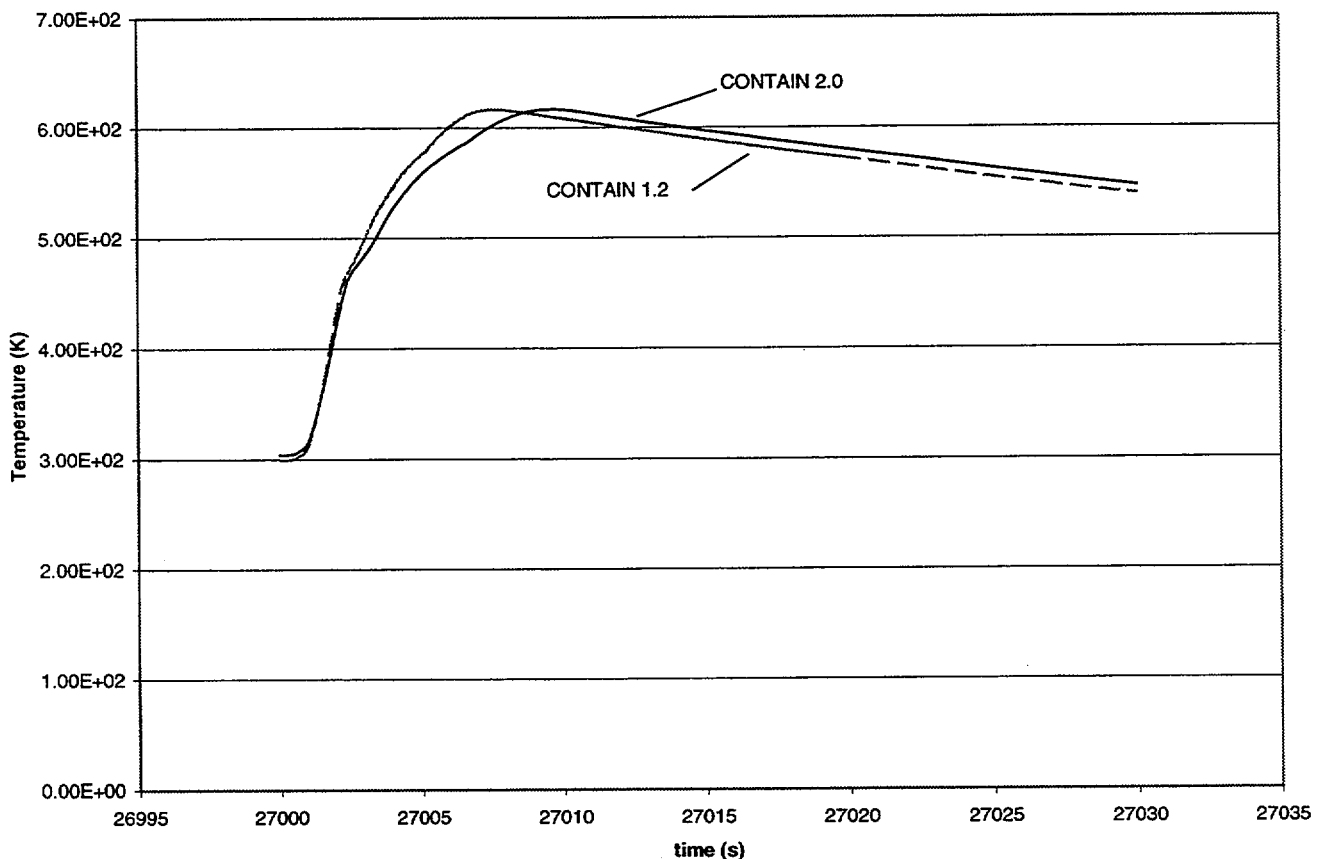


Figure 5.2 Comparison of predictions using CONTAIN 1.2 and CONTAIN 2.0 for Scenario VIa

recommended prescription for these choices and additional recommendations concerning which sensitivities are important. Appendix B discusses the assumptions made for the base case (or Reference Case) CONTAIN calculations in detail.

Also important is the characterization of the debris available for ejection at the time of vessel failure (i.e., debris in a molten pool in contact with the lower head). Melt mass distributions for 4-loop PWRs, with Zion as the prototype, were summarized in Table B.7 of NUREG/CR-6338. For the CONTAIN calculations discussed here, values were derived from the upper end (nominally the 99th percentile) of the distributions as listed in this table. However, some slight adjustments to the melt composition had to be made, reflecting differences between the Zion plant and typical reactor cores for ice condenser plants. Again, Appendix B has details.

5.3 Containment Response for DCH-Relevant Scenarios

5.3.1 Scenario VI-c: Non-Station Blackouts

This scenario is representative of DCH events in non-SBOs. AC power is available in the plant so that igniters, air return fans, and containment sprays are assumed available in the vast majority of cases. The availability of igniters and ARFs ensures that hydrogen concentrations never significantly exceed flammable limits throughout the containment. We focus first on the predicted ice inventory at vessel breach and then turn our attention to containment loads at vessel breach.

In the 1.2 Series discussed in Appendix B, steam and non-condensable gas sources were taken from an existing (Pilch et al. 1994b) SCDAP/RELAP5 calculation of a Station Blackout sequence with induced RCP seal failures for Zion, which is a four-loop Westinghouse plant similar to that in the ice condenser plants. In this calculation, each of the four RCPs introduced a 250 gpm coolant leakage into the containment. Vessel failure for this sequence occurred at 27000 seconds (7.5 hr) after scram. For many of the cases studied in the 1.2 Series, CONTAIN predicted that there would be no ice remaining in the ice chest after this sustained period of steam injection into the containment. Calculations of the DCH phase of the accident (assuming a dry cavity and no containment sprays) showed consistently that, in the absence of ice, peak pressures were high enough to threaten containment integrity for a wide range of assumptions about melt ejection and DCH phenomena. Thus, whether or not ice is available at the time of vessel breach is a potentially key issue for this scenario.

No new system level calculations were performed for this study. Unfortunately, the steam sources from the existing SCDAP/RELAP5 calculation are not ideally-suited for analyzing the non-SBO sequences prior to a DCH event:

- (1) The SCDAP/RELAP5 calculation is for a SBO; consequently, there is no auxiliary feedwater on the secondary side, which is available in the majority non-SBO PDSs.
- (2) Cooling water is generally available to the RCPs during non-SBOs; consequently, leakage through the RCP seals is not expected.
- (3) The SCDAP/RELAP5 calculation predicts a temperature-induced failure of the hot leg followed by complete depressurization of the RCS prior to vessel breach.

CONTAIN Calculations

The implications of these shortcomings are addressed next.

Auxiliary feedwater on the secondary side is available in many non-SBO PDSs. The available SCDAP/RELAP5 calculation is for a SBO, which does not have auxiliary feedwater available. That maximizes the load on the ice chest, which minimizes the ice inventory at vessel breach. As we will show, our base case calculations, tied to the existing SCDAP/RELAP5 calculation, lead to a bounding state with no ice inventory at vessel breach and a deeply flooded cavity. Consequently, additional cases, treated as sensitivity studies, were performed to explore the impact of substantial ice inventory at vessel breach. We note, however, that the cavity is deeply flooded with only 50% ice melt; consequently, a deeply flooded cavity is still likely even when substantial ice remains.

Cooling water is generally available to the RCPs during non-SBOs; consequently, leakage of the RCP seals is not expected. The SCDAP/RELAP5 calculation assumes that there is a temperature-induced RCP leak of 250 gpm/pump, which are classified as S2 leaks. Although RCP leaks are not expected in non-SBOs, their leakage is of the same general size as most LOCAs or a stuck open PORV that are associated with non-SBOs. Consequently, we conclude that incorrectly modeling the leak as a RCP leak rather than specifically as an initiator LOCA or a stuck open PORV is a second order effect that will not significantly change the steam load on the ice chest.

Figure 5.3 shows the CONTAIN 2.0 pressure trace in the upper containment during the period prior to vessel breach for Case VI using the same SCDAP/RELAP5 sources as were used in the 1.2 Series. One of the dominating events shown is the hot leg failure predicted by SCDAP/RELAP5 to occur at about 17000 seconds (4.7 hr) into the accident. This event results in rapid depressurization of the primary system, so that a high pressure melt ejection could not occur after that time; however, this steam source is largely responsible for melting any remaining ice in the 1.2 Series of calculations discussed in Appendix B.

Obviously, the event sequence predicted by SCDAP/RELAP5 is inconsistent with the postulated DCH scenario being studied. Because of that inconsistency, the 1.2 Series included numerous sensitivity cases in which the ice mass remaining was artificially restored to significant levels (typically 50%) before the vessel failed (which is the case for Figure 5.2), and other cases in which the steam sources prior to vessel breach were arbitrarily reduced in order to achieve conditions in which ice remained at the time of vessel failure. The motivation for these variations was not only the inconsistency of the SCDAP/RELAP5 sources with the postulated DCH event, but also because the NUREG-1150 quantifications for Sequoyah indicated substantial ice would remain at the time of any DCH event. We will return to this latter point later.

For the 2.0 Series, a different approach was taken for primary system sources prior to vessel breach. Because Scenario VI-c is based on the assumption that the hot leg does not fail, we removed the hot leg sources of steam and water from the CONTAIN input deck, then constructed an idealized source of steam from the leaking RCPs for the time period from the time of hot leg failure to the time of vessel failure (17000 to 27000 sec). This artificial source was necessary

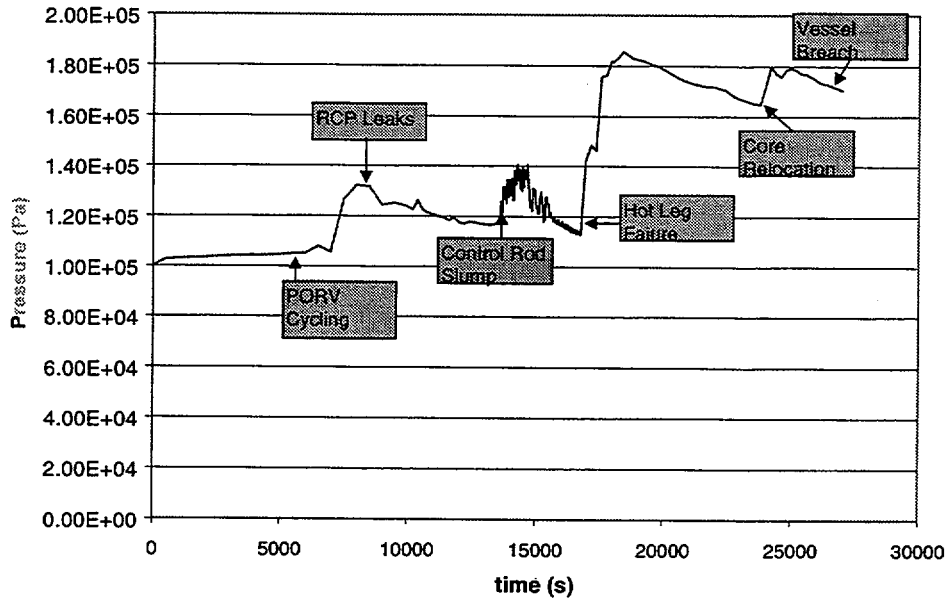


Figure 5.3 SCDAP/RELAP5 Upper containment pressure for Case VI using original SCDAP/RELAP5 sources

because the depressurization at 17000 seconds resulted in very low steam sources from the SCDAP/RELAP5-calculated RCP leaks.

The prescription for the artificial steam source was to inject steam at approximately the specific enthalpy characteristic of the vessel atmosphere at the time of hot leg failure, and at a mass flow rate determined such that the energy injection rate into the containment was approximately equal to the decay heat of the core.

The decay power was approximated by the Wigner formula:

$$P = 0.062 P_0 t^{-0.2} \quad (5.1)$$

where P_0 is the plant thermal power and t is the time since scram. Figure 5.4 compares the integrated energy injection from Eq. (5.1) to the SCDAP/RELAP5 calculations prior to hot leg failure (the sum of the leaks from all four RCPs and the PORV are included).

At the transition between the SCDAP/RELAP5 sources and the artificial decay heat source, the slope of the former (i.e., power) is less than that of the latter, which might suggest that our artificial prescription is conservative. On the other hand, exothermic energy from zircaloy oxidation is not included in the prescription, and a low value of core power was used for these calculations (3000 MW vs. the actual 3579 MW for Sequoyah), so some aspects of this

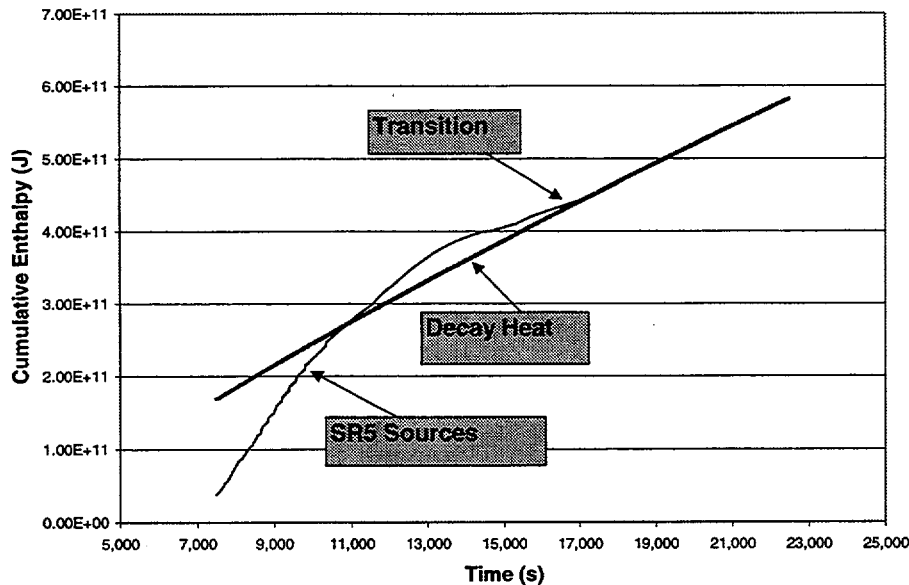


Figure 5.4 Energy injected into containment from coolant

calculation are non-conservative. The assumption that water is available (possibly from accumulator discharges) to carry decay power into containment as steam is justified by SCDAP/RELAP5 calculations for a best estimate RCP leak because the accumulators discharge. Sources of non-condensables from SCDAP/RELAP5 were not modified for this prescription; however, the SCDAP/RELAP5 calculations showed that most hydrogen was released into containment during the core degradation phase. Consistency with the prescription for the steam sources might be achieved by spreading the residual hydrogen release out over time, but this was not done; the purpose of constructing this source prescription was strictly to achieve a somewhat more realistic treatment of steam leaks, not to create a self-consistent substitute for detailed invessel code calculations. With this "extrapolated" steam source, CONTAIN 2.0 predicted that all ice was depleted well before 27000 seconds (the time predicted by SCDAP/RELAP5 for vessel failure). This is illustrated in Figure 5.5. The results of Figure 5.5 are strictly applicable only to the limiting (low probability case) of no auxiliary feedwater, and a natural consequence of ice melting in excess of about 50% is a deeply flooded cavity.

Best estimate SCDAP/RELAP5 calculations (with auxiliary feedwater), carried through to vessel breach without hot leg failure, would be desirable for completeness. We already predict complete ice melting, so there is no potential for any mitigation of loads at vessel breach associated with the ice chest; however, the cavity would be deeply flooded changing the nature of containment loads from DCH to steam spike. Significant ice could persist up to vessel breach if auxiliary feedwater is modeled. With this ice inventory, we still expect the cavity to be deeply flooded; but in this case, the remaining ice will be available to mitigate loads at vessel breach.

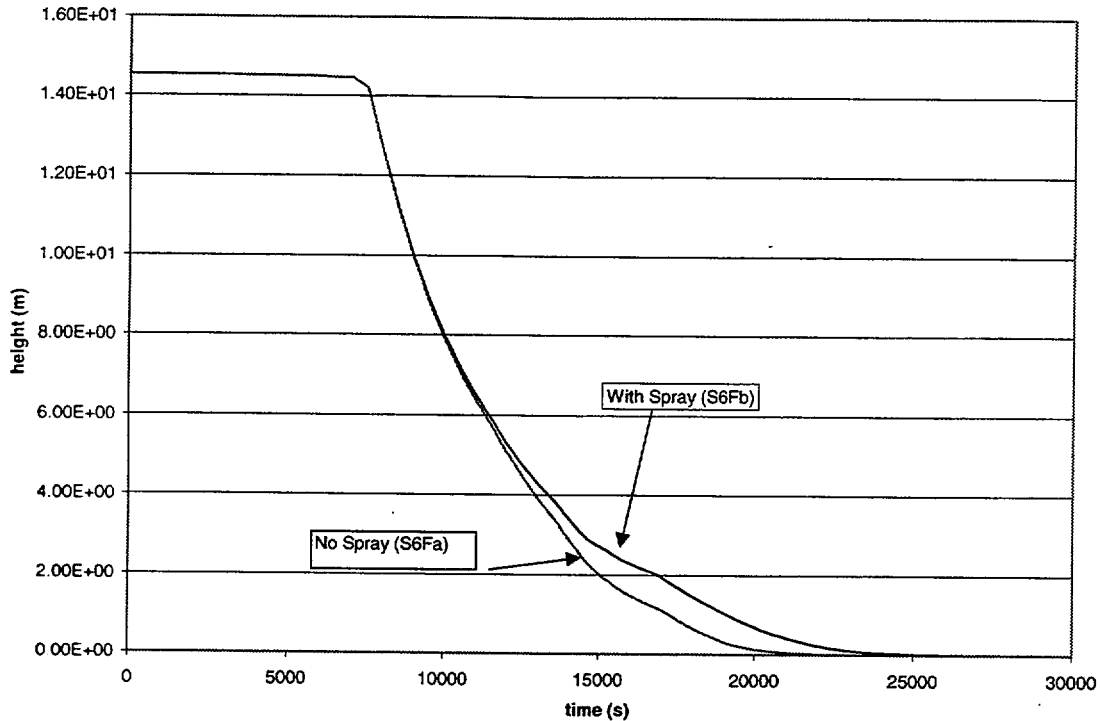


Figure 5.5 Predicted ice inventory in non-SBOs with bounding steam sources representative of scenarios with ARFs and no auxiliary feedwater

The deeply flooded cavity and resulting steam spikes are addressed in Section 5.5. The remainder of this section quantifies loads under the assumption of a dry cavity. As we will show, best estimate steam spike loads or dry cavity DCH loads are not containment threatening even when the ice is depleted. Consequently, we conclude that the availability of more representative system level calculations would not change the conclusions of this study.

For non-SBOs, we can anticipate that the RWST will be drained and the ice inventory completely melted for the bounding steam sources described previously; consequently, the reactor cavity will be deeply flooded. Consistent with NUREG-1150, we treat HPME events as if they were steam spikes from a flooded cavity. As sensitivity studies show, it is insightful to perform DCH calculations under the assumption of a dry cavity or limited melt/water interactions in the cavity.

When cases like this were run in the 1.2 Series, pressurization during the DCH event posed a severe challenge to the containment, assuming the ice was depleted and the containment sprays were not operational. The treatment of this scenario is different in the 2.0 Series from the earlier calculations because of the inclusion of containment sprays. One of the two redundant spray systems in the dome was assumed to be operational throughout the accident.¹¹ The result was a significant reduction in peak pressure.

¹¹ We note that D.C. Cook also has lower compartment sprays.

CONTAIN Calculations

Table 5.4 shows peak pressure calculated by CONTAIN 2.0 for several variations of Scenario VI-c. In the base case (VI-c/1, the peak pressure is considerably reduced from the "no ice" cases studied in the 1.2 series. A second case was run with no sprays; it gives a large pressure rise similar to the cases studied in the 1.2 Series (the DCH assumptions used here were the Reference case from Table B.9, which showed a pressure rise of 4.04 MPa, very comparable with the 3.95 MPa rise calculated here). Case 1 in Table B.9 is the steam spike calculation (sprays, no ice) comparable to Case VI-c/1 here. The predicted pressures are containment threatening, in part because the base pressure is higher and in part because the pressure rise is larger. We see that the steam spike loads actually exceed the dry cavity DCH loads when the upper end of the mass distribution is used in both calculations and when there is no ice in the ice chest.

The combined effect of sprays and ice are shown in the next variation (VI-c/3): this case addresses the possible state where auxiliary feedwater is available reducing the load to the ice chest, which potentially leaves substantial ice at the time of vessel breach. Here the ice was arbitrarily restored to 50% of its initial inventory. The pressure rise was very small in this case compared to a pure steam spike or a case with no ice and containment sprays. We conclude, therefore, that any combination of sprays or ice are effective at mitigating dry cavity DCH loads.

The next case shown in the table (VI-c/4) illustrates that the mitigating effect of the sprays is caused by keeping the base pressure low at the time of vessel failure. In this case, sprays were terminated at the time of vessel failure, but the peak DCH pressure was only slightly increased compared to the base case. The containment sprays kept the base pressure very close to one atmosphere, compared with 0.23 MPa in the case with no sprays. The DCH event injected approximately the same amount of energy in the two cases, but the pressure rise tends to be close to proportional to the pressure at the start of the DCH event. This is because the heat capacity of all dispersed debris is large compared to the heat capacity of the atmosphere.

The last two cases illustrate the effects of different assumptions about the DCH event itself. They are parameter variations selected from the options studied in the 1.2 Series. The variation VI-c/5 shows the potential effect of co-dispersed water: in this case, it is assumed that there is

Table 5.4 Dry-Cavity DCH pressures for Scenario VI-c; non-SBO

| Case | Scenario VI-c Assumptions | Base P (MPa) | Delta P (MPa) | Peak P (MPa) | CFP Sequoyah IPE |
|--------|--------------------------------------|--------------|---------------|--------------|------------------|
| VI-c/1 | Base Case: No ice, sprays on | 0.104 | 0.199 | 0.303 | 0.00 |
| VI-c/2 | No ice, no sprays | 0.231 | 0.395 | 0.625 | 0.93 |
| VI-c/3 | Sprays and 50% ice restored | 0.104 | 0.064 | 0.168 | 0.00 |
| VI-c/4 | No ice, sprays fail at vessel breach | 0.104 | 0.233 | 0.337 | 0.00 |
| VI-c/5 | Base Case with 10 mt water in cavity | 0.104 | 0.520 | 0.651 | 0.99 |
| VI-c/6 | VI-c/5 with steel insulation | 0.104 | 0.556 | 0.661 | 0.99 |

10,000 kg of water in the reactor cavity that becomes entrained in the high pressure melt ejection from the RPV. We note that such calculations are strictly parametric. Pilch et al. (1997b) discuss some of the difficulties in parametric modeling of cavity water with CONTAIN. More phenomenological attempts at modeling cavity water and limited experiment data generally do not support the enhancement of containment pressures shown in Case VI-c/5. Sarget & Lundy (Kolflax 1960; Thompson and Beckerley, 1973) performed experiments with downward-facing high-pressure flashing jets discharging directly into accumulated cold water on the floor of a containment vessel. The accumulated water was very effective at suppressing peak containment pressures on a transient response time (a few seconds) as is of interest to DCH.

The final variation (VI-c/6) introduces the sheet steel from the RPV insulation as a source of molten metal into the debris jet; it corresponds to case 2 in Table B.9 (except that corrected insulation sources are used). These cases show that when key DCH parameters are set at values that are conservative, peak pressures are reduced by the effects of containment sprays, but they are still challenging to containment integrity.

We conclude from these results that for Case VI-c with the nominal assumption of a dry cavity

- the ice inventory is completely melted before vessel breach when ARFs and sprays are operational, but auxiliary feedwater is not available;
- steam spike loads can exceed DCH loads for some conditions for the limiting case of no ice in the ice chest;
- with ARFs and igniters operating, but sprays inoperable, the absence of ice in the ice condenser system implies containment challenging pressures;
- any combination of sprays or ice would effectively mitigate dry-cavity DCH loads.

5.3.2 Scenario VI-d: Station Blackouts

This scenario is important because the assumption of no electrical power to igniters, air return fans, and containment sprays is consistent with failure of operators to restore cooling to the core. In the absence of ARFs, steam from the lower compartment can follow two parallel paths to the upper containment: through the ice condenser system and through leakage paths that bypass the ice condenser. These leakage paths are not fully characterized in ice condenser plants. According to the Sequoyah FSAR, the leaks consist of two types: a well-characterized pathway through the refueling drains, and various unspecified leakage paths that are lumped together conservatively as having an area of 0.29 m² or less. The drain portion of the leakage will be closed off when the water level in the lower containment floods the drain openings. At that point the leakage consists solely of the unspecified pathways.

Flow of steam and other gases into the upper containment will be driven by very small pressure differences, so it is important to capture the behavior of the doors in the ice condenser as carefully as possible. Again, information on the behavior of the containment systems under these conditions is limited. Williams and Gregory (1990) cite a variety of industry sources on the behavior of the three levels of doors and create a relatively detailed model for the CONTAIN input decks. Appendix B includes a detailed discussion.

Response of the containment to this DCH scenario is dominated by the presence of high concentrations of unburned hydrogen throughout the containment at the time of vessel failure. Hydrogen production and heat transfer from the ejected debris during the DCH event exacerbate these conditions, and the debris is calculated to provide an ignition source where hydrogen and oxygen concentrations are in the flammable range. Figure 5.6 shows the pressurization calculated in the base case and also in a second case characterized by a factor-of-ten reduction in deck leakage (i.e., to 0.029 m^2). In both cases, the DCH pressurization is very challenging to containment integrity.

While the upper compartment pressurization is similar for the two choices of deck leakage, other aspects of the accident are not. For example, there is a significant difference in the rate of ice melting prior to vessel breach, as shown in Figure 5.7. (Without AFRs, the flow stagnates in the upper compartment producing the knee in the curve after some initial steam release.) Also, the concentrations of hydrogen occurring in the ice condenser during the long pre-DCH portion of the accident are different, as shown in Figure 5.8. We note that a gradient in the hydrogen concentration (low at the inlet, high at the outlet) is expected in the ice chest, but this effect is not captured by the nodalization used here. Very high hydrogen concentrations in the ice chest are possible, but the potential for detonations, although acknowledged, is not quantified in this study. Williams and Gregory (1990) concluded that proper characterization of detonable gas mixtures in parts of the containment would require a more detailed representation of the plant (greater than the 26 cells that they used and certainly greater than the 9 cells used here). Not modeled in the current nodalization are 20 ft^2 openings that bypass the intermediate deck and upper deck doors. These bypass areas would permit natural circulation flows between the ice chest and the upper plenum as well as between the upper plenum and the containment dome that would mitigate the local development of high hydrogen concentrations in this region.

These results demonstrate that both ice melting rate and hydrogen concentrations in the ice condenser are controlled by a delicate balance between flows passing through the three ice condenser doors and flows that bypass the ice condenser. While these differences might have implications with respect to detonations in the ice chest, the important fact about these two cases is that they result in a high hydrogen concentration in the upper containment at the time of vessel failure and pressurized melt ejection.

The delicate balance of flows is not only uncertain because of uncertainty in the leakage pathways, but also because the behavior of the ice condenser doors is not well characterized. The pressure differences occurring across the various flow paths for the time period shown in Figure 5.7 are hundreds of Pa (e.g., about 1 psf).

The concentration of hydrogen in the dome for either of the two leakage treatments is around 13% prior to vessel failure, with oxygen at about 18%. These conditions by themselves represent a severe threat, even without the added energy from the DCH event itself. Cases studied in the 1.2 Series demonstrated that the combustion of pre-existing hydrogen is the dominant source of pressurization (see Table B.8). The principal effect of the high pressure melt ejection is that it is a mechanism to ignite the hydrogen-air mixture for the situation in which igniters are not operating. The presence of ice has a modest mitigative effect, about equal in size to the increase in pressure caused by the DCH event.

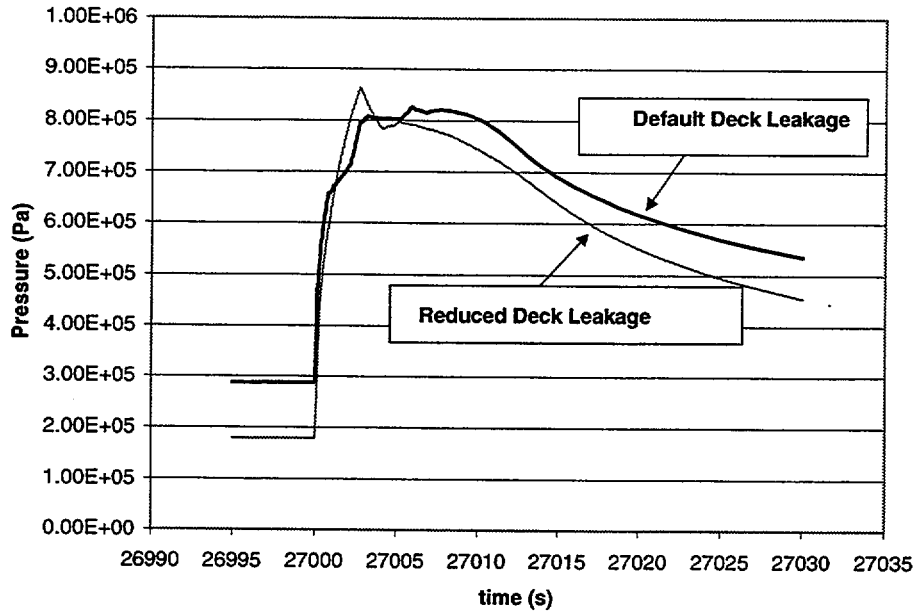


Figure 5.6 DCH pressure excursion in the upper compartment for Scenario VI-d for different deck leakage assumptions

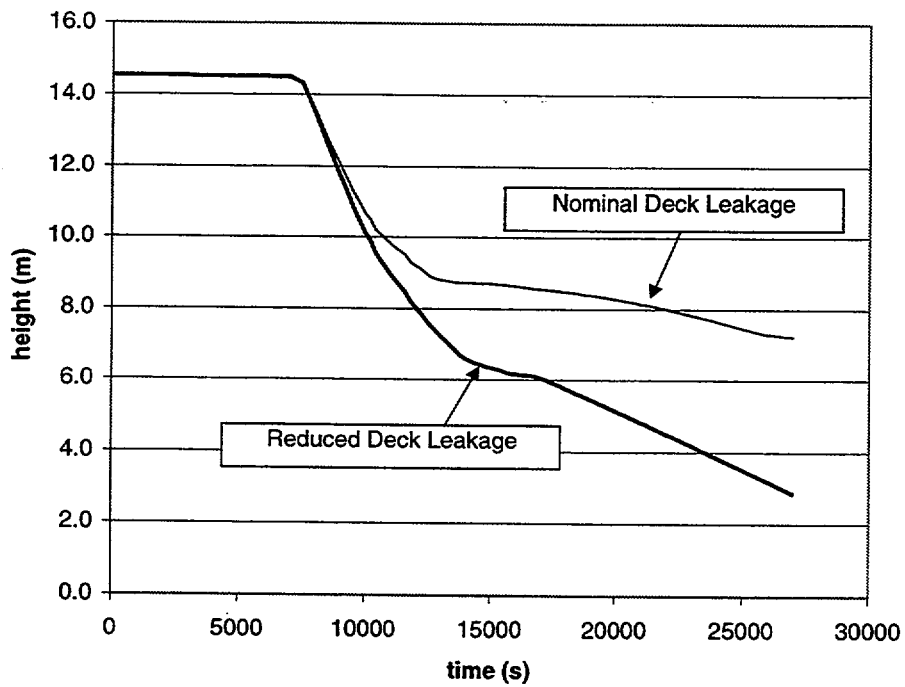


Figure 5.7 Ice remaining for different deck leakage assumptions

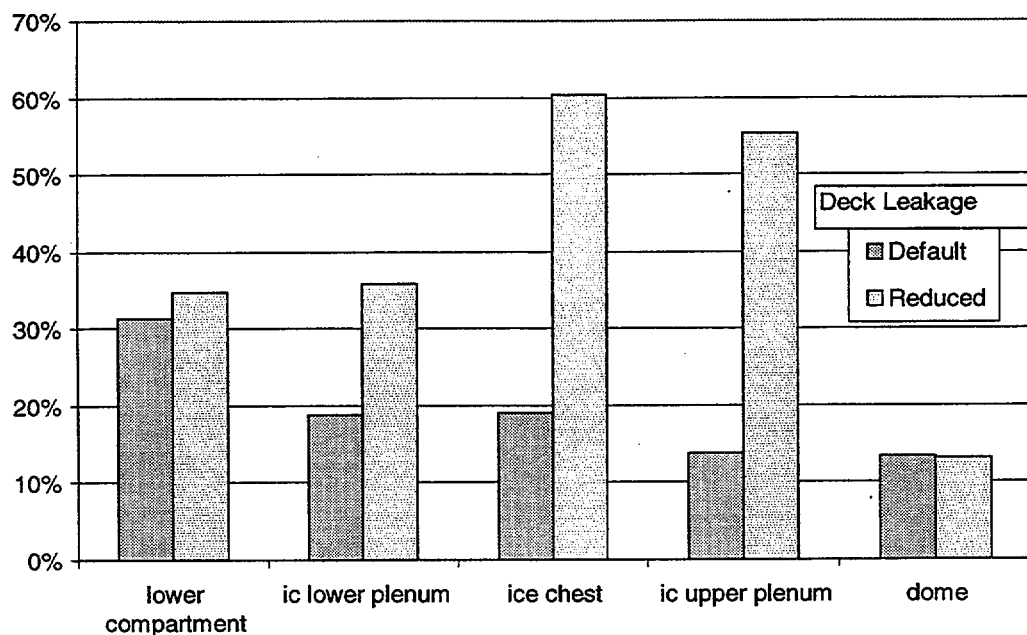


Figure 5.8. Peak hydrogen concentrations for Scenario VI-d (SBOs)

5.4 Insights on Predictions of Ice Inventory at Vessel Breach

Peer Reviewers criticized the draft Ice Condenser Report (NUREG/CR-6427), because SNL treated the containment as a “small dry” containment without taking mitigation credit for ice in the ice beds. CONTAIN calculations, using SCDAP/RELAP5 steam sources from a Zion calculation, predicted complete melting of ice prior to vessel breach (Appendix B). Fauske and Associates, Inc. (FAI) had provided a MAAP calculation showing half the ice remaining for a TMLB’ accident. Henry, in his review of draft NUREG/CR-6427, outlined a hand calculation that resulted in approximately 40% of the ice remaining. The peer reviewers generally characterized the no-ice scenario as physically impossible. Additional CONTAIN calculations performed in support of this study (Section 5.3.2) confirm that about half the ice inventory remains at vessel breach for SBOs.

Quantification of the remaining ice in NUREG-1150 (Table 5.5) shows that significant ice remains for the spectrum of initiating or induced leak sizes that could lead to HPME/DCH events. Consequently, NUREG-1150 quantifications support peer reviewer beliefs that significant ice will remain in the ice beds for all HPME/DCH relevant scenarios. However, Table 5.5 does support the trend for less ice inventory at vessel breach for SBOs.

We still predict (Section 5.3.1) that the ice inventory can be depleted for certain non-SBOs. We have identified two reasons for this unexpected result. First, the steam sources available to

Table 5.5 NUREG/CR-4551, Vol. 5, Rev. 1, Part 2, Quantification (Q29) of ice remaining at vessel breach for the NUREG-1150 study

| Case # | Sprays | Leak Size | Probability. of ice remaining in the stated Range | | | Comment |
|--------|--------|----------------|---|-----------|-----------|---------------------|
| | | | 1.0 – 0.5 | 0.5 – 0.1 | 0.1 – 0.0 | |
| 2 | Yes/No | None | 100% | 0% | 0% | |
| 5 | Yes | S ₃ | 95% | 5% | 0% | |
| 6 | No | S ₃ | 70% | 30% | 0% | SBO with RCP leak |
| 7 | Yes | S ₂ | 20% | 80% | 0% | |
| 8 | No | S ₂ | 0% | 99% | 1% | SBO with stuck PORV |

(1) Typical RCP leak classified as a S₃ leak.

(2) One stuck open PORV classified as a S₂ leak.

(3) No sprays is representative of SBO accidents but can occur in other accident with power in the plant.

use are for a SBO; consequently, the steam load on the ice chest is maximized and the ice inventory at vessel breach is minimized. Second, current generation codes predict that core melt progression through vessel breach proceeds much slower than code predictions at the time of NUREG-1150. This historical perspective is addressed further in Section 5.4.1. Section 5.4.2 provides some analytical insights into the predicted ice inventory that results from using the SCDAP/RELAP5 steam sources (no auxiliary feedwater) and a containment model that assumes the ARFs are operational.

5.4.1 Historical Perspective

The NUREG-1150 quantifications should first be examined in light of the calculational tools available at the time. Table A.3-4 in NUREG/CR-4551 Vol. 5, Rev. 1, Part 2 shows some representative sequence timings for a TMLB' accident. The codes of that time predicted that only one hour would elapse between UTAF¹² and vessel breach. Typically, those codes would relocate molten core material directly to the lower plenum or accumulate material on the core plate, which quickly failed from the thermal and structural loads. In either case, thermal attack of the lower head was initiated early and lower head failure was often predicted on contact (tube ejection) or after only a few minutes. Consequently, core melt progression was highly time compressed, limiting the quantity of coolant that could be boiled and released to the containment prior to vessel breach.

Sequoyah is a 4-loop Westinghouse plant, so it is useful to examine best estimate SCDAP/RELAP5 calculations for Zion as reported in NUREG/CR-6075, which were performed in support of DCH resolution activities for Zion. Table 5.6 reproduces here the timing of key

¹² Uncovery of top of active core.

**Table 5.6 SCDAP/RELAP5 sequence timings for case of best estimate
(250 gpm/pump) RCP leaks**

| Event | Time(s) | Time (hr) |
|--|-----------|--------------|
| TMLB' initiation | 0 | 0 |
| Introduction of seal leaks of 21 gpm per RCP; leak diameters = 0.00327 m | 0 | 0 |
| Steam generators dryout (pressurizer/non-pressurizer loops) | 4801/5003 | 1.33/1.39 |
| Onset of pressurizer PORV cycling | 5680 | 1.58 |
| RCP saturation; seal leaks increased to 250 gpm per RCP; leak diameters = 0.0137 m | 7466 | 2.07 |
| End of full loop (liquid) natural circulation | 7526 | 2.09 |
| Collapsed liquid level falls below the top of the fuel rods | 8944 | 2.48 |
| Vapor in the core exit begins to superheat; hot leg countercurrent circulation begins | 9045 | 2.51 |
| End of pressurizer PORV cycling | 10 320 | 2.87 |
| Pressurizer drains | 10 575 | 2.94 |
| Collapsed liquid level falls below the bottom of the fuel rods | 11 196 | 3.11 |
| Onset of fuel rod oxidation | 11 235 | 3.12 |
| First slumping into lower head begins; 2115 kg Ag-In-Cd over ~360 s | 13 616 | 3.78 |
| 27.5 kg of upper plenum stainless steel melts and slumps into lower head | 14 018 | 3.89 |
| First appearance of an in-core molten pool; by fuel dissolution in third channel | 14 057 | 3.90 |
| 71.5 kg of upper plenum stainless steel melts and slumps into in-core molten pool | 14 219 | 3.95 |
| Slumping into lower head begins; 235 kg Ag, 112.7 kg SS, 2406 kg UO ₂ 452 kg Zr over ~420 s | 14 250 | 3.96 |
| Accumulator injection begins | 14 414 | 4.00 |
| First heatup to molten fuel temperatures; in first channel | 14 976 | 4.16 |
| First fuel rod fragmentation; in the fifth channel | 15 371 | 4.27 |
| 501.7 kg of upper plenum stainless steel melts and slumps into in-core molten pool | 15 410 | 4.28 |
| 131.9 kg of upper plenum stainless steel melts and slumps into in-core molten pool | 15 566 | 4.32 |

**Table 5.6 SCDAP/RELAP5 sequence timings for case of best estimate (250 gpm/pump)
RCP leaks (continued)**

| Event | Time(s) | Time (hr) |
|---|---------|-----------|
| 632.0 kg of upper plenum stainless steel melts and slumps into in-core molten pool | 16 115 | 4.48 |
| 620.2 kg of upper plenum stainless steel melts and slumps into in-core molten pool | 16 558 | 4.60 |
| 749.5 kg of upper plenum stainless steel melts and slumps into in-core molten pool | 16 849 | 4.68 |
| Non-pressurizer loop hot leg nozzle fails by creep rupture | 16 925 | 4.70 |
| Hot leg break initiated; break diameter = 0.166 m | 16 925 | 4.70 |
| Core is reflooded; collapsed liquid level rises above the top of the fuel rods | 17 163 | 4.77 |
| Accumulators empty; injection ends | 17 169 | 4.77 |
| Second core dryout; collapsed liquid level falls below the bottom of the fuel rods | 17 748 | 4.93 |
| Core slumping into lower head; 62 930 kg UO ₂ , 16 350 kg ZrO ₂ | 23 938 | 6.65 |
| 5300 kg of submerged 'thin' stainless steel added to lower head debris | 24 000 | 6.67 |
| Slumping into lower head; 3556 kg UO ₂ , 1039 kg ZrO ₂ | 24 536 | 6.82 |
| Slumping into lower head; 2240 kg UO ₂ , 569 kg ZrO ₂ | 24 612 | 6.84 |
| Slumping into lower head; 2240 kg UO ₂ , 569 kg ZrO ₂ | 24 723 | 6.87 |
| Slumping into lower head; 2240 kg UO ₂ , 569 kg ZrO ₂ | 25 233 | 7.01 |
| Slumping into lower head; 4697 kg UO ₂ , 1193 kg ZrO ₂ | 25 302 | 7.03 |
| Slumping into lower head; 2240 kg UO ₂ , 569 kg ZrO ₂ | 26 205 | 7.28 |
| Lower head failure; by creep rupture approximately 0.80 m above the inside bottom surface of the head | 26 915 | 7.48 |
| End of calculation | 28 915 | 8.03 |

core melt progression events for a TMLB' accident where high temperatures induce a best-estimate 250 gpm leak through the seals in each of the 4 RCP pumps. The time from UTAF to vessel breach is approximately 5 hr, which is five times longer than code predictions available to NUREG-1150.

Some of this difference can be attributed to SCDAP/RELAP5-predicted hot leg failure, which leads to additional cooling of an incore crucible and lower stress states on the lower head. The codes prior to NUREG-1150 did not have the capability to properly model processes leading to hot leg failure. However, the primary differences between then and now are that current codes like SCDAP/RELAP5 all predict accumulation of core melt in an incore crucible that greatly delays core relocation of material into the lower plenum. Furthermore, SCDAP/RELAP5 predicts that it takes nearly one hour (after relocation) for the lower head to fail. These modeling differences explain why the time from UTAF to vessel breach is so much longer in modern core predictions. The bottom line, however, is that there is substantially more time to boil and release coolant to containment (assuming availability of water), and this means more steam loading on the ice beds.

5.4.2 Analytic Insights on Ice Inventory

Peer reviewers recommended a simple hand calculation equating decay heat levels with ice melting. This simple approximation has been implemented as follows:

- (1) After scram, decay energy first goes into boiling dry the secondary side of the steam generator and heating the RCS to the point that RCP leak. The onset of temperature-induced RCP leaks is taken from Table 5.6 as 7460 s.
- (2) Decay heat boils the reactor coolant, which is assumed to be immediately released from the RCS and completely condensed in the ice beds. The cumulative decay heat available to melt ice,

$$E = \int_{t_{leak}}^t P(t) dt = .07775 P_o [t^{0.8} (s) - t_{leak}^{0.8}] , \quad (5.2)$$

is obtained by integrating the Wigner Decay Power formula. This assumes adequate water in the core region to carry the decay heat into containment as steam. It also assumes that decay heat is not transferred to the secondary side (i.e. no auxiliary feedwater).

- (3) The fraction of ice remaining at any given time after PORV cycling is calculated from

$$f = 1 - \frac{E}{h_{s1} + C_p \Delta T} , \quad (5.3)$$

where $h_{s1} = .334$ MJ/kg is the heat of fusion, $C_p = 4.184 \times 10^3$ J/(kg K) is the ice/water specific heat, ΔT is the temperature rise associated with heating the ice from its storage

state to the melting point plus any additional temperature rise as the melted ice falls through the ice chest.

- (4) The Sequoyah IPE states that the storage state of ice is 270 K (i.e., 3 K below freezing). CONTAIN calculations show that gas in the ice chest is approximately 308 K for a large portion of the accident; consequently, we take $\Delta T=38$ K. This characterizes the sensible heat required to bring stored ice up to melting and the sensible heat required to heat water from melting ice up to the gas temperature in the ice chest.

Results of the approximate decay heat model are compared to the SCDAP/RELAP5/CONTAIN results in Figure 5.9. The approximate analytic-solution shows that the ice inventory should be depleted prior to vessel breach and that this result is not conservative for non-SBOs and in substantial disagreement with SCDAP/RELAP5/CONTAIN results for SBOs. Initially, the CONTAIN calculations with SCDAP/RELAP5 sources melt faster than the analytic solution suggests. This is because inventory loss and depressurization (accompanied by flashing in the RCS) are significant (if not dominant) sources of steam release from the RCS. Clad oxidation is an additional heat source that enhances steam production, which is more evident in the non-SBO SCDAP/RELAP5/CONTAIN calculation. For non-SBOs without auxiliary feedwater, the CONTAIN calculations show that not all steam that is released to the lower compartment is fully condensed as it passes through the ice beds. However, the ARFs quickly recycle this bypass steam (even if sprays are operational) back into the ice beds where it is further condensed. These additional sources of significant steam release, in conjunction with atmosphere recirculation, explain why SCDAP/RELAP5/CONTAIN calculations deplete the ice inventory more quickly than the analytic solution for non-SBO scenarios.

This situation is different in SBOs because the ARFs are not operational. CONTAIN calculations show that the initial steam release pushes lower compartment non-condensables into the upper compartment. The flow quickly stagnates because the ARFs cannot recycle gas back into the subcompartment. Additional steam release into the lower compartment will pressurize the containment, but very little of this additional steam passes through the ice beds where it can be condensed. This violates the key assumptions of the analytic model and explains why SCDAP/RELAP5/CONTAIN predict that half the ice remains at vessel breach in SBO accidents.

5.5 Containment Response for Non-DCH Relevant Scenarios

Because the probabilistic analysis in Section 4.0 addresses all containment failure modes, a number of CONTAIN calculations have been carried out for situations in which DCH does not occur. These are primarily low pressure scenarios. Having calculations from CONTAIN that use assumptions consistent with the DCH series is important for assessing the relative importance of DCH compared to other containment failure threats. Guided by the logic of NUREG-1150, we have addressed three scenarios that differ from the ones discussed earlier only in what happens at vessel breach:

- (1) non-DCH combustion of hydrogen in a SBO;
- (2) power available to containment ESFs with steam spike (i.e., igniters, sprays, and ARFs available);

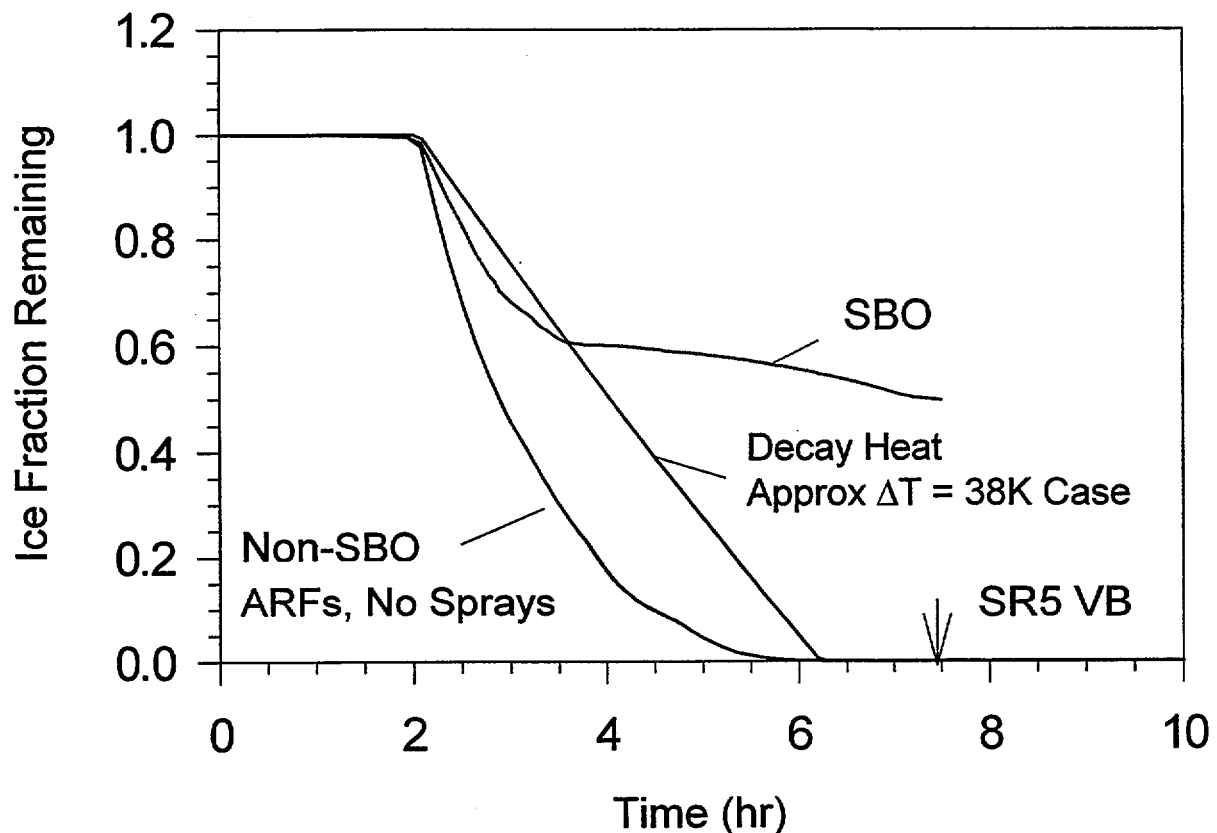


Figure 5.9 Prediction of ice inventory for various modeling approaches

- (3) power available with failure to switch to recirculation mode (i.e., sprays not available, igniters and ARFs available).

For the steam spike, we assume that the molten debris (approximately 88 mt) was quenched by cavity water over a 5 s period, corresponding to the debris pour time. We note that the melt mass corresponds to the extreme upper bound of the expected distribution. The 5 s quench time represents an extreme lower bound. Taken together, the steam spike is maximized; however, the underlying assumptions are low probability combinations of events.

Steam was assumed to be generated at more or less saturated conditions, and injected into the containment atmosphere. These are conservative assumptions, since the amount of water available is very large, and some of the thermal energy would go into heating the liquid that is not boiled or ejected into the atmosphere. In addition, cavity pressurization from initial melt water interactions could delay the ejection of remaining melt into the cavity.

Table 5.7 lists the assumptions used in the steam spike analysis. We acknowledge the potential for explosive melt water interactions in the cavity and speculate that such events might

blowout the walls of the freestanding cavity or displace the RPV. A steam spike is still possible in this scenario, but it is outside the scope of this study to judge if dynamic loads will couple with the containment shell or displace the RPV. We note, however, there is now a significant body of experimental evidence (Huhtiniemi et al., 1995, 1996; Kato et al., 1999; and Magallon et al., 1998) suggesting that molten UO_2 - ZrO_2 mixtures poured or injected into water do not lead to spontaneous explosive events.

For the CONTAIN calculations, base case assumptions, as specified in Sections 5.2 are used for the powered and unpowered cases, respectively. Table 5.8 gives highlights of the results.

The first case shows that a rapid debris quench creates a steam spike that is moderate in the powered situation (no ice with one of two redundant spray systems operational). The next two cases are the unrecovered station blackout, and show significantly higher peak pressures resulting from hydrogen deflagrations, in part because the base pressure was high. The pressure rise in the second case, caused by combustion only, is comparable to that in the first case, caused by the steam spike only (because igniters had kept hydrogen concentrations very low). The third case has the combined effect of the steam spike and hydrogen combustion under the assumption that global hydrogen combustion can be ignited at the same time as the steam spike. The pressure rise is significantly less than the sum of cases 1 and 2, but the peak pressure poses a significant challenge to containment integrity. The fourth case corresponds to a non-SBO scenario with operational igniters, but there is a failure to switch to recirculation mode before the RWST runs dry at 36 minutes. For case 4, the sprays are not operational for any time after 36 minutes. The steam spike loads in case 4 are quite similar to the hydrogen combustion loads in case 2, but the

Table 5.7 Conditions assumed for steam spike

| Quantity | Value |
|---|--------------------|
| Debris mass (kg) | 8.77×10^4 |
| Enthalpy transferred (J) | 1.14 E+11 |
| Steam enthalpy relative to 273 K liquid (J) | 2.72 E+06 |
| Cavity water enthalpy (J) | 2.17 E+05 |
| Quench time (s) | 5 |

Table 5.8. Cases without DCH (combustion enabled at VB)

| Case # | ESF Power? | Steam Spike? | Base P (MPa) | Delta P (MPa) | Peak P (MPa) | Peak Dome T (K) | Comment |
|--------|------------|--------------|--------------|---------------|--------------|-----------------|---------|
| 1 | Yes | Yes | 0.116 | 0.370 | 0.474 | 450 | Non-SBO |
| 2 | No | No | 0.287 | 0.357 | 0.644 | 1169 | SBO |
| 3 | No | Yes | 0.287 | 0.506 | 0.793 | 1196 | SBO |
| 4 | Yes/No | Yes | 0.231 | 0.412 | 0.643 | 500 | Non-SBO |

CONTAIN Calculations

dome temperatures are much lower. We examined the gas compositions in the lower compartment during the steam spike. Steam concentrations exceeded 60% and oxygen concentrations were less than 5%; consequently, the lower compartment is highly inerted and there is essentially no chance of a steam spike inducing a global hydrogen burn.

We emphasize that the non-SBO cases in Table 5.8 were performed under the bounding assumption of no ice and only one train of containment sprays (if operational). As noted previously, significant ice remains in the ice chest for non-SBOs if auxiliary feedwater is available. In addition, it is likely that both trains of sprays are operational in most scenarios. For these more likely situations, we expect the pressure rise from a steam spike to be non-threatening and limited by the pressure rise expected under DBA conditions.

5.6 Conclusions from the CONTAIN Studies

If all engineered safety features (ESFs) in the ice condenser containment are fully functional, the calculations presented here and in Appendix B indicate that, even when conservative assumptions on melt mass are used, containment integrity is not seriously threatened by DCH events, hydrogen combustion events, or steam spike events. However, if one or more of the ESFs is compromised, peak pressures could challenge containment. Specifically, hydrogen combustion events in a SBO (no igniters) are containment threatening and a DCH event (in conjunction with high H₂ concentrations) in a SBO are even more threatening.

In the 1.2 Series, for a given state of ESF availability, variations in uncertain aspects of DCH phenomenology introduced a spread in peak pressure loads that was on the order of 20% in either direction. Variations from one scenario to another were typically much larger and clearly distinguish different classes of containment vulnerability to DCH.

For the unrecovered station blackout (Scenario VI-d), the absence of igniters throughout the accident progression has severe implications for pressure loads, even though some ice is expected to remain in the ice condenser very late in the accident.

For the case with power available for air return fans, igniters, and containment sprays (Scenario VI-c), CONTAIN predicts that very little ice will remain at the specified time of vessel failure. Lack of auxiliary feedwater in the SCDAP/RELAP5 model and predicted delays in core relocation and lower head failure (relative to calculations at the time of NUREG-1150) were identified as key reasons why the ice inventory was depleted. However, containment sprays are effective in controlling the base pressure prior to vessel breach, and as a result, peak pressures are not very threatening for base case DCH assumptions. For more pessimistic assumptions concerning co-dispersed water, the resulting pressurization is significant to the containment, though not as high as in Case VI-d. We note that NUREG-1150 quantifications suggest that significant ice remains a vessel breach when auxiliary feedwater is available.

6.0 QUANTIFICATION OF CONTAINMENT FRAGILITY

This section characterizes the strength of a reactor containment in probabilistic terms, which are required for load/strength comparisons. The pressure capacity of a reactor containment is treated as a random variable because of the variability in material properties, unknown differences between the as-built and design conditions, and modeling uncertainties. The probability that the containment failure pressure is less than a specified pressure is known as the containment overpressure fragility curve.

Fragility curves represent a probabilistic estimate of the capacity of the containment. In general, the fragility curve could be derived from data and full-scale experiments. However, the containment fragility curves are dependent on site-specific detail and, without detailed model tests, they must be derived from analysis. As a practical matter, the fragility curves are derived from a combination of material property data, tolerances in dimensions from drawings, and judgment of the analyst. Judgment is used in determining what level of analysis is required and what failure mechanisms are considered to govern the containment capacity. Typically, adequate material property data exist to characterize variability in material properties. Finally, analyst judgment is used to assign modeling uncertainty to the models to characterize the analyst's confidence in the ability of the selected models to represent the actual failure mechanisms involved. Modeling uncertainty could, in principle, be reduced with further analysis or testing. Funding constraints, however, usually require the analyst to exercise his or her judgment to reflect the uncertainty involved.

The IPEs for all operating PWRs in the U.S. were assembled and containment fragility curves were obtained for each plant as part of DCH resolution activities for the Westinghouse plants (Pilch et al., 1996). The containment capacity results from each of the IPEs were examined and briefly reviewed, and the probability of containment failure was taken from them. In many cases, this consisted of fragility curves showing pressure versus cumulative failure probability. In other cases, a mean or median failure pressure was specified along with uncertainty bounds. In some cases, only curves or points for various failure modes were given and a total probability of failure had to be constructed. In all these situations, a single fragility curve resulted that was intended to reflect both modeling uncertainty and stochastic uncertainties caused by material property variations. A detailed assessment of the technical basis for the IPE fragility curves has not been performed and the IPE assessments are not always based on detailed information and analyses.

For those IPEs presenting only a single curve, the curve was digitized and curve-fit with a spline program. Failure probabilities were determined at intervals of 1 psig. For IPEs that reported medians and uncertainties, a curve was developed and failure probabilities were determined at intervals of 1 psig. The few that reported only median values (5% and 95%) were fit to either a log-normal distribution, normal distribution or third-order spline function in order to get the best fit and failure probabilities determined at 1 psig intervals. In most situations where this occurred, only a third-order spline provided an adequate fit to the three constraints.

Many of the IPE containment capacity analyses did not consider temperature or stated that increased temperatures would have little effect on the capacity. Other IPEs performed the

Quantification of Containment Fragility

analysis at either single or multiple accident temperatures. For those that determined the capacity at different temperatures, the analysis closest to 400 K (260°F) was selected as best representing the accident temperatures expected in the reactor containment building during vessel breach.

We observed that the licensee's level of effort and our estimate of the reliability of these containment fragility curves varied significantly. In some cases, a detailed analysis was performed for every possible failure mode. An overall cumulative failure curve was determined by combining each mode of failure, while some IPEs simply used containment fragility curves derived from other containments or simply shifted other plant's fragility curves based on their determination of the difference in ultimate capacity.

Appendix D in Pilch et al. (1996) briefly discusses (when given enough information) how the fragility curves were determined from each IPE. In addition, the process of digitizing, fitting and tabulating the curves or data given in the IPEs is discussed for every plant, and the detailed results are also tabulated

Functional representations of fragility are subject to possible error when extrapolated to low failure frequencies, because excessive extrapolation to low failure frequencies could lose or violate the physical basis most of the curve rests on. In other cases, some IPEs conservatively tie the low end of the fragility curve to the design pressure. Consequently, the IPE fragility curves might be quite conservative in the tails. On the other hand, the digitizing process is subject to human error and is dependent on the quality of the working curve. In a few cases, we supplied a curve fit to median values (5% and 95%), and extrapolation to lower failure frequencies may involve error. It will be shown that the assessment of early containment failure probability can be sensitive to uncertainties in the fragility curves.

Table 6.1 provides a concise summary of key plant-specific fragility data for each Westinghouse plant with an ice condenser containment. We note that all ice condenser containments are free-standing steel shells, except DC Cook, which is a reinforced concrete containment. We see that large variations in containment strengths exist. DC Cook is the least robust containment with a failure pressure of 45 psig, at a failure frequency of 10%. Watts Bar and Catawba are the strongest containments with failure pressures of 71 psig, at the same failure probability. Thus, we conclude that a containment's fragility is plant-specific. This is illustrated further in Figure 6.1 which compares the fragility curves for all the plants. We note in Table 6.1 that IPE assessments of fragility for Sequoyah suggest that the containment is more robust (particularly in the low-end tail) compared to NUREG-1150 assessments of the containment fragility for Sequoyah.

We note that the ice condenser plants are substantially less robust than other Westinghouse plants with large dry or subatmospheric containments. Table 6.1 shows that the mean of the containment failure pressure for all ice condenser plants is 62.8 psig at a failure frequency of 10%. The comparable value for all Westinghouse plants with large dry or subatmospheric containments is 113.1 psig. Ice condenser containments can afford to be less robust because of their reliance on ice beds as a pressure suppression feature for design basis accidents.

Table 6.1 Containment fragility

| PLANT | Design Press. psig | Cont. Press (psig) @ | | | Cont. Press/Design Press. @ | | |
|-----------------|-----------------------|----------------------|----------|----------|-----------------------------|----------|----------|
| | | Freq=0.01 | Freq=0.1 | Freq=0.5 | Freq=0.01 | Freq=0.1 | Freq=0.5 |
| Catawba | 15 | 61 | 71 | 85 | 4.07 | 4.73 | 5.67 |
| Cook | 12 | 37 | 45 | 58 | 3.08 | 3.75 | 4.83 |
| McGuire | 15 | 57 | 65 | 77 | 3.80 | 4.33 | 5.13 |
| Sequoyah | 10.8 | 55 | 62 | 69 | 5.09 | 5.74 | 6.39 |
| Sequoyah-N/1150 | 10.8 | 28 | 47 | 64 | 2.59 | 4.35 | 5.93 |
| Watts Bar | 15 | 56 | 71 | 90 | 3.73 | 4.73 | 6.00 |
| Summary Info.* | | | | | | | |
| Mean | 19.2 | 53.2 | 62.8 | 75.8 | 3.2 | 3.8 | 4.6 |
| STD | 8.2 | 8.4 | 9.6 | 11.4 | 1.1 | 1.3 | 1.5 |
| STD/Mean | 0.43 | 0.16 | 0.15 | 0.15 | 0.36 | 0.35 | 0.34 |

*Does not include Sequoyah-N/1150.

It is to be anticipated that the fragility curves derived for a specific containment are sensitive to local design details, tolerances, and the design philosophy used for that particular containment. While it is likely that various submodels representing different local containment failure modes may be applicable to a variety of containments of a given type, it is also true that the combination of failure mechanisms existing in a given containment is unique. Thus, the reader is cautioned against reading any generic applicability into the fragility curves developed for any specific containment. We, therefore, use the plant-specific IPE fragility curve in our analyses, consistent with previous DCH resolution activities (NUREG/CR-6338).

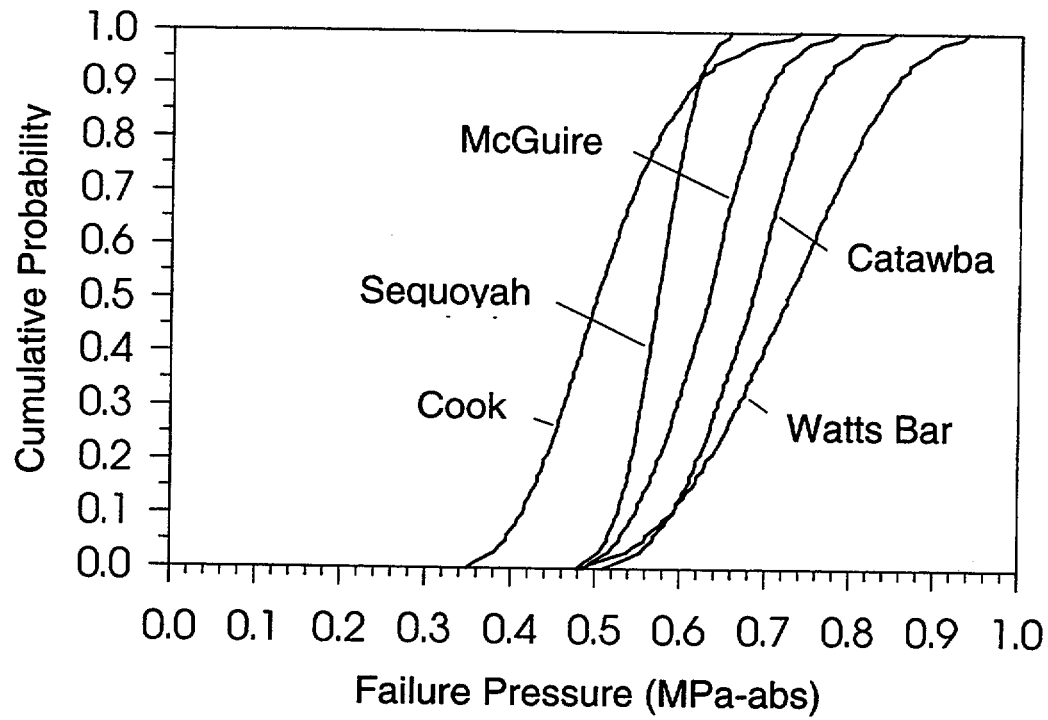


Figure 6.1 Fragility curves for all Westinghouse plants with ice condenser containments

7.0 RESULTS AND SENSITIVITIES

7.1 Benchmark Evaluations

The simplified CET described in Section 4.0 was evaluated for Sequoyah using quantifications consistent with NUREG-1150 quantifications for Sequoyah. The objective of this "benchmark" evaluation was to verify the adequacy of a simplified CET in reasonably representing the NUREG-1150 intent. Specifically, we wanted to ensure that all the *key* top events that influence early containment failure in NUREG-1150 were identified and adequately represented in the simplified CET.

Table 7.1 summarizes key results of the benchmark evaluations related to core damage arrest and the RCS pressure at vessel breach if core damage arrest does not occur. Results of the benchmark evaluations are compared to results obtained from NUREG-1150. The comparisons, on a CDI-specific basis and on a CDI-weighted based, confirm that the logic and quantifications related to HPME probabilities are adequately understood and captured in our CET.

Specific results are of interest as well. Despite the importance of core damage arrest (approximately 39%), the HPME probability is still quite large (approximately 35%). This is because hot leg or surge line failures are only significant in NUREG-1150 when the PORVs are cycling at the system setpoint.

Table 7.2 summarizes key results of the benchmark evaluation related to early containment failure modes and probabilities. Results of the benchmark evaluation are compared with results obtained from NUREG-1150. The comparisons, on a CDI-specific basis and on a CDI-weighted basis, confirm the logic and quantifications related to early containment failure. Specific comparisons are of interest as well. Note that non-DCH overpressure failures (approximately 5.4%) are comparable (on a CDI-weighted basis) to the sum (approximately 5.6%) of DCH overpressure failures and liner failures. Furthermore, the total early containment failure probability is comparable to the CCFP less than 10% criterion established by the NRC. Consequently, DCH must be evaluated in the context of all significant early containment failure modes.

7.2 Extrapolation Evaluations

The CET for extrapolation evaluations was simplified even further, as described in Section 4.0, relative to the already simplified CET used in the benchmark evaluations. This added simplification in logic is derived from the following:

- (1) Initiator leaks being associated only with LOCAs.
- (2) The elimination of recovered station blackouts as low probability events.
- (3) Core damage arrest is limited to some LOCAs and core damage arrest only occurs when the RCS pressure is low.

Table 7.1 Detailed comparison of (benchmark) lower head failure probabilities with Full NUREG-1150 results

| Core Damage Initiator | Mean CDI Cond Freq | CDI Conditional | | | | | Total LH Failures Press > 100 psi | |
|--------------------------|--------------------|--------------------|--------------------------|---------------------------|--------------------------|---------------|-----------------------------------|--|
| | | Core Damage Arrest | LH Failures At SSP Press | LH Failures At High Press | LH Failures At Int Press | | | |
| 1 Slow SBO | 0.0827 | 0.6161 | 0.0006 | 0.1173 | 0.1237 | 0.2416 | SNL | |
| | | 0.5400 | 0.0050 | 0.0970 | 0.1100 | 0.2120 | N/1150 | |
| 2 Fast SBO | 0.1671 | 0.3388 | 0.0336 | 0.0734 | 0.1406 | 0.2477 | SNL | |
| | | 0.3500 | 0.0200 | 0.0720 | 0.1630 | 0.2550 | N/1150 | |
| 3 LOCAs | 0.6289 | 0.3878 | 0.0000 | 0.1930 | 0.2324 | 0.4254 | SNL | |
| | | 0.3690 | 0.0000 | 0.1700 | 0.2000 | 0.3700 | N/1150 | |
| 4 Interfacing LOCA | 0.0.117 | | | | | | | |
| 5 Transients | 0.0413 | 0.7956 | 0.1160 | 0.000 | 0.0100 | 0.1260 | SNL | |
| | | 0.7900 | 0.1100 | 0.0000 | 0.0110 | 0.1210 | N/1150 | |
| 6 ATWS | 0.0377 | 0.0951 | 0.0013 | 0.1205 | 0.2010 | 0.3228 | SNL | |
| | | 0.1000 | 0.0030 | 0.0800 | 0.2200 | 0.3030 | N/1150 | |
| 7 SGTR | 0.0306 | | | | | | | |
| 8 Internal Flood | 0.0000 | | | | | | | |
| Total CDI Weighted Total | 1.0000 | 0.3879 | 0.0105 | 0.1479 | 0.1879 | 0.3463 | SNL | |
| | | 0.3716 | 0.0084 | 0.1300 | 0.1709 | 0.3093 | N/1150 | |
| Mean CD Freq | 5.57E-05 | | | | | | | |

Note: Table entries here and in subsequent tables are typically to four significant figures. This is not to imply that the listed probabilities are known to this accuracy. The four digits allow the reader to more clearly follow the arithmetic without roundoff reducing, small but finite, values to zero.

Table 7.2 Comparison of (benchmark) early containment failure modes with full NUREG-1150 results

| Core Damage Initiator | Mean CDI Cond Freq | CDI Conditional | | | | | Total Early Cont Fail Prob | |
|--------------------------|--------------------|-------------------------|-------------------------|-------------------------|-------------------------|-------------------------|----------------------------|--|
| | | Core Damage Arrest | VB > 200 psi Prob | DCH Or Liner Fail Prob | Non-DCH Op Fail Prob | | | |
| 1,2 SBO | 0.2498 | 0.4306 0.4140 | 0.2456 0.2390 | 0.0700 0.0640 | 0.1603 0.1060 | 0.2303 0.1700 | SNL N/1150 | |
| 3 LOCAs | 0.6289 | 0.3878 0.3690 | 0.4254 0.3700 | 0.0574 0.0310 | 0.0186 0.0200 | 0.0759 0.0510 | SNL N/1150 | |
| 4 Interfacing LOCA | 0.0117 | | | | | | | |
| 5 Transients | 0.0413 | 0.7956 0.7900 | 0.1260 0.1210 | 0.0179 0.0140 | 0.0088 0.0050 | 0.0267 0.0190 | SNL N/1150 | |
| 6 ATWS | 0.0377 | 0.0951 0.1000 | 0.3228 0.3030 | 0.0464 0.0230 | 0.0539 0.0270 | 0.1004 0.0500 | SNL N/1150 | |
| 7 SGTR | 0.0306 | | | | | | | |
| 8 Internal Flood | 0.0000 | | | | | | | |
| Total CDI Weighted Total | 1.0000 | 0.3879 0.3719 | 0.3463 0.3088 | 0.0561 0.0369 | 0.0541 0.0403 | 0.1102 0.0772 | SNL N/1150 | |
| Mean CDI Freq | 5.57E-05 | | | | | | | |

Results and Sensitivities

- (4) The evaluation of DCH loads for only one value (8 MPa rather than three ranges) of RCS pressure at vessel breach.

The net impact of some of these simplifications is to introduce a small conservative bias towards high pressure failure mechanisms, i.e., DCH overpressure failures and containment liner failures more likely. The benefits are that the CET logic and quantifications become more scrutable. The HPME and containment failure elements of these simplified trees were illustrated in Figures 4.1-4.12 for each CDI in the extrapolation evaluation for the Sequoyah plant. The logic remains the same for the remaining ice condenser plants; however, some of the branch probabilities are different as described in Section 4.

Table 7.3 provides insight into the dominant contributors to early containment failure modes for Sequoyah; however, these insights are equally applicable to all the ice condenser plants. Non-DCH containment overpressure processes are the dominant contributors to early containment failure (approximately 90%) in ice condenser plants. These non-DCH processes are dominated by hydrogen burns in SBO accidents. In the absence of hydrogen control (i.e., igniters not operational in SBOs), ice condenser plants are known to be vulnerable to hydrogen combustion events alone, and the results of Table 7.3 clearly reflect this vulnerability as well. The importance of hydrogen is further evidenced by that fact that approximately 2/3 of the pressure rise in a DCH event (SBO) is attributable to combustion of the pre-existing hydrogen, with the remaining approximately 1/3 attributable to the more fundamental DCH processes of debris dispersal, debris fragmentation, and debris/gas heat transfer. **The relative non-significance of DCH to integral assessments of early containment failure is the most important result of this study.** This means that safety considerations should focus first on hydrogen combustion issues and not on DCH processes.

Table 7.3 also shows that the probability of liner failure is zero in the base case evaluations. There are two reasons. First, in SBO the DCH overpressure failure probability is essential unity.¹³ Second, the logic does not allow for liner failures when the cavity is deeply flooded, which is the case here for non-SBOs. Sensitivity study 10 addresses the case when substantial ice remains and the cavity is essentially dry, which allows the possibility of liner failures.

The contribution of DCH overpressure failures and containment liner failures are not dominant in this study for two reasons. First, the dominant sequences are non-SBOs for which the cavity is deeply flooded and the DCH event is treated as a non-threatening steam spike. Secondly, the SBO frequency is small (approximately 0.03 for Sequoyah) and the HPME probability is small (approximately 0.07) so that the CDI-weighted probability of DCH overpressure failure is smaller still ($P \sim 0.03 \times 0.07 \sim 0.002$) even if the containment fails every time there is a DCH event in a SBO.

Table 7.3 shows the probability of core damage arrest, which occurs in the current study only for the LOCA CDI and only for those sequences that evolve to lower pressure.

¹³ Note that the HPME probability and the DCH overpressure failure probability (both conditional on core damage in a SBO) are identical to three significant digits.

Table 7.3 Summary of base case results using Sequoyah IPE input

| Core Damage Initiator | Mean CDI Cond Freq | CDI Conditional | | | | | Total Cont Fail Prob |
|-----------------------|-----------------------|-----------------------|--------------|---------------------|--------|----------------------|-------------------------|
| | | Core Damage Arrest | HPME Prob | DCH OP Fail Prob | Liner | Non-DCH Fail Prob | |
| 1 Slow SBO | 0.0103 | 0.0000 | 0.0718 | 0.0718 | 0.0000 | 0.9021 | 0.9739 |
| 2 Fast SBO | 0.0207 | 0.0000 | 0.0718 | 0.0718 | 0.0000 | 0.9021 | 0.9739 |
| 3 LOCAs | 0.1802 | 0.6312 | 0.0649 | 0.0000 | 0.0000 | 0.0000 | 0.0000 |
| 4 Interfacing LOCA | 0.0001 | | | | | | |
| 5 Transients | 0.6684 | 0.0000 | 0.0718 | 0.0000 | 0.0000 | 0.0000 | 0.0000 |
| 6 ATWS | 0.0413 | 0.0000 | 0.0718 | 0.0000 | 0.0000 | 0.0000 | 0.0000 |
| 7 SGTR | 0.0395 | | | | | | |
| 8 Internal Flood | 0.0395 | 0.0000 | 0.0718 | 0.0000 | 0.0000 | 0.0000 | 0.0000 |
| Total | 1.0000 | | | | | | |
| Mod CDI Wgted Total | | 0.1137 | 0.0677 | 0.0022 | 0.0000 | 0.0280 | 0.0302 |
| Mean CD Freq | 1.70E-04 | | | | | | |

Results and Sensitivities

Consequently, core damage arrest might only be important in determining non-DCH loads at low RCS pressures. Because best estimate steam spike loads are not containment threatening, core damage arrest has no impact on the results of this study. Core damage arrest played a much more important role in the NUREG-1150 study because it *also* precluded lower head failure for other CDIs and in some additional scenarios that otherwise would have lead to containment threatening DCH and liner attack events.

Table 7.4 shows that all plants, except McGuire, have early containment failure probabilities (full power internal events given core damage) in the range of 0.35% to 5.8%. These integral results of early containment failure are qualitatively consistent with published IPE results for these plants. The early containment failure probability was 13.9% for McGuire. The higher containment failure probability is dominated by the high SBO frequency and the relatively weak containment for McGuire. We have not investigated why our assessment for McGuire is seven times larger than the IPE value of 2%.

For perspective, we note that the DCH overpressure failure probability was less than or equal to 10^{-3} for the vast majority of PWRs with large dry or subatmospheric containments (Pilch et al. 1996 and Pilch et al. 1997). Because DCH is thought to be the dominant mode of early containment failure in most of these PWRs, we conclude that ice condenser plants are at least two orders of magnitude more vulnerable to early containment failure than other types of PWRs. This relative ranking of ice condenser plants with the remaining PWRs is generally consistent with perceived notions; but surprisingly, it is not consistent with results summarized from the IPEs themselves. Summarizing IPE results, NUREG-1560 (NRC 1996) showed that a large number of PWRs with large dry or subatmospheric containments report mean early containment failure probabilities in excess of 10%, while none of the ice condenser plants reported early failures greater than 2.4%. NUREG-1560 further cites DCH processes as the main contributor to early containment failure in PWRs with large dry or subatmospheric containments. In light of more recent NRC estimates (Pilch et al. 1996 and Pilch et al. 1997), we conclude without judging the relative quality of the IPEs, that many utilities with large dry or subatmospheric containments must have been overly conservative in their treatment of HPME probabilities and DCH loads.

The early containment failure estimates of this study are restricted to full power internal events. Bypass events, low power shutdown events, and external events must be considered to have a complete risk informed perspective of early containment failure risk. We note, however, that bypass events have nothing to do with DCH. Furthermore, HPME/DCH processes are not likely to occur in low power shutdown events because the RCS pressure is expected to be low; however, there are some scenarios where loss of RHR could lead to repressurization if the pressure boundary is sealed.

The core damage phenomenology for external events is similar to that for internal events. Risk-informed regulation could be better served if insights from this study were factored into fully integrated assessments of risk for ice condenser plants.

Table 7.5 shows the relative contributions of external events and internal events to total core damage frequency. For Catawba and McGuire, the CDF associated with external events can be a

Table 7.4 Early containment failure probability for all ice condenser plants

| | Sequoyah NUREG- 1150 | Catawba | D.C. Cook | McGuire | Sequoyah | Watts Bar | |
|--------|----------------------------|---------------|--------------|-------------|---------------|---------------|---|
| | 0.0772 | 0.0048 | 0.015 | 0.02 | 0.0165 | 0.0235 | Early containment failure from NUREG-1150 or IPE |
| Case # | | | | | | | Case Description |
| 1 | 0.1102 | | | | | | Benchmark of simplified tree to full NUREG-1150 results |
| 2 | | 0.0035 | 0.0170 | 0.1392 | 0.0302 | 0.0582 | Base case |
| 3 | | 0.0035 | 0.2051 | 0.1404 | 0.0352 | 0.0613 | Sensitivity: Revised steam spike loads using UB of mass distribution, sprays, no ice |
| 4 | | 0.0035 | 0.0170 | 0.1392 | 0.0302 | 0.0582 | Sensitivity: Case 2 + intentional depress (accident mgmt strategy) |
| 5 | | 0.0035 | 0.0170 | 0.1397 | 0.0302 | 0.0588 | Sensitivity: Case 2 + stuck open PORV (P=0.0) |
| 6 | | 0.0055 | 0.0173 | 0.1699 | 0.0304 | 0.0980 | Sensitivity: Case 2 + hot leg failure suppression to P=0.5 for SBOs, P=0.1 for non-SBOs |
| 7 | | 0.0002 | 0.0006 | 0.0041 | 0.0005 | 0.0038 | Sensitivity: Case 2 + DC igniters for SBOs (accident mgmt strategy) |
| 8 | | 0.0035 | 0.0257 | 0.1392 | 0.0302 | 0.0582 | Sensitivity: Sprays not available in LOCA, steam spike with BE core mass |
| 9 | | 0.0035 | 0.2646 | 0.1404 | 0.0677 | 0.0744 | Sensitivity: Sprays not available to LOCA, steam spike with UB core mass |
| 10 | | 0.0203 | 0.0310 | 0.1517 | 0.0459 | 0.0703 | Sensitivity: Dry cavity, non-SBO with ice |
| 11 | | 0.0087 | 0.0268 | 0.2319 | 0.0082 | 0.1291 | Sensitivity: -0.1 MPa fragility bias (weaker containment) |
| 12 | | 0.0008 | 0.0130 | 0.0369 | 0.0082 | 0.0177 | Sensitivity: +0.1 Mpa fragility bias (stronger containment) |

Table 7.5 Comparison of external events and internal events core damage frequencies

| | Fire | Seismic | Total External¹ | Total Internal² | Total |
|-----------|--|----------------------|-----------------------------------|-----------------------------------|-----------------------|
| Sequoyah | 1.6×10^{-5} | Margin ³ | 1.6×10^{-5} | 1.7×10^{-4} | 1.86×10^{-4} |
| Watts Bar | 7.0×10^{-6} | Margin | 7.0×10^{-6} | 8.0×10^{-5} | 8.70×10^{-5} |
| Catawba | 4.7×10^{-6} | 1.6×10^{-5} | 2.1×10^{-5} | 5.8×10^{-5} | 6.01×10^{-5} |
| McGuire | 2.3×10^{-7} | 1.1×10^{-5} | 1.1×10^{-5} | 4.0×10^{-5} | 5.1×10^{-5} |
| Cook | 3.8×10^{-6} | 3.2×10^{-6} | 7.0×10^{-6} | 6.3×10^{-5} | 7.0×10^{-5} |
| 1 | IPEEE | | | | |
| 2 | IPE | | | | |
| 3 | Some plants performed a margin analysis rather than quantify the core damage frequency for seismic events. | | | | |

significant contributor (21% and 35%, respectively) to the total CDF for these types of events. SBO-like events have a very high containment failure probability. Seismic (external) events often lead to loss of offsite power. Internal fires¹⁴ can also lead to loss of offsite power; however, the vulnerability is more plant specific. The IPEEEs should be useful in quantifying the SBO frequency associated with internal events, but it is outside the scope of this report to summarize this information. Consideration of lower power shutdown events and internal events will increase the total early containment failure probability; however, it will not change the basic conclusion that hydrogen, not the more fundamental DCH process, is the dominant contributor to early failures.

7.3 Sensitivity Studies

It is outside the scope of this study to perform a fully integrated uncertainty study as was done for NUREG-1150. We note, however, that the uncertainties in early containment failure are large for Sequoyah in NUREG-1150 with the early containment failure probability ranging from 0.02% to 70%. Although specific to the NUREG-1150 study and the Sequoyah plant, we might reasonably expect large uncertainties from this study for all ice condenser plants if a fully integrated uncertainty study were performed. However, we concluded here that DCH processes are second order contributors to early containment failure; consequently, we believe that uncertainties in early containment failure will be dominated by contributors other than the dispersal processes, fragmentation processes, and debris/gas heat transfer processes that are fundamental to DCH. We recognize that PRA studies ideally should be accompanied by uncertainty quantification for a more complete risk-informed assessment. However, the NRC has traditionally regulated on mean values and has required uncertainty studies only when utilities petition the NRC for regulatory relief on some issue.

In lieu of a formal sensitivity study, we perform selected sensitivity studies to further illuminate the importance of certain quantifications and assumptions and to examine the possible consequences of certain accident management procedures that might be proposed. The results of these one-at-a-time sensitivity studies are summarized in Table 7.4.

A sensitivity study (case 3) was performed using high-mass steam spike loads (assuming sprays are operating but no ice) for all plants. Only D.C. Cook shows a dramatic increase in early containment failure probabilities. We acknowledge that this sensitivity exists because this study also concluded that the ice inventory would be completely melted by the time of vessel breach in non-SBO accidents without auxiliary feedwater. In this case where auxiliary feedwater is available, substantial ice could remain and we expect this ice to be effective at suppressing even upper bound steam spike loads. D.C. Cook's sensitivity to steam spike loads is also attributable to the fact that we took no credit for lower compartment sprays, which are unique to D.C. Cook.

We consider next the impact of various quantifications on HPME probabilities and their subsequent impact on early containment failures. Lacking a credible human reliability analysis and consistent with NUREG-1150, we take no credit for intentional depressurization of the RCS

¹⁴ Classified as an external event in the IPEEEs.

Results and Sensitivities

after UTAF. As a sensitivity study, we assumed that the operators would successfully execute intentional depressurization after UTAF with a 90% probability for all sequences where AC power was available. The HPME probability is reduced by an order of magnitude while Table 7.4 shows that this reduction in HPME probability has negligible impact on early containment failure probabilities.

With the RCS initially cycling at the SSP, NUREG-1150 assigned a mean value of $P = 50\%$ to the probability of a PORV sticking open, while acknowledging large uncertainties with a uniform distribution ranging from $P = 0\%$ to $P = 100\%$. We explored the lower bound ($P = 0\%$) with a sensitivity study (case 5). Table 7.4 shows that the probability of a sticking PORV has negligible impact by itself on early containment failure probabilities. This is because the sticky PORV event is always backed up by a high-probability (90%) hot leg failure event.

Experts for NUREG-1150 assigned the same probabilities of hot leg failure to all CDIs, and we adopted this logic as our base case. At TMI-II, the hot leg did not fail and the reason has not been fully explained to everyone's satisfaction. With AC power available, however, the operators have the added means (e.g., toggling RCS pumps) to disrupt buoyancy-driven flows to the loops or convective drive flows to a stuck open PORV. As a sensitivity, we suppressed the probability of hot leg or surge line failure to 50% for SBOs and 10% for non-SBOs. Table 7.4 shows that early containment failure probabilities increase for plants with large SBO frequencies, but not to the point that conclusions regarding compliance with NRC goals would change.

This insensitivity to depressurization is a surprising result that is explained in three ways. First, the high pressure events and the low pressure events in the non-SBOs are modeled as the same non-threatening steam spike load, because the cavity is deeply flooded. Second, the incremental increase in failure probability in shifting from a hydrogen combustion event to a DCH event during a SBO is relatively small. Third, the SBO probability is small and there are multiple ways for the RCS to depressurize. We note that dry-cavity DCH loads in non-SBOs are nonthreatening as well; consequently, the non-sensitivity of DCH failures to RCS pressure remains for those scenarios where the cavity is not deeply flooded.

Ice condenser plants employ AC-powered igniters for hydrogen control; consequently, igniters are not available in SBO accidents. Control of hydrogen levels is important, because ice condenser plants have a small containment volume and can be sensitive to hydrogen combustion events if hydrogen is allowed to accumulate in the containment. As a sensitivity study, we postulate that DC igniters are available in SBO accidents to limit hydrogen concentrations to "low" values. Table 7.4 shows that early containment failure probabilities are reduced by more than an order of magnitude in all plants and especially McGuire. Previous cost/benefit studies by the utilities generally do not justify the expense in providing hydrogen control in SBO because the core damage frequency is low and because the SBO probability is a small fraction of the core damage frequency for internal events.

The containment event trees were greatly simplified in this study by assuming there is only one dominant plant damage state for each core damage initiator. We recommend that the results of this study be implemented into more complete PRAs, in order to ensure more complete

estimates of early containment failure probabilities. We can explore the impact of some sequence variations through sensitivity studies.

For the class of non-SBO accidents, we assume that the ARFs, hydrogen igniters, and containment sprays are all available. In NUREG-1150 the availability of ARFs (Q14) and igniters (Q13) was 99.9% and 99%, respectively (given AC power); consequently, there is no significant limitation in assuming their availability in general.

Containment sprays (Q6), however, were available only about 49% of the time in Sequoyah (NUREG-1150) for the class of LOCA initiators. Activation or reliability of the containment sprays, pumps, and valving are not the limitation here; instead, the dominant limitation is the short time available to complete a semi-manual switchover to recirculation when the RWST runs dry. Sequoyah and Watts Bar have a semi-automatic switchover that requires manual isolation of the RWST. D.C. Cook requires both manual switchover and manual isolation of the RWST. The IPEs for these plants identified this issue as a vulnerability and remediations were proposed. It remains to be confirmed that appropriate actions were fully implemented and that these actions are effective at ensuring reliable switchover to recirculation mode and the continued availability of sprays for all accident sequences. Catawba and McGuire have a fully automatic switchover to recirculation mode, so this is not an issue for these two plants.

As a sensitivity study (Table 7.4, cases 8 and 9), we examined the impact on early containment failure under the assumption that sprays are not available 50% of the time during LOCA initiators. The results remain the same for Catawba and McGuire because they have a fully automatic switchover to recirculation mode and are not vulnerable to this issue. Early containment failures increase for D.C. Cook, Sequoyah, and Watts Bar, but only D.C. Cook increases beyond a 10% early containment failure probability in the limited case where the steam spike is calculated with the upper bound melt mass. As noted previously, we expect no sensitivity to steam spike loads for those scenarios where significant ice remains. D.C. Cooks sensitivity to UB steam spike loads is also attributable, in part, to the fact that we took no credit for lower compartment sprays.

The results of this study take on a binary characteristic (containment fails in SBO and survives in non-SBOs), which can be attributed to simplifications in the CET and the use of point values. Here we examine how these binary results might change in consideration of uncertainties in the sequence frequency, phenomenological uncertainties, and uncertainties in fragility.

We used a simplified CET that assumes that all sequences within a class of core damage initiators has the same plant damage state. We examined as a sensitivity study the possibility that switchover to recirculation mode might not be achieved in a timely manner for those plants that have a manual procedure. This could lead to spray failure in some LOCAs, but the containment failure probability was not significantly altered. More important might be CDIs, such as transients, that might include sequences that evolve into a SBO-like scenario where igniters and ARFs are not available. We could find no such PDS in NUREG-1150, and the binning of such sequences might be a plant specific issue.

Results and Sensitivities

Table 7.6 summarizes key phenomenological uncertainties and assumptions. During SBOs, uncertainties in containment loads are dominated by uncertainties in hydrogen combustion phenomena and the amount of clad oxidized during core degradation. For non-SBOs, uncertainties in containment loads are dominated by uncertainties in steam spike modeling, the availability of sprays, and the melt mass that participates in the steam spike. As explained previously, this study concludes that early containment failure is relatively insensitive to intentional or unintentional depressurization mechanisms.

Peer reviewers have commented on previous DCH resolution documents, stating that the low end tails of the fragility curve might be uncertain or arbitrary. As a sensitivity, we arbitrarily bias the IPE-reported fragility curves to the left (weaker) or to the right (stronger) by 0.1 MPa. Similar sensitivity studies have been performed in previous DCH reports. The results are summarized as cases 11 and 12 in Table 7.4. Assuming the weaker containment, only Watts Bar exhibits an increase in the early containment failure probability above 10% when the base case is below 10%. Assuming the stronger containment, all plants exhibit an early containment failure probability less than 10%.

Having examined DCH issue in some detail and in the context of all early containment failures, we can summarize our insights for DCH alone in a simple way for the most sensitive plant, McGuire, as shown in Table 7.7. We divide the sequences in SBOs and non-SBOs and note that the SBO probability is generally low. We divide the RCS pressure at vessel breach (assuming it occurs) into high (DCH-relevant) and low categories. RCS depressurization after UTAF can occur because of initiator leaks, induced leaks, and intentional depressurization. Discussions in this report suggest that an upper bound to the probability of high pressure at vessel breach is 10%.

Steam spike loads and dry-cavity DCH loads are not containment threatening for any reasonable PDS associated with non-SBO events. Hydrogen combustion alone can be containment threatening in SBO events because igniters are not available to control hydrogen concentrations before vessel breach. Although a significant threat if they occur, DCH events in SBOs are unlikely because the SBO probability is low and because the probability of DCH-relevant RCS pressures at vessel breach are low. Furthermore, combustion of pre-existing hydrogen can be the most significant contributor to DCH loads rather than the more fundamental DCH processes of dispersal, fragmentation, and debris/gas heat transfer. In summary, hydrogen combustion issues, not DCH, dominate contributors to risk in ice condenser plants.

Table 7.6 Summary of key phenomenological assumptions, uncertainties, and their implications

| | SBO | Non-SBO |
|-------------------------------------|---|--|
| Plant Damage State | <ul style="list-style-type: none"> Igniters and ARFs are not available-<i>This leads directly to high hydrogen concentrations and hydrogen combustion loads.</i> Sprays are not available. Significant ice remains at vessel breach. Cavity is dry. | <ul style="list-style-type: none"> Igniters are available. ARFs are available Sprays are available, except possibly in some LOCAs where the operators fail to switch to recirculation mode. Auxiliary feedwater-<i>Plays a key role in determining if ice remains at vessel breach and if the cavity is deeply flooded..</i> |
| Hydrogen Combustion Loads (non-DCH) | <ul style="list-style-type: none"> Random ignition prior to vessel breach is not quantified-<i>Random ignition could lead to less threatening loads if it occurs before the full potential for hydrogen release from the RCS has occurred.</i> 49% clad oxidation assumed- <i>Clad oxidation could be on the range of 15-65% with 35-45% taken as a best estimate. This range of clad oxidation translates into a range of hydrogen combustion loads.</i> Detonations in the ice chest or upper plenum are not quantified-<i>Hydrogen release from the RCS that is sufficient to create detonable concentrations in the ice chest or upper plenum are also sufficient to lead to energetic deflagrations in the upper dome. For our hydrogen concentrations on the dome, deflagrations would fail containment 97% of the time in Sequoyah while detonations in the upper plenum would fail containment ~30% of the time. As a practical matter, detonations in the ice chest or upper plenum can be neglected.</i> | <ul style="list-style-type: none"> Igniters are assumed effective at keeping both global and local hydrogen concentrations below flammable levels. Detonations in the ice chest or upper plenum are not quantified-<i>NUREG-1150 experts judged that detonable concentrations of hydrogen will not accumulate in the upper plenum or ice condenser if the ARFs are running.</i> ARFs do not allow locally high concentrations of hydrogen to develop. |
| Steam Spike Loads | <ul style="list-style-type: none"> The cavity is dry, steam spikes are not possible. | <ul style="list-style-type: none"> Cavity deeply flooded (Y/N)-<i>Steam spikes are only an issue if the cavity is deeply flooded.</i> In the CONTAIN analyses, debris energy that goes into heating water to saturation (sensible heat) is neglected and steam is sourced into containment over 5 s-<i>This maximizes the steam source while minimizing the impact of structures and sprays on mitigating the steam spike.</i> Best estimate (BE) melt mass used in the loads calculations assuming sprays are operational-<i>There is no benefit from lower bound (LB) melt masses because the BE masses are already non-threatening. If sprays are not operational, containment-threatening loads are realized for all plants for upper bound (UB) (but low probability) melt masses. No credit for lower compartment spray in D.C. Cook.</i> |

Table 7.6 Summary of key phenomenological assumptions, uncertainties, and their implications (continued)

| | SBO | Non-SBO |
|--|---|---|
| Steam Spike Loads (continued) | | <ul style="list-style-type: none"> Dynamic loads from steam explosions not quantified-<i>This treatment is consistent with NUREG-1150. In addition, structures are typically more sensitive to static loads than to dynamic loads, and the containment is sensitive to steam spike loads only for a limited range of conditions.</i> |
| DCH Loads Coupled with Hydrogen Combustion Loads | <ul style="list-style-type: none"> Loads calculated for UB of mass distribution and 49% clad oxidation- <i>The DCH threat cannot be reduced below the hydrogen threat and hydrogen combustion is already threatening in most plants. Reducing the DCH threat would be partially offset by liner failures, which becomes possible if the containment does not fail by DCH.</i> Phenomenological uncertainties that might lead to higher loads are not addressed explicitly- <i>DCH loads are already containment threatening (83-100%) and other assumptions leading to higher loads cannot make things significantly worse.</i> | <ul style="list-style-type: none"> Dry-Cavity DCH loads are non-threatening. No hydrogen combustion contribution-<i>Igniters are operational.</i> DCH treated as a "steam spike" in a deeply flooded cavity-<i>This is treatment consistent with NUREG-1150, and there is limited experiment data to confirm this assumption</i> In the CONTAIN steam spike analyses, sensible heat of water is neglected and steam is sourced into containment over 4s-<i>This maximizes the steam source and minimizes the impact of structures and sprays on mitigating the steam spike.</i> BE melt mass used in the loads calculations assuming sprays are operational-<i>There is no benefit from LB melt masses because the BE masses are already non-threatening. If sprays are not operational, containment-threatening loads are realized for all plants for UB (but low probability) melt masses. No credit for lower compartment sprays in D.C. Cook.</i> Dynamic loads from steam explosions not quantified-<i>This treatment is consistent with NUREG-1150. In addition, structures are typically more sensitive to static loads than to dynamic loads, and the containment is sensitive to steam spike loads only for a limited range of conditions.</i> |
| Hot Leg Failure Probability | <ul style="list-style-type: none"> Hot leg failure probability determines split between HPME events and non-HPME events-<i>Results are not sensitive to hot leg failure probability because hydrogen combustion events are already containment threatening (22-100%) and hydrogen combustion events coupled with DCH cannot be any worse than assured containment failure; consequently, any switch from a DCH event to a hydrogen combustion event does not generally realize a large incremental reduction in containment failure.</i> | <ul style="list-style-type: none"> Hot leg failure probability determines split between HPME events and non-DCH events-<i>Results are not sensitive to hot leg failure probability because both high pressure and low pressure events are both treated as a BE (non-threatening) steam spike in this analysis.</i> |

Table 7.7 Simplified snapshot of DCH assessments for McGuire

| | | Sequence | |
|-------------------------------|--------------------------------------|--|--|
| | | SBO $p_1 = 0.239$ | Non-SBO $P_1 = 0.761$ |
| RCS Pressure at Vessel Breach | High ($P > 200$ psi) $P_2 = 0.1$ | <ul style="list-style-type: none"> • DCH (1/3) with combustion of pre-existing hydrogen (2/3). • Loads are threatening $p_{fail} = 0.98$. • Likelihood is very low $P_3 = P_1P_2 = 0.024$ • Conditional Failure $P = P_3P_{fail} = 0.024$ | <ul style="list-style-type: none"> • Steam spike or DCH. • Loads are non-threatening $P_{fail} = 0$ • Likelihood is low $P_3 = P_1P_2 = 0.076$ • Conditional Failure $P = P_3P_{fail} = 0$ |
| | Low ($P < 200$ psi) $P_2 = 0.9$ | <ul style="list-style-type: none"> • Non-DCH hydrogen combustion • Loads are threatening $P_{fail} = 0.55$ • Likelihood is low $P_3 = P_1P_2 = 0.215$ • Conditional failure $P = P_3P_{fail} = 0.118$ | <ul style="list-style-type: none"> • Steam spike or gravity pour into dry cavity • Loads are non-threatening $P_{fail} = 0$ • Likelihood is high $P_3 = P_1P_2 = 0.685$ • Conditional failure $P = P_3P_{fail} = 0$ |

8.0 SUMMARY AND RECOMMENDATION

This report (NUREG/CR-6427) addresses the DCH issue for all Westinghouse plants with ice condenser containments. There are ten operating ice condenser plants located at five sites in the U.S. DCH phenomena in ice condenser plants are different in some important aspects from DCH phenomena in plants with large dry or subatmospheric containments. Ice condenser plants are unique among PWRs in that they have ice beds to suppress DBA steam loads, AC-powered igniters to control hydrogen concentrations in the atmosphere, small containment volumes, and containment buildings with low ultimate capacities for pressure.

The most significant finding of this study was that the early containment failure probability is dominated by non-DCH hydrogen combustion events (which only occur during station blackouts) rather than DCH events. This is because the station blackout (SBO) probability is small, the HPME probability is small, and because containment loads are non-threatening for any reasonable plant damage state (PDS) associated with a non-SBO.

Initially, the methodology developed in NUREG/CR-6075 and NUREG/CR-6075, Supplement 1, was used to perform a load versus strength evaluation for each of these plants using plant-specific data gathered from IPEs, Final Safety Analysis Reports (FSARs), and direct contacts with plant personnel (when necessary). The same enveloping accident scenarios (splinters) that were used in NUREG/CR-6075, Supplement 1, and NUREG/CR-6109 were used for these plant evaluations under the assumption that a DCH event occurs. One additional splinter scenario, unique to plants with ice condenser containments, was also considered. These splinter scenarios establish important input parameters for the DCH load calculations, e.g., the RCS pressure at vessel breach, the melt mass and composition, the RPV breach size, the containment pressure and atmosphere composition at vessel breach, etc. The initial approach taken was to model the ice condenser plant as a small dry containment without taking credit for the passive pressure suppression afforded by the ice beds or the active pressure suppression afforded by containment sprays. Scenarios with deeply flooded cavities were not analyzed. Assuming core damage and a HPME/DCH event, all ice condenser plants exceeded the metric (conditional containment failure probability, CCFP ≤ 0.1) based on DCH-induced overpressure failures alone. Consequently, the DCH issue could not be resolved based on load/strength evaluations alone if a DCH event was postulated, and credit for ice beds, sprays, and igniters is not taken.

This initial assessment of DCH in ice condenser plants was reviewed by a NRC-sponsored panel of six experts who are familiar with the phenomenology and the DCH issue resolution process. Reviewer comment and recommendations fell into three general categories:

- (1) Expand the probabilistic framework to include sequence probabilities.
- (2) Validate CONTAIN's ice condenser models if CONTAIN is to be used in the load calculations.
- (3) Model the ice condenser explicitly in the loads calculations.

Summary and Recommendation

This final revision of NUREG/CR-6427 explicitly addresses these peer review comments. The approach taken is to provide an expansion of the probabilistic framework, which represents a simplification of the NUREG-1150 containment event tree for Sequoyah. The probabilistic framework addresses DCH-induced overpressure failures in the context of all significant early containment failure modes. These include DCH overpressure failures, thermal failures of the containment liner, non-DCH hydrogen combustion overpressure failures, and non-explosive steam spike overpressure failures.

The following practical approach was adopted for assessing the importance of HPME/DCH to early containment failure for all ice condenser plants.

- (1) Develop a simplified version of the NUREG-1150 containment event tree (CET) that operates on each core damage initiator (CDI) as a class (e.g., LOCAs) and not on the hundreds of plant damage states (PDS) that might be members of a given class.
- (2) Benchmark the simplified tree by demonstrating that the simplified tree, with NUREG-1150 consistent input, reproduces (in a reasonable fashion) the results documented in NUREG-1150 for Sequoyah. This ensures that all significant top events have been identified from the NUREG-1150 study.
- (3) Update specific quantifications in the simplified tree if significant new work since the time of NUREG-1150 justifies the revision. Significant quantifications that were updated include the hot leg failure probabilistic and a reassessment of containment loads using CONTAIN. Additional simplifications of the CET are possible to produce a more scrutable result for extrapolation evaluations.
- (4) Use the more simplified logic CET to evaluate, in a consistent manner, the early containment failure probability for all ice condenser plants (including a reevaluation for Sequoyah) using plant specific information (e.g., fragility and CDI frequencies) to the extent that information is available from the IPEs.

A simplified CET was developed to quantify the HPME probability and the early containment failure probability for each of the six core damage initiator (CDI) classes: slow station blackout, fast station blackout, LOCAs, transients, ATWS, and internal floods. We focus on full power internal events and exclude bypass events such as interfacing LOCAs and steam generator tube ruptures. The HPME portion of the CET quantifies whether core damage is arrested in vessel and at what RCS pressure does vessel failure occur if core damage is not arrested in vessel. The top events are the following:

- (1) RCS leak size at uncover of top of active fuel (UTAF).
- (2) Stuck open PORV during cycling at system setpoint (SP).
- (3) Temperature-induced leak in reactor coolant pump (RCP) seals.
- (4) Intentional depressurization of the RCS.

- (5) Temperature-induced failure of the surge line or hot leg.
- (6) RCS pressure prior to possible vessel failure.
- (7) AC power recovery after UTAF and before vessel breach.
- (8) Core damage arrest in vessel.

The containment failure portion of the CET addresses vessel breach mode/size, the quantity of water in the cavity, and each of the four containment failure mechanisms noted above.

The CONTAIN code was used exclusively to calculate containment loads resulting from DCH, non-DCH hydrogen combustion, and non-explosive steam spikes for representative station blackout and non-station blackout scenarios. The ice condenser model in CONTAIN was recently benchmarked against Waltz Mill data (full-height tests for ice condenser performance) for DBA conditions. CONTAIN has also been benchmarked against key experiments that emphasize each of the three sources of containment loads noted above. However, there are no integral DCH tests in ice condenser geometry to fully validate CONTAIN for this application.

Steam sources were taken from a SCDAP/RELAP5 SBO calculation and used as input to a CONTAIN code model of the ice condenser containment. CONTAIN predicted that approximately half the ice remained at the time of vessel breach. A fully consistent calculation of ice inventory for non-SBO events was not performed as part of this study, but a review of NUREG-1150 quantifications shows that 10-50% of the ice remains at the time of predicted vessel breach for DCH relevant scenarios. NUREG-1150 quantifications showed total or almost total ice melt for a number of scenarios; these tended to be cases involving large LOCAs or induced large LOCAs that preclude DCH.

CONTAIN calculations performed in support of the present effort show that there is a potential for the ice to be considerably more effective in preventing threatening DCH loads than indicated by the earlier studies, provided igniters (and ARFs) are operating prior to vessel breach. The principal reason is that the combination of limited metal in the melt and oxygen starvation in the lower containment resulted in a much smaller contribution from the combustion of DCH-produced hydrogen, and the ice was calculated to be very effective in suppressing pressurization owing to superheated gas and steam.

CONTAIN calculations showed that no ice condenser plant is inherently robust to all credible DCH or hydrogen combustion events in an SBO accident. The containment is threatened by hydrogen combustion events alone because AC-powered igniters are not available to mitigate the accumulation of very high concentrations of hydrogen in the containment. Hydrogen combustion, initiated by and in conjunction with a DCH event, is even more threatening. The ice beds were found to significantly reduce DCH loads in a SBO accident, but not to a level that did not threaten the containment. CONTAIN predicted non-threatening containment loads for non-SBOs provided ice or one train of containment sprays is available. If the refueling water storage tank has emptied and approximately 50% or more of the ice is melted,

Summary and Recommendation

the reactor cavity will be deeply flooded and the nature of containment loads change from DCH to non-threatening steam spikes.

The containment event tree is intended to give each containment challenge its proper probabilistic weighting based on plant specific core damage frequencies, phenomenological probabilities, and plant specific fragility curves. The CET event tree was benchmarked against NUREG-1150 to ensure that all significant top events were reasonably represented in a simplified CET patterned after NUREG-1150. Detailed comparisons proved this to be the case. The CET was further simplified by introducing some conservative assumptions and specific quantifications were updated based on more recent NRC-sponsored research.

A plant-specific evaluation of the CET showed that all plants, except McGuire, had an early failure probability (given core damage) within the range of 0.35% to 5.8% for full power internal events. These integral estimates of early containment failure are qualitatively consistent with published IPE results for these plants. The early containment failure probability, as computed here, was 13.9% for McGuire. This higher containment failure probability for McGuire is dominated by the relatively high SBO frequency and the relatively weak containment for McGuire. The IPE assessments of early containment failure at McGuire (2%) are significantly lower than our assessments; however, we have not investigated the reasons for the difference.

Phenomenological uncertainties are large, but a fully integrated uncertainty study was outside the scope of this effort. However, selected sensitivity studies were performed here to illuminate the importance of certain quantifications and to examine the importance of certain accident management procedures that might be proposed. Reduction in the hot leg failure probability and the probability of a stuck open PORV after UTAF had no significant impact of the results of this study. Reduction in the hot leg failure probability increases the probability of early containment failure for those plants with a large SBO frequency, but not to the point that conclusions regarding compliance with NRC goals would change. An additional sensitivity study assuming intentional depressurization by the operators after UTAF had no impact on the conclusions of this study. All plants, especially McGuire, would benefit from a reduction in SBO frequency or some means of hydrogen control that is effective in SBOs. The resulting risk reduction is greater than an order of magnitude for all plants.

Assuming igniters and air return fans are not operational (e.g. SBOs), uncertainties in containment loads are dominated by uncertainties in hydrogen combustion phenomena and the amount of clad oxidized during core degradation. For non-SBOs, uncertainties in containment loads are dominated by uncertainties in modeling, the availability of sprays, the ice inventory at vessel breach, and the melt mass. We use the mean fragility curves as reported in the IPEs, which have not been reviewed. These fragility curves are steep with a short low-end tail, and any uncertainties in these fragility curves could have a significant impact on computed containment failure probabilities.

Consistent with perceptions of the technical community, this study shows that ice condenser plants are substantially more sensitive to early containment failure than PWRs with large dry or subatmospheric containments. These perceptions, however, are not consistent with IPE results summarized in NUREG-1560 that show many PWRs with large dry or subatmospheric

containments report early containment failure probabilities in excess of 10% given a core damage accident, while none of the ice condenser plants reported early failures greater than 2.4%. NUREG-1560 cites DCH processes as the main contribution to early containment failure in PWRs with large dry or subatmospheric containments. In light of more recent NRC estimates of DCH-induced containment failure probabilities, we conclude that many utilities with large dry or subatmospheric containments were overly conservative in their treatment of HPME probabilities and DCH loads.

To develop a more integrated perspective for risk-informed regulation, it is recommended that the insights of this study be factored into more complete Level II analyses for each significant plant damage state and that the evaluation of early containment failure be evaluated not only for internal events, but also for external events, low power shutdown events, and bypass events. For completeness, we recommend that a formal uncertainty study be performed to quantify the impact of identified uncertainties on early containment failure; however, uncertainties in the fundamental DCH processes of dispersal, fragmentation, and debris/gas heat transfer are not likely to contribute significantly to the overall uncertainty in early containment failure because these DCH processes are such a small contributor to containment early failure. Containment sprays are important in mitigating loads in non-SBOs if the ice inventory is depleted, but it remains to be confirmed that plants with identified vulnerabilities in switching to recirculation mode have implemented proposed remediations.

9.0 REFERENCES

- Allen, M.D. et al. (1991). *Experiments to Investigate the Effect of Flight Path on Direct Containment Heating (DCH) in the Surtsey Test Facility: The Limited Flight Path (LFP) Tests*, NUREG/CR-5728, SAND91-1105, Sandia National Laboratories, Albuquerque, NM.
- Allen, M.D. et al. (1992). *Experiments to Investigate the Effect of Water in the Cavity on Direct Containment Heating (DCH) in the Surtsey Test Facility - The WC-1 and WC-2 Tests*, SAND91-1173, Sandia National Laboratories, Albuquerque, NM.
- Allen, M.D. et al. (1993). *Experiments to Investigate the Effects of Fuel/Coolant Interactions on Direct Containment Heating*, The IET-8A and IET-8B Experiments, SAND92-2849, Sandia National Laboratories, Albuquerque, NM.
- Allen, M.D. et al. (1994). *Experiments to Investigate Direct Containment Heating Phenomena with Scaled Models of the Zion Nuclear Power Plant in the Surtsey Test Facility*, NUREG/CR-6044, SAND93-1049, Sandia National Laboratories, Albuquerque, NM.
- Atwood, C.L. et al. (1998). *Evaluation of Loss of Offsite Power Events at Nuclear Power Plants: 1980 - 1996*, NUREG/CR-5496, INEEL/EXT-97-00887, Idaho National Engineering and Environmental Laboratory, Idaho Falls, ID.
- Binder, J.L. et al. (1994). *Direct Containment Heating Integral Effects Tests at 1/40 Scale in Zion Nuclear Power Plant Geometry*, NUREG/CR-6168, ANL-94/18, Argonne National Laboratory, Argonne, IL.
- Blanchat, T.K. et al. (1994). *Experiments to Investigate Direct Containment Heating Phenomena With Scaled Models of the Surry Nuclear Power Plant*, NUREG/CR-6152, SAND93-2519, Sandia National Laboratories, Albuquerque, NM.
- Blanchat, T.K., M.M. Pilch, and M.D. Allen (1996). *Experiments to Investigate Direct Containment Heating Phenomena with Scaled Models of the Calvert Cliffs Nuclear Power Plant*, NUREG/CR-6469, Sandia National Laboratories, Albuquerque, NM.
- Blanchat, T.K., and M.M. Pilch et al. (1999). *Direct Containment Heating Experiments at Low Reactor Coolant System Pressure in the Surtsey Test Facility*, NUREG/CR-5746, SAND99-1634, Sandia National Laboratories, Albuquerque, NM.
- Boyack, B.E. et al. (1995). *CONTAIN Independent Peer Review*, LA-12866, Los Alamos Scientific Laboratory, Los Alamos, NM.
- Chu, T.Y., and M.M. Pilch et al. (1999). *Lower Head Failure Experiments and Analyses*, NUREG/CR-5582, SAND98-2047, Sandia National Laboratories, Albuquerque, NM.

References

- Denny, V.E., and B.R. Sehgal (1983). "Analytical Prediction of Core Heatup/Liquefaction/Slumping," *Proceedings International Meeting on Light Water Reactor Severe Accident Evaluation*, Aug. 28-Sept. 1, 1983, Cambridge, MA.
- Dingman, S.E. and A.L. Camp (1985). "Pressure-Time Response in an Ice-Condenser Containment for Selected Accidents," in *Proceedings of the 13th Water Reactor Safety Research Information Meeting*, Gaithersburg, MD, October 22-26 1985.
- Epstein, M., and H.K. Fauske (1989). "The Three Mile Island Unit 2 Core Relocation -- Heat Transfer Mechanisms," *Nuclear Technology*, Vol. 87, p. 1021.
- Gauntt, R.O., R.D. Gasser, and L.J. Ott (1989). *The DF-4 Fuel Damage Experiment in ACRR With a BWR Control Blade and Channel Box*, NUREG/CR-4671, SAND86-1443, Sandia National Laboratories, Albuquerque, NM.
- Gregory, J.J. et al. (1990). *Evaluation of Severe Accident Risks: Sequoyah, Unit 1*, NUREG/CR-4551, SAND86-1309, Vol. 5, Rev. 1, Parts 1 & 2, Sandia National Laboratories, Albuquerque, NM.
- Hammersley, R.J. et al. (1993). "Experiments to Address Lower Plenum Response Under Severe Accident Conditions," *Proceedings of the International Topical Meeting on Probabilistic Safety Assessment (PSA93)*, Clearwater Beach, FL.
- Harper et al. (1991). *Evaluation of Severe Accident Risks: Quantification of Major Input Parameters*, NUREG/CR-4551, SAND86-1309, Vol. 2, Rev. 1, Part 2, Sandia National Laboratories, Albuquerque, NM.
- Harper et al. (1992). *Evaluation of Severe Accident Risks: Quantification of Major Input Parameters*, NUREG/CR-4551, SAND86-1309, Vol. 2, Rev. 1, Part 3, Sandia National Laboratories, Albuquerque, NM.
- Heames, T.J., and R.C. Smith (1987). "Integrated MELPROG/TRAC Analyses of a PWR Station Blackout," *Nuclear Engineering and Design*, Vol. 125, pp. 175-188.
- Henry, R.E. et al. (1991). "Direct Containment Heating Experiments in a Zion-like Geometry," in *26th National Heat Transfer Conference*, Vol. 87.
- Huhtiniemi, I. et al. (1995). "FCI Experiments in the Corium/Water System," *Proceedings of the International meeting on Nuclear Reactor Thermal-Hydraulics, NURETH-7*, NUREG/CP-0142, Saratoga Springs, New York, pp. 1712-1927, Sept. 10-15.
- Huhtiniemi, I. et al. (1996). "Test Results and Analysis of Recent KROTOS Experiment," *ANS Proceedings National Heat Transfer Conference*, Aug. 3-6, Houston, Texas, pp. 27-42.

- IDCOR (1985). *Technical Support for Issue Resolution*, IDCOR, Technical Report 85.2, Fauske and Associates, Inc., Burr Ridge, IL.
- Kato, M. et al. (1998). "Fuel Coolant Interaction Tests Using UO₂ Corium Under Ex-Vessel Conditions," paper presented at the SARJ-98 Meeting, JAERI-Conf-99-005, Tokyo, Japan.
- Kelly, J.E. et al. (1987). *MELPROG-PWT/MODI Analysis of a TMLB' Accident Sequence*, NUREG/CR-4742, SAND86-2175, Sandia National Laboratories, Albuquerque, NM.
- Knudson, D.L. (1993). Transmittal of SCDAP/RELAP5/MOD3 Results for the Zion Power Station, Letter Report to NRC.
- Knudson, D.L., and C.A. Dobbe (1993). *Assessment of the Potential for High Pressure Melt Ejection Resulting from a Surry Station Blackout Transient*, NUREG/CR-5949, EGG-2689, EG&G Idaho, Inc., Idaho Falls, ID.
- Kolflax, A. (1960). *Results of 1959 Nuclear Power Plant Containment Tests*, Sargent and Lundy Report SL-1800.
- Magallon, D. (1995). "HCEH Pressure Calcium Melt Quenching Tests in FARO," *Nuclear Engineering and Design*, V155, 1-2, pp 253-270.
- Magallon, D. et al. (1998). "FARO in the 5th Framework Programme of the European Commission (1999-2002)," paper presented at the SARJ-98 Meeting, Tokyo, Japan.
- Marshall, B.W. (1988). *Reactor Safety Research Semi-annual Report July-December 1987*, NUREG/CR-5039, SAND87-2411, Vol. 2, p. 244, Sandia National Laboratories, Albuquerque, NM.
- Murata, K.K. et al. (1997). *Code Manual for CONTAIN 2.0: A Computer Code for Nuclear Reactor Containment Analysis*, NUREG/CR-6533, SAND97-1735, Sandia National Laboratories, Albuquerque, NM.
- NRC (1989). *Severe Accident Risks: An Assessment for Five U.S. Nuclear Power Plants*, NUREG-1150, Vol. 1, U.S. Nuclear Regulatory Commission, Washington, DC.
- NRC (1990). *Severe Accident Risks: An Assessment for Five U. S. Nuclear Power Plants*, Final Summary Report, NUREG-1150, U. S. Nuclear Regulatory Commission, Washington, DC, December 1990.
- NRC (1992). *Severe Accident Research Program Plan Update*, NUREG-1365, Rev. 1, U.S. Nuclear Regulatory Commission, Washington, DC.

References

NRC (1996). *Individual Plant Examination Program: Perspectives on Reactor Safety and Plant Performance*, NUREG-1560, Vol. 1, Part 1, U.S. Nuclear Regulatory Commission, Washington, DC.

OECD (1998). "In-Vessel Core Debris Retention and Coolability," OECD/CSNI Workshop, NEA/CSNI/R(98)21, Garching, Germany

Pilch, M.M. et al. (1992). "Counterpart and Replicate DCH Experiments Conducted at Two Different Physical Scales: The SNL/IET-1, 1R and the ANL/IET-1R, 1RR Experiments," Letter Report to the NRC, Sandia National Laboratories, Albuquerque, NM.

Pilch, M.M. et al. (1994a). *The Probability of Containment Failure by Direct Containment Heating in Zion*, NUREG/CR-6075, SAND93-1535, Sandia National Laboratories, Albuquerque, NM.

Pilch, M.M. et al. (1994b). *The Probability of Containment Failure by Direct Containment Heating in Zion*, NUREG/CR-6075, Supplement 1, Sandia National Laboratories, Albuquerque, NM.

Pilch, M.M. et al. (1995). *The Probability of Containment Failure by Direct Containment Heating in Surry*, SAND93-2078, NUREG/CR-6109, Sandia National Laboratories, Albuquerque, NM.

Pilch, M.M. (1995b). "Splinter Scenarios for DCH Evaluation in Ice Condenser Plants," Letter to R. Lee, USNRC, September 6, 1995.

Pilch, M.M. et al. (1996). *Resolution of the Direct Containment Heating Issue for all Westinghouse Plants with Large Dry Containments or Subatmospheric Containments*, SAND95-2381, NUREG/CR-6338, Sandia National Laboratories, Albuquerque, NM.

Pilch, M.M. et al. (1997). *Resolution of the Direct Containment Heating Issue for Combustion Engineering Plants and Babcock & Wilcox Plants*, NUREG/CR-6475, Sandia National Laboratories, Albuquerque, NM.

Pilch, M.M. et al (1997b). "Heat Transfer During Direct Containment Heating," *Advances in Heat Transfer*, Vol. 29, p. 215.

Rempe, J.L. et al. (1993). *Light Water Reactor Lower Head Failure Analysis*, NUREG/CR-5642, EGG-2618, Idaho National Engineering Laboratory, Idaho Falls, ID.

Russell, N.A., and D.C. Williams (1990). "Comparison of CONTAIN Code Simulations to Experimental Ice Condenser Data," SAND89-3096C, *Proceedings of the Second International Conference on Containment Design and Operation*, Toronto, Canada, October 14-17, 1990.

Stickler, L.A. et al. (1993). *Calculations to Estimate the Margin to Failure in the TMI-II Vessel*, TMI V(93)EG01, Idaho National Engineering Laboratory, EG&G Idaho, Inc., Idaho Falls, ID.

- Tarbell, W.W. et al. (1986). "High Pressure Melt Ejection and Direct Containment Heating in Ice Condenser Containments," SAND86-2141C, International ANS/ENS Topical Meeting on Operability of Nuclear Power Systems in Normal and Adverse Environments," October 1, 1986.
- Theofanous, T.G. (1988). "Some Considerations of Severe Accidents at Loviisa," Report prepared for Imatron Voima 04, Helsinki, Finland, 2000
- Thompson, T.J., and J.G. Beckerley (1973). *The Technology of Nuclear Reactor Safety, Volume 2: Reactor Materials and Engineering*, Edited by Thompson and Beckerley, the MIT Press, Massachusetts Institute of Technology, Cambridge, MA, pp. 767-769.
- Tills, J.L., K.K. Murata, R.G. Gido, and A. Notafrancesco (to be published). *CONTAIN Code Qualification Report/User Guide for Auditing Design Basis PWR Calculations*.
- Tutu, N.K. et al. (1986). *Trapping of Melt Droplets in Ice Condenser Channels During High Pressure Melt Ejection Accident: Preliminary Scoping Experiments and Analysis*, Tech. Report A-3024 9-16-86, Brookhaven National Laboratory, Upton, NY.
- WEC (1974). *Final Report Ice Condenser Full-Scale Section Tests at the Waltz Mill Facility*, WCAP-8282, Westinghouse Electric Corporation.
- Wheeler, T.A. et al. (1989). *Analysis of Core Damage Frequency From Internal Events: Expert Judgment Elicitation*, NUREG/CR-4550, SAND86-2084, Vol. 2, Sandia National Laboratories, Albuquerque, NM.
- Williams, D.C. et al. (1987). *Containment Loads Due to Direct Containment Heating and Associated Hydrogen Behavior: Analysis and Calculations with the CONTAIN Code*, NUREG/CR-4896, SAND87-0633, Sandia National Laboratories, Albuquerque, NM.
- Williams, D.C., and J.J. Gregory (1990). *Mitigation of Direct Containment Heating and Hydrogen Combustion Events in Ice Condenser Plants*, NUREG/CR-5586, SAND90-1102, Sandia National Laboratories, Albuquerque, NM.
- Williams, D.C. et al. (1995a). "CONTAIN Code Analyses of Direct Containment Heating Experiments: Model Assessment and Phenomenological Interpretation," *Eleventh Proceedings of Nuclear Thermal Hydraulics, 1995 ANS Meeting*, October 29 - November 2, San Francisco, CA.
- Williams, D.C. et al. (1995b). *Assessment of CONTAIN Direct Containment Heating (DCH) Model: Analysis of DCH Integral Experiments*, Letter report to the Accident Evaluation Branch, USNRC.
- Wong, C.C. (1988). *HECTR Analysis of the Nevada Test Site (NTS) Premixed Combustion Experiments*, NUREG/CR-4916, SAND87-0956, Sandia National Laboratories.

References

Zuber, N. et al. (1991). *An Integrated Structure and Scaling Methodology for Severe Accident Technical Issue Resolution*, Draft for Comment, NUREG/CR-5809, EGG-2659, EG&G Idaho, Inc., Idaho Falls, ID.

APPENDIX A
**Extension of Zion SCDAP/RELAP5 Analysis Supporting DCH Issue Resolution for PWRs
with Ice Condenser Containments**

K.S. Quick
Idaho National Engineering Laboratory

The previously released document in this appendix is included in its entirety as the best available copy for ready reference and use with the main report. While the style of this previously released document differs somewhat from the main report, the style is consistent and useable. Citations in the main report use the numbering system of that document for all figures, tables, and sections in this appendix (e.g., A.1, A.2, etc.). The document in this appendix numbers the same figures, tables, and sections without the leading appendix letter identifier.

EXTENSION OF ZION SCDAP/RELAP5 ANALYSIS SUPPORTING DCH ISSUE RESOLUTION FOR PWRs WITH ICE CONDENSER CONTAINMENTS

K. S. Quick
Idaho National Engineering Laboratory

1. INTRODUCTION

Molten core materials could be ejected into the containment building by a high pressure RCS (reactor coolant system) following reactor vessel failure during certain severe accidents. A rapid rise in containment temperature and pressure, or DCH (direct containment heating), could result from that HPME (high pressure melt ejection). In an extreme case, the pressurization associated with DCH could lead to containment failure. The potential for such a failure has driven a number of DCH-related studies, including analyses to support resolution of the issue for the Zion PWR (pressurized water reactor).^{1,2,3} In the Zion analyses, creep rupture failures of ex-vessel piping were predicted due to the natural circulation of superheated steam that developed in the absence of operator actions. The ex-vessel failures allowed RCS depressurization prior to lower head failure, which reduced the potential for HPME and DCH.

The purpose of this report is to compare characteristics of Zion and PWRs with ice condenser containments that could affect RCS depressurization (and the potential for HPME and DCH). If PWRs with ice condenser containments are found to be similar to Zion (with respect to those characteristics), it is assumed that RCS depressurization in ice condenser plants and Zion will be similar. The appropriate comparisons are discussed in the following section. Associated conclusions are summarized in section 3.

2. PLANT COMPARISON

There are ten PWRs with ice condenser containments. They are Catawba Units 1 and 2, D.C. Cook Units 1 and 2, McGuire Units 1 and 2, Sequoyah Units 1 and 2, and Watts Bar Units 1 and 2 (which are not yet in commercial operation). A comparison of these plants with Zion was made for two reasons. First, the general design is similar - Zion and the ice condenser plants are all 4-loop Westinghouse PWRs with U-tube steam generators (SGs). And second, the comparison was made because RCS depressurization results have been established for Zion. The comparison

will address characteristics that may have an impact on RCS depressurization. Those characteristics are identified based on experience with similar analyses.^{1,4,5} They are:

1. Power density - core power divided by the fuel volume, which could affect the heatup rates and the timing of events.
2. Bypass configuration - core bypass or downcomer bypass, which could affect natural circulation flow patterns.
3. Hot leg piping geometry - which could affect ex-vessel heat transfer.
4. Steam generator geometry - which could affect natural circulation flows and decay heat removal rates.

2.1 Power Density

The power density of the plants is of interest because it could impact the timing of events. In particular, if the power density was such that it could lead to core melt and relocation prior to ex-vessel failure, the probability of RCS depressurization prior to lower head failure would be lower than in Zion. When a comparison of the Surry and Zion calculations was made, the Surry calculations were measurably longer for the full range of RCP seal leak rates.¹ It was concluded that one of the primary reasons for this difference was the higher power density of Zion, which shortened the time to the various events of the transient.

Table 1 contains a list of the power densities for Zion and the ice condenser plants. The power densities of the ice condenser plants are very close to that of Zion. Therefore, the timing of transient events should be similar. In comparing Surry and Zion, it was noted that the sequence of events (i.e., ex-vessel failure, core relocation, and lower head failure) stayed the same even though the Surry transient was longer in duration. Therefore, based on this comparison of power densities, it appears reasonable to assume that transient duration and event sequence should be similar in Zion and the ice condenser plants.

Table 1. Comparison of power density.

| Plant | Power Density (MW/m ³) |
|--------------------------|------------------------------------|
| Zion | 100.0 |
| Catawba 1 | 103.5 |
| Catawba 2 | 104.6 |
| D.C.Cook 1 | 98.0 |
| D.C.Cook 2 | 103.8 |
| McGuire 1/McGuire 2 | 103.5 |
| Sequoyah 1/ Sequoyah 2 | 103.5 |
| Watts Bar 1/ Watts Bar 2 | 103.5 |

2.2 Bypass Configuration

There are two basic bypass configurations - core bypass and downcomer bypass. The difference between core bypass and downcomer bypass flow configurations is not significant under normal operating conditions. However, the bypass configuration can influence in-vessel natural circulation and core degradation during severe reactor accidents. In particular, previous analyses have shown that a core bypass configuration can delay lower head failure.¹ There are two reasons for this, and the first pertains to in-vessel natural circulation flow patterns. In-vessel natural circulation occurs when the hottest steam in the center part of the core rises into the upper plenum. Heat transfer to upper plenum structures cools the steam. The cooler steam tends to sink along the outer edges of the upper plenum and the core where it is reheated to complete the circulation cell. The core bypass provides a relatively cool return flow path for the steam but in the downcomer bypass configuration, the return flow must progress downward through the outer-most fuel assemblies. Most of that flow will begin to rise due to heating before reaching the bottom of the assemblies, resulting in a semi-stagnant zone in the lower portions of the core. The second reason that the core bypass configuration could delay lower head failure is that it provides an alternate path for accumulator water to reach the core (via the core bypass and holes in the core baffle plates) if core blockage has occurred.

In Catawba Units 1 and 2, McGuire Units 1 and 2, and Watts Bar Units 1 and 2, holes in the top of the core baffle plates just below the upper core plate result in a core bypass flow as shown in Figure 1. Most of the flow goes upward through the fuel assemblies while a fraction bypasses

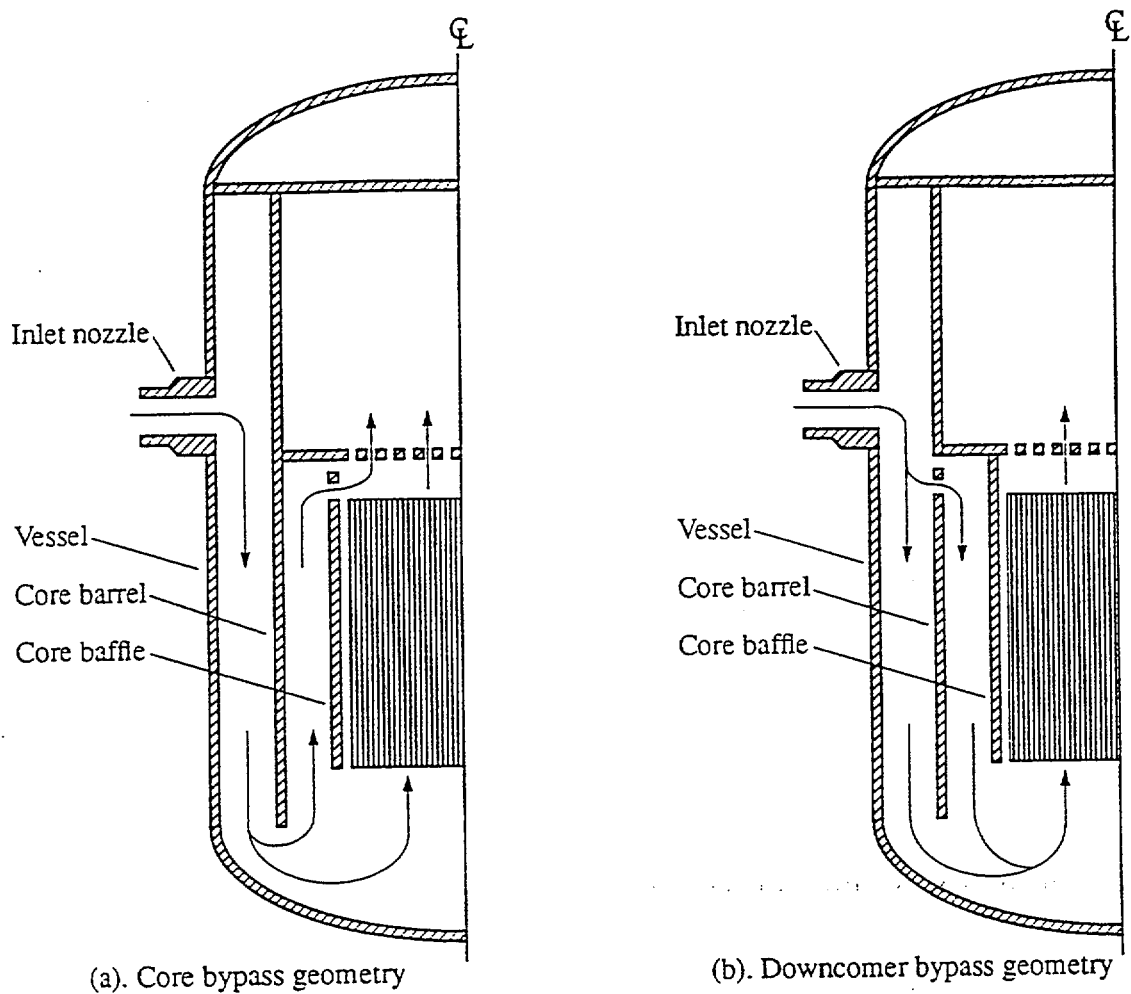


Figure 1. Normal flow patterns for core and downcomer bypass geometries.

the core through the baffle plate holes. In Zion as well as D.C. Cook Units 1 and 2, and Sequoyah Units 1 and 2, holes in the core barrel just below the upper core plate result in a downcomer bypass flow (also shown in the figure). Most of the flow goes through the downcomer annulus while a fraction bypasses the downcomer through the core barrel holes.

Table 2 summarizes the bypass configurations of Zion and the ice condenser plants. As described above, some of the ice condenser plants have downcomer configurations and some have core bypass configurations. However, the most recent analyses indicate that RCS depressurization

should occur before lower head failure with either configuration.^{3,5} Therefore, the bypass configuration of the ice condenser plants should not adversely impact RCS depressurization (and the potential for HPME and DCH) compared to Zion.

Table 2. Comparison of bypass configurations.^{1,7}

| Plant | Bypass Configuration |
|-------------------------|----------------------|
| Zion | downcomer |
| Catawba 1/Catawba 2 | core |
| D.C.Cook 1/ D.C.Cook 2 | downcomer |
| McGuire 1/McGuire 2 | core |
| Sequoyah 1/ Sequoyah 2 | downcomer |
| Watts Bar 1/Watts Bar 2 | core |

2.3 Hot Leg Piping Geometry

The hot leg geometry is of interest when hot leg countercurrent natural circulation flows develop during a severe accident. The development of such flows takes place after saturated liquid in the hot legs flashes and/or drains to the vessel. Temperature gradients from the core to the SG U-tubes can then drive steam flow along the top half of the hot leg, through a portion of the SG U-tubes, and back to the vessel through a cooler portion of the SG U-tubes and the lower half of the hot leg. The piping can affect the development of the countercurrent natural circulation flow since the geometry is a factor in the associated heat transfer. A comparison between the hot leg geometries for Zion and the ice condenser plants is given in table 3. As indicated, the hot leg diameter is the same in Zion as in the ice condenser plants and the lengths are very similar. Therefore, the hot leg piping geometry should not adversely impact RCS depressurization of ice condenser plants as compared to RCS depressurization in Zion.

Table 3. Hot leg piping comparison.^{6,7}

| Plant | ID (ft) | Length (ft) |
|-------------------------|---------|-------------|
| Zion | 2.42 | 17.79 |
| Catawba 1/Catawba 2 | 2.42 | 17.05 |
| D.C.Cook 1/ D.C.Cook 2 | 2.42 | 17.05 |
| McGuire 1/McGuire 2 | 2.42 | 17.05 |
| Sequoyah 1/ Sequoyah 2 | 2.42 | 17.02 |
| Watts Bar 1/Watts Bar 2 | 2.42 | 16.85 |

2.4 Steam Generator Geometry

SG tube diameters and lengths can affect the development of natural circulation flows since the surface area of the tubes is a factor in core decay heat removal by the secondaries. Therefore, these parameters are relevant to the topic of RCS depressurization. Zion has the same type of steam generator (series 51) as D.C. Cook 1, McGuire 1, McGuire 2, Watts Bar 1, and Watts Bar 2. The remaining ice condenser plants employ other steam generators which use smaller tubes in larger numbers as indicated in Table 4.

The SGs which use smaller tubes are not expected to adversely impact RCS depressurization because surface areas are similar and it is therefore reasonable to assume that natural circulation and heat transfer should be similar. Consequently, it does not appear as if the differences in the tube geometries will play a role in changing the RCS depressurization results for the ice condenser plants.

Table 4. Comparison of steam generator geometries.^{6.7}

| Plant | Tube OD (in) | Wall Thickness (in) | # Tubes | Avg Tube Length (in) | Surface Area of Tubes (ft ²) |
|-------------------------|--------------|---------------------|---------|----------------------|--|
| Zion | .875 | .05 | 3388 | 838.280 | 54216 |
| Catawba 1 | .75 | .043 | 4674 | 669.690 | 51217 |
| Catawba 2 | .75 | .043 | 4570 | 686.280 | 51318 |
| D.C. Cook 1 | .875 | .05 | 3388 | 838.280 | 54216 |
| D.C Cook 2 | .875 | .05 | 3592 | 837.562 | 57431 |
| McGuire 1/McGuire 2 | .75 | .043 | 4674 | 669.690 | 51217 |
| Sequoyah 1/Sequoyah 2 | .875 | .05 | 3388 | 838.280 | 54216 |
| Watts Bar 1/Watts Bar 2 | .75 | .043 | 4674 | 669.690 | 51217 |

3. CONCLUSIONS

A comparison between the Zion PWR and PWRs that use ice condenser containments was made in order to determine if the RCS depressurization results of Zion could be extended to the ice condenser plants. Four characteristics were compared including the power density, bypass configuration, hot leg geometry, and steam generator geometry. The following summarizes the conclusions derived from the comparisons.

1. The power densities for Zion and the ice condenser plants are nearly identical. Therefore, the power densities of the ice condenser plants should not adversely impact RCS depressurization (and the potential for HPME and DCH) compared to Zion.
2. Zion has a downcomer bypass configuration as do four of the ice condenser plants. The remaining ice condenser plants have core bypass configurations and, while the core bypass configuration has been shown to delay the progression of core degradation and lower head failure during station blackout accidents, the most recent calculations indicate RCS depressurization will occur before lower head failure with either configuration. Therefore, the bypass configuration should not result in RCS depressurization behavior unlike Zion.
3. The hot leg geometries of the ice condenser plants are nearly identical to Zion. Therefore, hot leg geometry should not be significant in changing RCS depressurization results.
4. Five of the ice condenser plants use the same steam generator design as Zion. The remaining plants use steam generators characterized by smaller tubes in larger numbers. However, surface areas are compatible and it can therefore be assumed that SG geometry will not adversely impact RCS depressurization.

Based on these comparisons it can be concluded that PWRs which use ice condenser containments will behave like Zion relative to RCS depressurization. As a result, there should be no significant difference between Zion and the ice condenser PWRs with respect to the probability for HPME and DCH.

4. REFERENCES

1. Knudson, D. L., et al., "Assessment of the Potential for HPME During a Station Blackout in the Surry and Zion PWRs," *Twenty-First Water Reactor Safety Meeting*, Bethesda, MD, October 1993.
2. Pilch, M. M., et al. (1994). *The Probability of Containment Failure by Direct Containment Heating in Zion*, NUREG/CR-6075, SAND93-1535, Sandia National Laboratories, Albuquerque, NM.
3. Pilch, M. M., et al. (1994). *The Probability of Containment Failure by Direct Containment Heating in Zion*, NUREG/CR-6075, SAND93-1535, Supp. 1, Sandia National Laboratories, Albuquerque, NM.
4. Knudson, D. L., and C. A. Dobbe (1993). *Assessment of the Potential for High Pressure Melt Ejection Resulting from a Surry Station Blackout Transient*, NUREG/CR-5949, EGG-2689, Idaho National Engineering Laboratory, Idaho Falls, ID.
5. Quick, K. S., and D. L. Knudson (1995). *A SCDAP/RELAP5 Analysis Supporting DCH Issue Resolution for the Surry PWR*, Letter Report, Idaho National Engineering Laboratory, Idaho Falls, ID.
6. Brownson, D. A., et al. (1993). *Intentional Depressurization Accident Management Strategy for Pressurized Water Reactors*, NUREG/CR-5937, EGG-247, Idaho National Engineering Laboratory, Idaho Falls, ID.
7. Fax Transmission, from Dr. Richard Lee (NRC) to D. L. Knudson (INEL), July 11, 1994, containing letter from Safeguards Analysis I to L. E. Hochreiter, WIN: 284-5575, "Ice Condenser Plant RCS Data", March 7, 1994.

APPENDIX B

CONTAIN Code Analyses of DCH in Ice Condenser Plants

David C. Williams and S.W. Hong
Sandia National Laboratories

B.1 Introduction

This document describes CONTAIN analyses performed for the DCH issue resolution effort for ice condenser plants. Major features of what was done and what results were obtained are included, but a number of details have been omitted.

The present ice condenser issue resolution effort includes both a screening analysis and a scoping study intended to provide guidance as to what might be needed in order to resolve DCH for ice condenser plants if the screening analysis cannot provide a complete resolution. The screening analysis employs TCE/LHS in a manner similar to that used for the PWR large dry containments in NUREG/CR-6338 (Pilch et al., 1996); complete success in this phase would eliminate any need for additional effort. In the TCE/LHS screening analysis, the effects of the ice condenser are neglected, an assumption that is thought to be conservative in terms of the overall results (although this assumption may be best-estimate for certain specific scenarios in which the ice condenser has been rendered ineffective owing to ice depletion, damage, etc.). This approximation will be referred to here as the "small dry" containment approximation, since the governing phenomena are expected to be qualitatively similar to those controlling DCH in large dry containments, except for differences reflecting the smaller capacity of ice condenser containments.

One purpose of the present effort is to support the screening analysis by providing CONTAIN calculations for point comparisons with loads calculated by TCE/LHS. In addition, the possible importance of uncertainties resulting from phenomena not modeled in TCE/LHS is considered. This includes examination of the potential for mitigation of DCH loads by the ice condenser. The role of this study is similar in some respects to the role played by the CONTAIN calculations that were performed for the Surry plant in NUREG/CR-6109 (Pilch et al., 1995). However, ice condenser analysis is more complex than PWR large dry analysis, and the calculations summarized here are more extensive than those that were performed for the Surry plant.

It is also important to understand what the present work does not attempt to do. In most instances, there is no attempt to bound the various effects considered; this study is not a bounding analysis. No attempt is made to assign quantitative probabilities to the various scenarios considered, even in a relative sense, except that the various cases are considered to be within the credible range of interest. In some instances, judgments are offered as to whether a particular input assumption is conservative or nonconservative. Use of these terms should only be understood as implying a bias in the indicated direction relative to a best estimate; it does not imply that the assumptions are bounding unless this is explicitly stated to be the case.

In addition, the present study has considered only quasi-static containment loading as a result of DCH and related phenomena (e.g., hydrogen burns). There has been no consideration of other issues such as dynamic loads associated with accelerated flames or detonations, fuel coolant interaction (FCI) effects, cavity pressurization following vessel breach and its consequences, or thermal failure of the containment resulting from debris accumulating against the shell.

In Section B.2, the CONTAIN input and modeling assumptions are summarized. Section B.3 provides the main results of the calculations, including the containment initial conditions for the various scenarios, point calculations of DCH loads for comparison with TCE/LHS, and assessing the potential impact of the ice condenser and other phenomena not considered by TCE/LHS. Section B.4 summarizes the major conclusions that can be drawn from this work.

B.2 CONTAIN Input and Modeling

The problem description as analyzed by the CONTAIN code is summarized in this section. Some details of the input description have been omitted, but the features known to be important are included.

B.2.1 CONTAIN Version 1.2

The calculations summarized here were performed using CONTAIN 1.2, which is a new release. There are numerous major model enhancements over prior code releases, although some have been available in various developmental versions of CONTAIN. Two major features that have not been generally available even in developmental versions include:

- Use of a new solution scheme for solving intercell flows, commonly called the "hybrid flow solver" because the differencing scheme employed can depend upon the conditions that are encountered.
- Modeling for detailed tracking of pools and liquid flows.

The old flow solution scheme in CONTAIN is known to overpredict downward mixing in situations that actually should be stably stratified, and the new hybrid flow solver prevents this overmixing in some instances. The hybrid solver was used in the present calculations. It is potentially of interest because, under some conditions, calculations using the hybrid solver might be capable of capturing the effects of stratification in the dome volume, which may be a factor in determining whether pre-existing hydrogen can burn in some DCH scenarios. However, use of this approach for DCH conditions has not been validated, and no attempt to represent stratification effects was made in the present work.

The pool tracking capability includes the ability to model heat transfer from pools to structures in some detail. However, using this capability requires more detailed information on the containment geometry than was readily available. Hence, all structures were modeled as being in contact with the containment atmosphere, as was done in the past in CONTAIN. Since this assumption is correct for the large majority of the heat sink surfaces within containment,

uncertainties resulting from this approximation are minor. The enhanced pool tracking capabilities were used in modeling the refueling drains as is noted below.

B.2.2 Plant Representation

The Sequoyah plant was selected as the representative plant for analysis. The input deck used was derived from the 6-cell representation of Sequoyah employed in NUREG/CR-5586 (Williams and Gregory, 1990). The topology of this representation is summarized in Figure B.1 for the volumes inside the containment. There have been numerous modeling enhancements to the CONTAIN code since the time the earlier work was performed, and a number of modifications were made to the deck in order to accommodate these enhancements.

In addition to the 6-cell representation of the containment, Williams and Gregory (1990) also utilized a considerably more detailed 26-cell deck in some of their analyses. Adapting this deck to the present application would have required more effort than was feasible for the present scoping study. Williams and Gregory (1990) found that the DCH loads calculating using the 6-cell and 26-cell representations did not differ very significantly, and thus their results support the use of the 6-cell representation in the present work. Their results also indicated that the more detailed representation would be needed if it were desired to expand the scope of the ice condenser DCH analyses to include issues involving uneven melting of ice and gas distribution issues, including existence of detonable gas mixtures in parts of the containment. Consideration of these questions is outside the scope of the present study.

Modeling of the Shield Building. The Sequoyah containment is a free-standing steel shell which is surrounded by a concrete shield building; there is a substantial gap (~1.5 m) between the shield building and the shell. In the earlier work, the shield building was not modeled. However, more recent studies of passively-cooled containments with a similar configuration have indicated that radiative heat transfer from the shell to the shield building can be important. Although this heat transfer is much too slow to affect the DCH response directly, it was thought that it could affect the containment initial conditions for DCH. Modeling of the shield building was therefore included.

In order to model the shield building, an additional cell (Cell 8) was added to the deck to represent the annular gap. Steel structures representing the outer surface of the shell were provided as were concrete structures representing the shield building. The steel structures were connected to the corresponding structures representing the shell in the various interior cells, in order to model thermal conduction through the shell. The radiative energy transfer between the shell and the shield building was modeled using the CONTAIN net enclosure model. The cell representing the shield building annulus was connected by a 0.1 m^2 flow path to a very large "environment" cell in order to permit pressure equalization with the environment.

Containment Volume. Based upon information from the Sequoyah individual plant examination (IPE), the free volume of the containment interior was taken to be $3.37 \times 10^4 \text{ m}^3$. The volumes of the various cells in the CONTAIN representation are summarized in Table B.1. Some of these volumes differ slightly from those used in the previous work.

Initial Atmosphere. At the time of reactor shutdown ($t=0$ s in the calculations), the containment pressure was assumed to be 0.1 MPa. The atmospheric temperature was taken to be 311 K, except for the ice condenser volumes, which were at 273.5 K.

Bypass Paths. The design intent of the containment is to force flow between the lower compartment and the dome to pass through the ice condenser. However, a limited amount of direct flow between the lower containment and the upper containment is possible. When the total flow rates are large (which includes flows during DCH), the great majority of the flow does pass through the ice condenser. However, when flow rates are low, and the ice condenser doors therefore closed, much of what flow does exist may pass to the upper containment via the paths that bypass the ice condenser. As described in (Williams and Gregory, 1990), this bypass flow can have a considerable effect on conditions at vessel breach if the air return fans (ARFs) are not operating. Containment pressures and dome steam concentrations are increased by the bypass flow. If the ARFs are operating, the bypass flow is too small relative to the flow forced by the fans to have a significant effect.

Two sources of bypass are modeled. One bypass flow path is the refueling drains, modeled as a flow path from Cell 2 to Cell 3 at an elevation of 6.47 m. The other is defined in the FSAR as unspecified deck leakage with an effective flow area ≤ 0.29 m². A value of 0.29 m² is used here. Since the FSAR value is an upper bound, actual leakage could be substantially smaller. A sensitivity calculation was therefore performed with an effective deck leakage flow area of 0.029 m².

Because the refueling drains are located at a relatively low elevation in the lower compartment, they are expected to flood when the volume of water exceeds about 750 m³, which happens well before vessel breach in the calculations. Flooding terminates the contributions of this flow path to the bypass flow. This flooding could not be directly modeled in the older versions of CONTAIN; however, it was modeled in the present calculations using the new pool tracking capabilities of CONTAIN 1.2.

Air Return Fans. In ice condenser plants, air return fans are provided which return air from the dome to the lower compartment, forcing enhanced flow through the ice condenser. This promotes containment mixing and helps to prevent detonable hydrogen concentrations from developing in the ice condenser volumes. It also accelerates steam and energy transport to the ice condenser and therefore enhances ice melt. In Sequoyah, the fans boot automatically when the containment pressure rises to 3 psig (Gregory et al., 1990); however, the fans are not always available in some core melt accidents of potential interest for DCH.

The ARFs were modeled by defining a flow path between Cells 2 and 6 with a user-specified flow rate from Cell 6 to Cell 2 of 54.7 m³/s. This rate corresponds to both trains of fans operating. Actuation was specified to begin at 7426 s, which is the time the containment pressure was calculated to rise to 3 psig.

Igniters. The Sequoyah plant is equipped with igniters for intentional ignition of hydrogen in the lower compartment, the upper plenum, and the dome; there are no igniters in the cavity, lower plenum, or ice condenser. In CONTAIN, availability of igniters was modeled by allowing ignition whenever the gas composition was within the flammable range. CONTAIN default flammability limits were used except for the minimum combustible mole fraction for ignition, which was set to 5.5 mole percent (m/o). This value is the same as what was assumed in the NUREG-1150 (NRC, 1990) analyses of the Sequoyah plant (Gregory et al., 1990). In cells that contained no igniters, ignition was prevented by setting the ignition criteria to impossible values. Burns initiating in cells with igniters could still propagate into the cells without igniters, however. (In CONTAIN, criteria for propagation are specified independently of the ignition criteria, and the propagation criteria were left at default values.) For calculations in which it was assumed that igniters do not operate, all hydrogen combustion prior to vessel breach was suppressed.

Ice Condenser. The initial height of the ice column was taken to be 14.53 m, the initial ice mass was 1.11×10^6 kg, and the effective surface area available for heat transfer was 2.48×10^4 m². As ice melts, these three quantities are decreased proportionately in the CONTAIN model. In some sensitivity studies, it was desired to run the DCH calculation with amounts of ice that differed from the amounts CONTAIN calculated to remain at the time of vessel breach. This was accomplished by restarting the calculation at vessel breach with the desired quantities of ice specified.

Ice Condenser Doors. There are three sets of doors that open in response to a forward pressure. The first set is between the lower compartment and the lower plenum; it is hinged to open with a minimal forward pressure. Unless the hinges are damaged, they can fully reclose, although a slight back pressure is required for full closure. The hinges are crushable and can deform if the doors are opened with sufficient violence, in which case they will not reclose. It has not been assessed whether this should be expected to occur in a DCH event. In the present study, the doors have been assumed to reclose in the absence of a continuing forward pressure.

There are also doors between the ice condenser and the upper plenum, and between the upper plenum and the upper containment. These require a larger forward pressure to open them and, if fully opened, they will only partially reclose.

In CONTAIN, all three sets of doors were modeled using flow paths in which the flow area is a function of the forward pressure differential. The lower plenum doors were assumed to be fully reversible. The partially irreversible behavior of the other two sets of doors was modeled. Additional detail on modeling the ice condenser doors is given in Williams and Gregory (1990).

B.2.3 RCS Sources

CONTAIN does not include modeling for the primary system and the in-vessel melt progression; hence, CONTAIN calculations must be provided with source tables that describe the releases from the primary system to the containment. State-of-the-art calculations for the in-vessel accident progression for the Sequoyah plant are not available. However, calculations for selected station blackout scenarios were performed for the Zion plant using SCDAP/RELAP5 (SR5) as described in Supplement 1 of NUREG/CR-6075 (Pilch et al., 1994b). Since both Zion and

CONTAIN Code Analyses

Sequoyah are 4-loop Westinghouse nuclear steam supply systems, sources for the present work were based upon the Zion SR5 calculations.

RCS sources were reported for three cases in (Pilch et al., 1994b). These were distinguished by the magnitude of the pump seal leakage assumed to occur. Case 1 was run without pump seal leakage, Case 2 was run with a best-estimate leakage of 250 gallons per minute (gpm), and Case 3 was run assuming 450 gpm, which was estimated to be the maximum possible. Case 2 was selected for the present study because it represented the best estimate of the expected leakage rate. In addition, it is potentially the most conservative case because it resulted in the largest hydrogen releases to the containment, and the analysis indicated that the hydrogen would not autoignite upon entering the containment.

For application to Sequoyah, the Zion sources were scaled by multiplying the hydrogen source rates by the Sequoyah/Zion zirconium inventory ratio ($23115 \text{ kg}/20208 \text{ kg} = 1.14385$), and sources of steam and liquid water were scaled by multiplying by the power ratio ($3570 \text{ MW}/3238 \text{ MW} = 1.1025$). The (small) nitrogen sources, which represent releases from the accumulator, were used as given for Zion, without scaling.

The rationale for scaling the hydrogen sources used here is straight-forward, but the rationale for scaling the water sources is less clear. It might be argued that the scale factor should be based upon the water inventories, which are almost equal. The argument used here is that an important parameter is the amount of ice melted prior to vessel breach (VB), and this is determined primarily by the energy released to the containment, not the total water mass.

In the SR5 analyses, sources were released from 6 different locations: the PORV, the four reactor coolant pump (RCP) seals, and a break in the hot leg. However, all these locations are within the lower compartment as defined here; hence, all sources were introduced in Cell 2.

The SR5 sources were calculated for a "hands off" station blackout accident, with no power recovery, no operator intervention, and no heat rejection via the secondary side. A thermally-induced hot leg failure was calculated to occur prior to vessel breach, completely depressurizing the primary system. Except for thermal energy that remains in the primary vessel and the degraded core, most of the energy initially stored in the primary system at reactor shutdown, plus the decay energy and zirconium reaction energy, is discharged to the containment in this scenario. These conditions tend to maximize the thermal load on the ice condenser.

There is some mismatch between the scenario calculated by SR5 and the postulated DCH event, because the SR5 scenario included complete depressurization owing to a hot leg failure at 16925 s, which is well before the calculated time of vessel breach (26915 s; for convenience, vessel breach was taken to be at exactly 27000 s in the CONTAIN analyses). This depressurization would, of course, preclude occurrence of HPME and DCH. Furthermore, Pilch et al. (1994b) concluded that all unrecovered station blackouts would similarly depressurize, precluding DCH. Hence only station blackout scenarios with power recovery and operator intervention were judged to be of interest for DCH in this treatment. Other accidents potentially of interest include certain transients and small-break LOCAs.

In many of the accident scenarios potentially of interest (including long-term station blackouts), secondary side cooling may be available for at least part of the time preceding vessel breach, reducing the energy discharged to the containment and, hence, reducing the thermal load on the ice condenser. Thus, the degree of ice melt prior to vessel breach that is calculated using the SR5 sources may be too high for at least some of the scenarios that would be of interest in a complete integrated systems analysis of DCH in ice condenser plants.

B.2.4 RCS Initial Conditions

In NUREG/CR-6338, RCS conditions (including melt masses and compositions) were defined for two scenarios, designated Scenarios V and VI. These were slightly modified versions of scenarios that were first defined in Supplement 1 of NUREG/CR-6075. In Scenario V, it was assumed operator intervention resulted in full repressurization prior to vessel breach. A relatively large amount (75000 kg) of water was assumed to overlie the melt at the time of vessel breach, and melt masses were moderate. In Scenario VI, repressurization was only partial (to 8 MPa), melt masses were larger, and only 10000 kg of water was assumed to overlie the melt at vessel breach.

Melt mass distributions for 4-loop PWRs, with Zion as the prototype, were summarized in Table B.7 of NUREG/CR-6338. Values used in the present work were derived from the upper end (nominally the 99th percentile) of the distributions as listed in this table. The tabulated values for UO_2 were scaled by the Sequoyah/Zion mass ratio for UO_2 (1.030), and values for Zr and ZrO_2 were scaled by the Zr inventory ratio (1.144). In NUREG/CR-6338, molten steel was estimated by considering the amount of thin lower-internals steel that would be submerged in the melt accumulating in the lower head. Since the determining feature is the volume of melt, the principal component of which is UO_2 , steel inventories were scaled by the UO_2 inventory ratio. The rationale for this scaling is admittedly approximate, but the effect is small in comparison with other uncertainties in the melt masses and compositions, and is therefore not considered to be a major source of uncertainty in these analyses.

RCS conditions and melt masses are summarized in Table B.2 for Scenarios V and VI. Quantities marked by an asterisk were not considered in NUREG/CR-6338 and hence could not be derived from information given there. The rationale for the values assumed is therefore summarized below.

Water Temperature. Although the quantities of water overlying the melt were specified in NUREG/CR-6338, this water was not actually included in the analyses; hence, its temperature (or enthalpy) did not have to be considered and was never specified. Since the water is overlying the melt, it is expected to be ejected with, and/or immediately after, melt ejection. CONTAIN calculations exploring the potential effects of this water require a specification of its enthalpy.

Although water temperature was not specified in NUREG/CR-6338, it was argued there that substantial subcooling could exist in Scenario V, based upon estimated RCS conditions during

the TMI-II accident; this subcooling could be as much as 100 K.¹ At 16 MPa, the saturation temperature is 620 K. Hence the water temperature was taken to be 520 K in the base case. Sensitivity to this assumption of strong subcooling was explored in calculations run with a temperature of 620 K.

In Scenario VI, it was judged implausible that the relatively small amount of water overlying the large mass of melt could be significantly subcooled. Hence the water was assumed to be saturated which, at a pressure of 8 MPa, corresponds to a temperature of 568 K.

RPV Insulation. Reactor pressure vessels are provided with thermal insulation to prevent excessive heat losses. Typically this insulation consists of stainless steel foils held in place between thin stainless steel sheeting. Discussion of modeling of the insulation in CONTAIN, and the rationale for the treatment assumed, will be deferred to Section B.6; however, for the sake of completeness, the masses assumed are tabulated in Table B.2.

B.2.5 Containment Scenarios

For both Scenarios V and VI, three different sets of containment conditions were initially defined. These are designated Scenarios V, Va, and Vb when combined with the Scenario V RCS conditions, and Scenario VI, VIa, and VIb when combined with the Scenario VI RCS initial conditions. The rationale for these scenarios has been addressed previously in Section 5.2. The scenarios are defined as follows:

V,VI: Igniters operate prior to vessel breach but the ARFs do not operate.

Va,VIa: Both igniters and the ARFs operate prior to vessel breach.

Vb,VIb: ARFs operate, but igniters do not operate and there is no ignition of hydrogen prior to vessel breach.

The combination with neither igniters nor ARFs is not included because it was assumed that this combination would arise principally in station blackouts with no recovery, and this accident category was assumed to always depressurize fully prior to vessel breach and therefore not contribute to the spectrum of DCH events.

Prior to vessel breach, the containment scenarios are assumed to be identical for both the Scenario V and Scenario VI variants, and they therefore have the same containment conditions at vessel breach. These conditions will be referred to as the "containment initial conditions for DCH", or simply the "initial conditions", in the present work.

When these cases were run on CONTAIN, it was found that complete ice melt was calculated to occur prior to vessel breach for the containment scenarios with ARFs operating. Consequently, the calculated initial conditions for V (and VI) did not differ as greatly from initial

¹ M.M. Pilch, personal communication to the authors.

conditions for Va (VIa) has had been expected. As noted previously, the SR5 sources used in these calculations may provide a greater thermal load on the ice condenser than would actually be expected in at least some of the accident scenarios of interest for DCH. In order to provide a case with initial conditions representative of those expected with ARFs and igniters operating and with ice still present at vessel breach, Scenarios Va' and VIa' were defined with the SR5 sources of steam and water coming from the PORV and RCP3 and RCP4 seals deleted. With these reductions in the energy input to the containment, some ice was calculated to remain at vessel breach even when ARFs and igniters were both operating.

Analogous Scenarios Vb' and VIb' were also defined, but only one calculation was run for VIb' and none was run for Vb'. In addition, one calculation was run for a variant of Scenario VI in which the effective area of the deck leakage bypass flow path was reduced by a factor of 10.

In addition to being needed for the CONTAIN DCH calculations, the initial conditions calculated by CONTAIN for these scenarios are also used in the TCE/LHS calculations.

B.2.6 DCH-Related Modeling

As part of the CONTAIN validation effort, an extensive series of CONTAIN analyses of DCH experiments was recently performed. Results are summarized in Williams et al. (1995a), with a much more detailed discussion being given in Williams et al. (1995b). The design of the calculations summarized in this report is based in part upon results described in Williams et al. (1995b).

CONTAIN includes a large number of input and modeling options for DCH and related phenomena such as hydrogen combustion and atmosphere-structure heat transfer. This flexibility is essential for assessing uncertainties in the results of CONTAIN analyses, but can pose QA problems for CONTAIN DCH calculations and code users generally if guidance as to appropriate choices for the various options were not provided. Hence, a standardized input prescription was defined and frozen in the CONTAIN validation study, with all experiments being analyzed using the standard prescription. In the sensitivity studies that were also performed, all input variations with respect to the standard prescription were explicitly noted.

In Williams et al. (1995a, 1995b), it was concluded that the standard prescription used for the experimental analysis was also applicable to NPP analysis, provided a few modifications were made in order to reflect lessons learned in the course of the study. It was also noted that the standard input prescription was not to be treated as a rigid recipe that must be followed in all cases, or that would guarantee good results if it were followed. Instead it was viewed as a starting point for defining CONTAIN DCH calculations, with modifications introduced as appropriate, and with the specific modifications used and the reasons for them being documented. This approach will be used here; hence, the discussion is largely limited to the rationale for certain departures from the standard prescription, and to issues not clearly covered by the standard prescription.

B.2.6.1 Hydrogen Combustion

CONTAIN has three models for hydrogen combustion: deflagrations in pre-mixed atmospheres containing hydrogen, a model for diffusion-flame burning (DFB) applicable when hydrogen-rich gases enter a receiving cell containing oxygen, and a bulk spontaneous reaction (BSR) model applicable when temperatures become sufficiently high that any oxygen and hydrogen within a volume are expected to react even if normal flammability limits are not satisfied. Initiation of deflagrations is controlled by composition thresholds, initiation of DFB is controlled by both composition and temperature thresholds, while the BSR model has only a temperature threshold. Unfortunately, the composition thresholds do not depend upon temperature in the CONTAIN model, nor do the temperature thresholds depend upon composition.

Parameters controlling hydrogen combustion prior to vessel breach in the CONTAIN model are not appropriate to DCH conditions. Hence, in all calculations, the initial calculation was stopped at vessel breach and restarted with altered hydrogen combustion parameters for the DCH event.

Combustion Prior to Vessel Breach. Modeling of deflagrations prior to vessel breach in scenarios with operating igniters was discussed in Section B.2.2. Prior to vessel breach, the DFB threshold temperature (applied to the incoming flow, not the receiving cell) was set to 1000 K, corresponding approximately to the autoignition temperature. However, this threshold temperature was only applied to flows entering from another cell; it cannot be applied to source tables. If conditions are otherwise appropriate for DFB, incoming hydrogen sources will burn off as they enter, no matter what the temperature. Since it was previously estimated (Pilch et al., 1994b) that hydrogen would not autoignite as it entered from the primary system in the Case 2 Zion analyses, burning the hydrogen as it enters is unrealistic. Hence DFB was suppressed in Cell 2 prior to vessel breach.

Combustion During DCH. The combustion models are largely based upon experiments performed under non-DCH conditions, and fully mechanistic combustion modeling for DCH is not available. Hence, the recommended procedure is to specify the controlling combustion parameters so as to assure one obtains the combustion behavior considered to be reasonable for the conditions at hand, and to perform sensitivity studies if necessary to investigate alternative combustion behaviors that cannot be ruled out. Experimentally, DCH-produced hydrogen was observed to burn in the large majority of those experiments in which the containment atmosphere was not very heavily inerted; hence the standard prescription is to set DFB parameters so as to favor combustion of DCH-produced hydrogen whenever it entered an oxygen-bearing volume, unless the molar ratio of diluent gas to hydrogen is greater than a threshold value. The CONTAIN default value (9.0) was used for this threshold, which is also the DCH standard prescription for NPP analysis. No temperature threshold was specified, since hot debris particles will provide more than adequate ignition sources.

For the same reason, it was assumed that, during DCH, ignition sources for deflagrations would be available in all cells. The minimum hydrogen concentration for ignition was taken to be 5.5 m/o, which is the same value as that used prior to vessel breach in the presence of igniters. The

standard prescription calls for specifying deflagration flame speeds to be ≥ 10 m/s, because debris particles flying through a flammable atmosphere are expected to provide multiple ignition sites, substantially shortening combustion times. Flame speeds of 20 m/s in Cells 1-4 and 10 m/s in Cells 5 and 6 were therefore specified. It is less clear that multiple ignition sources greatly affect burn completeness, however, and the default completeness correlations are therefore used in the standard prescription. Except in the Vb and VIb scenarios, deflagrations did not play a major role in the results.

In the standard prescription for application of the BSR model to NPP DCH events, the standard prescription was to leave the threshold temperature equal to the CONTAIN default value, 773 K. Considerable uncertainty is acknowledged concerning this value. For a well mixed volume, this uncertainty may be in either direction. In the present instance, it is believed that the standard value may be overly conservative because BSR is primarily important for hydrogen combustion in the dome. However, the hot gases containing hydrogen enter the dome at the top of the upper plenum, which is high in the containment. This geometry is thought likely to favor stratification in the dome, with much of the pre-existing hydrogen and much of the dome oxygen supply residing in the cooler gases below the hot plume. Strong stratification effects were observed in the Surry IET experiments, in which the geometry was somewhat similar to Sequoyah in this regard.

As has been done in TCE/LHS calculations (Pilch et al., 1996), the effects of stratification were nominally compensated for by setting the BSR threshold to a higher value, 950 K in this work. This approach is basically unsatisfactory in that it uses a chemistry parameter (i.e., a reaction temperature threshold) as a surrogate for what is fundamentally a gas mixing uncertainty. Hence, in cases in which the threshold was calculated to be exceeded in the dome, sensitivity of the results to the hydrogen combustion assumption was investigated by setting the threshold to a sufficiently high value (2000 K) that BSR could never occur.

B.2.6.2 Atmosphere-Structure Heat Transfer

The standard prescription uses the CONTAIN default modeling for atmosphere-structure heat transfer except for radiant energy transfer. The normal default model for thermal radiation takes into account optically active gases but does not provide mechanistic modeling for the effects of aerosols upon the atmospheric emissivity. Experimentally, dense aerosol clouds are observed to accompany DCH events, and these are expected to assure high emissivity values. An option is available in CONTAIN that permits the default emissivity model to be overridden with a fixed user-specified value. In the standard prescription, this option is used to specify an atmosphere emissivity of 0.8.

The standard prescription emissivity is not appropriate for the period prior to vessel breach, for which the normal default emissivity model should be used. Unfortunately, it is not possible to invoke the user-specified emissivity option in a restart; hence one model or the other must be used for the entire calculation.² The choice made here is to use the user-specified standard prescription

² This limitation is being eliminated, starting with CONTAIN release 1.21.

value. A sensitivity calculation provided results that support this choice; the results also indicated that the sensitivity of the calculated DCH loads to the choice of emissivity model is small.

B.2.6.3 DCH Models

RCS Blowdown. A cell representing the primary system is provided to generate the blowdown. This cell is initially filled with high pressure steam and is opened to the cavity at vessel breach. The flow path connecting the primary system to the cavity is kept closed until vessel breach. The area of this flow path is increased linearly to its maximum value over a time of duration t_h , which was estimated to be about 2 seconds using a correlation described in Williams et al. (1995b).

For the RCS conditions of Scenario VI, steam properties do not deviate greatly from ideality and the CONTAIN ideal gas EOS was used. The volume of the RCS was increased slightly (to 351.33 m³) in order to permit the cell to hold the correct mass of steam (6090 kg) for the indicated temperature and pressure. Departures from ideality are much greater for the conditions of Scenario V and the CONTAIN real EOS for steam was therefore used. The steam mass in the RCS is 21746 kg for the specified conditions when co-ejected water is not modeled. This mass was reduced to 15820 kg in calculations that included the 75000 kg of water, in order to take into account the reduction in RCS free volume associated with the water.

Debris-Water Interactions. Debris-water interactions can arise in DCH in either or both of two basic contexts: water initially in the cavity can be co-dispersed with the debris, and RPV water overlying the debris prior to vessel breach can be co-ejected with the debris. In compartmentalized containment geometries (which includes all ice condenser containments), water has the potential to either mitigate or augment DCH loads. Possible mitigation effects include quenching of debris, suppression of hydrogen combustion, and quenching of hydrogen combustion energy by aerosolized water. Possible augmentation effects include increasing the supply of steam available for thermal and chemical interactions with the debris, accelerating the transport of energy and hydrogen to the dome, and reducing subcompartment temperatures for the same amount of sensible heat transfer to the gas. The accelerated transport and reduced temperatures tend to reduce the calculated mitigating effect of atmosphere-structure heat transfer (Williams et al., 1987).

CONTAIN has no FCI model and no interactions of debris directly with liquid water are modeled. Instead it is assumed that the water is present as dispersed as drops small in comparison with the debris drops and that direct contact between debris and the water drops is not the dominant process. Under these conditions, the primary rate-limiting processes are the debris-atmosphere interactions, and it is these processes that are modeled. In scenarios involving large amounts of co-dispersed cavity water, the neglect of debris interactions directly with liquid water is an important limitation and CONTAIN analyses of the SNL/IET-8B experiment overpredicted the mitigating effect of the relatively large amount (62 kg) of water in the cavity. Underprediction of the heat transfer that results from direct contact of debris with liquid water was hypothesized to be a cause of the nonconservative result obtained.

Analyses performed in support of NUREG-1150 for the Sequoyah plant (Gregory et al, 1990) indicated that the cavity would be dry (except for condensate levels of water) in any scenario in which the RWST had not dumped. Given RWST dump, water from the lower compartment would overflow into the cavity if ice melt exceeded 25 percent, and the cavity would be completely flooded if ice melt exceeded 50 percent. Complete cavity flooding was assumed to preclude DCH, and we have adopted the same assumption in the present effort. In all the CONTAIN analyses, ice melt was calculated to exceed 50 percent at the time of vessel breach although the SR5 sources used here may overestimate the thermal load on the ice, as noted previously. Hence it appears likely that the cavity will either contain only very limited water (if the RWST has not dumped) or else be flooded (if the RWST has dumped), thereby precluding DCH; only for a limited range will there be sufficient water to be a major factor without also preventing DCH. Hence only one sensitivity case involving cavity water was run.

On the other hand, all the scenarios include at least some co-ejected RPV water and the possible effects of this water must be considered. Co-ejected RPV water differs from co-dispersed cavity water in that the RPV water is expected to be highly superheated with respect to cavity conditions. For water temperatures of 520 K to 620 K, about 25 percent to 50 percent of the water can flash to steam upon ejection, and the water that does not flash is likely to be highly fragmented. Hence the situation may correspond more closely to the assumptions of the CONTAIN model than is the case for scenarios involving large amounts of co-dispersed cavity water.

The only experimental data for testing the CONTAIN treatment of co-ejected water scenarios in compartmentalized containment geometries is provided by the CED-2 experiment. A CONTAIN calculation for this experiment gave ΔP and hydrogen production values agreeing with experiment to within 7.5 percent. It also yielded the correct order of magnitude of cavity pressurization (only approximate estimates of the experimental value are available) and provided a plausible explanation for the damage to subcompartment structures that was observed in the experiment. The fact that reasonable agreement was obtained for both ΔP and hydrogen production indicates that there was no substantial imbalance in the heat/mass transfer ratio, in contrast with the IET-8B results cited above. Since the CONTAIN heat/mass transfer analogy is not expected to apply when debris interactions with liquid water are dominant, success of the analogy in the CED-2 analysis suggests the dominant rate-limiting processes may have been debris-gas interactions, rather than interactions with the liquid water.

In the CED-2 experimental analysis, the experimental results were used to estimate the time interval (which was very short) over which debris was dispersed from the cavity. Since experimental information is obviously unavailable for the scenarios analyzed here, sensitivity studies were included for the debris dispersal interval and the degree of debris coherence with the ejected water and with blowdown steam.

Debris Sources. Williams et al. (1995b) presented sensitivity studies indicating that, for the case considered, DCH loads were very insensitive to the exact details of the time-dependence of the debris source, provided the fraction of the debris dispersed from the cavity was correct and the degree of coherence between debris dispersal and the steam blowdown was correct. Hence, use of debris sources with a simple trapezoidal time-dependence was judged adequate.

CONTAIN Code Analyses

For both Scenario V and Scenario VI, the debris fraction dispersed from the cavity was taken to be 0.9. Three different approaches were used to estimate the coherence:

1. The coherence ratio, R_t , was calculated from the semi-empirical model given by Eq. (5.2) of NUREG/CR-6338. The value of the multiplicative constant appearing in this model used here was the value obtained by fitting to the Surry-geometry experiments (12.2), as the Sequoyah cavity was judged to be more nearly Surry-like than Zion-like. This coherence will be referred to as the "NUREG/CR-6338 coherence."
2. The standard prescription of Williams et al. (1995b) was used. This is based upon a simplified version of the NUREG/CR-6338 model and the dominant parameter dependencies are the same; however, the multiplicative constant was obtained in a manner considered to be more appropriate for use with CONTAIN. This coherence will be referred to as the "standard coherence".
3. In calculations including co-ejected water, it was considered plausible that enhanced steam supplies associated with vaporizing water could enhance debris dispersal rates, reducing the degree of coherence of the debris dispersal with the blowdown steam and/or with the water. Hence some of the cases involving co-ejected water were calculated assuming accelerated dispersal. The accelerated dispersal rates were estimated assuming the dispersal rate is proportion to the square root of the steam flow rate, which is the dependence implied by both the NUREG/CR-6338 and the standard coherence formulae. Steam flow rates were estimated by estimating the water ejection rate and assuming that, during dispersal, heat transfer from the debris would be sufficient to vaporize what water does not flash. These debris sources will be referred to as the "accelerated-dispersal sources". It is recognized that there are large uncertainties in these estimates; for example, the CED-2 experiment appears to have yielded dispersal rates much more rapid than this approach implies.

Information on the timing of the debris and water sources and the debris coherence with respect to the blowdown is summarized in Table B.3. R_t is the coherence ratio as defined by Pilch et al. (1994a), t_e is debris entrainment interval assumed, and f_{coh} is the fraction of the blowdown steam, or the co-ejected water, that is coherent with the debris entrainment interval. In the second column, "N6338" means that coherence was figured using Eq. (5.2) of NUREG/CR-6338.

"Coherence" is only an approximate concept in the context of CONTAIN calculations, and values of R_t and f_{coh} exactly equivalent to those specified for TCE/LHS cannot be defined. In the case of Scenario VI, at least, the standard value may actually correspond more closely to the value used in TCE than does the value identified as "N6338" in the table. Most calculations were made with the standard value and it is recommended that these results be used in comparisons with TCE results. The point is somewhat academic, as CONTAIN calculations are expected to be quite insensitive to moderate variations in coherence; factor-of-two variations in coherence typically result in ~10 percent variations in the calculated ΔP values (Williams and Louie, 1988; Williams et al., 1995b), although greater sensitivity cannot be ruled out for all cases.

In the accelerated dispersal cases, R_1 values are not given because flashing RPV water, not blowdown steam, was assumed to drive dispersal of the debris. There is little or no overlap between the debris dispersal and the steam blowdown in these instances, and the effective coherence with blowdown steam is small or zero. For Scenario VI, the accelerated dispersal time was comparable to the estimated time required to eject the 10000 kg of water from the vessel; hence, the coherence between debris and water was assumed to be large in this case. An essentially arbitrary case postulating low coherence with both co-ejected water and steam was run to examine sensitivity to this issue. In Scenario V, the time required to eject the 75000 kg of water is long compared with the accelerated dispersal time and coherence is therefore relatively low.

RPV Insulation. Prior to the SNL/IET-11 experiment (Blanchat et al., 1994), it had been suggested that the insulation surrounding the RPV might crumple up and jam in the annular gap surrounding the RPV, thereby preventing transport of debris to the containment dome via this path. In IET-11, however, it was found that the insulation was almost totally removed from the annular gap, completely opening it up. Furthermore, most of the insulation appeared to have been removed by ablation (i.e., melting) rather than mechanical stripping. Hence, the insulation is expected to interact with blowdown steam and/or the containment atmosphere much as does the steel in the melt ejected from the RPV. Blanchat et al. (1994) note that the insulation may have contributed to hydrogen production in IET-11.

In the standard input prescription defined by Williams et al. (1995a,b), it was assumed that insulation from the lower part of the vessel would mix with debris churned up in the cavity, while insulation from the upper part of the vessel sides would mix with debris already committed to exiting via the annular gap. Hence, in the standard prescription, half the insulation is added to the debris as it is introduced into the cavity atmosphere and half is added to the debris that enters the dome via the annular gap. CONTAIN analyses of this experiment with the insulation included in this manner gave better agreement with experiment for both ΔP and H_2 production than did otherwise identical analyses not including the insulation.

A similar treatment was recommended for PWR large dry containment analysis. However, in ice condenser plants, the RPV gap does not communicate to the dome; it communicates only to a relatively constricted volume located above the RPV and below the deck separating the upper and lower compartments. In the CONTAIN deck, the volume is included as part of Cell 2. In reality, there are only limited connections with the main volume of Cell 2, and the volume involved is only a small fraction of the total volume of Cell 2. Hence it was judged that including the insulation from the upper part of the vessel would be overly conservative.

In our best-estimate calculations, therefore, only the half of the insulation added to debris in the cavity is included in the present calculations. In addition, for Scenario V cases in which the 75000 kg of co-ejected water was included, it was judged likely that the water could prevent most of the insulation from being melted. Hence insulation was not included at all in these analyses. Because the RPV insulation has been neglected in most past DCH analyses, a number of sensitivity cases including no insulation have also been performed even for Scenario VI and for Scenario V analyses not including large amounts of water. It should be kept in mind that these cases are potentially nonconservative, relative to what is considered to be the best estimate.

The estimates of insulation mass used in the initial phase of this study (5340 kg) were derived by scaling to the mass cited for Surry (4500 kg) in Blanchat et al., 1994. The basis for scaling was the estimated RPV surface area ratio. However, it was subsequently recognized that the estimate cited for Surry corresponded to the entire vessel surface, including the upper head. It seems unlikely that insulation above the vessel flange can melt and mix with the debris. Using an areal density estimate of 4.2 lb/ft² obtained from a vendor³, the mass of insulation below the flange was recalculated. Both the original and the revised estimates are tabulated in Table B.2. Calculations performed using the original estimate were not rerun, but they are identified where results are presented in Section B.3. The values given in Table B.2 refer to the total masses and the values actually input to the code are therefore half the tabulated values.

Other DCH Modeling Input. Other models important to DCH are those controlling heat transfer from airborne and nonairborne debris with steam and gas, chemical reactions of airborne and nonairborne debris, debris transport, and debris de-entrainment by interactions with structures (trapping). No modifications to the standard input prescription were required for these models and the details will not be given here.

B.2.7 Perspectives on Containment Fragilities

It is not intended that the present work be used to estimate conditional containment failure probabilities (CCFP), but it would be somewhat fatuous to assert that one should not be interested in comparing loads calculated here with the estimated containment failure pressures. In Table B.4, the absolute containment pressure (in MPa) corresponding to 1 percent and 10 percent failure probability in the various ice condenser containments is given. These values are designated $P_{0.01}$ and $P_{0.1}$, respectively. Also given is the difference $P_{0.1} - P_{0.01}$. This quantity is of interest because it represents the margin implied by using a CCFP of 0.01 in screening analyses. Among other things, this margin is intended to provide an allowance for residual modeling uncertainties in the loads calculations used in the screening analysis. Hence, any modeling uncertainty greater than $P_{0.1} - P_{0.01}$ is potentially of interest. The data in Table B.4 are taken from Appendix D of NUREG/CR-6338, which in turn is based upon the IPE evaluations of fragility.

The margins $P_{0.1} - P_{0.01}$ in the ice condenser containments are smaller than is the case for many large dry containments. In Zion and Surry, for example, this margin is 0.142 MPa and 0.135 MPa, respectively. The especially low value (0.043 MPa) for Sequoyah in Table B.4 is worth noting.

If these fragility measures are compared with loads calculated in Section B.3, it must be remembered that the melt masses assumed correspond to the 99th percentile of the distributions assumed in NUREG/CR-6338. Failure to allow for this fact could yield excessively pessimistic conclusions.

³ M.M. Pilch, private communication to the author.

B.3 Results of the CONTAIN Calculations

We consider first the initial conditions for DCH and the containment pressurization expected from blowdown alone. We next provide reference calculations with input assumptions comparable to those used in TCE/LHS, insofar as this is practicable. In Section B.3.3, we then present analyses of scenarios in which igniters do not operate, which are relatively simple in the sense that they are dominated by combustion of the pre-existing hydrogen. In Sections B.3.4 and B.3.5, we present additional analyses for RCS Scenarios VI and V, respectively. Scenario VI was analyzed prior to Scenario V, primarily because it was desired to start with the case for which complications associated with large amounts of co-ejected water were not as severe.

B.3.1 Initial Conditions and ΔP from Blowdown

B.3.1.1 Containment Initial Conditions for DCH

Initial conditions for DCH are tabulated in Table B.5. These are the conditions that CONTAIN calculated to exist at the time of vessel breach for the various containment scenarios described in Section B.2.5. The quantities tabulated are the containment pressure; the number of kmoles (1 kmole = 1000 g-moles) of steam and of the gases N_2 , O_2 , and H_2 ; the total number of atmosphere kmoles; the kmoles of hydrogen burned prior to vessel breach; and the fraction of the initial ice inventory that remains unmelted at vessel breach.

From the table, it is evident that, in the scenarios that include operating igniters, almost half the initial oxygen inventory (262.15 kmoles) has been consumed prior to vessel breach. This reduction in oxygen inventory helps to reduce the role played by hydrogen combustion in some of the DCH calculations.

For the scenarios with operating igniters, there is not much variation in the amount of hydrogen remaining unburned, and the principal variations are in the pressure (P_0) and in the amount of steam. Scenarios Vb and VIb, of course, have considerably more oxygen and much more hydrogen present at vessel breach than do the others. The numbers in the table give only the total gas inventories and ignore differences in distribution. As would be expected, the distribution is much less uniform for the cases without ARFs, with steam mole fractions in the lower compartment exceeding 60 percent at the time of vessel breach.

In Scenario VI, the effect of reducing the deck leakage is significant, with there being less steam and lower containment pressures at vessel breach in this case. There is also less ice remaining at vessel breach, since more of the steam is forced to flow through the ice condenser in this case.

B.3.1.2 Pressurization from Blowdown Alone

Because the containment volume is small in ice condenser plants, the pressurization that can result from RCS blowdown alone is significant if there is no ice, or if the "small dry" approximation is being used. It is of interest, therefore, to estimate this component of the total

pressurization that occurs following vessel breach. The containment response to the blowdown was therefore evaluated for the various RCS initial conditions of interest in this work. No ice was included in the calculations. For the sake of convenience, the blowdown calculations were performed at time zero, not for the conditions existing at vessel breach. This means that the heat sink structures were unheated at the start of blowdown, maximizing the mitigating effect on the blowdown. In order to bound this effect, calculations were also performed with all atmosphere-structure heat transfer turned off.

The calculations performed at time zero (i.e., with unheated heat sink structures) actually do provide a reasonable approximation for the containment conditions at vessel breach for Scenarios Va', Vb', VIa', and VIb' since the combination of operating ARFs and ice remaining until vessel breach keeps the containment cool in these cases. For the other cases, the structures would be warmer. Two cases were calculated for the containment conditions existing at vessel breach in containment Scenario VI (standard deck leakage assumed).

Results are summarized in Table B.6. The following points may be noted:

- Flashing of RPV water adds significantly to the blowdown pressurization in Scenario V, with a substantial increase resulting if the water is close to saturation.
- RPV water does not increase the blowdown ΔP for Scenario VI; in fact, a slight decrease results. The reason is that the RCS temperatures are initially relatively high (1000 K) in Scenario VI, and the blowdown heats the containment as well as adding steam to the atmosphere. Flashing of the RPV water does add additional steam, but this effect is counterbalanced by cooling owing to the water that does not flash.
- The ΔP values calculated when the heat sinks are included is about 70-80 percent of the adiabatic values.
- Evaluating the blowdown with the heat sinks conditioned as they were in containment Scenario VI increases the calculated pressurization slightly, but the effect was small.

B.3.2 Reference Case Calculations for Comparison with TCE/LHS

CONTAIN point calculations were performed in order to assist in benchmarking TCE/LHS in the "small dry" approximation; i.e., neglecting ice in the ice condenser. The results are summarized in Table B.7. These calculations will be referred to here as the "reference cases". TCE/LHS does not model either RPV insulation or co-ejected primary system water, and hence the reference cases do not include insulation or co-ejected water. It must be remembered that the best estimate CONTAIN assumptions are that the insulation and co-ejected water do participate in some degree and hence the reference cases are potentially nonconservative with respect to a best estimate. (It does not, of course, follow that the corresponding TCE/LHS calculations are necessarily nonconservative.) Possible effects of ice, insulation, and co-ejected water are considered separately, in Sections B.3.4 and B.3.5

As was discussed in Section B.2, it is recommended that comparisons with TCE/LHS use the CONTAIN calculations with coherence based upon the CONTAIN standard prescription because completely equivalent definitions for "coherence" in CONTAIN and TCE/LHS are not possible. For comparison, several cases were rerun with coherence based upon the NUREG/CR-6338 formula and these results are presented here also.

Table B.7 presents results for all the scenarios for which initial conditions are identified in Table B.5, with the exception of Scenarios Vb' and VIb'. Quantities tabulated include ΔP , the maximum temperature calculated to occur in the dome, the amount (in kmoles) of hydrogen left unburned after the DCH event, the amount of hydrogen produced, and the amount of hydrogen produced by metal-steam reactions. The hydrogen numbers cited are for 20 s following vessel breach, which is after the peak containment pressure in all cases. The maximum temperature calculated in the dome is reported because it is of interest in assessing whether the modeling of pre-existing hydrogen is reasonable. Several points may be noted in connection with the tabulated results:

- Severe loads are obviously calculated for the scenarios without igniters (Vb and VIb).
- Calculated ΔP values are very similar for Scenarios V and Va, and for VI and VIa. This also includes the variant of Scenario VI in which the deck leakage is reduced a factor of 10 below the FSAR values.
- For Scenarios Va' and, especially, VIa', the calculated ΔP values are considerably less. The reason is that the reduced initial atmosphere inventory in Scenarios Va' and VIa' mean that there is a smaller atmospheric heat sink available to be heated in the subcompartment, and temperatures are higher for a given energy transfer which results in more rapid energy transfer to structures. Inspection of the detailed code output showed that, in Scenario VIa', energy remaining in trapped debris and energy transferred from the atmosphere to structures were both higher than in Scenario VI; hence, the net energy residing in the gas at any one time was smaller in VIa'.
- Dome temperatures do not approach the presumed BSR threshold of 950 K, and combustion of pre-existing hydrogen played little role in the calculations, except for Vb and VIb.
- There is substantial unburned hydrogen remaining after the event. This includes not only pre-existing hydrogen (except in Vb and VIb) but also over half the DCH-produced hydrogen remains unburned. One reason is that the lower compartment quickly becomes oxygen-starved. There is substantial hold-up of hydrogen in the lower compartment in Scenario VI, where the amounts of blowdown steam are insufficient to flush most of the hydrogen to the dome, which contains the remaining oxygen supply. In Scenario V, the ratio of diluent/combustible generally exceeded the presumed inerting threshold (9.0) in the DFB model; hence, most hydrogen entering the dome was not calculated to burn.

CONTAIN Code Analyses

The debris fraction transported to the dome (not tabulated) was less than 0.01 in all cases; hence, dome transport did not contribute to pressurization in the calculations and debris quantities entering the dome are unlikely to be large enough to significantly alter hydrogen combustion behavior, other than to assure multiple ignition sources.

The above statements should not be overgeneralized; as given, they are intended to apply only to the reference cases.

One other feature of some of the calculations should be mentioned at this point. Scenario VI reference case pressure-time histories for the lower and upper compartments are plotted in Figure B.2. At early times in the DCH event, the pressures in the two compartments are nearly equal. However, at later times, the lower compartment cools more rapidly than the upper compartment, in part because the lower compartment is initially hotter and in part because it has a considerably higher surface/volume ratio available for heat transfer. As the lower compartment pressure falls below the upper compartment pressure, the lower plenum doors close, permitting large pressure differentials to develop. A number of other calculations exhibited similar behavior.

It is possible that the lower plenum doors would not reclose, if the hinges are crushed as a result of the initial flow surge associated with the onset of the DCH event. If the doors do reclose, structural failure of some type might preclude development of such large reverse pressures. The nature of any such failure, and whether it poses a potential threat to containment integrity, has not been assessed in this work.

B.3.3 Scenarios Without Igniters

Scenarios Vb and VIb results in Table B.7 obviously represent severe loads, and DCH is unlikely to be favorably resolved for these scenarios if important mitigating effects cannot be identified. We briefly consider this possibility in the present section. We also consider the loads associated with hydrogen combustion alone. Some cases were run with the CONTAIN default flame speed correlation for deflagrations instead of the DCH standard prescription values; however, for the high hydrogen concentrations involved, the default flame speeds are generally as high as, or higher than, the DCH prescription.

Some results are summarized in Table B.8. Cases Vb-1 and VIb-1 are the reference cases for these scenarios, given in Tables B.7. In Case Vb-2, 50 percent of the ice was artificially restored to the ice condenser, in order to investigate how much mitigation the ice condenser might provide. Although the loads are reduced, the resulting containment pressurization is still severe.

Case Vb-2 is unrealistic in the sense that the initial conditions are those of Scenario Vb, which are not appropriate for a scenario in which ARFs operate and ice remains at vessel breach. Case VIb'-2 was run with the initial conditions of Scenario VIb' and, in addition, the ice remaining at vessel breach was artificially increased to 50 percent. Finally, Case VIb-3 was run (with the Scenario VIb initial conditions) with HPME completely omitted; only the blowdown was modeled, in addition to the hydrogen burns.

The cases with ice in the ice condenser are actually rather similar to the case with no HPME at all (which was, however, run without ice). The dominant contribution to the loads is hydrogen combustion in these scenarios. Among other things, the fact that these cases were run with a large melt mass is not very significant in interpreting these results, because even a minimal melt mass will yield at least the hydrogen combustion pressurization, which is itself large. However, the SR5 calculations used to define hydrogen sources to the containment may be higher than median or best-estimate values.

At vessel breach, hydrogen concentrations are 14-15 percent in Scenario Vb and VIb, and 18-19 percent in Scenarios Vb' and VIb'. These concentrations are within the range for which dynamic loading associated with large-scale accelerated flames or even detonations can occur. Given the large concentrations of hydrogen, these hydrogen combustion threats do not require HPME to occur; hence they are considered to be an issue separate from DCH and will not be considered further here.

B.3.4 Scenario VI With Igniters Operating

The ice condenser analysis has required consideration of several containment scenarios for each RCS scenario, and addressing DCH-related loading issues in detail for all combinations would be prohibitive. Hence a number of exploratory calculations were performed to determine what is potentially important and which scenarios need not be considered in detail. It was found that Scenarios VI and VIa generally responded similarly, while Scenario VIa' revealed distinct differences. Hence only Scenarios VI and VIa' are considered in any detail, and Scenario VIa may be assumed to be similar to Scenario VI. The variant of Scenario VI in which deck leakage is reduced is also believed to respond to DCH similarly to Scenario VI, although only a single calculation (see Table B.7) has been performed for this case.

Not all the calculations that have been performed will be discussed here. Table B.9 summarizes the results of greatest interest. Cases are numbered for ease of reference. In the text, the case number is preceded by the scenario when necessary for clarity; e.g., Case VIa'-3. Following the case number, the next three columns indicate whether RPV insulation was included, the mass of co-ejected water included (if any), the fraction of the original inventory of ice assumed to be present at vessel breach, and any other variations. Blank entries in the table indicate cases that were not run.

We consider first the "small dry" approximation in which no credit is given for ice in the ice condenser. Although no effort is made to bound the loads in the "small dry" analyses, some reasonably severe cases are identified, partly in order to test the potential of the ice condenser to mitigate DCH loads under a range of conditions. Using the insights obtained concerning the major factors that might affect the loads, we then consider cases with ice that show, for the range of conditions considered here, postulating that the ice condenser remains effective at vessel breach can result in a high degree of mitigation, even for cases with relatively high loads in the "small dry" approximation. Note, however, that the cases with ice do not apply for Scenario VIa, in which ice is completely exhausted prior to vessel breach.

B.3.4.1 "Small Dry" Approximation

Potential Effects of Co-Ejected Water. In Case 2, co-ejected RPV water was included, using the standard prescription for coherence. An enhancement in ΔP of about 0.2 MPa results for Scenario VI, and an enhancement of over 0.3 MPa results for Scenario VIa'. Since there are many uncertainties involved in modeling DCH scenarios involving water, these results may best be thought of as representing the potential effects of co-ejected water if efficient interactions with debris do occur, rather than representing a prediction of what will actually happen. Several sensitivity cases were run to investigate how sensitive this enhancement is to the specific assumptions made in Case 2.

One of the most important of the uncertainties involved is the coherence between debris, water, and blowdown steam, as this is a major factor controlling how much interaction with debris can actually occur. Case 3 was run with the accelerated debris dispersal assumption (see Section B.2.6.3 and Table B.3), which almost eliminates debris coherence with blowdown steam although the coherence with water is still high. There is little change with respect to the standard case. Case 4 was run with the reduced coherence assumption of Section B.2.6.3, in which there is little coherence with steam and coherence of debris dispersal with water is only 25 percent. The effect of the water is reduced appreciably, but it is still substantial, relative to the reference case.

The decrease in ΔP in Case 4 relative to Case 3 is considerably larger for Scenario VIa' than for Scenario VI. However, in Cases VIa'-2 and Cases-VIa'-3, the maximum dome temperatures show that BSR initiated in the dome, while peak temperatures dropped below the presumed BSR threshold of 950 K in Case VIa'-4. Part of the decrease in this case is due to the failure to initiate BSR; sensitivity to this issue is briefly considered later in this section.

Case 5 was run with a low water temperature (320 K, as might exist in the cavity); results indicate that the calculation is not very sensitive to water temperature. Assuming 5000 kg of water interacts, with the rest of the water not included in the calculation at all, also reduces the pressurization but it is still significantly above the reference case.

It is worth considering the reasons for the calculated effects. In RCS Scenario VI, the mass of steam in the vessel is relatively low, 6090 kg; considering only the coherent blowdown steam, the debris/steam heat capacity ratio, ψ , is fairly high, about 4. The energy required to vaporize that portion of the water which does not flash is small compared with the total energy available, and the increased steam supply much more than compensates for this energy. Inspection of the detailed code output showed that less energy remained in the debris in the cases with water and, in addition, less energy was transferred from the atmosphere to the structures, because the increased steam supply implies that lower gas temperatures result from the same amount of sensible heat transfer to the gas.

Again, it is to be remembered that the effects calculated here for co-ejected water should not be viewed as definite predictions, because a detailed mechanistic model for predicting how much water will actually interact with the debris is not available. The results do show that significant

effects are calculated for a considerable range of assumptions concerning interaction timing and debris-water coherence.

RPV Insulation. Comparison of Case VI-1 with Case VI-8, and Case VI-7 with Case VI-3, indicates that the insulation is not a major factor contributing to the calculated containment pressurization. Although there is a significant increase in the hydrogen produced, most of the additional hydrogen does not have an opportunity to burn. Some calculations not reported here showed somewhat larger effects of the insulation (up to 0.03 MPa.) If all the additional hydrogen produced could burn adiabatically, the increase in ΔP would be about 0.075 MPa for the cases with the corrected insulation mass. None of the calculations closely approached this value. The overall behavior indicates that the insulation is not likely to be a major effect. One reason is that it is difficult for the extra hydrogen produced to find oxygen in time to burn on DCH time scales.

Completeness of Reaction. The calculated results for hydrogen production show little variation except for cases with different amounts of insulation participating, principally because virtually all the metal was calculated to react in most cases. The reason is that the standard input prescription assumes that the turbulence of the DCH event keeps the debris well-mixed. Williams (1992) cites evidence supporting this treatment. With this assumption, chemical reaction rates are assumed to be limited only by gas-phase mass transport rates. Analyses of the DCH experiments using this assumption generally yielded good results (Williams et al., 1995b).

The well-mixed assumption, combined with the assumption that there are no drop-side reaction rate limits, result in very rapid reaction of the metal when the amounts of metal are small, because the full surface area of the debris is credited, no matter how small the metal content. This tendency can be increased further because the CONTAIN model, as used here, will mix aged debris that contains no metal with fresh debris that still contains metal, which can exaggerate the surface area of the debris. CONTAIN includes a feature that permits separating the debris into time-resolved groups, such that debris introduced at early times is kept in fields separate from the debris introduced later. Running a case similar to the Scenario VIa reference case with 30 time-resolved groups affected the parameters of interest (ΔP , hydrogen production) by less than 1 percent, relative to an equivalent calculation without time resolution. It is possible, however, that 30 groups is insufficient to completely suppress the effect. Since even 30 groups results in a prohibitively slow calculation, this effect was not investigated further. It is planned to improve the efficiency of this feature in a future code release.

A more extreme limitation to reaction rates results if drop-side reaction rate limits are imposed (Baker, 1986). Case VI-9 was run with drop-side reaction rate controlled by an assumed drop diffusivity, D_d , of 10^{-8} m²/s. This value is appropriate for the materials and temperatures of interest if the drops are completely stagnant (Williams et al., 1987). Comparison with Case VI-2 shows a reduction in hydrogen production of 44 percent, and ΔP is reduced by almost 0.06 MPa. While this reduction is not trivial, it does not represent a dominant effect. More importantly, Case VI-9 almost certainly overpredicts any possible impact of drop-side reaction rate limits, even as a bound. Analysis of the SNL/IET-1R and SNL/IET-3 experiments with $D_d=10^{-8}$ m²/s underpredicts hydrogen production by more than a factor of two and, in SNL/IET-3 (where the hydrogen could burn), it underpredicts ΔP by about 35 percent. Clearly, there can be no justification in the

CONTAIN validation base for imposing drop-side reaction rate limits this large. It is concluded, therefore, that any tendency of CONTAIN to overpredict the extent of reaction in these calculations has at most a minor effect upon the results and it will not be considered further.

Hydrogen Combustion in the Dome. Since these scenarios postulate operational igniters prior to vessel breach, dome hydrogen concentrations are generally below the deflagration flammability limits at the time of DCH initiation. Combustion in the dome is therefore limited principally to the BSR model in the CONTAIN calculations. Dome temperatures exceeded the presumed BSR threshold of 950 K in Cases VIa'-2 and VIa'-3, and combustion of pre-existing hydrogen in the dome contributed to the calculated loads. Since hydrogen behavior under these conditions is uncertain, Case VIa'-10 was run with BSR suppressed in the dome. Comparison with Case VIa'-3 shows that the calculated ΔP is reduced by about 0.04 MPa. The amount of hydrogen burned is reduced by about 60 kmoles, which could result in a much larger difference, almost 0.15 MPa, if the hydrogen were assumed to burn adiabatically. The reason is that the fractional burn rate in this calculation (0.185 s^{-1}) results in burn times considerable longer than the debris dispersal interval (1.41 s), which permits substantial mitigation by heat transfer. This burn rate is, of course, quite uncertain. None of the Scenario VI cases initiate BSR in the dome, although some come within 50 K of the presumed threshold.

Substantial uncertainties can exist (in either direction) in the present treatment of combustion in the dome. If the dome is truly well-stratified, pre-existing hydrogen below the mixing interface may be almost immune to combustion, even if the temperatures calculated by CONTAIN for a single well-mixed dome cell become very high. On the other hand, questions also exist as to whether the argument that stratification inhibits combustion of pre-existing hydrogen will always be valid. For example, in the accelerated dispersal cases, flow velocities of 50-100 m/s arise at the entrance to the dome during the initial pressurization period. The resulting turbulence may prevent the presumed stratification from developing. In addition, flammability limits for deflagrations become broader as temperatures rise, something the CONTAIN model does not take into account.

Application of the stratification stability correlations given in Pilch et al. (1994b) might provide some insights as to whether stratification should be presumed for all cases in the ice condenser analysis. In addition, application of the temperature-dependent flammability correlations given there might provide additional guidance as to whether deflagrations could occur in the dome as it heats and pressurizes. However, further investigation of these issues is not considered necessary for the present study because the goals of this work do not include a full quantification of uncertainties, and the major conclusions that can be drawn from the work are not sensitive to whether one does or does not assume that the suppression of hydrogen combustion in the dome will always apply. Hence the issue will not be considered further here.

Nonairborne Debris. Williams et al. (1995a,b) acknowledged substantial uncertainties in the modeling of nonairborne debris interactions and recommended supplementing the standard prescription calculations with sensitivity studies designed to illustrate the possible uncertainty range. The recommended cases were to eliminate the nonairborne model completely to provide a lower bound, and to consider a conservative case in which the nonairborne model is applied as it

was in the 1/10-scale experiments, without taking credit for the scaling rationale that was developed for NPP analysis.

Limited investigation of the sensitivity to uncertainties in the nonairborne model was performed for Scenario VIa (not VIa'). For the case without water, results were virtually insensitive to any assumptions concerning nonairborne debris. This result was unsurprising, since the nonairborne model contributes primarily by permitting interactions to occur with the noncoherent portion of the blowdown, and most of the blowdown is coherent in Scenario VI. In the case with co-ejected water, deleting the nonairborne model reduced loads by ~0.02 MPa. The more conservative case, in which no credit is taken for scaling, resulted in an increase in ΔP of about 0.12 MPa; however, a considerable part of this increase was the result of exceeding the threshold for BSR in the dome, which did not happen in the standard prescription case. There was no evidence that uncertainties associated with the nonairborne model could alter any important findings of the present effort.

Transport to the Dome. Calculated dome carryover fractions were < 1 percent in the cases without water and ~ 2 percent in the cases with water and the standard coherence. The high flow rates in the accelerated dispersal cases resulted in carry-over fractions of 5-10 percent. The debris that did reach the dome had cooled to about 1700 K (accelerated dispersal case), versus its initial temperature of 2800 K. There can be considerable uncertainty in the CONTAIN models for debris transport and trapping; with the standard input prescription, Williams et al. (1995a,b) considered the model more likely to overestimate dome transport fractions than to underestimate them. All things considered, transport to the dome is not a major factor controlling containment pressurization in the calculations and is not likely to be very important in reality. Uncertainties in the calculated loads resulting from the uncertainties in dome carryover fractions were considered very unlikely to be large enough to significantly affect the conclusions to be drawn from this work, and sensitivity studies to evaluate these uncertainties were not performed.

B.3.4.2 Potential Mitigation Effects of the Ice Condenser

The DCH calculation in Case 11 in Table B.9 was run with whatever amount of ice was calculated to remain at vessel breach, which was about 35 percent in Scenario VI and about 16 percent in Scenario VIa'. No water was included in these cases. The calculated loads are very mild. There is no significant threat to containment integrity.

The amount of ice left at vessel breach is determined largely by the steam and water sources input to the containment. Section B.2.3 noted that the SR5 sources used here may not be representative of all the scenarios of potential interest here; indeed, the SR5 sources are not fully consistent with a DCH event occurring at all, since the scenario analyzed with SR5 included full primary system depressurization as the result of a hot leg failure. The major purpose of the present study is to ascertain whether the ice condenser has the potential to mitigate DCH across a wide spectrum of possible scenarios. It was not desired to have this judgment contingent upon the exact amount of ice remaining at vessel breach for the particular SR5 sources used in the calculation. Hence, other calculations were performed assuming 50 percent of the ice would remain. This may be optimistic for some cases of possible interest. However, this is not of concern when the intent is

only to determine whether a potential for important mitigation does exist provided the amount of ice assumed is within the range of interest, which is the case here (Gregory et al., 1990). There is, of course, no expectation that the present study alone can "resolve" DCH for scenarios in which ice is available in the ice condenser.

For both Scenario VI and Scenario VIa', the two most threatening cases in the "small dry" approximation were Cases 2 and 3. In addition, Case 3 is also of potential interest because it might be supposed that the high flow rates associated with the accelerated dispersal cases could reduce the effectiveness of the ice condenser.

Cases 12 and 13 are analogous to Cases 2 and 3, respectively, except for the assumption that 50 percent ice remains at vessel breach. The resulting events are relatively innocuous. The accelerated dispersal case does enhance loads somewhat but even it represents a minimal threat. For example, if the initial pressures from Table B.5 are added to the indicated ΔP , only for Case 6-13 in the D. C. Cook containment is the 1 percent CCFP pressure exceeded, and even for D. C. Cook, the 10 percent CCFP pressure is not exceeded. For all other combinations of cases and plants, the 1 percent CCFP pressure is not equaled or exceeded. In assessing the significance of this result, it is worth recalling that all calculations were performed for a melt mass corresponding to the 99th percentile of the NUREG/CR-6338 uncertainty distributions.

An interesting point is that steam stripping results in high hydrogen concentrations developing in the ice condenser. Ice condenser gas compositions during and immediately after DCH are shown for Case VIa'-13 in Figure B.3. Hydrogen concentrations reach 40 percent at one point. The ice condenser is inerted at this time and no immediate combustion threat exists. If oxygen-bearing gases from the dome mix in with the hydrogen-rich ice condenser atmosphere, it is possible that mixtures capable of supporting accelerated flames and/or detonations might develop. The rate of mixing cannot be inferred from the present results because the plant model used possesses insufficient detail to address gas mixing problems. In the present scenario, the dome oxygen concentrations are only ~10 percent and it is possible that the locus of composition states achievable as the gases mix would never pass through a dangerous regime. However, the fact that the SR5 sources used here involve hydrogen production at the high end of the uncertainty distributions for in-vessel zirconium oxidation is *nonconservative* in the present context; that is, with less hydrogen entering the containment, less oxygen would be consumed prior to vessel breach. (To a certain extent, similar considerations apply to all the "small dry" approximation DCH calculations, except for the scenarios with no igniters prior to vessel breach.)

Since the most threatening of the "small dry" scenarios are rendered relatively nonthreatening when the ice condenser is included, there is little need to consider additional sensitivity cases involving DCH-related phenomena. There are, of course, uncertainties involved in the CONTAIN model for the ice condenser. Performing sensitivity studies on the ice condenser model may prove useful as part of a broader effort to assess the validity of the modeling. It is not, however, needed for the present goal of establishing that the potential for effective mitigation does indeed exist for a considerable range of DCH scenarios.

B.3.5 Scenario V with Igniters Operating

Many of the issues discussed in connection with Scenario VI apply to Scenario V also, and the discussion can be shorter than was the discussion of Scenario VI. We first consider a number of cases analogous to those considered in Scenario VI, in which either no co-ejected water is modeled or else in which only a small amount (i.e., 10000 kg) is included. The possible effects of the full 75000 kg of water postulated to be present in Scenario V are then considered. Finally, we consider the potential for the ice condenser to mitigate DCH in Scenario V.

We acknowledge that there is no mechanistic justification for the cases with the smaller amount of water, or with no water; the 75000 kg of water overlying the vessel is obviously going to be ejected with and/or immediately after the debris and it must be considered. However, calculations not including the full amount of water provide insights into other differences (as well as similarities) between Scenarios V and VI and provide a basis for comparison with TCE/LHS. In addition, calculations involving large amounts of water may be especially uncertain, to say nothing of being potentially controversial, and cases involving more familiar DCH analyses should be available for comparison.

Results for Scenarios V and Va' are summarized in Table B.10. Case 1 is the reference case. Loads are higher than in the analogous RCS Scenario VI cases, owing to the larger steam supply in the accumulator. The contribution of the blowdown itself is larger than in Scenario VI (see Table B.6). In addition, the debris/steam heat capacity ratio, ψ , is about 1.45 for Scenario V, versus about 4.0 for Scenario VI. Even allowing for the smaller melt mass in Scenario V, more energy can be transferred to blowdown steam.

Case 2 was run with the RPV insulation included as described in Section 2.6.3. The effect is somewhat larger than in Scenario VI, but it is still not a major effect. Note also that all Scenario V cases that include insulation were run with the original uncorrected mass estimate, which is probably too large.

Case 3 included 10000 kg co-ejected water for comparison with the Scenario VI analyses. The impact of the water is considerable less for the RCS Scenario V cases (especially in containment Scenario V); with more atmospheric heat sink available from the blowdown steam, the potential for the additional steam supplied by the water to enhance loads is less.

The drop-side reaction rate model was imposed with $D_d = 10^{-8} \text{ m}^2/\text{s}$ in Case V-4. The effect upon ΔP is small, even though it had a significant impact upon hydrogen production.

Case 5 was run with 75000 kg of 520 K co-ejected water and the accelerated dispersal prescription. For Scenario V, the enhancement over the case without water is comparable to what might be expected based upon the blowdown pressures alone that are given in Table B.6. There is a larger effect in Scenario Va'.

Case V-6 was run to examine the extent of quenching by airborne water in the CONTAIN calculations. In the cases with water, heat transfer is calculated to supply sufficient energy to

vaporize the water that is introduced during the debris dispersal period. However, in the cases involving 75000 kg of water, the water source is assumed to continue longer than the debris dispersal interval. Once debris dispersal is largely complete, the available energy is not sufficient to vaporize all the water. In the CONTAIN model, water that does not flash is assumed to condense as a water aerosol. De-entrainment of airborne water is not modeled in the sense that de-entrainment of debris is modeled; only the normal CONTAIN aerosol models are available. With the exception of the model for aerosol removal in the ice condenser, the aerosol models remove the water aerosol only slowly. There is therefore a potential for the water aerosol to remain airborne too long, which could cool the containment more than is realistic and result in calculated loads that are too low.

Case Va'-6 was run using the 'dropout' option. When this option is used, water that cannot be accommodated in the vapor phase is immediately placed in a pool where it is no longer available for rapid heat transfer with the atmosphere. The postulated behavior of the water in this case is not realistic; the option is not recommended for general use. However, it does provide a means of investigating whether there is a spurious quenching of DCH loads as a result of airborne water not being de-entrained sufficiently rapidly. In the present instance, specifying 'dropout' made very little difference. Other calculations (not tabulated) for Scenario V using 'dropout' yielded similar results. Hence it is not believed that any spurious quenching effects are very important in these calculations.

Case 7 was run assuming the water is saturated, $T=620$ K. (It is recognized that this case may be excessively conservative; it was run partly to provide a comparison case for the ice condenser calculations to follow.) Calculated loads are higher, especially in Case Va'-7 in which BSR was initiated in the dome. Rerunning this case with BSR suppressed in the dome (Case Va'-8) shows that the contribution from BSR initiation is larger in Scenario Va than it was in Scenario VIa. As a practical matter, the issue is not very important because calculated loads are high even without BSR in the dome.

With the exception of the case in which BSR occurred in the dome, the effect of the large amounts of co-ejected water upon ΔP in the Scenario V cases is comparable to the extra pressurization that the co-ejected water contributes to the pressurization calculated for blowdown alone. As a first approximation, then, the contribution of the co-ejected water appears to be an additive contribution associated with water flashing in these calculations. This situation differs from the Scenario VI calculations, in which the water contributed by increasing the atmospheric heat sink available for DCH heat transfer. In Scenario Va', the enhanced atmospheric heat sink does contribute some, but the effect is still considerably smaller than it was in Scenario VIa'.

Potential Mitigation Effects of the Ice Condenser. In Case 9, the DCH calculation of the reference case in Table B.7 was run with whatever amount of ice was calculated to remain at vessel breach, which was about 35 percent in Scenario VI and about 16 percent in Scenario VIa'. No water was included in these cases. The calculated loads are very mild, even for the Scenario VIa' case, for which the ice remaining is small. These cases do not imply any significant threat to containment integrity.

Case 10 is analogous to Case 3 except that 50 percent of the ice is assumed to remain at vessel breach. Again, the ice is highly effective in suppressing containment pressurization. Case 11 is analogous to Case 7 except for the presence of 50 percent ice, and thus provides a severe test of the potential for the ice condenser to mitigate the loads; the resulting event is still quite mild. Even when the ice inventory is reduced to 25 percent (Case V-12), the calculated loads are only somewhat higher and there is little threat to containment integrity except, possibly, in the case of the D. C. Cook containment.

B.4. Discussion and Conclusions

The results presented here concerning DCH loads support sorting the various issues involved in the ice condenser according to a four-level hierarchy, such that the issues involved at any given level are important only given certain outcomes at the higher level(s). In descending order, these issues are as follows:

1. Availability of ignition sources prior to vessel breach.
2. Availability and effectiveness of ice in the ice condenser.
3. Loads modeling uncertainties related to co-ejected RPV water.
4. Other loads modeling uncertainties.

We next discuss these issues in a little more detail, and compare their roles in ice condenser containments and PWR large dry containments.

1. Availability of Ignition Sources Prior to Vessel Breach.

The overriding issue is the availability of igniters or other ignition sources prior to vessel breach. If hydrogen released to containment is allowed to accumulate until vessel breach, the DCH event need do little more than provide the ignition source in order to produce threatening loads. No other factor identified is capable of providing sufficient mitigation to reverse this conclusion. The principal qualification here is that the hydrogen sources assumed in this work are based upon a single SR5 calculation, and the amount of hydrogen produced in these calculations corresponds to oxidation of 58.8 percent of the total core zirconium inventory. This corresponds to the high end of the distribution for the fraction of zirconium oxidized as given in NUREG/CR-6338; the median there is about 40 percent oxidized. Averaging over the distribution would give a somewhat lower loads spectrum. It is doubtful, however, that there would be any major change to the conclusion that the availability of igniters prior to vessel breach is a crucial issue.

This situation is quite different from that in PWR large dry containments, in which the question of whether pre-existing hydrogen can burn prior to vessel breach played a relative minor role in assessing DCH threats. If engineered safety features (ESFs) are unavailable, flammable conditions may be unlikely to develop before vessel breach and, even if ESFs are available, there are no igniters to provide deliberate ignition sources. This issue was not considered to be

sufficiently important to require detailed assessment in NUREG/CR-6338 and its predecessor documents, and no splinters were defined based upon this issue. Some consideration was given as to whether hydrogen could autoignite as it enters the containment from the primary system (Pilch et al., 1994b).

2. Availability and Effectiveness of Ice in the Ice Condenser

If the hydrogen is burned off prior to vessel breach, the ice condenser effectiveness becomes the dominant issue controlling DCH loads, by wide margins. If the ice is available, the ice condenser is calculated to have the potential to mitigate any of the scenarios (other than VIb and Vb) that have been considered, even if when assumptions thought to be conservative are made in the loads modeling. No calculation with ice exceeded the 1 percent CCFP pressure for any containment other than D. C. Cook, and even in this case, the 10 percent failure probability was not exceeded. This fact is all the more significant when one takes into account that all the calculations were performed with melt masses corresponding to the 99th percentile of the NUREG/CR-6338 melt distributions.

It must be remembered, however, that this optimistic picture is contingent upon resolution of three questions:

- Is sufficient ice remaining at vessel breach to be effective?
- Even if ice is available, can ice condenser effectiveness be defeated by uneven ice melting, damage to the ice condenser owing to detonations, etc?
- Is the CONTAIN model for ice condensers valid under the conditions of interest? (Even for DBAs, there has not been a major effort to validate the CONTAIN ice condenser model, and there is no data base for validation under DCH conditions.)

It is interesting to compare the current findings with respect to the potential of the ice condenser to mitigate DCH threats with the results of the earlier study by Williams and Gregory (1990). In this study, it was found that the ice condenser could not prevent the development of threatening loads in many of the scenarios of interest, even if it were assumed that igniters were operating prior to vessel breach. In part, this difference reflects refinements that have been made to CONTAIN's models for DCH and hydrogen combustion phenomena since that time. At least as important, however, is the change in the assumed initial conditions. The earlier study assumed melt compositions based upon BMI-2104 (Gieseke et al., 1984), which had a high metal content. As a result, large amounts of hydrogen were produced during the DCH event itself in those calculations, and its combustion produced a threat that neither igniters nor the ice condenser could control effectively. In the present study, the metal content is limited and much of what hydrogen is produced does not find sufficient oxygen for combustion on DCH time scales, or is sufficiently diluted with steam that combustion is not predicted to occur.

The ice condenser issue has no analogue in PWR large dry containment analysis. Although questions exist concerning what ESFs might be operating, the answers to these questions do not

exert the dominant influence over DCH loads that is potentially exerted by the ice condenser question.

3. Effects of Co-Ejected RPV Water on DCH Loads

If hydrogen is burned off prior to vessel breach and there is little or no ice remaining, or if the "small dry containment" approximation is being used, the dominant issue appears to be the effect of co-ejected water on the calculated loads. If optimistic assumptions are made concerning this water (e.g., if it is ignored), the calculated loads suggest that resolution could be achieved for at least some combinations of plants and scenarios. However, most calculations including the water (even cases not judged to be particularly conservative) result in threatening loads. This result is only suggestive, not conclusive, in part because of the large melt mass assumed; folding in these uncertainties with the melt mass distributions assumed in previous work (Pilch et al., 1996) could moderate this conclusion somewhat.

There are large uncertainties in modeling the impact of co-ejected RPV water on DCH loads; the CONTAIN calculations involving water are better thought of as illustrating the potential consequences of a given degree of debris-water interaction rather than a prediction of what will actually happen. Thus they define an uncertainty range, not a point estimate. An important contributor to the uncertainty is the degree of coherence between debris dispersal and water ejection, which is highly uncertain. The success of the CONTAIN analysis of the CED-2 experiment, for which an approximate experimental estimate of the coherence was available, suggests that CONTAIN can be useful for examining the implications of any specified degree of coherence. Note also that much of the potential impact of water in the Scenario V calculations appeared to be that associated with flashing of the water upon depressurization. Uncertainties in this contribution are governed more by uncertainties in the amounts and enthalpies of water remaining in the RCS at vessel breach than they are governed by uncertainties in DCH phenomenology.

Phenomenologically, co-ejected water can have qualitatively similar effects upon DCH in PWR large dry containments. However, the larger containment volume will result in the change in ΔP being smaller (by about a factor of two) for a given energy input. Furthermore, the much greater margin to failure reduces the practical import of these uncertainties.

4. Other Uncertainties in Loads Modeling.

In addition to the co-ejected water issue, a number of other loads uncertainties were also considered here. These include hydrogen combustion issues other than the igniter question, effects of RPV insulation, completeness of metal reaction, debris transport to the dome, and coherence between debris dispersal and blowdown steam. Some of these should be included in a complete and quantitative treatment of loading uncertainties. However, there is no evidence that these questions have significant potential to modify the major conclusions offered here. That is, if these uncertainties were completely eliminated, it is not expected that any of the conclusions concerning the first three levels of the hierarchy would be seriously affected.

References

- Baker, L., Jr. (1986). "Droplet Heat Transfer and Chemical Reactions During Direct Containment Heating," *Proceedings of the International ANS/ENS Topical Meeting on Thermal Reactor Safety*, San Diego, CA.
- Blanchat, T.K. et al. (1994). "Experiments to Investigate Direct Containment Heating Phenomena With Scaled Models of the Surry Nuclear Power Plant," NUREG/CR-6152, SAND93-2519, Sandia National Laboratories, Albuquerque, NM.
- Gieseke, J.A. et al. (1984). Radionuclide Release Under Specific LWR Accident Conditions: PWR Ice Condenser Containment Design," (Vol. IV), BMI-2104, Battelle Columbus Laboratories, Columbus, OH.
- Gregory, J.J. et al. (1990). "Evaluation of Severe Accident Risks: Sequoyah, Unit 1," NUREG/CR-4551, SAND86-1309, Vol. 5, Rev. 1, Parts 1 & 2, Sandia National Laboratories, Albuquerque, NM.
- Pilch, M.M., H. Yan, and T.G. Theofanous (1994a). "The Probability of Containment Failure by Direct Containment Heating in Zion," NUREG/CR-6075, SAND93-1535, Sandia National Laboratories, Albuquerque, NM.
- Pilch, M.M. et al. (1994b). "The Probability of Containment Failure by Direct Containment Heating in Zion," NUREG/CR-6075, Supplement 1, Sandia National Laboratories, Albuquerque, NM.
- Pilch, M.M. et al. (1995). "The Probability of Containment Failure by Direct Containment Heating in Surry," NUREG/CR-6109, SAND93-2078, Sandia National Laboratories, Albuquerque, NM.
- Pilch, M.M. et al. (1996). "Resolution of the Direct Containment Heating Issue for All Westinghouse Plants with Large Dry Containments or Subatmospheric Containments," NUREG/CR-6338, SAND95-2381, Sandia National Laboratories, Albuquerque, NM.
- NRC (1990). *Severe Accident Risks: An Assessment for Five U. S. Nuclear Power Plants*, Final Summary Report, NUREG-1150, U. S. Nuclear Regulatory Commission, Washington, DC, December 1990.
- Williams, D.C. et al. (1987). "Containment Loads Due to Direct Containment Heating and Associated Hydrogen Behavior: Analysis and Calculations with the CONTAIN Code," NUREG/CR-4896, SAND87-0633, Sandia National Laboratories.
- Williams, D.C. and D.L.Y. Louie (1988). "CONTAIN Analyses of Direct Containment Heating Events in the Surry Plant," Proceedings of the ANS/ENS Winter Meeting, Thermal Hydraulics Division, Washington DC.

Williams, D.C. and J.J. Gregory (1990). "Mitigation of Direct Containment Heating and Hydrogen Combustion Events in Ice Condenser Plants," NUREG/CR-5586, SAND90-1102, Sandia National Laboratories, Albuquerque, NM.

Williams, D.C. (1992).

Williams, D.C. et al. (1995a). "CONTAIN Code Analyses of Direct Containment Heating Experiments: Model Assessment and Phenomenological Interpretation," Eleventh Proceedings of Nuclear Thermal Hydraulics, 1995 ANS Winter Meeting, Oct. 29 - Nov. 2, 1995, San Francisco, CA.

Williams, D.C. et al. (1995b). "Assessment of the CONTAIN Direct Containment Heating (DCH) Model: Analysis of DCH Integral Experiments," Letter report to the Accident Evaluation Branch, USNRL.

Table B.1 CONTAIN representation of the Sequoyah containment

| Cell No. | Containment Region Represented | Volume (m ³) |
|----------|--------------------------------|--------------------------|
| 1 | Reactor Cavity | 420 |
| 2 | Lower Compartment | 8962 |
| 3 | Lower Plenum | 685 |
| 4 | Ice Chest | 2444 |
| 5 | Upper Plenum | 1330 |
| 6 | Upper Compartment ("Dome") | 19859 |
| 7 | Reactor Coolant System (RCS) | 344* |
| 8 | Shield Building Annulus | 9143 |
| 9 | Environment | 10 ²⁰ |

*Used to generate blowdown steam sources. Volume = 351.33 m³ for Scenario VI calculations; see Section 2.6.

Table B.2 RCS initial conditions for Sequoyah DCH calculations

| Parameter | Scenario V | Scenario VI |
|---|--|---------------------------|
| RPV Pressure (MPa) | 16.0 | 8.0 |
| RPV Temperature (K) | 700 | 1000 |
| RPV Failure Size (Diameter, m) | 0.45 | 0.5 |
| Debris Temperature (K) | 2800 | 2800 |
| Total Debris Mass (kg) | 61880 | 87700 |
| UO ₂ | 51500 | 72000 |
| ZrO ₂ | 6290 | 8810 |
| Zr | 1720 | 2290 |
| Steel (Total) | 2370 | 4530 |
| Fe | 1710 | 3264 |
| Cr | 450 | 866 |
| Ni | 210 | 399 |
| RPV Water | | |
| Mass (kg) | 75000 | 10000 |
| Temperature (K) [*] | 520 (620) ^a | 568 |
| Enthalpy (J/kg) [*] | 1.070x10 ⁶ (1.644x10 ⁶) ^a | 1.316x10 ⁶ |
| RPV Insulation [*] | | |
| Temperature (K) [*] | 600 | 600 |
| Total Mass (kg) [*] | (5340 ^b) | 3355 (5340 ^b) |
| Fe [*] | (3950 ^b) | 2482 (3950 ^b) |
| Cr [*] | (960 ^b) | 603 (960 ^b) |
| Ni [*] | (430 ^b) | 270 (430 ^b) |
| [*] Values not derivable from NUREG/CR-6338 and were estimated for this work. | | |
| ^a Values used in some sensitivity calculations. | | |
| ^b These values were used in some calculations, but are now believed to be too high; values not enclosed in () are the corrected values. | | |

Table B.3 Timing and coherence information for debris, steam, and water sources

| RCS Scenario | R _t Correl. | Water (kg) | Comments | R _t | t _e | f _{coh} | |
|--------------|------------------------|------------|--|----------------|----------------|------------------|-------|
| | | | | | | Steam | Water |
| V | N6338 | 0 | | 0.602 | 5.22 | 0.437 | --- |
| V | Std. | 0 | | 0.448 | 4.02 | 0.351 | --- |
| V | Std. | 10000 | Reduced water case | 0.448 | 4.02 | 0.351 | 1.0 |
| V | --- | 75000 | Accelerated dispersal | --- | 1.41 | 0.0 | 0.27 |
| VI | N6338 | 0 | | 1.63 | 9.34 | 0.764 | --- |
| VI | Std. | 0 | | 1.12 | 6.46 | 0.642 | --- |
| VI | Std. | 10000 | Std. water prescription * | 1.12 | 6.46 | 0.642 | 1.0 |
| VI | --- | 10000 | Accelerated dispersal | --- | 1.41 | < 0.05 | 1.0 |
| VI | --- | 10000 | Accelerated dispersal, reduced coherence | --- | 1.41 | < 0.05 | 0.25 |

*In the standard prescription, water is introduced in parallel with the debris sources and the fraction of the water that participates is varied. The prescription was defined primarily for co-dispersed cavity water.

Table B.4 Ice condenser containment fragility measures

| | Fragility Measures (MPa absolute) | | |
|------------------|-----------------------------------|--------------------|-------------------------------------|
| | P _{0.01} * | P _{0.1} * | P _{0.1} - P _{0.1} |
| Catawba 1 & 2 | 0.518 | 0.588 | 0.070 |
| D. C. Cook 1 & 2 | 0.353 | 0.412 | 0.059 |
| McGuire 1 & 2 | 0.489 | 0.545 | 0.066 |
| Sequoyah 1 & 2 | 0.482 | 0.525 | 0.043 |
| Watts Bar 1 & 2 | 0.489 | 0.586 | 0.097 |

*Absolute pressures at which estimated containment failure probabilities are 0.01 and 0.1, respectively.

Table B.5 Containment conditions at vessel breach

| Parameter | --- Containment Scenario --- | | | | | |
|--------------------------------|------------------------------|-----------|---------|-----------|---------|-----------|
| | V, VI | (V, VI) * | Va, VIa | Va', VIa' | Vb, VIb | Vb', VIb' |
| Pressure, P ₀ (MPa) | 0.1819 | 0.1402 | 0.1707 | 0.1016 | 0.1856 | 0.1264 |
| Atmosphere (kmoles) | | | | | | |
| Steam | 732.9 | 358.1 | 584.2 | 58.1 | 451.7 | 52.3 |
| N ₂ | 1046.0 | 1046.0 | 1046.0 | 1046.0 | 1046.0 | 1046.0 |
| O ₂ | 150.6 | 153.2 | 150.3 | 146.7 | 262.2 | 262.2 |
| H ₂ | 74.9 | 80.1 | 74.3 | 67.1 | 298.0 | 298.0 |
| Total | 2004.4 | 1637.4 | 1854.8 | 1317.9 | 2057.9 | 1658.5 |
| H ₂ Burned | 223.1 | 217.9 | 223.6 | 230.0 | 0 | 0 |
| Ice Fraction Unmelted | 0.351 | 0.136 | 0.0 | 0.159 | 0.0 | 0.219 |

*Variation of Scenarios V and VI with deck leakage reduced to 10 percent of FSAR value.

Table B.6 Containment pressurization from blowdown alone

| RCS Scenario | Containment Conditions | --- RPV Water --- | | Containment ΔP (MPa) | |
|--------------|------------------------|-------------------|-----------------|------------------------------|-----------|
| | | Mass (kg) | Temperature (K) | Heat Sinks Included | Adiabatic |
| V | t = 0 s | 0 | --- | 0.1262 | 0.1771 |
| V | t = 0 s | 75000 | 520 | 0.1662 | 0.2115 |
| V | t = 0 s | 75000 | 620 | 0.2645 | 0.327 |
| VI | t = 0 s | 0 | --- | 0.0665 | 0.0940 |
| VI | Scen. V, VI | 0 | --- | 0.0737 | --- |
| VI | t = 0 s | 10000 | 568 | 0.0636 | 0.0761 |
| VI | Scen. V, VI | 10000 | 568 | 0.0729 | --- |

Table B.7 Reference calculations for comparison with TCE/LHS

| Scenario | Coherence | ΔP (MPa) | $T_{\max}(\text{dome})$ (K) | Hydrogen Data (kmoles) | | |
|----------|-----------|------------------|-----------------------------|------------------------|--------|----------|
| | | | | Remaining | Burned | Produced |
| V | Std. | 0.476 | 743 | 131.7 | 34.5 | 81.3 |
| Va | Std. | 0.462 | 741 | 120.2 | 35.4 | 81.3 |
| Va | N6338 | 0.466 | 736 | 120.4 | 35.2 | 81.2 |
| Va' | Std. | 0.380 | 787 | 101.6 | 46.9 | 81.3 |
| Vb | Std. | 0.940 | 1658 | 30.6 | 348.7 | 81.3 |
| VI | Std. | 0.404 | 718 | 156.3 | 52.2 | 133.5 |
| VI | N6338 | 0.387 | 697 | 169.9 | 48.6 | 133.6 |
| VI* | Std. | 0.384 | 757 | 170.6 | 43.1 | 133.6 |
| Vla | Std. | 0.361 | 673 | 158.6 | 49.4 | 133.6 |
| Vla | N6338 | 0.347 | 651 | 161.8 | 46.0 | 133.8 |
| Vla' | Std. | 0.234 | 616 | 149.5 | 51.2 | 133.6 |
| Vla' | N6338 | 0.232 | 609 | 150.0 | 50.7 | 133.6 |
| Vlb | Std. | 0.821 | 1605 | 80.4 | 351.2 | 133.6 |
| Vlb | N6338 | 0.788 | 1601 | 80.9 | 350.6 | 133.6 |

*Variant of Scenario VI with deck leakage reduced a factor of ten.

Table B.8 Cases without igniters

| Case | Description | ΔP (MPa) | $T_{\max}(\text{dome})$ (K) | Hydrogen Data (kmoles) | | |
|--------|---|---------------------|--------------------------------|------------------------|--------|----------|
| | | | | Remaining | Burned | Produced |
| Vb-1 | Reference case | 0.940 | 1840 | 30.6 | 348.7 | 81.3 |
| Vb-2 | 50 percent ice restored | 0.628 | 1627 | 45.0 | 334.3 | 81.3 |
| VIb-1 | Reference case | 0.821 | 1605 | 80.4 | 351.2 | 133.6 |
| VIb'-2 | Scenario VIb', 50 percent ice restored* | 0.652 | 1914 | 68.7 | 362.8 | 133.6 |
| VIb-3 | No HPME* | 0.656 | 1640 | 1.4 | 296.7 | 0 |

*Run with default flame speed, which actually exceeds the standard DCH value. All cases probably should have used the default values, but the point is of no practical significance.

Table B.9 Summary of Scenario VI and Scenario VIa' results

| Case | Insul. | Water | Coh. | Comments | Scenario VI | | | | Scenario VIa' | | | |
|------|--------|-------|--------|----------------------------------|---------------------|------------------|----------------|-------|---------------------|------------------|----------------|-------|
| | | | | | ΔP (MPa) | T_{max} (K) | H_2 (kmoles) | | ΔP (MPa) | T_{max} (K) | H_2 (kmoles) | |
| | | | | | | | Burn | Prod. | | | Burn | Prod. |
| 1 | N | 0 | Std. | Reference Case | 0.404 | 718 | 52.2 | 133.6 | 0.2335 | 616 | 51.2 | 133.6 |
| 2 | Y* | 10000 | Std. | | 0.605 | 867 | 55.0 | 179.8 | 0.550 | 1095 | 128.9 | 179.7 |
| 3 | Y | 10000 | Accel. | | 0.613 | 914 | 65.1 | 161.3 | 0.555 | 1153 | 128.3 | 161.2 |
| 4 | Y | 10000 | Accel. | Reduced coherence | 0.558 | 902 | 71.4 | 157.3 | 0.418 | 923 | 79.3 | 156.2 |
| 5 | Y* | 10000 | Std. | $T_{water}=320$ K | 0.556 | 817 | 52.9 | 179.5 | --- | --- | --- | --- |
| 6 | Y* | 5000 | Std. | | 0.516 | 809 | 52.6 | 179.0 | --- | --- | --- | --- |
| 7 | N | 10000 | Accel. | | 0.595 | 885 | 47.9 | 130.5 | --- | --- | --- | --- |
| 8 | Y* | 0 | Std. | | 0.405 | 731 | 57.0 | 182.0 | --- | --- | --- | --- |
| 9 | Y* | 10000 | Std. | $D_d=10^{-8}$ m ² /s | 0.547 | 782 | 32.1 | 100.1 | --- | --- | --- | --- |
| 10 | Y | 10000 | Accel. | No dome BSR | --- | --- | --- | --- | 0.513 | 1019 | 69.2 | 161.2 |
| 11 | N | 0 | N6338 | 35.1 percent, 15.9 percent ice** | 0.118 | 458 | 42.9 | 133.6 | 0.130 | 454 | 46.5 | 133.6 |
| 12 | Y* | 10000 | Std. | 50 percent ice | 0.154 | 502 | 46.9 | 179.8 | 0.150 | 487 | 58.2 | 179.7 |
| 13 | Y | 10000 | Accel. | 50 percent ice | 0.193 | 549 | 60.0 | 161.2 | 0.206 | 607 | 68.8 | 161.0 |

*Run with the original estimate of insulation mass; cases without asterisk were run with the corrected mass. See Section B.2.6.3.

**Fraction of ice calculated to be left in Scenario VI and VIa, respectively.

Table B.10 Summary of Scenario V and Scenario Va' results

| Case | Insul. | Water | Coh. | Comments | Scenario V | | | | Scenario Va' | | | |
|------|--------|-------|--------|--|---------------------|------------------|-------------------------|-------|---------------------|------------------|-------------------------|-------|
| | | | | | ΔP (MPa) | T_{max} (K) | H ₂ (kmoles) | | ΔP (MPa) | T_{max} (K) | H ₂ (kmoles) | |
| | | | | | | | Burn | Prod. | | | Burn | Prod. |
| 1 | N | 0 | Std. | Reference Case | 0.476 | 743 | 34.5 | 81.3 | 0.3802 | 787 | 46.9 | 81.3 |
| 2 | Y* | 0 | Std. | | 0.5122 | 802 | 55.8 | 130.5 | 0.3955 | 828 | 58.7 | 130.5 |
| 3 | Y* | 10000 | Std. | $T_{water} = 568$ K | 0.5536 | 763 | 31.5 | 130.5 | 0.523 | 899 | 49.2 | 130.5 |
| 4 | Y* | 10000 | Std. | $T_w = 568$ K, $D_d = 10^{-8}$ m ² /s | 0.5357 | 743 | 25.4 | 71.2 | --- | --- | --- | --- |
| 5 | N | 75000 | Accel. | $T_w = 520$ K | 0.5561 | 739 | 26.1 | 81.2 | 0.5338 | 865 | 36.8 | 81.3 |
| 6 | N | 75000 | Accel. | $T_w = 520$ K; with 'dropout' | --- | --- | --- | --- | 0.5378 | 852 | 36.2 | 81.3 |
| 7 | N | 75000 | Accel. | $T_w = 620$ K | 0.7170 | 825 | 25.3 | 81.3 | 0.8021 | 1162 | 116.7 | 81.3 |
| 8 | N | 75000 | Accel. | $T_w = 620$ K, no dome BSR | --- | --- | --- | --- | 0.6872 | 962 | 36.0 | 81.9 |
| 9 | N,Y* | 0 | Std. | 35.1 percent, 15.9 percent** ice | 0.1441 | | 41.5 | 81.3 | 0.1386 | 485 | 57.2 | 130.5 |
| 10 | Y* | 10000 | Std. | $T_w = 568$, 50 percent ice | 0.1439 | | 47.8 | 130.5 | 0.1603 | 515 | 56.0 | 130.5 |
| 11 | N | 75000 | Accel. | $T_w = 620$ K, 50 percent ice | 0.1573 | 493 | 33.7 | 81.3 | 0.1748 | 533 | 52.1 | 81.3 |
| 12 | N | 75000 | Accel. | $T_w = 620$ K, 25 percent ice | 0.2254 | 553 | 36.3 | 81.3 | --- | --- | --- | --- |

*Run with the original estimate of insulation mass; cases without asterisk were run with the corrected mass. See Section 2.6.3.
**Fraction of ice calculated to be left in Scenario V and Va, respectively.

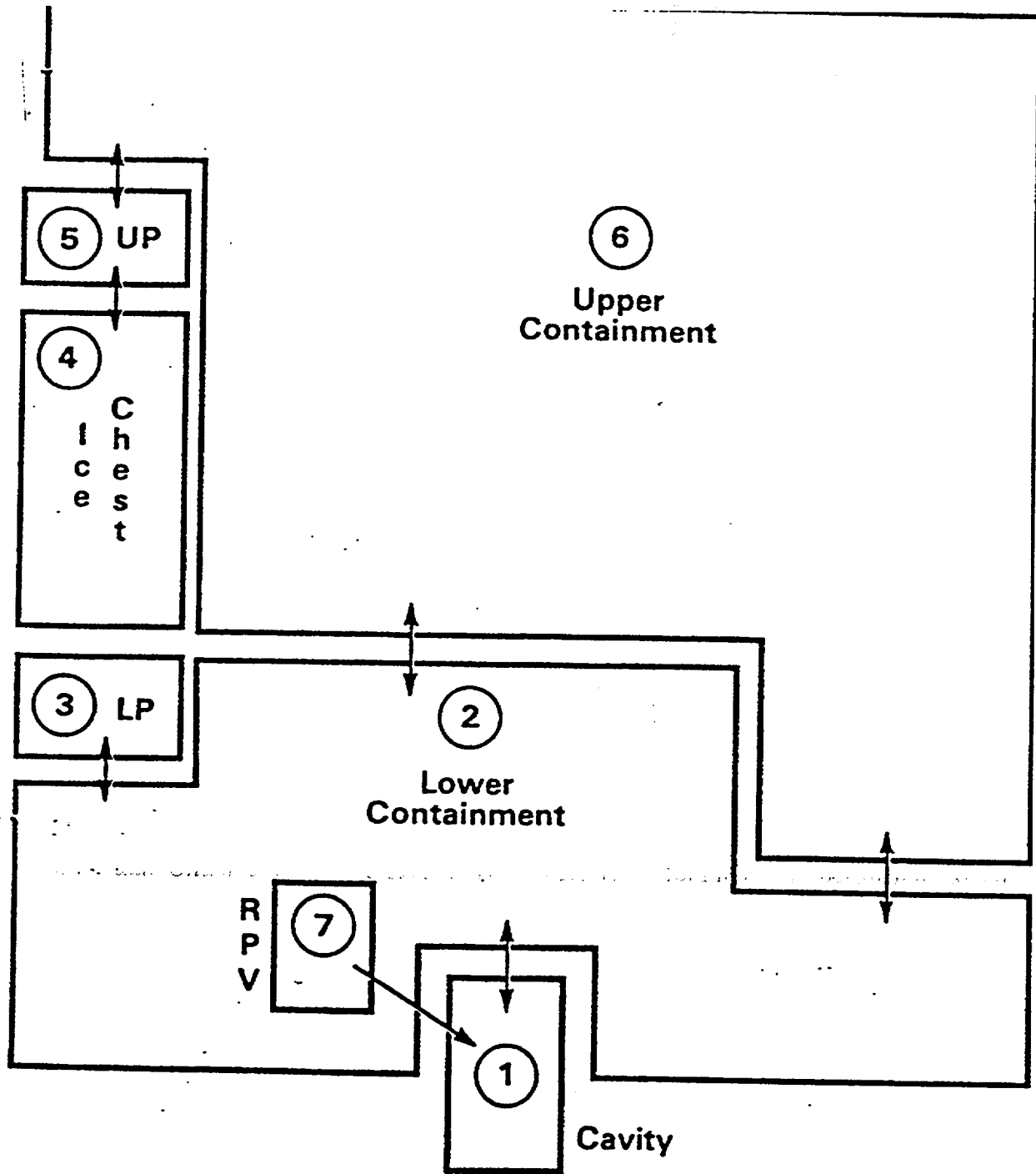
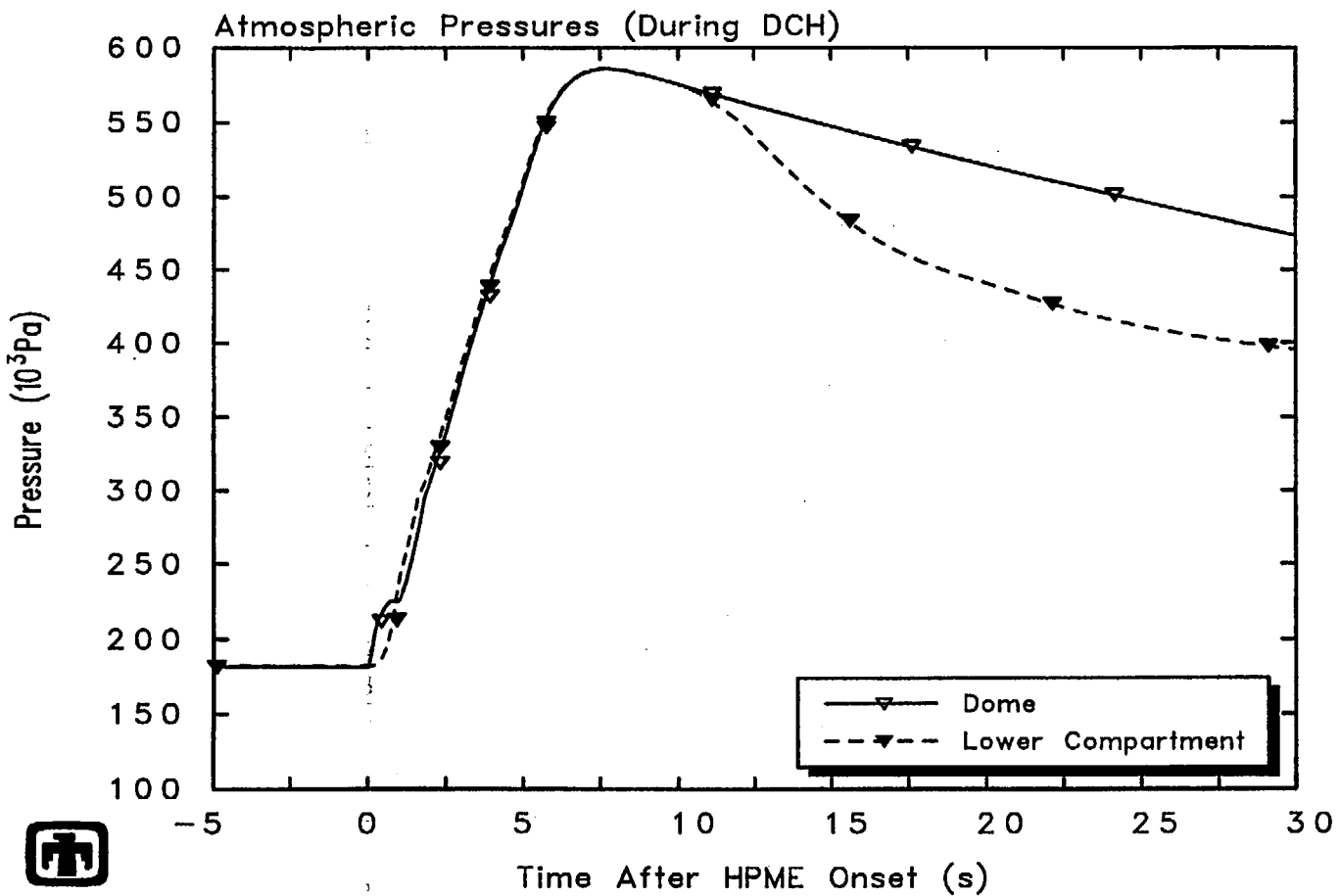


Figure B.1. CONTAIN nodalization of the Sequoyah containment.



Scenario 6, Reference Case
27Sep95 00:46:41 contain

Figure B.2. Pressure histories in the upper and lower compartments for the reference case.

APPENDIX C Plant Geometry

Martin M. Pilch
Sandia National Laboratories

C.1 Introduction

This appendix summarizes plant-specific information on the reactor cavity and subcompartment region for each operating Westinghouse plant with an ice condenser containment. This information serves four needs:

1. To quantify debris dispersal fractions and to provide assessments of dispersal pathways,
2. To quantify the coherence ratio,
3. To quantify transport of debris to the dome, and
4. To catalog the potential for the reactor cavity to be deeply flooded.

Plant data used as input to our quantifications is obtained primarily from the IPEs. These quantifications are discussed below in greater detail.

C.2 Reactor Cavity Geometry

IDCOR (1985) categorized cavity geometries in 14 classes and provided a subjective assessment of the dispersive qualities of each cavity. For completeness, the IDCOR descriptions for all cavity types are listed below. The IDCOR descriptions refer to some plants that are no longer operational, but we have made no attempt to update the discussion. Figure C.1 provides a schematic of each of the IDCOR cavities and Table C.1 associates an IDCOR cavity type with each Westinghouse plant with an ice condenser containment. All ice condenser containments have cavity geometries which are described as Type C in the IDCOR scheme. D.C. Cook was not characterized by IDCOR, but IPE drawings clearly indicate that it is an IDCOR Type C cavity like all the other ice condenser plants. Our review of the IPEs show that the basic cavity geometry is almost identical amongst the ice condenser plants with only some differences in volume. This is also true of the basic containment geometry, which is illustrated in Figure C.2 for Watts Bar. We note, however, that D.C. Cook has a reinforced concrete containment, like all the other ice condenser plants which have free standing steel shell containments like Watts Bar.

The cavity geometry potentially impacts debris dispersal, coherence ratio, and the possible impact of cavity water. Specific quantifications for these issues are addressed in Sections C.2.1, C.2.2, and C.2.3, respectively. The following is the IDCOR discussion of reactor cavity groups:

Plant Geometry

IDCOR Type A

This configuration is representative of Braidwood 1 & 2, Byron 1 & 2, and Zion 1 & 2, all of which are Westinghouse/Sargent & Lundy plants. This configuration would allow debris dispersal during a high pressure blowdown of the primary system as predicted in the Zion Probabilistic Safety Study and confirmed by the ANL and SNL experiments. The containment structures that could possibly entrap debris after it was ejected from the reactor cavity and instrument tunnel would be the lower side of the seal table room and two of the nearby walls.

IDCOR Type B

This configuration is representative of Seabrook, Indian Point 2 & 3, and Trojan which are Westinghouse/United Engineers and Constructors and Bechtel plants. This geometry would also not retain much debris after high-pressure melt ejection. It also has an additional manway which would serve as a vent during such an event. The debris that would be ejected and propelled upward from this type cavity would impact upon the bottom of the floor of the seal table room. There is somewhat more surface area for the debris to impact upon than for a type A configuration and thus more potential for aerosol generation.

IDCOR Type C

This configuration is representative of Sequoyah 1 & 2, Catawba 1 & 2, McGuire 1 & 2, Diablo Canyon 1 & 2, Vogtle 1 & 2, and Watts Bar 1 & 2. These plants all have a Westinghouse NSSS but a variety of containment A/Es (TVA, Duke, Pacific Gas & Electric, Southern Services, and Bechtel). This type has a reduced potential for direct entrainment and an increased potential for retaining a considerable amount of debris at steps and standoff regions away from the main gas flow. The manway into this reactor cavity would serve as a vent during such an event. The impingement locations for any ejected debris from the reactor cavity from which an aerosol could perhaps be produced would be under the floor containing the seal table and on the edges of some of the adjacent walls.

IDCOR Type D

This configuration is representative of Millstone 3, Beaver Valley 1 & 2, Ginna, Harris 1, North Anna 1 & 2, Robinson 2, and Surry 1 & 2. All these plants have a Westinghouse NSSS, and the containment A/Es were Stone & Webster, Gilbert & Associates, and Ebasco. This configuration is expected to retain essentially all of the debris. Most of the debris would be anticipated to initially accumulate at the sump end of this reactor cavity type. Authors Note: Since the time of the IDCOR study, many experiments using low-temperature and high-temperature simulant fluids have demonstrated that Surry-like cavities are not retentive as the IDCOR study suggested.

IDCOR Type E

This is the configuration of South Texas 1 & 2, which are Westinghouse/Bechtel plants. Little debris will escape this reactor cavity because the instrument tubes are individually sealed through the concrete wall in the reactor cavity and the manway represents a tortuous path to the upper compartments in the containment. The manway continues around in a circular pattern for about 45° from the door location after which it starts up a flight of stairs. It is the horizontal surface area of the roof in this stairwell compartment that provides nearly all the impaction area for the hypothetical generation of an aerosol that could then possibly be carried up further into the containment.

IDCOR Type F

This configuration is representative of Calvert Cliffs 1 & 2, Arkansas 2, Millstone 2, and Palisades which are all Combustion Engineering/Bechtel plants. Most all of the debris would escape through the annulus between the reactor vessel and the biological shield. Most of the ejected debris would then impact on the missile shield over the control rod drive mechanisms and be accumulated in the refueling pool.

IDCOR Type G

This is the configuration of Oconee 1, 2, and 3 which are Babcock & Wilcox/Duke-Bechtel plants. Not much core debris is expected to escape from this reactor cavity since the instrument tunnel is dead ended. The instrument tubes are individually sealed as they pass through separate penetrations in the floor before they enter the seal tank. Hence, significant fractions of the debris inventory could not migrate up into the containment via this path. The ~0.76 m diameter access passage to the reactor cavity is brick filled but without any mortar. If this is opened by the blowdown, debris would be distributed onto the containment floor and would not provide for significant direct heating.

IDCOR Type H

This configuration is representative of Summer 1, Maine Yankee, Palo Verde 1, 2, 3, WNP 3, Farley 1 & 2, Prairie Island 1 & 2, and Turkey Point 3 & 4. These plants have Combustion Engineering & Westinghouse NSSS, and the containment A/Es were Stone & Webster, Bechtel, Ebasco, Southern Services, Gilbert & Associates, and Pioneer. Little debris is expected to escape from this configuration partially because of the trapping of such material at the sump end of the lower cavity. The upper wall adjacent to where debris would accumulate at the sump is also chambered thus providing additional flow area for the gas/vapor flow to negotiate the turns without entraining the heavier debris.

IDCOR Type I

This configuration is representative of St. Lucie 1 & 2, Point Beach 1 & 2, and Waterford 3. These plants have Westinghouse and Combustion Engineering NSSS, and the containment

Plant Geometry

A/Es were Bechtel and Ebasco. Not much core debris is expected to migrate to the upper regions of the containment primarily because of the tortuous path involved in this configuration. Furthermore, the flow area enlarges as the upper floor is approached, reducing the velocity of the debris.

IDCOR Type J

This is the configuration of San Onofre 2 & 3 which are Combustion Engineering/Bechtel plants with top-mounted in-core instrumentation. A considerable amount of core material is expected to escape from this reactor cavity through the cooling ducts and up around the RPV. Most of the debris would probably pass up around the RPV since the total cooling duct flow area is only about 40 percent of that around the RPV. Consequently, most of the debris impaction area for possible aerosol generation would be on the main coolant lines just outside of the RPV before they penetrate the concrete biological shield and also on the missile shield over the control rod drive mechanisms.

IDCOR Type K

This configuration is representative of Arkansas Nuclear One and WNP 1 which have Babcock & Wilcox NSSS and containments designed by Bechtel and United Engineers & Constructors, respectively. Not much core material is expected to escape from this type even with the large volume of the instrument tunnel because it is dead ended where the instrument tubes pass through individually sealed penetrations in the floor supporting the seal tank. The most likely debris migration path in such an event would be up around the RPV where the impaction area would be that imposed by the main coolant lines between the RPV outer wall and concrete biological shield as well as on the missile shield.

IDCOR Type L

This is the configuration of Bellefonte 1 & 2, which are Babcock & Wilcox/Tennessee Valley Authority plants. Even though the instrument tunnel and the ventilating ducts are shown in the same plant for simplicity, they are actually rotated about 120° from each other. Some core material would be anticipated to escape from this configuration. Most is expected to traverse up around the RPV and also out through the outboard cooling duct. Not much is anticipated to migrate through the smaller flow area, inboard cooling duct, or through the large volume instrument tunnel because it is sealed where the instrument tubes pass through the floor supporting the seal tank. The impaction of core debris would most likely occur on the structure above the outboard cooling duct exit and on the main coolant line in the annulus surrounding the RPV.

IDCOR Type M

This configuration is representative of Callaway 1, Comanche Peak 1 & 2, Wolf Creek, and Davis Besse 1. These plants have Westinghouse and Babcock & Wilcox NSSS and containments designed by Bechtel, Gibbs & Hill, and Sargent & Lundy. This particular reactor

cavity arrangement is expected to retain a good fraction of the core material ejected from the RPV. Most of this debris is anticipated to accumulate in the corner opposite the RPV which contains the sump. The debris retention capabilities are enhanced by the manway which could serve as a vent and the chamfered wall adjacent to the sump which would create more flow area to relieve the gas/vapor flow during the blowdown.

IDCOR Type N

This is the configuration of Yankee Rowe which is a Westinghouse/Stone & Webster plant. It is expected that a reasonable fraction of the core material ejected from the RPV would exit this cavity. The debris would most likely traverse up around the RPV because there are apparently no penetrations nor vents in the lower region of the reactor vessel cavity. One of the few structures that would most likely impede the debris migration out of the LRC would be the borated water tank surrounding the RPV. Impaction of core debris on the main coolant lines would occur as the debris exited the cavity. Authors' Note: No operational reactors have this cavity type.

C.2.1 Debris Dispersal

Debris dispersal from the reactor cavity has been the focus of many programs since the Zion Probabilistic Safety Study (ZPSS, 1981). Spencer et al. (1982; 1983) showed that the threshold for dispersal from the Zion reactor cavity is reasonably predicted by the Kutateladze criterion proposed in the Zion Probabilistic Safety Study. IDCOR (1985) categorized existing cavity geometries into 14 classes and provided a subjective assessment of the dispersive or nondispersive qualities of each class. The IDCOR notion that cavity geometry influences debris dispersal has been confirmed only partially by more recent experiments. Separate effects experiments using low-temperature simulant fluids in the Zion, Surry, and Watts Bar geometries (Tutu et al., 1988a; b; Tutu, 1990; Tutu and Ginsberg, 1990), in the Sizewell B geometry (MacBeth and Trenberth, 1987; Rose, 1987; MacBeth et al., 1988), in Korean designs (Kim et al., 1992; Chun et al., 1991), and in certain combustion engineering designs with annular cavities (Bertodano, 1993), all show that cavity geometry is important only at low RCS pressures where dispersal is incomplete. However, correlations proposed by these authors and independent correlations (Levy, 1991) based on some of the same data all suggest that debris dispersal is nearly complete at reactor scale for RCS pressures in excess of about 4 MPa, regardless of the cavity geometry.

Typical dispersal fractions of 62 - 89 percent have been observed in large-scale integral-effects DCH experiments (Allen et al., 1994a; Blanchat et al., 1994) and some smaller-scale counterparts at ANL (Binder et al., 1994). These tests were conducted in Zion and Surry geometry (Westinghouse plants); however, more recent tests (Blanchat et al., 1996) in Calvert Cliffs geometry (Combustion Engineering) showed similar dispersal fractions, i.e., 57 - 87 percent. The retained material predominantly appears as a thin frozen crust on all cavity surfaces. This retention by freezing did not occur in dispersal experiments using low temperature simulant fluids.

Henry (1989) and Ishii et al. (1993) analyzed the dispersal process as a competition between film sweepout and surface entrainment. Ishii's predictions have been confirmed qualitatively by recent separate effects tests conducted at Purdue University (Ishii et al., 1993) using water as a simulant for molten core material in Zion geometry. These models, although differing in their details, both predict that surface entrainment dominates the dispersal process for representative conditions of interest if heating of the blowdown gas is significant. These predictions and conclusions are consistent with the Ishii and Mishima (1989) correlation for the entrained liquid flux in annular two-phase flow.

The experiments of MacBeth et al. (1988) for a sizewell-like cavity suggest that the fraction of melt swept from the cavity is independent of physical scale. Correlations by Tutu and Ginsberg (1990) for the Zion and Surry cavities (based on 1/42 scale experiments conducted at BNL and unpublished 1/10 scale experiments conducted at SNL) suggest that the extent of dispersal is nearly independent of physical scale. The correlations of Levy (1991) for Zion and Surry, which are based on the same data suggest that dispersal increases with physical scale. Other experiments (Kim et al., 1992; Chun et al., 1991) also show that the extent of dispersal is nearly independent of physical scale for Korean cavity designs. More recently, the large-scale (1:10) integral effects DCH experiments (high temperature melts) conducted at SNL (Allen et al., 1992c-h, Allen et al., 1993) and their smaller-scale counterparts (1:40) at ANL (Binder et al., 1992a-f) show that the extent of melt dispersal is independent of physical scale.

Reactor cavities normally exist so in-core instrument guide tubes can have access to the lower head of the RPV. Most dispersal experiments have been conducted without these structures in the cavity. Rose (1987) found that modeling the guide tubes and their supports dramatically reduced dispersal of low temperature simulant fluids from a model of the Sizewell B cavity. The support structures are much more massive in the Sizewell reactor than typical U.S. reactors. Allen et al. (1990), however, found that the guide tubes and their supports were forcibly ejected from a model of the Surry cavity during the dispersal process. The distinguishing feature here is that a high temperature melt cut (by ablation) the supports free from the anchors in the floor of the cavity.

Surface entrainment results in fine fragmentation of the melt. Particle sizes have been measured in some high temperature DCH experiments (Zion or Surry geometry) using either a Fe/Al₂O₃ thermite (Tarbell et al., 1987; Allen et al., 1991, 1992a,b, 1994a,b) or a uranium thermite (Blomquist et al., 1985, 1986). Particle sizes for the Zion or Surry geometry are distributed lognormally with a sieve mass mean diameter of ~0.5 - 1.5 mm and a geometric standard deviation of ~4. Sienicki and Spencer (1986) showed that the mass mean sizes in these experiments are qualitatively consistent with the correlation of Kataoka and Ishii (1982). Ishii et al. (1993) and Zhang et al. (1994) have performed separate effects tests in Zion geometry with water and woods metal and found that the Kataoka correlation can underpredict the particle size by as much as a factor of two. Zhang and Ishii (1995) attribute this to entrance region effects. In a Calvert Cliffs geometry, (Blanchat et al., 1996) also reports lognormally distributed particle sizes with a mass mean size of 0.3 - 0.6 mm, which is consistent with particle sizes reported by Bertodano (1993) for a Calvert Cliffs-like cavity.

The Kataoka correlation sometimes predicts particle sizes from entrainment that are sufficiently large that secondary fragmentation ($We \geq 12$) can occur in the gas core (Sienicki and Spencer, 1986; Ishii et al., 1993). Using mean gas velocities and ignoring heating of the blowdown gas, Ishii et al. (1993) predict a mass mean particle size of ~0.6 mm for a representative set of DCH conditions in Zion geometry. Larger particles are expected if secondary fragmentation does not go to completion or if entrained debris slows the gas. On the other hand, smaller particles are expected if localized gas velocities near the entrainment surface significantly exceed the mean gas velocity or if heating of the blowdown gas is significant.

In summary, we expect that debris dispersal will be complete for RCS conditions of most interest to DCH, except for some retention by freezing on cavity surfaces, for the cavity design employed in all Westinghouse plants with ice condenser containments. We also expect that dispersal will be dominated by surface entrainment and that the melt will be fragmented to sizes of ~1 mm.

We now seek a first order accounting of the quantity of melt that can freeze on cavity structures. The fraction of melt that can disperse (with freezing on cavity structures as the sole mechanism for retention) is approximated by

$$f_{disp} = 1 - \frac{\delta A_s \rho_d}{M_d^o} \sim 1 - \frac{2\lambda_c (\alpha_c R_\tau \tau_b)^{1/2} 6V_c^{2/3} \rho_d}{M_d^o} \quad (C.1)$$

The definition of each of these terms is given in the nomenclature section, C.5. The crust growth constant ranges from $\lambda \sim 0.14$ (0.32 when there is no superheat) for thermite on concrete to $\lambda_c \sim 0.48$ for corium on concrete. We assume that freezing occurs on cavity surfaces during the debris dispersal interval $t = R_\tau \tau_b$ where R_τ is the coherence ratio as discussed later in Section C.2.2 and τ_b is the characteristic blowdown time given by

$$\tau_b = \frac{1}{C_{d,h}} \left(\frac{\gamma + 1}{2} \right)^{\frac{\gamma + 1}{2(\gamma - 1)}} \frac{V_{RCS}}{A_h} \left(\frac{MW_{g,RCS}}{R_u T_{RCS}^o} \right)^{1/2} \quad (C.2)$$

Table C.2 shows that this simple model reasonably bounds the observed retention of melt in the cavity. Reactor applications are both plant-specific and scenario-specific. The former is true because of geometric differences and the latter is true because of the scenario dependent melt masses and RCS pressures. Evaluations were performed for the upper end of the mass distributions for each plant and scenario. It was found that freezing on cavity surfaces retains only ~7 percent of the melt for each plant and scenario.

C.2.2 Coherence Ratio

The TCE model assumes that debris/gas interactions are limited to that portion of the blowdown gas that is coherent with the dispersal process. The ratio of the characteristic dispersal time to the characteristic time constant for blowdown is termed the coherence ratio. Smaller

values of the coherence ratio means that the primary heat sink for debris/gas thermal interactions is smaller and that metal/steam reactions are more likely to be steam limited.

The notion that noncoherence (between debris dispersal and RCS blowdown) can limit DCH interactions is not unique to the TCE model. Ginsberg and Tutu (1987) were the first to suggest this limitation. Early CONTAIN calculations (Williams and Louie, 1988) also exhibited some sensitivity to coherence, though the effect found was not large. The CLCH model (Yan and Theofanous, 1993) also considers noncoherence as a basic modeling process. These analytic reflections all have a solid basis in experiment observations. Unpublished real-time flash x-rays taken at SNL show that dispersal is complete well before blowdown. In addition, many experiments have been conducted (e.g., Allen et al., 1991; Allen et al., 1992a,b) with pyrometers focused on the cavity exit. Pyrometer signals also confirm the notion of noncoherence, and they suggest that cavity pressurization records can also be used to define the coherent interval. Despite this physical evidence, no systematic experiments have ever been performed for the purpose of directly validating the impact of noncoherence on DCH loads.

The database for the coherence ratio largely overlaps the range of individual parameters that are of interest to reactor applications. However, the database does not include all possible combinations of parameters for each of the potential applications; consequently, a correlation for the coherence ratio is required in order to fill gaps in the database. It is significant that any such process is more closely analogous to interpolation rather than order of magnitude extrapolation.

Pilch (Appendix E in Pilch et al., 1994a) developed a correlation for the coherence ratio based on momentum considerations. The Pilch correlation can be expressed as

$$R_{\tau} = \frac{\tau_e}{\tau_b} = C_{R\tau} f_{disp} \left(\frac{T_{RCS}^o}{T_{d,i}^o} \right)^{1/4} \left(C_{d,h} \frac{M_d^o}{M_g^o} \frac{A_h V_c^{1/3}}{V_{RCS}} \right)^{1/2}, \quad (C.3)$$

where $C_{R\tau}$ is a constant that is determined from experiment data. The multiplier was only a weak function of cavity geometry for Zion or Surry-like cavities; however, it will be seen that $C_{R\tau}$ is substantially smaller for Calvert Cliffs-like cavities. For an isentropic blowdown of the RCS, the fraction of blowdown gas that is coherent with debris dispersal is given by

$$f_{coh} = 1 - \frac{M_g^o}{M_{g,e}} = 1 - \left(\frac{P_{e,RCS}}{P_{RCS}^o} \right)^{\frac{1}{\gamma}} = 1 - \left(1 + \frac{\gamma-1}{2} R_{\tau} \right)^{\frac{-2}{\gamma-1}}. \quad (C.4)$$

for $R_{\tau} \leq 0.5$, $f_{coh} \sim R_{\tau}$, so that R_{τ} is directly proportional to the amount of blowdown gas that can react with the debris.

Table C.1 summarizes information needed to quantify the coherence ratio for each plant. Specifically, the coherence ratio correlation contains a lead constant that is a function of plant geometry. Our goal is to quantify the multiplier and other geometric information needed to compute the coherence ratio for each plant. In addition, we must specify a relative standard

deviation in our quantification of the coherence ratio. Consistent with experiment observations, the coherence for Calvert Cliffs-like cavities with Bechtel annular cavities is ~5-6 smaller than Westinghouse designs that have a more U-tube configuration to accommodate the in-core instrument lines. Even with this reduced coherence in Calvert Cliffs-like cavities, there is sufficient coherent steam to oxidize all the metal in the dispersed melt.

The database on which the coherence ratio correlation is based contains Zion-like geometries, Surry-like geometries, and Calvert Cliffs-like geometries. Consistent with previous efforts (NUREG/CR-6338 and NUREG/CR-6475) we reduce the IDCOR categorization into 5 groups for the purpose of quantifying the coherence ratio: Zion-like, Surry-like, other Westinghouse, Calvert Cliffs-like, and other CE/B&W. We define Zion-like cavities as having a U-tube layout with a slanted riser section, and we define Surry-like cavities as having a U-tube layout with a vertical riser section. The U-tube layout of these cavities facilitates transfer of the in-core instrument guide tubes to the lower head. Many CE plants do not have lower head penetrations so the cavity resembles a pot with the dominant dispersal path up through the annulus around the RPV.

Having further grouped the cavity designs, we assign the lead constant and relative standard deviation appropriate to Zion to all Zion-like cavities. A similar procedure is followed for Surry and Calvert Cliffs. Some cavities are significantly outside the database; consequently, we recommend biasing the results for the most relevant database by one standard deviation and applying an uncertainty distribution. Uncertainties are bounded in this fashion while still maintaining a broad uncertainty distribution. The recommended coherence constant and the relative standard deviation for each class of cavity are tabulated in Table C.3.

The reactor cavity of ice condenser plants has features of both Surry-like (vertical to step to cavity exit) and Zion-like cavities (scoped section to cavity exit). The value of the multiplicative constant appearing in the coherence correlation was assigned a value and uncertainty appropriate to Surry-like cavities because the large vertical step in ice condenser cavities rendered them more Surry-like than Zion-like.

C.2.3 Cavity Water

NUREG/CR-6075 (Pilch et al., 1994a) identified the need to catalog the extent of cavity flooding prior to vessel breach. The need is born from three questions:

- What impact does cavity water have on DCH loads?
- Can explosive or non-explosive FCIs in the cavity cause structural damage to the cavity?
- In-vessel retention

This section catalogs the necessary information (to the extent available) to address these issues.

All reactor cavities will always contain some water due to condensation on cavity surfaces. This water will typically collect in the cavity sump, so we refer to this situation as "dry." The issue then becomes whether the cavity can act as a collection point for condensate

Plant Geometry

from the entire containment or act as a collection point for RWST water should it be injected into the containment during spray operation, emergency core cooling system (ECCS) operation, or operator action.

The IPEs generally assessed the likelihood that water will be present in the reactor cavity. We consider three categories:

- *Dry* cavities which contain only condensate levels of water,
- *Wet* cavities which are only partially full and does not submerge the lower head, and
- *Flooded* cavities which will overflow onto the basement floor.

We note, however, that a flooded cavity does not always mean that the lower head of the RPV is submerged. A catalog of the IPE assessments of cavity water is provided at the end of this section. These assessments are summarized in Table C.4. The IPE descriptions are sometimes supplemented with our own subjective interpretations of the IPE descriptions in order to categorize each cavity.

Reactor cavities are more likely to be dry if the RWST water is not injected into the containment. Figure C.2 shows that the containment basement must be deeply flooded before water can overflow into the reactor cavity. In general, reactor cavities in ice condenser plants will remain dry until the RWST and approximately half the ice has melted.

Reactor cavities can be excavated or free standing. Free standing cavities are potentially vulnerable to damage in the event of high cavity pressures resulting from explosive FCIs, non-explosive FCIs, or the debris dispersal process itself. Excavated cavities should not be vulnerable to damage from high cavity pressures. Table C.4 shows that all ice condenser plants have excavated cavities.

The following catalog of cavity water assessments was compiled from IPE and other PSA reports.

Catawba

No discussion found in the IPE.

D.C. Cook

Floodup level in the Cook Nuclear Plant containment is to approximately 614' if the entire contents of the RWST, accumulators, reactor coolant system (RCS), and ice condenser are considered. Because of the piping sleeves mentioned above, injection of the RWST alone will probably not allow water to spill from the lower compartment into the cavity until sufficient ice has melted to raise the water level in both the lower and annular compartments to the 610'-0" elevation.

McGuire

No discussion found in the IPE.

Sequoyah

No discussion found in the IPE.

Watts Bar

No discussion found in the IPE.

C.3 Debris Transport to the Containment Dome

There are two primary debris transport pathways from the cavity to the containment dome in plants with large dry or subatmospheric containments: (1) through the annular gap between the RPV and the biological shield wall, and (2) from the in-core instrument tunnel or manways through the lower compartments. The only potentially significant pathway for dispersed debris to enter the upper dome is for it to pass through the ice compartment. Tutu et al. (1986) concluded, through extrapolation of experiment results, that ~80 percent of all debris entering the ice chest would be trapped before entering the dome. Examination of the lower compartment geometry in an ice condenser plant suggests that particles would have a hard time negotiating the turns necessary for gas to carry melt particles into the ice chest. Hence, the extent of debris transport to the dome is not believed to be an important issue in ice condenser plants.

C.4 References

Allen, M.D. et al. (1990). *A Demonstration Experiment of Steam-Driven, High-Pressure Melt Ejection: The HIPS-10S Test*, NUREG/CR-5373, SAND89-1135, Sandia National Laboratories, Albuquerque, NM.

Allen, M.D. et al. (1991). *Experiments to Investigate the Effect of Flight Path on Direct Containment Heating (DCH) in the Surtsey Test Facility: The Limited Flight Path (LFP) Tests*, NUREG/CR-5728, SAND91-1105, Sandia National Laboratories, Albuquerque, NM.

Allen, M.D. et al. (1992a). *Experiments to Investigate the Effect of Water in the Cavity on Direct Containment Heating (DCH) in the Surtsey Test Facility - The WC-1 and WC-2 Tests*, SAND91-1173, Sandia National Laboratories, Albuquerque, NM.

Allen, M.D. et al. (1992b). *Experimental Results of Tests to Investigate the Effects of Hole Diameter Resulting from Bottom Head Failure on Direct Containment Heating (DCH) in the Surtsey Test Facility - The WC-1 and WC-3 Tests*, SAND91-2153, Sandia National Laboratories, Albuquerque, NM.

Plant Geometry

Allen, M.D. et al. (1992c). *Experiments to Investigate the Effects of 1:10 Scale Zion Structures on Direct Containment Heating (DCH) in the Surtsey Test Facility: The IET-1 and IET-1R Tests*, SAND92-0255, Sandia National Laboratories, Albuquerque, NM.

Allen, M.D. et al. (1992d). *The Third Integral Effects Test (IET-3) in the Surtsey Test Facility*, SAND92-0166, Sandia National Laboratories, Albuquerque, NM.

Allen, M.D. et al. (1992e). *The Effects of Condensate Levels of Water on Direct Containment Heating (DCH) in Zion-Like Geometry: The Fourth Integral Effects Test (IET-4) Conducted in the Surtsey Test Facility*, SAND92-1241, Sandia National Laboratories, Albuquerque, NM.

Allen, M.D. et al. (1992f). *Experimental Results of an Integral Effects Test in a Zion-Like Geometry to Investigate the Effects of a Classically Inert Atmosphere on Direct Containment Heating: The IET-5 Experiment*, SAND92-1623, Sandia National Laboratories, Albuquerque, NM.

Allen, M.D. et al. (1992g). *An Integral Effects Test in a Zion-Like Geometry to Investigate the Effects of Preexisting Hydrogen on Direct Containment Heating in the Surtsey Test Facility - The IET-6 Experiment*, SAND92-1802, Sandia National Laboratories, Albuquerque, NM.

Allen, M.D. et al. (1992h). *An Integral Effects Test to Investigate the Effects of Condensate Levels of Water and Preexisting Hydrogen on Direct Containment Heating in the Surtsey Test Facility - The IET-7 Experiment*, SAND92-2021, Sandia National Laboratories, Albuquerque, NM.

Allen, M.D. et al. (1993). *Experiments to Investigate the Effects of Fuel/Coolant Interactions on Direct Containment Heating: The IET-8A and IET-8B Experiments*, SAND92-2849, Sandia National Laboratories, Albuquerque, NM.

Allen, M.D. et al. (1994a). *Experimental Results of Integral Effects Tests with Zion-Like Structures to Investigate Direct Containment Heating*, NUREG/CR-6044, SAND93-1049, Sandia National Laboratories, Albuquerque, NM.

Allen, M.D. et al. (1994b). *Test Results on Direct Containment Heating by High-Pressure Melt Ejection into the Surtsey Vessel: The TDS Test Series*, SAND91-1208, Sandia National Laboratories, Albuquerque, NM.

Bertodano, M. Lopez de (1993). *Direct Containment Heating DCH Source Term Experiment for Annular Reactor Cavity Geometry*, Ninth Proceedings of Nuclear Thermal Hydraulics, 1993 ANS Winter Mtg., Nov. 14-18, 1993, San Francisco, CA, p. 111-120.

Binder, J.L. et al. (1992a). *Quick Look Data Report on the Integral Effects Test 1R in the Corexit Facility at Argonne National Laboratory*, draft for review, Argonne National Laboratory, Argonne, IL.

- Binder, J.L. et al. (1992b). *Quick Look Data Report on the Integral Effects Test IRR in the Corexit Facility at Argonne National Laboratory*, draft for review, Argonne National Laboratory, Argonne, IL.
- Binder, J.L. et al. (1992c). *Quick Look Data Report on the Integral Effects Test-3 in the Corexit Facility at Argonne National Laboratory*, draft for review, Argonne National Laboratory, Argonne, IL.
- Binder, J.L. et al. (1992d). *Quick Look Data Report on the Integral Effects Test-6 in the Corexit Facility at Argonne National Laboratory*, draft for review, Argonne National Laboratory, Argonne, IL.
- Binder, J.L. et al. (1992e). *Quick Look Data Report on the Integral Effects Test-7 in the Corexit Facility at Argonne National Laboratory*, draft for review, Argonne National Laboratory, Argonne, IL.
- Binder, J.L. et al. (1992f). *Quick Look Data Report on the Integral Effects Test-8 in the Corexit Facility at Argonne National Laboratory*, draft for review, Argonne National Laboratory, Argonne IL.
- Binder, J.L. et al. (1994). *Direct Containment Heating Integral Effects Tests at 1/40 Scale in Zion Nuclear Power Plant Geometry*, NUREG/CR-6168, ANL-94/18, Argonne National Laboratory, Argonne, IL.
- Blanchat, T.K. et al. (1994). *Experiments to Investigate Direct Containment Heating Phenomena with Scaled Models of the Surry Nuclear Power Plant*, NUREG/CR-6152, SAND93-2519, Sandia National Laboratories, Albuquerque, NM.
- Blanchat, T.K., M.M. Pilch, and M.D. Allen (1996). *Experiments to Investigate Direct Containment Heating Phenomena With Scaled Models of the Calvert Cliffs Nuclear Power Plant*, NUREG/CR-6469, Sandia National Laboratories, Albuquerque, NM.
- Blomquist, C.A. et al. (1985). "Data Report for Corium/Water Thermal Interaction Test CWTI-13," Argonne National Laboratory, Argonne, IL.
- Blomquist, C.A. et al. (1986). "Data Report for Corium/Water Thermal Interaction Test CWTI-14," Argonne National Laboratory, Argonne, IL.
- Chun, M.H. et al. (1991). "A Parametric Study of the High Pressure Melt Ejection from Two Different Scale Reactor Cavity Models," *Int. Con. Heat Mass Trans.*, Vol. 18, pp. 619-628.
- Ginsberg, T. and N.K. Tutu (1987). *Safety Research Programs Sponsored by Office of Nuclear Regulatory Commission*, Quarterly Progress Report, NUREG/CR-2331, Vol. 7, No. 2.

Plant Geometry

Henry, R.E. (1989). "Evaluation of Fission Product Release Rates During Debris Dispersal," PSA 1989, *Proc. of the ANS/ENS International Topical Meeting: Probability Reliability and Safety Assessment*, p. 375-383.

IDCOR (1985). *Technical Support for Issue Resolution*, IDCOR, Technical Report 85.2, Fauske and Associates, Inc., Burr Ridge, IL.

Ishii, M. and K. Mishima (1989). "Droplet Entrainment Correlation in Annular Two-Phase Flow," *Int. J. Heat Mass Transfer*, Vol. 32, No. 10, pp. 1835-1846.

Ishii, M. et al. (1993). *Separate Effects Experiments on Phenomena of Direct Containment Heating - Air-Water Simulation Experiments in Zion Geometry*, PU NE-93/1, Purdue University, West Lafayette, IN.

Kataoka, I. and M. Ishii (1982). *Mechanism and Correlation of Droplet Entrainment and Deposition in Annular Two-Phase Flow*, NUREG/CR-2885, ANL-82-44, Argonne National Laboratories, Argonne, IL.

Kim, M. et al. (1992). "Experimental Study on Direct Containment Heating Phenomena," in *ANS Winter Meeting*, Chicago, IL.

Levy, S. (1991). "Debris Dispersal From Reactor Cavity During Low Temperature Simulant Tests of Direct Containment Heating. Part I: Tests with Constant Gas Flow Rates; Part II: Tests with Blowdown Gas Conditions," *Proceedings of National Heat Transfer Conference*, Minneapolis, MN.

MacBeth, R.W., and R. Trenberth (1987). *Experimental Modeling of Core Debris Dispersion from the Vault Under a PWR Pressure Vessel - Part 1*. "Preliminary Experimental Results," AEEW-R1888, UK Atomic Energy Authority, AEE Winfrith, UK.

MacBeth, R.W. et al. (1988). *Experimental Modeling of Core Debris Dispersion from the Vault Under PWR Pressure Vessel - Part 3*. "Results of Varying the Size Scaling Factor of the Model Use," AEEW-R2426, UK Atomic Energy Authority, AEE Winfrith, UK.

Pilch, M.M. et al. (1994a). *The Probability of Containment Failure by Direct Containment Heating in Zion*, NUREG/CR-6075, SAND93-1535, Sandia National Laboratories, Albuquerque, NM.

Pilch, M.M. et al. (1994b). *The Probability of Containment Failure by Direct Containment Heating in Zion*, NUREG/CR-6075, Supplement 1, Sandia National Laboratories, Albuquerque, NM.

Pilch, M.M. et al. (1995). *The Probability of Containment Failure by Direct Containment Heating in Surry*, SAND93-2078, NUREG/CR-6109, Sandia National Laboratories, Albuquerque, NM.

- Rose, P.W. (1987). *Experimental Modeling of Core Debris Dispersion from the Vault Under a PWR Pressure Vessel - Part 2. Results of Including the Instrument Tubes Support Structure in the Experiment*, AEEW-R2143, UK Atomic Energy Authority, AEE Winfrith, UK.
- Sienicki, J.J. and B.W. Spencer (1986). "Corium Droplet Size in Direct Containment Heating," *Transactions of the ANS*, TANSO 53, pp. 557-558.
- Spencer, B.W. et al. (1982). *Sweepout Thresholds in Reactor Cavity Interactions*, ANL/LWR/SAF 82-1, Argonne National Laboratory, Argonne, IL.
- Spencer, B.W. et al. (1983). *Hydrodynamics Aspects of Ex-Vessel Debris Dispersal in Zion-Type Containment Design*, ANL/LWR/SAF 83-1, Argonne National Laboratory, Argonne, IL.
- Tarbell, W.W. et al. (1987). *Results from the DCH-1 Experiment*, NUREG/CR-4871, SAND86-2483, Sandia National Laboratories, Albuquerque, NM.
- Tutu, N.K. et al. (1986). *Trapping of Melt Droplets in Ice Condenser Channels During High Pressure Melt Ejection Accident: Preliminary Scoping Experiments and Analysis*, Tech. Report A-3024 9-16-86, Brookhaven National Laboratory, Upton, NY.
- Tutu, N.K. et al. (1988a). *Debris Dispersal from Reactor Cavities During High Pressure Melt Ejection Accident Scenarios*, NUREG/CR-5146, BNL-NUREG-52147, Brookhaven National Laboratory, Upton, NY.
- Tutu, N.K. et al. (1988b). "Low Pressure Cutoff for Melt Dispersal from Reactor Cavities," *Fourth Proc. of Nuclear Thermal Hydraulics*, 29-37.
- Tutu, N.K. (1990). *Melt Dispersal Characteristics of the Watts Bar Cavity*, Technical Report A-3024, Brookhaven National Laboratory, Upton, NY.
- Tutu, N.K., and T. Ginsberg (1990). "The Results of Melt Dispersal Experiments with Surry and Zion Cavity Models," Letter Report, Brookhaven National Laboratory, NY.
- Williams, D.C. and D.L.Y. Louie (1988). "CONTAIN Analyses of Direct Containment Heating Events in the Surry Plant," *Proceedings of the ANS/ENS Winter Meeting*, Thermal Hydraulics Division, Washington, DC.
- Yan, H. and T.G. Theofanous (1993). "The Prediction of Direct Containment Heating," *ANS Proceedings*, 1993 National Heat Transfer Conference, Atlanta, GA, p. 294-309.
- Zhang, G.J. et al. (1994). "Simulation Experiment on Corium Dispersion in Direct Containment Heating Using Air-Water and Air-Woods Metal," *Tenth Proceedings of Nuclear Thermal Hydraulics*, 1994 ANS Winter Meeting. Washington, DC.

Plant Geometry

Zhang, G.J. and M. Ishii (1995). "Entrance Effect on Droplet Entrainment in DCH," *ANS Proceedings*, 1995 National Heat Transfer Conference, Portland, OR.

ZPSS (1981). *Zion Probabilistic Safety Study*, Commonwealth Edison Co., Chicago, IL.

Table C.1 Cavity dispersal summary

| PLANT | ARCHITECT/ ENGINEER | FOUNDATION | CAVITY | IDCOR | COHERENCE | CAV. VOL. | COH. MUL. | COH. REL. |
|-----------|------------------------|------------|--------|-------|-----------|-----------|-----------|-----------|
| | | SUPPORT | WATER | TYPE | CATEGORY | m**3 | | STD. DEV. |
| Catawba | Duke Power | Excavated | Dry | C | Surry | 429 | 12.2 | 0.18 |
| Cook | AEP | Excavated | Dry | (C) | Surry | 474 | 12.2 | 0.18 |
| McGuire | Duke Power | Excavated | Dry | C | Surry | 336 | 12.2 | 0.18 |
| Sequoyah | TVA | Excavated | Dry | C | Surry | 420 | 12.2 | 0.18 |
| Watts Bar | TVA | Excavated | Dry | C | Surry | 522 | 12.2 | 0.18 |
| | | | | | | | | |

Table C.2 Validation of melt retention by freezing during cavity dispersal

| Parameter | SNL/IET Allen et al. 1994b | ANL/IET Binder et al. 1994 | SNL/IET Blanchat et al. 1994 | SNL/CES/CE Blanchat et al. 1996 |
|----------------------------|---------------------------------------|---------------------------------------|---------------------------------------|---------------------------------------|
| Cavity | Zion | Zion | Surry | Calvert Cliffs |
| Scale | 1:10 | 1:40 | 1:5.75 | 1:10 |
| Melt Simulant | Fe/Al ₂ O ₃ /Cr | Fe/Al ₂ O ₃ /Cr | Fe/Al ₂ O ₃ /Cr | Fe/Al ₂ O ₃ |
| f _{disp} observed | 0.62 - 0.89 | 0.69 - 0.80 | 0.73 - 0.89 | 0.57 - 0.87 |
| f _{disp} Eq. C.1 | 0.91 | 0.85 | 0.88 | 0.89 |

Table C.3 Input for coherence ratio correlation

| Cavity Type | Coherence Constant | Relative Standard Deviation |
|---------------------|--------------------|--------------------------------|
| Zion-like | 9.661 | 0.29 |
| Surry-like | 12.2 | 0.18 |
| Other Westinghouse | 14.6 | 0.33 |
| Calvert Cliffs-like | 1.717 | 0.585 |
| Other CE/B&W | 2.302 | 0.585 |

Table C.4 Cavity water summary

| PLANT | ARCHITECT/ | CONTAINMENT | CAVITY WATER | | FOUNDATION |
|-----------|------------|---------------|--------------|-------------|------------|
| | ENGINEER | | TYPE | NO RWST INJ | |
| Catawba | Duke Power | Ice Condenser | Dry | Wet | Excavated |
| Cook | AEP | Ice Condenser | Dry | Wet | Excavated |
| McGuire | Duke Power | Ice Condenser | Dry | Wet | Excavated |
| Sequoyah | TVA | Ice Condenser | Dry | Wet | Excavated |
| Watts Bar | TVA | Ice Condenser | Dry | Wet | Excavated |

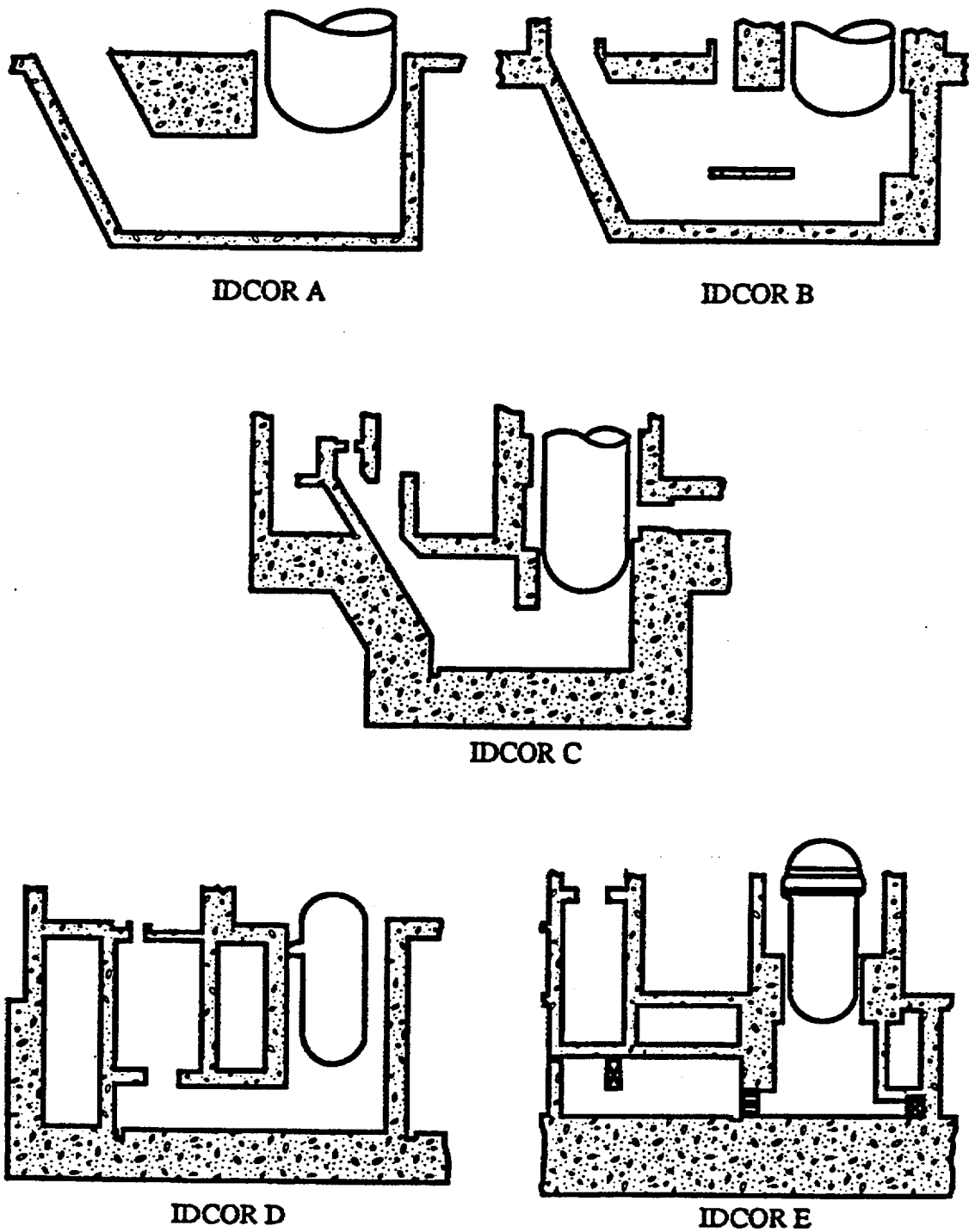


Figure C.1. Schematic drawings of the IDCOR cavity groups.

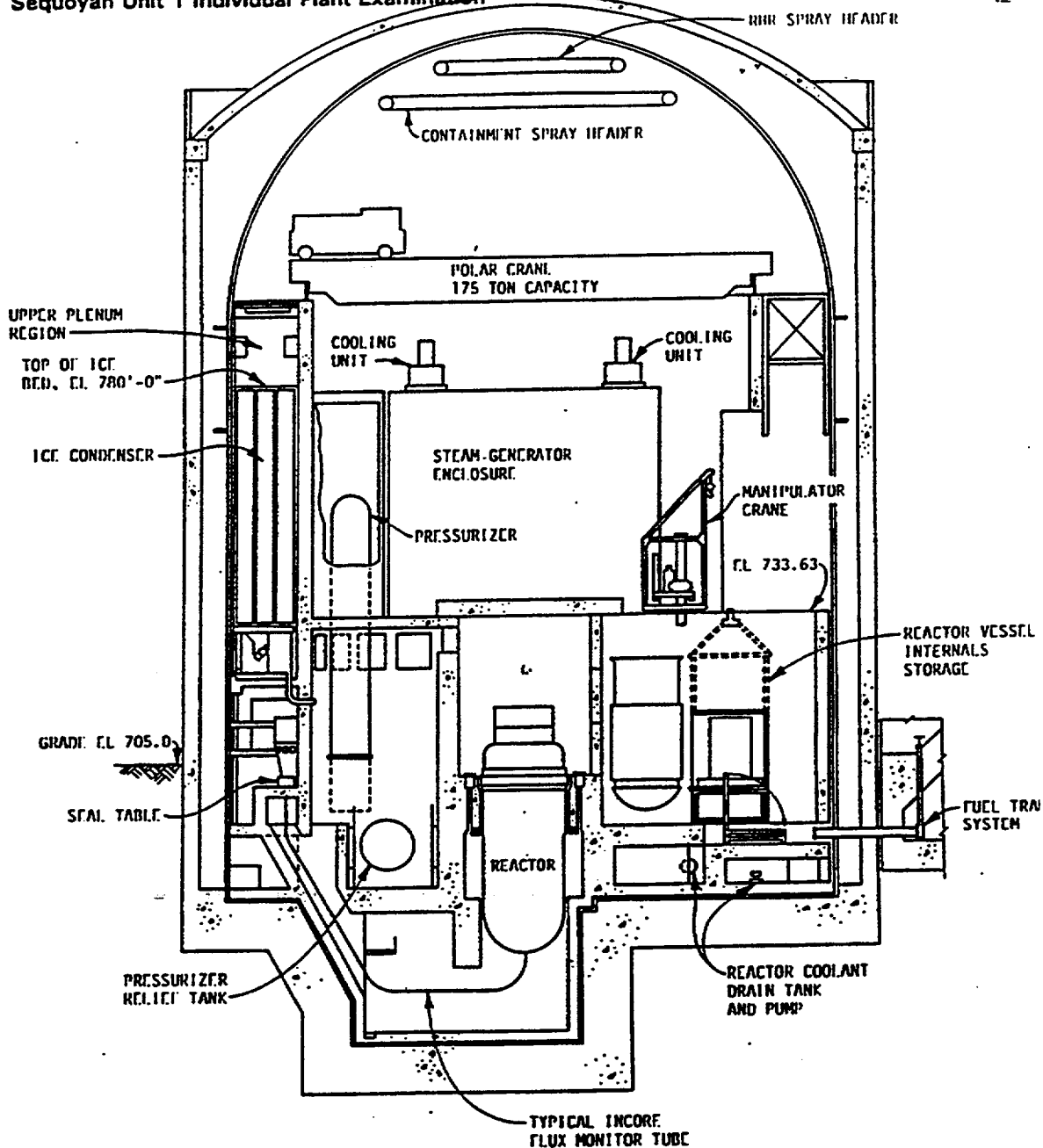


Figure C.2. Layout of an ice condenser typical containment (taken from the Watts Bar IPE).

APPENDIX D

A Splinter Scenario Approach to DCH Resolution

M. M. Pilch, M. D. Allen, and D. C. Williams
Sandia National Laboratories

D.1 Introduction

Initially, the methodology developed in NUREG/CR-6075 and NUREG/CR-6075, Supplement 1, was used to perform a load versus strength evaluation for each of these plants using plant-specific data gathered from IPEs, Final Safety Analysis Reports (FSARs), and direct contacts with plant personnel (when necessary). The same enveloping accident scenarios (splinters) that were used in NUREG/CR-6075, Supplement 1, and NUREG/CR-6019 were used for these plant evaluations. One additional splinter scenario, unique to plants with ice condenser containments, was also considered. These splinter scenarios establish important input parameters for the load calculations, e.g. the RCS pressure at vessel breach, the melt mass and composition, the RPV breach size, the containment pressure and atmosphere composition at vessel breach, etc.

The initial approach taken was to model the ice condenser plant as a small dry containment without taking credit for passive pressure suppression afforded by the ice beds or active pressure suppression afforded by containment sprays. Scenarios with deeply flooded cavities were not analyzed as part of the effort documented in Appendix D. Assuming a HPME/DCH event for these assumptions, all ice condenser plants violated the success criteria ($CCFP \leq 0.1$) based on DCH-induced overpressure failures alone. Those sections of draft NUREG/CR-6427 that deal with this splinter scenario approach are preserved in their entirety as Appendix D of this report. Appendix D also documents peer review comments on draft NUREG/CR-6427. We acknowledge that the underlying assumptions of Appendix D are overly conservative and physically inconsistent with the expected evolution of accident scenarios in ice condenser plants. Sensitivity studies performed as part of Appendix D show that the ice beds could be effective at suppressing DCH loads if the igniters are also operational.

D.2 Probabilistic Framework

Two approaches are taken to address the key uncertainties in our analyses. When the range of behavior is deemed too wide and the conservative trend is unclear, we resort to an appropriate number of "splinter scenarios"; that is, a number of qualitatively different scenarios that together envelop the physically possible behavior. Rather than attempting to assign probabilities, each splinter is pursued to quantification. Section D.3.2 defines the six splinter scenarios addressed in this work.

If the conservative trend is clear, we seek the adequately conservative distribution with the aim that it can envelop what any expert might expect. The probabilistic framework can be structured in the manner illustrated in Figure D.1. As shown in this figure, the initial melt

Splinter Scenario Approach

parameters are to be quantified as independent probability density functions, representing modeling uncertainty in the parameters. Variations from stochastic processes are assessed as insignificant relative to modeling uncertainty. These functions are formed into a joint probability density function and then combined with CR1, under the parameter distribution function that represents model uncertainty for the DCH process, coherence ratio (R_t), to obtain a probability density function for the peak containment pressure. This distribution function for peak containment pressure is combined (CR2) with the set of containment fragility curves (probabilistically distributed themselves⁴) to obtain a probability distribution of containment failure frequency.⁵ This process is repeated for each of the splinter scenarios noted above.

Sandia has developed software to perform either traditional Monte Carlo sampling or stratified Monte Carlo sampling. The software, called LHS, is user friendly and has an established quality assurance pedigree, including code assessment and verification. Sandia chose to use this numerical tool based on Latin hypercube sampling (LHS) to propagate distribution through the probabilistic framework. The resulting software was applied to NUREG/CR-6075, Supplement 1 (Pilch et al., 1994b), where it is described more fully in Appendix B. The same software was used in NUREG/CR-6109 (Pilch et al., 1995), NUREG/CR-6338 (Pilch et al., 1996), and NUREG/CR-6475 (Pilch et al., 1997) and it is used here without modification.

Our approach here recognizes that variability (i.e., statistical variations for nominally similar conditions) will probably be smaller than uncertainties in the phenomena themselves. We chose to use artificial probabilities as a tool to demonstrate relative variations in the probabilities of different outcomes. The numbers themselves have no quantitative value; they are important only in a relative sense. We used a physically based probability scale (Table 3.1) to quantify inputs and used the same scale to convert bottom-line results to a physical interpretation. The physical interpretations have been selected for the case of DCH within the context of the entire risk picture. We recognize that a probability of 0.01 might be considered very high in another context where the numbers carry a frequensic interpretation.

Empirically, it can be shown that the physical interpretation of the probability calculation is invariant relative to the numbers assigned to the judgmental degrees of belief, as long as the same geometrical progression is preserved. With our recommended assignment, the product of two "edge of spectrum" events ($p \sim 10^{-1}$) is 10^{-2} , which should be interpreted as an "upper bound." The interpretations in Table 3.1 might be given the alternative assignments: 1, 1/3, 1/9. Once again, the product of two "edge of spectrum" events ($p \sim 1/3$) is 1/9, which should be interpreted physically as an "upper bound" with the new assignments. Therefore, the specific value of a judgmental degree of belief has no intrinsic meaning; it is only meaningful when measured against the physical assignment.

⁴ In the current assessments, only a single fragility curve is available, but the discussion here has been generalized to accommodate desired improvements in information.

⁵ Each fragility curve is expressed in terms of failure frequency, and this frequency expresses the statistically meaningful variations (based on actual experience) in containment strength. These containment strength variations are due to variations in material and workmanship and are characterized by the fraction that failed in a nominally similar population of structures subjected to the same load. On the other hand, the probability assigned to each fragility curve expresses a subjective degree of belief as to the appropriateness of it in meeting the intended task.

Our judgmental degree of belief for any process can be characterized as likely ($p \sim 1$), as unlikely ($p \sim 10^{-2}$), or as something in between ($p \sim 10^{-1}$). As a practical matter, we assign $p \sim 1$ to our best estimate and $p \sim 10^{-2}$ to our estimate of a reasonable upper bound (assuming we have a reasonable expectation that the upper bound is unlikely). The working group for NUREG/CR-6075, Supplement 1 concurred with this interpretation (Pilch et al., 1994b).

Table D.1. Definition of Probability Levels

| Process Likelihood | Process Characteristics |
|--------------------|--|
| ~ 1 | Behavior is within known trends - best estimate. |
| 10^{-1} | Behavior is within known trends but obtainable only at the edge of spectrum parameter. |
| 10^{-2} | Behavior cannot be positively excluded - upper bound. |

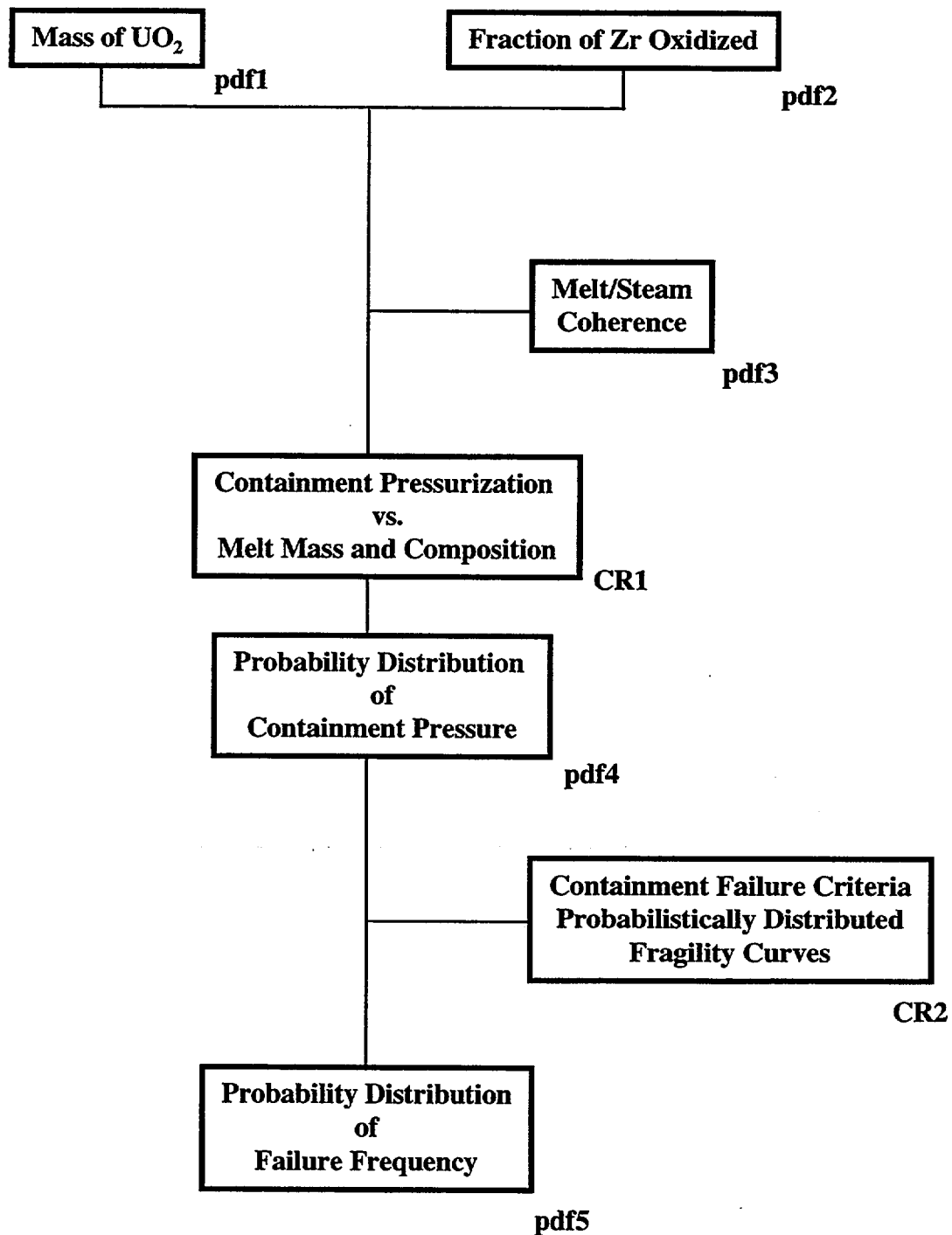


Figure D.1. The probabilistic framework for containment failure under direct containment heating scenarios. The (J) and (F) are the “joint” and “function” operations, respectively.

D.3 Quantification of Initial Conditions

D.3.1 Introduction

Quantification of melt release conditions was developed by attempting to envelop physically possible behavior in a comprehensive and systematic manner. This means that we needed to examine all reasonably conceivable severe accident scenarios, identify key aspects of their phenomena and respective ranges of behavior, and establish the few splinter scenarios that envelop the DCH challenge to the containment.

Reviewers raised the following questions (Appendix A in Pilch et al. 1994b) regarding the completeness of the splinter scenarios considered in NUREG/CR-6075 (Pilch et al. 1994a) for the Zion application:

1. Can full-system pressure cases be ruled out?
2. Should operator intervention scenarios be analyzed?
3. Can dry core scenarios lead to melting and relocation of the metal (Zr) blockage from the core to the lower plenum?

Generally, the reviewers characterized initial condition quantifications in NUREG/CR-6075 (Pilch et al. 1994a) for Zion as "optimistic." Specifically, they expressed concern that ~8 MPa RCS pressure might not be adequately bounding, that the melt mass distributions were too narrow, and that the melt composition did not contain sufficient Metals (Zr and steel). The reviewers also stressed that SCDAP/RELAP5 analyses should be performed and used in a consistent manner in establishing initial conditions.

The NRC convened a working group to make recommendations on how to resolve these concerns for Zion. Their minutes are included in Appendix A of Pilch et al. (1994b) and summarized here in Section D.3.2, where additional splinter scenarios are defined. Residual concerns were fully resolved for Zion (Appendix A in Pilch et al. 1994b) and it is our intent to follow the prescription for quantifying initial conditions for all Westinghouse plants with ice condenser containments. SCDAP/RELAP5 calculations were performed to provide confirmatory insight into the working group recommendations for Zion (Knudson, Appendix E in Pilch et al. 1994b) and for Surry (Knudson and Dobbe, 1993; Quick and Knudson, Appendix E in Pilch et al. 1995). Best estimate SCDAP/RELAP5 calculations were also performed for representative CE plants (ANO-2 and Calvert Cliffs) and for representative B&W plants (Oconee and Davis Besse) in Pilch et al. (1996). The relevant insights are summarized in Section D.3.3. Quantifications for the new scenarios are presented in Sections D.3.5, D.3.6, and D.3.7.

D.3.2 Splinter Scenarios

DCH is only of concern if the RPV fails while the RCS is still at elevated pressure. Figure D.2 depicts the four splinter scenarios analyzed in NUREG/CR-6075 (Pilch et al., 1994a). The complex phenomena of core melt progression leads to the possibility of two divergent scenarios

Splinter Scenario Approach

or bifurcations: one concerned with the quantity of melt that accumulates in the core region prior to its release and relocation into the lower plenum, and the other concerned with the mode and timing of lower head failure. Analysis of the first bifurcation considers crucible formation or failure versus gradual relocation (no crucible) as the mechanism for melt relocation into the lower plenum. Analysis of the second bifurcation considers a localized penetration failure of the lower head versus rupture.

Working group recommendations focused on four new splinter scenarios as shown in Figure D.3. These new splinter scenarios include some minor modifications to the previous splinter scenarios, some deletions of previous splinter scenarios, and the addition of new splinter scenarios. The intent was to place greater reliance on systems-level codes (SCDAP/RELAP5) in order to achieve better consistency between RCS pressure at vessel breach with melt mass and composition. Specifically, the working group emphasized that there were correlations between RCS pressure and melt composition; high RCS pressures and oxidic melts are correlated predominantly with operator intervention where water is added to the RCS (as occurred at TMI-II); metallic melts are more likely to be correlated with station blackout accidents with reduced RCS pressures associated with pump seal leaks of sufficient magnitude that hot leg failure does not occur. The working group minutes (Appendix A in Pilch et al., 1994b) refer to the new splinters as Scenarios II, IIa, IIb, and III; however, to avoid confusion with the scenarios already analyzed in NUREG/CR-6075, we refer to the new splinters in this report as Scenarios V, VI, VII, and VIII. The new scenarios either bound the scenarios in NUREG/CR-6075 or stress greater consistency in the conditions at vessel breach; thus, the new scenarios are intended to replace those in NUREG/CR-6075. The rationale leading to these new splinter scenarios is discussed next.

The working group felt that there was no compelling need to further analyze scenarios with penetration failures. A prototypic experiment (LHF-4; Chu et al., 1996) has been performed since the time of working group discussions. The experiment employed a 15th scale mock-up of a RPV lower head with scaled penetrations. As in a NPP, the penetrations are slipped through holes in the RPV and held in place with a shallow weld on the inside of the vessel. The test apparatus was pressurized to a steady 10 MPa, and the vessel was heated from the inside with resistive heaters to produce a uniform temperature on the lower head. The penetration weld was found to fail as the vessel began to balloon, and this failure occurred well before global failure strains (as determined from the LHF-1 test) were achieved. Consequently, we currently expect only penetration type failures, enlarged by ablation as the melt is ejected from the RPV. For DCH relevant melt masses, NUREG/CR-6075 (Pilch et al., 1994a) showed that a penetration failure, enlarged by ablation, would produce a hole about the same size as would be expected for a local rupture of the lower head. For consistency with prior work, we will use a local rupture of the lower head. We expect that the DCH loads will be insensitive to the initial hole size.

Scenario VI is very similar to Scenario II in NUREG/CR-6075. Here, the working group wanted to emphasize the presence of water in the lower head. They recommended the addition of a new TMI-like scenario (Scenario V) characterized by reflooding and repressurization (~16 MPa) of the RCS as a result of operator actions. Scenarios V and VI were envisioned as having water in the core (at least covering the bottom) during much of the core melt progression; consequently, slumping core material would form a crucible which could fail only locally. The

melt composition would be largely oxidic, with most unoxidized Zr permanently retained as a metal blockage in the core. Scenarios V and VI envelop those scenarios in which operators attempt to manage or recover an accident by adding water to the RCS but fail to prevent severe core damage, which then leads to failure of the RPV lower head.

The working group then recommended consideration of scenarios (VII and VIII) in which core melting would proceed without water in the core region and largely without water in the lower plenum. It was their expectation that these scenarios would evolve to much lower RCS pressures (< 4 MPa) at vessel failure for typical small break loss-of-coolant accidents (SBLOCAs). At the lower pressures, the possibility of the upper plenum steel melting without also failing the hot leg becomes possible; thus, both scenarios VII and VIII augment the oxidic component of the melt with large quantities of upper plenum steel. Scenario VIII is distinguished from Scenario VII in that the metal blockage is also assumed to remelt, allowing large quantities of unoxidized Zr to also relocate to the lower plenum.

NUREG/CR-6075 (Scenario IV) considered a gradual relocation that progressed under high pressure (~ 8 MPa) with complete melting of upper plenum steel. Working group discussions pointed out that this scenario is overly conservative and that melting of upper plenum steel is strongly correlated with hot leg failure. In fact, gradual relocation has been predicted in only one MELPROG calculation for the Surry plant (Heames and Smith, 1987); and even here, hot leg failure was predicted to occur before core relocation into the lower plenum. Should a gradual relocation occur, working group members believed that it would look like Scenario VIII at the time of vessel failure, thus Scenario IV should be replaced with Scenario VIII.

SCDAP/RELAP5 calculations have been performed (based on working group recommendations) for a station blackout accident to confirm the basic features of Scenarios VII and VIII for Zion (Appendix C in Pilch et al. 1994b). Three cases (representing short-term station blackout accidents) were run for Zion with SCDAP/RELAP5 representing the full spectrum of expected pump seal loss of coolant accidents (LOCAs): no leaks, 250 gallons per minute (gpm)/pump, and 480 gpm/pump. The key conclusion for Zion, however, is that hot leg failure will occur before core relocation for all pump seal LOCAs, leading to complete depressurization of the RCS before lower head failure.

INEL has made a comparison (Appendix A) between the Zion PWR and PWRs that use ice condenser containments in order to determine if the RCS depressurization results of Zion could be extended to the ice condenser plants. Four characteristics were compared including the power density, bypass configuration, hot leg geometry, and steam generator geometry. The following summarizes the conclusions derived from the comparisons.

1. The power densities for Zion and the ice condenser plants are nearly identical. Therefore, the power densities of the ice condenser plants should not adversely impact RCS depressurization (and the potential for HPME and DCH) compared to Zion.
2. Zion has a downcomer bypass configuration as do four of the ice condenser plants. The remaining ice condenser plants have core bypass configurations and, while the core bypass configuration has been shown to delay the progression of core degradation and lower head

Splinter Scenario Approach

failure during station blackout accidents, the most recent calculations indicate RCS depressurization will occur before lower head failure with either configuration. Therefore, the bypass configuration should not result in RCS depressurization behavior unlike Zion.

3. The hot leg geometries of the ice condenser plants are nearly identical to Zion. Therefore, hot leg geometry should not be significant in changing RCS depressurization results.
4. Five of the ice condenser plants use the same steam generator design as Zion. The remaining plants use steam generators characterized by smaller tubes in larger numbers. However, surface areas are comparable and it can therefore be assumed that SG geometry will not adversely impact RCS depressurization.

Based on these comparisons it can be concluded that PWRs with ice condenser containments will behave like Zion relative to RCS depressurization. As a result, there should be no significant difference between Zion and the ice condenser PWRs with respect to the probability for HPME and DCH.

In addition to RCS conditions, we must envelop the range of containment conditions that can exist at vessel breach. Hydrogen igniters, air return fans (ARFs), and ice beds differentiate ice condenser plants from plants with large dry or subatmospheric containments. These features have significant impact on the containment conditions (as discussed below) prior to vessel breach. Figure D.4 depicts the six splinter scenarios we propose to analyze as part of the ice condenser DCH evaluation. This figure does not depict logical events where neither the ARFs or the igniters are available. Such events are associated with unrecovered station blackout accidents, which have been shown to lead to creep rupture of the hot leg nozzles and complete depressurization of the RCS. The six splinter scenarios are intended to envelop the expected range of sequences and phenomenological uncertainties that are DCH relevant. We assign no probabilities to the various splinters. Each of the splinters will be run through TCE/LHS to compute the CCFP for each plant. We intend to do point comparisons between CONTAIN and TCE for each of the splinters. The remaining sequences in the event tree are candidates for additional CONTAIN calculations to gain insight and to assure that the splinters are adequately bounding.

The state of the igniters and air return fans prior to vessel breach plays an important role in defining atmosphere conditions. These primarily determine the conditions of the containment atmosphere prior to vessel breach. If the igniters are energized during most of the core melt progression, then the hydrogen concentration in the building will be no more than ~5 percent; otherwise the hydrogen concentration in the building could be very high (perhaps detonable) at the upper end of the core oxidation distribution. This combustion of hydrogen prior to vessel breach could also reduce the oxygen concentration in the building.

Operation of the ARFs forces steam through the ice beds, which reduces the steam concentration in the building and increases the rate of ice remaining in the ice beds. If the ARFs are not operational, then more ice will remain and up to ~0.1 MPa of steam could remain in the building. The presence or absence of steam in the building parallels a similar situation in large dries (or subatmospherics) associated with the operation of fan coolers (which occurred at TMI).

In NUREG/CR-6338 (Pilch et al., 1996), we added the designator "a" to denote the absence of steam in the building atmosphere.

A review of the Sequoyah IPE shows that small LOCAs or sequences with failure of certain electrical panels can lead to core melt and vessel breach while the RCS is still pressurized. Such sequences occur with total or partial power within the plant. The most DCH significant sequence in the Sequoyah IPE was initiated by failure of an electrical panel. The igniters were energized but the ARF were unavailable due to loss of DC control power. The Sequoyah IPE also identified other high pressure sequences where the igniters and ARFs were both powered.

Station blackout (SBO) sequences do not appear to play a significant role in Sequoyah's IPE containment event tree, but they do in NUREG-1150. The probability of a SBO is plant-specific and may be unusually low for Sequoyah because Sequoyah can draw power from two different grids. In the absence of any recovery attempts, INEL calculations for Zion (very similar to the NSSS in ice condenser plants) predict hot leg failure and complete depressurization long before (166-210 min) lower head failure. Sequences that spontaneously depressurize are of no concern to DCH.

The potential for power recovery prior to predicted hot leg failure must also be considered for SBO accidents. We acknowledge that recovery might terminate the accident in-vessel as occurred at TMI. The current knowledge base, however, cannot preclude the possibility that the accident will progress to lower head failure even with recovery (the margin appeared to be small at TMI). The possibility of recovery precluding hot leg failure but not vessel breach is implicitly recognized and enveloped by the Scenarios V and VI established in prior resolution reports, and this possibility should also be considered in ice condenser plants.

A recovered SBO in an ice condenser plant is unique, however, in that the status of igniters on recovery strongly determines the amount of hydrogen that remains in the building prior to vessel breach. The Sequoyah IPE states that the igniters do not energize automatically if power is recovered. Positive operator action is required. In a SBO accident, the operators are instructed to secure (i.e., turn off) the igniters. The igniters do not energize automatically when power is recovered, it requires deliberate operator action to energize the igniters. The operator is allowed to energize if hydrogen instrumentation is on-line and indicates that the hydrogen concentration is less than 6 percent. Otherwise, the operators should seek guidance from the NRC's technical support center. Consequently, we assume that the igniters remain off in many recovered SBOs.

The Sequoyah IPE states that the ARFs will automatically reboot after a ten minute time delay when power is recovered. This raises the possibility of a chance ignition of preexisting hydrogen. NUREG-1150 assumed that chance ignition was certain following recovery of the ARFs to be assigned a 100 percent probability to the event. A chance ignition occurred at TMI-II with operating fan coolers, but not before the hydrogen concentration reached ~8 percent. We assume as a bound that ignition sources (igniters or chance) do not exist in recovered accidents.

Figure D.5 summarizes the timing of key core melt progression events in a SBO, as predicted by SCDAP/RELAP5 for Zion with a 250 gpm/pump seal leak. Recovery prior to the onset of clad oxidation will likely terminate the accident in-vessel. Recovery after clad oxidation begins

Splinter Scenario Approach

and prior to calculated hot leg failure likely will preclude failure of the hot leg but it may not terminate the accident in-vessel. Recovery after hot leg failure is of no significance to DCH since the RCS will already be depressurized. Consequently, the time window for recovery is ~95 minutes if recovery is going to turn a depressurization scenario (hot leg failure) into a DCH scenario. Perhaps more importantly, clad oxidation has progressed as far as it will after only ~60 minutes; and as a result, it is likely that the hydrogen concentration in the building will be near its full potential when power is recovered and the potential for chance ignition exists. The threat to containment resulting from a hydrogen burn alone has been addressed in other programs and the IPEs, and this issue will not be addressed further in this document.

The reactor cavity can be flooded only if the entire RWST is dumped into the containment and some significant fraction of the ice is melted. Activation of the containment spray is an important mechanism for RWST injection into the containment, and the setpoint for spray actuation is plant-specific. The amount of melted ice (in addition to RWST injection) required to flood the cavity is also plant-specific and ranges from 20 - 80 percent. Lower head failure could be precluded altogether if the lower head is submerged in water. NUREG-1150 considered both flooded and dry reactor cavities in its containment event tree for Sequoyah, and the Sequoyah IPE adopted the same logic. Containment loads are likely to be higher for a dry cavity, and we adopt this as our splinter branch. We note that NUREG-1150 experts judged DCH loads to be negligible when the cavity was flooded, and we endorse this assumption in the current study. Considering only dry cavities is consistent with our modeling capabilities using TCE/LHS.

In many, but not all, scenarios involving complete melting of ice, we can expect the reactor to also be deeply flooded thus precluding significant DCH loads. Exceptions will be certain scenarios (e.g., station blackouts) where the RWST is not fully ejected into the containment. Our splinters are intended to be bounding, but the utilities might find benefit in the wire integrated perspective offered by their plant PSAs.

Operation of the ARFs has a large impact on the amount of ice remaining at vessel breach. About a third of the ice will remain if the ARFs *are not* operational, while little or no ice will remain when the ARFs *are* operational. In the latter case, the remaining ice may not be fully effective due to channeling or asymmetric flow through the ice beds. NUREG-1150 considered both cases (i.e., effective and ineffective ice beds) and the Sequoyah IPE appears to also. As a bound to both sequence permutations and phenomenological uncertainties, we assume that the ice beds are not effective for our splinter scenarios. In effect, we treat the plant as a "small dry," which is consistent with TCE/LHS capabilities. CONTAIN calculations will be performed to assess the potential impact of the remaining ice and to ensure that the defined splinters are adequately bounding.

In summary, DCH is only of concern if the reactor pressure fails while the RCS is still at elevated RCS pressure. Consequently, we exclude here from further analysis any scenarios with low RCS pressure at the onset of core damage, scenarios where the RCS is intentionally depressurized in compliance with accident management procedures or other forms of operator intervention, and sequences where the RCS unintentionally depressurizes as a natural consequence of core melt progression. SCDAP/RELAP5 calculations show that hot leg failure and RCS depressurization is likely if the core is not reflooded. We envelop the RCS pressure

with high pressure (16 MPa) and intermediate pressure (8 MPa) splinter scenarios, which are noted as Scenarios V and VI, respectively. We envelop containment conditions by considering splinters with and without active cooling in the containment (i.e., no steam or steam in the atmosphere respectively); these are noted as Scenarios Va and VIa, respectively, depending on whether the RCS is at high or intermediate pressure. These four scenarios are consistent with previous assessments of DCH in plants with large dry or subatmospheric containments. We consider two additional scenarios characterized by low steam and high hydrogen concentrations in the atmosphere; which are unique to plants with ice condenser containments. These scenarios, denoted as Scenarios Vb and VIb, address recovered station blackout sequences where containment cooling is restored but hydrogen igniters are de-energized. These scenarios are characterized by low steam concentrations and high hydrogen concentrations.

INEL notes that the bypass configuration can have some effect on core melt progression; however, any differences do not alter the basic conclusion that RCS depressurization is expected before core relocation into the lower plenum and well before lower head failure. This conclusion follows from an examination of the NSSS and from SCDAP/RELAP5 calculations performed from both Zion and Surry. Some ice condenser plants employ a "downcomer bypass configuration." Zion has a downcomer bypass configuration while Surry has a core bypass configuration. Previous SCDAP/RELAP5 calculations for Zion and Surry show that any differences in core melt progression do not violate the prescription used here to define the melt mass and composition at vessel breach. These six splinter scenarios adequately envelop the full range of RCS and containment conditions for the few DCH relevant scenarios.

D.3.3 Summary of SCDAP/RELAP5 and CONTAIN Insights

The initial and boundary conditions for the scenarios analyzed in this report are based in part on insights from SCDAP/RELAP5 and CONTAIN calculations. These system code calculations are used to better quantify a consistent set of initial and boundary conditions for the splinter scenarios discussed in Section D.3.2. In this regard, we do not blindly use the results of system-level code calculations; rather, we use the codes as one form of input when forming our expert judgments. For example, we include zirconium in our melts when SCDAP/RELAP5 predicts essentially none.

SCDAP/RELAP5 calculations have been performed for Zion (W 4-loop plant), Surry (W 3-loop plant), Calvert Cliffs (CE lowest power density), ANO-2 (CE highest power density), Oconee (B&W low loop), and Davis Besse (B&W raised loop). These calculations are reported as appendices in Pilch et al. (1994, 1995, 1996). The credible range of pump seal leaks have been examined for each plant and sensitivity studies have been performed. SCDAP/RELAP5 has now analyzed each of the major reactor types from each supplier of PWR nuclear steam supply systems in the U.S. All of the cases analyzed so far produced "dry core" conditions, so the potential existed for metallic blockages to relocate to the lower plenum. However, relocation of metallic blockages were not predicted by SCDAP/RELAP5.

Zion is a four-loop Westinghouse nuclear steam supply system. Three dry core cases were run with SCDAP/RELAP5 for Zion at different leak rates: (1) no leaks, (2) 250 gpm per pump leaks, and (3) 480 gpm per pump leaks. The results of these calculations are discussed in

Splinter Scenario Approach

Appendix C of Pilch et al. (1994b). The goal of these calculations was to develop a better understanding of the melt mass, melt composition, and RCS pressure at the time of lower head failure for dry scenarios. In each case, hot leg failure was allowed to occur, if predicted during the calculation. This failure would lead to depressurization and complete accumulator discharge.

The SCDAP/RELAP5 calculations for Zion predicted that hot leg failure occurred prior to melt relocation into the lower plenum in all cases. The failure resulted in depressurization and accumulator discharge. In all cases, the RCS pressure was at containment pressure at the time of lower head failure. Owing to the significant amount of time between hot leg failure and lower head failure, we conclude that the sequences, as calculated by SCDAP/RELAP5, will not result in a DCH threat. This supports the assessment in NUREG/CR-6075 that full system pressure scenarios can be excluded (except operator intervention accidents such as TMI-II). The SCDAP/RELAP5 calculations also confirm that the ~8 MPa bound in NUREG/CR-6075 is not only conservative, but perhaps excessively so unless the operator intervenes in the accident. This assumes, of course, that water injection does not arrest melt progression.

Surry is a three-loop Westinghouse nuclear steam supply system that does not have the core by-pass feature found in Zion. Existing SCDAP/RELAP5 calculations (Knudson and Dobbe, 1993), which were intentionally biased to accelerate core melt progression and lower head failure, were examined for insights on core melt progression. Three different RCP leak rates were examined: (1) no leaks, (2) 250-gpm/pump leaks, and (3) 480-gpm/pump leaks. In addition, a best-estimate calculation for the 480-gpm/pump case was performed for the NUREG/CR-6109 study (Pilch et al., 1995). These calculations provide additional insight into melt mass, melt composition, and RCS pressure at the time of lower head failure.

The existing SCDAP/RELAP5 calculations for Surry indicated that hot leg or surge line failure occurred prior to melt relocation into the lower plenum in all but the 480-gpm/pump case. The existing calculations were intentionally biased to accelerate core melt progression and lower head failure in order to bound the likelihood that lower head failure could occur while the RCS was still at elevated pressure. Consequently, the NRC asked INEL to perform a best-estimate calculation of the 480-gpm/pump case. This best estimate also led to hot leg failure. These conclusions are fully consistent with those reached for Zion.

Sensitivity studies were performed for the biased SCDAP/RELAP5 calculations (Appendix F in Pilch et al., 1995) in order to assess the potential impact of uncertainties on these conclusions. The probability that the RCS pressure would exceed 1.38 MPa (200 psig) is ~1.1 percent conditional on a short-term station blackout accident. This insensitivity occurs because of the significant amount of time between hot leg failure and lower head failure. As a result, we conclude that the probability of an HPME is small for a station blackout accident, without operator intervention or recovery.

An insight from the SCDAP/RELAP5 calculations is related to the amount of metallic debris present in the melt in the lower plenum. We noted that the degree of upper plenum steel melting is limited in all cases and is strongly correlated with hot leg failure. The maximum amount of upper plenum steel that was predicted to melt was much less than 1 mt for Surry and ~3 mt for Zion. We also noted that lower plenum steel was assumed to melt in all cases, representing an

additional ~5 mt of steel. Melting of lower plenum steel occurs only to the extent that thin lower plenum steel is submerged in the relocated core material. Lower plenum water always existed in the SCDAP/RELAP5 calculations, even in the absence of operator interaction; consequently, radiative melting of lower plenum steel is not expected.

With respect to zirconium in the melt, SCDAP/RELAP5 indicates that very little zirconium is predicted to relocate into the lower plenum for Zion and Surry. The maximum amount of zirconium in the lower plenum melt is ~0.13 mt for Surry and ~0.5 mt for Zion. This implies that meltout of the metallic blockage in the core region is not predicted, even in dry core scenarios.

The reason for this behavior can be seen by a careful review of the calculations. In all cases, the melt that relocated into the lower plenum is predicted to quench, but not all of the available water is vaporized. This is most likely due to displacement of water from the lower plenum as the melt relocates. The water eventually settles back into the lower plenum, but a stratified condition exists, i.e., the water overlies the debris residing on the lower head. Owing to inefficient heat transfer between the debris and the water, the water is vaporized slowly and water remains in the lower plenum at the time of lower head failure. The presence of water and its slow vaporization appears to be sufficient to prevent meltout of the in-core blockages. Hence, we conclude that the amount of zirconium in the melt in the lower plenum will be very limited. We acknowledge uncertainties in modeling of late-phase core melt progression; consequently, additional Zr will be treated in our melt composition quantifications as discussed in Sections D.3.5 and D.3.6.

A third insight is related to the amount of hydrogen generated for Zion and Surry, which corresponds to from ~20 to 60 percent oxidation of the initial zirconium inventory in the core. Our expectation is that the 60 percent level is a likely upper bound since much of the remaining zirconium is contained in metallic blockages that are difficult to oxidize.

The fourth insight is related to the amount of molten material at the time of lower head failure. We noted that the amount of oxide material that was available to relocate into the lower plenum for Zion varies from approximately 77 mt to 104 mt for the three Zion cases, but the amount of *molten* oxide varies from 55 mt to 66 mt. We noted that the maximum amount of oxide material available to relocate into the lower plenum was ~75 mt for Surry. The biased SCDAP/RELAP5 calculations for Surry indicate that virtually all of the core debris relocated in the lower plenum is solid at the time of lower head failure. This is a consequence of attempts to accelerate lower head rupture. If best estimate rupture times are assumed, then SCDAP/RELAP5 indicates that ~13 mt of relocated material will be solidified leaving ~62 mt molten at the time of lower head failure.

Our prescription for quantifying molten oxide masses conservatively envelope available SCDAP/RELAP5 predictions for Westinghouse plants. Plant calculations and sensitivity studies with SCDAP/RELAP5 show that plants with lower power densities will have lower melt masses at vessel breach. This is because reheating of lower power density debris is slower allowing vessel heatup to more closely follow debris heatup. Our approach to quantifying melt masses takes no credit for this fact in plants with low power densities.

Splinter Scenario Approach

The flow of steam, water, hydrogen, and nitrogen (from accumulator discharge) into the containment for Zion was provided to Sandia by INEL for use in CONTAIN to determine the containment conditions at the time of lower head failure. The hydrogen flow into the containment was assessed to determine if the hydrogen would burn as it entered the containment. A number of important insights were obtained from these calculations.

Insights were obtained on non DCH-induced hydrogen combustion in Zion using both the SCDAP/RELAP5 and CONTAIN calculations. The SCDAP/RELAP5 predictions were analyzed to determine what fraction, if any, of the hydrogen injected into the Zion containment would be consumed as an autoigniting jet. Furthermore, since the scenarios analyzed were station blackout scenarios, the autoigniting jets were considered to be the only possible ignition source for deflagrations in the containment. Therefore, CONTAIN predictions of the source compartments were analyzed to determine if mixtures were flammable at the time the jets autoignited. It was determined that the only possibility of jet autoignition in Zion would occur at the hot leg break in the case of no pump seal leak or in the case of a 480 gpm/pump leak, and these cases would depressurize so quickly that they would not be a DCH threat. Otherwise, the temperatures of the gases (~600 K) released from the power-operated relief valves (PORVs) were too low for autoignition for all cases, and the hydrogen concentration in the jet never exceeded ~5 percent and usually was zero. Likewise, gases released from the RCPs likely would not autoignite in all of the cases analyzed because hydrogen concentrations in the jets were very low (~5 - 15 percent) during periods of high gas temperatures. Thus, the hydrogen concentration in the Zion containment just prior to vessel failure can be simply determined by summing all hydrogen released from the RCS.

Analogous calculations were not performed specifically for the ice condenser plants, however, insights from the Zion analyses regarding autoigniting jets are applicable to ice condenser plants. In Zion, hot jets did not ignite deflagrations in the containment atmosphere because hydrogen concentrations were too low. However, hydrogen concentrations in the atmosphere of an ice condenser plant can be ~2.4 times higher because of the much smaller containment volume. Figure C.25 (Pilch et al., 1994b) shows that virtually all hydrogen is released to containment prior to calculated hot leg failure; consequently, flammable hydrogen concentrations can exist in the atmosphere prior to expected hot leg failure. Figure D.7 (Pilch et al., 1994b) shows that gas temperatures venting from the RCPs can be far in excess of the ~1100 K ignition temperature for deflagrations in the atmosphere (even though autoignition conditions do not exist for the jet itself). Consequently, it is likely that deflagrations will be ignited in flammable atmospheres prior to hot leg failure in unrecovered SBO accidents. Although not addressed explicitly in Pilch et al., 1994b, the operations may vent cases directly through the upper head vents, and we expect that these gases are also capable of igniting containment hydrogen.

These conditions are of no interest to DCH because hot leg failure is directly related to the high jet temperatures. DCH relevant scenarios are most likely to evolve from managed accidents where water injection cools the RCS gas to the point that hot leg failure is not assured. Jet temperatures may still be high enough to ignite flammable atmosphere, but we have no assurance that this is the general expectation. Consequently, we cannot conclude definitively that gases discharge from the RCS will act as an ignition source for flammable atmospheres.

Consequently, the hydrogen concentration in an ice condenser containment just prior to vessel failure can be simply determined by summing all hydrogen released from the RCS in those scenarios where hydrogen igniters are de-energized.

Pressure suppression is a distinguishing feature in ice condenser plants. CONTAIN calculations (Appendix B) for Sequoyah (using RCS sources from a Zion SBO) indicate that the containment will be pressurized to ~0.10 - 0.18 MPa at the time of vessel breach for all scenarios. If the ARFs are operating (Scenarios Va, Vb, VIa, VIb), CONTAIN predicts that the containment is well mixed and that all the ice is melted prior to vessel breach. CONTAIN predicts that ~35 percent of the ice remains when the ARFs are not operating (Scenarios V, VI) and that the lower compartment is steam rich.

D.3.4 TCE/LHS Summary Quantifications

Table D.2 provides a description of the TCE/LHS data input. Tables D.3 – D.8 provide a concise summary of the TCE/LHS quantifications for every plant and for each scenario.

D.3.5 Scenario V - SBLOCA with Repressurization of the RCS by Operator Intervention

Scenario V represents a core melt accident that progresses with water still present in the lower portions of the core. Such conditions lead to formation of a crust within the core followed by a massive release of melt when the crust fails. Accumulation of core material on the lower head of the RPV causes the lower head to heat up, eventually to the point where its structural strength is so degraded it can no longer withstand the stresses induced in the lower head by elevated RCS pressures. Thus, creep rupture of the lower head is the expected failure mechanism. The distinguishing feature of Scenario V is that operator actions are assumed to refill the RPV with water and to fully repressurize the RCS. Analysis of DCH for a repressurized RCS is deemed conservative because we expect operators to depressurize the RCS in a core damage accident.

Operator actions are assumed to repressurize the RCS to 16 MPa. Operator intervention refills the RPV with water to the hog leg nozzles and quenches any steam remaining in the RCS to near saturation (~700 K). Recall that at TMI-II a noncondensable gas bubble prevented operators from refilling the entire RCS. The RPV lower head must be heated by accumulated core material to the point that steel loses its strength (~1000 K), which leads to rupture of the lower head. The initial hole diameter is ~0.40 m (Pilch et al., 1994a) because of the likely presence of hot spots and because of stress concentrations associated with the existence and spacing of lower head penetrations (for those plants with lower head penetrations). A 1:5th scale experiment recently conducted by SNL (LHF-4, Chu et al., 1996) included scaled lower head penetrations. The experiment showed that gross strain in the lower head induced failure of a penetration weld well before global creep rupture of the lower head would be expected. We note that this experiment did not represent all the loads on penetrations and these loads would increase likelihood that a penetration failure would occur.

We note that TMI-II exhibited a ~1 m hot spot on the lower head, and some have argued that a ~1 m hole might be more appropriate for those CE plants that do not have lower head

Splinter Scenario Approach

penetrations. A 1:5th scale experiment recently conducted by SNL (LHF-2, Chu et al., 1996) simulated a ~2 m hot spot, while the resulting rupture size was ~0.38 m (full scale equivalent). This rupture size is in accordance with prior working group recommendations (Appendix A in Pilch et al., 1994b) observed for Zion (~0.4 m).

As TMI suggests, hot spots may generally be expected due to nonuniform accumulation and quenching of debris in the lower plenum. In certain situations, multiple relocations for the core might be expected; consequently, the bottom portions of the lower head will have a "head start" in heating over higher portions of the lower head. Systems code modeling generally cannot capture fully the types of expected nonuniformities. Thus, we expect localized failure as exhibited in the LHF-2 experiment (bottom peaked heating, no penetration) or the LHF-4 experiment (uniform heating, with penetration), even in CE plants with integral lower heads, but especially in plants with lower head penetrations.

SNL recently observed a nearly completely circumferential "unzipping" of a lower head in the LHF-5 experiment⁶ conducted at pressures of 7-10 MPa. This experiment employed an inductively-heated graphite heater that produced ~625 K on the vessel bottom and ~1050 K at an azimuthal location corresponding to the (scaled) top of ~75 percent of the core relocated into the lower plenum.

These test conditions favor global failure rather than the local failure expected in DCH-relevant scenarios. Strongly side peaked heating might occur in high pressure scenarios if there is a single massive relocation and if there is no quenching of debris with lower plenum water so that the molten pool starts convecting immediately. These conditions are considered unreasonable for DCH relevant scenarios. Strongly side-peaked heating might also be expected in low pressure scenarios where volumetric heating has had time to fully remelt the relocated core debris forming well established convecting pools in the lower head. This scenario is of no interest to DCH System code calculations for the plant also indicate that the location of peak heating, although side-peaked, occurs about midway between the bottom and the top surface of the melt pool. Most significantly, however, the heaters in the LHF tests do not simulate the nonuniformities or time sequencing of relocation that drive our expectation of localized failure in the plant.

We note that the SNL LHF experiments exhibit very large strains prior to rupture for the likely case of a hot spot or even uniform heating of the head. These strains are comparable to the clearance between the RPV and the cavity floor, so the possibility exists that the deforming lower head could become supported by the cavity floor before rupture occurs. This external support could promote the potential of external failure or it could delay or even prevent creep rupture of the lower head. B&W plants are unique amongst PWRs in that the RPV is supported by a skirt. The skirt is expected to act as a local heat sink, thus preserving local strength. In addition, the skirt provides additional structural support. Since B&W plants have lower head penetrations, we expect the presence of a skirt to make penetration failure even more likely.

⁶ This experiment was conducted August 1, 1997, just prior to the publication of this report. Posttest analyses are being conducted and experiment results have not yet been published.

Experiments (Allen et al., 1991) at ~4 MPa driving pressures and the TCE model do not show a strong sensitivity to the initial hole size. The final hole size is computed with the ablation model, Eq. (D.8) for each plant, scenario, and Monte Carlo sampling; however, ablation is not important for the large initial hole sizes associated with rupture of the lower head.

Oxidation of Zr occurs predominantly before significant core degradation, as demonstrated in various calculations. In earlier two-dimensional MELPROG calculations performed by Kelly et al. (1987), 80 percent of the Zr oxidation occurred prior to formation of a molten pool. SCDAP/RELAP5 calculations (Appendix C in Pilch et al., 1994b) performed for Zion confirm these early assessments and show that nearly 100 percent of the hydrogen is produced before core slump. SCDAP/RELAP5 predicts similar behavior for Surry (Appendix E and Knudson and Dobbe, 1993). A dramatic reduction in oxidation is expected after clad relocation and freezing in the lower portions of the core as qualitatively observed in the DF-4 experiment (Gauntt et al., 1989). To a first order then, Zr oxidation is independent of the core melt progression that follows the main oxidation event; and since oxidation occurs predominantly before formation of the molten pool, existing system-level computer codes are technically adequate to assess the range of possible oxidation.

Referring then to SCDAP/RELAP5 calculations (Knudson and Dobbe, 1993; Knudson, 1993; Appendix C in Pilch et al., 1994b; and Appendix E in Pilch et al., 1995), MELPROG/PWR-MOD1 calculations (Kelly et al., 1987), and CORMLT calculations (Denny and Sehgal, 1983), we find that the fraction of Zr oxidized ranges from 20 to 60 percent, with a mean around 40 percent. Observations from TMI-II fall into this range. The distribution is shown in Figure D.6. The calculations cited were chosen because of their explicit treatment of recirculating flow patterns in the core.

Consistent with TMI-II, the potential release of molten material to the lower head is controlled by the formation of a hemispherical crucible that excludes only the outer assemblies of the core (Figure D.7). The outer assemblies are generally not expected to be in a severely degraded state because the RPV is flooded. We note that SCDAP/RELAP5 does predict melting of the outer assemblies in the region of the in-core crucible. It is an imposed code requirement (resulting in a bigger in-core crucible and more melt relocation) that the crucible grow to the core edge before relocation is allowed. We feel that asymmetries in crucible growth ensure that localized penetration of the outer assembly and the core barrel would most likely occur when the crucible has grown (on average) to the outer assembly. This is consistent with the observed end state at TMI-II.

We expect the melt mass to be a function of the core size for each plant; fortunately, all four-loop Westinghouse plants (including the ice condenser plants) have the same core sizes. The distribution for molten UO_2 at vessel breach has been quantified previously for all Westinghouse, CE, and B&W plants by Pilch et al. (1996, Appendix B). The UO_2 distributions for the ice condenser plants are repeated here as Tables D.9 and D.10 for Scenarios V and VI, respectively. Figure D.8 shows the distribution of molten UO_2 in the lower plenum at the time of vessel rupture for Scenarios V, Va, and Vb. The upper end of the distribution corresponds to a bottom failure of the crucible with the best estimate corresponding to a side failure of the crucible as observed in TMI-II. The quantifications recognize that ~15 percent of the material contained in

Splinter Scenario Approach

the crucible is ZrO_2 . Furthermore, the quantifications take nominal credit for relocating melt that freezes (~ 10 mt) as a necessary condition to heat the lower head to rupture.

We conservatively assume bottom failure of the RPV so that all molten material is available for ejection into the cavity. Side peaked heat fluxes could cause the lower head to fail near the pool surface if convecting molten pools are established in the lower plenum. For the same hole size (~ 0.4 m), scoping analyses based on published hydrodynamic entrainment criteria indicate that ~ 25 - 50 percent of the melt in the lower plenum cannot be entrained out the hole. The presence of an oxidic crust overlying the melt pool would likely enhance melt retention in the RPV. We note that credit was taken in NUREG-1150 for side failure of the RPV for Sequoyah as part of its DCH assessment.

The amount of molten ZrO_2 in the melt is controlled by the amount of clad oxidation that

$$M_{ZrO_2} = \frac{M_{UO_2}(melt)}{M_{UO_2}(core)} M_{Zr}^0 f_{Zr} \frac{123}{91} \quad (D.1)$$

occurs prior to core melt. The amount of molten ZrO_2 can be estimated from

This expression assumes that ZrO_2 is contained in the melt in the same fraction to which the core is degraded $M_{UO_2}(degraded)/M_{UO_2}(core)$ and that ZrO_2 relocates to the lower plenum in the same manner as the UO_2 , that is, $M_{UO_2}(melt)/M_{UO_2}(degraded)$.

The relocation of Zr metal within the core plays a key role in the ultimate formation of core blockages. Upon melting, most of the Zr metal and $(U,Zr)O_2$ relocates downward until it freezes in cooler portions of the core, forming partial or complete blockages, depending on the amount of relocating material. The subsequent melting of UO_2 and ZrO_2 allows molten oxides (at least initially) to settle and refreeze on top of the metallic blockages. In this way, the accumulating melt forms a crucible on top of the metallic blockage. This picture is consistent with SC-DAP/RELAP5 calculations and TMI-II observations. This separation of molten oxides from the blockage, which consists of unoxidized clad and dissolution products, ensures that little metal enters the melt, except possibly through some additional formation of $(U,Zr)O_2$ eutectics, dripping of Zr from fuel stubs above the degraded region, or when the crust fails. However, SC-DAP/RELAP5 predicts only negligible additional formation of eutectics, and dripping is not predicted even in scenarios in which the core is completely dry. As observed in TMI-II, the crust is expected to fail locally (from inhomogeneities in the crust and asymmetries in crucible growth), carrying only small quantities of metal from the blockage into the lower plenum. The flooded core scenario precludes melting out of the blockage. Thus, little or no Zr is expected in the melt.

We note that SC-DAP/RELAP5 calculations predict little or no Zr in the melt. However, to account for uncertainties in eutectic formation and crucible failure (and consistent with the working group recommendations), we assume that the molten Zr mass is proportional to the mass of molten UO_2 . Thus, the amount of molten Zr can be computed from

$$M_{Zr} = 0.029 M_{UO_2} \quad (D.2)$$

The constant of proportionality (0.029), as estimated for Zion (Pilch et al., 1994b), is assumed to be applicable to all plants. We conservatively assume that any Zr that relocates with the melt does not oxidize as it falls through the water pool. Additional perspectives on this formulation are discussed in Section D.3.7.

In a wet core scenario such as this, the control rod material will be an initial contributor to the metal blockage in the core and the flooded core scenario precludes melting out of the blockage. Consequently, only trivial quantities (~0 mt) of control rod will be present in the melt at the time of vessel breach.

Melting of upper plenum steel is strongly correlated with failure of the surge line or hot leg nozzle at high system pressures (~8 MPa). Specifically, gas temperatures that are hot enough to melt upper plenum steel (~1700 K) are also hot enough to induce rupture (under pressure) of the hot leg or surge line. Upper plenum steel is a potential contributor to melt mass and composition only in those scenarios (Scenarios VII and VIII) that proceed to relatively low pressures at the time of vessel breach; and even then, SCDAP/RELAP5 predicts failure of the hot leg when upper plenum steel is predicted to melt. In any case, melting of upper plenum steel cannot be important when operators reflood the RPV as they did in TMI-II. The small amount of steel initially in the core, like cladding and control rod material, is largely retained in core blockages, which cannot melt out in a flooded core scenario.

The melting of lower plenum steel by relocated core material is the only source of molten steel of potential importance in a DCH event. SCDAP/RELAP5 calculations show that some water is nearly always present in the lower plenum, so the core debris cannot radiate to structures. Only thin lower plenum steel (e.g., nozzles) that is submerged in the accumulating core material is assumed to melt. The quantity of submerged steel depends on the volume of core material in the lower plenum and can be computed from

$$M_s = M_{s,LP} \frac{\frac{M_{UO_2}}{\rho_{UO_2}} + \frac{M_{ZrO_2}}{\rho_{ZrO_2}} + \frac{10 \times 10^3}{\rho_{UO_2/ZrO_2}} + \frac{M_{Zr}}{\rho_{Zr}} + \frac{M_{CRM}}{\rho_{CRM}}}{V_{LP}} \quad (D.3)$$

where the densities (kg/m³) are $\rho_{UO_2} = 10,400$, $\rho_{ZrO_2} = 5,900$, $\rho_{UO_2/ZrO_2} = 9,660$, $\rho_{Zr} = 6,500$, and $\rho_{CRM} = 9,250$. Note that the quenched 10 mt must be taken into account because it is part of the volume of core material. We note that submerged nozzles at TMI-II did not all melt; consequently, Eq. (D.3) gives a conservative result.

Consideration of natural convection in volumetrically heated pools (Theofanous, 1988; Epstein and Fauske, 1989) indicates that the melt superheat cannot exceed ~200 K under steady-state conditions. The UO₂/ZrO₂ eutectic melts at about 2800 K, so the maximum temperature on relocation is about 3000 K (~2900 K has been estimated for TMI-II), but some cooling on

Splinter Scenario Approach

relocation is expected. Thus, we believe that a conservative bounding value of ~2800 K is appropriate for Scenario V.

CONTAIN calculations were performed to gain insight into containment conditions prior to vessel breach. RCS sources were taken from an existing SCDAP/RELAP5 calculation of a station blackout accident in Zion. The containment pressure at vessel breach was found to be ~0.18 MPa in all scenarios if active containment cooling is not operational. The ice is predicted to be completely melted in scenarios Va and Vb and the atmosphere is well mixed because the ARFs are operational. CONTAIN predicts that significant (~35 percent) ice remains in Scenario V and the lower compartment is steam rich because the ARFs are not available.

The containment conditions discussed above assume that active containment cooling systems (i.e., fan coolers or sprays) are not operational. We note that fan coolers were operational at TMI-II and that containment conditions were $P \sim 0.11$ MPa, $T \sim 326$ K, $X_{STM} \sim 0.035$, and $X_{H2} \sim 0.079$. Thus, there was little steam in the containment and the hydrogen concentration was high. In an ice condenser plant, we must also distinguish if the igniters are available as this controls the hydrogen concentrations. Scenario Va is characterized by low hydrogen concentrations (~5.5 percent) and low steam concentrations ($X_s \sim 0$ percent) because igniters and active cooling are available. Scenario Vb is characterized by high hydrogen concentrations (Eqs. D.4 and D.5) and low steam concentrations ($X_s \sim 0$ percent) because igniters are not available while active cooling is available.

The core-wide oxidation of Zr also controls the amount of preexisting hydrogen that can exist in the containment building at the time of vessel breach (when igniters are not available). The RCS retains very little of this hydrogen because it is produced early in the accident and most is vented to the containment. This is supported by earlier SCDAP/RELAP5 calculations (Knudson, 1993) where more than 90 percent of the H_2 was released to the containment. Recent SCDAP/RELAP5 calculations performed for Zion (Appendix C in Pilch et al., 1994b) indicate that essentially all the hydrogen produced in-vessel will be released to the containment. Steam and H_2 sources from SCDAP/RELAP5 are sometimes very hot (Appendix D in Pilch et al., 1994b) and there is a possibility that hydrogen jets will burn as it enters the containment. However, recent CONTAIN assessments for Zion (Pilch et al., 1994b) and Surry (Pilch et al., 1995) using SCDAP/RELAP5 sources suggest that this effect is minimal except possibly in the event of a hot leg failure, which precludes a DCH event. Consequently, we conclude that all hydrogen produced in-vessel will be released to containment, where it will not burn prior to vessel breach. The moles of preexisting hydrogen in the containment are given by

$$N_{H2} \text{ (g \cdot mole)} = \frac{2}{0.091} f_{Zr} M_{Zr}^0 \text{ (core)}, \quad (D.4)$$

or alternatively, a concentration can be specified

$$X_{H2} = \frac{N_{H2}}{N_{ATM}^0} \quad (D.5)$$

We note that at TMI-II there was ~7.9 percent H_2 in the atmosphere and essentially no steam. Even though these conditions are in the flammable regime, we cannot guarantee that a random ignition source (unless intentional) will burn off the hydrogen prior to vessel failure if the flammability limits are exceeded.

Igniters (if available) are effective at keeping the hydrogen concentrations below ~5.5 percent regardless of the hydrogen released to the containment. This controlled and deliberate combustion of hydrogen prior to vessel breach also consumes oxygen in the atmosphere. At the extremes of the invessel oxidation (~65 percent), this controlled combustion of hydrogen could reduce the global oxygen concentration to ~6-7 percent in Scenario V and 10-11 percent in Scenarios Va and Vb. In our TCE modeling, hydrogen combustion is allowed provided the oxygen concentration exceeds 5 percent and the hydrogen concentration is sufficiently high. Consequently, the deliberate combustion of hydrogen prior to vessel breach is not expected to significantly alter the potential to burn available hydrogen after the DCH event. As a matter of implementation into TCE, we hardwire a maximum hydrogen concentration of 5.5 percent and ignore changes in oxygen concentration resulting from deliberate combustion of preexisting hydrogen prior to vessel breach.

D.3.6 Scenario VI - SBLOCA Under Wet Core Conditions

In the absence of any RCS leaks, SCDAP/RELAP5 (Pilch et al., 1994b, 1995) predicts surge line failure or hot leg failure long before bottom head failure. These cases fully depressurize and are of no interest for DCH. We then sought SBLOCAs of just the right size to depressurize sufficiently that natural circulation degrades to the point that surge line or hot leg failure is not assured. Such an intermediate state was not found. In fact, SCDAP/RELAP5 predicts hot leg failure before core relocation for the full spectrum of SBLOCAs; consequently, Scenario VI can only exist as the consequence of partial operator intervention. For the expected SBLOCAs, SCDAP/RELAP5 predicts depressurization to the ~4 MPa range. However, repressurization spikes due to accumulator injection or melt relocation could sometimes repressurize the RCS to ~8 MPa, which is consistent with NUREG/CR-6075 (Pilch et al., 1994a) assessments. Thus, the ~8 MPa RCS pressure used in NUREG/CR-6075 is adequately bounding, particularly in light of SCDAP/RELAP5 predictions that the hot leg will fail before core relocation. Owing to similarity in Scenarios V and VI, we emphasize only the differences in RCS temperature, melt mass, and composition, with all other parameters developed in a manner similar to that for Scenario V.

The RCS gas at the time of vessel breach clearly must be superheated. In conjunction with the pressure and volume, the moles of gas in the RCS can be computed with the RCS temperature. The gas temperatures in each region of the RCS are estimated from SCDAP/RELAP5 output for Zion (Pilch et al., 1994b). Given this assessment, a lower bound of ~1000 K is assigned to this scenario.

The potential release of molten material to the lower head is again controlled by the formation and failure of a crucible in the core region. Water occupies only the lowest regions of the core, so radial cooling of a growing crucible is reduced in this situation, and consistent with SCDAP/RELAP5 predictions, the crucible could take on the bounding shape of an upright cylinder as depicted in Figure D.9. We note that SCDAP/RELAP5 conservatively assumes that

Splinter Scenario Approach

the melt pool must grow to the core boundary as a condition for core relocation, thus SCDAP/RELAP5 shows some localized involvement of the outer assemblies. We expect, however, that asymmetries in crucible growth ensure that localized penetration of the outer assembly and core barrel would likely occur when the crucible has grown (on average) to the outer assembly. Consequently, the outer assemblies are excluded from our assessments.

We expect the melt mass to be a function of the core size for each plant; fortunately, all ice condenser plants have the same core size. The distribution for molten UO_2 at vessel breach has been quantified previously for all Westinghouse, CE, and B&W plants by Pilch et al. (1996, Appendix B). The UO_2 distributions for ice condenser plants are repeated here as Tables D.9 and D.10 for Scenarios V and VI, respectively.

Figure D.10 shows the distribution of molten UO_2 in the lower plenum at the time of vessel rupture for Scenarios VI, VIa, and VIb. As expected, the melt mass decreases with decreasing core size. The upper ends of the distributions correspond to a bottom failure of the crucible with the best estimate corresponding to a side failure of the crucible as observed in TMI-II. The quantifications recognize that some of the material contained in the crucible is ZrO_2 . Furthermore, the quantifications take nominal credit for relocating melt that freezes (~ 10 mt) as a necessary condition to heat the lower head to rupture.

Scenario VI is envisioned as having water in the lower plenum, but not to the extent that it submerges the bottom of the core. Under such circumstances, it is possible for low melting point control rod material to relocate to the lower plenum.

We note that SCDAP/RELAP5 calculations predict little or no Zr in the melt because most of the Zr relocates and forms blockages in the lower core before significant melting of fuel occurs. However, to account for uncertainties in eutectic formation and crucible failure, we assume that the molten Zr mass is 2.9 percent of the molten UO_2 mass (Eq. D.2). Although SCDAP/RELAP5 does not predict relocation of the metallic blockage, we acknowledge that scenarios where the bottom of the core is not submerged in water have an increased potential for partial melting and relocation of the metallic blockage into the lower plenum. We note, however, that complete oxidation of the Zr in reactor material melts was observed in a FARO experiment (Magallon 1995) involving melt drainage into a pressurized water pool. More importantly, however, are SCDAP/RELAP5 predictions that the RCS will be depressurized in those scenarios that have the greatest potential for relocation of the metallic blockage.

It is useful to examine the recommended Zr content of the melt from alternative perspectives. The recommended formulation is equivalent to a hypostoichiometry of urania, which can be expressed as UO_{2-x} , where $x \sim 0.17$. One can also perform a mass balance on the Zr inventory. For instance, the core contains 23.1 mt of Zr in Catawba. On a core-wide basis, ~ 40 percent of Zr is oxidized, so ~ 13.9 mt of Zr metal remains. About 24 percent of the initial Zr inventory resides in the cooler outer assemblies, which are not part of the degraded core debris. Assuming ~ 20 percent oxidation in the outer assemblies, about 4.4 mt of Zr will remain in the outer assemblies and the remaining 9.9 mt will be retained in the core blockage. At the upper end of the Scenario VI UO_2 distribution, ~ 2 mt of Zr will relocate to the lower plenum. This represents ~ 21 percent of the Zr inventory in the metal blockage. These perspectives on possible Zr

relocation coupled with the likelihood of complete Zr oxidation when melt relocates to the lower head and low RCS pressures, support the bounding nature of our assessments, even in scenarios where the core is not submerged in water.

The fraction of Zr oxidized envelops the range of expected behavior here also. In fact, the code calculations cited previously are more closely analogous to this scenario. This, in conjunction with the causal relations (Eqs. D.1 - D.4) developed in Section D.3.5, defines the remaining melt constituents and atmosphere compositions. We acknowledge that active containment cooling could produce conditions in the containment atmosphere with little or no steam as occurred at TMI-II and we must consider the availability of igniters. These situations will also be analyzed as Scenarios VIa and VIb in this report to better envelop the range of containment conditions.

D.3.7 Comparison of Melt Masses and Composition with Prior Work

Because many of the melt constituents are correlated, it is useful to tabulate the lower bound, best-estimate, and upper bound masses for a more direct comparison of quantifications for the current assessments with prior work. This is done in Table D.11 for Zion. The lower and upper bounds are taken at the ~1 percent probability level.

Consider first the comparison of Scenarios V and VI by composition using the prescription. The ZrO_2 values are a function of both the UO_2 mass and the fraction of Zr oxidized. For this comparison, the three UO_2 masses are used in conjunction with the best estimate for the fraction of Zr oxidized. This ensures that lower and upper bounds to the ZrO_2 values are also at the ~1 percent probability level; however, this prescription is not unique. For instance, it is possible to use the best estimate for the UO_2 mass in conjunction with the lower, best-estimate, and upper bound values for the fraction of Zr oxidized. This procedure, however, gives somewhat less ZrO_2 mass for the best-estimate and upper bound value.

At the outset, we should state that no potential comparisons are fully consistent with the plant and scenarios discussed in this report, so some compromise is necessary to make suitable comparisons. Prior summary efforts (i.e., NUREG-1150 and SASM) are therefore the most useful for comparison since these activities employed panels of knowledgeable experts who were able to synthesize the experimental and analytical information available at the time. Since the time of these summary efforts, new information in the form of best estimate SCDAP/RELAP5 calculations have become available and these new data are reflected in our current quantifications.

NUREG-1150 was the first summary assessment of core melt progression parameters and this study only addressed the core fraction that is molten and the fraction of cladding oxidized. NUREG-1150 assessments were largely based on MARCH, early MAAP, and preliminary MELPROG calculations. The distribution of the molten core fraction in Scenario VI is in good agreement with the expert elicitation results in NUREG-1150.

Table D.11 summarizes the melt mass predicted by SCDAP/RELAP5 at the time of vessel failure for the spectrum of credible pump seal leaks. Current quantifications (Scenario VI) for

Splinter Scenario Approach

oxide mass are in general agreement with the system code predictions. These code predictions are interpreted as upper bounds because SCDAP/RELAP5 assumes complete drainage of the in-core molten pool, because the molten pool must grow to the core boundary before SCDAP/RELAP5 relocates material, and because SCDAP/RELAP5 always predicted complete depressurization of the RCS. Complete depressurization delays bottom head failure and increases the time available for frozen material to remelt on the lower head. Here, we compare only to Scenario VI because Scenario V progresses with water in the core (operator action), which was not modeled in the SCDAP/RELAP5 calculations. SCDAP/RELAP5 predicts essentially no Zr in the melt while our quantifications chose to bound the amount. The amount of lower plenum steel predicted by SCDAP/RELAP5 is somewhat greater than the current assessments for Zion.

Table D.2 Description of TCE/LHS summary quantifications

| Variable | Units | Description |
|----------|----------------|--|
| tlhead | m | Thickness of RPV lower head. Used in hole ablation calculations. |
| vlp | m ³ | Volume of RPV lower plenum, which is defined as that portion of the RPV volume located below the core. Determines how much thin lower plenum steel is submerged by melt. |
| dh0 | m | Initial diameter of lower head failure site before hole ablation occurs. Used in hole ablation calculations. |
| tw0 | K | Outside surface temperature of lower head at vessel breach. Used in hole ablation calculations. |
| crmm | kg | Mass of control rod material in the melt. |
| uo2m0 | kg | Total inventory of UO ₂ in the core prior to core damage. |
| zrm0 | kg | Total mass of zircaloy in the core prior to core damage. |
| stlmlp | kg | Total mass of thin (melttable) steel in the lower plenum. |
| cohmul | ---- | Plant-specific constant in coherence ratio correlation. |
| prcs | Pa | RCS pressure at vessel breach. |
| vrsc | m ³ | RCS volume. |
| trcs | K | Average RCS gas temperature at vessel breach. |
| prcboc | Pa | Pressure in the reactor containment building at operating conditions. |
| trcboc | K | Atmosphere temperature in the reactor containment building at operating conditions. |
| prcb | Pa | Pressure in the reactor containment building at vessel breach. |
| trcb | K | Atmosphere temperature in the reactor containment building at vessel breach. |
| vrcb | m ³ | Volume of the reactor containment building. |
| vcav | m ³ | Volume of the reactor cavity. |
| fasub | ---- | Fraction of dispersed debris retained in the subcompartments (vs. bypass plus carryover to the dome). |
| fvsb | ---- | Volume of the subcompartment region that predominantly traps debris normalized by the containment volume. Set to an arbitrarily small value in this study. |
| tautoig | K | Autoignition temperature for sudden volumetric combustion of hydrogen in the dome. |
| tdeb | K | Temperature of molten debris as it is ejected from the RPV. |
| fzrel | ---- | Fraction of Zr blockage relocated to lower head. This parameter is disabled and is no longer used. The default of 0.0 should always be used. |
| fh2rcs | ---- | Fraction of all hydrogen production by Zr/steam reactions in the RPV that remains in the RCS at the time of vessel breach. |
| feject | ---- | Fraction of melt in the lower head of the RPV that is ejected into the reactor cavity. |
| fdisp | ---- | Fraction of melt ejected from RPV into the cavity that is then dispersed from the reactor cavity. |

Table D.2 Description of TCE/LHS summary quantifications (Continued)

| Variable | Units | Description |
|----------|-------|---|
| zro2ml | ---- | Multiplier on calculation of ZrO_2 . This parameter is no longer used and the default value of 1.0 should always be used. |
| stlmul | ---- | Multiplier on steel mass. This parameter is no longer used and the default value of 0.0 should always be used. |
| uo2m | kg | Piecewise linear, cumulative distribution of UO_2 mass. |
| stlmi | ---- | Piecewise linear, cumulative distribution of molten steel in addition to lower plenum steel that is submerged. Set to an arbitrarily small value in this study. |
| fzrox | ---- | Piecewise, linear, cumulative distribution of core zirconium oxidized prior to vessel breach. |
| cohdis | ---- | Distribution of the coherence ratio. |
| subdis | ---- | Distribution for fraction of dispersed melt trapped in subcompartment (fasub). The distribution is normal with a default mean of 0.0. Any other value would represent a relative bias. The relative standard deviation must also be input. Set to an arbitrarily small value in this study. |
| zdist | ---- | Distribution on the Kg-Zr per Kg- UO_2 in the melt. The distribution is normal with a default mean of 0.0. Any other value would represent a relative bias. The relative standard deviation must also be input. Set to an arbitrarily small value in this study. |
| tcedist | ---- | Distribution for modeling uncertainty in TCE pressure rise predictions. The distribution is normal with a default mean of 0.0. Any other value would represent a relative bias. The relative standard deviation must also be input. Set to an arbitrarily small value in this study. |
| pfail | ---- | Piecewise linear, cumulative distribution for the containment fragility. |

Splinter Scenario Approach

Table D.4 Model input for Scenario Va

| | Catawba 1,2 | Cook 1 | Cook 2 | McGuire 1,2 | Sequoyah 1,2 | Watts Bar 1,2 |
|--|-------------|------------|------------|-------------|--------------|---------------|
| tthead | 0.14 | 0.14 | 0.14 | 0.14 | 0.17 | 0.17 |
| vlp | 28.14 | 28.14 | 28.14 | 28.14 | 24.3 | 28.12 |
| dh0 | 0.4 | 0.4 | 0.4 | 0.4 | 0.4 | 0.4 |
| tw0 | 1000 | 1000 | 1000 | 1000 | 1000 | 1000 |
| crmm | 0 | 0 | 0 | 0 | 0 | 0 |
| uo2m0 | 101245 | 88292 | 92816 | 101245 | 101202 | 101202 |
| zrm0 | 23142 | 19783 | 18072 | 23142 | 21360 | 21360 |
| stlmlp | 10000 | 10000 | 10000 | 10000 | 10000 | 10000 |
| cohmul | 12.2 | 12.2 | 12.2 | 12.2 | 12.2 | 12.2 |
| prcs | 16.0E+6 | 16.0E+6 | 16.0E+6 | 16.0E+6 | 16.0E+6 | 16.0E+6 |
| vrcs | 347 | 366 | 366 | 363 | 344 | 352 |
| trcs | 700 | 700 | 700 | 700 | 700 | 700 |
| prcboc | 1.00E+05 | 1.00E+05 | 1.00E+05 | 1.00E+05 | 1.00E+05 | 1.00E+05 |
| trcboc | 316 | 316 | 316 | 316 | 316 | 316 |
| prcb | 1.80E+05 | 1.80E+05 | 1.80E+05 | 1.80E+05 | 1.80E+05 | 1.80E+05 |
| trcb | 380 | 380 | 380 | 380 | 380 | 380 |
| vrcb | 3.396E+04 | 3.679E+04 | 3.68E+04 | 3.51E+04 | 3.37E+04 | 3.37E+04 |
| vcav | 429 | 474 | 474 | 336 | 420 | 522 |
| fasub | 0.99 | 0.99 | 0.99 | 0.99 | 0.99 | 0.99 |
| fvsb | 0.25 | 0.25 | 0.25 | 0.25 | 0.25 | 0.25 |
| tautoig | 950 | 950 | 950 | 950 | 950 | 950 |
| tdeb | 2800 | 2800 | 2800 | 2800 | 2800 | 2800 |
| fzrrel | 0 | 0 | 0 | 0 | 0 | 0 |
| fh2rcs | 0 | 0 | 0 | 0 | 0 | 0 |
| fejec | 1 | 1 | 1 | 1 | 1 | 1 |
| fdisp | 0.93 | 0.93 | 0.93 | 0.93 | 0.93 | 0.93 |
| zro2ml | 1 | 1 | 1 | 1 | 1 | 1 |
| stlmul | 0 | 0 | 0 | 0 | 0 | 0 |
| uo2m | Tbl 5.9 | Tbl 5.9 | Tbl 5.9 | Tbl 5.9 | Tbl 5.9 | Tbl 5.9 |
| stlmi | 0 | 0 | 0 | 0 | 0 | 0 |
| fzrox | Figure 5.5 | Figure 5.5 | Figure 5.5 | Figure 5.5 | Figure 5.5 | Figure 5.5 |
| cohdist | 0.18 | 0.18 | 0.18 | 0.18 | 0.18 | 0.18 |
| subdis | 0,1.0E-3 | 0,1.0E-3 | 0,1.0E-3 | 0,1.0E-3 | 0,1.0E-3 | 0,1.0E-3 |
| zdist | 0,1.0E-3 | 0,1.0E-3 | 0,1.0E-3 | 0,1.0E-3 | 0,1.0E-3 | 0,1.0E-3 |
| tcedist | 0,1.0E-3 | 0,1.0E-3 | 0,1.0E-3 | 0,1.0E-3 | 0,1.0E-3 | 0,1.0E-3 |
| pfail | N/CR-6338 | N/CR-6338 | N/CR-6338 | N/CR-6338 | N/CR-6338 | N/CR-6338 |
| Note: hydrogen concentration limited to a maximum of 5.5 percent | | | | | | |

Table D.5 Model input for Scenario Vb

| | Catawba 1,2 | Cook 1 | Cook 2 | McGuire 1,2 | Sequoyah 1,2 | Watts Bar 1,2 |
|---------|-------------|------------|------------|-------------|--------------|---------------|
| tthead | 0.14 | 0.14 | 0.14 | 0.14 | 0.17 | 0.17 |
| vlp | 28.14 | 28.14 | 28.14 | 28.14 | 24.3 | 28.12 |
| dh0 | 0.4 | 0.4 | 0.4 | 0.4 | 0.4 | 0.4 |
| tw0 | 1000 | 1000 | 1000 | 1000 | 1000 | 1000 |
| crmm | 0 | 0 | 0 | 0 | 0 | 0 |
| uo2m0 | 101245 | 88292 | 92816 | 101245 | 101202 | 101202 |
| zrm0 | 23142 | 19783 | 18072 | 23142 | 21360 | 21360 |
| stlmlp | 10000 | 10000 | 10000 | 10000 | 10000 | 10000 |
| cohmul | 12.2 | 12.2 | 12.2 | 12.2 | 12.2 | 12.2 |
| prcs | 16.0E+6 | 16.0E+6 | 16.0E+6 | 16.0E+6 | 16.0E+6 | 16.0E+6 |
| vrsc | 347 | 366 | 366 | 363 | 344 | 352 |
| trcs | 700 | 700 | 700 | 700 | 700 | 700 |
| prcboc | 1.00E+05 | 1.00E+05 | 1.00E+05 | 1.00E+05 | 1.00E+05 | 1.00E+05 |
| trcboc | 316 | 316 | 316 | 316 | 316 | 316 |
| prcb | 1.10E+05 | 1.10E+05 | 1.10E+05 | 1.10E+05 | 1.10E+05 | 1.10E+05 |
| trcb | 320 | 320 | 320 | 320 | 320 | 320 |
| vrcb | 3.396E+04 | 3.679E+04 | 3.68E+04 | 3.51E+04 | 3.37E+04 | 3.37E+04 |
| vcav | 429 | 474 | 474 | 336 | 420 | 522 |
| fasub | 0.99 | 0.99 | 0.99 | 0.99 | 0.99 | 0.99 |
| fvsb | 0.25 | 0.25 | 0.25 | 0.25 | 0.25 | 0.25 |
| tautoig | 950 | 950 | 950 | 950 | 950 | 950 |
| tdeb | 2800 | 2800 | 2800 | 2800 | 2800 | 2800 |
| fzrrel | 0 | 0 | 0 | 0 | 0 | 0 |
| fh2rcs | 0 | 0 | 0 | 0 | 0 | 0 |
| fejec | 1 | 1 | 1 | 1 | 1 | 1 |
| fdisp | 0.93 | 0.93 | 0.93 | 0.93 | 0.93 | 0.93 |
| zro2ml | 1 | 1 | 1 | 1 | 1 | 1 |
| stlmul | 0 | 0 | 0 | 0 | 0 | 0 |
| uo2m | Tbl 5.9 | Tbl 5.9 | Tbl 5.9 | Tbl 5.9 | Tbl 5.9 | Tbl 5.9 |
| stlmi | 0 | 0 | 0 | 0 | 0 | 0 |
| fzrox | Figure 5.5 | Figure 5.5 | Figure 5.5 | Figure 5.5 | Figure 5.5 | Figure 5.5 |
| cohdist | 0.18 | 0.18 | 0.18 | 0.18 | 0.18 | 0.18 |
| subdis | 0,1.0E-3 | 0,1.0E-3 | 0,1.0E-3 | 0,1.0E-3 | 0,1.0E-3 | 0,1.0E-3 |
| zdist | 0,1.0E-3 | 0,1.0E-3 | 0,1.0E-3 | 0,1.0E-3 | 0,1.0E-3 | 0,1.0E-3 |
| tcedist | 0,1.0E-3 | 0,1.0E-3 | 0,1.0E-3 | 0,1.0E-3 | 0,1.0E-3 | 0,1.0E-3 |
| pfail | N/CR-6338 | N/CR-6338 | N/CR-6338 | N/CR-6338 | N/CR-6338 | N/CR-6338 |

Splinter Scenario Approach

Table D.6 Model input for Scenario VI

| | Catawba 1,2 | Cook 1 | Cook 2 | McGuire 1,2 | Sequoyah 1,2 | Watts Bar 1,2 |
|--|-------------|------------|------------|-------------|--------------|---------------|
| tlhead | 0.14 | 0.14 | 0.14 | 0.14 | 0.17 | 0.17 |
| vlp | 28.14 | 28.14 | 28.14 | 28.14 | 24.3 | 28.12 |
| dh0 | 0.4 | 0.4 | 0.4 | 0.4 | 0.4 | 0.4 |
| tw0 | 1000 | 1000 | 1000 | 1000 | 1000 | 1000 |
| crmm | 2280 | 2280 | 2280 | 2280 | 2280 | 2280 |
| uo2m0 | 101245 | 88292 | 92816 | 101245 | 101202 | 101202 |
| zrm0 | 23142 | 19783 | 18072 | 23142 | 21360 | 21360 |
| stlmlp | 10000 | 10000 | 10000 | 10000 | 10000 | 10000 |
| cohmul | 12.2 | 12.2 | 12.2 | 12.2 | 12.2 | 12.2 |
| prcs | 8.0E+6 | 8.0E+6 | 8.0E+6 | 8.0E+6 | 8.0E+6 | 8.0E+6 |
| vrcs | 347 | 366 | 366 | 363 | 344 | 352 |
| trcs | 1000 | 1000 | 1000 | 1000 | 1000 | 1000 |
| prcboc | 1.00E+05 | 1.00E+05 | 1.00E+05 | 1.00E+05 | 1.00E+05 | 1.00E+05 |
| trcboc | 316 | 316 | 316 | 316 | 316 | 316 |
| prcb | 1.80E+05 | 1.80E+05 | 1.80E+05 | 1.80E+05 | 1.80E+05 | 1.80E+05 |
| trcb | 380 | 380 | 380 | 380 | 380 | 380 |
| vrcb | 3.396E+04 | 3.679E+04 | 3.68E+04 | 3.51E+04 | 3.37E+04 | 3.37E+04 |
| vcav | 429 | 474 | 474 | 336 | 420 | 522 |
| fasub | 0.99 | 0.99 | 0.99 | 0.99 | 0.99 | 0.99 |
| fvsb | 0.25 | 0.25 | 0.25 | 0.25 | 0.25 | 0.25 |
| tautoig | 950 | 950 | 950 | 950 | 950 | 950 |
| tdeb | 2800 | 2800 | 2800 | 2800 | 2800 | 2800 |
| fzrrel | 0 | 0 | 0 | 0 | 0 | 0 |
| fh2rcs | 0 | 0 | 0 | 0 | 0 | 0 |
| fejec | 1 | 1 | 1 | 1 | 1 | 1 |
| fdisp | 0.93 | 0.93 | 0.93 | 0.93 | 0.93 | 0.93 |
| zro2ml | 1 | 1 | 1 | 1 | 1 | 1 |
| stlmul | 0 | 0 | 0 | 0 | 0 | 0 |
| uo2m | Tbl 5.9 | Tbl 5.9 | Tbl 5.9 | Tbl 5.9 | Tbl 5.9 | Tbl 5.9 |
| stlmi | 0 | 0 | 0 | 0 | 0 | 0 |
| fzrox | Figure 5.5 | Figure 5.5 | Figure 5.5 | Figure 5.5 | Figure 5.5 | Figure 5.5 |
| cohdist | 0.18 | 0.18 | 0.18 | 0.18 | 0.18 | 0.18 |
| subdis | 0,1.0E-3 | 0,1.0E-3 | 0,1.0E-3 | 0,1.0E-3 | 0,1.0E-3 | 0,1.0E-3 |
| zdist | 0,1.0E-3 | 0,1.0E-3 | 0,1.0E-3 | 0,1.0E-3 | 0,1.0E-3 | 0,1.0E-3 |
| tcedist | 0,1.0E-3 | 0,1.0E-3 | 0,1.0E-3 | 0,1.0E-3 | 0,1.0E-3 | 0,1.0E-3 |
| pfail | N/CR-6338 | N/CR-6338 | N/CR-6338 | N/CR-6338 | N/CR-6338 | N/CR-6338 |
| Note: hydrogen concentration limited to a maximum of 5.5 percent | | | | | | |

Table D.7 Model input for Scenario VIa

| | Catawba 1,2 | Cook 1 | Cook 2 | McGuire 1,2 | Sequoyah 1,2 | Watts Bar 1,2 |
|---------|-------------|------------|------------|-------------|--------------|---------------|
| tthead | 0.14 | 0.14 | 0.14 | 0.14 | 0.17 | 0.17 |
| vlp | 28.14 | 28.14 | 28.14 | 28.14 | 24.3 | 28.12 |
| dh0 | 0.4 | 0.4 | 0.4 | 0.4 | 0.4 | 0.4 |
| tw0 | 1000 | 1000 | 1000 | 1000 | 1000 | 1000 |
| crmm | 2280 | 2280 | 2280 | 2280 | 2280 | 2280 |
| uo2m0 | 101245 | 88292 | 92816 | 101245 | 101202 | 101202 |
| zrm0 | 23142 | 19783 | 18072 | 23142 | 21360 | 21360 |
| stlmlp | 10000 | 10000 | 10000 | 10000 | 10000 | 10000 |
| cohmul | 12.2 | 12.2 | 12.2 | 12.2 | 12.2 | 12.2 |
| prcs | 8.0E+6 | 8.0E+6 | 8.0E+6 | 8.0E+6 | 8.0E+6 | 8.0E+6 |
| vrsc | 347 | 366 | 366 | 363 | 344 | 352 |
| trcs | 1000 | 1000 | 1000 | 1000 | 1000 | 1000 |
| prcboc | 1.00E+05 | 1.00E+05 | 1.00E+05 | 1.00E+05 | 1.00E+05 | 1.00E+05 |
| trcboc | 316 | 316 | 316 | 316 | 316 | 316 |
| prcb | 1.10E+05 | 1.10E+05 | 1.10E+05 | 1.10E+05 | 1.10E+05 | 1.10E+05 |
| trcb | 320 | 320 | 320 | 320 | 320 | 320 |
| vrcb | 3.396E+04 | 3.679E+04 | 3.68E+04 | 3.51E+04 | 3.37E+04 | 3.37E+04 |
| vcav | 429 | 474 | 474 | 336 | 420 | 522 |
| fasub | 0.99 | 0.99 | 0.99 | 0.99 | 0.99 | 0.99 |
| fvsb | 0.25 | 0.25 | 0.25 | 0.25 | 0.25 | 0.25 |
| tautoig | 950 | 950 | 950 | 950 | 950 | 950 |
| tdeb | 2800 | 2800 | 2800 | 2800 | 2800 | 2800 |
| fzrel | 0 | 0 | 0 | 0 | 0 | 0 |
| fh2rcs | 0 | 0 | 0 | 0 | 0 | 0 |
| fejec | 1 | 1 | 1 | 1 | 1 | 1 |
| fdisp | 0.93 | 0.93 | 0.93 | 0.93 | 0.93 | 0.93 |
| zro2ml | 1 | 1 | 1 | 1 | 1 | 1 |
| stlmul | 0 | 0 | 0 | 0 | 0 | 0 |
| uo2m | Tbl 5.9 | Tbl 5.9 | Tbl 5.9 | Tbl 5.9 | Tbl 5.9 | Tbl 5.9 |
| stlmi | 0 | 0 | 0 | 0 | 0 | 0 |
| fzrox | Figure 5.5 | Figure 5.5 | Figure 5.5 | Figure 5.5 | Figure 5.5 | Figure 5.5 |
| cohdist | 0.18 | 0.18 | 0.18 | 0.18 | 0.18 | 0.18 |
| subdis | 0,1.0E-3 | 0,1.0E-3 | 0,1.0E-3 | 0,1.0E-3 | 0,1.0E-3 | 0,1.0E-3 |
| zdist | 0,1.0E-3 | 0,1.0E-3 | 0,1.0E-3 | 0,1.0E-3 | 0,1.0E-3 | 0,1.0E-3 |
| tcedist | 0,1.0E-3 | 0,1.0E-3 | 0,1.0E-3 | 0,1.0E-3 | 0,1.0E-3 | 0,1.0E-3 |
| pfail | N/CR-6338 | N/CR-6338 | N/CR-6338 | N/CR-6338 | N/CR-6338 | N/CR-6338 |
| | | | | | | |
| | | | | | | |

Note: hydrogen concentration limited to a maximum of 5.5 percent

Table D.8 Model input for Scenario VIb

| | Catawba 1,2 | Cook 1 | Cook 2 | McGuire 1,2 | Sequoyah 1,2 | Watts Bar 1,2 |
|---------|-------------|------------|------------|-------------|--------------|---------------|
| tlhead | 0.14 | 0.14 | 0.14 | 0.14 | 0.17 | 0.17 |
| vlp | 28.14 | 28.14 | 28.14 | 28.14 | 24.3 | 28.12 |
| dh0 | 0.4 | 0.4 | 0.4 | 0.4 | 0.4 | 0.4 |
| tw0 | 1000 | 1000 | 1000 | 1000 | 1000 | 1000 |
| crmm | 2280 | 2280 | 2280 | 2280 | 2280 | 2280 |
| uo2m0 | 101245 | 88292 | 92816 | 101245 | 101202 | 101202 |
| zrm0 | 23142 | 19783 | 18072 | 23142 | 21360 | 21360 |
| stlmlp | 10000 | 10000 | 10000 | 10000 | 10000 | 10000 |
| cohmul | 12.2 | 12.2 | 12.2 | 12.2 | 12.2 | 12.2 |
| prcs | 8.0E+6 | 8.0E+6 | 8.0E+6 | 8.0E+6 | 8.0E+6 | 8.0E+6 |
| vrsc | 347 | 366 | 366 | 363 | 344 | 352 |
| trcs | 1000 | 1000 | 1000 | 1000 | 1000 | 1000 |
| prcboc | 1.00E+05 | 1.00E+05 | 1.00E+05 | 1.00E+05 | 1.00E+05 | 1.00E+05 |
| trcboc | 316 | 316 | 316 | 316 | 316 | 316 |
| prcb | 1.10E+05 | 1.10E+05 | 1.10E+05 | 1.10E+05 | 1.10E+05 | 1.10E+05 |
| trcb | 320 | 320 | 320 | 320 | 320 | 320 |
| vrcb | 3.396E+04 | 3.679E+04 | 3.68E+04 | 3.51E+04 | 3.37E+04 | 3.37E+04 |
| vcav | 429 | 474 | 474 | 336 | 420 | 522 |
| fasub | 0.99 | 0.99 | 0.99 | 0.99 | 0.99 | 0.99 |
| fvsb | 0.25 | 0.25 | 0.25 | 0.25 | 0.25 | 0.25 |
| tautoig | 950 | 950 | 950 | 950 | 950 | 950 |
| tdeb | 2800 | 2800 | 2800 | 2800 | 2800 | 2800 |
| fzrrel | 0 | 0 | 0 | 0 | 0 | 0 |
| fh2rcs | 0 | 0 | 0 | 0 | 0 | 0 |
| fejec | 1 | 1 | 1 | 1 | 1 | 1 |
| fdisp | 0.93 | 0.93 | 0.93 | 0.93 | 0.93 | 0.93 |
| zro2ml | 1 | 1 | 1 | 1 | 1 | 1 |
| stlmul | 0 | 0 | 0 | 0 | 0 | 0 |
| uo2m | Tbl 5.9 | Tbl 5.9 | Tbl 5.9 | Tbl 5.9 | Tbl 5.9 | Tbl 5.9 |
| stlmi | 0 | 0 | 0 | 0 | 0 | 0 |
| fzrox | Figure 5.5 | Figure 5.5 | Figure 5.5 | Figure 5.5 | Figure 5.5 | Figure 5.5 |
| cohdist | 0.18 | 0.18 | 0.18 | 0.18 | 0.18 | 0.18 |
| subdis | 0,1.0E-3 | 0,1.0E-3 | 0,1.0E-3 | 0,1.0E-3 | 0,1.0E-3 | 0,1.0E-3 |
| zdist | 0,1.0E-3 | 0,1.0E-3 | 0,1.0E-3 | 0,1.0E-3 | 0,1.0E-3 | 0,1.0E-3 |
| tcdist | 0,1.0E-3 | 0,1.0E-3 | 0,1.0E-3 | 0,1.0E-3 | 0,1.0E-3 | 0,1.0E-3 |
| pfail | N/CR-6338 | N/CR-6338 | N/CR-6338 | N/CR-6338 | N/CR-6338 | N/CR-6338 |

Table D.9 Distribution of molten UO₂ mass at the time of vessel breach for Scenario V, and Va, and Vb

| UO ₂ Mass (mt) Range | Discrete Probability | UO ₂ Mass (mt) | Cumulative Probability |
|--|-------------------------|---------------------------|---------------------------|
| W 4-Loop Plants (3.37m Core Dia.) | | | |
| 0 - 10.0 | 0.10 | 0 | 0 |
| 10.0 - 30.0 | 0.79 | 10.0 | 0.10 |
| 30.0 - 40.0 | 0.10 | 30.0 | 0.89 |
| 40.0 - 50.0 | 0.01 | 40.0 | 0.99 |
| | | 50.0 | 1.00 |

Table D.10 Distribution of molten UO₂ mass at the time of vessel breach for Scenarios VI, VIa, and VIb

| UO ₂ Mass (mt) Range | Discrete Probability | UO ₂ Mass (mt) | Cumulative Probability |
|--|-------------------------|---------------------------|---------------------------|
| W 4-Loop Plants (3.37m Core Dia.) | | | |
| 0 - 5.0 | 0.01 | 0 | 0 |
| 5.0 - 20.0 | 0.10 | 5.0 | 0.01 |
| 20.0 - 40.0 | 0.78 | 20.0 | 0.11 |
| 40.0 - 55.0 | 0.10 | 40.0 | 0.89 |
| 55.0 - 70.0 | 0.01 | 55.0 | 0.99 |
| | | 70.0 | 1.00 |

Table D.11 Comparison with prior work for Zion

| Parameter | Scenario V | Scenario VI | NUREG-1150 | SCDAP/RELAP5 NUREG/CR-6075, Sup. 1 Case 1-2-3 |
|--|-----------------|-----------------|----------------|---|
| UO ₂ mass (mt) | 0/20/50 | 0/30/70 | | 43.3-52.8-44.4 |
| ZrO ₂ mass (mt) | 0/2.2/5.5 | 0/3.3/7.7 | | 11.2-13.4-12.3 |
| Zr mass (mt) | 0/0.6/1.5 | 0/0.9/2.0 | | 0-0.5-0 |
| Steel mass (mt) | 0.3/1.1/2.3 | 0.3/1.8/4.4 | | 4.8-8.2-5.0 |
| CRM mass (mt) | 0 | 0 | | 0-3.3-2.2 |
| Total melt mass (mt) | 0.3/23.9/59.3 | 0.3/36.0/84.1 | | 59.3-78.2-63.9 |
| Core fraction molten | 0.002/0.19/0.47 | 0.002/0.29/0.67 | 0/0.28/0.60 | 0.47-0.63-0.51 |
| Fraction Zr oxidized | 0.15/0.40/0.65 | 0.15/0.40/0.65 | 0.08/0.32/0.76 | 0.53-0.59-0.48 |
| Case 1 = 0 gpm/pump (minimum); Case 2 = 250 gpm/pump (best estimate); Case 3 = 480 gpm/pump (maximum). | | | | |

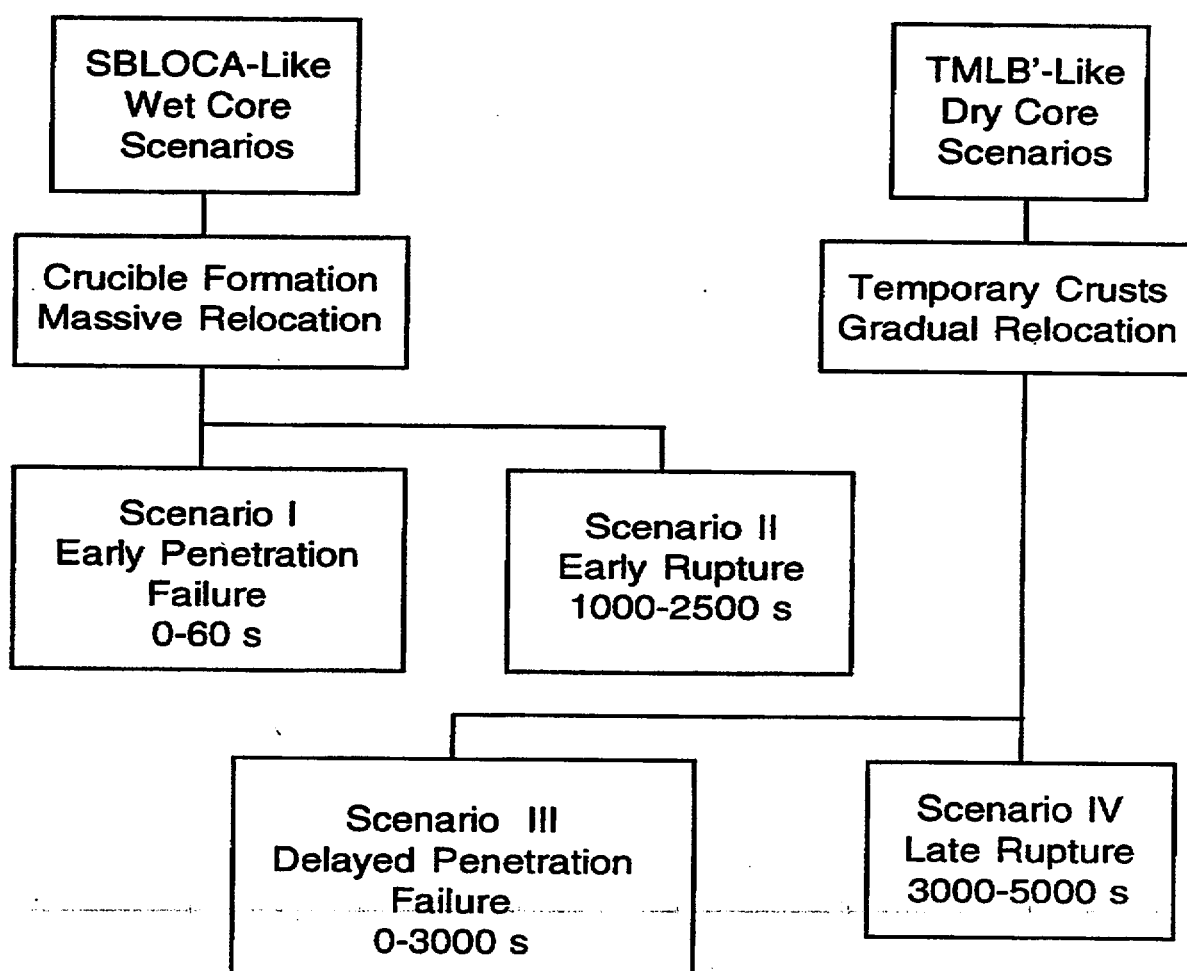


Figure D.2. Splinter DCH scenarios used in NUREG/CR-6075.

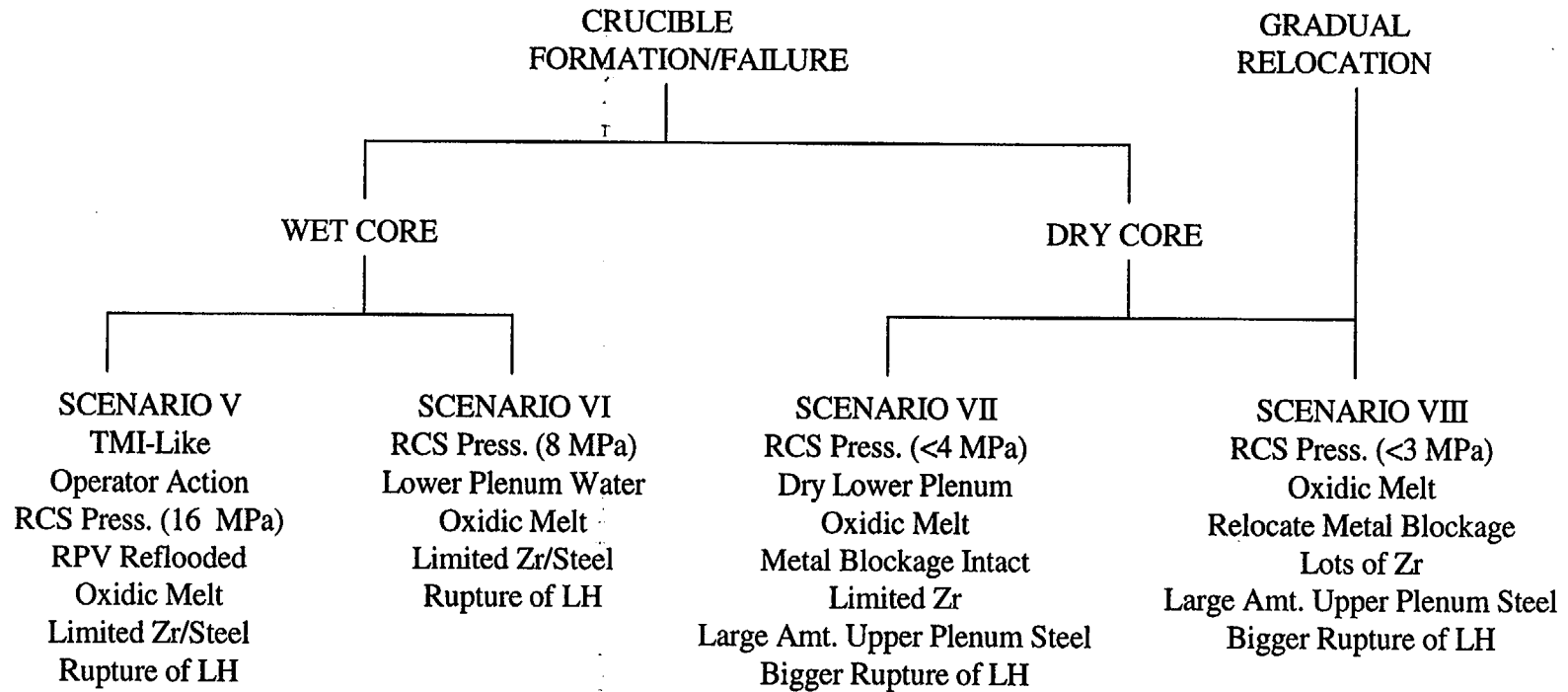


Figure D.3. Splinter DCH scenarios reflecting working group recommendations.

Splinter Scenario Approach

| Core Melt Progression | Igniter/ARF Available | Cavity Flooded | Ice Condenser Effective | |
|-----------------------|-----------------------|----------------|-------------------------|---|
| Scenario V | On/Off | Y | No DCH | |
| | | N | | Y |
| | On/On | Y | No DCH | |
| | | N | | Y |
| | Off/On | Y | No DCH | |
| | | N | | Y |
| | | | | Scn. V; low H ₂ high steam |
| | | | | Scn. Va; low H ₂ low steam |
| | | | | Scn. Vb; high H ₂ low steam |
| Scenario VI | On/Off | Y | No DCH | |
| | | N | | Y |
| | On/On | Y | No DCH | |
| | | N | | Y |
| | Off/On | Y | No DCH | |
| | | N | | Y |
| | | | | Scn. VI; low H ₂ , high steam |
| | | | | Scn. VIa; low H ₂ low steam |
| | | | | Scn. VIb; high H ₂ low steam |

Figure D.4. Further definition of splinter scenarios for ice condenser plants.

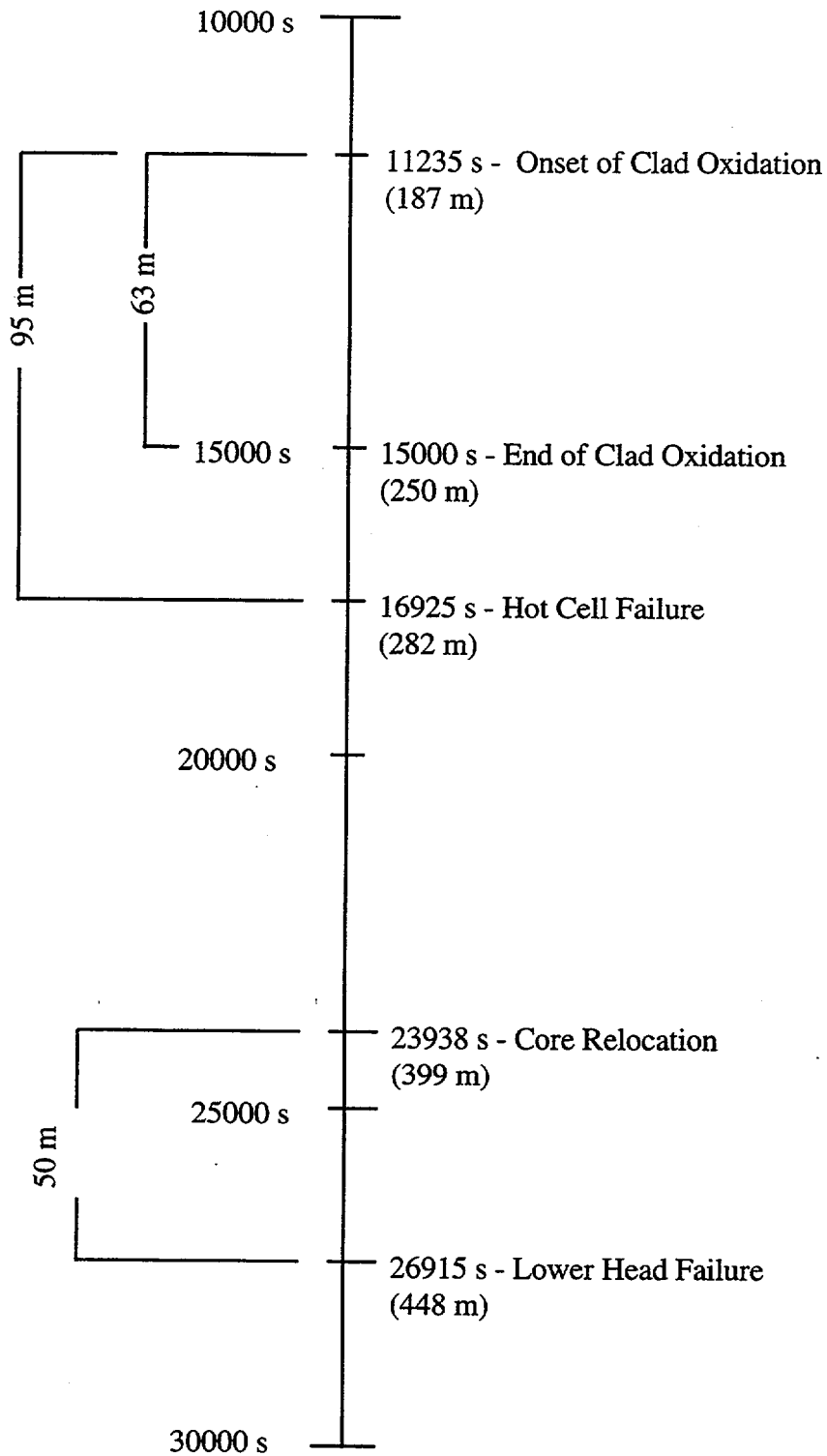


Figure D.5. Timing of key core melt progression events for a SBO with a 250 gpm/pump leak.

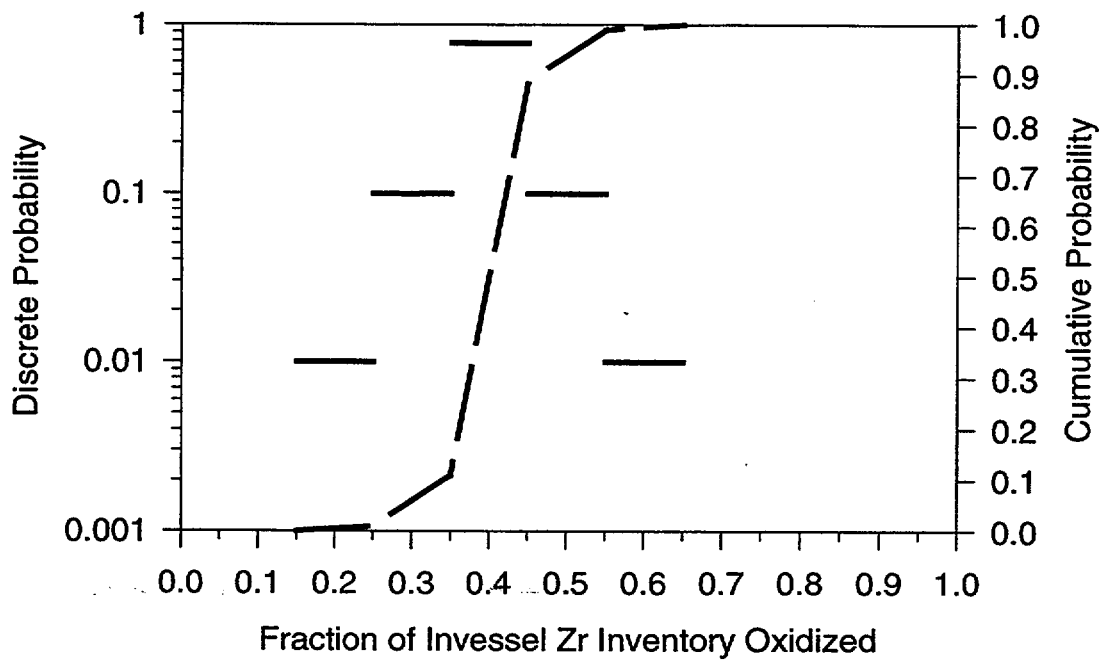


Figure D.6. Distribution for fraction of Zr oxidized (core-wide) in Scenarios V and VI.

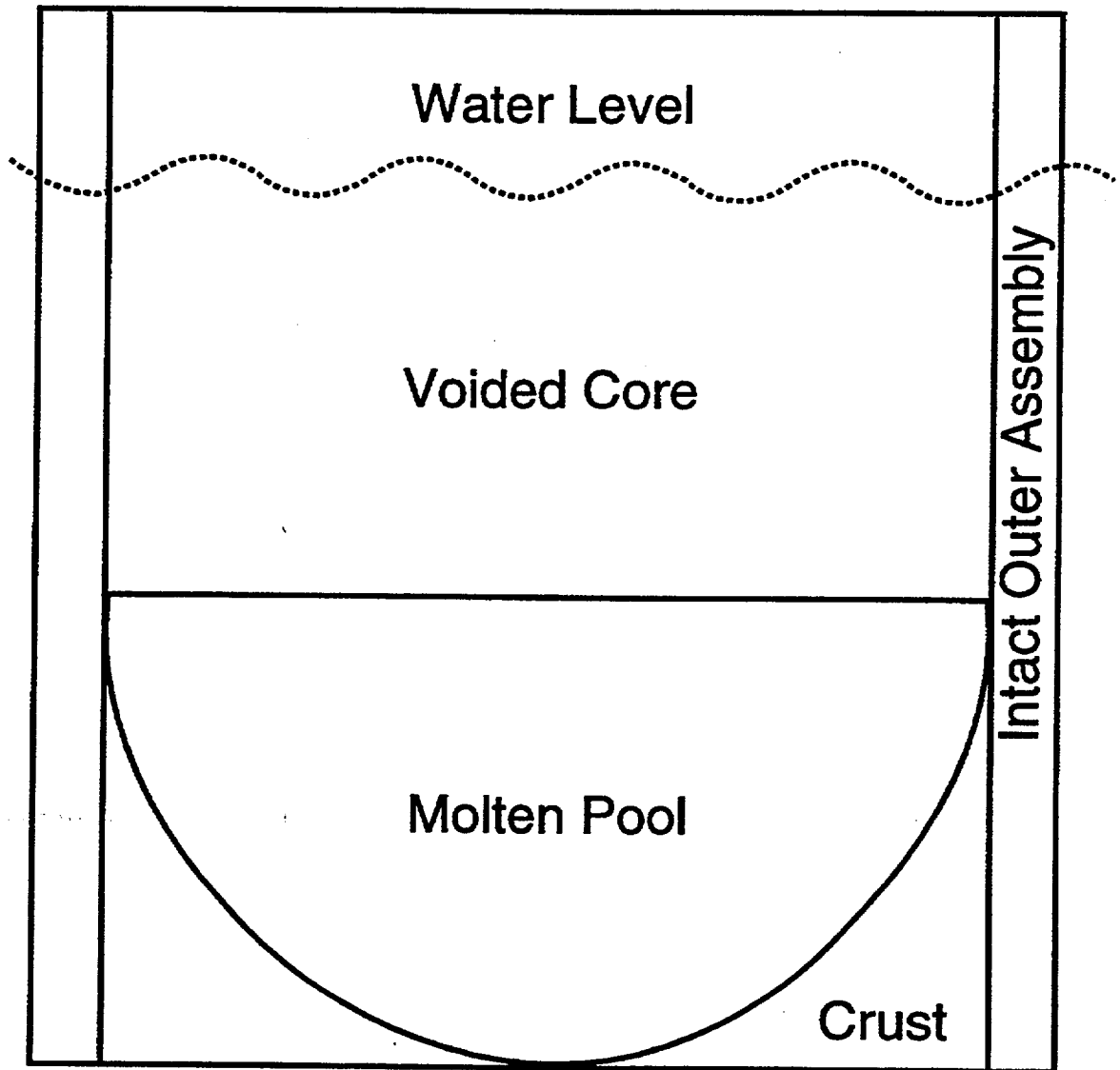


Figure D.7. Crucible formation in a flooded RPV - Scenarios V, Va, and Vb.

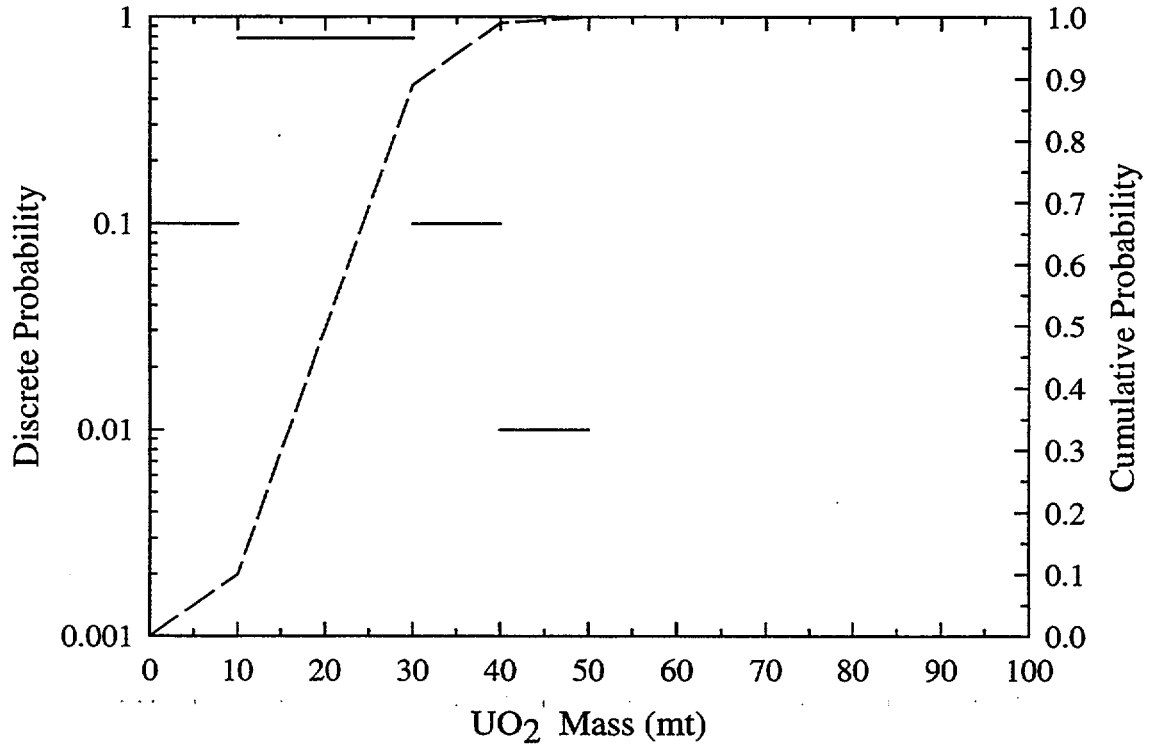


Figure D.8. Distribution of molten UO₂ in the lower plenum at the time of vessel rupture for Scenarios V, Va, and Vb.

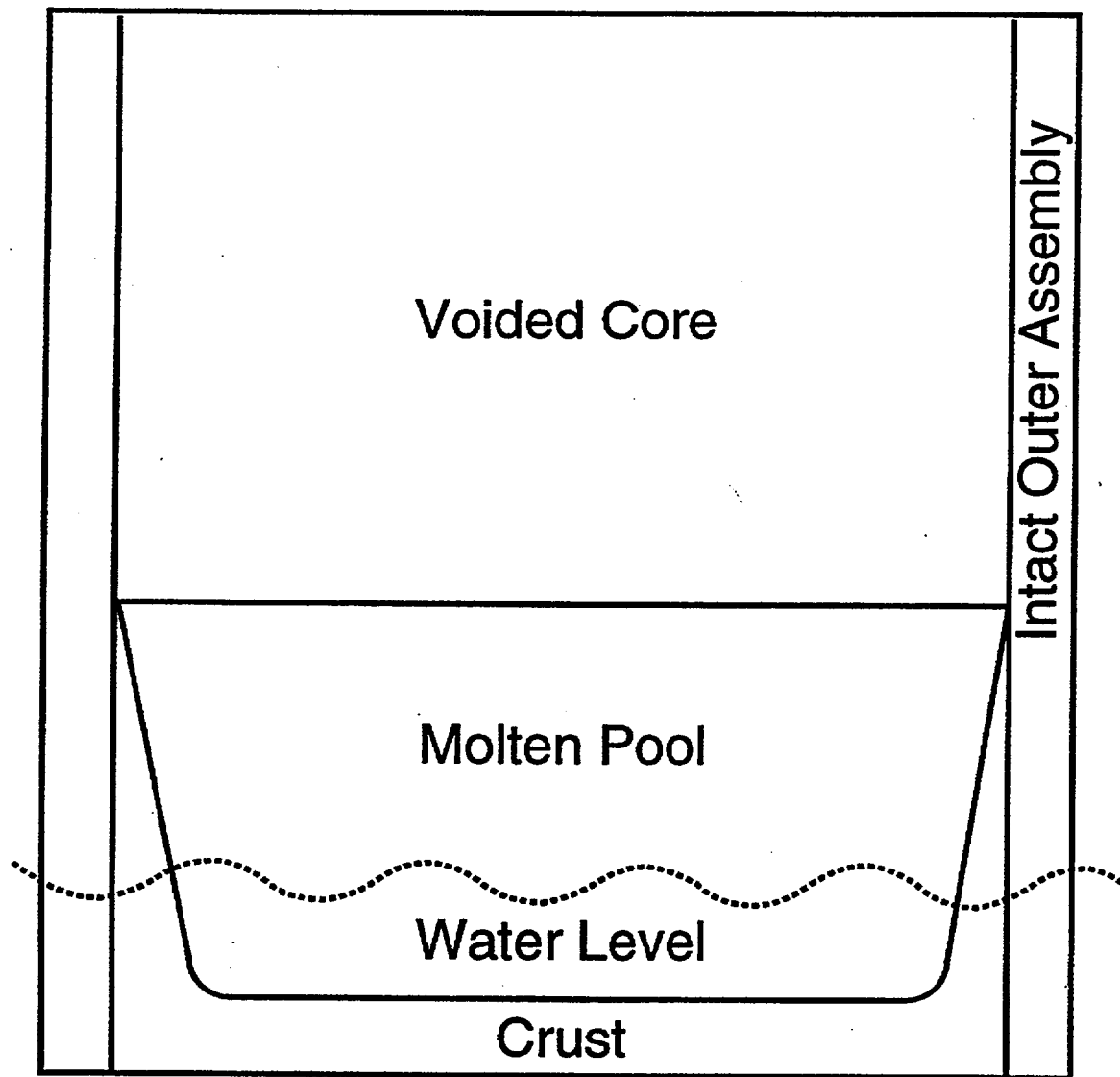


Figure D.9. Crucible formation in wet core scenarios with partial operator intervention – Scenarios VI, VIa, and VIb.

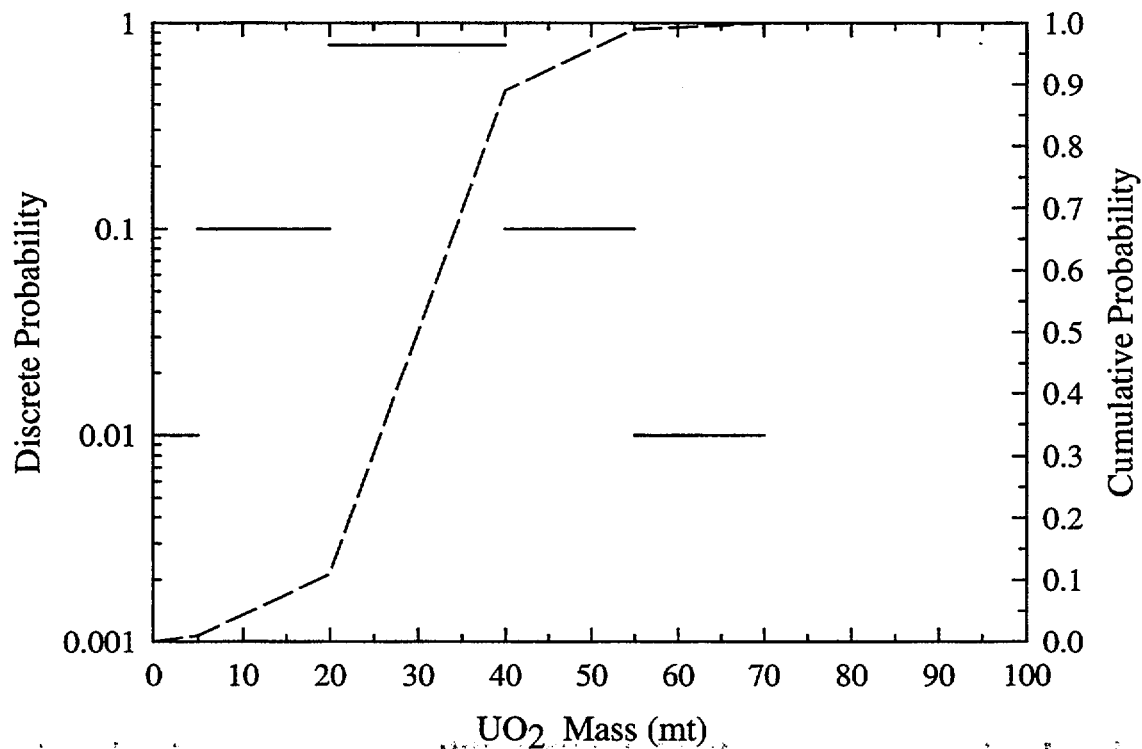


Figure D.10. Distribution for molten UO₂ in the lower plenum at the time of vessel rupture for Scenarios VI, VIa, and VIb.

D.4 Quantification of the DCH Phenomena

The quantification of the DCH phenomenon is carried out by means of a causal relation (CR1) for the containment load. CR1 is fulfilled here by the two-cell equilibrium model, which is developed in Appendix E of NUREG/CR-6075 (Pilch et al., 1994a). Refinements to the hydrogen combustion models are documented in Appendix E of NUREG/CR-6075, Supplement 1 (Pilch et al., 1994b). In the TCE model, the containment pressurization can be written in terms of the various energy sources (blowdown, latent and sensible heat of debris, oxidation of metallic debris constituents, and hydrogen combustion) that can contribute to DCH,

$$\frac{\Delta P}{P_c^0} = \eta \frac{\sum \Delta E_i}{U^0(1 + \psi)}, \quad (\text{D.6})$$

where η is an efficiency of containment pressurization due to the combined processes of blowdown, heating of the atmosphere, and hydrogen combustion. The efficiency accounts for compartmentalized geometry of the containment and accounts for mitigation that is due to the noncoherence of debris dispersal and blowdown processes. The TCE model has been validated against the extensive database that is summarized in Table D.12. The TCE model represents the dominant processes contributing to DCH loads using a fast running code that meets the needs of the issue resolution effort; there is no claim that it captures every detail of DCH phenomenology.

Figure D.11 compares model predictions with the relevant database for plants where most debris is sourced into subcompartments below the operation deck. Such a database is largely relevant to Westinghouse plants with large dry or subatmospheric containments. There is no database directly relevant to DCH in ice condenser containments, and the TCE model does not represent the ice beds in our current assessments. Consequently, we treat ice condenser plants as if they are “small dry” containments. Section D.3.5 concludes that this approach is bounding, but not excessively so in all cases.

Point comparisons of TCE with CONTAIN have been performed for conditions near the upper bound of the distributions for each of the scenarios. The results are summarized in Table D.13. TCE always predicts loads greater than CONTAIN. It should be noted that TCE burns all DCH produced hydrogen while CONTAIN does not. In CONTAIN, most of the DCH produced hydrogen resided in the oxygen starved lower cell (at the time of peak pressure) or was steam inerted as it was pushed into the oxygen-bearing upper dome. These differences in modeling approaches can lead to substantial differences (~0.2 MPa) in loads predictions in some scenarios. However, we note that the contain calculations performed for comparison with TCE were restricted in a way believed to be nonconservative by the contain modeler, as noted in Appendix B. Given the sensitivity of ice condenser plants to DCH, it may be fruitful to create a response surface to CONTAIN predictions and use the response surface instead of TCE in the Monte Carlo framework. This is outside the scope of the current efforts.

NUREG/CR-6075 (Pilch et al., 1994a) identified the need to catalog the extent of cavity flooding prior to vessel breach. This is accomplished in Section C.2.3, where assessments are taken from the IPEs under two limiting cases: with/without injection of the refueling water

Splinter Scenario Approach

storage tank (RWST) into the containment. The assessments are plant-specific: cavities are dry if the RWST is not injected and are flooded if the RWST discharges fully and 20-80 percent of the ice is melted. A deeply flooded cavity usually, but not always, means that the lower head of the RPV is at least partially submerged in water increasing the potential for in-vessel retention. We endorse NUREG-1150 judgments that a deeply flooded cavity will not lead to significant DCH loads.

Figure D.12 explores the potential impact of cavity water on containment loads in plants with large dry or subatmospheric containments. Three experiments with cavity water from the DCH database have counterparts with essentially dry cavities (thin films of condensate water was present in the SNL tests): FAI/DCH-2, 3 (Henry et al., 1991), SNL/WC-1,2 (Allen et al., 1992), and SNL/IET-7,8B (Allen et al., 1993). The WC tests were conducted in an open vessel, while the FAI/DCH tests and the SNL/IET tests were conducted in a Zion-like compartmentalized geometry. We note that only SNL/IET-8B had a reactive atmosphere. The data suggest that DCH loads are insensitive to water mass. In the IET-8B experiment, the containment atmosphere exceeded the saturation temperature only slightly indicating that DCH energies (including hydrogen combustion) went into vaporizing water, so that most of the resulting pressurization came from added moles.

Validation of models predicting the impact of cavity water on DCH (even for large dry or subatmospheric containments) has been problematic. Boyack et al. (1995) performed an NRC sponsored peer review of the CONTAIN code. With regard to the modeling of possible debris/water interactions in CONTAIN, Boyack et al. concluded that energetic FCIs are poorly understood and are not modeled. Less energetic interactions are better understood but there are no features in the code to predict processes such as water slug ejection from the cavity. Heat transfer and oxidation of the debris can be represented parametrically but without capturing the essential features of the physical processes. Within these limitations, it is typical to parametrically treat the interactions of the user-defined amount of water with debris. Parametric calculations of this sort (e.g., curve a in Figure D.12) suggests that water has the potential to either mitigate or augment DCH loads. Simple parametric models for cavity phenomena with ejection of a water slug are incorporated in the CORDE code, but more detailed modeling would be required to determine the appropriate values for the parameters in such a model. Figure D.12 shows, however, that initial attempts to model ejection of water slugs eliminates any potential sensitivity of DCH loads to cavity water in a PWR with a large dry containment.

Ice condenser cavities are all excavated and are not vulnerable to damage from potential steam explosions. For large dry containments, the IET-8 experiment (Allen et al., 1994) showed that DCH loads were predominately from vaporized water and that the load was comparable or less than cases without the cavity water. In an ice condenser plant, the impact of cavity water is expected to be further reduced in those scenarios (Figure D.4) with effective ice beds because the additional steam will be quenched in the ice beds.

The working group discussions from NUREG/CR-6075, Supplement 1 (Appendix A in Pilch et al., 1994b) defined two new scenarios (V and VI) which involve significant quantities (~10-75 mt) of water that would be coejected with the melt into the reactor cavity. The working group (Appendix A in Pilch et al., 1994b) expressed an opinion that water in the primary system at

vessel breach is expected to mitigate the impact of DCH. RPV water (unlike cavity water) will partially flash to steam during isentropic blowdown. The contribution to containment pressure from this mechanism is less than ~0.075 MPa for ~75 mt of water in Zion if flashing and DCH loads are simply additive. These assessments were performed without the benefit of experiment insight. There are substantial uncertainties concerning the amounts and enthalpies of RPV water present at vessel breach, and additional study of the effects of coejected water would be warranted if future work indicates that large amounts of near-saturated water could be present. The CES/CE tests (Blanchat et al., 1996) addressed the issue of coejected water for the Calvert Cliffs geometry. Table D.14 shows that tests with coejected water resulted in lower loads than comparable steam-driven tests. Consistent with this limited experiment data and some preliminary calculations with MAAP3B (Fontana et al., 1990) for ALWRs, we ignore the impact of water coejected from the RCS during HPME. In an ice condenser plant, the impact of coejected water is expected to be further reduced in those scenarios (Figure D.14) with effective ice beds because the additional steam from flashing will be quenched in the ice beds. We acknowledge, however, that there is no direct experimental validation of this point in ice condenser geometry.

Most inputs to the TCE model are related to initial conditions and material properties. Four supplemental phenomenological models are required to complete evaluation of the TCE model:

1. a model for the coherence ratio as a function of hole size and cavity geometry,
2. a model for the hole size,
3. a model for the amount of preexisting hydrogen burned on DCH time scales, and
4. a model for the amount of debris transported to the dome.

A key modeling parameter in the TCE model is the melt-to-steam coherence ratio. Because the entrainment time is short compared with the blowdown time, molten debris is exposed to a small fraction of the primary system steam during the dispersal process. Since this steam is the medium oxidizing metal and carries the melt energy and the hydrogen produced by steam-metal interactions to the main containment volume, this incoherence can be an important mitigating factor, particularly if the metal content is high. We note, however, that only limited sensitivity to R_τ is observed for the melt compositions identified in our study. With this understanding, it is possible to reduce most of the complexity of cavity phenomena to the coherence ratio ($R_\tau = \tau_e/\tau_b$ in the TCE model). We now focus on the coherence ratio and its quantitative representation in the calculations.

Appendix E in NUREG/CR-6075 (Pilch et al., 1994a) develops a correlation for the coherence ratio based on experiment values obtained by a procedure best suited to the TCE model. The correlation can be expressed as

$$R_\tau = \frac{\tau_e}{\tau_b} = C_{R\tau} f_d \left(\frac{T_{RCS}^0}{T_d^0} \right)^{1/4} \left(C_d \frac{M_d^0}{M_g^0} \frac{A_h V_{cav}^{1/3}}{V_{RCS}} \right)^{1/2}, \quad (D.7)$$

where $C_{R\tau}$ is a cavity-specific multiplier that is determined from experiment data.

Splinter Scenario Approach

The database on which the coherence ratio correlation is based contains Zion-like geometries and Surry-like geometries, and Calvert Cliffs-like geometries. Figure D.13 compares the coherence ratio correlation with the Zion, Surry, and Calvert Cliffs database. For the purpose of quantifying the coherence constant and a relative standard deviation for each plant, we have categorized all Westinghouse cavities into one of four groups: Zion-like, Surry-like, Calvert Cliffs-like, and other. We have consulted the IDCOR descriptions of reactor cavities and applied our own subjective assessments when making the assignments. Our basis is described more fully in Appendix C.

We define Zion-like cavities as having a U-shaped layout with a slanted riser section, and we define Surry-like cavities as having a U-shaped layout with a vertical riser section. Calvert Cliffs-like cavities are characterized by large debris transport up around the annular gap around the RPV. Our assessments are summarized in Table C.1 where we note that all ice condenser cavities have a Surry-like cavity for the purpose of quantifying the coherence.

The Zion, Surry, and limited Calvert Cliffs database for the coherence ratio largely overlaps the range of individual parameters that are of interest to reactor applications (Table D.15). However, the database does not include all possible combinations of parameters for each of the potential applications; consequently, the correlation for the coherence ratio is required to fill gaps in the database. It is significant that this process is one of interpolation rather than extrapolation for Zion, Surry, and Calvert Cliffs. This argument is based upon recognized *nondimensional* parameters. We do not imply that the database includes full scale reactor cavities.

Rapid ejection of hot melt through a breach in the RPV leads to ablation, which increases the initial hole size. Appendix J in NUREG/CR-6075 (Pilch et al., 1994a) develops a model for hole ablation. The final hole size can be computed from

$$\frac{\Delta D_h}{D_h^0} = \frac{\tau_M}{\tau_D} \left[1 + 0.6934 \left(\frac{\tau_M}{\tau_D} \right)^{2/3} \right] \quad (\text{D.8})$$

where

$$\tau_M = \frac{M_d^0}{\dot{M}_d} = \frac{M_d^0}{\rho_d C_d \frac{\pi (D_h^0)^2}{4} \left(\frac{2}{\rho_d} (P_{RCS}^0 - P_c^0) \right)^{1/2}} \quad (\text{D.9})$$

is the characteristic time to eject all the melt from the RPV in the absence of ablation and where

$$\tau_D = \frac{D_h^0}{\dot{D}_h} = \frac{D_h^0}{\left(\frac{2 h_{d,w} (T_d^0 - T_{mp,w})}{\rho_w [C_{p,w} (T_{mp,w} - T_w) + h_{f,w}] } \right)} \quad (\text{D.10})$$

is the characteristic time to double the initial hole size by ablation. Figure D.14 validates the model against the existing database. This figure also illustrates that ablation increases the hole size only slightly for initial hole sizes characteristic of lower head rupture; consequently, ablation will not have a strong influence on the calculations performed for this report. Although a point estimate of the initial hole size is specified in this report, a distribution of final hole sizes results because the causal relation (Equation D.8) is evaluated for a distribution of melt masses.

A second phenomenological uncertainty concerns hydrogen combustion during DCH. The working group for Zion resolution (Appendix A in Pilch et al., 1994a) emphasized that hydrogen combustion should be treated in a manner consistent with the expected conditions in the containment. Appendix E (Pilch et al., 1994b) addresses the issue of jet combustion, entrainment into a jet, stratification, global mixing, and volumetric combustion phenomenology in more detail. Our conclusions regarding hydrogen combustion during DCH events can be summarized as follows:

1. DCH-produced hydrogen (plus some entrainment of H₂ from the preexisting atmosphere) can burn as a jet in the dome and contribute to peak containment pressures. These burning jets would represent an adequate ignition source for deflagrations if flammable conditions exist in the containment.
2. Stratification of hot jet combustion products will occur in the dome if sprays are not operational, thus impeding the mixing of combustion products with the cooler preexisting atmosphere. Thus, we picture hot nonflammable gases accumulating in the upper dome and the cooler, potentially flammable, preexisting atmosphere displaced downward in the lower dome regions.
3. Flame propagation is difficult to achieve in stratified containment atmospheres with ~50 percent steam, and the burning process is too slow and inefficient to contribute to peak loads except possibly at the upper end of H₂ distribution. Explicit treatment of deflagrations to better define and bound uncertainties in hydrogen combustion (Pilch et al., 1995; Pilch, 1995) was included in the Zion supplement (Pilch et al., 1994b) and our current analyses. The fraction of the preexisting hydrogen that can burn on DCH time scales and contribute to peak loads is given by

$$f_{pre} = \eta_c \left(1 - \frac{\dot{E}_{HT}}{\dot{E}_{H2}} \right). \quad (\text{D.11})$$

Splinter Scenario Approach

Even for finite combustion completeness (η_c), heat transfer to structures can exceed the energy release rate that is due to the deflagration so that the deflagration does not contribute to peak DCH loads. The deflagration model also handles the continuum of cases where deflagrations can contribute to peak DCH loads depending on atmosphere composition and temperatures induced by the DCH event itself. Deflagration-enhanced DCH loads are predicted for a TMI-like scenario with essentially no steam in the atmosphere, but the increased pressure is offset by the lower initial pressure in the containment.

4. Slow volumetric combustion of preexisting hydrogen can occur in parallel with potential deflagrations, but slow volumetric combustion does not contribute to peak loads.
5. Sudden volumetric combustion (autoignition) of preexisting hydrogen is essentially impossible in a stratified atmosphere because heating of the containment atmosphere is limited by mixing. However, to better bound uncertainties in hydrogen combustion phenomena, we recommend a bulk averaged autoignition temperature of 950 K based on separate effects data.
6. Combustion initiated by passive mixing (i.e., sprays are not operational) of hot gases with the preexisting atmosphere is too slow to contribute to peak pressure. This is because the mixing time scale of the atmosphere is long compared with the time scale for structure heat transfer. Here, we refer to global mixing of the atmosphere, not entrainment into a burning jet, which is already accounted for in item 1 above. This mixing limited combustion occurs in parallel with potential deflagrations and volumetric combustion.

These insights and recommendations are consistent with peer review comments for NUREG/CR-6075 (Pilch et al., 1994a) concerning the autoignition temperature and the need to consider partial combustion of the preexisting hydrogen. These recommendations have been factored into the calculated results presented in Section D.6.

The IET-11 experiment (Blanchat et al., 1994) showed that stainless steel insulation around the RPV was largely dispersed with the molten debris. Little of the intact insulation was recovered posttest. The interaction of steam with the insulation has the potential to be a source of additional hydrogen that could burn and contribute to peak containment loads. High hydrogen production values reported in IET-11 compared to IET-9 and IET-10 can be partially explained in terms of differences in initial conditions or the stochastic range of possible hydrogen production. The Cr content of the insulation is the most likely source of any additional hydrogen because of thermodynamic limitations to Fe oxidation and because of coherent steam limitations in the annulus. In the Surry plant, oxidation of the Cr content of the insulation would produce $\sim 1.45 \times 10^4$ additional moles of hydrogen resulting in an additional load of ~ 0.023 MPa if all the hydrogen burns. In addition, melting of the insulation comes at the expense of quenching the molten core materials. Lastly, significant quantities of cavity water or water coejected from the RCS may reduce the tendency of the insulation to melt and thus mitigate the possible production of additional hydrogen. The analyses do not model this potential source of additional hydrogen.

The amount of material participating in DCH is typically less than the melt mass on the lower head at the time of bottom head failure. Experiments show melt retention in both the crucible

(scaled to the bottom head of the RPV) and the reactor cavity below the RPV. On average, ~93 percent of the melt in the Zion experiments (Allen et al., 1994; Binder et al., 1994) and 99 percent of the melt in the Surry experiments (Blanchat et al., 1994) was ejected into the cavity. These results are for a hole centered on the lower head. Additional retention may occur for off-center holes. A conservative upper bound of 100 percent is used for all the scenarios in this report.

Section C.2.1 provides a comprehensive review of debris dispersal phenomena. Experiments typically show 60-90 percent dispersal with the retained material appearing as a thin crust of frozen material on all surfaces. To summarize, we expect that debris dispersal will be complete for RCS conditions of most interest to DCH, except for some retention by freezing on cavity surfaces. We also expect that the melt will be fragmented to sizes ~1 millimeter (mm) or less.

The DCH database indicates that melt retention occurs predominantly as a thin crust (~1 mm) of frozen material plated out on all cavity surfaces. A first order correction to the dispersal fraction, which accounts for surface freezing

$$f_{disp} = 1 - \frac{\delta(t) A_s \rho_d}{M_d^o} \sim 1 - \frac{2\lambda_c (a_c R_c \tau_b)^{1/2} 6V_c^{2/3} \rho_d}{M_d^o}, \quad (D.12)$$

is developed in Section C.2.1. This simple model is validated against the database in Table D.16 where it is shown to conservatively underpredict the amount of retention by freezing.

Reactor applications are both plant-specific and scenario-specific. The former is true because of geometric differences and the latter is true because of the scenario dependent melt masses and RCS pressures. Section C.2.1 computes the fraction dispersed for each plant and for each scenario, with the evaluation being performed for the upper end of the mass distributions. Freezing on cavity surfaces retains only ~7 percent of the melt for each plant and scenario. A single representative value of ~93 percent is used for the dispersal fraction for all plants and scenarios.

Table D.12 Survey of DCH-relevant experiments

| Experiment Series | Number of Tests | Nominal Scale | Cavity Type | Cavity Water |
|-------------------|-----------------|---------------|-------------------|-----------------------------|
| SNL/DCH | 4 | 1:10 | Zion | None |
| SNL/TDS | 7 | 1:10 | Surry | None |
| SNL/LFP | 6 | 1:10 | Surry | None |
| SNL/WC | 3 | 1:10 | Zion | None Cavity |
| SNL/IET-Zion | 9 | 1:10 | Zion | Cavity Cavity/basement |
| SNL/IET-Surry | 3 | 1:5.75 | Surry | None Cavity/basement |
| ANL/CWTI | 2 | 1:30 | Zion-like | Cavity/basement |
| ANL/IET | 6 | 1:40 | Zion | None Cavity |
| ANL/U | 3 | 1:40 | Zion | None |
| FAI/DCH | 4 | 1:20 | Zion | Basement Cavity/basement |
| SNL/CES/CE | 7 | 1:10 | Calvert Cliffs | Dry, Condensate Levels |

Table D.12 (continued)
Survey of DCH-relevant experiments

| Experiment Series | Driving Gas | Driving Pressure (MPa) | Melt Mass (kg) | Melt Composition | Hole Size |
|-------------------|-------------------------------------|------------------------|----------------|--|-------------|
| SNL/DCH | N ₂ | 2.6 - 6.7 | 20, 80 | Fe/Al ₂ O ₃ | 0.06 |
| SNL/TDS | H ₂ O | 3.7 - 4.0 | 80 | Fe/Al ₂ O ₃ /Cr | 0.065 |
| SNL/LFP | H ₂ O | 2.5 - 3.6 | 50, 80 | Fe/Al ₂ O ₃ /Cr | 0.04 - 0.09 |
| SNL/WC | H ₂ O | 3.8 - 4.6 | 50 | Fe/Al ₂ O ₃ /Cr | 0.04 - 0.10 |
| SNL/IET Zion | H ₂ O | 5.9 - 7.1 | 43 | Fe/Al ₂ O ₃ /Cr | 0.04 |
| SNL/IET Surry | H ₂ O | 12 | 158 | Fe/Al ₂ O ₃ /Cr | 0.072-0.098 |
| ANL/CWTI | N ₂ | 4.7 - 5.0 | 4.1 | UO ₂ /ZrO ₂ /SS | 0.13 |
| ANL/IET | H ₂ O | 5.7 - 6.7 | 0.72, 0.82 | Fe/Al ₂ O ₃ /Cr | 0.011 |
| ANL/U | H ₂ O | 3.0 - 6.0 | 1.13 | UO ₂ /Zr/ZrO ₂ /SS | 0.011 |
| FAI/DCH | N ₂ , H ₂ O | 2.4 - 3.2 | 20 | Fe/Al ₂ O ₃ | 0.025 |
| SNL/CES/CE | N ₂ , steam, steam/water | 8 | 33 | Fe/Al ₂ O ₃ | 0.04-0.05 |

Table D.12 (concluded)
Survey of DCH-relevant experiments

| Experiment Series | Containment Pressure (MPa) | Annular Gap Around RPV | Atmosphere Composition | Containment Structures |
|-------------------|----------------------------|------------------------|--|---------------------------------------|
| SNL/DCH | 0.08 | No | Air, Ar | Open containment |
| SNL/TDS | 0.09 - 0.23 | No | Air, Ar | Open containment |
| SNL/LFP | 0.16 | No | Ar | Compartmentalized by slab |
| SNL/WC | 0.16 | No | Ar | Essentially open |
| SNL/IET Zion | 0.2 | No | N ₂ , N ₂ /Air, N ₂ /Air/H ₂ , CO ₂ /Air/H ₂ | Zion subcompartment structures |
| SNL/IET Surry | 0.13-0.19 | No partial insulation | Air/H ₂ O/H ₂ | Surry subcompartment structures |
| ANL/CWTI | 0.1 | No | Ar | Compartmentalized by baffle |
| ANL/IET | 0.2 | No | N ₂ , N ₂ /Air, N ₂ /Air/H ₂ , H ₂ O/Air/H ₂ | Zion subcompartment structures |
| ANL/U | 0.2 | No | N ₂ /Air/H ₂ | Zion subcompartment structures |
| FAI/DCH | 0.1 | No | N ₂ | Zion (Like) subcompartment structures |
| SNL/CES/CE | 0.2-0.23 | Yes | N ₂ /Air/H ₂ O/H ₂ | Calvert Cliffs-like |

Table D.13 CONTAIN/TCE comparisons

| Scenario | ΔP (MPa) | | H ₂ Burn (kg) | |
|----------|----------|-------|--------------------------|-------|
| | CONTAIN | TCE | CONTAIN | TCE |
| V | 0.476 | 0.502 | 34.5 | 94.9 |
| Va | 0.466 | 0.570 | 35.2 | 94.8 |
| Vb | 0.940 | 1.034 | 348.7 | 304.0 |
| VI | 0.387 | 0.598 | 48.6 | 142.5 |
| VIa | 0.347 | 0.586 | 46 | 142.4 |
| VIb | 0.788 | 0.979 | 350.6 | 298.5 |

Table D.14 Experiment insights on “coejected” water for Calvert Cliffs geometry

| Test | Driving Medium | Atmosphere | ΔP_{HPME} |
|-------|----------------|------------|-------------------|
| CES-2 | steam | inert | 0.316 |
| CES-3 | sat. water | inert | 0.293 |
| CES-1 | cold water | inert | 0.234 |
| CE-3 | steam | reactive | 0.253 |
| CE-2 | sat. water | reactive | 0.208 |

Table D.15 Applicability of the database to reactors

| | CAVITY | f_{disp}^* | T_d^0/T_{RCS}^0 | M_d^0/M_r^0 | $A_h V^{1/3} \sqrt{V_{RCS}}$ |
|--|-------------|--------------|-------------------|---------------|------------------------------|
| Complete database | Zion, Surry | 0.6 - 1.0 | 3.0 - 11.0 | 2.8 - 21.4 | 0.001 - 0.014 |
| SNL/ANL IET Zion tests $P_{RCS}^0 = 6 \text{ MPa}$ | Zion | 0.6 - 0.9 | 4.2 | 3.9 - 6.0 | 0.0027 |
| SNL/IET Surry tests $P_{RCS}^0 = 13 \text{ MPa}$ | Surry | 0.9 | 3.2 | 2.9 | 0.0033 |
| NPP $P_{RCS}^0 = 8 \text{ MPa}$ $D_h^0 = 0.4 \text{ m}$ $T_{RCS}^0 = 1000 \text{ K}$ $M_d^0 = 50 \text{ mt}$ | Zion | ~1 | 3.5 | 6.2 | 0.002 |
| NPP $P_{RCS}^0 = 16 \text{ MPa}$ $D_h^0 = 0.4 \text{ m}$ $T_{RCS}^0 = 800 \text{ K}$ $M_d^0 = 50 \text{ mt}$ | Zion | ~1 | 2.8 | 3.9 | 0.002 |

*Only experiments where dispersal is complete or nearly complete ($f_{disp} > 0.5$) considered.

Table D.16 Validation of melt retention by freezing during cavity dispersal

| Parameter | SNL/IET-1 to 8B Allen et al., 1994 | ANL/IET-1R to 8 Binder et al., 1994 | SNL/IET-9 to 11 Blanchat et al., 1994 | SNL/CES-2/CE-3 |
|---------------------|---------------------------------------|--|--|-----------------------------------|
| Cavity | Zion | Zion | Surry | Calvert Cliffs |
| Scale | 1:10 | 1:40 | 1:5.75 | 1:10 |
| Melt simulant | Fe/Al ₂ O ₃ /Cr | Fe/Al ₂ O ₃ /Cr | Fe/Al ₂ O ₃ /Cr | Fe/Al ₂ O ₃ |
| f_{disp} observed | 0.62 - 0.89 | 0.69 - 0.80 | 0.73 - 0.89 | 0.64 - 0.85 |
| f_{disp} Eq. C.1 | 0.91 | 0.85 | 0.88 | 0.88 |

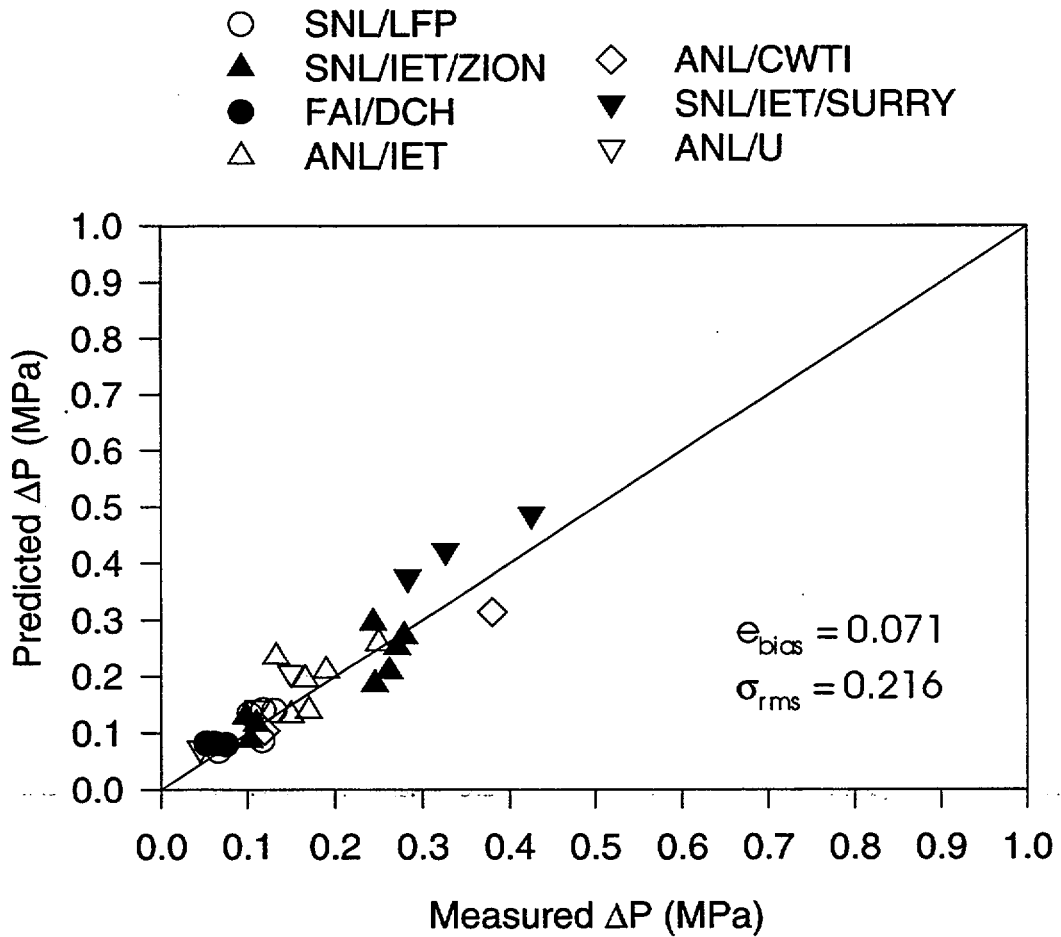


Figure D.11. Validation of the two-cell equilibrium model against all experiments with compartmentalized geometry.

- a Surry, CONTAIN Code, Williams et al. 1987
- b Surry, Darwish 1991
- c Ringhalls, CONTAIN/CORDE Code, Gustavsson 1992
- d Sizewell, CONTAIN/CORDE Code, Sweet and Roberts 1994
- e ALWR, MAAP3B Code, Fontana et al. 1990
43 mt Flashing Water
- f ALWR, MAAP3B Code, Fontana et al. 1990
43 mt Flashing Water + 227 mt Cavity Water
- g SNL/WC-2, Cavity Water, Allen et al. 1992
- h FAI/DCH-2, Cavity Water, Henry et al. 1991
- i SNL/ET-8B, Cavity Water, Allen et al. 1993
- j SNL/CES-1, Coejected Room Temperature Water, Blanchat et al. 1996
- k SNL/CES-3, Coejected Flashing Water, Blanchat et al. 1996
- l SNL/CE-2, Coejected Flashing Water, Blanchat et al. 1996

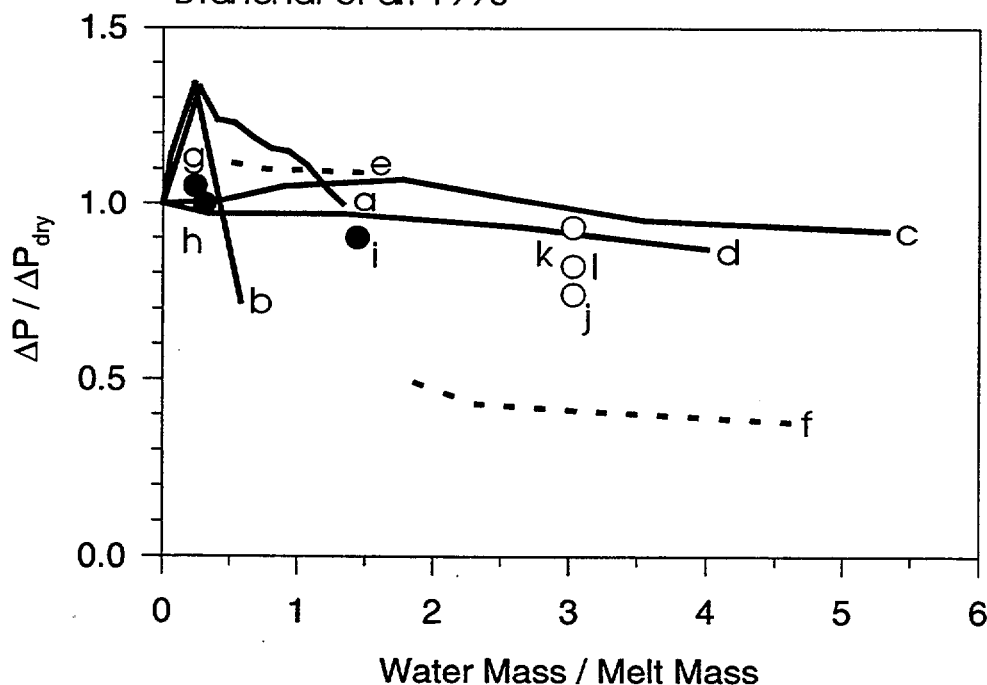


Figure D.12 Potential impact of codispersed water on DCH loads.

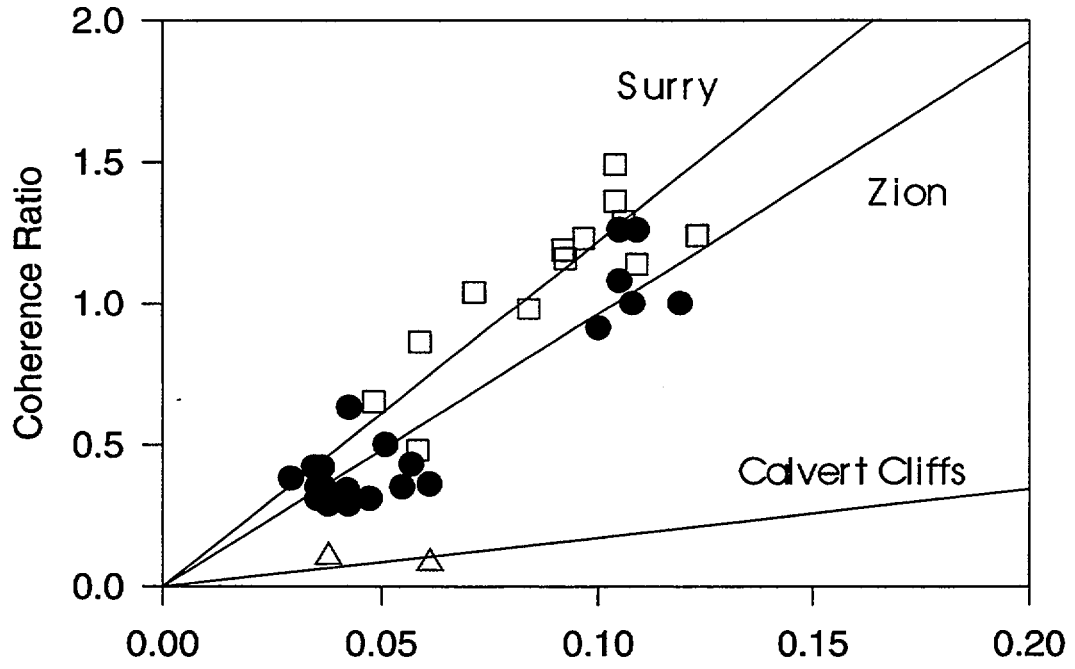


Figure D.13. Validation of the coherence ratio for scenarios without coejected water.

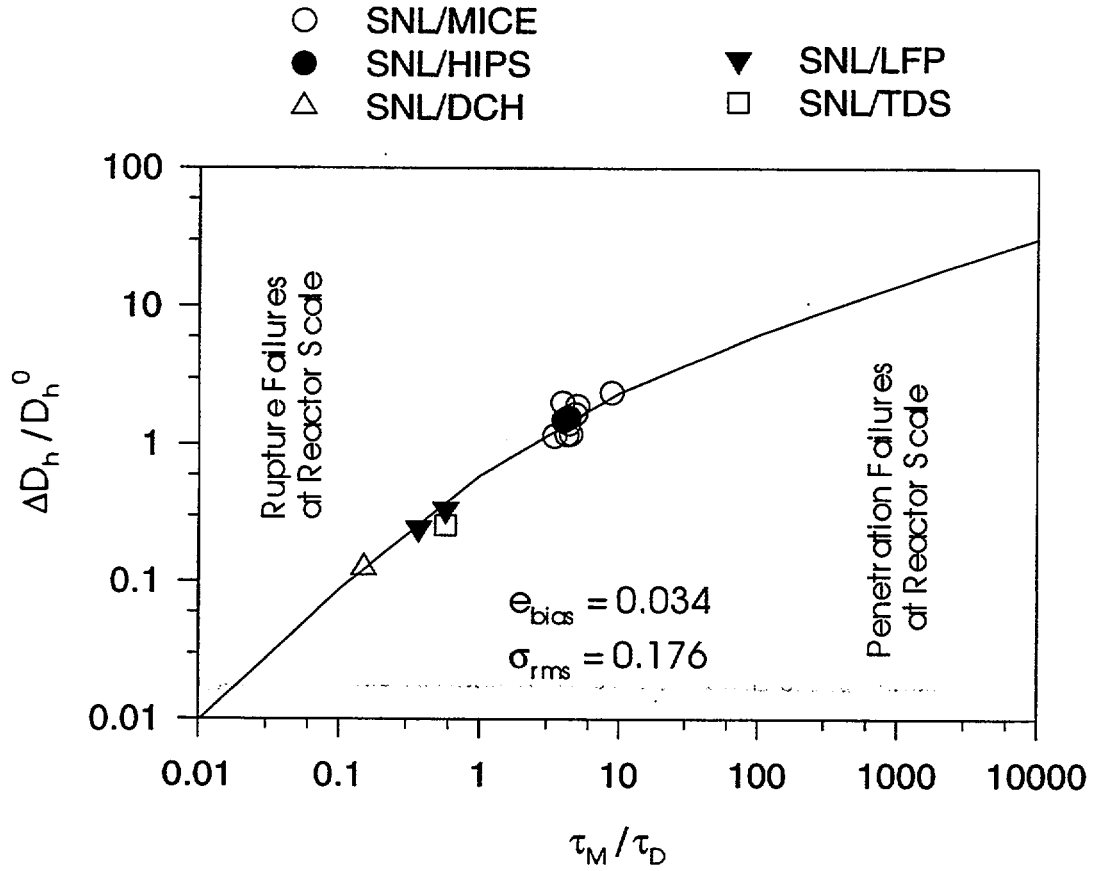


Figure D.14. Validation of the hole ablation model.

D.5 Quantification of Containment Facility

This section characterizes the strength of a reactor containment in probabilistic terms, which are required for TCE/LHS evaluations. The pressure capacity of a reactor containment is treated as a random variable because of the variability in material properties, of unknown differences between the as-built and design conditions, and modeling uncertainties. The probability that the containment failure pressure is less than a specified pressure is known as the containment overpressure fragility curve.

Fragility curves represent a probabilistic estimate of the capacity of the containment. In general, the fragility curve could be derived from data and full-scale experiments. However, the containment fragility curves are dependent on site-specific detail and, without detailed model tests, they must be derived from analysis. As a practical matter, the fragility curves are derived from a combination of material property data, tolerances in dimensions from drawings, and judgment of the analyst. Judgment is used in determining what level of analysis is required and what failure mechanisms are considered to govern the containment capacity. Typically, adequate material property data exist to characterize variability in material properties. Finally, analyst judgment is used to assign "modeling" uncertainty to the models to characterize the analyst's confidence in the ability of the selected models to represent the actual failure mechanisms involved. Modeling uncertainty could, in principle, be reduced with further analysis or testing. Funding constraints, however, usually require the analyst to exercise his or her judgment to reflect the uncertainty involved.

The Individual Plant Examinations (IPEs) for all operating Pressurized Water Reactors (PWRs) in the U.S. were assembled and containment fragility curves obtained for each plant as part of DCH resolution activities for the Westinghouse plants (Pilch et al., 1996). The containment capacity results from each of the IPEs were examined and briefly reviewed and the probability of containment failure was taken from them. In many cases, this consisted of fragility curves showing pressure versus cumulative failure probability. In other cases, a mean or median failure pressure was specified along with uncertainty bounds. In some cases, only curves or points for various failure modes were given and a total probability of failure had to be constructed. In all these situations, a single fragility curve resulted that was intended to reflect both modeling uncertainty and stochastic uncertainties due to material property variations. In only two cases, confidence limits were derived and reported. Confidence limits are used to separate modeling uncertainties from stochastic uncertainties. A detailed assessment of the technical basis for the IPE fragility curves is beyond the scope of this study.

For those IPEs presenting only a single curve, the curve was digitized, curve-fit with a spline program and failure probabilities determined at intervals of 1 psig. For IPEs which reported medians and uncertainties, a curve was developed and failure probabilities determined at intervals of 1 psig. The few which reported only median, 5 percent and 95 percent values, were fit to either a log-normal distribution, normal distribution or 3rd order spline function in order to get the best fit and failure probabilities determined at 1 psig intervals. In most situations where this occurred, only a third order spline provided an adequate fit to the three constraints.

Many of the IPE containment capacity analyses did not consider temperature or stated that increased temperatures would have little effect on the capacity. Other IPEs performed the analysis at either single or multiple accident temperatures. For those which determined the capacity at different temperatures, the analysis closest to 400 K (260°F) was selected as best representing the accident temperatures expected in the reactor containment building at the time of vessel breach.

We observed that the licensee's level of effort and our estimate of the reliability of these containment fragility curves varied significantly. In some cases, a detailed analysis was performed for every possible failure mode and an overall cumulative failure curve was determined by combining each mode of failure, while some IPEs simply used containment fragility curves derived from other containments or simply shifted other plant's fragility curves based on what they determined to be the difference in ultimate capacity.

Appendix D in Pilch et al. (1996) briefly discusses (when given enough information) how the fragility curves were determined from each IPE. In addition, the process of digitizing, fitting and tabulating the curves or data given in the IPEs is discussed for every plant, and the detailed results are also tabulated. We interpret our fragility curves as *mean* values, and our compilations, to the extent possible, strive for consistency in this regard. None of IPEs from ice condenser plants presented families of fragility curves from which a high confidence or a mean curve could be explicitly identified.

Functional representations of fragility are subject to possible error when extrapolated to low failure frequencies because excessive extrapolation to low failure frequencies could lose or violate the physical basis on which most of the curve rests. In other cases, some IPEs conservatively tie the low end of the fragility curve to the design pressure. Consequently, the IPE fragility curves might be quite conservative in the tails. On the other hand, the digitizing process is subject to human error and is dependent on the quality of the working curve. In a few cases, we supplied a curve fit to median, 5 percent, and 95 percent values, and extrapolation to lower failure frequencies may involve error. However, it will be shown the potential uncertainties in the tails of the fragility distributions are not dominating the results of this study.

Table D.17 provides a concise summary of key plant-specific fragility data for each Westinghouse plant with an ice condenser containment. We note that all ice condenser containments are free standing steel shells; except DC Cook, which is a reinforced concrete containment. We see that large variations in containment strengths exist. DC Cook is the least robust containment with a failure pressure of 45 psig, at a failure frequency of 10 percent. Watts Bar and Catawba are the strongest containments with failure pressures of 71 psig, at the same failure probability. Thus, we conclude that a containment's fragility is plant-specific. This is illustrated further in Figure D.15 which compares the fragility curves for all the plants.

We note that the ice condenser plants are substantially less robust than other Westinghouse plants with large dry or subatmospheric containments. Table D.17 shows that mean of the containment failure pressure for all ice condenser plants is 62.8 psig at a failure frequency of 10 percent. The comparable value for all Westinghouse plants with large dry or subatmospheric

Splinter Scenario Approach

containments is 113.1 psig. Ice condenser containments can afford to be less robust because of their reliance on ice beds as a pressure suppression feature for design basis accidents.

It is to be anticipated that the fragility curves derived for a specific containment are sensitive to local design details, tolerances, and the design philosophy used for that particular containment. While it is likely that various submodels representing different local containment failure modes may be applicable to a variety of containments of a given type, it is also true that the combination of failure mechanisms existing in a given containment is unique. Thus, the reader is cautioned against reading any generic applicability into the fragility curves developed for any specific containment. We, therefore, use the plant-specific IPE fragility curve in our analyses, consistent with previous DCH resolution activities (NUREG/CR-6338).

Table D.17 Containment fragility

| PLANT | Design Press. psig | Cont. Press (psig) @ | | | Cont. Press/Design Press. @ | | |
|---------------|-----------------------|----------------------|----------|----------|-----------------------------|----------|----------|
| | | Freq=0.01 | Freq=0.1 | Freq=0.5 | Freq=0.01 | Freq=0.1 | Freq=0.5 |
| Catawba | 15 | 61 | 71 | 85 | 4.07 | 4.73 | 5.67 |
| Cook | 12 | 37 | 45 | 58 | 3.08 | 3.75 | 4.83 |
| McGuire | 15 | 57 | 65 | 77 | 3.80 | 4.33 | 5.13 |
| Sequoyah | 10.8 | 55 | 62 | 69 | 5.09 | 5.74 | 6.39 |
| Watts Bar | 15 | 56 | 71 | 90 | 3.73 | 4.73 | 6.00 |
| Summary Info. | | | | | | | |
| Mean | 19.2 | 53.2 | 62.8 | 75.8 | 3.2 | 3.8 | 4.6 |
| STD | 8.2 | 8.4 | 9.6 | 11.4 | 1.1 | 1.3 | 1.5 |
| STD/Mean | 0.43 | 0.16 | 0.15 | 0.15 | 0.36 | 0.35 | 0.34 |

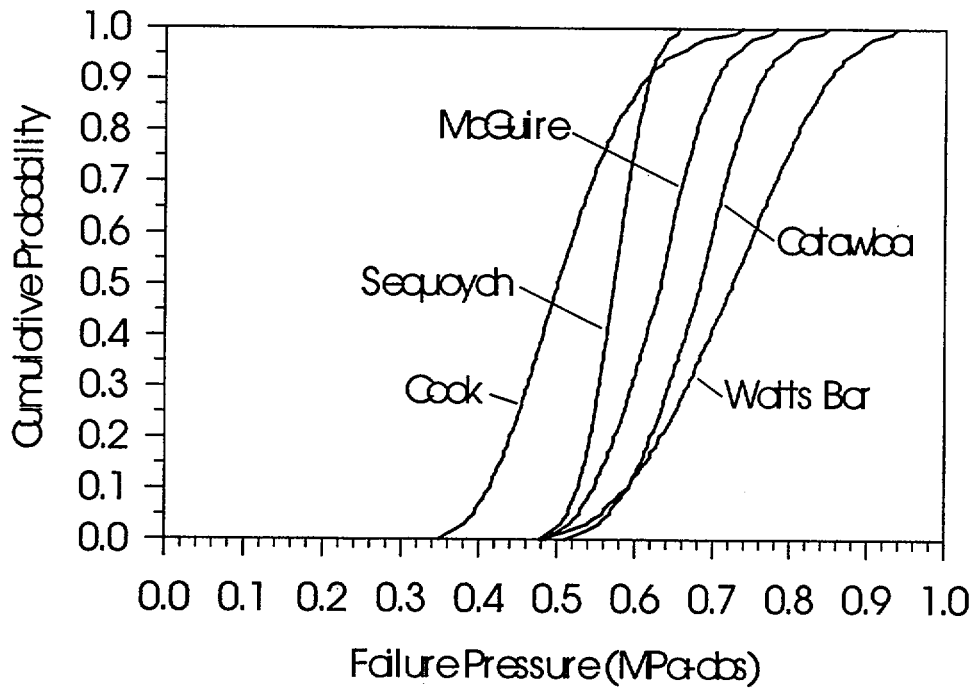


Figure D.15. Fragility curves for all Westinghouse plants with ice condenser containments.

D.6 Results

Each scenario identified in Section D.3.2 supplemented by the respective coherence ratio distribution as discussed in Section D.4 and the fragility curve of Section D.5, was run through the arithmetic defined by the probabilistic framework of Section D.2 to produce a probability distribution for the containment pressure. Finally, the containment failure probability was computed. The process was repeated for all Westinghouse plants with ice condenser containments. The calculations were carried out using the computer code TCE/LHS as listed in Appendix B of NUREG/CR-6075, Supplement 1 (Pilch et al., 1994b) with 10,000 samples.

DCH resolution is judged by the mean (best estimate) conditional containment failure probability, which is based on the mean containment fragility curve. Table D.18 summarizes the CCFP for each plant and for each scenario. Containment failure probabilities exceeding 0.1 occur for all plants when ignitors are not energized prior to vessel breach (Scenarios Vb and VIb). Containment failure probabilities also exceed 0.1 for all plants for one or more of the remaining scenarios.

Point comparisons between TCE and CONTAIN suggest that TCE predicted loads may be overly conservative, even for the small dry approximation. CONTAIN burns substantially less DCH-produced hydrogen than TCE because CONTAIN predicts that much of the DCH-produced hydrogen still resides in the oxygen starved subcompartments at the time of peak containment pressure. CONTAIN also predicts some additional mitigation due to heat transfer to structures. The TCE model burns all DCH-produced hydrogen and treats the containment as essentially adiabatic on DCH time scales.

Sensitivity studies have been performed using loads more representative of what CONTAIN might predict. This is accomplished by applying a relative bias to all TCE predictions, for all combinations of distribution parameters. The relative bias,

$$bias = \frac{\Delta P_{CONTAIN}}{\Delta P_{TCE}}, \quad (D.13)$$

is the ratio of the CONTAIN prediction to the TCE prediction for the point comparison (upper end of the distribution for melt mass). The bias is constant for all calculations within a given scenario, but it varies from scenario to scenario, as noted in Table D.19

The use of a bias in this fashion is only indicative of how improved modeling might impact the containment failure probabilities. Additional CONTAIN calculations are required to confirm that a constant bias for a given scenario is adequate for a broader range of the parameter space. Alternatively, a response surface could be constructed as a surrogate for the CONTAIN in the Monte Carlo simulations. These options, however, are beyond the scope of the current work.

Table D.19 shows containment failure is still calculated (small dry approximation) when the bias is applied to the TCE load prediction for scenarios where ignitors are not energized prior to vessel breach. Containment failure probabilities are reduced slightly for other scenarios, but the

fact remains that the failure probabilities significantly exceed 0.1 for all plants in one or more scenarios, even if the ignitors are operational prior to vessel breach.

The small dry approximation is itself be overly conservative for those scenarios where ice remains at the time of vessel breach. Using sources from SCDAP/RELAP5, CONTAIN calculations (Appendix B) suggest that ~35 percent of the ice will remain for scenarios where the ARFs are not operational, i.e., Scenarios V and VI. Sensitivity studies for Scenario V using CONTAIN (Appendix B) show that DCH loads will be reduced from $\Delta P = 0.476$ MPa (small dry approximation) to $\Delta P = 0.144$ MPa if the ice is modeled. Thus, the ice condenser can be effective at mitigating loads when ice remains. Similar results were found for Scenario VI.

A sensitivity was performed with TCE/LHS to explore the impact that ice might have on the CCFPs for Scenarios V and VI where ice is predicted to remain. A sensitivity was also performed for Scenario Vb under the arbitrary assumption that ice remains. These three sensitivities are made possible by the fact that CONTAIN calculations (with and without the ice) are available to quantify the bias. CONTAIN calculations are not available for the other scenarios in Table D.20. A constant relative bias, as noted in Table D.20, is applied to all calculations within a given scenario, but it varies between scenarios.

Table D.20 lists CCFP results under the assumption the TCE predictions are biased to match CONTAIN predictions when ice remains. The presence of ice reduces CCFPs, but the reduction is not significant relative to the success criterion (CCFP = 0.1) for the case where ignitors are not available (i.e., Scenario Vb). Predicted CCFPs are reduced to below the screening criterion (0.01) for all plants in Scenarios V and VI. Similar results could be expected for Scenarios Va and VIa if it could be demonstrated that ice remains in these scenarios.

The preceding discussions show that a decisive resolution of the DCH issues does not exist for ice condenser plants based on the inherent capacity of the containment to withstand all credible DCH loads, particularly in those scenarios where ignitors are not available prior to vessel breach. Ultimate disposition of the issue might therefore require an integrated risk analysis that puts into perspective the probabilities of the various sequences that lead to a HPME/DCH event. NUREG-1150 (NRC, 1989) provided an integrated risk analysis for the Sequoyah plant, so it would be useful to compare the loads elicited provided then with the loads computed for this study. This is accomplished in Table D.21.

The high pressure (2000 - 2500 psi) and intermediate pressure (500 - 1000 psi) events can be compared with our Scenarios V and VI, respectively. NUREG-1150 elicited distributions quantified a distribution on the containment load at vessel breach. Here, we list the NUREG-1150 pressure rise at the 50 percentile. Point analyses using CONTAIN and TCE have been performed for the upper end of our melt mass distributions, and these point comparisons are best compared to the NUREG-1150 distributions at the 50 percentile because the NUREG-1150 distributions represented uncertainty in the loads modeling. In this way, we are comparing our nominal results with their nominal results.

Consider first the case with no ice in the containment. TCE and CONTAIN calculated loads (at the upper end of the mass distribution) are comparable to or less than the NUREG-1150

Splinter Scenario Approach

distribution. We note that the NUREG-1150 distributions also include contributions from steam explosions. CONTAIN predictions for the cases with ice are dramatically lower than loads estimates at the time of NUREG-1150. CONTAIN played a large role in establishing the NUREG-1150 distribution, and its DCH modeling has improved since that time. However, the major difference in loads predictions is likely due to differences in melt composition. Core melt progression analyses performed for the DCH resolution efforts with SCDAP/RELAP5 predict far more oxidic melts now compared to assessments at the time of NUREG-1150.

NUREG-1150 found that the mean early containment failure probability was less than 10 percent for Sequoyah, which was the success criterion established by the NRC. The Sequoyah IPE used the mean pressure rises from the NUREG-1150 elicitation, and also concluded, from an integrated risk perspective, that DCH and early containment failure meet all NRC guidelines. The loads predicted as part of this study are substantially less than loads used in these prior efforts, which reinforces these prior conclusions. In addition, the probability of HPME in a station blackout accident (without operator intervention) was refined in NUREG/CR-6109 for Surry, and the resulting probabilities (~0.077) are lower than values (~0.2) used in NUREG-1150. The plant owners may wish to confirm the analyses and conclusions reached in this report and to interpret these findings in the context of their own PRA activities.

The ice condenser plants are all of similar size and have similar nuclear steam supply systems. Consequently, we expect the DCH loads to be similar amongst the plants. All ice condenser plants, except D.C. Cook 1,2, have containments stronger than Sequoyah. Thus, it seems promising that DCH can be resolved from an integrated risk perspective for most if not all of the plants. However, a firm conclusion cannot be defended at this time because sequence probabilities can be plant and site specific. D.C. Cook 1,2 warrant closer attention because their containments are weaker than Sequoyah.

Table D.18 CCFP results using TCE/LHS with the small dry assumption

| PLANT | Scn V | Scn Va | Scn Vb | Scn VI | Scn VIa | Scn VIb |
|---------------|-------|--------|--------|--------|---------|---------|
| Catawba 1,2 | 0.049 | 0.013 | 0.947 | 0.667 | 0.199 | 0.976 |
| Cook 1 | 0.520 | 0.211 | 0.914 | 0.936 | 0.784 | 0.987 |
| Cook 2 | 0.508 | 0.199 | 0.837 | 0.935 | 0.776 | 0.979 |
| McGuire 1,2 | 0.097 | 0.020 | 0.954 | 0.761 | 0.361 | 0.988 |
| Sequoyah 1,2 | 0.311 | 0.078 | 0.968 | 0.950 | 0.780 | 0.998 |
| Watts Bar 1,2 | 0.052 | 0.017 | 0.822 | 0.501 | 0.162 | 0.890 |

Table D.19 CCFP results biasing TCE predictions to be more representative of CONTAIN predictions with the small dry approximation

| PLANT | Scn V | Scn Va | Scn Vb | Scn VI | Scn VIa | Scn VIb |
|--|-------|--------|--------|--------|---------|---------|
| bias = $\Delta P(\text{CONTAIN})/\Delta P(\text{TCE})$ | 0.95 | 0.82 | 0.91 | 0.65 | 0.59 | 0.80 |
| Catawba 1,2 | 0.028 | 0.002 | 0.902 | 0.046 | 0.000 | 0.798 |
| Cook 1 | 0.452 | 0.061 | 0.879 | 0.553 | 0.071 | 0.923 |
| Cook 2 | 0.439 | 0.055 | 0.781 | 0.548 | 0.068 | 0.884 |
| McGuire 1,2 | 0.062 | 0.002 | 0.931 | 0.118 | 0.000 | 0.889 |
| Sequoyah 1,2 | 0.216 | 0.011 | 0.958 | 0.362 | 0.001 | 0.974 |
| Watts Bar 1,2 | 0.035 | 0.003 | 0.682 | 0.052 | 0.001 | 0.518 |

Table D.20 CCFP results biasing TCE predictions to match point comparisons with CONTAIN assuming ice remains in the ice chest

| PLANT | Scn V | Scn Va | Scn Vb | Scn VI | Scn VIa | Scn VIb |
|--|-------|--------|--------|--------|---------|---------|
| bias = $\Delta P(\text{CONTAIN})/\Delta P(\text{TCE})$ | 0.3 | | 0.67 | 0.29 | | |
| Catawba 1,2 | 0.000 | | 0.403 | 0.000 | | |
| Cook 1 | 0.000 | | 0.524 | 0.006 | | |
| Cook 2 | 0.000 | | 0.343 | 0.006 | | |
| McGuire 1,2 | 0.000 | | 0.541 | 0.000 | | |
| Sequoyah 1,2 | 0.000 | | 0.739 | 0.000 | | |
| Watts Bar 1,2 | 0.000 | | 0.213 | 0.000 | | |

Table D.21 Comparison of NUREG-1150 loads elicitation with DCH loads predicted in this study

| NUREG-1150 Events | NUREG-1150 Load Percentile | Pressure Rise (MPa) No Ice | | | | | Pressure Rise (MPa) With Ice | | |
|---|----------------------------|----------------------------|---------|----------|---------|----------|------------------------------|---------|----------|
| | | | TCE | | CONTAIN | | | CONTAIN | |
| | | NUREG-1150 | Scn. V | Scn. Va | Scn. V | Scn. Va | NUREG-1150 | Scn. V | Scn. Va |
| 2000-2500 psi high core fraction large hole | 50% | 0.62 | 0.50 | 0.47 | 0.48 | 0.47 | 0.42 | 09.14 | 0.14 |
| NUREG-1150 Events | NUREG-1150 Load Percentile | Pressure Rise (MPa) No Ice | | | | | Pressure Rise (MPa) With Ice | | |
| | | | TCE | | CONTAIN | | | CONTAIN | |
| | | NUREG-1150 | Scn. VI | Scn. VIa | Scn. VI | Scn. VIa | NUREG-1150 | Scn. VI | Scn. VIa |
| 500-1000 psi high core fraction large hole | 50% | 0.60 | 0.60 | 0.59 | 0.40 | 0.35 | 0.38 | 0.12 | 0.13 |

D.7 Conclusions and Recommendations

This study shows that no ice condenser plant is inherently robust against all possible DCH threats. The magnitude of the DCH threat is largely controlled by whether ignitors are operational prior to vessel breach. Such scenarios are dominated by combustion of preexisting hydrogen in the atmosphere during the DCH event. If hydrogen released to the containment is allowed to accumulate until vessel breach (as may occur in a recover station blackout), the DCH event need do little more than provide the ignition source to produce containment threatening loads. The containment threat from hydrogen combustion alone has been previously recognized, and DCH does nothing to improve the perspective. We acknowledge, however, that recovered station blackouts where RPU failure occurs at high RCS pressure may be relatively rare in the plants risk profile.

The ice condenser effectiveness becomes the dominant issue controlling DCH loads, by wide margins if the hydrogen is burned off prior to vessel breach. If the ice is available, the ice condenser is calculated to have the potential to mitigate any of the scenarios (other than Vb or VIb) that have been considered, even when assumptions thought to be conservative are made in the loads modeling. No point calculation with ice exceeded the 1 percent CCFP pressure for any containment other than D.C. Cook, and even in this case, the 10 percent failure probability was not exceeded. This fact is all the more significant when one takes into account that all the calculations were performed with melt masses corresponding to the 99th percentile of the NUREG/CR-6338 (Pilch, et al., 1996) melt distributions.

It is appropriate to consider how resolution might be achieved in future work. We offer a general approach that could be adopted for future issue resolution work on ice condenser plants.

Quantify Spectrum of Scenarios Leading to HPME. The spectrum of accident scenarios of potential concern for HPME could be evaluated using PRA techniques based upon those of NUREG-1150 (NRC, 1989), with information updated from the IPEs and other sources as needed. Goals would include answering the following questions:

- In what fraction of the HPME-relevant cases will hydrogen be burned off prior to vessel breach?
- In what fraction of accident sequences will ice be present in the ice condenser?
- Will sprays play a significant role in DCH-relevant scenarios?
- In what fraction of accident sequences will there be sufficient cavity water to preclude DCH and/or liner failure by direct contact? In what fraction of accident sequences will cavity water be sufficient to play a significant role in HPME, but insufficient to preclude DCH and/or preclude liner failure by direct contact?
- What are the probabilities of the various combinations of the conditions enumerated above?

Splinter Scenario Approach

Evaluate Role of Scenarios Without Hydrogen Ignition Prior to Vessel Breach. If the spectrum of HPME-relevant scenarios is dominated by events in which ignition sources are not available prior to vessel breach, a severe hydrogen burn problem likely exists at vessel breach and additional detailed consideration of DCH as such may not be warranted unless the hydrogen issue is resolved. Scenarios such as these can be remediated through accident management measures that might include the use of DC powered ignitors.

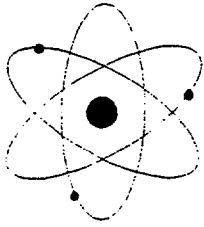
Improve Validation Basis of the CONTAIN Ice Condenser Model. Mitigation by the ice condenser offers the potential for large improvements in the prospects for DCH issue resolution if scenarios in which hydrogen is burned prior to vessel breach *and* unmelted ice remains at vessel breach are important to the spectrum of DCH-relevant events. The validation basis of the CONTAIN ice condenser model could be substantially improved by comparing its predictions with the results of experiments such as the Waltz Mill test data and the results of licensing code calculations for ice condenser plants. These comparisons would directly address validity only for DBA conditions; additional analysis would be needed in order to assess uncertainties under DCH conditions. Issues related to compromise of ice condenser efficiency by uneven ice melting would also require attention, at least in scenarios in which ice melt exceeded 50 percent of the initial inventory.

Quantification of Uncertainties in Loads Modeling. If scenarios in which hydrogen does burn prior to vessel breach but ice is *not* effective are important to the spectrum of DCH-related events, issue resolution may require a more quantitative treatment of the various uncertainties in loads modeling that were itemized in Section 3. The scoping calculations described in Section B.3 of this report provide considerable insight as to which of these uncertainties are potentially important, but no effort is made there to assign probabilities to the cases that are considered or to develop uncertainty distributions for the loads. A response surface can be developed and used as a surrogate for CONTAIN in Monte Carlo assessments of the DCH threat.

HPME Threats to Containment Other than DCH. The present report does not consider in detail HPME-related threats other than DCH pressurization. However, it will be necessary to consider these threats in order to achieve full closure on HPME-related issues for ice condenser plants. The review of the NUREG-1150 assessment of HPME-related threats in Section 3 indicates that the potentially significant threats are direct contact of the liner by molten debris and hydrogen detonations. The NUREG-1150 analyses did not indicate that the CCFP associated with any of the other threats discussed in Section 3 could exceed 0.01.

PRA activities performed by the utilities for their own plants is the best framework for integrating load/strength analyses, sequence probabilities, and HPME probabilities. NUREG-1150 (Sequoyah) and the Sequoyah individual plant examination (IPE) report mean early containment failure probabilities less than 0.1 (given core damage); consequently, the utility concluded that DCH was resolved for their plant. These integrated utility assessment account for sequence probabilities and temperature induced hot leg failure. DCH load distributions used in NUREG-1150 and the Sequoyah IPE are comparable or greater than the loads distributions calculated for this study. The plant owners may wish to confirm the analyses and conclusions reached in this report and to interpret these findings in the context of their own PRA activities.

D.8 Peer Review of Draft NUREG/CR-6427



ENERGY RESEARCH, INC.

P.O. Box 2034
Rockville, Maryland 20847
(301) 881-0866 / FAX 881-0867

March 26, 1998

Dr. Richard Lee
Accident Evaluation Branch
Division of Systems Technology
Office of Nuclear Regulatory Research
U. S. Nuclear Regulatory Commission
Washington, D. C. 20555-0001

Dear Dr. Lee:

Attached please find copies of the review comments on NUREG/CR-6427 (July 1997) by F. Moody, M. Ishii, M. Modarres, R. Henry, and D. Stamps. The comments by S. Levy was sent directly to Mr. Wayne Hodges. If you have any further questions, please do not hesitate to contact me.

Sincerely,

H. Esmaili

H. Esmaili

xc: ERI/NRC-046 file

ASSESSMENT OF THE DCH ISSUE FOR PLANTS
WITH ICE CONDENSER CONTAINMENTS, NUREG/CR-6427

Comments by F. J. Moody
March 9, 1998

SUMMARY

The DCH resolution methodology involves a multilayered procedure of screens or filters to determine a conditional containment failure probability (CCFP) for a nuclear power plant. The procedure is designed to incorporate various stages of refinement, as needed, in order to provide increased rigor in CCFP distributions. If the first screening does not provide a CCFP which is within established limits for DCH issue resolution, the next screen with more refinement is applied, and so on.

The study reported in NUREG/CR-6427 led to the conclusion that none of the ice condenser plants has the capacity to withstand credible DCH events, unless H₂ ignitors are available and ice remains at the time of DCH. That is, the determination of CCFP for the ice condenser plants needs further refinement in order to demonstrate values of the CCFP of 0.1 or less. Sandia has outlined a path of progressive refinement in the procedure, which leads to high expectation that further reduction of the CCFP values can be justified at a level for which the DCH issue for ice condenser plants can be closed. The refinement path requires more fine structure analysis and processing of elements in the CCFP determination. The plan Sandia has offered involves refinement of the load/strength analyses, consideration of the HPME probabilities conditional on core damage, and if necessary, an integration of load/strength analyses and HPME probabilities.

I think that the steps outlined by Sandia are reasonable. The resolution plan discussed is based on a laboratory team who function openly with acknowledged experts from industry and academia, who demonstrate substantial familiarity and accountability in advancing a complex but relatively mature technology. It was noted that PRA techniques can be employed in evaluating the potential concern for HPME, using updated information from IPEs. The ice condenser model in CONTAIN could be evaluated from available data, and comparison with licensing code calculations. The outlined steps to closure involve thoughtful, rigorous "pencil and paper" exercises and computational work by experienced practitioners. One item that could be more fully discussed is the kind of attention that may be required to determine ice condenser efficiency by uneven ice melting. It is not clear if this step would require further experimental studies.

Sandia has a good track record for helping in the closure of DCH issues. Since current analysis refinements for ice condenser plants at this point have not resulted in CCFP values low enough to close the DCH issue, additional effort is needed. One possibility mentioned is to remedy the hydrogen problem through accident management by the use of DC powered ignitors. However, it seems that the preferred steps to resolution

have been outlined by Sandia. Sandia has the expertise and in-depth understanding of DCH phenomena and has developed a layered resolution methodology for closing DCH issues for the PWR fleet. It is preferable to use validated analysis with the hope of showing that a problem does not exist before installing additional devices.

I think that the most reasonable choice is to ask Sandia to perform sequential selected refinements from their proposal until it is demonstrated that the CCFP is 0.1 or less. Selection of the refinement which appears to dominate should come first, followed by the next, and the next...most important steps. When success is achieved, there is no need to further refine.

Several questions follow, for which answers may provide additional confidence in the likelihood of success for the proposed Sandia closure of DCH issues in ice condenser plants.

QUESTIONS

1. What study is envisioned for quantifying the ice condenser efficiency? The accepted pattern is a combination of theoretical model development and validation experiments in order to predict actual phenomena, before incorporating into a system level program. Would this require something like a full height, partial segment of an ice condenser? Or is there sufficient available data to develop, validate, and apply to containment analyses with reasonable confidence?
2. Exactly what kind of DCH mitigative features of the ice condenser (suggested in the report) have not yet been adequately modeled to take advantage of their influence?
3. Direct contact of molten debris on the containment wall was mentioned as an attack mechanism not included in determination of CCFP. What kind of further assessment does this possibility require?
4. Since DCH is less of an issue with lower vessel pressure at breach, would the probability of HPME be the most likely contributor to a successful closure, followed, as mentioned in NUREG/CR-6427, by convolution with the containment fragility properties, for the worst splinter scenario if it could be identified beforehand?
5. It has been determined that if operable prior to vessel breach, the ignitors would reduce CCFPs to within the closure range. Realizing that unrecovered SBO events can preclude the ignitor function, would the addition of DC ignitors to accommodate SBO introduce major concerns and further probability distributions of their own, making them much less preferred than reducing the CCFPs by successive refinement? We know the pros. What are the cons of DC ignitors?
6. In what way would sprays affect DCH scenarios?

The rest of this discussion is a rambling commentary on those discussion points in NUREG/CR-6427 which appear to be significant in arriving at DCH issue resolution in the ice condenser plants. It also will serve to display any erroneous concepts I may have adopted.

CONTEXT OF DCH RESOLUTION AND ICE CONDENSER PLANTS

My conclusion from this study is that further refinement by Sandia experts is probably the best choice for achieving DCH issue closure on ice condenser plants. A particular "momentum" seems to be present in the performance that Sandia has delivered in the past, which leads to anticipated acceptable CCFP determinations for ice condenser plants. This anticipation is largely based on earlier opportunities to peer-review their work on DCH closure for other PWRs.

CCFP Determinations

The CCFP is structured around the two-cell-equilibrium, TCE, model, which employs macroscopic gas state equations to relate containment pressure to the internal energy, resulting from steam discharge convected energy, and thermal energy transfer from molten debris, as well as metal/water interaction, hydrogen production, and burning. The DCH load can be determined for a range of parameters, including debris mass and metal content, vessel pressure at the time of breach, and containment geometry and initial state. Comparison or convolution with the containment strength properties yields a CCFP value to be compared with the limit established for issue closure.

System programs like SCDAP/RELAP5 are used to predict the core melt progression, leading to debris conditions at the time of discharge. The CONTAIN program is employed in establishing initial conditions in the containment, including the presence of water, at discharge.

It follows that a rigorous multisource energy addition can be obtained for use in the TCE to predict the distribution of possible containment pressures and other state properties.

Zion and Surry Plants

The DCH issue resolution methodology was developed and applied to the Zion and Surry plants. The procedure involved initial screening, and subsequent refinement as needed to demonstrate acceptable CCFP values. Currently, when the initial screening criterion is satisfied, for which the $CCFP < 0.01$ for a given plant, the DCH issue is resolved without further consideration. Other plants that do not pass the initial screening criterion have been shown, with further refinement, to have $CCFP < 0.1$, for which the DCH issue is considered resolved. Plants with $CCFP > 0.1$ determinations at some stage of consideration require more detailed analysis to obtain a more accurate CCFP, by either

removing layers of excess conservatism, incorporating probability distributions for the likelihood of an event or condition in the process, or a combination of steps that include successive increments of available information.

The Zion and Surry exercises established the depth and flexibility of the methodology. The DCH load distributions were convoluted with the containment fragility properties to demonstrate CCFP values less than 0.1 for issue resolution. Both cases were based on the occurrence of an HPME. The likelihood of an HPME could have been factored into the determination, leading to a lower CCFP, but this was unnecessary because there were no intersections with the fragility curves. One of the proposed steps of refinement for the ice condenser plants is to include the HPME likelihood.

Ice Condenser Plants

The subject report notes that CCFPs below 0.1 were reported for ice condenser plants in early risk assessments of NUREG 1150. However, the present methodology, incorporated with splinter scenarios selected to bound all DCH loads for a credible range of initial states, showed that none of the ice condenser plants passed the criterion for DCH issue resolution. It is expected that additional analysis (refinement steps proposed by Sandia), involving the probability of high pressure at breach, a more rigorous load/strength analysis, and possibly integration of both, will demonstrate CCFP values less than 0.1. The current CCFP determinations are based on the assumption that the splinter scenarios do occur, without regard to their likelihood.

The plants without ice condensers (large dry or subatmospheric containments) passed either the initial screening $CCFP < 0.01$ (41 plants), or $CCFP < 0.1$. The ice condenser plants have smaller containments and higher hydrogen concentrations, causing the CCFPs to exceed 0.1 unless hydrogen is burned by the ignitors prior to breach.

If the ignitors are not available prior to vessel breach to control atmospheric hydrogen, it was found that the probability of hydrogen burning and significant containment pressurization was high. The presence of ice removes vapor from the atmosphere, leading to a richer hydrogen concentration. When ignitors are available prior to breach, the ice bed effectiveness appears to dominate CCFP. If ice does not remain at breach, or if it is not effective (uneven melting, etc.) the ice condenser plants do not achieve CCFPs less than 0.1. That is, CCFP determinations at the present level of refinement are less than 0.1 if atmospheric hydrogen is controlled prior to breach, and the ice condensers are effective. If these conditions are not satisfied, more refinement is needed to incorporate more detailed technology into the CCFP determination, as proposed by Sandia. Furthermore, the report notes that there are mitigative features of ice condensers, which require additional tools to analyze.

It was noted that the NSSSs for the ice condenser plants all have the same core size. Also, the containments were similar. Consequently, if one CCFP exceeded 0.1, the same result would be expected for each containment.

It was noted that the TCE model does not have the capacity for handling the effects imposed by the ice condenser. However, the TCE model is employed in a bounding approach to predict ice condenser containment pressure distribution from a dry basis. Pressure distributions from Zion were modified for ice condenser plants by incorporating ratios of containment gas energy changes per unit of available UO_2 and Zr masses (to account for energy addition from hydrogen) with that of Zion, based on the assumption of linear scaling.

It appears that the TCE model determination of DCH loads for ice condenser plants has proceeded rationally, capturing the differences in an acceptable way which is representative of expected results if the Zion plant was replaced by an ice condenser plant.

PURDUE UNIVERSITY



SCHOOL OF NUCLEAR ENGINEERING

March 13, 1997

Dr. M. Wayne Hodges, Director
Division of Systems Technology
Office of Nuclear Regulatory Commission
Washington, DC 20555-0001

Re: Review of a Draft NUREG/CR-6427 Report "Assessment of the DCH Issue with Ice Condenser Containments"

Dear Dr. Hodges:

In response to your request of January 21, 1998, I have reviewed the above draft NUREG report prepared by M. M. Pilch, et al. My comments are as follows:

1. Overall Evaluation

The report evaluates the effects of the DCH and related containment phenomena for the nuclear power plants with ice condensers in the containment. This report focuses on the possibility of extending the well-established methodology which is developed for the dry and large containment. The basic approach in this report is to highlight the three major characteristics. These are:

- small containment size
- ignitor effectiveness
- ice condenser effectiveness

I agree with this basic approach. However, the study in the draft NUREG/CR-6427 indicated that ice condenser containments as a group have the following characteristics:

- a) If they are treated as a small dry containment, the analysis shows that CCFP far exceeds the acceptable value of 0.01 for many scenarios. Therefore, this containment does not have the inherent robustness against DCH which is typical of the large dry containments studied previously.
- b) If the ignitors are available prior to the vessel breach to reduce the hydrogen concentration, the DCH load can be reduced. However, in many cases the CCFP far exceeds the value of 0.01. Therefore, the effectiveness of the ignitors alone may not lead to the DCH resolution.



c) The effective ice-condenser has the potential of mitigating the DCH problem. However, there is no ice-condenser model based on the first principles. Therefore, at this point we can only speculate on its effectiveness. This problem should be addressed in a scientific manner. Well scaled experiments and mechanistic model should be developed, and it should be implemented in the CONTAIN code or other simple stand-alone codes to evaluate the effectiveness of the ice.

2. Splinter Scenarios (Sections 5 and 8)

The splinter scenarios V, VI, VII and VIII with more detailed scenarios V, Va, Vb, VI, VIa, and VIb are introduced in Section 5. I agree that these are good splinter scenarios which highlight the special characteristics of the ice-condenser containments. In Section 8, the results of the analysis are presented for only V, Va, Vb, VI, VIa, and VIb. It is not clear what has happened to scenarios VII and VIII. There should be some statement on these.

3. Global Scaling Parameters (Section 4.2.1)

The four scaling factors introduced in this section are useful parameters to highlight the difference between the ice-condenser containments and dry containments. In the fifth paragraph on page 16, it is stated that "These differences occur because ice condenser containments are not as strong as large dry containments, and they are not as big." These two important characteristics of the ice condenser containments are reflected in the dimensionless parameter Φ_R . However, it will be useful for the readers of this report, if the authors can present actual typical differences in terms of the containment volume and the containment strength separately between the ice condenser containments and the large dry containments. This information can be useful and supplement Tables 5.1 to 5.8.

4. Sensitivity Study and CONTAIN Calculations (page 91 - 95)

Based on the assumption that the TCE model is overly conservative relative to the CONTAIN code predictions, sensitivity studies have been performed, and the relative bias is introduced. This bias is the ratio of the pressurization predicted from the CONTAIN to that of TCE. The bias was shown to be between 0.59 and 0.95. I am not sure that these numbers can be used to state that the TCE model is overly conservative and the CONTAIN prediction is closer to reality. It should be remembered that the TCE model is a very simple control volume approach; however, the coefficients of the models such as the coherency ratio are adjusted using the integral test data. The model, therefore, takes into account all the effects in an integral manner for the dry containment case. The CONTAIN code itself is a control volume based code with many non-physical models or correlations. The extrapolation of this code to the conditions beyond the data base is questionable. For the TCE model, we know the limitation and capability.

5. CONTAIN Code Use in Quantification (Section 6)

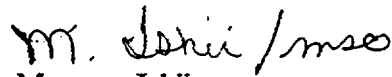
The use of the CONTAIN code for quantitative evaluation for the following phenomena is questionable. Even the qualitative evaluation of those can be considered questionable.

- FCI energetics in the reactor cavity.
- Water-debris interactions in the cavity .
- Ice condenser performance in general, and in particular, its performance during the DCH.

6. Minor Comments

page xii, 2nd paragraph, leach → each
page 17, item 1; $\Phi_R \rightarrow \Phi_m$?

Sincerely,



Mamoru Ishii

Professor of Nuclear Engineering

MI/mso



UNIVERSITY OF MARYLAND AT COLLEGE PARK

GLENN L. MARTIN INSTITUTE OF TECHNOLOGY ♦ A. JAMES CLARK SCHOOL OF ENGINEERING

CENTER FOR TECHNOLOGY RISK STUDIES

Dr. Mohsen Khatib-Rahbar
Energy Research, Inc.
P.O. Box 2034
Rockville, MD 20847-2034

February 23, 1998

Dear Dr. Khatib-Rahbar:

I have reviewed the draft copy of "Assessment of the DCH Issue for Plants with Ice Condenser," NUREG/CR-6425, dated October 1997. As in the previous reviews, I mainly focused on the probabilistic treatments discussed in the report. Therefore, views expressed in this letter reflect the process of assessing the containment failure probability, but not the adequacy of the physical processes involved. I have summarized a general comment first followed by a number of specific comments.

General Comment

I believe that if we estimate probabilities of events: "Igniter/ARF Available," "Cavity Flood," and "Ice Present in the Ice Condenser" instead of "splintering," and recalculate CCFPs for each plant, most likely CCFPs will be less than the 0.1 criterion. Since all these splintered events are assumed to occur independent of the HPME, the use of the criterion 0.1 for CCFP should still be valid. This seems to be more straightforward than pursuing HPME frequency estimation, or refining containment fragilities. I recommend that this be the next step to resolve the DCH issue for the ice condenser plants.

Specific Comments

1. Page xii , 2nd paragraph, line 8. Change "contain" to "CONTAIN."
2. Page 9, last paragraph. I have semantic problems with the discussions in this paragraph. The term "variability" when it is used to describe variations inherent in a given model due to nominally similar conditions (as preferred by ACRS) should be termed "aleatory uncertainty." Also, our lack of knowledge in constructing such a model should be called "epistemic uncertainty."

Accordingly the inherent variability observed by using the probabilistic framework in Figure 3.1 is the aleatory uncertainty, but the uncertainties expressed by pdf1-pdf5, CR1, and CR2 are epistemic uncertainties. Usually the epistemic uncertainty dominates aleatory uncertainty. Is it the case here too? I cannot find a convincing argument for this.

Further, I would avoid using "artificial probabilities," since other probabilities are not "natural probabilities." Using just "probability" or "degree of belief" would be better.

Finally, the last sentence of this paragraph: "We recognize. . ." is vague. I am not sure what is the point here and how significance it is.

3. Page 10 first paragraph. While it is true conceptually that multiplication of two "edge of spectrum" events based on the definition provided in Table 3.1 yields an "upper bound" event, the concept cannot be extrapolated to any other event likelihood values. For example, if one selects process likelihood assignments (1, 1/2, 1/10) then the argument no longer holds. Therefore, contrary to the conclusion of the paragraph, the judgmental degree of beliefs used for "process likelihood" have intrinsic meanings. These values are used to show our "relative degree of belief" on some process characteristics that are described in a convenient, but imprecise form. This qualitative form facilitates assignments of actual events and processes to these characteristics, and to the corresponding relative likelihood values. The qualitative grades used for these "relative likelihood" values are quite influential on the end results that we get.

4. Page 19, 3rd Paragraph. Some discussions about the type of events or class of scenarios that lead complete or partial melting of the ice would be helpful. Also, identifying the type or class of PRA level-1 scenarios that lead to the detonation following a vessel breach that may bypass remaining ice would enhance the discussions.

5. Page 64, Figure 5.3. The event "Ice Condenser Effective" has been referred in the text as situations where partial ice is available at the time of the vessel breach. There have been no discussions as to what percent of the ice remaining would make the ice condenser "effective." Also, it is not clear whether any other event would make the condenser ineffective. For example, there was a discussion earlier about the possibility of bypassing the ice condenser. Is this also included in this splinter event?

6. Page 87, 3rd Paragraph, 4th line from the bottom. As a matter of semantics I would delete ". . . stochastic uncertainty . . ." from the sentence. I would also change "confidence limits" to "probability limits." Finally the sentence before last in this paragraph is vague. Usually confidence limits (I prefer probability limits since this is not a classical statistical analysis) are used to show the quantiles of a random variable, not to differentiate between model and "stochastic" uncertainties.

7. Page 89, Table 7.1. The summary information provided in the last three rows which average all plants has no significance. I suggest deleting the last three rows.

8. Page 91, Equation 8.1. The concept of defining a physically-based measure of "bias" is good so long as assuming CONTAIN and TCE models contain the totality of all modeling uncertainties. Otherwise the ways that this problem was handled (i.e., using arbitrarily large biases) would be more appropriate. When the upper bound values of ΔP_{TCE} are used to calculate the "bias," is it mean or 95% quantile? Why not using a wider range of quantiles of ΔP_{TCE} (for example, mean, 90%, and 99%).

9. Page 93, First complete paragraph. NUREG-1150 calculations are "conditional" containment failure probabilities (conditional on having an HPME). I would eliminate the last sentence of this paragraph. Why should the NRC suggests to the plant owners what should they do, especially when the state of knowledge is still evolving?

10. Page 93, last paragraph. I would eliminate this whole paragraph. The discussions are too speculative.

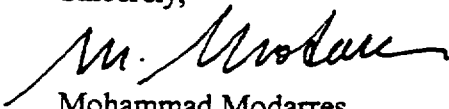
11. Page 94, Table 8.3. As a matter of completeness it would be important to repeat the calculations for Scenarios Va, VIa, and VIb.

12. Page 94. In light of the recommendation given in the comment No. 8, I would repeat Tables 8.2 and 8.3 for other bias values to effectively see the trends in the sensitivity of the CCFP to the pressure rise due to DCH.

13. Page 95, Table 8.4. Correct the value of "pressure rise" with ice present for the 2000-2500 psi events.

Thank you for giving me the opportunity to comment on this report. Please don't hesitate to call me at (301) 405-5226, if I can be of further help.

Sincerely,



Mohammad Modarres
Professor



Fauske & Associates, Inc.

March 13, 1998

Mr. Wayne Hodges, Director
Division of Systems Technology
Office of Nuclear Regulatory Research
U.S. Nuclear Regulatory Commission
Washington, DC 20555

Dear Mr. Hodges:

As you requested in your letter of January 21, 1998, I have reviewed the draft of NUREG/CR-6427, "Assessment of the DCH Issue for Plant With Ice Condenser Containments". To the extent that the objective of the effort is to document the results obtained when applying the previous resolution process for large dry subatmospheric containments to ice condenser containments, I find that the report is clearly written and a logical extension of the previous assessments. Furthermore, the report correctly incorporates the recent observations from the Sandia lower head failure test and also the extensive and continually developing literature basis for external RPV cooling.

However, the use of the TCE approach to evaluate ice condenser containments as "small dry" systems is, in fact, the application of an existing experimental basis to a pressure suppression containment that is fundamentally different than the scaled containment systems used to develop the experimental basis. The authors correctly identified this in the report. As a result, the conclusion developed is that "no ice condenser plant is inherently robust against all possible DCH threats" is developed assuming no contribution from the ice condenser. Since this is a fundamental part of the design, I am lead to the conclusion that the previous issue resolution process for large dry and subatmospheric containments is insufficient when applied to pressure suppression designs.

Given this, how should the process continue such that these types of containments can be evaluated? The authors provide directions in the conclusions and recommendations and these are certainly important elements to the evaluations. I suggest that the authors consider expanding the probabilistic framework for containment failure shown in Figure 3.1 to include additional elements along with the splinter scenarios considered for the different containment conditions. In this regard, the major questions are

- What are the conditions that would have to occur for insufficient ice to be available?
- What are the conditions necessary for hydrogen combustion event sufficient to challenge containment integrity with, and without, ice available?
- What are the necessary conditions to have a deeply flooded cavity to prevent lower head failure?

By increasing the probabilistic framework to include these questions, I believe that the important features of the ice condenser containment can be adequately represented and examined with respect to the subject of issue resolution. If this is the intention of the section in Chapter 9 identified as "Quantified Spectrum of Scenarios Leading to HPME", then I endorse the authors suggested approach. However, an important part of this is to include the pressure suppression containment response as part of the evaluation process since this is fundamental to the containment design.

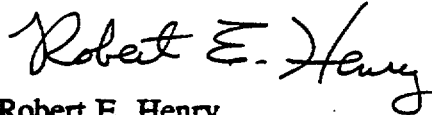
In this regard, there is a statement on page 48 that CONTAIN calculations were performed for scenarios Va and Vb and these calculate that the ice is completely melted in these evaluations. This is somewhat puzzling since small break LOCA sequences for the Westinghouse RCS designs have heat removal through the steam generators as long as water is available on the secondary side, which is approximately 1 hour without AFW injection. Furthermore, a typical licensing basis for an ice condenser containment is an ice mass of about 2.1 million lbm (955,000 kg) with the actual ice load being about 2.5 million lbm (1,136,000 kg). Assuming that decay heat is 30 MW and that the steam formed in the core melts the ice, about 3 to 3-1/2 hours is required to melt all of the ice. Moreover, there is additional energy absorption by the cold water as it spills out of the ice condenser drains and falls through the lower compartment which is approximately 40% of the melting energy. This adds at least another hour to the time necessary for complete ice melting. With no RCS injection, core damage would occur within 3 hours and the water inventory vaporized before core damage would be about 180,000 kg. Assuming this melts the ice and increases the water sensible heat by 30°C results in 576,000 kg melted. Therefore, at least 40% of the ice would remain. The fact that complete ice melt is calculated for the two scenarios mentioned is surprising and should be examined carefully in terms of how the sequences are defined. This would be an important element of an expanded evaluation that would investigate the ice condenser transient response to such postulated severe accident conditions.

In summary, within the framework of the previous issue resolution analyses, the result of this study is not surprising. However, this simply shows that the previous framework, which was experimentally based using DCH experiments for large dry and subatmospheric containment types is not sufficient to address the issue for ice condenser containments. The probabilistic framework identified for the resolution process has the proper format to be expanded to incorporate pressure suppression designs. Within this framework, the evaluation for the different system responses must be based more on integral analyses, rather than an experimental database. One should view this

report as the first step in the evaluations for ice condenser containments for this issue resolution process.

Should you have any comments or questions regarding by review, please feel free to call me at any time.

Sincerely yours,

A handwritten signature in cursive script that reads "Robert E. Henry".

Robert E. Henry
Senior Vice President

REH:lab

**Comments on the Review of the Report
"Assessment of the DCH Issue for Plants with
Ice Condenser Containments" (NUREG/CR-6427) by
M.M. Pilch, M.D. Allen, D.C. Williams, K.D. Bergeron, K.S. Quick,
and S.W. Hong**

General Comments

DCH is a complicated issue involving many phenomena. The issue is complicated even further by the number of engineered safety features found in the ice condenser plants. Because of the complexity of the issue, the authors frequently must make generalizations, use codes when data are not available, and rely on informed judgements in their attempt to resolve this issue. On the other hand, such an approach does not always lend itself to a rigorous treatment of the issues. However, within this context, the authors did a credible job of addressing the issues.

The following examples are given to illustrate the above points and are not intended to be inclusive.

1. Some times generalizations were made when the likelihood of a special case was small. However, it would be helpful for the authors to speculate on what would happen if the exception occurred. For example, even though the likelihood is considered small that a rapid release of steam and hydrogen could occur from the primary just before vessel breach (pg 23), what would the consequences be if it did happen? Even though the authors suggest that after examining the lower compartment geometry of an ice condenser plant, particles would have a hard time negotiating the turns necessary to be transported into the ice chest (pg 28), what would happen if they did? Other examples exist, but the main point here is whether the authors can comment on the consequences of special cases when generalizations are made.
2. Some of the conclusions are based on informed judgements, which can change with experience and new knowledge. For example, this was already discussed in terms of our improved understanding of metallic versus oxidic melt compositions from the early to the current predictions. Other examples that may be subject to change include the judgement required to assign values to η (Eq. 6.1, pg 71) when applying the TCE model to real plants, whose scales are significantly larger and geometries possibly different than test data. Another example involves a structural analyst's judgement of the actual failure mechanism for each specific and unique containment (pg 87), which affects the fragility curves. Other examples exist. Perhaps the authors can summarize parameters that require informed judgement prior to the method of solution, maybe at the beginning of Chapter 8.

3. The report relies on the SCDAP/RELAP5 code calculations for source terms to the containment, conditions inside the reactor pressure vessel (melt composition, primary water, etc.) prior to vessel breach. It would be helpful for the authors to comment to what extent the code has been validated under conditions pertinent to this report, like the quantities just mentioned. As another example, arguments have been constructed that depressurization will occur for many sequences due to the failure of the hot leg. Have there been any experiments to validate these predictions? If so, then the authors should include a discussion of these assessments in the report.
4. It would be convenient if assumptions that are key to the resolution issue are summarized prior to the method of solution, say at the beginning of Chapter 8. For example, it was assumed that PWRs with ice condenser containments will behave like Zion relative to RCS depressurization. Other assumptions are made for the TCE model, like ignoring the coejected water from the RCS during HPME (pg 73). This is not a requirement since the assumptions are interspersed throughout the report but it would aid the reader in assessing the model and method of solution.

Specific Comments

1. Why was a splinter scenario not considered for the case with igniters and ARFs both off (pg 39)? This would result in both high steam and high hydrogen content, which can produce higher combustion pressures than when the steam is removed, depending on the mixture composition. Was this explored as a bounding case versus Scenarios Vb and VIb when hydrogen burns augment DCH loads?
2. Water sprays were mentioned several times throughout the report but their effect was not explicitly included in the analyses. For example, the question was asked in Chapter 9 (pg. 96) if sprays will play a significant role in DCH-relevant scenarios. Why were the effects of sprays not included in this initial assessment? Water sprays have the potential to rapidly mix the dome region to create uniform conditions. This could be important prior to vessel breach (pg. 36, 5 paragraph), especially for the case that was ignored when large quantities of hydrogen and steam may be injected into the containment just before vessel breach and ARFs do not have time to mix. Or, as mentioned on page 75, the ability to mix hot jet combustion products during the DCH event. One caveat, however, is that the water spray flow rate may be substantially reduced or eliminated during the DCH event if the containment pressure (back pressure) exceeds the spray water system pressure.

3. As the report discusses, combustion of DCH-produced and pre-existing hydrogen can potentially augment DCH loads. The authors have limited the treatment of hydrogen combustion to time scales that contribute to peak loads. This approach is correct for pressure sensitive structures, like containments that have steel shells. However, containments that have lower frequency responses like reinforced concrete containments, are generally impulse sensitive. DC Cook may be a candidate to this type of loading since it has a reinforced concrete containment and is one of the least robust containments among the ice condenser plants considered in this report. The additional impulse could come from the combustion of DCH-produced hydrogen and deflagrations of pre-existing hydrogen that burn too slowly to contribute to peak pressure but still contribute to the impulse. Volumetric combustion may contribute although its time scale can be slower than deflagrations.
4. The point comparisons between TCE and CONTAIN in Table 6.2 suggest that TCE is conservative when predicting DCH loads when similar initial conditions are assumed. This result is not too surprising since, for the same conditions, one would expect CONTAIN to predict lower loads with the inclusion of several mitigative effects (heat transfer to structures, ice condenser, holdup of hydrogen, etc) not included in TCE. The authors did note that the CONTAIN calculations may have been nonconservative because of constraints placed on CONTAIN to compare with TCE. Instead of simply referring the reader to Appendix B, something that many readers may not take the time to do, it would be interesting to make at least some comparisons to illustrate the nonconservatism in the main body of the report, like in Table 6.2.
5. The report states that the working group expressed an opinion that water in the primary system at vessel breach is expected to mitigate the impact of DCH loads (pg. 72) although this opinion is balanced by the CONTAIN calculations (pg. B-18) that show the RPV water can both augment or mitigate DCH loads, depending on the scenario. Perhaps the authors could provide a balanced statement on page 72 and refer the reader to Appendix B for more details.
6. The clarity of the report would be improved if the description of the solution method at the beginning of Chapter 8 was expanded. The solution method depends on the material in Chapter 3 as well, which I sometimes found difficult to read. Chapter 3 could also be improved with additional detail. If possible, an example problem in Chapter 8 would greatly benefit the clarity of the solution method.
7. The report discusses the mitigative effect of atmosphere-structure heat transfer in the Zion and Surry geometries (pg. 28) and the authors feel that qualitatively similar

mitigative effects are expected for ice condenser plants. In an attempt to quantify this effect, is there more or less structure surface area (or mass) per containment volume in the ice condensers than Zion or Surry?

8. Were the hydrodynamic entrainment criteria (pg. 46) developed based on hole diameters as large as 0.4 m? If not, what uncertainty could exist on the amount of material that could remain in the vessel?
9. The report discusses that flame propagation is difficult to achieve in steam-laden atmospheres. However, since the DCH jet is a vertical "linear" ignition source, propagation can occur horizontally and not just downwards, relaxing the hydrogen concentration requirements for propagation.
10. Other minor comments and editorial corrections are included in the draft report.

LEVY & ASSOCIATES

3880 S. Bascom Ave., Suite 112
San Jose, CA 95124
408/369/6500
FAX 408/369-8720

February 18, 1998

M. Wayne Hodges, Director
Division of Systems Technology
Office of Nuclear Regulatory Research
Nuclear Regulatory Commission
Washington, D.C. 20555-0001

Dear Mr. Hodges:

As per your request of January 21, 1998, I have reviewed the draft copy of NUREG/CR-6427 and my comments, arranged in the increasing order of page number, are as follows:

1. Page iii, the Abstract does not describe the significant results of the study. For instance it could include the sentence from the Executive Summary "It was found that no ice condenser plant had a CCFP less than 0.1 for all possible scenarios, thus no ice condenser has the inherent capacity to withstand all credible DCH events." However, as explained later, I strongly urge that such a sentence be qualified here and every other place in the report by stating that no credit was taken for the ice condenser in those DCH calculations.
2. There is disagreement about the calculated DCH loads. In the Abstract and your letter, they are characterized as significantly lower than those in NUREG-1150, while on page xiii they are stated to be comparable. This needs to be fixed.
3. The Preface, the Introduction and the Executive Summary repeat themselves about the process and basis for DCH calculations. I recommend the repetition be reduced if not eliminated. Also, there is a large number of typos.
4. There is confusion about the CCFP value needed to resolve DCH. My understanding was that
 - a screening criterion $CCFP < 0.01$ was set originally to account for potential non conservatisms (e.g. in degree of metallics present in the molten material and the amount of molten material being ejected) or possible residual modeling concerns (e.g. coherence factor or lack of test data). This is so stated on page 6.
 - when potential non conservatisms or modeling uncertainties are shown to be small,

then a CCFP<0.1 becomes acceptable but it applies to all potential containment failure modes.

5. The confusion about the required CCFP value comes about from such statements as "the DCH issue is considered resolved for a given plant if the CCFP<0.1 for each of the splinter scenarios" (see first paragraph of page xiv). Furthermore, because of the complex behavior and the lack of DCH tests with ice condensers one might question the use of CCFP<0.1.
6. In my opinion, this DCH study for ice plants is not representative of their performance because it neglects the presence of the ice condensers. The CONTAIN study in Appendix B is much more typical of ice plants performance during DCH with ice condensers available. As stated in the last paragraph of page B-26, the "small dry" scenarios described in the main body of the report "are rendered relatively non threatening when the ice condenser is included. It would be my recommendation to rewrite the report so it is clear that all the DCH results derived up to Chapter 9 exclude ice condensers and are mostly atypical. Also, the CONTAIN results with ice condensers should be given preferred rather than second class status. This situation is recognized on page 4 where it is stated that "the TCE model has no features to model the impact of ice beds on DCH loads, so a bounding approach is adopted that models the containment with a "small dry" approximation. Lacking a fully relevant database for DCH in ice condenser plants, TCE predictions are supplemented with CONTAIN DCH predictions to explore the potential impact of ice beds on DCH loads. The CONTAIN assessments are given in Appendix B. The bounding TCE approach is not appropriate in my opinion and the CONTAIN results are much more relevant.
7. On page 7, first paragraph, it is stated that additional analyses for plants that do not meet the success criterion for the initial screening phase (i.e. CCFP≤0.01) will be formally documented in a separate report to the NRC. I am not aware that such a strategy has been pursued. Furthermore, the methodology of Figure 2-1 has not been applied to my knowledge to plants with CCFP≥0.1 after load strength evaluations.
8. The treatment of global scaling parameters starting on page 13 is unfair to ice condenser plants because it again neglects the ice condensers and the igniters. I recommend that we also show them at their best potential by plotting the pressure ratio after removing from the energy input to the containment the energy which could be quenched by the ice condensers. Similarly, it may be desirable to show the hydrogen concentration if the igniters are functioning. The ice plants most likely will fall between the worst and best of those ratio values.
9. At the bottom of page 17, it is stated that crediting these features (ice condenser and the igniter systems) will require tools for analyzing their effects as well as determining to what extent these systems will be available in the spectrum of accident scenarios of interest. Without crediting those features and having those tools, I doubt that one can get a fair picture of the performance of ice plants and it may be best to rely upon NUREG-

1150 or an upgraded version of it to get that picture. By the way, the sentence at the bottom of page 17 is incorrect.

10. On page 19, it is noted that the CONTAIN ice condenser model is not validated specifically for DCH conditions. There is a need to further discuss the impact of that statement upon Appendix B results.

11. The discussion in Section 4.2.2 shows that the CCFP for ice containment is much more complicated than for dry containment. It, also, points out that

- the melts used in NUREG/CR-6427 contain considerably less metal so that the ice condensers would be much more effective than in NUREG-1150.
- the bypass around the ice condensers may have been optimistic in NUREG-1150 and highly uneven ice melts could result from the use of the HECTR Code.
- there has been no effort to validate the CONTAIN ice condenser model and the model uncertainties may be large.
- the integrity of the ice condenser doors is not established fully.
- the availability of ignition sources prior to vessel breach is crucial to containment integrity.
- the operation of the air return fans (ARFs) would increase the degree of ice melt prior to vessel breach.
- global flame acceleration and/or detonations were not considered in NUREG-1150.
- molten debris could accumulate against the inner surface of the containment shell and cause its loss of integrity.
- when the cavity is flooded with water, it could react with the ejected melt and the "possibility of vessel displacement and its implications may merit further investigation".
- a large percentage of the debris entering the ice chest could be trapped there.

These items are listed here to reinforce the idea that the small dry model used in NUREG/CR-6427 is most likely inadequate and that even the results of NUREG-1150 deserve scrutiny if not an upgrade.

12. Section 5.0 is not very different from previous coverage for other PWRs. The following points may deserve more attention:

- on page 38, it is noted that only dry cavities were considered when there is a high chance that due to the ice melting the cavity would be flooded.
- the SCDAP/RELAP5 insights on page 39 fail to recognize the much closer coupling between the Reactor Coolant System (RCS) and the containment for ice containments and, in particular, that the containment pressure and compartment temperatures could be very different.
- the amount of Zr is 14% greater, the weight of UO₂ and the power density are 3% greater in ice vs Zion dry containments and they deserve some discussion.
- side peaked melt relocation and breaks were considered unreasonable; yet, they may have impact upon ice condenser bypass.

- trapping of hydrogen into the ice condensers and its burning impact within the condenser was not considered before the vessel breach. Also, trapping of molten materials within the ice condensers was not included.

13. Sections 6,7, and 8 again follow previous coverage for other PWRs except for the following points:

- on page 71, it is stated that there is no database directly relevant to DCH in ice condenser containments (which might require a CCFP goal of <0.01).
- on page 72, it is reported that validation of models predicting the impact of cavity water on DCH (even for large dry or subatmospheric containment) has been problematic. Yet the judgment is made at the top of the same page that a deeply flooded cavity will not lead to significant DCH loads.
- the fragility curve for the Cook containment is much worse than for other ice containments on page 90. This may deserve further study or discussion with the utility.
- the calculated CCFP for Scenarios Vb, VI, Via, VIB on page 94 are quite high and could provide the wrong picture. When CONTAIN was used with ice present, only Scenario Vb gave high CCFP values. That scenario deals with station blackout where containment cooling is restored but hydrogen igniters remain deenergized; i.e. the scenario is characterized by low steam concentration and high hydrogen concentration which might fail the containment if it burns.
- This result is not influenced much by the occurrence of DCH except that it provides an ignition source. The lack of igniters is best dealt with probabilistically and a summary of the licensing submittals would help diffuse this issue.

14. The following issues are raised in Appendix B.

- on page B-2, it is stated that in Appendix B “there has been no consideration of other issues such as dynamic loads associated with accelerated flames or detonation, fuel coolant interaction (FCI) effects, cavity pressurization following vessel breach and its consequences or thermal failure of the containment resulting from debris accumulating against the shell”.
- on page B-3, the issue of uneven melting of ice and of gas distribution is raised; on page B-4 the possibility of detonable hydrogen mixtures in the ice condenser volume is mentioned; page B-5 damage and lack of full reclosure of the ice condenser doors is discussed briefly; on page B-10, questions are raised about the hydrogen combustion models; on page B-12, it is noted that CONTAIN has no fuel coolant interaction model.
- on page B-14, the uncertainties associated with co-ejected water are raised and on page B-31, it is stated that co-ejected water becomes the dominant issue when the hydrogen is burned off and there is no ice remaining.
- on page B-30, it is noted that there has been no major effort to validate the CONTAIN ice condenser model and that there is no data under DCH conditions and the crowning blow appears on page B-26 when it is stated that “there is, of course, no expectation that the present study alone can resolve DCH for scenarios in which ice is available in the ice condenser”.

The above statements jeopardize any reliance that might be placed upon the CONTAIN results provided in NUREG/CR-6427 and they also raise questions about the validity of NUREG-1150 results.

CONCLUSIONS

1. I recommend against publishing NUREG/CR-6427 in its present form.
2. The small dry containment TCE method for DCH may do more harm than good to ice containments because it neglects the benefits of ice condenser and igniter systems. Its only benefit, in fact, is to show that, when there is no ice left, the TCE method calculates equivalent or lower loads than those reported in NUREG-1150. This is not surprising because NUREG/CR-6427 ejects less molten material and less metallics than NUREG-1150.
3. When ice is present the TCE method is over conservative and inappropriate and CONTAIN should be the tool of choice to calculate CCFP. However, most of the concerns raised in item 14 must be dealt with if the CONTAIN results are to be believed. In particular, lack of DCH test data for ice containments, verification of CONTAIN, bypass or uneven melting of ice condensers, damage to ice condenser doors, and coejection of water must be assessed and shown to produce reasonable uncertainties.
4. When the igniter system is unavailable neither the TCE or CONTAIN are the correct tools. This issue is best handled probabilistically and an Appendix summarizing licensing submittals on that topic should be included to explain why the present designs were accepted.
5. Similar conclusions to the above proposal are reached on pages 71, 96, and 97 of NUREG/CR-6427. They are the only way to present a fair picture of ice containments. The magnitude of such a task, however, should not be underestimated.

I hope that the preceding comments are helpful to you and the authors. I shall be glad to explain them further if necessary.

Sincerely yours,


Salomon Levy

cc Dr. R. Lee, NRC

APPENDIX E
Peer Review of Revised NUREG/CR-6427



UNIVERSITY OF MARYLAND

GLENN L. MARLEN INSTITUTE OF TECHNOLOGY,
A. JAMES CLARK SCHOOL OF ENGINEERING,
DEPARTMENT OF MATERIALS AND NUCLEAR ENGINEERING,
RELIABILITY ENGINEERING PROGRAM

2100 Marie Mount Hall
College Park, Maryland 20742-7531
301.405.6659 TEL 301.314.9601 FAX

1 November, 1999

Dr. Mohsen Khatib-Rahbar
Energy Research, Inc.
P.O. Box 2034
Rockville, Maryland 20847-2034

Dear Dr. Khatib-Rahbar

I have reviewed the new draft of NUREG/CR-6427 (October 1999), "Assessment of the DCH Issue for Plants with Ice Condenser Containment." As before, I concentrated on the probabilistic evaluations. In my earlier review of this report I suggested to perform uncertainty calculations. The current report recognizes this need and only suggests that it be done in the future. Clearly any regulatory decision based on the results of this study without a clear representation of uncertainty would be difficult. I had also suggested to closely tie the actual frequency of core damage for high-pressure scenarios, with the total unconditional LERF/DCH frequency, whereby making them within the ranges of acceptable risk-informed guidelines (e.g., Reg. Guide 1.174.) The process would have been more consistent with the current trends and approaches proposed for risk-informed calculations in Reg. Guide 1.174.

I have no reservations or concerns regarding the technical accuracy and adequacy of this report. My major concerns discussed in my September 13, 1999 letter have been adequately addressed. The report is commendable and the Sandia team should be congratulated.

Thank you for giving me the opportunity to comment on this report.

Sincerely yours,

A handwritten signature in cursive script, appearing to read "Mu. Modarres".

Mohammad Modarres
Professor



UNIVERSITY OF MARYLAND AT COLLEGE PARK

GLENN L. MARTIN INSTITUTE OF TECHNOLOGY ♦ A. JAMES CLARK SCHOOL OF ENGINEERING

CENTER FOR TECHNOLOGY RISK STUDIES

13 September, 1999

Dr. Mohsen Khatib-Rahbar
Energy Research, Inc.
P.O. Box 2034
Rockville, Maryland 20847-2034

Dear Dr. Khatib-Rahbar

I have reviewed NUREG/CR-6427, "Assessment of the DCH Issue for Plants with Ice Condenser Containment." My review was limited to the probabilistic assessments and calculations, and due to the limited scope of my review I did not attempt to independently verify the adequacy, technical basis and accuracy of the various probabilities used. Nor I examined adequacy of the simplified event trees. Therefore, my comments are limited to the probabilistic process itself and I have identified obvious errors or inconsistencies. I have three general comments and a number of more specific comments.

General Comments

1. The study did not perform uncertainty calculations because this was "out of scope." I believe that while the probabilities used are quite uncertain and some appear to be highly subjective guesses, use of the results without proper uncertainty considerations for decision making is impractical and contrary to a valid risk-informed approach. Considering the fact that uncertainty estimates in the NUREG-1150 results for similar events usually spread over two orders of magnitude, it is necessary to perform uncertainty calculations. The amounts of effort to do this analysis, especially since small event trees are developed and used, should not be large. I recommend to include uncertainty calculations, not only for this effort but also for any other best estimate calculation in which highly uncertain data are used and the results are employed in regulatory decision making.
2. Considering the actual frequency of core damage for high-pressure scenarios, for the resolution purpose I would prefer using the total LERF/DCH frequency value instead of the conditional probability of HPME/DCH. I suspect that the LERF/DCH values will be below 10^{-6} /year for all ice condenser plants, whereby making them within the ranges of acceptable risk-informed guidelines (e.g., Reg. Guide 1.174.) The process will also be more consistent with the

current approaches proposed for risk-informed calculations in Reg. Guide 1.174.

3. In many places the report interchangeably uses "frequency" and "probability." This must be corrected. Typically, in PRAs scenarios involving an initiating event is measured by frequency (per year). Probability is used when the scenario is conditional upon occurrence of an initiating event and possibility some other events.

Specific Comments

1. Page 7; 4th line. Change "interval" to "internal."
2. It is unclear that by using class of core damage initiators instead of class of core damage states, how the frequencies of scenarios leading to high-pressure core damage were selected? A discussion may clarify the process.
3. A benchmark of the simplified event trees against NUREG-1150 trees only verify conformance with NUREG-1150 results. It does not necessarily prove that the trees are adequate or accurate.
4. Table 4.2; 2nd Column. Use $D > 2$ " instead of $D < 2$ ".
5. Table 4.2. Are the probabilities for Slow and Fast SBO represent "induced LOCAs"? Are LOCA probabilities include both transient-induced and actual LOCA initiators? Please clarify this in the table.
6. Table 4.2. Probabilities for "Transient" CDI are missing.
7. Table 4.3. While I did not independently verify the probabilities in this and other tables, the report provides no discussion of the technical basis for these probabilities. Also in Table 4.1 it showed that IPEs only consider 0.375" - 6 " breaks for small LOCAs. Accordingly, I am not sure how accurate the leak data will be if IPE results are not used (since only break sizes of NUREG-1150 are employed).
8. Section 4.1.2. Use of a uniform distribution from 0 to 1 with mean of 0.5 for PORVs and SRVs sticking open confirm importance and need for a well-organized uncertainty calculation in this study.
9. Table 4.7. It is not clear what leak rates for RCPs are used for Catawba, McGuire, and D.C. Cook.
10. Page 40. 2nd Paragraph. It is indicated that because of a lack of reliable HRA methodology no credit is given to operator intentional RCS depressurizations after UTAF, whereas Table 4.8 suggests probabilities for this action. Are these used or not? If not, then Table 4.8 adds confusion. In general, I feel that intentional depressurization should be carefully studied as an accident management measure for the future. For example what is its impact, should operators be required to depressurize.
11. Section 4.1.5. It appears that the most significant difference with NUREG-1150 and this study is the inclusion of a better pump seal leak modeling, characterization and probability estimation. It is important to note the impact of this event on the HPME conditional probability. For large-scale leaks the impact should be high. I am not sure if this is clarified well enough in this report.
12. Reducing the probability of hot leg or surge line failure from 90% to 50% will clearly result in no major changes. Sensitivity studies should go to some extreme values to measure the rate of change. For example 0.05 may be more appropriate.
13. Page 46. Last paragraph. The AC recovery in slow SBOs is not credited because the

probability of its success is 0.153 (or about 0.85 probability non-recovery). This value seems to be in line with other events in the simplified event tree. So, this value is relatively significant and should be included.

14. Page 57. Table 4.19 and 4.20 are out of order.
15. Page 57. It is indicated that McGuire and Watts Bar have high frequency of SBO frequency. The data in Table 4.20 show that D.C. Cook and Sequoyah have high SBO frequencies. Is this an error? The data in Table 4.23 appear to be correct. The data for SBO frequency in Table 4.23 are inconsistent with those in Table 4.20.

Thank you for giving me the opportunity to comment on this report. If you have more questions please don't hesitate to contact me at modarres@eng.umd.edu or (301)405-5226.

Sincerely,



Mohammad Modarres
Professor

PURDUE UNIVERSITY



SCHOOL OF NUCLEAR ENGINEERING

November 3, 1999

Dr. M. Khatib-Rahbar
Energy Research, Inc.
PO Box 2034
Rockville, MD 20847

Re: Review of the final draft NUREG/CR-6427

Dear Dr. Khatib-Rahbar:

I have reviewed the final draft of NUREG/CR-6427, "Assessment of the DCH Issue for Plants with Ice Condensor Containments." I have already reviewed the draft report twice. The authors responded to the comments and the last draft report was reasonably satisfactory. As I stated in the last review of the draft report, the authors did quite a good job in assessing the DCH issue in the ice condensor plants with the given conditions of the available data and budget.

I addressed one point, which was not directed to the author, but to the NRC. This is related to the inconsistency in terms of the early containment failure analysis between the present NUREG/CR-6427 and the NUREG-1560. The NUREG/CR-6427 showed that the ice condensor plants are substantially more sensitive to early containment failure than PWRs with large dry or subatmospheric containments. However, NUREG-1560 showed that many PWRs with large dry or subatmospheric containments reported early containment failure probabilities in excess of 10% given a core damage, while all the ice condensor plants reported much less probabilities. The conclusion of NUREG-1560 seems to be wrong after the detail evaluation of the DCH issue for the large dry containments. It may be necessary for the NRC to amend the conclusion of the NUREG/CR-1560 in view of the new insight to the DCH issue.

As far as the NUREG/CR-6427 is concerned, the author did an excellent job and considerably improved the early draft report in view of the comments from the peer review as stated in the Executive Summary. At this point I am satisfied with the report and recommend the NRC to publish it as it is.

Sincerely,

A handwritten signature in cursive script, likely belonging to M. Ishii.

M. Ishii
Professor of Nuclear Engineering

MI/mog



PURDUE UNIVERSITY



SCHOOL OF NUCLEAR ENGINEERING

September 17, 1999

Dr. M. Khatib-Rahbar
Energy Research, Inc.
PO Box 2034
Rockville, MD 20847

Dear Dr. Khatib-Rahbar:

I have reviewed the draft report NUREG/CR-6427 and the Sandia's response to the reviewer's comments.

Unlike the review of the earlier DCH issue resolution reports, this time Sandia did not prepare the point-by-point reply and subsequent revision outlined for each comment. Instead, Sandia added two essentially new sections of i) event tree analysis and ii) CONTAIN code predictions. It was a little more difficult to evaluate what exactly has been done to each comment than the previous DCH report cases. However, the overall strategy was clear and the conclusion was also clear.

The direct application of the DCH issue resolution methodology in NUREG/CR-6075 (using the probabilistic comparison of DCH loads versus containment strength) to the Westinghouse plants with ice condenser containments leads to considerable difficulties due to two major uncertainties. One is the general behavior of the ice up to the vessel breach and the corium dispersion with or without ice during the DCH event.

The revised draft report NUREG/CR-6427 addresses those points from several angles. For the effect of the ice beds, the CONTAIN code which was benchmarked against Waltz Mill data for the design base accidents was used. Although the data do not represent the DCH condition, the prediction of the ice condenser behaviors before the vessel breach by the CONTAIN code becomes much more credible following this benchmark.

The accurate prediction of the DCH itself for the plants with the ice condenser remains to be difficult as pointed out in the report. The debris dispersion process and the interaction of the debris and ice during the DCH for these plants are not extensively studied. Both the TCE model and CONTAIN model are not benchmarked against well scaled realistic integral test data, nor they are based on the detailed mechanistic models. As such large uncertainties remain in the DCH prediction of the plant with ice condensers.



The Sandia researchers went around this problem by demonstrating:

1. Non-DCH hydrogen combustion and non-explosive steam spike for station black out (SBO) and non-SBO cases dominate the overall early containment failure probability.
2. High pressure melt ejection probability is relatively small.
3. SBO frequencies are small.
4. In non-SBO events melt is ejected into deeply flooded cavities which tend to reduce the DCH load.

When these results from the event tree analysis and others were combined, a major conclusion was reached. This essentially states that the early containment failure probability is dominated by non-DCH hydrogen combustion events rather than DCH or linear melt through. However, it also can be said that the DCH with the hydrogen combustion will certainly threaten the containment. In essence the containment of the ice condenser plants can be challenged even without considering the DCH. The DCH contribution for the total early containment failure probability is relatively small.

This approach based on the event tree analysis did not lead to the accurate prediction of the containment failure probability due to the DCH phenomena. However, it made the DCH as a side issue in the overall evaluation of the containment effectiveness. The ice condenser plants are substantially susceptible to early containment failure than plants with large dry containment.

The authors mentioned that this conclusion is not consistent with the individual plant examinations reported in NUREG/1560. It is now the responsibility of the NRC to resolve these differences. The NRC cannot stand on these inconsistent conclusions and accept both of them as accurate and reliable analyses.

Sincerely,



M. Ishii

MI/mog



Fauske & Associates, Inc.

November 8, 1999

Dr. Mohsen Khatib-Rahbar
Energy Research, Inc.
Post Office Box 2034
Rockville, Maryland 20847-2034

Dear Mohsen:

As you requested I have reviewed the latest revision of draft NUREG/CR-6427 relating to direct containment heating loads in ice condenser containments. Since my comments on the previous draft focused on Chapter 5, I have concentrated on that aspect in this review. In general my comments have been address in the text. There are additional experiments that can be referenced that are relevant to these evaluations which can, and should be, referenced. These are detailed below.

In the previous review, I asked to be provided the information on the benchmark activities of the CONTAIN code with the Waltz Mill ice condenser experiments (Appendix Z). These have been provided, I have reviewed the information and I find that the appropriate comparisons have been made. In particular, the focus of the benchmarks was on calculating the containment pressure history for both large break and small break conditions as well as the code capabilities to calculate the water drain temperatures in the bottom of the ice box as well as in the simulated lower compartment for the experiments. Through these comparisons with large scale experiments, the reviewer can have confidence that the CONTAIN models are adequately representing the ice melt behavior for the spectrum of accident sequences addressed. Thus, this has adequately addressed my questions posed in the previous review. I strongly recommend that such benchmarking activities be made a permanent part of plant evaluations for future assessments of all plants and for future assessments of ice condenser plants if the CONTAIN model has any updates/error corrections, etc.

I am somewhat confused by the discussion of the dry cavity cases summarized on page 94. In particular, the third bullet says "the absence of ice in the ice condenser system implies containment challenging pressures, but neither is containment threatening". There evidently are words missing here and it is an important point. This needs to be examined and clarified.

There is a substantial discussion related to the influence of deeply flooded cavities given a DCH event and how this relates to both SBO and non-SBO sequences. One of the important aspects discussed in this revision is the extended time interval between core damage and the failure of the reactor vessel. Certainly the available experimental results and the TMI-2 accident experience demonstrate that there would be a substantial interval before the vessel would fail and as a result, there would be additional ice melted. This would leave less ice available to mitigate the consequences of a DCH event, but would also increase the ice inventory in the containment lower compartment. There are leakage paths between the lower compartment and the reactor cavity through the ex-vessel nuclear instrumentation that penetrates the

biological shield. Consequently, this extended interval before RPV failure also provides time for water to drain into the reactor cavity. Hence, this would increase the water inventory in the reactor cavity at the time of vessel failure.

The draft report has a discussion on the influence of accumulated water in the reactor cavity and previous CONTAIN calculations (version 1.2) have suggested that a water inventory of approximately 10 tons would augment the containment pressurization. The current draft states that "More phenomenological attempts at modeling cavity water and limited experimental data generally do not support the enhancement of containment pressures shown in case VI-c/5". As additional support for this state, I suggest referencing the experimental data on the influence of accumulated water in containment reported by Sargent & Lundy and documented by Kolflat (1960) as well as Thompson and Beckerley (1973). Figure 1 illustrates the configuration used for these experiments with the rapid blowdown of high pressure saturated water into a containment vessel with varying masses of cold water in the bottom. Figure 2 illustrates the results in terms of the net containment pressurization as a function of the break location and initial mass of cold water in containment. A rupture location at the bottom of the high pressure vessel is the most pertinent set of experiments for this evaluation and these data show that cold water in the containment is very influential in terms of limiting the containment pressurization. Even though these experiments are for discharging of high pressure flashing two-phase mixture into cold water, the net influence of discharging directly into an accumulated cold water mass is clearly evident on a similar transient response time (a few seconds) as is of interest for DCH. These results are relevant to the conclusion and should be added as supporting evidence. Moreover, before CONTAIN is used to assess the relevance of accumulated water in containment, the code models should be compared to these experiments in the same manner that they were compared to the large scale Waltz Mill ice condenser experiments.

Another aspect of the extended time to vessel breach is the length of time that the reactor vessel would be at an elevated temperature. If there is a significant hydrogen concentration in the lower compartment and the reactor cavity, the natural circulation flow between these two regions should also circulate the high hydrogen content next to the overheated reactor vessel. As a result, one would expect that the reactor vessel would act as an igniter for hydrogen-oxygen recombination in the near vicinity reactor vessel during this extended interval. It is not necessary that such calculations be added to the report, but it should be noted that the high temperature surface of the reactor vessel would act as a source for ignition that would promote recombination during some of the extended interval that the vessel could be at high temperatures before failing. Certainly the technical basis suggests that hydrogen-oxygen mixtures exposed to such temperatures would react and this could also enhance the natural circulation flows between the reactor cavity and the lower compartment.

On page 105, it is stated that "We acknowledge the potential for explosive melt-water interactions in the cavity and speculate that such events might blow out the walls of the free standing cavity or displace the RPV." While the potential for explosive melt-water reactions should always be acknowledged when there is a high temperature melt contacting water, the numerous KROTOS experiments with melt uranium dioxide and $\text{UO}_2\text{-ZrO}_2$ mixtures should be referenced here as part of the technical basis. While these experiments demonstrated strong explosive interactions for molten aluminum oxide and water, no significant explosive interactions were observed when reactor materials were used in the same test apparatus (see the attached references). This was also the conclusion from the COTELS experiments (Kato, 1999) injecting molten uranium dioxide into water. Hence, significant steaming rates are part of the accident scenario, but the experimental basis does not support that molten $\text{UO}_2\text{-ZrO}_2$ mixtures poured or injected into water would cause such explosive events. I recommend that these references and a statement of their important findings be added to provide the necessary experiments perspective.

Lastly, there are several typos that should be corrected in Section 5 since this is the heart of the conclusions. These are listed below.

1. Second sentence of page 87 should read "...Zion plant and typical reactor cores for ice condenser plants."
2. Page 91, the middle of the second paragraph should read "As we will show, ...".
3. At the end of the second paragraph in page 91, "id" should be "is".
4. First sentence in the second paragraph on page 93, "o" should be "to".
5. In the third paragraph on page 93 "2.3 MPa" should be "0.23 MPa".
6. On page 98 the last sentence of the first paragraph should read "...the predicted ice inventory that results from using...".

In summary, the authors have been responsive to the comments provided in my previous review. I have provided some additional experimental references that would be helpful to the authors in supporting their conclusions. Since this also provides the necessary technical basis for the Nuclear Regulatory Commission, I suggest that these be added to the technical basis to further support these conclusions. Should you have any questions regarding my review, please feel free to call at any time.

Sincerely yours,



Robert E. Henry
Senior Vice President

REH-lab

References

Kolflat, A., 1960, "Results of 1959 Nuclear Power Plant Containment Tests," Sargent and Lundy Report SL-1800.

Thompson, T. J. and Beckerley, J. G., 1973, The Technology of Nuclear Reactor Safety. Volume 2: Reactor Materials and Engineering, Edited by Thompson and Beckerley, the MIT Press, Massachusetts Institute of Technology, Cambridge, Massachusetts, pp. 767-769.

REFERENCES

- Hohmann, D. et al., 1995, "FCI Experiments in the Aluminum Oxide/Water System," Nuclear Engineering and Design, Vol. 155, pp. 391-403.
- Huhtiniemi, I. et al., 1995, "FCI Experiments in the Corium/Water System," Proceedings of the International Meeting on Nuclear Reactor Thermal-Hydraulics, NURETH-7, Saratoga Springs, New York, Sept. 10-15, NUREG/CP-0142, pp. 1712-1927.
- Huhtiniemi, I. et al., 1996, "Test Results and Analysis of Recent KROTOS Experiments," ANS Proceedings National Heat Transfer Conference, Aug. 3-6, 1996, Houston, Texas, pp. 27-42.
- Kato, M. et al., 1999, "Fuel Coolant Interaction Tests Using UO_2 Corium Under Ex-Vessel Conditions," Paper Presented at the SARJ-98 Meeting, JAERI-Conf-99-005, Tokyo, Japan, pp. 304-309.
- Magallon, D. et al., 1998, "FARO in the 5th Framework Programme of the European Commission (1999-2002)," Paper Presented at the SARJ-98 Meeting, Tokyo, Japan.

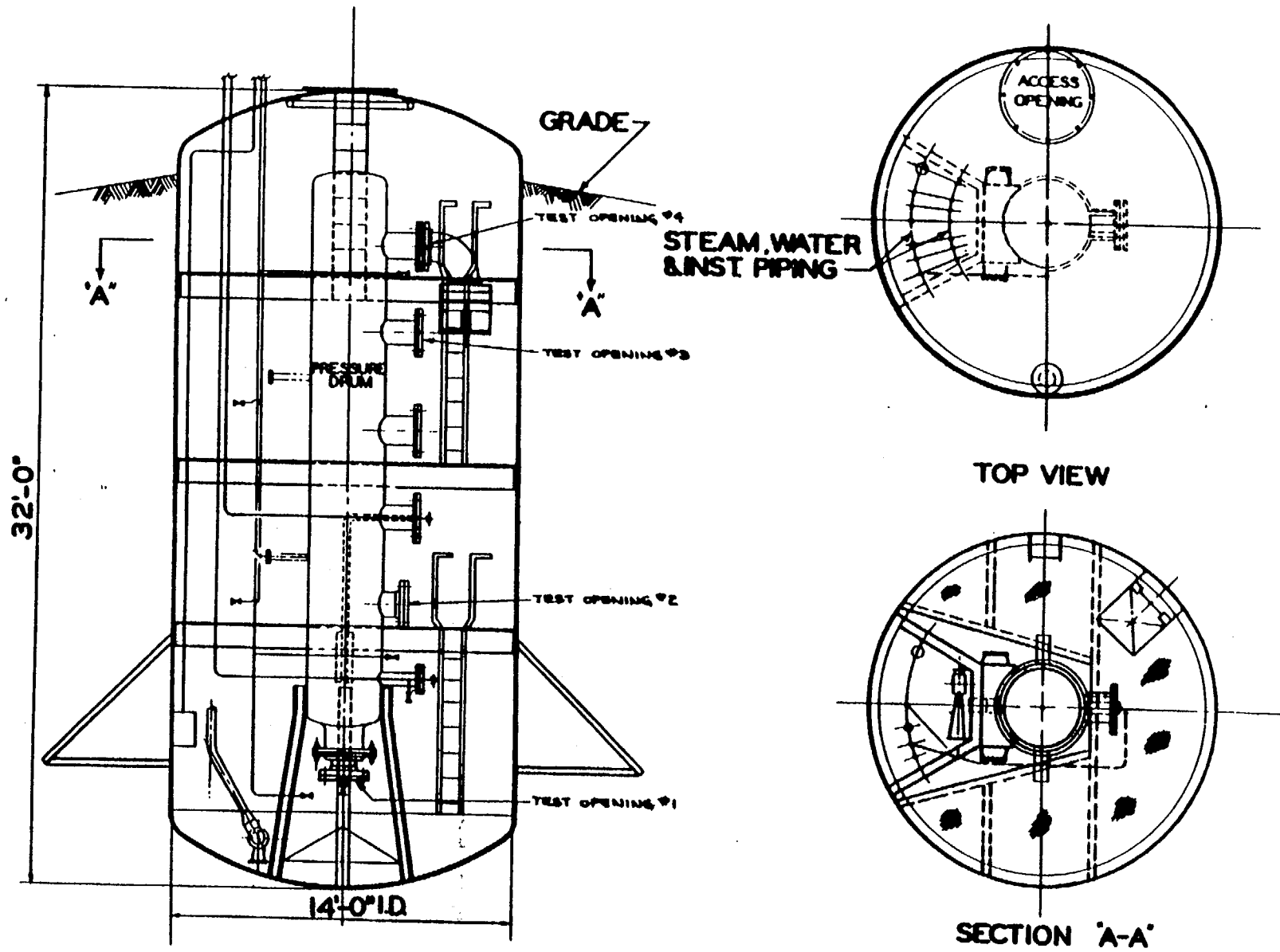


Figure 1 General arrangement containment test.

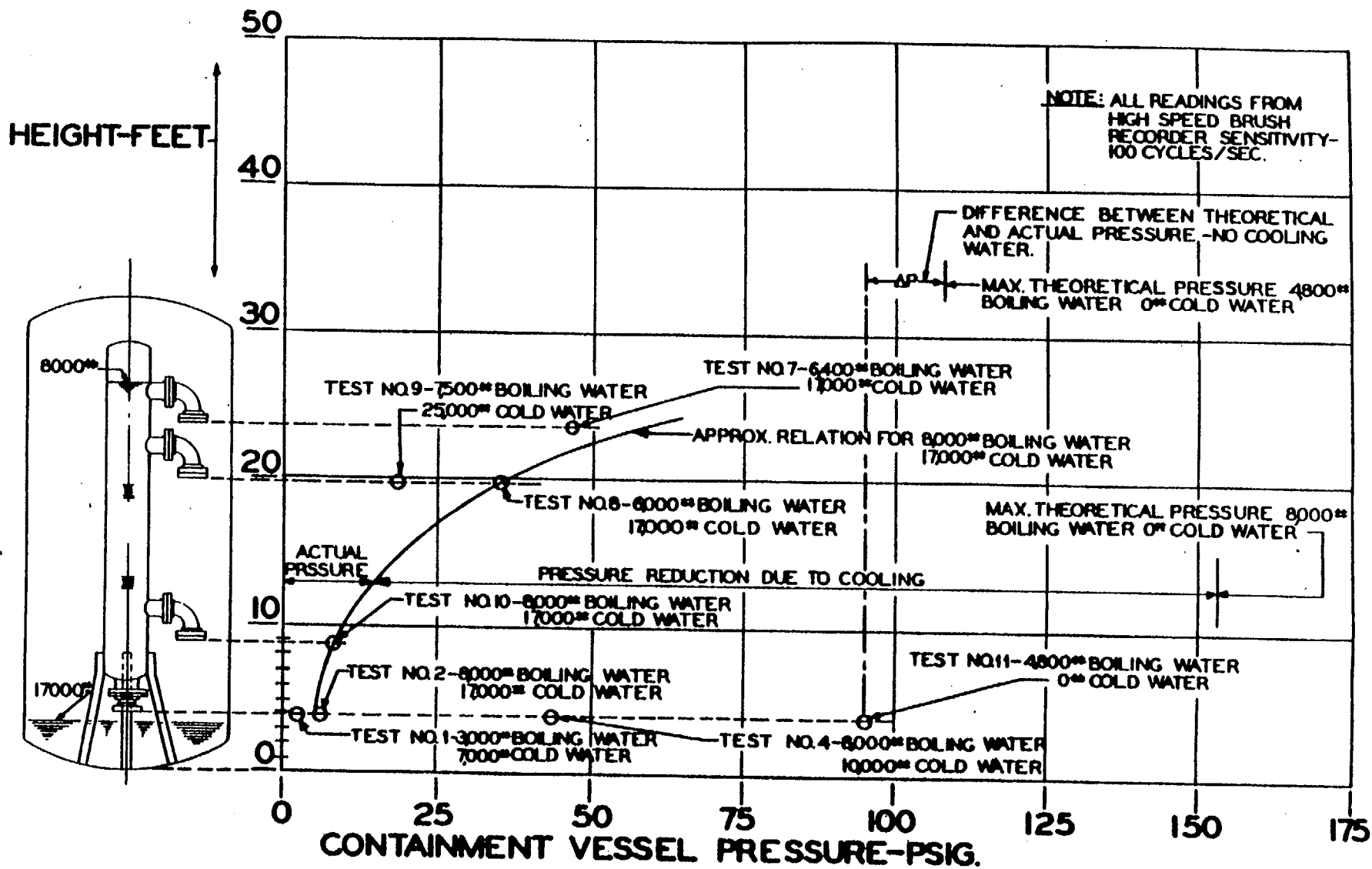


Figure 2 Containment vessel pressure vs. height.

Stamps

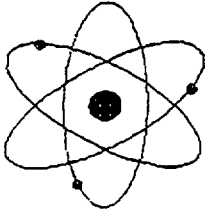
**Comments on the Review of the Final Draft Report
"Assessment of the DCH Issue for Plants With Ice Condenser Containments"
(NUREG/CR-6427) by**

M. M. Pilch, K. D. Bergeron, and J. J. Gregory

General Comments

I have reviewed the NUREG/CR-6427 report and found that my specific comments have generally been addressed.

I would recommend that a new statement added to the Abstract be moved to the Summary and Recommendations chapter. The new statement discusses the justification provided by the utilities not to install additional hydrogen control for SBO because of cost/benefit studies. The reason I suggest moving this statement is that the Abstract should be a terse summary of the work performed *in this project*, not a study performed by the utilities.



ENERGY RESEARCH, INC.

P.O. Box 2034
Rockville, Maryland 20847

FAX NUMBER: (301) 881-0867

VERIFICATION: (301) 881-0866

| | |
|---|------------------|
| TO: | Richard Lee |
| ORGANIZATION: | NRC |
| FAX NUMBER: | (301) 415-5074 |
| VERIFICATION NUMBER: | (301) 415-6795 |
| FROM: | Tracey Mullinix |
| DATE: | October 29, 1999 |
| NUMBER OF PAGES: (INCLUDING COVER) | 2 |

REMARKS:

Doug Stamps review attached.

305-845-3117
To: Marty →
From: Richard
10/29/99

- 1 -

**Comments on the Review of the Revised Report
"Assessment of the DCH Issue for Plants With Ice Condenser Containments"
(NUREG/CR-6427) by**

M.M. Pilch, M.D. Allen, K.D. Bergeron, D.C. Williams,
J.J. Gregory, K.S. Quick, and S.W. Hong

General Comments

The authors made significant changes to this report based, at least in part, on the comments of the peer reviewers. These changes have resulted in an improvement in the approach taken in this report.

The approach taken was to expand the probabilistic framework by developing a simplified containment event tree to quantify the HPME probability and early containment failure probability for a set of core damage indicator classes. Four phenomena were identified that could contribute to early containment failure and the CONTAIN code was used in part to quantify containment loads under representative conditions.

The CONTAIN code was used in this revised report instead of the TCE code to calculate containment loads. This is an improvement since CONTAIN can model the mitigative features of an ice condenser plant that otherwise could not be included in the TCE calculations. However, it should also be recognized that there are certain limitations to the current use of CONTAIN for predicting loads in an ice condenser plant. These limitations include the use of source terms computed for Zion, a large dry containment, for the ice condenser study and limited assessment of the CONTAIN models for the mitigative features of ice condenser plants. For example, the assessment of CONTAIN's ice condenser model was for DBA conditions, not for DCH and severe accident conditions.

I was somewhat surprised by the absence of a statement in the report regarding the resolution of the DCH issue for ice condenser plants. Unlike in previous reports, the reader is left without any definitive position in this regard. However, given the number of recommendations, there is at least some indication that the issue is not fully resolved. If further work is to be done in this area, issue resolution appears to depend, at least in part, on the use of CONTAIN and/or experiments to quantify loads. I can think of at least three options: (1) present approach using CONTAIN with the current limitations on loads calculations, (2) more prototypical source terms for CONTAIN and more prototypical assessment of CONTAIN's models that pertain to ice condenser mitigative features, and/or (3) prototypical DCH experiments in scaled ice condenser models.

Additionally, issue resolution also involves placing DCH-induced overpressure failures in the proper probabilistic framework. In this regard, the report recommends external events, low power shutdown events, and bypass events be evaluated in addition to the internal events to develop a more integrated perspective for risk-informed regulation. This would be the third attempt to resolve the DCH issue for ice condenser plants: the

first attempt being the probabilistic comparison of containment loads versus containment strength used for large dry containments and subatmospheric containments and the second being the expanded probabilistic assessment used in this report. The recommendation to expand the PRA analyses for a more complete Level II analysis has the potential to blur the distinction between a bona fide use of credible PRA analyses to address the DCH issue and "just one more attempt" to make PRA "resolve" the issue.

The authors also recommend an uncertainty study be performed to quantify the impact of identified uncertainties on early containment failure. I think this would be especially useful since the structural analysts judgment is an important part of the analysis of the containment's capacity. Furthermore, large uncertainties suggest a better understanding of the issue is needed.

Specific Comments

1. A potential difference between large dry and ice condenser plants is the type of load that can fail the containment, i.e. pressure sensitive versus impulse sensitive. The "pressurization energy ratio" (pg 12) appears to address only pressure sensitive containments by virtue of its definition. It seems that failure by impulse should be addressed since at least one containment has concrete and, therefore, may be sensitive to impulse for failure. The possibility of dynamic loads is mentioned on page 14 but stops short of actually quantifying it.
2. The report states that melts in earlier CONTAIN studies contained considerably more metal than current assessments. Why? What makes the current metal content assumed for the melt better than the old values?
3. Local detonations can also excite higher frequency failure modes in the containment (pg 20).
4. The argument that debris transport to the dome appears weak since it is based on extrapolations of data and opinion (pg 25).
5. What is the justification of assuming a hot leg failure of 90% (pg 41)?
6. Section 4.1.7 suggests that the recovery of AC power after UTAF provides a beneficial effect. That is, DCH loads can be reduced by the precombustion of hydrogen in the containment atmosphere by the energized igniters. However, ignition of the hydrogen at the concentration listed (~12%) may threaten the containment by itself and not provide the beneficial effect suggested. The same comment holds true on page 56.
7. The recommended DCH loads at vessel breach in Table 4.19 give the impression of more accuracy than actually exists.

8. It was stated that McGuire and Watts Bar have high SBO frequencies (pg 57) but it appears that Cook and Sequoyah are the ones that have high SBO frequencies from Table 4.20.

9. In the cell under SBO and Hydrogen Combustion Loads in Table 7.6, the statement that “deflagrations would fail containment 97% of the time in Sequoyah while detonations would fail containment ~30% of the time” doesn’t make sense to me. The equilibrium pressure after a detonation is the AICC pressure in an insulated vessel, the same pressure that would result if a deflagration occurred in the same mixture. However, the initial detonation wave has significantly higher peak pressure than a deflagration. So, if anything, the detonation would fail the containment a larger percentage of the time than a deflagration, all other things being equal.

Review of Final Draft NUREG/CR-6427
"Assessment of the DCH Issue for Plants with Ice Condenser Containments"

Reviewer: F. J. Moody

The final draft has incorporated changes from the earlier version, which substantially clarify some of the discussions. In some cases, the order of discussion has been revised, or the explanations have been expanded to make the document more easily understood. Tables have been added, showing some of the in-between assessments employed in the overall study. The authors have strengthened their assessment by offering a clear description of the extensive CONTAIN studies for specific scenarios. The present form of the final draft is essentially self-contained, and one that communicates a technological assessment, which is complete within the scope established. Recommendations are given for further assessment of the early containment failure probabilities of ice condenser plants. Aside from a few typographical errors, the document, in my opinion, accomplishes its task, and is ready for distribution.

Specific typographical (Etc.) errors and comments.

Page 11, Eq. (3.1) The ratio C_p/R can be expressed as $1/(k-1)$, where k is the ratio of specific heats, and might be better known for the gas mixture.

Page 34, Table 4.2: I think that $D < 0.5$ " is correct, although in the previous review draft, someone had painstakingly crossed out 0.5 and penciled in 0.05".

Page 55, item (6): "to this variable..." is repeated.

Page 58, second sentence in second paragraph, "...Watts Bar have high relatively SBO frequencies..." Change order of underlined words.

Page 91, next to last sentence, second paragraph, "...when the ice id depleted."

Page 99, item (3) should be shifted down to replace (4), and (4) should replace (5).

There was an extra page 108 and 109 in my copy.

Page 127 jumps to page 129.

Review of NUREG/CR-6427
"Assessment of the DCH Issue for Plants with Ice Condenser Containments"

Reviewer: F. J. Moody

PURPOSE OF THE REVIEW

The review of this document is part of the process for ensuring that the work has sufficient technical strength to support conclusions about the response of ice condenser containments to loads associated with direct containment heating.

The report contains numerous discussions and arguments, justifying the manner in which theoretical models were verified and applied to predict the containment responses for various accident scenarios. The work incorporates probabilities associated with dominant parameters, systems, and processes, including the time line of various events. A credible review generally applies critical judgement to each significant technical aspect of the report, thereby assessing its validity, based on consistency, available evidence, extensive experience, and whether or not the various models are representative of actual system responses.

Both strengths and weaknesses are appropriate in a review, but special focus on weaknesses may suggest the possibility that the conclusions from the study could be changed. The present report has provided such an in-depth, extensive analytical investigation that it is difficult to find weaknesses that are not already mentioned and/or quantified by the authors.

OVERALL ASSESSMENT

Earlier work on ice condenser containment response to DCH was based on the methodology established for resolving the Zion DCH issue (NUREG/CR-6075). A determination of the conditional containment failure probability (CCFP) no greater than 0.1 was deemed sufficient to close the DCH issue. The CCFP was determined by a combination of probability distributions on dominant parameters, causal relationships among state variables, and the containment fragility characteristic. Similar applications were made to CE and B&W plants. The methodology begins without taking credit for the probability of a HPME, and employs other conservatisms to determine if the CCFP is low enough to resolve the DCH issue. If it is not, then further credit can be taken for known conservatisms, which justifiably lower the CCFP, usually to the 0.1 value, for which the issue can be closed.

Preliminary application of the DCH issue methodology to ice condenser plants failed to reduce the CCFP to a level for issue closure, based on SBO scenarios without the availability of H₂ igniters and the presence of ice at the time of DCH. A peer review at that time expressed optimism that further refinements of ice condenser models,

elements in the CCFP determination, the containment load/strength characteristics, and consideration of the HPME probabilities conditional on core damage, would lead to a reduction of the overall CCFP to a level for closing the DCH issue.

The present work provides an exhaustive investigation, taking reasonable credit available to reduce the CCFP to acceptable levels for issue closure. The end result, though unfortunate, appears to give a solid technical basis for claiming that without igniter burning of the hydrogen released, the DCH issue could not be resolved in this study by incorporating the containment load/strength characteristic with the pressure load achieved. The CCFP limit of 0.1 is exceeded during SBO events, being dominated by hydrogen burning. The HPME probability is small, but does not counteract the potential for hydrogen domination of early containment failure.

The DCH issue is not resolved for ice condenser plants by the present work. The investigators offer suggestions for the individual plants to achieve resolution. These suggestions include: quantifying the spectrum of scenarios leading to HPME using PRA techniques of NUREG 1150, updated wherever possible; employing DC igniters to burn hydrogen as it is introduced; improving the validation of the CONTAIN ice condenser model; assigning probabilities to the loadings described in Section B3; incorporating HPME probabilities, more accuracy in containment load/strength characteristics, and refining sequence probabilities through PRA activities.

THE APPROACH TAKEN IN THIS STUDY

Since ice condenser plants are unique with respect to ice beds to suppress DBA steam loads, AC-powered igniters to control hydrogen inventory, smaller containment volumes, and containments with lower strength characteristics, previous scoping analyses did not achieve CCFP values low enough to close the DCH issue. It was recommended by the investigators, and supported by the peer review panel, that further refinements could result in CCFP values small enough to close the DCH issue.

The investigators proceeded in refining probabilities, benchmarking the containment ice condenser model with limited data, and employing steam sources from SCDAP/RELAP5 models for input to CONTAIN.

Numerous selected sensitivity studies are included to "illuminate" the importance of various phenomena and accident management procedures. Such sensitivity studies may provide a basis for plant specific analysis refinements.

IMPORTANT FINDINGS FROM THE STUDY

Analyses described in this study confirmed earlier expectations that about 40 percent of the ice remained at vessel breach in SBO scenarios. However, it was also confirmed that the major containment threat was associated with unburned hydrogen,

since AC igniters would not function during SBO. Moreover, analysis revealed, contrary to expectations, that the entire ice inventory could be melted prior to vessel breach for some non SBO scenarios, which would yield containment threatening loads unless sprays were available.

The methodology applied to large dry, subatmospheric, and ice condenser containments showed a reversal of earlier IPE results, which showed lower CCFP values for ice condenser plants. One reason noted was model improvements as the technology has advanced. Another reason suggested is that many utilities with large dry, or subatmospheric containments employed overly conservative approaches in their treatment of HPME on DCH loads.

RECOMMENDATIONS ARISING FROM THIS STUDY

Because phenomenological uncertainties in ice condenser containments are large, a fully integrated uncertainty analysis could not be addressed in this study. Mean fragility curves were employed, based on IPEs, which have not been reviewed. Since these curves are steep with many uncertainties, significant benefit to CCFPs might be realized by further refinements in the fragility properties.

It also is recommended that insights from this study be factored into more complete Level II analysis for each significant plant damage state. A formal uncertainty study was recommended to quantify the impact of identified uncertainties on early containment failure.

OPINION

A study of the extensive arguments, analyses, and discussions presented in this report have shown that the investigators have employed state-of-the-art models in their assessment of the DCH issue for plants with ice condensers. They have taken previous review comments seriously into account, and done a credible job in responding to them. Their arguments show accountability to the technical community, and their presentations give a solid basis for either present conclusions or extended refinements.

The structure of the report is such that current analytical methods are justified historically, experimentally, and practically in a defensible, traceable mode. They have included a collection of information and references that supports technical integrity. They have blended together information from many sources, including their own, to show a state-of-the-art consistency. Users of this report should perceive a high level of confidence in the abundance of material included. Furthermore, the authors have identified weaknesses, leaving the door open to further refinements, which may further reduce CCFP values for ice condenser containments. They have also made suggestions for individual plant analyses to improve their numbers, or provide design or operational procedures to resolve the early containment failure issue.

LEVY & ASSOCIATES

3880 S. Bascom Ave., Suite 112
San Jose, CA 95124
408/369/6500
FAX 408/369-8720

November 23, 1999

Dr. R. Lee
Division of Systems Technology
Office of Nuclear Regulatory Research
Washington, D.C. 20555

Dear Richard:

On November 23, 1999, a telephone conversation was held between yourself, M.M. Pilch and the writer of this letter. The subject of the conference call was to agree upon a response to my letter of comments about the latest version of NUREG/CR-6427. It was agreed that reservations or additions will be made to the final issue of this text instead of a substantial writeup. I agree with that approach and the proposed changes by M. M. Pilch are very responsive to my comments. I now consider my review role to be satisfactorily closed on NUREG/CR-6427.

Best wishes to you for the forthcoming holiday season.

Sincerely yours,


Salomon Levy

cc: M. M. Pilch

LEVY & ASSOCIATES

3880 S. Bascom Ave., Suite 112
San Jose, CA 95124
408/369/6500
FAX 408/369-8720

October 22, 1999

Dr. M. Khatib-Rahbar
Energy Research, Inc.
P.O. Box 2034
Rockville, Maryland 20847

Dr. R. Lee
Division of Systems Technology
Office of Nuclear Regulatory Research
U.S. Nuclear Regulatory Commission
Washington, D.C. 20555

Gentlemen:

Subject: Review of October Version of NUREG/CR-6427

While this October version is improved, it continues to fail to recognize the full benefits provided by the ice condenser. The ice beds provide a **passive** cooling system with very large heat removal capacity and there is no comparable passive system in dry containments. The ice condenser provides two important benefits. First, the ice condensers when they are not depleted can remove significant amounts of heat prior to the DCH and after the DCH. Second, when the ice beds are depleted (in fact, only 50 percent depleted) the reactor cavity is fully flooded.

When ice is present, as stated on page 16 of this report, "in contrast, CONTAIN calculations performed in support of the present effort (Section 5 and Appendix B) implied that there is a potential for the ice to be considerably more effective in preventing load threatening loads than indicated by the earlier studies, provided igniters (and ARFs) are operating prior to vessel break". (In other words, DCH loads are not threatening for non SBO conditions). When the reactor cavity is deeply flooded (i.e. RWST has emptied and approximately 50% or more of the ice has melted) as stated on page 19 of this report, "in which case DCH was assumed to be prevented in NUREG-1150. We have endorsed this assumption in the present study also".

Put simply, **either we have ice in the ice beds or the reactor cavity is flooded** and I do not understand why we keep calculating containment loads without ice or without a flooded cavity. Under SBO conditions, there is a high potential for containment failure due to hydrogen and the treatment of hydrogen in NUREG/CR-6427 is appropriate.

I have tried to mark the report to recognize the benefits provided by the passive cooling feature of ice beds and I have attached all my changes. They are so numerous and so significant that the rework is enormous and it might be preferable to start all over and to limit the scope of this report to DCH as stated in the report title. No matter what the decision to proceed is, my feelings are very strong on the following issues:

1. Appendix D should be removed or a strong statement made that it does not provide for the presence of ice or a fully flooded cavity. The probability of conditions analyzed in Appendix D is zero. Any use of the results of Appendix D in the main body of the report must recognize that shortcoming.
2. The parameters ϕ_R and ϕ_m as proposed fail to recognize the heat removal of the ice or the flooding of the cavity. A suggestion is made in the attached sheets how one might do so. Furthermore, it is important to emphasize that for the high probability case when the igniters are working the hydrogen conditions in dry and ice containers are about equivalent and that only for the small probability case of station blackouts the ice containment performance is inferior to the dry containment.
3. Considerable time is spent during the CONTAIN calculations (Section 5) to prove that the ice beds will be depleted before vessel breach and containment loadings for a dry cavity are provided. Those are irrelevant for several reasons: (1) the reactor cavity will be flooded and (2) there is a high probability that the plant will be depressurized. A correct SCDAP/RELAP/CONTAIN calculation would validate those results for non-SBO and SBO conditions. This also can be inferred from Figure 5.9.
4. The calculation of steam spike is very conservative in terms of mass release and quench time and it is contrary to having accepted NUREG-1550 position as already noted. According to the Zion DCH NUREG/CR-6075, the release of 40mt of UO_2 has a probability of 0.01 and it will be smaller in ice containments because of the flooded cavity and the formation of a crust within the vessel.

I also recommend that the redo of NUREG-1150 is unnecessary except as related to DCH. In the case of DCH the report should recognize the reduced probability of an HPME due to a temperature-induced failure of the hot leg; the increased risks of not burning the hydrogen due to new phenomena; and, the increased time for vessel breach. Thus the DCH risks are reduced in absolute value and relative to other early containment failure modes. The early ice containment failure risks with respect to dry containment are increased due to the possibility of not burning the hydrogen.

I am sorry that I cannot support the proposed revision and I hope that all the persons involved who have worked so hard will understand my position.

Sincerely yours,



Salomon Levy

ABSTRACT

This report (NUREG/CR-6427) addresses the Direct Containment Heating (DCH) issue for all Westinghouse plants with ice condenser containments. There are ten operating ice condenser plants located at five sites in the U.S. DCH phenomena in ice condenser plants are different in some important aspects from DCH phenomena in other Pressurized Water Reactors (PWRs) in that they have ice beds to suppress Design Basis Accident (DBA) steam loads, AC-powered igniters to control hydrogen concentrations in the atmosphere, small containment volumes, and containment buildings with low ultimate capacities to withstand internal pressures.

Unlike PWRs with large dry or subatmospheric containments, the DCH issue for ice condenser plants could not be resolved by a probabilistic comparison of containment loads versus containment strength. The approach taken here is to provide an expansion of a probabilistic framework, which represents a simplification of the NUREG-1150 containment event tree for Sequoyah. The containment event tree is intended to give each containment challenge its proper probabilistic weighting based on plant specific core damage frequencies, phenomenological probabilities, and plant specific fragility curves. The probabilistic framework addresses DCH-induced overpressure failures in the context of all significant early containment failure modes. These include DCH overpressure failures, thermal failures of the containment liner, non-DCH hydrogen combustion overpressure failures, and non-explosive steam spike overpressure failures.

The most significant finding of this study was that the early containment failure probability is dominated by non-DCH hydrogen combustion events rather than DCH events. This is because the HPME probability is small, the SBO probabilities are small, and because containment loads in non-station blackouts are not containment threatening. The CONTAIN code was used exclusively to calculate containment loads resulting from DCH, non-DCH hydrogen combustion, and non-explosive steam spikes for representative station blackout and non-station blackout scenarios. CONTAIN calculations show that no ice condenser plant is inherently robust to all credible DCH or hydrogen combustion events in station blackouts. CONTAIN predictions show that containment loads in nonstation blackout are not containment threatening for any reasonable plant damage state.

Consistent with perceptions of the technical community, this study shows that ice condenser plants are substantially more sensitive to early containment failure than PWRs with large dry or subatmospheric containments. A plant-specific evaluation of the containment event tree showed that all plants, except McGuire, have an early failure probability within the range 0.35% to 5.8% for full power internal events. The early containment failure probability was 13.9% for McGuire. The higher containment failure probability is dominated by the relatively higher station blackout probability and relatively weaker containment for McGuire.

One at a time variations in the hot leg failure probability and the probability of a struck open power-operated relief valve (PORV) after uncovering of the top of active fuel (UTAF) had no significant impact on the results of this study. An additional sensitivity study assuming intentional depressurization by the operators after UTAF (uncovering of top of active fuel) also had no impact on the conclusions of this study. All plants, especially McGuire, would benefit from some means of hydrogen control that is effective in station blackouts. The risk reduction was

reducing the probability of station blackouts or finding

Executive Summary

and the unavailability of ice the ice beds (an essential passive feature of ice containments)

developed in NUREG/CR-6075 and NUREG/CR-6075, Supplement 1, was used to perform a load versus strength evaluation for each of these plants using plant-specific data gathered from Individual Plant Examinations (IPEs), Final Safety Analysis Reports (FSARs), and direct contacts with plant personnel (when necessary). The same enveloping accident scenarios (splinters) that were used in NUREG/CR-6075, Supplement 1, and NUREG/CR-6109 were used for these plant evaluations under the assumption that a DCH event occurs. One additional splinter scenario, unique to plants with ice condenser containments, was also considered. These splinter scenarios establish important input parameters for the DCH load calculations, e.g., the RCS pressure at vessel breach, the melt mass and composition, the RPV breach size, the containment pressure and atmosphere composition at vessel breach, etc. Assuming core damage and a HPME/DCH event, all ice condenser plants exceeded the metric (conditional containment failure probability, $CCFP \leq 0.1$) based on DCH-induced overpressure failures alone. Consequently, the DCH issue could not be resolved based on load/strength evaluations alone if a DCH event was postulated.

This initial assessment of DCH in ice condenser plants was reviewed by a NRC-sponsored panel of six experts who are familiar with the phenomenology and the DCH issue resolution process. Reviewer comment and recommendations fell into three general categories:

1. Expand the probabilistic framework to ~~include sequence probabilities,~~ *of the DCH issue*
2. Validate CONTAIN's ice condenser models if CONTAIN is to be used in the load calculations, and
3. Model the ice condenser explicitly in the loads calculations.

*This report title deal with DC
Dry containments were confined to D*

This revision of draft NUREG/CR-6427 explicitly addresses these peer review comments. The approach taken is to provide an expansion of the probabilistic framework, which represents a simplification of the NUREG-1150 containment event tree for Sequoyah. *as related to DCH* The probabilistic framework addresses DCH-induced overpressure failures in the context of all significant early containment failure modes. ~~These include DCH overpressure failures, thermal failures of the containment liner, non-DCH hydrogen combustion overpressure failures, and non-explosive steam spike overpressure failures.~~

reality

The following practical approach was adopted for assessing the importance of HPME/DCH to early containment failure for all ice condenser plants.

1. Develop a simplified version of the NUREG-1150 containment event tree (CET) that operates on each core damage initiator (CDI) as a class (e.g., LOCAs) and not on the hundreds of plant damage states (PDS) that might be members of a given class.
2. Benchmark the simplified tree by demonstrating that the simplified tree, with NUREG-1150 consistent input, reproduces (in a reasonable fashion) the results documented in NUREG-1150 for Sequoyah. This ensures that all significant top events have been identified from the NUREG-1150 study.

3. Update specific quantifications in the simplified CET if significant new work since the time of NUREG-1150 justifies the revision. Significant quantifications that were updated include the hot leg failure probability and a reassessment of containment loads using CONTAIN. Additional simplifications of the CET are possible to produce a more scrutable result for extrapolation evaluations.
4. Use the more simplified logic tree to evaluate, in a consistent manner, the early containment failure probabilities for all ice condenser plants (including a reevaluation for Sequoyah) using plant specific information (e.g., fragility and CDI frequencies) to the extent that information is available from the IPEs.

A simplified CET was developed to quantify the HPME probability and the early containment failure probability for each of the six CDI classes: slow station blackout, fast station blackout, loss of coolant accident (LOCAs), transients, anticipated transients without scram (ATWS), and internal floods. We focus on full power internal events and exclude bypass events such as interfacing LOCAs and steam generator tube ruptures. The HPME portion of the CET quantifies whether core damage is arrested in vessel and at what RCS pressure does vessel failure occur if core damage is not arrested in vessel. The top events are:

1. RCS leak size at UTAF,
2. Stuck open PORV during cycling at system set point (SP),
3. Temperature-induced leak in reactor coolant pump (RCP) seals,
4. Intentional depressurization of the RCS,
5. Temperature-induced failure of the surge line or hot leg,
6. RCS pressure prior to possible vessel failure,
7. AC power recovery after UTAF and before vessel breach, and
8. Core damage arrest in vessel.

The containment failure portion of the CET addresses vessel breach mode/size, the quantity of water in the cavity, and each of the four containment failure mechanisms noted above.

The CONTAIN code was used exclusively to calculate containment loads resulting from DCH, non-DCH hydrogen combustion, and non-explosive steam spikes for representative station blackout and non-station blackout scenarios. The ice condenser model in CONTAIN was recently benchmarked against Waltz Mill data (full-height tests for ice condenser performance) for DBA conditions. CONTAIN has also been benchmarked against key experiments that emphasize each of the three sources of containment loads noted above. However, there are no integral DCH tests in ice condenser geometry to fully validate CONTAIN for this application.

Executive Summary

CONTAIN calculations showed that no ice condenser plant is inherently robust to all credible DCH or hydrogen combustion events in a station blackout (SBO) accident. The containment is threatened by hydrogen combustion events alone because igniters, which are AC-powered, are not available to mitigate the accumulation of very high concentrations of hydrogen in the containment. Hydrogen combustion, initiated by and in conjunction with a DCH event is even more threatening. The ice beds were found to significantly reduce DCH loads in a SBO accident, but not to a level that did not threaten the containment. CONTAIN predicted non-threatening containment loads for non-SBOs provided ice or one train of containment sprays is available.

The containment event tree is intended to give each containment challenge its proper probabilistic weighting based on plant specific core damage frequencies, phenomenological probabilities, and plant specific fragility curves. The CET event tree was benchmarked against NUREG-1150 to ensure that all significant top events were reasonably represented in a simplified CET patterned after NUREG-1150. Detailed comparisons proved this to be the case. The CET was further simplified by introducing some conservative assumptions and specific quantifications were updated based on more recent NRC-sponsored research.

Limit to DCH

A plant-specific evaluation of the CET showed that all plants, except McGuire, had an early failure probability (given core damage) within the range 0.35% to 5.8% for full power internal events. These integral estimates of early containment failure are qualitatively consistent with published IPE results for these plants. The early containment failure probability, as computed here, was 13.9% for McGuire. This higher containment failure probability for McGuire is dominated by the relatively high SBO frequency and the relatively weak containment for McGuire. The IPE assessments of early containment failure at McGuire (2%) are significantly lower than our assessments; however, we have not investigated the reasons for this difference.

Phenomenological uncertainties are large, but a fully integrated uncertainty study was outside the scope of this effort. However, selected sensitivity studies were performed here to illuminate the importance of certain quantifications and to examine the importance of certain accident management procedures that might be proposed. One at a time variations in the hot leg failure probability and the probability of a stuck open power-operated relief valve (PORV) after uncovering of the top of actual fuel (UTAF) had no significant impact on the results of this study. An additional sensitivity study assuming intentional depressurization by the operators after UTAF also had no impact on the conclusions of this study. All plants, especially McGuire, would benefit from some means of hydrogen control that is effective in SBOs. The risk reduction is greater than an order of magnitude for all plants.

a reduction in station blackout probability or

Assuming igniters and air return fans are not operational (e.g. SBOs), uncertainties in containment loads are dominated by uncertainties in hydrogen combustion phenomena and the amount of clad oxidized during core degradation. For non-SBOs, uncertainties in containment loads are dominated by uncertainties in modeling, the availability of sprays, the ice inventory at vessel breach, and the melt mass. We use the mean fragility curves as reported in the IPEs, which have not been reviewed. These fragility curves are steep with a short low-end tail, and any uncertainties in these fragility curves could have a significant impact on computed containment failure probabilities.

Consistent with perceptions of the technical community, this study shows that ice condenser plants are substantially more sensitive to early containment failure than PWRs with large dry or subatmospheric containments. These perceptions, however, are not consistent with IPE results summarized in NUREG-1560 that show many PWRs with large dry or subatmospheric containments report early containment failure probabilities in excess of 10% given a core damage accident, while none of the ice condenser plants reported early failures greater than 2.4%. NUREG-1560 cites DCH processes as the main contribution to early containment failure in PWRs with large dry or subatmospheric containments. In light of more recent NRC estimates of DCH-induced containment failure probabilities, we conclude that many utilities with large dry or subatmospheric containments were overly conservative in their treatment of HPME probabilities and DCH loads.

To develop a more integrated perspective for risk-informed regulation, it is recommended that the insights of this study be factored into more complete Level II analyses for each significant plant damage state and that the evaluation of early containment failure be evaluated not only for internal events, but also for external events, low power shutdown events, and bypass events. For completeness, we recommend that a formal uncertainty study be performed to quantify the impact of identified uncertainties on early containment failure; however, uncertainties in the fundamental DCH processes of dispersal, fragmentation, and debris/gas heat transfer are not likely to contribute significantly to the overall uncertainty in early containment failure because these DCH processes are such a small contributor to early containment failure. Containment sprays are important in mitigating loads in non-SBOs if the ice inventory is depleted, but it remains to be confirmed that plants with identified vulnerabilities in switching to recirculation mode have implemented proposed remediations.

mean → Not done for dry containment. Uncertainty very large as shown in NUREG-1150. In terms of DCH, we do not meet CCFP ≤ 0.1 and we will not meet with external events.

1.0 INTRODUCTION

In a light-water reactor core melt accident, if the reactor pressure vessel (RPV) fails while the reactor coolant system (RCS) is at high pressure, the expulsion of molten core debris may pressurize the reactor containment building (RCB) beyond its failure pressure. A failure in the bottom head of the RPV, followed by melt expulsion and blowdown of the RCS, will entrain molten core debris in the high-velocity steam blowdown gas. This chain of events is called a high-pressure melt ejection (HPME). Four mechanisms may cause a rapid increase in pressure and temperature in the reactor containment: (1) blowdown of the RCS, (2) efficient debris-to-gas heat transfer, (3) exothermic metal-steam and metal-oxygen reactions, and (4) hydrogen combustion. These processes, which lead to increased loads on the containment building, are collectively referred to as direct containment heating (DCH) when they have the potential to occur simultaneously. It is necessary to understand factors that enhance or mitigate DCH because the pressure load imposed on the RCB may lead to early failure of the containment.

DCH is a prominent severe accident issue because of its potential for early containment failure. Although the RPV did not fail at Three Mile Island II (TMI-II), some important and necessary conditions for HPME/DCH existed, e.g., the relocation of approximately 20 mt of core material to the lower head and high (approximately 10 MPa) RCS pressures. The Nuclear Regulatory Commission (NRC) has identified DCH as a major issue for resolution in the Revised Severe Accident Research Plan (NRC, 1992) and has sponsored programs at Sandia National Laboratories (SNL) to resolve the DCH issue.

NUREG-1150 was the first attempt to treat DCH from a probabilistic risk assessment (PRA) perspective that integrates sequence probabilities with uncertainties associated with initial/boundary conditions and phenomenological uncertainties associated with predicting containment loads. NUREG-1150 addressed only a small number of reference plants and the DCH database was largely nonexistent at the time, so there was no way to validate these early attempts to predict DCH loads. More recently, the IPEs have also addressed the DCH issue from a PRA perspective. Their strength is that plant-specific sequence information is fully integrated into the assessment for every plant. On the other hand, the approaches taken to assess containment loads are inconsistent and poorly tied to the existing database.

Section 2 of this report presents the overall methodology and success criteria for resolution of the DCH issue. Historically, the first step in the DCH issue resolution process for PWRs with large dry or subatmospheric containments was the writing and public review of NUREG/CR-6075 and its supplement, "The Probability of Containment Failure by Direct Containment Heating in Zion." NUREG/CR-6109, "The Probability of Containment Failure by Direct Containment Heating in Surry," applied the same methodology to the Surry plant as a second demonstration of the DCH resolution methodology. DCH was examined in a broader way for all Westinghouse (W) plants, excluding plants with ice condenser containments, in NUREG/CR-6338, "Resolution of the Direct Containment Heating Issue for all Westinghouse Plants With Large Dry Containments or Subatmospheric Containments." Most recently, the DCH issue was examined for all Combustion Engineering (CE) and Babcock & Wilcox (B&W) plants in NUREG/CR-6475, "Resolution of the Direct Containment Heating Issue for Combustion Engineering Plants and Babcock & Wilcox Plants." In the vast majority of PWRs with large dry

(The probability of auxiliary feedwater not being available is of the order of 0.01 and its presence will reduce the peak load on the ice chest and increase the ice inventory) Introduction
response for the steam loads. For non-SBOs, these steam sources maximize the load on the ice chest and minimize the ice inventory because auxiliary feedwater was not represented in the SCDAP/RELAP5 calculation. These calculations were used to define the ice inventory, the containment base pressure, and the DCH pressure rise at the time of vessel breach. These assessments are described in Section 5.0

The containment fragility curve was extracted from the IPE for each plant. The fragility assessments are summarized in Section 6.0 and are compiled previously in Appendix C (Pilch et al. 1996). Containment loads, for each end state in the containment loads tree, are convoluted with the plant specific fragility curve to determine the corresponding overpressure failure probability. The results of these calculations are presented in Section 7.0. The summary and conclusions are given in Section 8.0. Comments from a NRC-sponsored peer review of this revised document by experts in Reactor Safety are published in Appendix E.

↓
This is a significant shortcoming which I cannot accept. It can make a lot of difference. The probability of this occurring is 0.01 and the results need to be stated and taken into account. I have suggested a paragraph.

2.0 ASSESSMENT METHODOLOGY

Based on recommendations of the NRC, the methodology has traditionally aimed at grouping each PWR into one of two categories:

- (1) PWRs in which the threat of early containment failure, conditional on core damage, is shown to be ≤ 0.1 , and
- (2) PWRs in which the threat is > 0.1 .

We emphasize that the containment failure probability is conditional on core damage. More recently, the NRC has placed greater emphasis on the large early release fraction (LERF) of $< 10^{-5}$ as a safety goal. Ultimately, the resolution of any safety issue is based on a risk-informed assessment of the plant performance against safety goals, uncertainties in the plant performance relative to those safety goals, and cost/benefit analyses associated with any proposed changes in the plant. The metric used in this study is the CCFP for early containment failure, which serves the purpose here as a common metric by which the relative vulnerability of reactor containments can be assessed so that the results of this study can be compared to those of previous DCH resolution studies. We expect that the insights of this study ultimately will be factored into utility PRAs, and the revised results presented in the format that best addresses the regulatory goals in place at the time.

We recognize that DCH must be considered in the plant-specific context of all early containment failure modes¹ when the CCFP criterion is applied; however, DCH is thought to dominate early containment failure for most PWR plants with large dry or subatmospheric containments. Consequently, reasonable demonstration that the containment failure probability given a DCH event is less than 0.1 is sufficient to classify a plant into the first category. The DCH issue was previously resolved for all PWRs with large dry or subatmospheric containments through plant-specific probabilistic comparisons of DCH loads versus containment strength assuming that a HPME event occurred. For the vast majority of these plants, the containment failure probability was less than a 0.01 screening criteria without recourse to sequence or HPME probabilities. Although not examined in a general way, it was recognized that the DCH containment failure probability would be at least an order of magnitude lower if DCH was considered conditional on core damage (rather than conditional on a HPME event) because of the low HPME probability.

The DCH issue for ice condenser plants could not be resolved based on plant-specific probabilistic comparisons of DCH loads versus containment strength assuming that a HPME event occurs. An initial attempt along these lines is documented as Appendix D for reference. NUREG/CR-4551 for the Sequoyah plant was carefully reviewed for possible insights to an assessment methodology. Four key observations can be summarized as follows:

*assuming the unavailability of ice beds
and a dry cavity*

¹ We conservatively define early containment failure as occurring shortly after vessel breach. We note that the NRC is considering defining early in terms of the public evacuation time scale instead of vessel breach.

- (1) Develop a simplified version of the NUREG-1150 event tree that operates on each core damage initiator (CDI) as a class (e.g., LOCAs) and not on the more numerous plant damage states (PDS) that might exist at the time of core uncover.
 - (2) Benchmark the simplified tree by demonstrating that the simplified tree, with NUREG-1150 consistent input, reproduces (in a reasonable fashion) the results documented in NUREG-1150 for Sequoyah.
 - (3) Update specific quantifications (e.g., hot leg failure probabilities) in the simplified tree if significant new work since the time of NUREG-1150 justifies the revision.
 - (4) Calculate probability of DCH or containment failure, and its increase with respect to other NUREG-1150 early containment failures.
- This approach for assessing DCH in ice condenser plants is developed more fully in Section 4.0.

This report focuses on full power interval events. We acknowledge that risk-informed regulation must also address external events (fire and seismic) and low power shutdown events,² but these are outside the scope of the current effort. Core damage frequencies for full power internal events were previously quantified by the utilities in the individual plant examinations (IPes), while CDFs for external events were more recently quantified by some utilities in the individual plant examinations of external events (IPEEEs). In some cases, the CDF for external events can be comparable to the CDF for internal events. The CDF for low power shutdown events has not been systematically evaluated for all light water reactors (LWRs); but in a few cases where quantifications have been performed, the CDF can again be comparable to the CDF for full power internal events. As this study will show for full power internal events, the CCFPs for ice condenser plants can be comparable to or exceed the CCFP < 0.1 success criteria; consequently, a comprehensive assessment of early containment failure would benefit from additional consideration of external events and low power shutdown events. External events and low power shutdown events as initiators could introduce more early containment failures, which when combined with early failures for internal events, could exceed 10% of all core damage accidents. This is because external events could have a disproportionately large number of SBO-like sequences, which have a significant probability of early containment failure from hydrogen deflagrations or DCH processes.

CCFP < 0
would further
no basis for this

²Level II and Level III risks have not been assessed for low power shutdown accidents; however, DCH would not normally be possible in low power shutdown events because the RCS pressure is low.

Assessment Methodology

- (1) Given a "typical" DCH event, NUREG-1150 says there is approximately a 34% probability of containment overpressure failure; and if the containment does not fail by overpressure, then there is approximately 24% probability that the accumulation of dispersed debris against the containment liner will result in a thermal failure.
- (2) The probability of vessel breach with RCS pressure greater than 200 psi is approximately 35%.
- (3) The total mean early containment failure probability (weighted by the probability of all plant damage states) is approximately 7.6% with non-HPME failures making up about half of the total.
- (4) The uncertainties are large with the early containment failure probability ranging from approximately 0.02% to approximately 70% for the 5% and 95% confidence limits, respectively.

The implications for a DCH assessment study focused on ice condenser plants are fivefold:

- (1) Revised load/strength analyses for a small number of bounding "splinter scenarios" (assumed to be conditional on a DCH event) cannot produce DCH resolution because liner failures alone are greater than the 10% criteria for early containment failure.
- (2) It is unlikely that DCH resolution will be achieved in a general way based on HPME probabilities alone (although there is now a technical basis to take more credit for hot leg failures).
- (3) ~~DCH assessment must be approached from an integrated perspective that addresses all significant modes of early containment failure in a framework that places all significant failure modes in the proper and consistent probabilistic framework.~~
probabilistic deserves another evaluation which takes into account all the research work carried out in the recent years.
- (4) We must acknowledge that the uncertainties in early containment failure might be large, but it is outside the scope of this study to quantify uncertainties.
- (5) The DCH issue itself might be judged of secondary importance if the frequency-weighted DCH overpressure failures are shown to be small compared to other frequency-weighted contributors to early failure, ~~even if the probability of all early failures is comparable to or exceeds a CCFP of 10%.~~ *as taken from NUREG-1150.*

The best way to address these needs is through detailed and credible Level I and Level II probabilistic analyses, specific to each individual plant. This is outside the scope of the current assessment, and a cursory review of the IPE's for ice condenser plants shows that the Level II decompositions and quantifications differ from plant to plant. In this work, the following is proposed as a practical approach for assessing the importance of HPME/DCH to early containment failure for all ice condenser plants.

- (1) Develop a simplified version of the NUREG-1150 event tree that operates on each core damage initiator (CDI) as a class (e.g., LOCAs) and not on the more numerous plant damage states (PDS) that might exist at the time of core uncover.
 - (2) Benchmark the simplified tree by demonstrating that the simplified tree, with NUREG-1150 consistent input, reproduces (in a reasonable fashion) the results documented in NUREG-1150 for Sequoyah.
 - (3) Update specific quantifications (e.g., hot leg failure probabilities) in the simplified tree if significant new work since the time of NUREG-1150 justifies the revision.
 - (4) Calculate probability of DCH or containment failure, and its importance with respect to SBO. NUREG-1150 early containment failures.
- This approach for assessing DCH in ice condenser plants is developed more fully in Section 4.0.

This report focuses on full power interval events. We acknowledge that risk-informed regulation must also address external events (fire and seismic) and low power shutdown events,² but these are outside the scope of the current effort. Core damage frequencies for full power internal events were previously quantified by the utilities in the individual plant examinations (IPEs), while CDFs for external events were more recently quantified by some utilities in the individual plant examinations of external events (IPEEEs). In some cases, the CDF for external events can be comparable to the CDF for internal events. The CDF for low power shutdown events has not been systematically evaluated for all light water reactors (LWRs); but in a few cases where quantifications have been performed, the CDF can again be comparable to the CDF for full power internal events. As this study will show for full power internal events, the CCFPs for ice condenser plants can be comparable to or exceed the CCFP < 0.1 success criteria; consequently, a comprehensive assessment of early containment failure would benefit from additional consideration of external events and low power shutdown events. External events and low power shutdown events as initiators could introduce more early containment failures, which when combined with early failures for internal events, could exceed 10% of all core damage accidents. This is because external events could have a disproportionately large number of SBO-like sequences, which have a significant probability of early containment failure from hydrogen deflagrations or DCH processes.

CCFP < 0.1
no basis for this
would further

²Level II and Level III risks have not been assessed for low power shutdown accidents; however, DCH would not normally be possible in low power shutdown events because the RCS pressure is low.

3.0 ASSESSMENT OF ICE CONDENSER CONTAINMENT PHENOMENA

3.1 Introduction

The United States Nuclear Regulatory Commission (USNRC) and others have invested considerable effort towards understanding and resolving the DCH issue for commercial US power plants over the past ten years or so. These efforts have focused primarily on the phenomena that might occur during a HPME sequence in PWRs with large dry containments. In particular, the later phases of the experimental effort were guided by the Severe Accident Scaling Methodology (SASM) program which emphasized DCH in the large dry containments; subsequent experimental efforts focused on the study of DCH phenomena as they would be manifest in large dry containments and the initial conditions were defined to be appropriate for large dry containments. There were good reasons for that focus; DCH was shown by NUREG-1150 (NRC 1989) to be the only important mechanism of concern that could lead to early containment failure for large dry containments. Other plant types (i.e., the "pressure suppression containments"--BWRs and PWRs with ice condenser containments) had smaller populations in the plant fleet and had other early containment failure concerns associated with them.

At the present time, efforts toward resolution of the DCH issue for plants with large dry or subatmospheric containments are complete, and it is now appropriate to review how those results might be applied to these other plant types and what additional work might be needed to pursue resolution for the pressure suppression containments. Care must be taken in translating the results for plants with large dry containments to these specialized containments. Each has a different phenomenological "signature" in response to an HPME event. These differences could have a strong bearing on the relevance or applicability of the substantial knowledge base that has been developed to date for the large dry containments. None of the special characteristics of the pressure suppression containments have been factored into the experimental programs, and they received at most passing attention in the SASM effort. Hence there is less of a validation base for whatever analytical tools are available for addressing the specialized features of the pressure suppression containments.

The starting point for such an assessment should be a basic discussion of the nature of the threat posed by HPME to these containments, with a particular emphasis on the differences from the large dry containments. This section provides such a review for the ice condensers. Its purpose is not to delve deeply into any particular phenomenological sub-issue, but rather to provide a general context in which to view HPME in ice condensers compared with previous work on DCH in large dry containments.

We make an important distinction here between HPME and DCH. HPME is a mode of vessel failure that is the end point of the in-vessel part of the event trees used in PRAs. DCH is a set of phenomena that subsequently occur in the containment that represent a potential threat to containment integrity through global overpressurization. Other containment failure mechanisms besides DCH but resulting from HPME have been considered for plants with large dry containments, e.g., hydrogen combustion and in-vessel steam explosions. However, they have been largely dismissed on the basis of loads evaluations and probabilistic considerations.

IN PRA

NUREG/CR-6427

There is an important difference between dry and ice condenser containments; the ice containments have a passive cooling source which can reduce the energy deposited into the containment during HPME and DCHs

effects of rapid steam condensation in the ice condenser during a DCH event. The second involves phenomena that can occur in both types of containments, but with the boundary conditions for the processes being sufficiently different that quite different behaviors may actually result. A consideration of global scaling parameters provides some useful insights into the second class of differences, and we consider these in the next section. Specific instances of both classes of phenomena are then discussed in Section 3.2.2.

3.2.1 Global Scaling Parameters: Large Dry Containment vs. Ice Condenser Containments

In this section, we define three global scaling parameters that reflect containment resistance toward DCH, sensitivity of the margin to DCH uncertainties, and concentration regimes for hydrogen phenomenology. We then present two-dimensional maps comparing the location of the ice condenser containments with the location of Westinghouse large dry and subatmospheric containments in the parameter space defined by the scaling parameters. We conclude that ice condenser plants are potentially more susceptible to failure from DCH because the loads are potentially higher (small containment with higher hydrogen concentrations when igniters are not operational), and ~~because the containments are not as robust as large dry or subatmospheric containments.~~

Containment Pressurization Energy Ratio. One measure of a containment's resistance toward DCH can be defined by considering the ratio of the energy required to result in a pressure rise sufficient to threaten containment integrity to the energy available in the core debris. In the screening approach that was adopted for previous issue resolution efforts, the screening criterion has been that the conditional containment failure probability (CCFP) be less than 0.01 (conditional on core damage and a HPME event); hence, we define a "threatening" pressure to be $P_{0.01}$, the pressure corresponding to a 1% failure probability on the fragility curve. The energy input required to threaten the containment, $\Delta U_{0.01}$, is then given by

$$\begin{aligned} \Delta U_{0.01} &= V C_v \Delta P_{0.01} / R, \\ \Delta P_{0.01} &= P_{0.01} - P_c^0, \end{aligned} \tag{3.1}$$

where V is the containment volume, C_v is the constant-volume molar heat capacity of the containment atmosphere, R is the universal gas constant, P_c^0 is the containment pressure immediately prior to vessel breach, and where the number of moles of gas in containment is constant (neglects steam and hydrogen addition). Following NUREG/CR-6338 (Pilch et al., 1996), we take P_c^0 to be 0.25 MPa and 0.15 MPa for atmospheric and subatmospheric large dry containments, respectively; both values assume active engineered safety features (ESFs) are not available. Based upon CONTAIN calculations described in Appendix B, we take P_c^0 to be 0.18 MPa for ice condenser containments when active ESFs are unavailable. *In the case of ice containments, the ice beds will reduce the energy input because they are a passive system and*

The total energy (thermal and chemical) potentially available depends upon the core debris mass and the composition. For present purposes, we are interested only in relative measures, and we assume that the various energy sources scale as the core size, for which we take the measure to be the mass of UO_2 (M_{UO_2}). A possible concern is that there is some variation in the ratio of

$\Delta U_{0.01}$ needs to be changed to $(\Delta U_{0.01} - \Delta U_{IB})$; Eq. (3.1) assumes ΔU_{IB} to be zero which has a zero probability of occurrence. As discussed later, there are uncertainties that the full energy reduction of the ice beds may be available (where ΔU_{IB} is the energy reduction of the ice beds) NUREG/CR-6427

needs to be changed

zirconium inventory (M_{Zr}) to UO_2 inventory among the various plants and that this could distort comparisons based upon M_{UO_2} alone, because M_{Zr} largely governs the potential for hydrogen production and hydrogen can be a very important contributor to DCH loads. We examine this question further in connection with hydrogen phenomenology below and accept this approximation for now.

Because we are interested in relative measures, we define a "pressurization energy ratio," ϕ_R , by taking the ratio of $\Delta U_{0.01}/M_{UO_2}$ for the plant of interest to the value of $\Delta U_{0.01}/M_{UO_2}$ for the Zion plant, which we use as a typical PWR large dry containment for reference purposes:

$$\phi_R = \frac{M_{UO_2, Zion} \Delta P_{0.01} V}{M_{UO_2} (\Delta P_{0.01} V)_{Zion}} \quad (3.2)$$

wrong needs to be reduced

wrong for a reactor cooling system

where we have neglected any differences in C_v for different plant atmospheres.

Margin Provided by CCFP ≤ 0.01 in Screening Studies. The operational definition of "issue resolution" adopted in this program has been demonstration that the $CCFP \leq 0.1$. The value of 0.01 was adopted for previous screening studies in order to allow for uncertainties owing to plant-specific features that may not have been adequately considered and to allow for phenomenological uncertainties in the loads modeling. A question of some importance is then how robust this margin is toward DCH modeling uncertainties. That is, by how much would some unacknowledged uncertainty have to increase the efficiency of DCH in order to yield an actual $CCFP \geq 0.1$ when the screening calculations gave $CCFP \leq 0.01$? A measure ϕ_m of the robustness of this margin can be obtained by replacing $\Delta P_{0.01}$ in the definition of ϕ_R by $\delta P_m = P_{0.1} - P_{0.01}$, where $P_{0.1}$ is the pressure corresponding to a 10 percent failure probability on the containment fragility curve; thus,

$$\phi_m = \frac{M_{UO_2, Zion} \delta P_m V}{M_{UO_2} (\delta P_m V)_{Zion}} \quad (3.3)$$

A small value of ϕ_m results when the containment fragility curve is steep, implying that the pressures corresponding to the 10% and 1% failure probabilities do not differ greatly. A small value of ϕ_m does not necessarily imply a weak containment.

Hydrogen Phenomenology. We consider here the global hydrogen concentrations that can accumulate in the containment when igniters are not operational. In first approximation, the potential for hydrogen production scales as the mass of zirconium in the core, M_{Zr} . In defining ϕ_R above, we assumed that the ratio M_{Zr}/M_{UO_2} is the same in all PWR plants, and that M_{UO_2} could therefore be taken as a measure of the relative variation in total energy available for DCH among the various plants. In order to investigate this issue, we define a normalized Zr/ UO_2 ratio, ϕ_{Zr} , from the relation

When the igniters are available, the concentration of hydrogen in the dry containment and ice condenser containments are relatively the same & lower

$$\phi_{Zr} = \frac{M_{Zr} / M_{UO_2}}{(M_{Zr} / M_{UO_2})_{Zion}} \quad (3.4)$$

If values of ϕ_{Zr} show sufficiently small variability, we may conclude that variations in the Zr/UO₂ mass ratios among the plants will not seriously perturb the ϕ_R values calculated from Eq. (3.2). Similar considerations apply to the adequacy of Eq. (3.3) used to define the margin parameter, ϕ_m .

There are many features of hydrogen phenomenology for which ϕ_{Zr} is not a useful scaling parameter because these features show strong nonlinear dependencies upon the hydrogen mole fraction. Examples include burn completeness, burn rates, and the potential for flame acceleration and deflagration-to-detonation transition (DDT) that could produce dynamic containment loads. Flame speeds and burn completeness increase rapidly with increasing concentration; for example, burn completeness is very low near the upward flammability limit (approximately 4% H₂) but increases rapidly with mole fraction, becoming almost 100% complete for concentrations greater than or equal to 7-10% (Wong, 1988). The likelihood of flame acceleration and/or DDT are sensitive to hydrogen concentration and can show an approximate threshold behavior; for example, the NUREG-1150 study assessed DDT in certain Sequoyah scenarios and concluded DDT to be impossible for hydrogen concentrations less than 14 percent while the probability of DDT was taken to be > 0.6 if a deflagration initiated at concentrations ≥ 16 percent for the scenarios considered (see Section 4.2.2.2 for some details). We note, however, that if global hydrogen concentrations are high enough to support detonations then a deflagration with the same hydrogen concentration is sufficient to fail the containment with a high probability. As a practical matter, little is lost by ignoring global detonations in the upper dome.

In comparing the ice condenser and large dry containments, therefore, it is useful to define a global scaling parameter that reflects the potential for developing high hydrogen concentrations. A comparative measure for this purpose may be defined by taking the ratio of M_{Zr} to the number of moles of containment atmosphere and assuming that the latter is proportional to $P_c^0 V / T_c^0$:

$$\phi_{H_2} = \frac{M_{Zr} T_c^0 (P_c^0 V)_{Zion}}{(M_{Zr} T_c^0)_{Zion} P_c^0 V}, \quad (3.5)$$

where T_c^0 is the initial containment temperature. *This scaling parameter applies only when igniters are not available.*

Mapping of Ice Condenser and Large Dry Containments. In this section, we compare ice condenser and large dry containments in terms of the global scaling parameters defined above. The "large dry containments" considered are limited to the atmospheric and subatmospheric containments for Westinghouse plants, which are the plants that were addressed in NUREG/CR-6338. In the plots to be presented, some of the data points represent two containments when there are two units that are identical with respect to the scaling parameters.

In Figure 3.2, ϕ_m is plotted against ϕ_R for ice condenser containments (open symbols) and large dry containments (closed symbols). For the latter, all data required to evaluate the scaling parameters were taken from Tables 4.3 and 6.1 of NUREG/CR-6338 (Pilch et al., 1996). The values assumed for containment pressure at vessel breach are those that correspond to accident scenarios without active containment ESFs operating.

when the ice beds are available and unavailable

square and

It is immediately obvious that the ice condenser and large dry containments fall in quite different regions of the scaling parameter space. Much of this separation is because of the differences in ϕ_R . For the large dry containments, ϕ_R varies from 0.58 for H. B. Robinson to 1.74 for Seabrook. For the ice condensers, the range is only 0.16 to 0.27. For Sequoyah, $\phi_R = 0.24$; this means that DCH need be only 24% as efficient to threaten containment integrity in Sequoyah as is required in Zion and only approximately 40% as efficient as is required in H. B. Robinson.

relatively the same region when ice beds are available

Sequoyah

ice beds are not taken into account. Their performance would be lower than when the ice beds are available

These differences occur because ice condenser containments are not as strong or as big as large dry containments.

when ice beds are unavailable

Unlike the case for ϕ_R , there is a slight overlap between the ranges spanned by ϕ_m for ice condensers (0.12-0.27) and the large dry containments (0.20-1.0). However, the ice condenser values are all at or below the low end of the range for large dry containments. Sequoyah has the smallest value of ϕ_m , 0.12. In Sequoyah, therefore, the margin provided by screening with a CCFP of 0.01 could be overcome by uncertainties in DCH efficiency that are almost an order of magnitude smaller than those required to overcome the margin in Zion. Even for Watts Bar ($\phi_m = 0.27$), the difference with respect to Zion is almost a factor of four.

when the igniters are unavailable

Values of ϕ_{H_2} are plotted against ϕ_{Zr} in Figure 3.3. It is seen that the values ϕ_{Zr} do not span a wide range; in fact, the standard deviation in ϕ_{Zr} among all the plants considered is only 7%. Furthermore, there is no significant tendency for the ice condenser plants to differ from the large drys with respect to this parameter. Hence, we can conclude that variations in ϕ_{Zr} do not significantly perturb the comparisons presented in Figure 3.2 for ϕ_R and ϕ_m .

when the igniters are unavailable

In contrast, the values of the hydrogen concentration parameter ϕ_{H_2} for the ice condenser plants (2.5-3.5) are outside the ranges spanned by the large dry containments (1.0-1.7 for the atmospheric containments, 1.9-2.0 for the subatmospheric containments). In the absence of igniters, global hydrogen concentrations in the ice condenser plants can be approximately 2.5 times as great as in Zion, for equivalent metal oxidation fractions. This difference is large enough to put the containment into quite different phenomenological behavior regimes in Sequoyah. The value of ϕ_{H_2} does depend on the containment pressure at vessel breach, which in turn depends upon various details of the accident sequence including especially engineered safety feature availability. However, these variations will be insufficient to alter the conclusion that the range of ϕ_{H_2} values that must be considered for ice condenser plants is considerably higher than the range that has been necessary to consider in large dry containments.

Conclusions to be drawn from the comparisons of global scaling parameters considered here may be summarized as follows:

Summarize first when ice beds and igniters are available

neglecting the cooling provided by the ice beds

The values of ϕ_R show that there is a potential for margins to be much smaller, if they exist at all, in ice condenser plants than in large dry containments, implying that ice condenser plants may be more sensitive to phenomenological uncertainties in DCH loads modeling.

(2) The margin provided by screening at a CCFP level of 0.01 is smaller for ice condenser plants than for most (though not all) large dry containments.

due to absence of igniters

(3) The large values of ϕ_{H_2} for ice condenser plants indicate that there is a greater potential for flame acceleration or detonations to yield dynamic loads rather than only the quasi-static loads that were considered in the large dry containments; this result illustrates the potential need to consider threats other than quasi-static pressurization in evaluating HPME in ice condenser plants.

unrealistically

A key word here is "potential," because the scaling parameters do not take into account the special mitigative features of ice condenser plants, such as the ice condenser and the igniter systems. However, crediting these features will require tools for analyzing their effects as well as determining to what extent these systems will be available in the spectrum of accident scenarios of interest. These requirements obviously complicate the assessment process relative to the large dry containments *which do not have a passive cooling system because they*

unacceptable

not these CONTAINMENTS can do

3.2.2 Specific Issues Involving HPME in Ice Condenser Containments

In what follows, we consider the various issues relating to HPME and DCH in ice condenser plants in greater detail and compare them with analogous issues, if any, in large dry containments. First, we consider issues related to the availability of various ESFs. Next we consider HPME threats other than DCH pressure loads, and we conclude by considering other containment phenomenology. The latter phenomena are considered primarily in the context of DCH pressure loads. Much of what follows is based upon assessments performed for the NUREG-1150 effort, supplemented by more recent work where possible.

3.2.2.1 Availability of ESFs

In addition to the ice condenser itself, ice condenser containments include three other ESFs: ARFs, igniters, and sprays. Except for containment sprays, there is no analogue for these ESFs in large dry or subatmospheric containments. A large number of combinations of various levels of ESF availability are possible. The effect of these combinations on DCH threats can be complex and has not been fully delineated, nor has the question of ESF availability for the spectrum of events of potential interest to DCH and HPME been systematically addressed. Insights from NUREG-1150 have been factored into the simplified CETs developed in Section 4 of this report.

Effectiveness of Ice in the Ice Condenser. Prior to vessel breach, the ice condenser is expected to provide an efficient means of condensing steam released from the primary system. If the air return fans are operating, pressures, temperatures, and steam concentrations within containment at vessel breach may not be substantially greater than for normal operating

conditions. If ice is exhausted, pressures and steam concentrations will rise. However, if ice is exhausted prior to vessel breach, it is expected this will not happen until relatively late in the period preceding vessel breach; hence, large additional releases of steam and energy to the containment are not likely to occur between the time ice is exhausted and the time vessel breach occurs. Hence, very high pressures and steam concentrations at vessel breach are not expected, and the dome usually will not be inerted against hydrogen combustion. However, when ice is exhausted, the reactn cavity will be filled with water and the vessel breacher will generate steam to reach the dome and DCH is presented according to NUREG-1150

Handwritten mark

By design, the ice in the ice condenser is configured so as to provide for efficient condensation of steam in a DBA. This configuration also favors rapid transfer of thermal energy from the atmosphere in the ice chest. In a DCH event, superheated gas and steam are generated in the lower compartment, forcing flow through the ice condenser. There is a potential that the ice condenser will remove much of the energy and the steam from the gas flowing through it, substantially mitigating DCH. Note, however, that the ice condenser cannot remove hydrogen, although the removal of steam and sensible heat from the gases entering the ice condenser can delay the rate at which hydrogen from the lower compartment reaches the dome

Early CONTAIN calculations (Williams et al., 1987) indicated that the ice condenser could mitigate DCH significantly, but containment-threatening loads were still calculated for many of the scenarios considered. These calculations used melt mass representative of complete core melt and significant melting of structural steel. In the NUREG-1150 study, ΔP values were assumed to be 30-70% higher, depending upon the scenario, if ice were completely ineffective than if it were fully effective. An ice bed is considered ineffective if the ice is completely melted or if uneven melting allows gases to largely bypass any remaining ice. A more detailed CONTAIN study (Williams and Gregory, 1990) yielded qualitatively similar results. Nonetheless, in these calculations, the presence of ice did not prevent containment-threatening loads from developing in many of the scenarios considered, even if igniters were available prior to vessel breach. An important factor was that the melts assumed in these prior studies contained considerably more metal than our current assessments.³ Hydrogen produced during the DCH event itself was an important contributor to the calculated ΔP , and the ice condenser can have at most only a limited effect upon this component of the pressurization.

Very fair statement finally!!!

In contrast, CONTAIN calculations performed in support of the present effort (Section 5 and Appendix B) implied that there is a potential for the ice to be considerably more effective in preventing threatening DCH loads than indicated by the earlier studies, provided igniters (and ARFs)⁴ are operating prior to vessel breach. The principal reason is that the combination of limited metal in the melt and oxygen starvation in the lower containment resulted in a much smaller contribution from the combustion of DCH-produced hydrogen, and the ice was calculated to be very effective in suppressing pressurization owing to superheated gas and steam.

This belongs in Exec. Summary

³ The melt composition in this earlier study was taken from BMI-2104. Based on inventory arguments BMI-2104 assumed that all unoxidized cladding (~12 mt) and all structural steel (~62 mt) would be in the melt. Using more mechanistic modeling, current best estimate codes predict that most unoxidized cladding will be retained in an in-core crucible and that melting of structural steel is largely limited to small quantities of thin steel within the core regions.

⁴ The availability of igniters is greater than 99% and the availability of ARFs is greater than 99% given that there is power in the plant.

Containment threatening loads are still calculated for SBOs because DCH can only worsen an already threatening hydrogen combustion event.

Impaired Ice Condenser Efficiency. The preceding discussion of DCH mitigation by the ice condenser presumes that the ice condenser is in a condition to be effective at the time HPME occurs. There are three ways in which ice condenser effectiveness can be defeated:

- (1) Ice may be totally melted prior to vessel breach.
- (2) Ice may still be present, but uneven ice melting may have opened up sufficient channels that the remaining ice is effectively bypassed at vessel breach.
- (3) Detonations in the ice condenser at vessel breach may open up channels bypassing the remaining ice.

These issues were considered in some detail in the NUREG-1150 analyses. The detonation issue was addressed in Williams and Gregory, 1990, who concluded that detonable gas compositions under adverse circumstances could not be ruled out. Ice was totally or almost totally depleted in a number of scenarios; however, these tended to be cases involving large LOCAs or induced large LOCAs, which would preclude DCH. Cases in which any LOCAs were sufficiently small that primary system pressures were in the intermediate or high range at vessel breach generally had considerable ice remaining at vessel breach.

The NUREG-1150 (NRC, 1990) analysts also considered the bypass issues. Except when ice was almost depleted (greater than or equal to 90% ice melt), they concluded that any channeling would result in a bypass of less than 10% for both the uneven ice melt and the detonation-induced bypass case. However, calculations using the HECTR code (Dingman and Camp, 1985) and the CONTAIN code (Williams and Gregory, 1990) showed quite strong tendencies for recirculation flows to produce highly uneven ice melt in some of the scenarios considered. The degree to which control volume codes such as HECTR and CONTAIN can model these effects quantitatively is uncertain, and there is also uncertainty as to how much channeling can be tolerated without seriously degrading the ice condenser performance in the context of DCH mitigation.

Modeling of the Ice Condenser During DCH. To date, quantitative analyses of mitigation of DCH by the ice condenser have been limited to various analyses performed with the CONTAIN code. There has been recent effort to validate the CONTAIN ice condenser model for DBA conditions, and a prototypic data base for validation under DCH conditions is nonexistent. The model includes a user-specifiable multiplier on the heat and mass transfer coefficients for the ice, and it also includes a user-specifiable water film thickness on the ice. Heat conduction limitations through this water film can limit the rates of heat and mass transfer to the ice.

In the calculations described in Appendix B of this report, a major motivation was to determine whether the ice condenser offered the potential for significant mitigation; no claim is made that the calculations demonstrate a fully validated capability for DCH events. In this context, artificially eliminating a potentially promising mitigation effect by using overly

NUREG/CR-6338, it was concluded that, in general, the atmosphere will be flammable at vessel breach only if some degree of containment heat removal is available. The issue of burning off hydrogen prior to vessel breach is much less dominant in large dry containments and this question did not play an important role in NUREG/CR-6338 (it was assumed that the hydrogen would not burn prior to vessel breach). Flammable hydrogen concentrations can accumulate in the containment prior to vessel breach in some Combustion Engineering plants.

Air Return Fans. The ARFs require AC power. They actuate automatically when containment pressures reach 3 psig and will actuate in a recovered station blackout if other failures do not prevent their doing so. The ARFs will assure a generally well-mixed containment except at times of rapid influx of large quantities of steam and/or hydrogen from the primary system. Immediately prior to vessel breach, available SCDAP/RELAP5 calculations do not predict strong sources from the primary system, suggesting that the containment will be reasonably well mixed prior to vessel breach if the ARFs operate. If ARFs do not operate, steam concentrations will be considerably higher in the lower compartment than in the dome, and the lower compartment may be inert toward combustion prior to vessel breach as judged by conventional inerting criteria (these criteria probably do not apply at the very high temperatures that quickly develop in the lower compartment during DCH). Operation of the ARFs will decrease hydrogen concentrations in the ice beds and increase the degree of ice melt prior to vessel breach.

Containment Sprays. Long-term heat removal for the Sequoyah plant is provided by containment sprays with associated heat exchangers. Like the ARFs, they require AC power and actuate automatically when the containment pressure exceeds 3 psig, assuming they are in an operable condition. If sprays are operating, the refueling water storage tank (RWST) generally will have been exhausted prior to vessel breach, in which case the cavity will probably contain water, with the amount depending upon the amount of ice melted. If the RWST has emptied and approximately 50% or more of the ice has melted, the cavity will be deeply flooded, in which case DCH was assumed to be prevented in NUREG-1150. We have endorsed this assumption in the present study also. If sprays are operating at the time of vessel breach, there will be some airborne water in the dome atmosphere and evaporation of this water will tend to cool the dome and reduce pressures during DCH. The extent of this mitigation is addressed in Section 5.0 where it is shown that sprays are effective at mitigating DCH loads to non-threatening levels provided the igniters are operational, even when ice is depleted prior to vessel breach. Spray operation is stated to reduce ice melt in the NUREG-1150 study but a quantitative effect cannot be derived from the results given. Sprays operate only in the dome (except for the D.C. Cook Plant), and most of the gas and steam normally reaches the dome only after passing through the ice condenser. Nonetheless, Section 5.0 of this report shows that spray operation in the upper dome has a relatively small effect at preserving the ice inventory.

An important mechanism

Corresponding Large Dry Issues. Of the active ESFs in Sequoyah, the sprays are the only systems for which reasonable counterparts exist in large dry containments. Their direct effects upon DCH loads were not considered in NUREG/CR-6338; however, some of the possible consequences associated with spray operation (reduced containment pressures and steam concentrations at vessel breach, extent of cavity flooding) were considered. *The absence of a*

passive cooling system, such as the ice bed, will mean that dry containment has to deal with an increased energy input.

Because they will remove heat which will deplete ice when they are not operating

3.2.2.2 HPME Threats Other Than DCH

Talk first about burners being available

This report is not confined to use of NUREG-1150 in support of a summary of NUREG-1150. It should be enough.

Hydrogen Detonations and Accelerated Flames in the Upper Dome. If igniters do not function prior to vessel breach, the large values (2.5-3.5) of the global hydrogen scaling parameter ϕ_{H_2} , noted above suggests that hydrogen detonations in the upper dome are ~~much~~ ^{probably} more credible in ice condenser plants than in large dry containments. The initial conditions calculated by CONTAIN (Appendix B of this report) include molar hydrogen concentrations of 14-18% if ignition sources are absent. The calculations made use of hydrogen sources calculated by SCDAP/RELAP5 in which in-vessel zirconium oxidation was predicted to be 58%. This value is greater than the median (approximately 40%) assumed in NUREG/CR-6338, but it is less than the value of 75% that is postulated for the NRC's hydrogen rule for ice condenser plants (10 CFR 50.44). Operating igniters or the presence of other ignition sources preclude development of the high global hydrogen concentrations required for global detonations, whatever the extent of in-vessel zirconium oxidation.

In NUREG-1150, deflagration-to-detonation (DDT) in the ice condenser or the upper plenum was considered likely (probability greater than or equal to 0.45) whenever ignition occurred with hydrogen concentrations greater than or equal to 14%. DDT may be less likely in the open volumes of the dome (obstacles and channel geometries favor DDT) but turbulence and/or elevated temperatures associated with the DCH event could enhance detonability. Furthermore, a detonation initiated in the ice condenser or upper plenum region could propagate into the dome if gas compositions and temperatures there are within the detonable regime.

Accelerated flames occur when the combustion front accelerates to near-sonic velocities but does not become supersonic. Considerations for flame acceleration resemble those for DDT but the requirements are somewhat less stringent. Flame acceleration has been observed with hydrogen concentrations down to 10%, even with substantial steam present. Other things being equal, peak dynamic pressures for accelerated flames are lower than for detonations but the integrated dynamic load (i.e., the impulse) can be comparable.

Global flame acceleration and/or detonations apparently were not considered in NUREG-1150. If they occur, the threat to containment integrity would presumably be substantial because, at the high hydrogen concentrations required, even a simple deflagration can be threatening.

Obviously, if detonable hydrogen concentrations have developed, the potential threat is not limited to HPME events; any ignition source could initiate combustion and DDT. However, as noted above, HPME may provide conditions more favorable to detonation (turbulence and/or elevated temperatures) than would otherwise exist. If nothing else, HPME assures an ignition source.

Corresponding Large Dry Issues. Global detonations are generally not considered an important threat for PWR large dry containments because it is difficult to achieve the high hydrogen concentrations required in the larger containment volumes. Nonetheless, threats of dynamic loads are considered minimal for large dry containments and have received little emphasis in recent work.

if igniters do not function

if the igniters do not function

Local Detonations. Because the ice condenser can strip steam from the entering gas mixture, detonable gas compositions can develop in the ice condenser and the upper plenum even if atmospheric compositions are not susceptible to detonation elsewhere within containment. Although a potential detonation threat can develop independently of HPME, the occurrence of HPME may promote detonability as discussed under global detonations and, in any case, it will provide an ignition source. As noted previously, the NUREG-1150 containment loads expert panel considered DDT in the ice condenser and/or upper plenum to be likely if ignition occurred with hydrogen concentrations exceeding 14%. Given a detonation, the distribution of impulsive loadings overlapped the distribution of containment fragility with respect to impulse as defined by the structural response experts. Hence, containment failure as a result of detonations in the ice condenser and/or the upper plenum were an acknowledged failure mode.

It is generally assumed that, if igniters and ARFs are both operating, the containment will be sufficiently well mixed that high hydrogen concentrations cannot develop in the ice chest even though there are no igniters there. In principle, this may not be true for short periods of time during very rapid release of steam and hydrogen from the primary system (Williams and Gregory, 1990). The likelihood that this will happen just prior to vessel breach is probably sufficiently small that it may be discounted.

If igniters operate but ARFs do not, the lower compartment is typically steam-inerted; hence the igniters located there are ineffective. Code calculations (Dingman and Camp, 1985; Williams and Gregory, 1990) indicate that hydrogen can reach detonable concentrations in the ice condenser before concentrations in the upper plenum (where the closest igniters are located) are high enough to initiate a burn that can propagate downward into the ice condenser. If HPME occurs while these conditions exist, DDT may follow ignition. However, the detonation would be limited to the ice condenser in this scenario, and the NUREG-1150 structural response panel considered the containment boundary in the ice condenser to be less vulnerable to impulsive loading than in the plenum, although failure was still possible.

with or without burners?

During an HPME event, the mixture flowing into the ice condenser will include high concentrations of steam mixed with varying amounts of hydrogen. Condensation of steam can then lead to gas mixtures exiting the ice condenser with ~~very~~ high concentrations of hydrogen immediately after the HPME event. Since the HPME event will have depleted gas entering the ice condenser of oxygen, the high hydrogen concentrations are not necessarily combustible. However, if gases from the dome subsequently mix with the hydrogen-rich gas in the ice condenser, detonable compositions may develop at some point.

except in a few compartments

Corresponding Large Dry Issues. Large dry containments include no features capable of causing a large, local concentration of hydrogen analogous to the ice condenser. Detonations were not observed in the IET experiments and analyses conclude that mixing limitations would likely preclude the possibility of detonations in large dry containments.

OK

Containment Failure by Direct Contact with Molten Debris. In the Sequoyah plant, debris traveling up the in-core instrumentation tunnel in an HPME event can strike the seal table. It is possible that the seal table and/or adjacent paneling will fail owing to thermal and mechanical loading, in which case molten debris can enter the seal table room (STR). The STR is located in

IET did not simulate upper plenum and did not provide for an initial H2 input!

heavily flooded. NUREG-1150 considered the possibility that an ex-vessel steam explosion could cause containment failure. The only failure mode identified was the possibility that blast traveling up the in-core instrument tunnel to the seal table could create missiles that might fail the containment. This event was considered incredible except for the combination of a melt mass greater than or equal to 20% of the core being ejected into a deeply flooded cavity, and even in this case a conditional probability of only 0.01 was assigned.

Various experiments involving HPME and water have demonstrated a capability for severe cavity pressurization. Typically, the interactions have not been truly explosive, but cavity pressures of several MPa have resulted. The possibility of vessel displacement and its implications may merit further investigation for these conditions. The fragility of the cavity walls (if the walls are free standing) has not been addressed. The potential for missile generation, should the cavity walls fail, has also not been assessed.

Corresponding Large Dry Issues. For the specific failure mode identified in NUREG-1150, there is probably no analogue in large dry containments because the STR is located inside the crane wall. Any missile would have to penetrate the crane wall and still possess sufficient energy to fail the containment.

3.2.2.3 Other Phenomenological Issues

Here we briefly summarize other phenomenological issues affecting DCH loads in order to identify any potentially significant differences between large dry containments and ice condenser plants. We do not explicitly consider the effect of ice in the ice condenser, which was discussed in Section 3.2.2.1; however, we note that some of the effects mentioned here may be of significance only for scenarios in which ice is depleted.

Oxygen Depletion Prior to Vessel Breach. If igniters operate, or if other ignition sources are present, hydrogen burns prior to vessel breach may substantially reduce the available oxygen supply at the time of vessel breach. For example, given 58% in-vessel zirconium oxidation as in the calculations cited in Appendix B, combustion of all this hydrogen prior to vessel breach would consume about 56% of the initial inventory of oxygen in the containment. Complete combustion of the hydrogen is not to be expected; however, the CONTAIN calculations of initial conditions in Appendix B predict that over 40% of the oxygen will be consumed prior to vessel breach.

Although global oxygen starvation during a DCH event is not expected to occur, local oxygen starvation is expected in the lower compartment and the ice condenser. This can be a significant mitigator of DCH. In the Surry-geometry SNL/IET experiments performed in the CTTF, the measured ΔP values ranged from 0.283 MPa to 0.43 MPa, and CONTAIN analyses of these experiments indicated that over half of this range could be attributed to the differences in the initial oxygen inventories in these experiments, even though oxygen starvation on a global basis did not occur in any of the experiments.

In this context, a high degree of in-vessel zirconium oxidation is *nonconservative* in accident scenarios with igniters operating. This point needs to be kept in mind when assessing the

X
This applies to dry

hydrogen to the dome, reducing the effects of mitigation by atmosphere-structure heat transfer. On the other hand, large amounts of water are more likely to mitigate loads by quenching the debris, suppressing the combustion of hydrogen, and cooling the atmosphere by evaporation of aerosolized water. No fully mechanistic models are available for calculating the effect of water on DCH loads. Limited experiments suggest that DCH loads are insensitive to cavity water in large dry containments. If the ice beds are functional at vessel breach, there may be a net mitigative benefit in converting direct heating (i.e., an atmospheric temperature rise) into a scenario with additional steam loading. This is because the ice beds can be more efficient at condensing steam than cooling hot gases.

Corresponding Large Dry Issues. No important qualitative differences between ice condenser plants and large dry containments have been identified in connection with debris-water interactions. Quantitatively, however, the smaller values of ϕ_R and ϕ_m render the analysis of ice condenser containments considerably more sensitive to the potential effects of debris-water interactions upon DCH efficiency.

Atmosphere-Structure Heat Transfer. Atmosphere-structure heat transfer has been found to be an important mitigator in the CONTAIN analyses of the DCH IET experiments in both the Zion and Surry geometries. Delay of hydrogen combustion owing to hold-up in oxygen-starved subcompartments contributed to this effect by prolonging the time period over which heat transfer could act. Deleting the combined heat transfer and hydrogen hold-up effects increased the calculated ΔP by 60-75%. Because ice condenser containments represent a compartmentalized containment geometry, qualitatively similar mitigation effects are expected for these containments also.

Debris Transport to the Dome. Pilch et al. (1994b) have concluded that debris transport to the dome in large dry containments will be insufficient to have an important impact upon DCH loads except in cases in which line-of-sight paths connecting the cavity exits to the dome are important. No such line-of-sight transport paths exist in ice condenser containments. The only potentially significant pathway for dispersed debris to enter the upper dome is for it to pass through the ice compartment. Tutu et al. (1986) concluded, through extrapolation of experiment results, that approximately 80% of all debris entering the ice chest would be trapped by the ice baskets alone before entering the dome. Examination of the lower compartment geometry in an ice condenser plant suggests that particles would have a hard time negotiating the turns necessary for gas to carry melt particles into the ice chest. Furthermore, the gas expands and slows down significantly as it exits the cavity and enters the lower compartment, which further reduces the potential for debris (~1 mm) to follow gas into the ice chest. Hence, the extent of debris transport to the dome is not believed to be an important issue in ice condenser plants. This has been confirmed by CONTAIN calculations that assume (as a bound) that debris moves with gas and without slip into the ice chest, subject only to gravitational settling in the lower compartment. CONTAIN predicts very little debris transport to the upper dome.

RPV Insulation. In the SNL/IET-11 experiment, the stainless steel insulation surrounding the RPV was simulated. The insulation was almost totally stripped away, apparently by melting ablation, and the ablated insulation may have contributed to hydrogen production (Blanchat et al., 1994). However, the ablated insulation did not contribute to experiment loads in any significant

Assessment

or decisive fashion. In large dry containments, some of the ablated insulation can enter the dome via the annular gap around the RPV. This is not possible in ice condenser plants, which may reduce the potential contribution of the insulation to DCH loads. On the other hand, the reduced values of ϕ_R and ϕ_m enhance sensitivity to whatever contribution does exist.

wrong values again
Other DCH Phenomena: Other DCH-related phenomena include the rates of thermal and chemical interactions of gas and steam with airborne and nonairborne debris, debris airborne residence times, fraction of debris dispersed from the cavity, and coherence between debris dispersal and blowdown steam. No major differences between large dry containments and ice condenser containments have been identified concerning these phenomena.

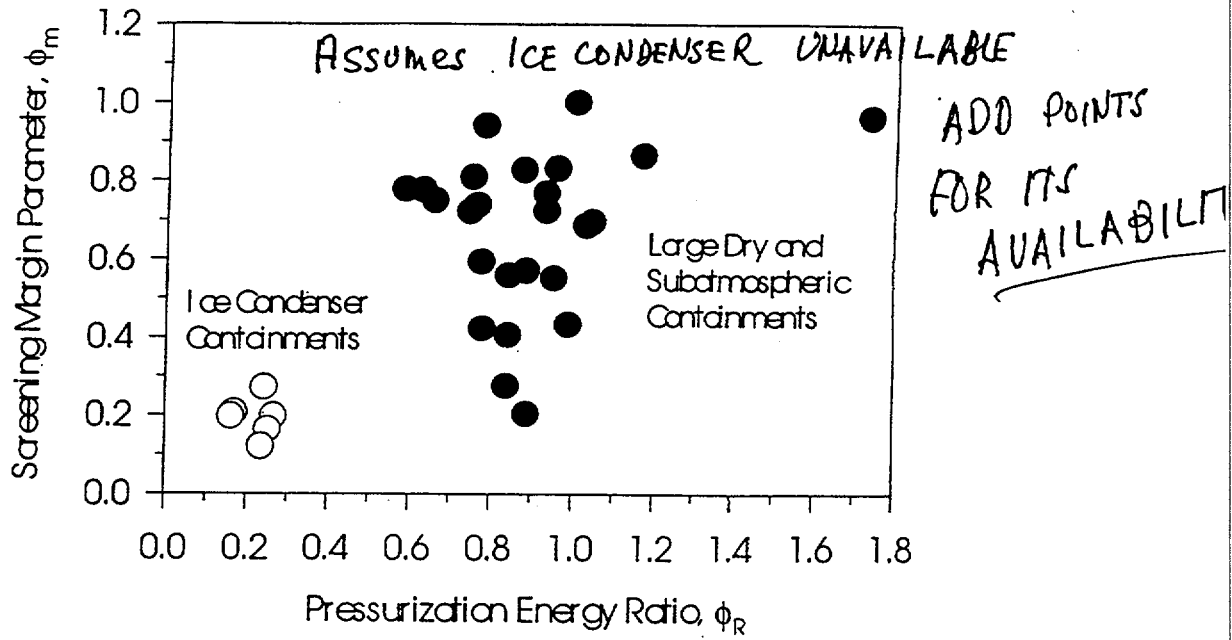


Figure 3.2 Screening margin and pressure energy ratio

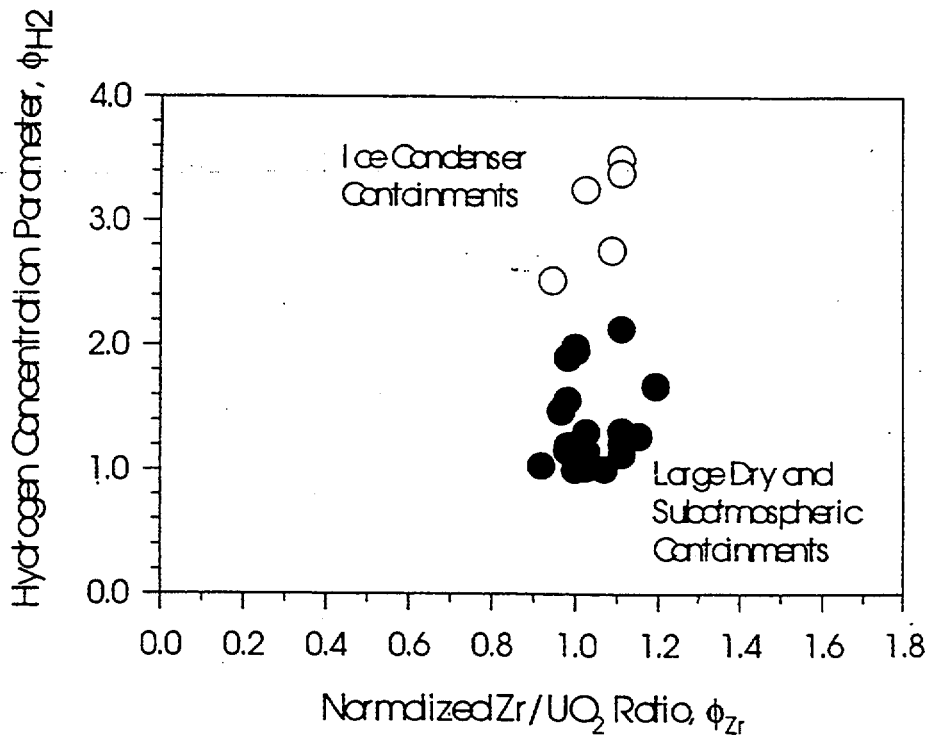


Figure 3.3 Hydrogen and Zr/ UO_2 ratio parameters

*Refer to
As discussed
Event to DCH*
*See herein
Comments*

4.0 QUANTIFICATION OF THE PROBABILISTIC FRAMEWORK

The best way to address the integration needs is through detailed and credible Level I and Level II probabilistic analyses, specific to each individual plant. This is outside the scope of the current assessment, and a cursory review of the IPE's for Ice Condenser plants shows that the Level II decompositions and quantifications for one plant are not always consistent with the decomposition and quantifications of another plant. To address these needs, the following practical approach was adopted for assessing the importance of HPME/DCH to early containment failure for all Ice Condenser plants.

- (1) Develop a simplified version of the NUREG-1150 event tree that operates on each CDI as a class (e.g., LOCAs) and not on the hundreds of PDS that might be members of a given class.
- (2) Benchmark the simplified tree by demonstrating that the simplified tree, with NUREG-1150 consistent input, reproduces (in a reasonable fashion) the results documented in NUREG-1150 for Sequoyah. This ensures that all significant top events have been identified in the NUREG-1150 study.
- (3) Update specific quantifications (e.g., hot leg failure probabilities) in the simplified tree if significant new work since the time of NUREG-1150 justifies the revision. Additional simplifications of the CET are possible to produce a more scrutable result for extrapolation evaluations.
- (4) Use the more simplified logic tree to evaluate, in a consistent manner, the early containment failure probabilities for all ice condenser plants (including a reevaluation for Sequoyah) using plant specific information (e.g., fragility and CDI frequencies) to the extent that information is available from the IPEs.

The DCH issue for ice condenser plants must be examined from the perspective of all early containment failure modes. The significant modes of early containment failure considered in NUREG-1150 and the current assessments are:

- (1) DCH overpressure failures,
- (2) Thermal failures of the containment liner resulting from accumulation of dispersed debris against the containment liner following HPME, *Refer to NUREG-1150*
- (3) Non-DCH hydrogen combustion overpressure failures in scenarios where core damage is arrested in vessel or when the RPV fails at low pressures, and *Refer to NUREG-1150*
- (4) Non-DCH steam spike overpressure failures when the lower head fails at low (less than 200 psi) RCS pressures. *(Refer to NUREG-1150)*

NUREG-1150 also considered α -mode failures, but the early containment failure probabilities were small and could be ignored in the current assessments.

leg nozzles and the surge line. If the RCS remains at high pressure during degradation, the hoop stress on the hot leg and the surge line will be high, and the elevated temperatures will weaken the metal considerably. It is possible that the piping may fail before vessel breach. Both the hot leg and the surge line are large pipes, so that all failures are of "A" size.

Table 4.10 summarizes NUREG-1150, IPE, and SNL-recommended quantifications for this issue. NUREG-1150 considered surge line or hot leg failures likely only when the RCS was at the system setpoint pressure (no leak except for cycling PORVs), and only limited credit was given for RCS pressures above 2000 psi (13.6 MPa). Surge line or hot leg failures were considered incredible when RCS pressures were below 2000 psi (13.6 MPa). We note also that NUREG-1150 assigns the same probability of surge line or hot leg failure to all CDIs. The IPEs generally adopted the NUREG-1150 quantifications with only minor adjustment of the probabilities while accepting the assessment that surge line or hot leg failures are only likely at system set point pressures.

Since the time of NUREG-1150, best estimate SCDAP/RELAP5 calculations have been performed for the spectrum of pump seal leaks in both Zion (Pilch et al. 1994b) and Surry (1995), which are both Westinghouse plants. The calculations all showed hot leg failure after the onset of core damage but well before core relocation to the lower plenum and well before lower head failure. The resulting depressurization of the RCS precludes HPME/DCH processes. The impact of varying key modeling parameters affecting core melt progression was examined in Pilch et al. (1995). For SBO sequences in Surry, the probability of hot leg failure was quantified as $P = 0.98$ for system setpoint pressures; $P = 0.98$ for 250 gpm RCP leaks; and $P = 1.0$ for stuck open or latched open PORVs.

We conclude from these calculations that hot leg or surge line failure is essentially assured for the full spectrum of RCS leak sizes that could leave the RCS at DCH-relevant pressures at vessel breach. We note that hot leg or surge line failure did not occur in TMI-II; and consistent with TMI-experience, the operators have means at hand that could disrupt natural and forced convective flows in the RCS if AC power is available. Consequently, we recommend that the hot leg or surge line failure probability be set to 90% for all CDIs and all leaks capable of leaving the RCS at DCH-relevant pressures at vessel breach. As a sensitivity study (case 6, Table 7.4, Section 7.0), the probability of hot leg or surge line failure will be reduced conservatively to 50% for SBOs and to 10% for non-SBOs.

Table 4.10 Probability of temperature induced failure of the surge line or hot leg

| | Probability of Failure | | |
|---------------------|------------------------|---------|---------|
| | No Leak | S3 Leak | S2 Leak |
| NUREG-1150 (Q21) | 0.768 | 0.035 | 0.000 |
| Sequoyah, Watts Bar | 0.768 | - | - |
| Catawba, McGuire | 0.900 | 0.001 | 0.001 |
| D.C. Cook | - | - | - |
| SNL Quantification | 0.900 | 0.900 | 0.900 |

New
Keep

The manway to the reactor cavity stands approximately 13 feet above the floor of the subcompartment; consequently, water cannot flow into the cavity unless significant water accumulates on the subcompartment floor. Typically, the RCS boiloff inventory plus the contents of the RWST plus approximately 50% ice melt is required to deeply flood the reactor cavity.

A deeply flooded reactor cavity will (at least partially) submerge the lower head, leading to the possibility that core melt can be retained within the lower head. NUREG-1150 and the Sequoyah/Watts-Bar IPE explicitly take no credit for this invessel retention. A recent OECD/CSNI-sponsored workshop (OECD 1998) on this issue concluded that invessel retention by exvessel cooling could not be assured for large core masses characteristic of many US pressurized water reactors (PWRs). Consequently, we take no credit in our studies for invessel retention resulting from exvessel cooling. Even if exvessel cooling does not prevent lower head failure, it is likely to delay the failure. This increases the likelihood that the hot leg, surge line, or even the upper head will fail leading to complete depressurization of the RCS before lower head failure. No credit is taken for this in the current study.

NUREG-1150 computes the amount of cavity water based on several PDS-specific conditionalities; the most important of which are the fraction of ice melted and whether the RWST is fully injected into the containment. The latter requires AC power; consequently, wet or deeply flooded cavities cannot be expected in unrecovered SBOs. These quantifications are themselves dependent on other PDS-specific parameters. We have extracted summary values of cavity water from the NUREG-1150 output files themselves (Table 4.18). Table 4.17 shows that a flooded cavity is not possible in SBOs because AC power is required for containment sprays or emergency core cooling; consequently, the RWST cannot be injected into the containment. The probabilities of a wet cavity (in NUREG-1150) follow closely the probabilities of AC recovery (Table 4.14) suggesting a partial discharge of the RWST. With AC power in the plant, a dry cavity is not likely while a deeply flooded cavity is possible when large (but not total) ice inventories are melted.

Our benchmark evaluations use Table 4.17 entries for all branches that lead to vessel breach. We simplify the CET even further for the extrapolation evaluations. Recovered SBOs are low probability events that are ignored here, so there is no possibility of wet or deeply flooded cavities. In any case, we note that DCH loads (see Section 4.2.3) are insensitive to cavity water; consequently, we do not consider cavity water for branches that lead to failure of the lower head with RCS pressures greater than 200 psi (1.4 MPa). CONTAIN calculations described in Section 5 show that the ice beds are completely melted in non-SBOs if auxiliary feedwater is not available. Because AC power is available, the RWST tank can be fully injected into the containment. Consequently, for the limiting case of no auxiliary feedwater, we expect a deeply flooded cavity because the RWST is drained into the containment and the ice is fully melted. Our recommended quantifications for the extrapolation evaluations are listed in Table 4.18.

We chose the limiting case of no auxiliary feedwater as our ^{inappropriate} base case for convenience (as described in Section 5) while acknowledging that many PDSs for non-SBO could have auxiliary feedwater available. If auxiliary feedwater is available, the steam load on the ice chest is reduced and the potential for significant ice at vessel breach exists. This scenario is treated as a sensitivity (case 10, Section 7.3).

5.0 CONTAIN CALCULATIONS IN SUPPORT OF CONTAINMENT LOADS AT VESSEL BREACH AND ICE INVENTORY

5.1 Introduction

The probabilistic framework defined in Section 4.0 requires, for completion, the quantifications of DCH loads, non-DCH related hydrogen combustion loads, and non-DCH related steam spike loads. The loads must be specified for two dominant scenarios: station blackouts and non-station blackouts. SBOs are characterized by high hydrogen concentrations, significant ice inventory remaining, and no active containment cooling (i.e., sprays). Non-SBOs are characterized by low hydrogen concentrations, no ice inventory, and containment sprays in the base case. Previous discussions noted that with auxiliary feedwater available, significant ice could remain at vessel breach and the cavity could still be flooded. Various deviations from the base case will also be quantified here.

Peer reviewers criticized the original draft of this report because DCH loads calculations were performed using the TCE model under the assumption of no ice and no sprays for all scenarios. Peer reviewers recommended

- (1) Validation of CONTAIN's ice condenser models if CONTAIN is to be used in the load calculations, and
- (2) Model the ice condenser explicitly in the loads calculations.

The peer reviewers were explicit in their belief that significant ice would be present at vessel breach in all credible scenarios.

This section addresses these peer review comments in two ways. First, containment loads calculations were performed with the CONTAIN code so that appropriate credit can be taken for the ice condenser and containment sprays. Since the time of the draft report, the CONTAIN code has been benchmarked against Waltz Mill data for ice condenser performance (WEC, 1974). The CONTAIN code has also been validated for hydrogen combustion and steam spike events. The CONTAIN code has also been benchmarked against the existing DCH database for large dry containments, and key code parameters will be selected in a manner consistent with other DCH resolution activities.

Secondly, this section will address peer reviewer comments that significant ice will remain at vessel breach in all credible scenarios. An expanded set of CONTAIN calculations were performed with steam sources taken from SCDAP/RELAP5 to better define the scenarios when ice would or would not be present at vessel breach. A simple hand calculation was used to lend credibility to code calculations that the ice inventory will be depleted before vessel breach in non-SBOs when auxiliary feedwater is not available. Furthermore, plausible reasons are presented as to why the current calculations lead to depleted ice inventories for non-SBOs while code calculations cited in NUREG-1150 generally predicted that significant ice would remain at vessel breach

with auxiliary feedwater

At the transition between the SCDAP/RELAP-5 sources and the artificial decay heat source, the slope of the former (i.e., power) is less than that of the latter, which might suggest that our artificial prescription is conservative. On the other hand, exothermic energy from zircalloy oxidation is not included in the prescription, and a low value of core power was used for these calculations (3000 MW vs. the actual 3579 MW for Sequoyah), so some aspects of this calculation are non-conservative. The assumption that water is available (possibly from accumulator discharges) to carry decay power into containment as steam is justified by SCDAP/RELAP5 calculations for a best estimate RCP leak because the accumulators discharge. Sources of non-condensables from SCDAP/RELAP-5 were not modified for this prescription; however, the SCDAP/RELAP-5 calculations showed that most hydrogen was released into containment during the core degradation phase. Consistency with the prescription for the steam sources might be achieved by spreading the residual hydrogen release out over time, but this was not done; the purpose of constructing this source prescription was strictly to achieve a somewhat more realistic treatment of steam leaks, not to create a self-consistent substitute for detailed invessel code calculations. With this "extrapolated" steam source, CONTAIN 2.0 predicted that all ice was depleted well before 27000 seconds (the time predicted by SCDAP/RELAP-5 for vessel failure). This is illustrated in Figure 5.5. *and Reactor cavity was fully flooded.*

Apply artificial

*Stop no aux cavity!!
feedwater!!*

*Also no loss to water in cavity...
etc*

Best estimate SCDAP/RELAP5 calculations, carried through to vessel breach without hot leg failure, would be desirable for completeness. We already predict complete ice melting, so there is no potential for any mitigation of loads at vessel breach associated with the ice chest *mitigation by the flooded cavity* except for significant ice could persist up to vessel breach if auxiliary feedwater is modeled. With this ice inventory, we still expect the cavity to be deeply flooded; but in this case, the remaining ice will be available to mitigate loads at vessel breach. The deeply flooded cavity, and resulting steam spikes, are addressed in Section 5.5. The remainder of this section quantifies loads under the assumption of a dry cavity. As we will show, best estimate steam spike loads or dry cavity DCH loads are not containment threatening even when the ice is depleted. Consequently, we conclude that the availability of more representative system level calculations would not change the conclusions of this study.

Remove section cavity full of water

For non-SBOs, we can anticipate that the RWST will be drained and the ice inventory completely melted for the bounding steam sources described previously; consequently, the reactor cavity will be deeply flooded. Consistent with NUREG-1150, we treat HPME events as if they were steam spikes from a flooded cavity. As sensitivity studies show, it is insightful to perform DCH calculations under the assumption of a dry cavity or limited melt/water interactions in the cavity.

Not real

↑ why?

When cases like this were run in the 1.2 Series, pressurization during the DCH event posed a severe challenge to the containment, assuming the ice was depleted and the containment sprays were not operational. The treatment of this scenario is different in the 2.0 Series than in the earlier calculations because of the inclusion of containment sprays. One of the two redundant spray systems was assumed to be operational throughout the accident. The result was a significant reduction in peak pressure.

Note: we have ice in the chest or we have a flooded cavity

CONTAIN Calculations

from the RPV. We note that such calculations are strictly parametric. Pilch et al. (1997b) discuss some of the difficulties in parametric modeling of cavity water with CONTAIN. More phenomenological attempts at modeling cavity water and limited experiment data generally do not support the enhancement of containment pressures shown in Case VI-c/5. The final variation (VI-c/6) introduces the sheet steel from the RPV insulation as a source of molten metal into the debris jet; it corresponds to case 2 in Table B.9 (except that corrected insulation sources are used). These cases show that when key DCH parameters are set at values that are conservative, peak pressures are reduced by the effects of containment sprays, but they are still challenging to containment integrity.

We conclude from these results that for Case VI-c with the nominal assumption of a dry cavity

Why talk about dry cavity water it is wet and full of water

- the ice inventory is completely melted before vessel breach when ARFs and sprays are operational, but auxiliary feedwater is not available;
- steam spike loads can exceed DCH loads for some conditions;
- with ARFs and igniters operating, but sprays inoperable, the absence of ice in the ice condenser system implies containment challenging pressures, but neither is containment threatening;
- any combination of sprays or ice would effectively mitigate dry-cavity DCH loads.

5.3.2 Scenario VI-d: Station Blackouts

This scenario is important because the assumption of no electrical power to igniters, air return fans, and containment sprays is consistent with failure of operators to restore cooling to the core. In the absence of ARFs, steam from the lower compartment can follow two parallel paths to the upper containment: through the ice condenser system and through leakage paths that bypass the ice condenser. These leakage paths are not fully characterized in ice condenser plants. According to the Sequoyah FSAR, the leaks consist of two types: a well-characterized pathway through the refueling drains, and various unspecified leakage paths that are lumped together conservatively as having an area of 0.29 m² or less. The drain portion of the leakage will be closed off when the water level in the lower containment floods the drain openings. At that point the leakage consists solely of the unspecified pathways.

Flow of steam and other gases into the upper containment will be driven by very small pressure differences, so it is important to capture the behavior of the doors in the ice condenser as carefully as possible. Again, information on the behavior of the containment systems under these conditions is limited. Williams and Gregory (1990) cite a variety of industry sources on the behavior of the three levels of doors and create a relatively detailed model for the CONTAIN input decks. Appendix B includes a detailed discussion.

Response of the containment to this DCH scenario is dominated by the presence of high concentrations of unburned hydrogen throughout the containment at the time of vessel failure. Hydrogen production and heat transfer from the ejected debris during the DCH event exacerbate these conditions, and the debris is calculated to provide an ignition source where hydrogen and oxygen concentrations are in the flammable range. Figure 5.6 shows the pressurization

5.5 Containment Response for Non-DCH Relevant Scenarios

Because the probabilistic analysis in Section 4 addresses all containment failure modes, a number of CONTAIN calculations have been carried out for situations in which DCH does not occur. These are primarily low pressure scenarios. Having calculations from CONTAIN that use assumptions consistent with the DCH series is important for assessing the relative importance of DCH compared to other containment failure threats. Guided by the logic of NUREG-1150, we have addressed three scenarios that differ from the ones discussed earlier only in what happens at vessel breach:

- (1) non-DCH combustion of hydrogen in a SBO;
- (2) power available to containment ESFs with steam spike (i.e., igniters, sprays, and ARFs available);
- (3) power available with failure to switch to recirculation mode (i.e., sprays not available, igniters and ARFs available).

For the steam spike, we assume that the molten debris (~88 mt) was quenched by cavity water over a 5 s period, corresponding to the debris pour time. Steam was assumed to be generated at more or less saturated conditions, and injected into the containment atmosphere. These are conservative assumptions, since the amount of water available is very large, and some of the thermal energy would go into heating the liquid that is not boiled or ejected into the atmosphere. In addition, cavity pressurization from initial melt water interactions could delay the ejection of remaining melt into the cavity. We emphasize here that the ~88 mt melt mass represents the upper bound of the expected melt mass distribution, which is considered unlikely.

In fact, under the Zion DCH report NUREG/CR-6075, the probability of releasing 40mt of UO₂ is 2.01 and it would lead to containment due to the cavity being flooded and the formation of a crust liquid the vessel.

Table 5.7 lists the assumptions used in the steam spike analysis. We acknowledge the potential for explosive melt water interactions in the cavity and speculate that such events might blowout the walls of the freestanding cavity or displace the RPV. A steam spike is still possible in this scenario, but it is outside the scope of this study to judge if dynamic loads will couple with the containment shell or displace the RPV.

For the CONTAIN calculations, base case assumptions, as specified in Sections 5.2 are used for the powered and unpowered cases, respectively. Table 5.8 gives highlights of the results.

Table 5.7 Conditions assumed for steam spike

| Quantity | Value |
|---|--------------------|
| Debris mass (kg) | 8.77×10^4 |
| Enthalpy transferred (J) | 1.14 E+11 |
| Steam enthalpy relative to 273 K liquid (J) | 2.72 E+06 |
| Cavity water enthalpy (J) | 2.17 E+05 |
| Quench time (s) | 5 |

← too low for low pressure scenarios!

September 8, 1999

Dr. M. Khatib-Rahbar
Energy Research, Inc.
P.O. Box 2034
Rockville, Maryland 20847

Subject: Comments about August 1999 version of NUREG/CR-6427

As per your request, I have reviewed the latest version of the subject report and this letter provides my comments. I have also attached a copy of my comments dated February 18, 1998 on the previous version of the report because they are not included with the comments of the other peer reviewers and because I plan to refer to them rather than repeat myself on some issues.

GENERAL COMMENTS

1. The scope and objective of the study have been broadened considerably in this latest version of NUREG/CR-6427 and they should be examined carefully to determine whether they should be retained and in what order they are presented.

To put this comment in perspective, it should be recognized that for large dry containments Direct Containment Heating (DCH) "was the dominant mode of early containment failures and the DCH issue was resolved through plant specific probabilistic comparisons of DCH loads versus containment strength without taking credit for low High Pressure Melt Ejection (HPME) probabilities. In a few cases, recourse to elementary assessments of HPME probabilities or other supplementary arguments were required to ensure that the DCH issues was adequately resolved"⁽¹⁾. Those studies were coupled with the formulation of splinter scenarios and several new severe accident tests for large dry containments to generate new predictive models and to reduce the DCH loads and their probability of occurrence. The net result was a significant reduction in DCH risks for large dry containments.

My recommendation would be to confine NUREG/CR-6427 in its initial Sections to the DCH issue and HPME Probabilities as was done first in the case of large dry containments. Also the DCH loadings should be predicted from only the CONTAIN code (at first initially) because it provides for the ice condensation feature and because, as

⁽¹⁾ Page vx of NUREG/CR-6427.

noted on page xviii, "the ice beds were found to significantly reduce DCH loads in a Station Black Out (SBO) accident". The calculated containment failure probabilities from DCH loadings with CONTAIN should be provided in those initial Sections and they should be compared to the two NRC conditional failure metrics, $0.01 \leq \text{CCFP} \leq 0.1$.

This recommendation is made for several reasons:

- The new version of NUREG/CR-6427 continues to be dominated by the TCE/LHS methodology results even though it is valid only when the ice inventory is depleted and it is debatable when such depletion will occur.
- The decision to expand the probabilistic framework came from the TCE/LHS DCH predictions instead of those from the CONTAIN code.
- As discussed later, I have reservations about the CONTAIN non-SBOs and steam spike prediction probabilities which reinforce my concerns about the expansion to non-DCH loads.

It is recognized that the above recommendations would yield DCH results only for the Sequoyah plant but they would provide an answer which is applicable to an ice condenser containment and which can be compared to the various large dry containments on an equivalent basis.

2. The reassessment of NUREG-1150 also deserves careful scrutiny.

Considerable formality, peer review, and participation of experts went into NUREG-1150. No similar conditions were applied to the proposed reassessment. For example, **it is not clear why under non SBO conditions the refrigeration equipment is not restarted and, in particular, why water is not added to the secondary side of steam generators.** Both actions would delay if not stop the depletion of ice.

3. The discussion of ice condenser containments is biased in favor of large dry containments.

As noted in comment 8 of my letter of 8/18/98, the treatment of global scaling parameters is unfair because it neglects the ice condensers and igniters. I urge that we show the global parameters recognizing those inherent features of ice condenser containments. Similarly, in Section 3.2.2 dealing with ice condenser containment phenomena, I question why it is necessary to say so many times that there "is no analogue in large dry containments". One single statement stating that pressure suppression phenomena have no analogue in large dry containments should suffice. Finally, there is no effort to recognize the advantages of pressure suppression over large dry containments. They include the facts that the containment pressure is suppressed after most accidents and that the water and ice can trap a significant portion of the fission products released. Those were the two fundamental reasons for their introduction even though it was recognized that their reduced volume and pressure capability would not be as effective to cope with extreme severe accidents.

SPECIFIC COMMENTS

These comments are arranged in the ascending order of page number:

1. On page iii first paragraph and many subsequent pages, insert the word pressure when talking about low capacity of ice condenser containment.
2. On page iii, third paragraph the words "were taken" are repeated. Also, as noted before, I disagree with the statement that "the ice inventory will be depleted prior to vessel breach for many non-station blackout scenarios." This is true because of the decision to not add water to the secondary side of steam generators as noted later. Also, there is no basis for the statement that "CONTAIN calculations show that no ice condenser plant is inherently robust to all credible DCH or hydrogen combustion events in station blackouts" since calculations were not performed for all ice condenser plants.
3. On page iii, fourth paragraph, the noted probabilities were obtained with TCE/LHS and if that is the case it should be so stated.
4. On page iii, fifth paragraph, insufficient emphasis is given to the fact that early containment failures due to DCH are small because the HPME and SBO frequencies are small and because melt ejection was into deeply flooded cavities in non-SBO events. That was the primary purpose of this report.
5. On page iv, the concept of means of hydrogen control that is effective in SBOs was considered during the licensing process and rejected due to cost-benefit. If that is the case, it should be so noted.
6. On page xv, last paragraph should state that the methodology developed in NUREG-6075 does not take into account the presence of ice. This is an important shortcoming and the conclusions on top of page xvi are subject to debate for that reason.
7. On page xvii, it should be noted that there was no benchmarking of CONTAIN against integral severe accident tests as was done for large dry containments. This is unfortunate because, as noted in later sections, the uncertainties of the predictions remain large particularly by comparison to large dry containments.
8. On page xvii, I disagree with the last paragraph as noted before.
9. On page xviii, second paragraph, it does not make sense to use a dry cavity for non SBO events and a depleted ice inventory. I also disagree that the steam spike produces containment threatening loads. That is a result of the calculation assumptions as noted later.
10. On page xviii, sixth paragraph, see specific comment (4).

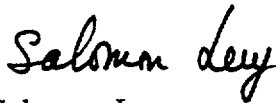
11. On page xix, third paragraph, I question whether this is the proper place to criticize IPE's. The same is true for third paragraph, page 1.
12. On page xix, last paragraph I am against the recommendation because I am not sure that it will change the current answers unless it is coupled with severe accident tests and a reexamination of severe accident management for ice condenser containments.
13. On page 2, last paragraph, it should be noted that the SCDAP/RELAP5 results were not specific to ice condenser studies and may have over estimated the steam sources as noted under the CONTAIN section.
14. On page 6, I disagree with item 5 because it is different from the criterion set for the large dry containment. With large uncertainties as in the case for ice condenser containments, the DCH loading failures need to produce a CCFP \leq 0.01 to be considered resolved irrespective of other early containment failure probabilities. Similarly, I do not agree with the last sentence on page 7 because the DCH issue needs to be resolved independently of other risks such as external events.
15. For section 3.0 see general comment (3). Also, it appears that an attempt is made to reopen issues previously settled in NUREG-1150, i.e. ice condenser bypass, ice door failing to reclose...etc. Some of those positions explain why I am reluctant to redo NUREG-1150.
16. On page 51 and 56, it is stated that DCH loads are relatively insensitive to hole size. This may not be true for pressure suppression containments because they are sensitive to rate of energy addition (for example, the peak dry well pressure in BWRs goes up as the energy input rises). Furthermore, in many of the accidents considered for ice condenser containment, the bottom of the reactor vessel will be submerged in water and the outside of the vessel would be cold and the propagation of the hole size may be reduced by comparison to tests performed for dry surfaces. Also, the hole may not be located at the bottom of the pressure vessel and the amount of material released could decrease significantly. On page 56, I have previously objected to the last sentence.
17. On page 60, I suggest that the liner failure probability be made a function of whether the reactor vessel is submerged in water.
18. On page 82, SCDAP/RELAP calculations for Sequoyah would have made more sense than the use of previous large dry containment and making all the adjustments on page 87. These difficulties are discussed on pages 87, 88 and 89.
19. On page 87, and under non-SBO conditions, it is not clear why pump seals leak when power is available to supply coolant to the seals. As noted previously, it is not clear why coolant is also not supplied to the secondary side of the steam generators to further delay or eliminate any hot leg failing (as in the TMI accident) and the depletion of ice. Finally, please note the conflict on page 92 of the assumption of a

dry cavity at the same time that the first bullet discusses a depleted ice inventory. With power available, the severe accident should develop as in the TMI-2 accident, i.e. no pump leak and decay heat removal through the steam generators.

20. On page 95, last line the statement that "ice inventory is exhausted for the more common case of non-SBOs" may not be appropriate as discussed under item 19.
21. On page 103, it is stated that "for the steam spike, we assume that the molten debris was quenched over a five second period, corresponding to the debris pour time". These conditions are noted to be conservative on the same page. I believe that they are very very conservative because of the previous comment 16 on hole size. Also, as the first molten material reaches the cavity, water will be thrown upwards and pressure will rise delaying the pour of the molten material. Finally the amount of material used is bounding rather than realistic and it will decrease sharply if the hole is not located at the bottom of the vessel.
22. The conclusions on pages 105 and 105 were obtained from CONTAIN and they are the only valid ones. They need to be more highlighted in the Abstract and Executive Summary because they show that the DCH loadings may not be as serious in terms of containment failure probability except for hydrogen combustion under SBO conditions. They provide less justification for a redo of NUREG-1150 and they tend to support my recommendation under the first general comment. A statement about uncertainties in phenomena and models may be appropriate at that same location to cover the discussion of uncertainties throughout the report.

I recognize that the preceding comments are extensive and sometimes challenging but they are made to provide a more realistic picture of ice condenser containments.

Sincerely yours,



Salomon Levy

P.S. I have just received the revisions to the Executive Summary. I disagree with the new statement on page 89a because as noted in previous comments there are other accident management actions which can be taken to avoid pump seal failures and encourage decay heat removal through the steam generators.

Cc Dr. R. Lee, NRC

BIBLIOGRAPHIC DATA SHEET

(See instructions on the reverse)

1. REPORT NUMBER
(Assigned by NRC, Add Vol., Supp. Rev.,
and Addendum Numbers, if any)
NUREG/CR-6427
SAND99-2553

2. TITLE AND SUBTITLE

**ASSESSMENT OF THE DCH ISSUE FOR PLANTS WITH ICE CONDENSER
CONTAINMENTS**

3. DATE REPORT PUBLISHED

| | |
|----------------|--------------|
| MONTH Apr 1 | YEAR 2000 |
|----------------|--------------|

4. FIN OR GRANT NUMBER

J6027

5. AUTHOR(S)

M. M. Pilch, K. D. Bergeron, J. J. Gregory (SNL)

6. TYPE OF REPORT

Technical

7. PERIOD COVERED *(inclusive Dates)*

8. PERFORMING ORGANIZATION - NAME AND ADDRESS *(If NRC, provide Division, Office or Region, U.S. Nuclear Regulatory Commission, and mailing address; if contractor, provide name and mailing address.)*

**Sandia National Laboratories
Albuquerque, NM 87185-1139**

9. SPONSORING ORGANIZATION - NAME AND ADDRESS *(If NRC, type "Same as above", if contractor, provide NRC Division, Office or Region, U.S. Nuclear Regulatory Commission, and mailing address.)*

**Division of Systems Analysis and Regulatory Effectiveness
Office of Nuclear Regulatory Research
U.S. Nuclear Regulatory Commission
Washington, DC 20555-0001**

10. SUPPLEMENTARY NOTES

Richard Y. Lee, NRC Project Manager

11. ABSTRACT *(200 words or less)*

This report (NUREG/CR-6427) addresses the Direct Containment Heating (DCH) issue for all Westinghouse plants with ice condenser containments. The approach taken here is to provide an expansion of a probabilistic framework, which represents a simplification of the NUREG-1150 containment event tree for Sequoyah. The containment event tree is intended to give each containment challenge its proper probabilistic weighting based on plant specific core damage frequencies, phenomenological probabilities, and plant specific fragility curves. The probabilistic framework addresses DCH-induced overpressure failures in the context of all significant early containment failure modes. These include DCH overpressure failures, thermal failures of the containment liner, non-DCH hydrogen combustion overpressure failures, and non-explosive steam spike overpressure failures.

The most significant finding of this study was that non-DCH hydrogen combustion events rather than DCH events dominate the early containment failure probability. This is because the HPME probability is small, the SBO probabilities are small, and because containment loads in non-station blackouts are not containment threatening. The CONTAIN code was used exclusively for predicting containment loads for representative station blackout and non-station blackout scenarios. CONTAIN calculations show that no ice condenser plant is inherently robust to all credible DCH or hydrogen combustion events in station blackouts. CONTAIN predictions show that containment loads in non station blackouts are not containment threatening for any reasonable plant damage state.

12. KEY WORDS/DESCRIPTORS *(List words or phrases that will assist researchers in locating the report.)*

*direct containment heating, ice condenser plants, severe accidents, CONTAIN Code,
hydrogen combustion, steam spike*

13. AVAILABILITY STATEMENT
Unlimited

14. SECURITY CLASSIFICATION
(This Page)
Unclassified

(This Report)
Unclassified

15. NUMBER OF PAGES

16. PRICE



Federal Recycling Program